

2022

# Identifying novel therapeutic targets for seizures and brain cancers

Ching, Jared

<http://hdl.handle.net/10026.1/19410>

---

<http://dx.doi.org/10.24382/695>

University of Plymouth

---

*All content in PEARL is protected by copyright law. Author manuscripts are made available in accordance with publisher policies. Please cite only the published version using the details provided on the item record or document. In the absence of an open licence (e.g. Creative Commons), permissions for further reuse of content should be sought from the publisher or author.*

## **Copyright Statement**

This copy of the thesis has been supplied on condition that anyone who consults it is understood to recognise that its copyright rests with its author and that no quotation from the thesis and no information derived from it may be published without the author's prior consent.



**UNIVERSITY OF  
PLYMOUTH**

**Identifying novel therapeutic targets for  
seizures and brain cancers**

by

**Jared Ching**

A thesis submitted to the University of Plymouth  
in partial fulfilment for the degree of

**DOCTOR OF PHILOSOPHY**

Peninsula Medical School

**October 2021**

## **Acknowledgements**

I would like to thank my Director of Studies, Professor David Parkinson, first and foremost for his enthusiasm and encouragement for me to undertake this PhD. Without him, this thesis would not be possible.

I would like to acknowledge all my previous laboratory and clinical supervisors, particularly those who were willing to consider my research proposals. I would like to thank Professor Colin McCaig for his immense support, sharing of knowledge, and imparting his wisdom over the years in both science and life matters. I am very fortunate to have had the pleasure of working in his outstanding laboratory in Aberdeen. I also would like to thank Dr Michal Pruski and Dr Hannah Clancy for their incredible hard work and persistence in our experiments on electric fields and glioblastoma.

My journey to pursue a Doctorate has not been typical or easy. I recall spending anywhere between 12 and 18 hours in the lab 7 days a week for many months to attempt to collect sufficient data for some of the projects described in this thesis. Prior to most of the lab work I performed, I would spend many hours reading the literature and attempting to ensure a robust experimental plan. In retrospect, I am not sure if I could repeat this kind of working schedule in the future but I certainly feel that it was worthwhile and fulfilling! It has also been a wonderful journey that has allowed me to make many friends from around the world and work with colleagues who have taught me so many things that I will probably never forget!

To my wife, Lisa, I am most fortunate that she has stuck by me throughout the years and helped me get through the tough times and rock bottoms. I am also so

happy to have welcomed Lucille into the world, during which time, I spent finalising this thesis.

Finally, I would like to acknowledge my parents for their undying support, inspiration, wisdom and willingness to never give up on anything. This thesis is dedicated to them.

## Declaration

All work enclosed in this research portfolio was carried out between the years 2011 and 2021. Research for each of chapter was undertaken at the indicated locations as follows:

Chapter 1: Department of Neurosurgery, Frenchay Hospital, Bristol, BS16 1LE (Closed 2014), UK

Chapter 2: Department of Neonatology, St Michael's Hospital, Bristol, BS2 8EG, UK

Chapter 3: Department of Neurosurgery, The Royal Melbourne Hospital, Melbourne, VIC 3050, Australia

Chapter 4: Departments of Neurosurgery and Neurology, The Royal Melbourne Hospital, Melbourne, VIC 3050, Australia

Melbourne Brain Centre, Kenneth Myer Building, Melbourne, VIC 3052

Chapter 5: Division of Neurosurgery, Addenbrooke's Hospital, Cambridge, CB2 0QQ, UK

Chapter 6: The Institute of Medical Sciences, University of Aberdeen, Aberdeen, AB25 2ZD, UK

Chapter 7: The Institute of Medical Sciences, University of Aberdeen, Aberdeen, AB25 2ZD, UK

At no time during the registration for the degree of Doctor of Philosophy has the author been registered for any other University award without prior agreement of the Doctoral College Quality Sub-Committee.

Work submitted for this research degree at the University of Plymouth has not formed part of any other degree either at the University of Plymouth or at another establishment.

Word count of main body of thesis: 16,590 words

Signed:

A handwritten signature in black ink, appearing to be 'A. King', written over a horizontal line.

Date: 21<sup>st</sup> October 2021

## Identifying novel therapeutic targets for seizures and brain tumours

Jared Ching

### Abstract

Epilepsy describes a range of conditions characterised by unprovoked recurring seizures that are due to multiple factors including the excitatory neurotransmitter glutamate. A subgroup of patients with epilepsy may not respond to systemic treatment and therefore would become candidates for surgical therapy. A less invasive approach is vagal nerve stimulation, which I demonstrated is safe and effective in 100 patients, in the first UK based large case series.

Another group of patients that suffer from intractable epilepsy are those with tumour associated seizures (TAS). In particular, patients diagnosed with glioblastoma multiforme can initially present with unexplained seizures or develop seizures later in the course of the disease. TAS is often pharmaco-resistant and treatment options are limited. Animal models of TAS demonstrated that the systemic  $X_c^-$  cysteine-glutamate exchange transporter (XCT) antagonist sulfasalazine reduced the frequency of seizures. In human studies of TAS, increased levels of glutamate, reduced excitatory amino acid transporter 2 (EAAT2) expression and reduced XCT were associated with greater frequency of TAS.

We found that EAAT2 single nucleotide mutations correlated with an increased susceptibility to cerebral palsy in pre-term infants, implicating glutamate excess as the underlying cause. Together with evidence of downregulation of EAAT at

the peri-tumoural region in TAS, it became evident that glutamate mediated excitotoxicity caused by dysfunctional EAAT2 may be a therapeutic target in such diseases. Therefore, I investigated strategies to modulate the expression of EAAT2, identifying peroxisome proliferator gamma (PPAR $\gamma$ ) agonists as a promising candidate.

I utilised Immortalised glioblastoma cell lines to investigate the role of the PPAR $\gamma$  agonist pioglitazone on glutamate transport in vitro. Pioglitazone was chosen for its established safety profile in type 2 diabetes and widely reported anti-neoplastic effects. I demonstrated that pioglitazone increases EAAT2 expression and reduces extracellular concentrations of glutamate in doses that do not affect cell viability. At the time of publication, this work identified a second drug candidate for the treatment of TAS in addition to sulfasalazine, which proved to be potentially unsafe in a clinical trial.

Glioblastoma is associated with a very poor prognosis due to its invasiveness and presence of cancer stem cells. We showed that the use of multimodal MRI can help delineate the invasive margin of glioblastoma but further therapeutic strategies would be needed. As such, my focus shifted to cancer cell migration since glioblastoma is known to be a highly infiltrative and diffuse disease, where glutamate mediate excitotoxicity was thought to facilitate this process. The concept of cancer stem cells offered a new explanation for treatment resistance, where this subpopulation of cells was shown to be resistant to conventional treatments. Further, I demonstrated that neural stem cells are directed by electric fields (EFs). As such, I investigated the role of EFs on both differentiated and cancer stem cells, finding that each cell type had opposing responses to EFs. I



subsequently investigated the role of pioglitazone, finding that directed cell migration was inhibited in both cells types, indicating that this drug class may have a further role in preventing glioblastoma recurrence.

## List of Contents

<b>INTEGRATIVE SUMMARY .....</b>	<b>11</b>
<b>CHAPTER 1: EPILEPSY AND VAGAL NERVE STIMULATION (VNS).....</b>	<b>12</b>
<b>CHAPTER 2: GLUTAMATE TRANSPORT IN NEONATAL BRAIN INJURY .</b>	<b>55</b>
<b>CHAPTER 3: GLUTAMATE TRANSPORT IN BRAIN TUMOURS .....</b>	<b>72</b>
<b>CHAPTER 4: MODULATING GLUTAMATE TRANSPORT IN BRAIN TUMOURS.....</b>	<b>84</b>
<b>CHAPTER 5: METABOLIC AND PERFUSION CHANGES IN BRAIN TUMOURS.....</b>	<b>103</b>
<b>CHAPTER 6: ELECTRIC FIELDS IN NEURAL STEM CELL MIGRATION ..</b>	<b>121</b>
<b>CHAPTER 7: ELECTRIC FIELDS IN BRAIN TUMOUR CELL MIGRATION</b>	<b>141</b>
<b>CHAPTER 8: GENERAL DISCUSSION AND CONCLUSIONS .....</b>	<b>181</b>
<b>EVIDENCE OF CONTRIBUTION.....</b>	<b>201</b>
<b>REFERENCES .....</b>	<b>207</b>
<b>PUBLISHED WORKS APPENDIX</b>	
<b>1) LONG-TERM EFFECTIVENESS AND TOLERABILITY OF VAGAL NERVE STIMULATION (VNS) IN ADULTS WITH INTRACTABLE EPILEPSY: A RETROSPECTIVE ANALYSIS OF 100 PATIENTS</b>	
<b>2) VARIANTS OF EAAT2 GLUTAMATE TRANSPORTER GENE PROMOTER ARE ASSOCIATED WITH CEREBRAL PALSY IN PRETERM INFANTS</b>	
<b>3) A NOVEL TREATMENT STRATEGY FOR GLIOBLASTOMA MULTIFORME AND GLIOMA ASSOCIATED SEIZURES: INCREASING GLUTAMATE UPTAKE WITH PPAR AGONISTS</b>	
<b>4) THE PEROXISOME PROLIFERATOR ACTIVATED RECEPTOR GAMMA AGONIST PIOGLITAZONE INCREASES FUNCTIONAL EXPRESSION OF THE GLUTAMATE TRANSPORTER EXCITATORY AMINO ACID TRANSPORTER 2 (EAAT2) IN HUMAN GLIOBLASTOMA CELLS</b>	

**5) MULTIMODAL MRI CAN IDENTIFY PERFUSION AND METABOLIC CHANGES IN INVASIVE MARGIN OF GLIOBLASTOMAS**

**6) PHYSIOLOGICAL ELECTRICAL SIGNALS PROMOTE CHAIN MIGRATION OF NEUROBLASTS BY UP- REGULATING P2Y1 PURINERGIC RECEPTORS AND ENHANCING CELL ADHESION.**

**7) GLIOBLASTOMA CELL MIGRATION IS DIRECTED BY ELECTRICAL SIGNALS**

## **Integrative Summary**

Research that I have undertaken over the last 10 years in neurosciences has predominantly been based on basic science enquiry that may have the potential to identify novel therapeutic targets in the future. I present my most relevant publications on the central nervous system (CNS) in the epilepsy, brain injury and brain cancer fields, summarising and identifying their significance in terms of scientific and clinical contributions. All research work included in these sections are based on studying diseases of the CNS with the unifying goal of identifying new treatment strategies. Each of the works presented in these sections acted as precursors for the next piece of work and ultimately form a body of evidence that indicates potential new ways of treating CNS disorders through neurochemical, cell signalling and electric field manipulation.

## **Chapter 1: Epilepsy and vagal nerve stimulation (VNS)**

### ***Introduction***

Epilepsy is a disorder of the brain characterised by an enduring predisposition to generate epileptic seizures, and by the neurobiologic, cognitive and psychological, and social consequences of this condition.<sup>1</sup> Where the definition of epilepsy requires the occurrence of at least one seizure according to the International League Against Epilepsy (ILAE) and the international Bureau for Epilepsy.<sup>1</sup> An epileptic seizure is defined as a transient occurrence of signs and/or symptoms due to an abnormal excessive or synchronous neural activity in the brain that have been classified according to onset, including focal, generalised and unknown.<sup>1,2</sup> The definition of epilepsy has been further clarified by the ILAE for clinical use to avoid ambiguity in certain clinical scenarios, such that a diagnosis of epilepsy can be made with any of the 3 definitions listed in Box 1.<sup>3</sup> The pathogenesis of epilepsy has a number of possible mechanisms, however animal studies have shown key roles for glutamate and gamma-amino butyric acid.<sup>4</sup> Gene mutations have been identified to have a role in hereditary epilepsy, such as faulty voltage gated sodium channels with prolonged opening times, where hyperexcitability may result and cause excessive glutamate release.<sup>5</sup> When glutamate transmission is uncontrolled, as is the case for epilepsy for example, excitotoxicity can ensue, which is characterised by cell injury or death secondary to overactivation of excitatory neurotransmitter receptors by substances such as glutamate.<sup>6</sup>

Approximately 50 million people worldwide are estimated to have epilepsy, of whom about one third will be resistant to treatment with medication and therefore

may require an epilepsy surgery workup.<sup>7,8</sup> Where resective surgery is not viable, for example if no discernible seizure focus was identified or multifocal in nature, palliative surgical options include vagal nerve stimulation (VNS), corpus callosotomy and multiple subpial resections.<sup>9</sup> Where cranial surgery fails, VNS has been shown to have a potential benefit on seizure frequency.<sup>10</sup>

Epilepsy is a disease of the brain defined by any of the following conditions:

1. At least two unprovoked (or reflex) seizures occurring more than 24 hours apart;
2. One unprovoked (or reflex) seizure and a probability of further seizures similar to the general recurrence risk (at least 60%) after two unprovoked seizures, occurring over the next 10 years;
3. Diagnosis of an epilepsy syndrome.

Box 1. Operational Clinical Definition of Epilepsy. Taken from Fisher et al.<sup>3</sup>

VNS is an invasive therapy that involves direct electrical stimulation of the vagus nerve via implanted electrodes powered by an impulse generator placed subcutaneously in the infraclavicular region. VNS is considered an adjunctive palliative treatment for intractable epilepsy where patients are not suitable for resective surgery or express a preference for an alternative to surgery requiring a craniotomy.

To date, studies of VNS have largely been based on cohorts in the USA, with no data published in the UK. While efficacy of VNS has been proven with randomised controlled trials, identifying individuals for whom VNS will benefit most is still challenging as only a proportion benefit and in a variable fashion. It has become increasingly recognised that “real world data” from non-randomised studies has value in assessing the efficacy of medical interventions.<sup>11</sup> In the UK,

the National Institute of Clinical Excellence has provided guidelines on the use of such data and regulatory agencies including the European Medicines Agency provide guidance in post-marketing effectiveness and safety studies.<sup>12,13</sup> As such, I completed a retrospective study in the Department of Neurosurgery, Frenchay Hospital Bristol to determine whether VNS was clinically efficacious and safe in accordance with the previous randomised controlled trials undertaken previously.<sup>14</sup> The results of this work would act to guide local policy as to whether to continue to fund VNS as a treatment option. As a prelude to this work, I reviewed the literature pertaining to the clinical studies to date of VNS, the role of neurotransmitters in epilepsy, neuroanatomy and neurochemistry of in VNS.

### ***Aims***

- Review the literature pertaining to clinical efficacy of VNS in epilepsy
- Review the physiological and pathological roles of neurotransmitters and ion channels
- Review the neuroanatomy and neurochemistry of VNS
- Undertake a retrospective study examining the efficacy of VNS in a UK population (published work)
- Summarise the current role of VNS in the context of existing and novel candidate treatments for pharmaco-resistant epilepsy
- Summarise the nature and significance of this work, and provide a critical appraisal of the published paper pertaining to this chapter

### ***Literature review***

*Clinical outcomes of vagal nerve stimulation in epilepsy:*

At the time of writing this original paper, the highest level of clinical evidence pertaining to the efficacy of VNS was a meta-analysis by Englot et al.<sup>15</sup> As of 2021, this still remains an important analysis in the field and has been frequently cited. In the field of treatment resistant depression, Bottomley et al. recently performed a systematic review and meta-analysis of VNS combined with treatment as usual, including systemic medications, psychotherapy, electroconvulsive therapy, repetitive transcranial magnetic stimulation, transcranial direct current stimulation or deep brain stimulation, finding it beneficial.<sup>16</sup>

In order to understand what data to collect in this retrospective study, I extensively reviewed the existing literature and summarised the most pertinent papers. This allowed me to define eligibility criteria, data collection parameters, set outcome measures and plan the type of analysis to perform in order to make this a relevant to the existing body of literature. Table VIII.<sup>14</sup> of this publication tabulates the most pertinent studies, a number of which I have summarised as follows:

Kuba et al. carried out a Czech Republic based retrospective, multicentre, open-label, study in all participants that received VNS over 5 years (90 patients). At 1 year no patients were seizure free, 3 patients (3.3%) experienced 90% reduction, 37 patients (41.1%) experienced 50% reduction, and the remaining 48 patients (53.3%) did not respond (defined as seizure reduction <50%, no change, or worsening of seizure frequency (Table 1.). Further increases in improvement were seen at 2 years and at 5 years: 5 patients (5.5%) seizure free, 9 patients (10%) experienced 90% seizure reduction, and the remaining 27 patients (30.1%) did not respond (Fig. 1).<sup>17</sup>



Responders	Non-responders
No seizures	Seizure reduction <50%
≥90% seizure reduction	No change in seizure frequency
≥50 seizure reduction	Worsening of seizure frequency

**Table 1:** Definition of responders and non-responders.<sup>17</sup>

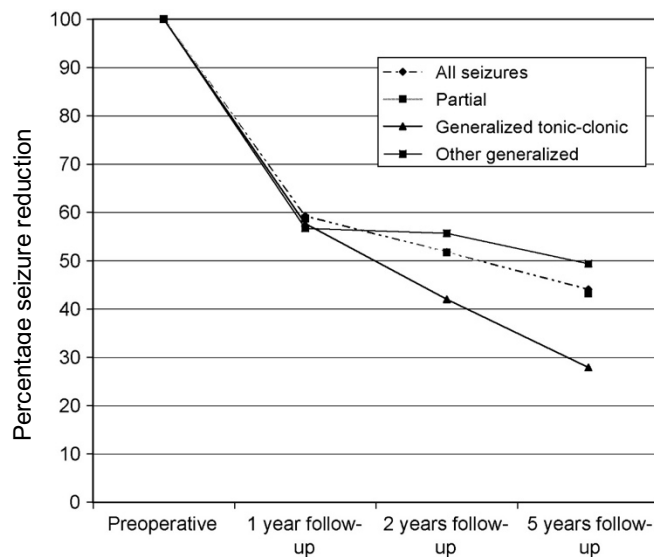


**Figure 1:** Summary of results, showing longitudinal reduction in all types of seizures at time points post VNS implantation.<sup>17</sup> NB: original graphs and images taken from certain publications are of a lower resolution due to printing limitations in the past.

Ardesch et al. performed a long-term descriptive study based in the Netherlands, recruiting 19 anti-epileptic drug (AED) resistant patients aged between 17-46 years not suitable for resective surgery to determine seizure reduction post VNS implantation. Gradual ramp up of current was performed in steps of 0.25mA every 3-4 weeks, with adjustments made for any side effects encountered. Mean seizure reduction progressively increased each year over the 6 year follow up in

a limited number of patients: year 1) 14%, (n=19), 2) 25%(n=19), 3) 29% (n=16), 4) 29% (n=15), 5) 43% (n=9), 6) 50% (n=7) (Fig. 2).<sup>18</sup>

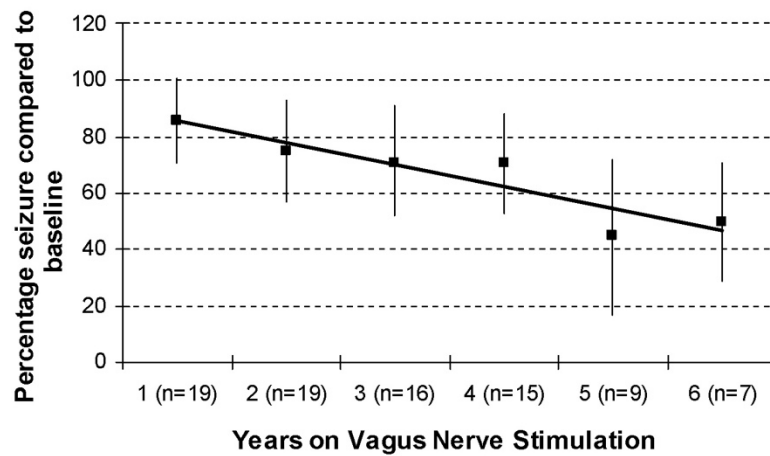


**Figure 2:** Percentage seizure frequency reduction over 6 years compared to 5-month baseline measurements, showing 95% confidence intervals.<sup>18</sup>

Spanaki et al. undertook a retrospective record review based in Wisconsin, Milwaukee, USA. Twenty-eight patients treated with VNS for  $\geq 5$  years were reviewed for changes in seizure frequency after 1 year of treatment and then followed up between 5-7 years. Median seizure frequency at baseline was 16.5 seizures per month (range 2-2,800), which reduced by 28% to 8.5 seizures per month (range 0-1400,  $p = 0.0053$ ) [Fig. 3].<sup>19</sup>

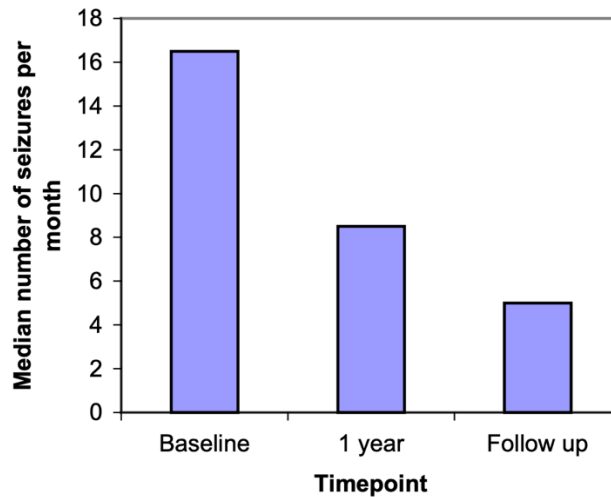


**Figure 3:** Median number seizures/month decreased from baseline to 12 months and follow up.<sup>19</sup>

DeGiorgio et al. performed the first long term prospective study of patients treated with VNS. One-hundred and ninety-five patients enrolled on the E05 Trial with  $\geq 6$  generalised or partial tonic-clonic seizures gave consent to be followed up over 12 months on the long-term safety and efficacy study of VNS - XE5. Mean reduction in seizure frequency at 3 months was 34% and at 12 months 45%. At 3 months 34% of participants had a 50-100% reduction in seizure frequency, of these 16% had >75% reduction in seizures frequency (Fig. 4).<sup>20</sup>

A prospective 3 year follow up study by Morris et al. based on the series of trials E01 to E05 undertaken between 1988 and 1997 (Fig. 5), recruited 440 patients. The following formula was used to assess the efficacy of VNS to determine a percentage change in seizure frequency:

**Efficacy** = [(daily seizure frequency during VNS stimulation – daily baseline seizure rate) x 100]/daily baseline seizure rate

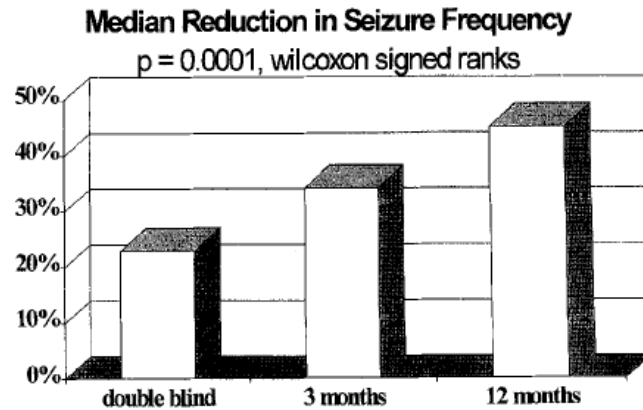


**Figure 4:** Median reduction in seizure frequency at end of DBRCT (E05) and long term follow up at 3 months and 12 months compared to 3 month prior to implantation seizure frequency.<sup>20</sup>

The formula above was used to determine efficacy over 3 years follow up. However, different analyses were used to take into account loss to follow including: 1) Last visit carried forward analysis, 2) Declining number, 3) Constant cohort.<sup>21</sup> It was found seizure frequency reduced over the period from 3 months to 3 years (Fig. 6).<sup>21</sup> >50% reduction in seizure frequency occurred post-implantation after: i. 1 year in 36.8% of patients, ii. 2 years in 43.2% of patients, and iii. 3 years in 42.7% of patients.<sup>21</sup>

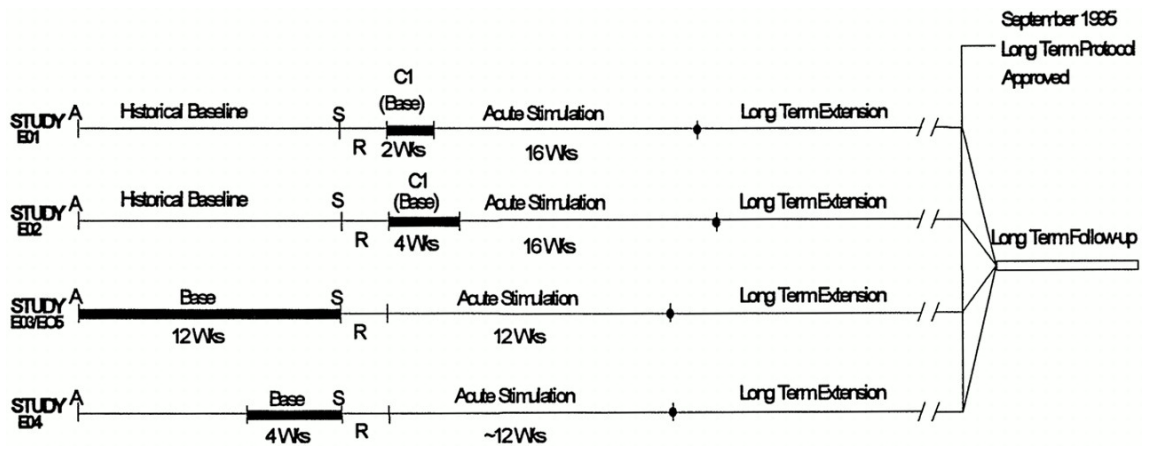


**Figure 5:** Study design of E01-E05. A = admission; S = surgery; R = postsurgical recovery; Base = baseline; C1 = control period (used as baseline period for seizure frequency comparisons).<sup>21</sup>

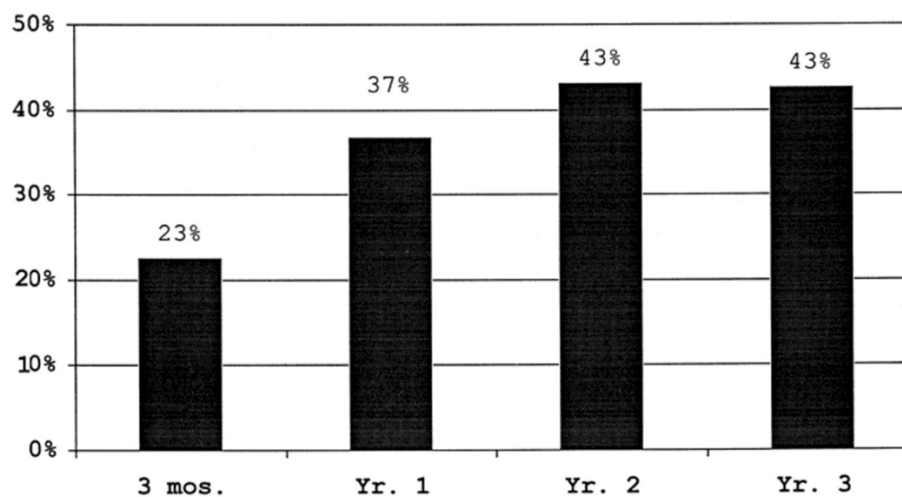


**Figure 6:** Percentage of patients (y-axis) experiencing a  $\geq 50\%$  seizure frequency reduction at 3 months, 1 year, 2 years and 3 years post-implantation (x-axis).<sup>21</sup>

The E05 randomised controlled trial (RCT) by Handforth et al. comparing VNS low and high stimulation settings in 254 patients with medically refractory partial onset seizures over 3 months. 94 patients receiving high stimulation (13-54 years old) had mean 28% seizure frequency reduction compared with 15% in the

active-control low stimulation group (152 patients, 13-60 years old), see Table 2.<sup>22</sup>

Menachem et al. performed a follow-up study after a 14-week blinded RCT with 67 patients, of whom 31 received therapeutic VNS and 36 receiving non-therapeutic VNS levels. 26 of the 31 who were randomised to treatment achieved a 52% mean seizure frequency reduction. For control patients converted to treatment VNS, 24 of 36 patients benefited from a mean reduction of seizure frequency of 38.1% (Fig. 7).<sup>23</sup>

Variable	Low	High
Patients (n)	102	94
Change in total seizure frequency from baseline (%)		
Mean $\pm$ SD	-15.2 $\pm$ 39.2	-27.9 $\pm$ 34.3
Mean difference and 95% CI	—	-12.7 (-2.3, -23.1)
Between-groups <i>p</i> value (aligned ranks)	—	0.04
Within-group <i>p</i> value (Wilcoxon)	<0.0001	<0.0001
Change in partial-onset seizures (%)		
With alteration of consciousness		
Mean $\pm$ SD	-13.4 $\pm$ 40.1	-26.6 $\pm$ 36.8
Mean difference and 95% CI	—	-13.2 (-2.3, -24.1)
Between-groups <i>p</i> value (aligned ranks)	—	0.03
Within-group <i>p</i> value (Wilcoxon)	<0.0001	0.0001
Patients with reduction in seizure frequency, n, %		
50% or more	16 (15.7)	22 (23.4)
75% or more	2 (2.0)	10 (10.6)*

\* *p* = 0.015, Fisher's exact test.

**Table 2:** Seizure frequency in active-control and treatment groups.<sup>22</sup>

### *Neurotransmitters in epilepsy*

Neurotransmitters are chemicals that permit transmission of signals across synapses and act by binding receptors that enable excitatory and inhibitory functions. Such neurotransmitters are largely stored in synaptic vesicles at the axon terminal of the presynaptic neuron, before release into the synaptic cleft following a signal such as an action potential. Released neurotransmitters

traverse the synaptic cleft and bind specific target receptors on a number of cell types.<sup>24,25</sup> Neurotransmitters that permit signal transduction across neurones are known to have an important role in epileptogenesis.<sup>26</sup> Seizures represent an imbalance between excitatory and inhibitory electrical activity amongst neurones.<sup>27</sup> The predominant neuronal excitatory and inhibitory neurotransmitters are glutamate and gamma-aminobutyric acid (GABA), respectively, which play an important role in neuronal excitability.<sup>28,29</sup> These and other neurotransmitters have important roles in epilepsy (Fig. 8), where the following focuses specifically on glutamate receptors and its transport.

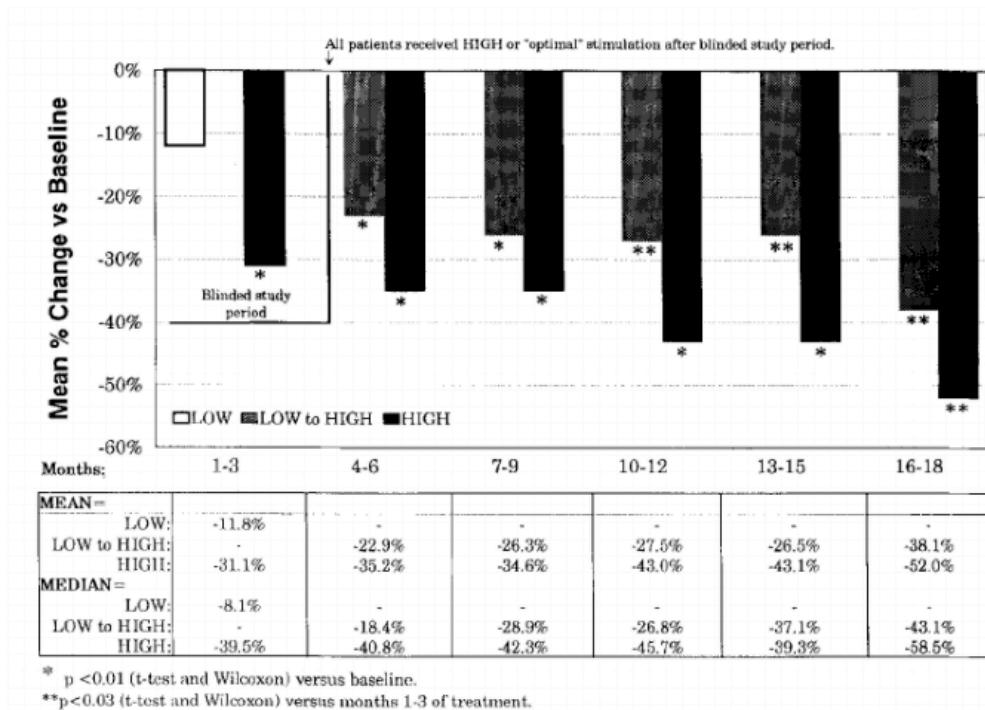


**Figure 7:** Mean seizure frequency percentage change over time. In months 1-3 the open column represents patients randomised to low VNS stimulation settings to act as an initial control and then after month 3, these patients were provided high optimal settings as per the treatment group.<sup>146</sup>

THE MAIN NEUROTRANSMITTERS in EPILEPSY

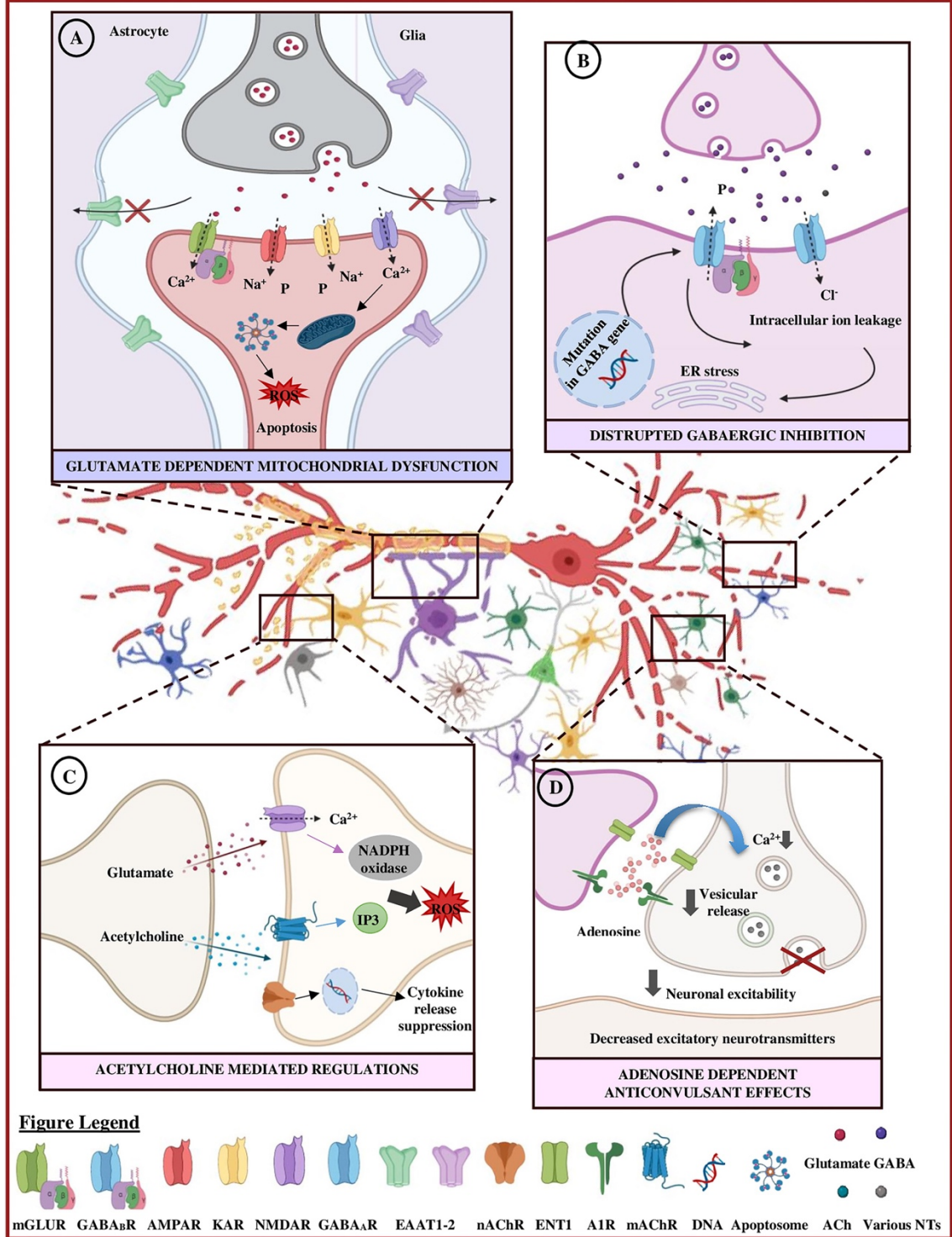


**Figure 8:** Key neurotransmitters involved in epilepsy. A. Glutamate binds NMDA and AMPA receptors causing increased calcium and reactive oxygen species formation, resulting in excitotoxicity in glutamate excess. Apoptotic pathways are activated during oxidative stress due to mitochondrial disturbance. B. GABA



mediates an inhibitory effect by binding to GABA<sub>A</sub>, which transports Cl<sup>-</sup> into the cell, while GABA<sub>B</sub> transports K<sup>+</sup> out. GABA subunit mutations in epilepsy can cause ER stress or intracellular ion leakage. C. Some nicotinic acetylcholine receptors suppress cytokine release and are therefore thought to contribute to neuroinflammation involved in epilepsy. Muscarinic acetylcholine receptor activation provides IP<sub>3</sub> and together with glutamate receptor activation, generate reactive oxygen species that activate apoptotic mechanisms involved in epilepsy. D. Adenosine reduces neuronal excitability by preventing vesicular neurotransmitter release by binding A<sub>1</sub>R and ENT1 receptors that are part of an anti-inflammatory cascade. Taken from Akyuz et al.<sup>27</sup>

### Glutamate receptors

Glutamate is the anion of glutamic acid and the predominant amino acid found in the brain.<sup>30</sup> Glutamate is generated by the glutaminase enzyme in the glutamate-glutamine cycle in the presynaptic neurones and adjacent glial cells.<sup>31</sup> Glutamate mediates its functions by binding cell surface receptors that include  $\alpha$ -amino-3-hydroxy-5-methyl-4-isoxazole propionate receptors (AMPA), N-methyl-D-Aspartate (NMDAR), kainate (KA) receptors, and metabotropic glutamate receptors (mGluR). AMPAR, NMDAR and kainate receptors are ionotropic receptors that permit ions to pass when in the activated state.<sup>32</sup> The ionotropic glutamate receptors are tetrameric, that is constituting of four proteins, each containing three transmembrane segments, and structurally have a ligand binding site and ion channel that undergoes conformational changes upon ligand binding to allow ion passage.<sup>33</sup> Each channel demonstrate selective ion permeabilities, for example NMDAR is mostly Ca<sup>2+</sup> permeable but also permeable to K<sup>+</sup> and Na<sup>+</sup>, whereas kainate receptors and AMPAR are almost

exclusively  $K^+$  and  $Na^+$  permeable.<sup>32,34</sup> AMPAR receptors lacking the GluA2 subunit are known to be  $Ca^{2+}$  permeable.<sup>35</sup> mGluR monomeric proteins comprise an intracellular domain that binds G-proteins and an extracellular domain that contains a binding site for neurotransmitters. Unlike ionotropic glutamate receptors, mGluRs do not have a ion pore and instead affect biochemical cascades that lead to modification of other proteins downstream, including ion channels.<sup>36,37</sup> As such, ion pore opening is mediated much more quickly by ionotropic glutamate receptor activation compared to mGluR, where the former facilitates rapid synaptic transmissions.

NMDA receptors have been shown to be dynamically expressed in the brain and are important regulators of synaptic plasticity.<sup>38</sup> Their structure is composed of 2 types of subunits that include GluN1 and GluN2, where D-serine or glycine is known to bind GluN1 and glutamate binds GluN2 (Fig. 9).<sup>39</sup> There are four subtypes of GluN2 subunits (GluN2A-D).<sup>40,41</sup> Each subunit type share features including a cytoplasmic C-terminal domain, a pore forming transmembrane domain and a large extracellular region composed of two clam shell like domains; the N-terminal domain and the ligand binding domain.<sup>40</sup> In resting conditions, concentrations of D-serine and glycine are thought to be sufficient to maintain binding on the GluN1 subunit, such that NMDA receptor activation is essentially reliant on glutamate binding to the GluN2 subunit.

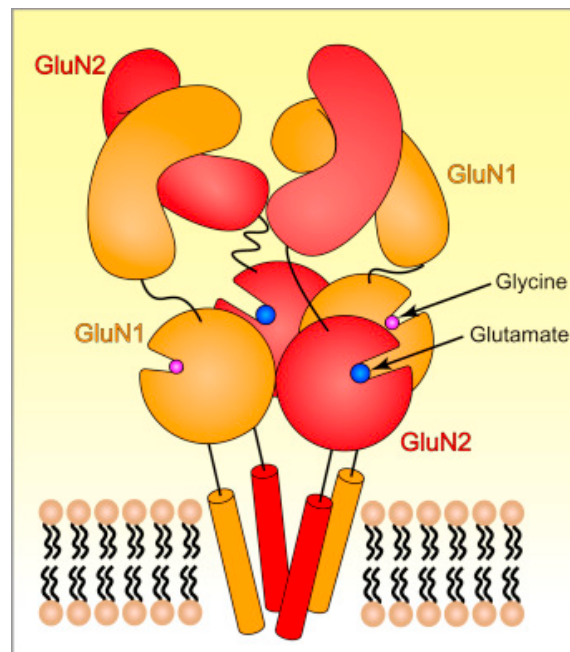


**Figure 9:** NMDA receptors are tetrameric, containing 4 protein subunits. The GluN1 subunit binds D-serine or glycine and the GluN2 subunit binds glutamate. The cytoplasmic or transmembrane domains are not represented in this simplified diagram. Diagram taken from Meriney and Fanselow.<sup>42</sup>

In the resting state, NMDA receptor ion pores are blocked by  $Mg^{2+}$  binding on a binding-site within the pore, which occurs due to the negative charge within the cell membrane attracting the  $Mg^{2+}$  ion. When depolarisation occurs, the  $Mg^{2+}$  ion is repelled by the change in membrane charge and in the presence of glutamate binding, the receptor permits ion flux.<sup>43</sup> Therefore, NMDA receptors are frequently called a “coincident detector” (Fig. 10).<sup>44</sup>

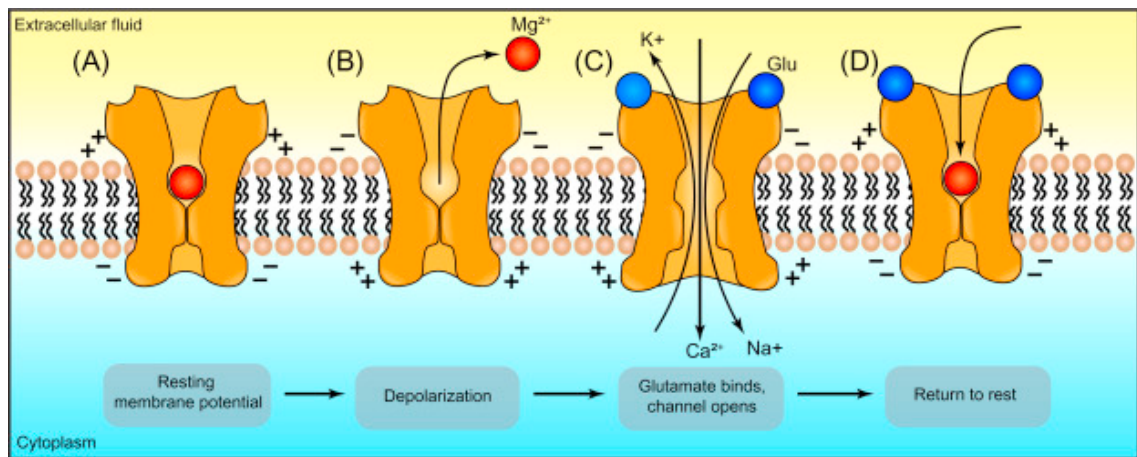


**Figure 10:** Magnesium blockade of NMDA receptor. (A) Magnesium is attracted into the ion pore due to the negative resting membrane potential, preventing ion flux when glutamate binds the NMDA receptor. (B) When the membrane is depolarised, magnesium is repelled. (C) If glutamate binds the NMDA receptor during depolarisation, calcium and sodium enter the cell through the pore, while potassium leaves. (D) When the resting potential is restored, the magnesium ion returns to block the ion pore. Diagram taken from Meriney and Fanselow.<sup>42</sup>

Dysfunction of NMDAR subunits is known to be associated with certain brain diseases. Synaptic NMDARs typically contain GluN2A subunits that are associated with faster kinetics and involved with synaptic plasticity.<sup>45</sup> Extrasynaptic NMDARs generally contain GluN2B, which displays slower kinetics and thought to be associated with excitotoxicity in Parkinson's disease for example.<sup>46,47</sup> Genetic variation in *Grin2a* and *Grin2b*, the genes encoding GluNR2A and GluNR2B subunits respectively, are associated with neurodevelopmental disorders that can be associated with a range of epilepsies and cognitive impairments such as Landau-Kleffner Syndrome and idiopathic focal epilepsy.<sup>48</sup> Numerous mutations in the NMDAR subunits have been identified in human epilepsy, where 12 mutations in *Grin1*, 82 mutations in *Grin2a*, and 13 mutations in *Grin2b* have so far been characterised.<sup>49</sup> By far the

most frequently occurring mutations of the NMDAR subunits are in Grin2a, where 28 of the 32 investigated, have been shown to have functional significance in epilepsy.<sup>50</sup> This suggests that Grin2a mutations are most closely associated with the epilepsy phenotype. Therefore, manipulation of NMDAR subunits to increase or decrease signalling to ameliorate diseases has become an area of therapeutic interest. For example, memory enhancement has been shown with inhibition of phosphorylation of Ser1116 on the GluNR2A subunit by cyclin-dependent kinase 5.<sup>51</sup>

Inflammatory mechanisms have been linked to some forms of epilepsy following the emergence of evidence linking immune system activation and epilepsy, the high incidence of epilepsy associated with auto-immune diseases and the discovery of limbic encephalitis (a group of auto-immune conditions associated with inflammation of the limbic system characterised by loss of short-term memory and a other neuropsychiatric features including epilepsy).<sup>52,53</sup> Brain inflammatory mediators are known to cause neuronal hyperexcitability and epilepsy, including interleukin-1 $\beta$  (IL-1 $\beta$ ), tumour necrosis factor (TNF), prostaglandin E2 (PGE2) and the complement cascade.<sup>54</sup> IL-1 $\beta$  has been found to induce tyrosine phosphorylation of GluNR2A/B subunits of hippocampal neurons, leading to raised NMDA mediated intracellular Ca<sup>2+</sup> flux.<sup>55</sup> There is clinical evidence to support these observations where elevated IL-1 $\beta$  in cerebral spinal fluid (CSF) has been detected in febrile seizures<sup>56</sup>, tonic clonic seizures<sup>57</sup>, and temporal lobe epilepsy.<sup>58</sup> Other inflammatory mediators associated with neuronal hyperexcitability include astrocytic glutamate release through TNF $\alpha$  signalling<sup>59</sup>, cytokine mediated glial glutamate uptake inhibition<sup>60</sup>, and glutamate receptor trafficking through TNF $\alpha$  signalling.<sup>61</sup> Inflammatory mediators can be

released from neurones, glial cells, peripheral immune cells and blood-brain-barrier endothelial cells, which may or may not be glutamate-mediated downstream and contribute to epileptogenesis in a variety of conditions.<sup>62</sup>

### Glutamate transporters

In the central nervous system, a small proportion of synaptic glutamate binds glutamate receptors, around 10 to 20%, while the remaining 80 to 90% or more is taken up via glutamate transporters in neurones and astrocytes.<sup>63</sup> There are two main types of glutamate transporters: Na<sup>+</sup>-independent and Na<sup>+</sup>-dependent transporters.<sup>64</sup> Na<sup>+</sup>-independent transporters are chloride dependent anti-porters that permit cysteine/glutamate exchange and uptake a relatively small proportion of glutamate.<sup>65</sup> In contrast, Na<sup>+</sup>-dependent transporters are termed excitatory amino acid transporters (EAAT) and uptake the majority of extracellular glutamate.<sup>66</sup>

### *Na<sup>+</sup>-independent transporters*

Na<sup>+</sup>-independent transporters are expressed in multiple cell types including astrocytes<sup>65</sup>, microglia<sup>67</sup>, retinal Müller cells<sup>68</sup> and glioma cells.<sup>69</sup> Such transporters were initially classified according to their functional properties that may have included substrate specificity, ion and pH dependence, kinetics and regulatory properties. Later, these transporters were classified as “systems” and a specific nomenclature ascribed that included distinction between Na<sup>+</sup> dependence, where uppercase letters would indicate Na<sup>+</sup> dependence (e.g. System L) and lower case letters would indicate independence (e.g. System y<sup>+</sup>).<sup>70</sup> Of importance to glutamate homeostasis, the system x<sub>c</sub><sup>-</sup> antiporter imports cystine (the oxidised form of cysteine) in exchange for exporting glutamate with

a stoichiometry of 1:1.<sup>71</sup> It is a transmembrane  $\text{Na}^+$  independent and  $\text{Cl}^-$  dependent electroneutral amino acid transporter with relatively low expression central nervous system in normal conditions.<sup>72,73</sup> The nomenclature of this system has been previously clarified, where  $x^-$  indicates a preference for dicarboxylic acid in their anionic form.<sup>74</sup> The system  $x_c^-$  is composed of a light chain, xCT, and heavy chain 4F2 (Fig. 11), and as such is part of a family of heterodimeric amino acid transporters.<sup>75</sup> The 4F2hc heavy chain is a single transmembrane glycoprotein that is thought to be universal across the heterodimer membrane transporter family system L.<sup>76</sup> 4F2hc does not function to transport amino acids, however it is essential for system  $x_c^-$  function as it brings xCT to the membrane.<sup>77,78</sup> xCT is encoded by the solute carrier family 7, member 11 (slc 7a11) gene and determines substrate specificity of system  $x_c^-$ .<sup>77</sup> The xCT subunit structure includes a 12 transmembrane domain with a re-entrant loop and cytosolic N- and C- termini.<sup>79</sup>

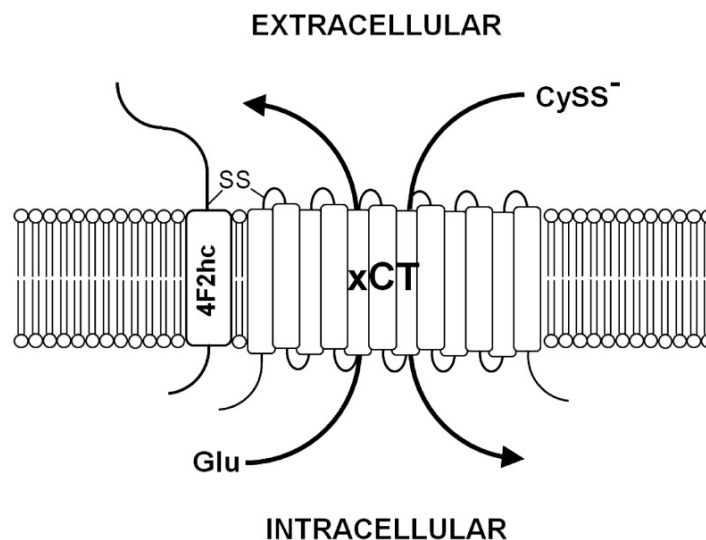


**Figure 11:** System  $x_c^-$  is composed of a heavy chain 4F2hc and light chain xCT which are bound by a disulphide bond. Cystine ( $\text{CySS}^-$ ) is exchanged for glutamate (Glu). Diagram taken from Lewerenz.<sup>76</sup>

Cystine imported intracellularly by the system  $x_c^-$  has an important antioxidant role whereby cysteine is formed from cystine following immediate reduction upon entering the intracellular space either by intracellular glutathione (GSH) via the formation of a mixed disulfide intermediate or by thioredoxin reductase 1 (TRR1).<sup>80</sup> GSH is a tripeptide containing glutamate, glycine and cysteine, and mediate antioxidant properties by: 1) Directly quenching reactive hydroxyl free radicals, oxygen-centred free radicals, and radicals on DNA, and 2) Acting as a co-substrate for glutathione peroxidase, which hydrolyse hydrogen and lipid peroxides.<sup>81</sup> Although astrocytes and neurones have been shown to express system  $x_c^-$ , aged neurones have little or no  $x_c^-$  activity, such that one of the important functions of astrocytic  $x_c^-$  is to provide neuroprotection during oxidative stress.<sup>82</sup> xCT is an inducible molecule that is dependent on transcriptional activation of NF-E2-related factor (Nrf2) or inducible factor 1 $\alpha$  (Hif-1 $\alpha$ ), where oxidative stress can increase its expression to increase cystine uptake but concomitantly release glutamate, which can be deleterious to surrounding neurones.<sup>83-85</sup> Glutamate has been shown to act as a competitive inhibitor for the uptake of cystine via system  $x_c^-$ , where  $K_i$  for glutamate inhibition of cystine uptake by system  $x_c^-$  is 150 $\mu$ M, while the  $K_i$  for cystine inhibition of glutamate uptake is 33 $\mu$ M.<sup>86</sup> The direction of transport is driven by high intracellular concentrations of glutamate and low concentrations of intracellular cystine.

There is emerging evidence for the role of system  $x_c^-$  in epileptogenesis and as a possible novel anti-convulsant target.<sup>87</sup> Leclercq et al. used a xCT deletion mouse model to investigate the effect of three different pro-convulsant models compared to control mice on the development and susceptibility to seizure induction.<sup>88</sup> These models included the self-sustained status epilepticus, corneal kindling and



pilocarpine models. These authors found that in all in epilepsy models used, a reduction in seizure frequency and severity was observed in xCT deletion mice compared to controls. Further, they found that sulfasalazine, a specific system  $x_c^-$  inhibitor, significantly reduced seizures in pilocarpine kindled mice where xCT expression was found to be increased. In another recent study investigating the role of system  $x_c^-$ , specifically in the pentylenetetrazole chemical kindling model of epilepsy, Sears et al. showed that  $x_c^-$  knock out mice demonstrated a significant resistance to epileptogenic kindling.<sup>89</sup> Therefore, this evidence points towards the therapeutic potential of inhibiting system  $x_c^-$  to modify export of glutamate. However, further research would be required to determine whether this is truly a translatable target, for example, does xCT deletion result in neural network alternations that cannot be recapitulated with pharmacotherapy in the acute phase of epileptogenesis? Further studies will be required to provide definitive evidence of the potential of system  $x_c^-$  in epilepsy. Prior to this work, the role of system  $x_c^-$  was well established in glioma-associated-seizures found to be due to overexpression of system  $x_c^-$  and reduced  $Na^+$  dependent glutamate transporters.<sup>90</sup> The same group later demonstrated that system  $x_c^-$  can be inhibited by sulfasalazine, resulting in reduced seizure frequency.

#### *Na<sup>+</sup>-dependent transporters*

$Na^+$ -dependent high affinity glutamate transporters, also known as excitatory amino acid transporters (EAAT), account for the majority of synaptic glutamate transport, approximately 80% of uptake.<sup>63</sup> EAATs belong to the solute carrier 1 (SLC1) family, where 5 subtypes EAAT1-5 have been identified.<sup>91</sup> Each of these subtypes demonstrate different expression patterns.<sup>92</sup> Glutamate transport by EAATs is coupled to ion flux, where the stoichiometry of EAATs 1-3 has been

established as co-transport of 3 Na<sup>+</sup> and 1 H<sup>+</sup>, followed by counter transport of K<sup>+</sup> (Fig. 12).<sup>93,94</sup> Substrate binding to EAATs also generates a thermodynamically uncoupled Cl<sup>-</sup> flux through the transporter (Fig. 12).<sup>95</sup> The stoichiometry of EAAT4-5 has not been established, however, it has been shown that neuronal EAAT4-5 behave predominantly as Cl<sup>-</sup> channels, whilst Cl<sup>-</sup> flux plays a much smaller role in EAAT1-3 transporter function.<sup>96</sup>

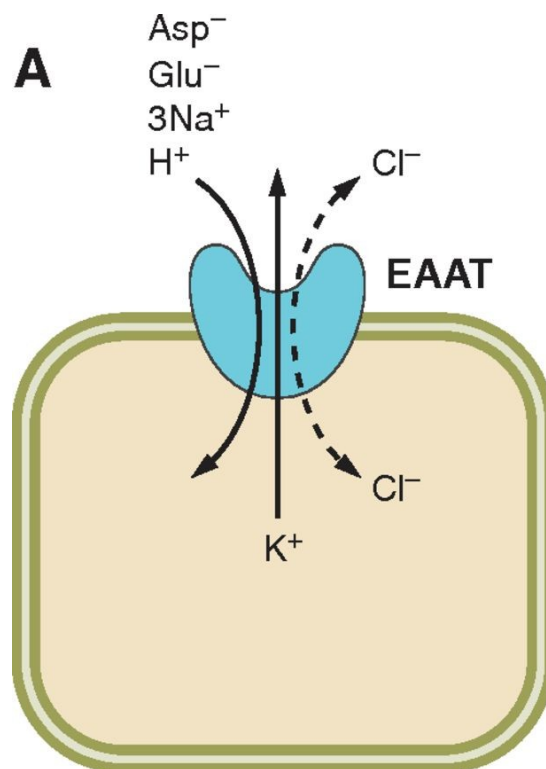


**Figure 12:** Stoichiometry of ion-flux coupling of EAAT. the stoichiometry of EAATs 1-3 has been established as co-transport of 3 Na<sup>+</sup> and 1 H<sup>+</sup>, followed by counter transport of K<sup>+</sup>. Substrate binding to EAATs also generates a thermodynamically uncoupled Cl<sup>-</sup> flux through the transporter (A). Image taken from Vandenberg et al.<sup>97</sup>

EAATs are secondary electrogenic transporters that were shown in early work to produce large rectifying inward currents between -160 and +80mV in response to the addition of extracellular glutamate in electrophysiological recordings.<sup>98</sup>

Initial transport kinetic experiments showed that membrane hyperpolarisation stimulated glutamate concentration dependent transport. Watzke et al. used a photo-releasable glutamate analogue to further elucidate glutamate binding and translocation, finding a very brief electrogenic component on glutamate release that rapidly decayed to steady state levels.<sup>99</sup> Glutamate translocation has been shown to be dependent on the binding and co-transport of several cationic species, where  $\text{Na}^+$  binding to the empty transporter has been shown to be a voltage dependent process.<sup>100</sup> Electrogenicity of EAATs has been further characterised using a combination of pre-steady state concentration and voltage jump experiments with computational modelling, where Grewer et al. found that negative charge generated by EAAT transporter is partially compensated by  $\text{Na}^+$ ,  $\text{H}^+$  and  $\text{K}^+$  ions.<sup>101</sup> Overall, the ion binding compensates the endogenous transporter charges, in addition to a defocused electric field and distribution of electrogenic steps, resulting in a highly regulated 4 state glutamate stoichiometry and ion movement (Fig 13).

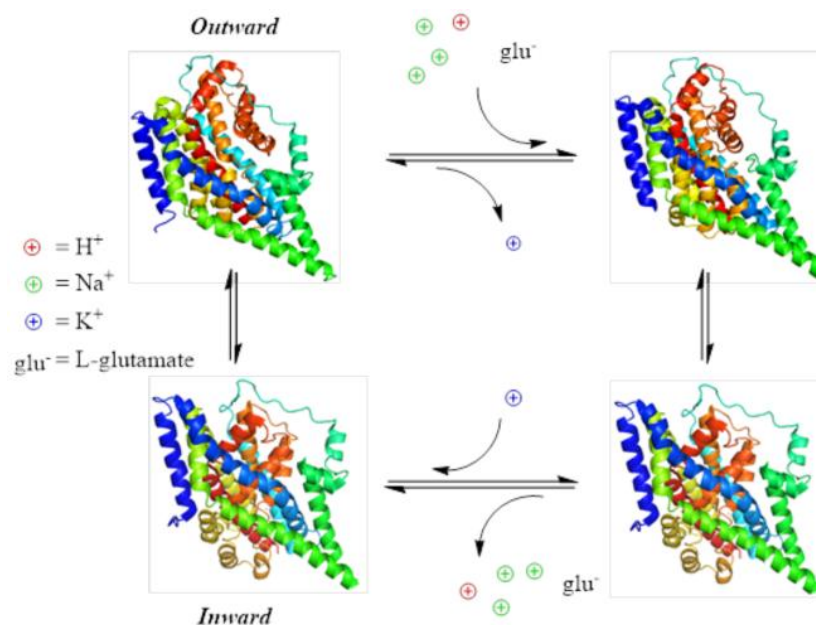


**Figure 13:** Electrogenicity and stoichiometry of EAATs. Four state diagram demonstrating the outward open state (upper left), outward bound occluded state

(upper right), inward occluded state (lower right), and the inward open state (lower left). Diagram take from Divito & Underhill.<sup>102</sup>

### *Ion channels in epilepsy*

There are 3 primary ways that ion channels are known to be involved with epilepsy: 1) Specific mutations in familial idiopathic epilepsies, 2) Specific antibodies in acquired seizure-related disorders, and 3) Ion channel changes in expression and function.<sup>103</sup> A number of ion channels are involved in these processes, including voltage gated sodium ( $\text{Na}_v$ ) channels, voltage gated potassium ( $\text{K}_v$ ), voltage gated calcium channels ( $\text{Ca}_v$ ), and nicotinic acetylcholine receptors (nACh). The role of such channelopathies has been reviewed elsewhere<sup>104</sup>, and the following discussion will focus on  $\text{Na}_v$  and their blockade as an anti-epileptic drug.

#### Voltage gated sodium channels ( $\text{Na}_v$ )

$\text{Na}_v$  are integral membrane proteins that change conformation in response to membrane potential depolarisation, resulting in transmembrane pore opening that allows inward  $\text{Na}^+$  ion conductance, propagating action potentials.<sup>105</sup> As such,  $\text{Na}_v$  have important roles in nerve conduction, cardiac and skeletal muscle contraction, neurotransmission, amongst other processes, and have also been shown to play a critical role in seizure initiation and spread.<sup>106,107</sup> There are three stages of sodium channel between inactivation and activation, including: 1) Resting phase (channel closed), 2) Active phase (channel open) and 3) Inactive phase (non-conductance) (Fig. 14).<sup>108</sup>

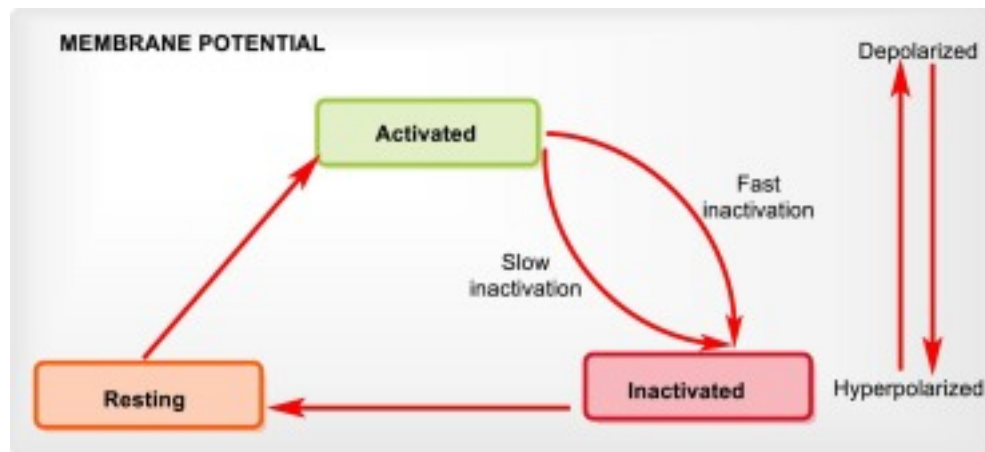


**Figure 14:** Schematic summarising the three stages of sodium channel. The cycle starts at the resting phase, and depolarisation occurs, the channel opens in the activated state, allowing inward  $\text{Na}^+$  flux for milliseconds, before the inactivated phase, characterised by non-conductance of  $\text{Na}^+$  ions. Slow inactivation occurs when there is repetitive or prolonged high firing of neurones. Schematic taken from Pal et al. <sup>109</sup>

Structurally,  $\text{Na}_v$  contain  $\alpha$ -subunits that can be coupled to one or two  $\beta$ -subunits. The different  $\text{Na}_v$  subtypes are defined by their distinctive  $\alpha$ -subunits, which include receptor sites for drugs and toxins that can modulate  $\text{Na}_v$  function. Accordingly, there are nine subtypes  $\text{Na}_v1.1$  to  $\text{Na}_v1.9$ , which can be further classified to their sensitivity to the guanidine-based tetrodotoxin (TTX) sensitivity, where  $\text{Na}_v1.1$ ,  $\text{Na}_v1.2$ ,  $\text{Na}_v1.3$ ,  $\text{Na}_v1.4$ ,  $\text{Na}_v1.6$ ,  $\text{Na}_v1.7$  are TTX-sensitive, whilst  $\text{Na}_v1.5$ ,  $\text{Na}_v1.8$ , and  $\text{Na}_v1.9$  are TTX resistant.<sup>110</sup> Each  $\text{Na}_v$  subtype is encoded by a specific gene, including *SCN2A*, *SCN3A*, *SCN4A*, *SCN5A*, *SCN8A*, *SCN9A*, *SCN10A*, *SCN11A*, in order of  $\text{Na}_v1.1$  to  $\text{Na}_v1.9$  (Table 3).

Channel Isoform	Gene	Inactivation Rate	Tissue Localization	TTX Sensitivity
NaV1.1	SCN1A	Fast	Mainly in CNS, also found in DRG	Sensitive
NaV1.2	SCN2A	Fast	Mainly in CNS	Sensitive
NaV1.3	SCN3A	Fast	Mainly in Embryos, also found in CNS	Sensitive
NaV1.4	SCN4A	Fast	Skeletal Muscle	Sensitive
NaV1.5	SCN5A	Slow	Mainly in heart, also in Embryos and DRG	Resistant
NaV1.6	SCN8A	Fast	Mainly in DRG and Motor neurons	Sensitive
NaV1.7	SCN9A	Fast	DRG and CNS	Sensitive
NaV1.8	SCN10A	Slow	Found in DRG only	Resistant
NaV1.9	SCN11A	Slow	Mainly in DRG, low levels in CNS	Resistant

**Table 3:** Sodium channel isoforms, corresponding gene, tissue localisation and tetrodotoxin (TTX) sensitivity. Table taken from Pal et al.<sup>109</sup>

The widely used anti-epileptic drugs (AEDs) phenytoin and carbamazepine block  $\text{Na}_v$  at therapeutic concentrations where it is thought that reducing  $\text{Na}^+$  influx via the fast inactivation state inhibition mediates its anti-epileptic activity.<sup>111,112</sup> Phenytoin was the prototypic  $\text{Na}_v$  specific AED that did not interfere with neurocognitive function. Its inhibition is both voltage and frequency-dependent, whereby phenytoin binds with greater affinity to  $\text{Na}_v$  in the inactivated channel states and high frequency channel activation (Fig. 15). The selective nature of phenytoin  $\text{Na}_v$  inhibition is thought to be derived from weak inhibition of  $\text{Na}^+$  currents during periods between seizures when neurones only depolarise intermittently. During seizure activity, prolonged neuronal discharges of action potentials are optimal for phenytoin binding. Thus, it is thought that this is how

phenytoin mediates its specific anti-epileptic effects with limited cognitive side-effects.<sup>113</sup>

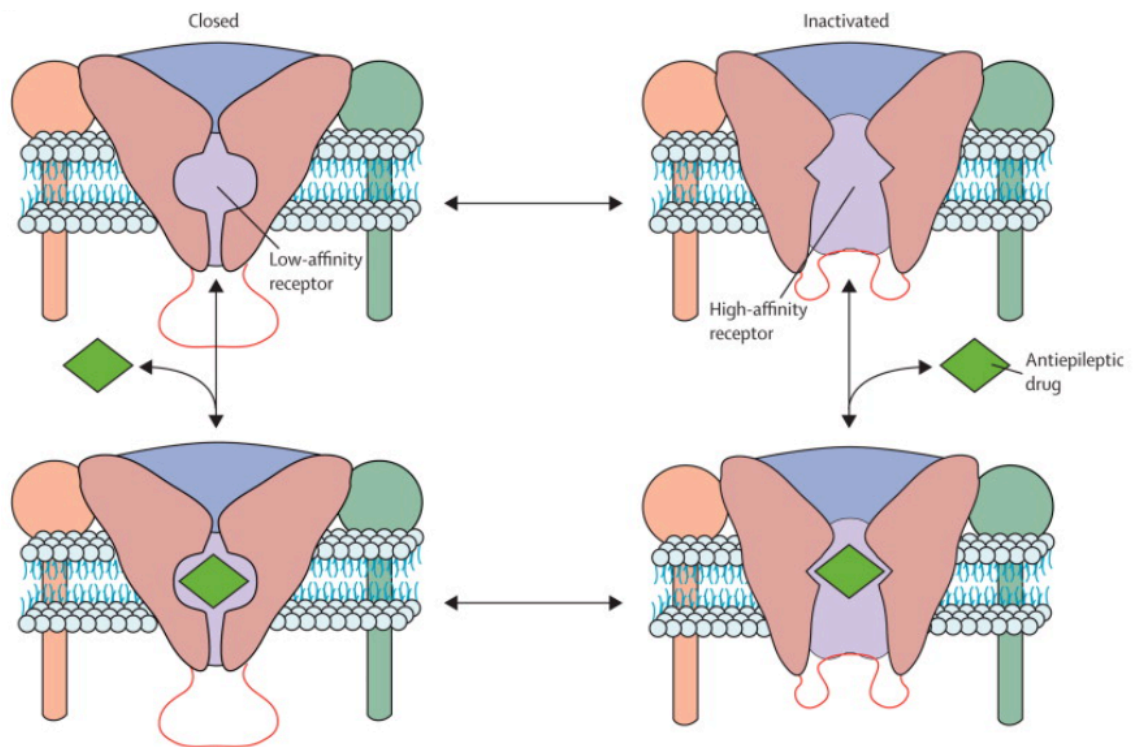


**Figure 15:** Schematic summarising voltage and frequency-dependent inhibition of sodium channels with phenytoin and AEDs or local anaesthetics with a similar mechanism of action (green diamond). The modulated receptor model is depicted here, whereby the drug binds the receptor with higher affinity in the inactivated state compared to the resting channel state.<sup>114</sup>

Carbamazepine works similarly to phenytoin by inhibiting  $\text{Na}_v$  in a voltage and frequency-dependent manner. It is effective against both generalised and partial tonic-clonic seizures. In comparison to phenytoin, carbamazepine has a 3 times lower binding affinity to depolarised channels but binds 5 times faster, which may make it more effective in seizures with shorter depolarising shifts that would be a possible explanation for variation in efficacy between patients.<sup>112</sup> Other AEDs that

act on Na<sub>v</sub> alongside other molecular targets include as valproate, lamotrigine, topiramate, and ethosuximide.

*Neuroanatomy and neurochemistry of Vagal Nerve Stimulation:*

The American neurologist Corning first investigated transcutaneous VNS and cervical sympathetic stimulation in combination with carotid artery compressors, he had devised previously, as a method to abort seizures in 1883<sup>115</sup>. Results were, however, not consistent and VNS was not re-visited until 1938 when Baily and Bremer in Brussels recorded cortical electrograms in the cat model when stimulating the vagus nerve(s), determining that when the central end of the vagus nerve is electrically stimulated, the orbital surface of the frontal lobe of the cerebral cortex is stimulated<sup>116</sup>. In 1988 Penry and colleagues performed the first human VNS implantation and went on to describe the surgical technique to implant the VNS device along with preliminary results (E01 and E02 trials).<sup>117-119</sup> They elucidated that stimulating the left vagal nerve reduced the risk of bradycardia compared to the right. This was later thought to be due to the higher density of right vagal nerve fibres innervating the atria compared to the left vagus nerve, which innervates the ventricles at a lower density.<sup>120</sup>

The vagus nerve (or cranial nerve X - CNX) contains ca. 100,000 axons, of this it has been shown that approximately 80% are afferent sensory and visceral fibres and the remaining 20% are made up of myelinated motor and parasympathetic fibres.<sup>121,122</sup> An average of  $5.2 \pm 3.5$  nerve fascicles have been found in 27 human cadaveric samples (Fig.16).<sup>123</sup> CNX sensory afferents terminate in the nucleus tractus solitarius (visceral), trigeminal sensory nucleus (general), area postrema, and nucleus cuneatus.<sup>124</sup> Afferent fibres begin at



receptors located in the lungs, heart, aorta, aortic chemoreceptors, gastrointestinal tract and concha of the ears.<sup>125</sup> Afferent fibre cell bodies are located in the jugular and nodose ganglia. Parasympathetic efferents to the heart, lungs, gastric tract and other intra-abdominal organs originate in the visceromotor dorsal nucleus.<sup>126</sup> Striated laryngeal and pharyngeal muscles are innervated by vagal efferents originating in the nucleus ambiguus.<sup>126</sup> CNX emerges from the medulla posterior to the olives and caudal to the glossopharyngeal nerve. CNX exits the skull via the jugular foramen with CNIX and the accessory nerve, to enter the jugular sheath between the carotid artery and jugular vein, which underlies the sternocleidomastoid muscle. From here it has the longest course of any of the cranial nerves, reaching as far as the colon (Fig. 17).

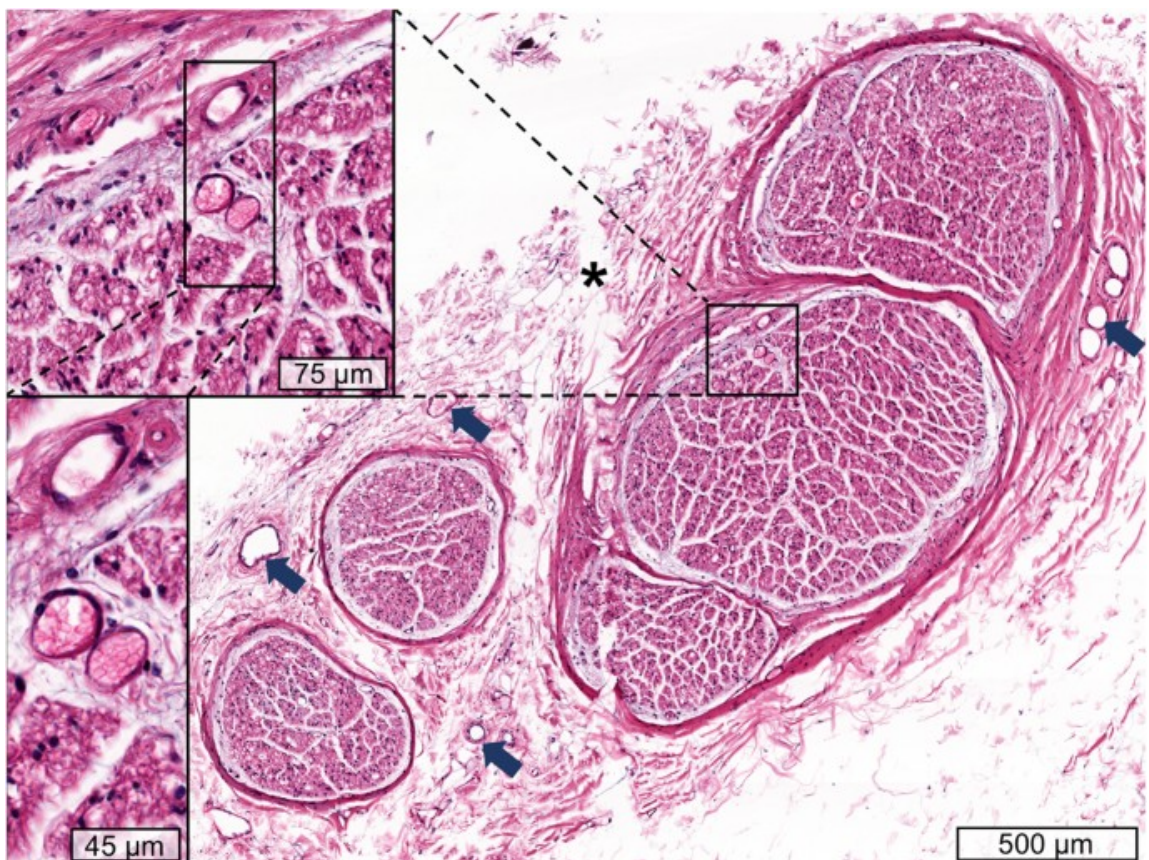


**Figure 16:** Hematoxylin-eosin stained vagus nerve showing numerous fascicles separated by perineurium and subepineural vascular supply present in this

sample (arrows) and magnified in the images on the left. Image taken from Hammer et al.<sup>123</sup>

The anatomical basis for VNS lies within the network of projections from the nucleus tractus solitarius to higher brain centres including the hypothalamus, thalamus, and amygdala which go on to innervate insular cortex.<sup>127</sup> Left and right vagal innervation to the heart is heterogeneous, where the right innervates the sinoatrial node and the left innervates the atrioventricular node. It was found that stimulation on the right nerve induced more profound bradycardia than the left in dogs.<sup>128</sup> More recent evidence demonstrated that the right nerve innervates ventricles with a higher density than atria, with the inverse being true for the left, giving further impetus for utilising the left rather than right vagus nerve for VNS.<sup>129</sup>

To date, a definitive mechanism for the anti-convulsant effect of VNS has yet to be elucidated. VNS has been shown to have an effect on cerebral blood flow, EEG and CSF constituents.<sup>130-132</sup> Stimulation of vagal C-fibres in VNS was previously thought to be essential for anti-seizure activity. However, this has been shown not to be true in rats with C-fibres destroyed with capsaicin.<sup>133</sup> Evidence to date favours the locus coeruleus (LC) as having the most important role in the mechanism of VNS.

The role of the LC has been implicated as having a crucial role for vagal pathways necessary for seizure suppression. In the rat model, chronic lesions and acute inactivation of the LC using infusions of 6-hydroxy-dopamine hydrobromide and lidocaine, respectively, significantly reduced the anti-seizure activity with vagal stimulation when compared to sham lesions (no infusion and saline infusion

respectively).<sup>133</sup> However, response to VNS was not completely obliterated by lesioning, where some residual seizure suppression remained, indicating that the LC does not act in solitude.<sup>134</sup>

Other nuclei may have a role whereby cross-talk may occur between nuclei innervated by NTS projections. When VNS was investigated for the treatment of depression, it was shown to be effective in the rat model when utilising the forced swim test and in a number of naturalistic human studies utilising the Hamilton Rating Scale for Depression.<sup>135</sup> As serotonin (5-HT) and noradrenaline (NA) are both implicated in the pathophysiology of depression, their respective major brainstem nuclei, the dorsal raphe nucleus (DRN) and LC, were investigated to determine a potential mechanism for VNS anti-depressant effect. It was found that basal LC firing rate was significantly greater than DRN in the rat model in the short-term term group but similar rises in firing rate were seen in both nuclei in the long-term (3 months), authors of this study postulated DRN activation was secondary to LC firing since it is known that co-innervation exists between the two nuclei.<sup>136</sup>

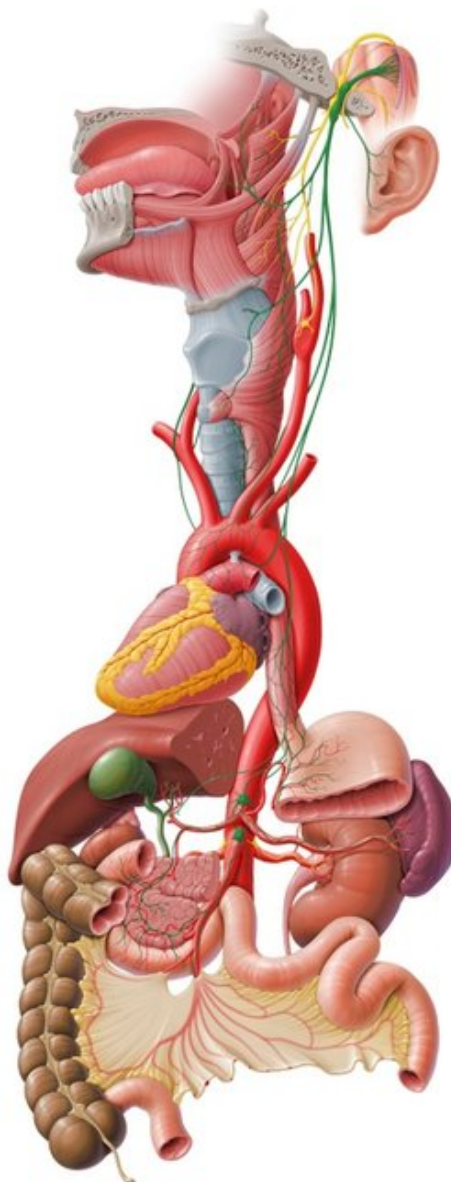


**Figure 17:** Diagram demonstrating the anatomical pathway of the vagus nerve (green) emerging from the medulla oblongata and distally innervating visceral tissues. Image adapted from [www.kenhub.com](http://www.kenhub.com).

This has relevance to the mechanism of LC mediated suppression of seizures since it has been shown that activation of DRN receptors with neuropeptide agonist galanin, and subsequent release of 5-HT, prevents limbic seizures in rats.<sup>137</sup> The role of serotonin in epilepsy has been established in experimental models where drugs that elevate exogenous 5-HT have been shown to mitigate

generalised seizure and focal seizures.<sup>138,139</sup> In contrast, depletion of 5-HT leads to an increased susceptibility to evoked convulsions and increased efficacy of anti-convulsant drugs.<sup>140,141</sup> It has been found that in many implicated pathways involved in epilepsy, excitability is decreased by hyperpolarisation of glutamatergic neurons by 5-HT<sub>1A</sub> receptors, depolarisation of antagonists of 5-HT<sub>2</sub> and 5-HT<sub>7</sub> and depolarisation of GABAergic neurons by 5-HT<sub>2C</sub> receptors.<sup>142</sup> Classically it has been known that the DRN does not receive direct inputs from the NTS, unlike the LC, however it is now clear from tracing methods using injections of free horseradish peroxidase that NTS projections reach the DRN via a medial system across the dorsomedial reticular formation<sup>143</sup>. This would therefore potentially allow LC-independent seizure suppression to occur via a NTS-DRN-5HT pathway and provide a basis for other intervening nuclei. Figure 18 highlights the pathways which VNS may activate to mediate seizure reduction.

When the LC is activated by VNS, NA is released which has been shown to have a protective effect against epileptogenesis. In limbic status epilepticus, inhibition of NA results in neuronal damage and conversion from intermittent seizures to status epilepticus.<sup>144</sup> However, VNS is delivered intermittently in cycles, with a common setting of 30 seconds “on” and 5 minutes “off”. This indicates that VNS must have a long-lasting effect on seizure mediating pathways in the brain. Indeed, it has been shown that LC neurones alter cortical excitability via synaptic plasticity.

In summary, the role of the LC and NA in VNS has been studied in depth, providing a basis for a possible neurochemical mode of action for VNS. An extensive review on this subject has been previously published.<sup>145</sup>

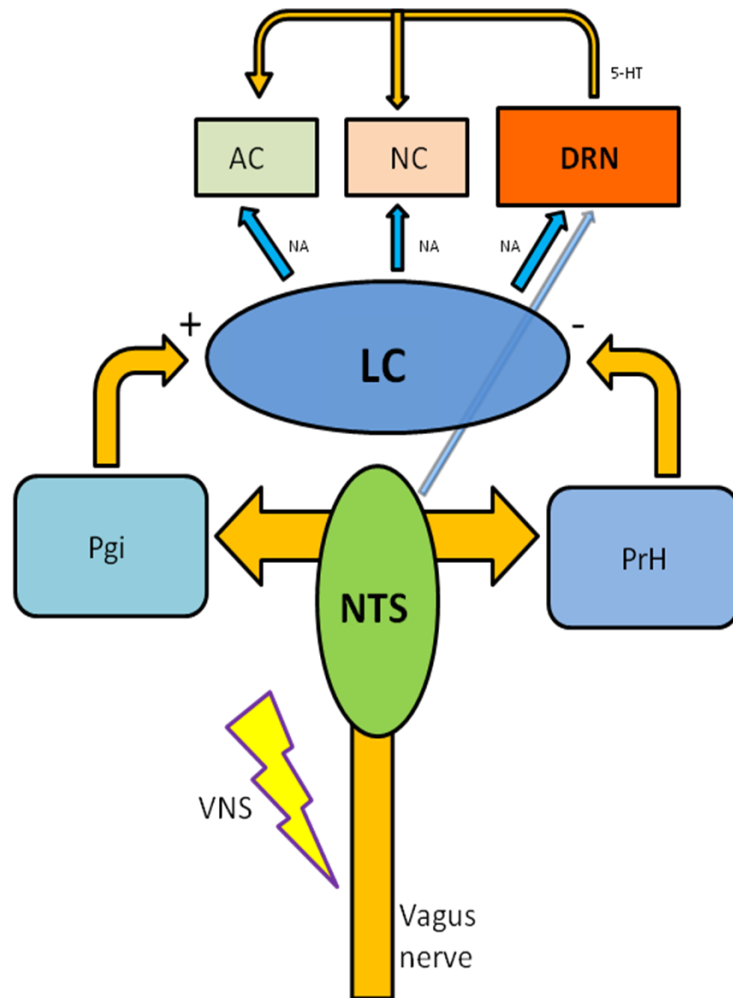


**Figure 18:** Afferent pathway between the vagus nerve and locus coeruleus (LC), diagram modified and adapted.<sup>134</sup> Afferent vagal fibres innervate the nucleus tractus solitarius (NTS) that follow a disynaptic projection pathway via the excitatory nucleus paragigantocellularis (Pgi) and inhibitory nucleus propositus hypoglossi (PrH) that together mediate noradrenaline neurone (NA) activity projecting from the LC in to allocortex (AC), neocortex (NC) and the dorsal raphe nucleus (DRN). DRN releases 5-HT directly and indirectly from NTS activation to AC and NC. Direct efferents from the NTS to the DRN are depicted by a semi-transparent arrow as demonstrated by a tracing study previously.<sup>143</sup> Activation of VNS causes an increase in NA and 5-HT firing.<sup>136</sup>

### ***Methodological overview***

The literature was reviewed by completing searches in Web of Science, PubMed and handpicking relevant papers. I carried this out by using key search terms including: “vagal nerve stimulation”, “drug resistant epilepsy” and “vagus nerve”.

Surgical records were used to identify 220 patients with VNS implants. Patients were excluded where medical records were incomplete or where insufficient long term follow up data was available, leaving 100 eligible patients.

The Senior Author, Mr David Sandeman, was a Consultant Neurosurgeon who I designed the study with. I collected all data retrospectively using the patient records database. Based on the previous RCTs and observational studies reviewed in the literature, the data collected included patient demographic information, VNS device models, presurgical evaluation findings, diagnosis(es), epilepsy risk factors, associated past medical history, seizure frequency per month at baseline (prior to VNS implantation) and at future intervals (6 months, 1, 2, 3, 4, 5, 6, 8, 10, and 12 years), the total number of AEDs tried in the past, AEDs prescribed prior to and after VNS implantation, neuropsychiatric results, complications resulting from surgery, VNS on time, and AEDs, VNS battery replacements, VNS removal, last VNS settings, number of admissions, days spent in hospital as an inpatient and total outpatient appointments attended.

I undertook statistical analysis using GraphPad Prism, however in order to ensure validity, my calculations were confirmed or corrected by collaborating with Dr Paul

White, Associate Professor of Applied Statistics at the University of the West of England. For the main outcome measure, seizure frequency, the Wilcoxon signed-rank test was used to compare seizure frequency at baseline and at each follow-up time point. Pearson's correlation coefficient was used to assess the strength of the relationship between the change in seizure frequency and independent variables. The independent t-test was used to compare differences between the responder and non-responder groups in this study. The chi-squared test was used to compare categorical variables.

***The current role of VNS in the context of existing and novel candidate treatments for pharmaco-resistant epilepsy***

Of all patients affected by epilepsy, around 30% or more will be resistant to AEDs, which is defined by the ILAE as the failure of two AEDs as monotherapy or combination therapy to achieve seizure freedom.<sup>147</sup> Further, it is known that after failing to respond to 2 AEDs, the chances of responding to additional AEDs falls to 12.5-22.2%), making it necessary to consider alternative treatment modalities.<sup>148</sup> Combination therapy using valproic acid with lamotrigine as an add on therapy, compared with lamotrigine, phenytoin and carbamazepine, has been shown in human studies to be a more effective synergistic combination.<sup>149</sup> Other effective combinations that have been studied, include lamotrigine with levetiracetam, and lacosimide with levetiracetam.<sup>150,151</sup> These combinations may be more effective than monotherapy as the different mechanisms of action may act in concert and can be considered in the management of pharmaco-resistant epilepsy. For example, lacosimide enhances voltage gated sodium channels slow inactivation, while levetiracetam binds SV2A to modulate synaptic neurotransmitter release.<sup>152</sup>



The more recently approved AEDs perampanel and brivaracetam have been licensed for focal seizures with or without secondary generalisation. Perampanel is a non-competitive, first in class, antagonist of AMPA receptors that has randomised controlled trial evidence of efficacy in resistant epilepsy.<sup>153</sup> Brivaracetam acts on SV2A vesicles, similar to levetiracetam, and is licensed for focal onset seizures. However, further studies will be needed to elucidates its efficacy in patients who have not received prior treatment levetiracetam therapy.<sup>154</sup> Newer pharmacotherapies include cannabidiol and fenfluramine. Cannabidiol acts on multiple targets relevant to epilepsy including GABA receptors and transient receptor of vanilloid type 1 (TRPV1) channels where its efficacy in a pharmaco-resistant form of paediatric epilepsy has been proven as an add-on therapy in a randomised controlled trials.<sup>155</sup> Fenfluramine exerts its anti-seizure activity by disrupting vesicular storage of serotonin via sigma 1 receptor binding and serotonin receptor binding, specifically 5HT2C and 1D).<sup>156</sup> Trials for fenfluramine on treatment resistant epilepsy are ongoing and its efficacy has not yet been established.<sup>157</sup> Other promising drugs on the horizon include cenbamate and padsevonil, which are both undergoing clinical trials. The future of medication-based treatment for pharmaco-resistant epilepsy may lie in the refinement of genomic “precision medicine”, where detected genetic mutations may guide the clinical treatment and pre-clinical drug development in the future.

VNS has been refined since publication of the study presented in this chapter, where hardware improvements, software upgrades and a name change from NeuroCybernetic Prosthesis to the VNS Therapy System has been made (Fig

19).<sup>158</sup> The cumulative number of patients treated with VNS since its first FDA approval in 1997 is over 125,000 as of 2020.<sup>159</sup> Single and dual pin VNS Therapy generators are available presently, with complimentary software, which all have advantages and disadvantages that make them more or less practical in certain circumstances. The indications for VNS have also been extended to treat adults over 18 years old with treatment resistant epilepsy, defined as at least one episode of major depression that did not respond to any of four different antidepressant drugs.<sup>160</sup> There are wide range of other conditions that VNS may be have a therapeutic role in the future, including neonatal sepsis for example, where VNS has been shown to reduce the expression of IL-6 and TNF- in response to VNS stimuli in preterm neonatal rat models.<sup>161</sup> In the field of pain management, VNS has been shown have potential benefits in fibromyalgia and cluster headaches.<sup>162,163</sup> Given the range of vagal afferents and efferents, VNS has been investigated in other organ systems including cardiac atherosclerosis, obesity, pulmonary injury, stroke, traumatic brain injury and rheumatoid arthritis.<sup>164</sup>

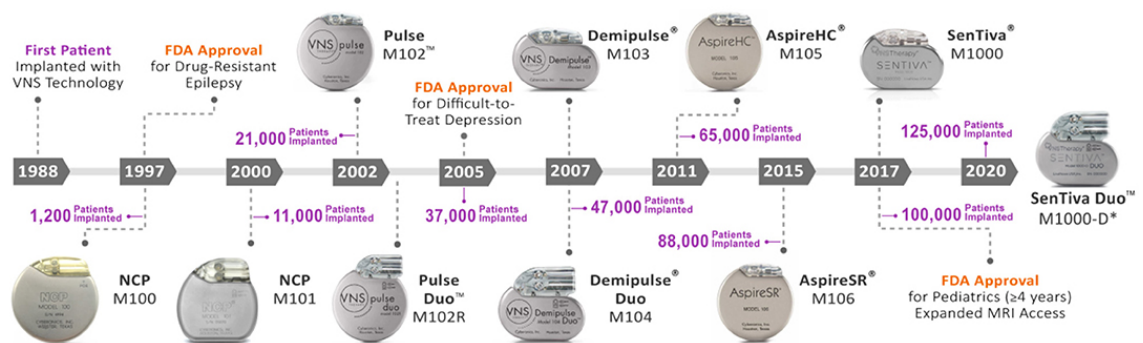


**Figure 19:** Evolution of the VNS therapy system. Timeline of FDA approvals of each iteration of VNS devices with cumulative number of patients treated over time. The indications for use of VNS was approved in 2005 for resistant depression and in 2017 for children over 4 years old. HC – High capacity, M –

Model, MRI – Magnetic resonance imaging, NCP – NeuroCybernetic Prosthesis, SR – sense and respond. Image taken from Afra et al.<sup>158</sup>

While VNS is the most studied and established neuro-stimulatory device for drug resistant epilepsy, other modalities are available that can be divided into invasive and non-invasive. Invasive modalities include deep brain stimulation (DBS), responsive neurostimulation (RNS), and chronic subthreshold cortical stimulation (CSCS). Non-invasive forms include transcutaneous VNS (tVNS), trigeminal nerve stimulation (TNS), transcranial magnetic stimulation (TMS), and transcranial direct current stimulation (tDCS).<sup>165</sup> DBS involves implantation of electrodes into deep brain structures that include the anterior nucleus of the thalamus, hippocampus, centromedian nucleus of the thalamus, cerebellum, and globus pallidus. The electrodes are connected to a pulse generator and have been shown to be effective in reducing seizure frequency by 40% and 69%, in the short and long term respectively, in patients with drug resistant epilepsy where surgical resection was contraindicated in the Stimulation of the Anterior Nucleus of the Thalamus for Epilepsy trial (SANTE).<sup>166</sup> RNS is a closed loop device that includes a cranially seated neurostimulator and 4 electrode contacts that are surgically implanted at seizure foci. This system detects epileptogenic activity and delivers focal stimulation to abort seizure activity. It has been shown in an RCT to reduce seizure frequency by 53% in adults with drug resistant epilepsy.<sup>167</sup> CSCS is similar to VNS, in as much that is an open loop system, which targets ictal cortical focus areas with continuous subthreshold stimulation. There is limited clinical data to support the widespread use of CSCS, but it is an emerging alternative modality for drug resistant epilepsy.<sup>168</sup> TMS utilises an magnetic flux applied externally that generates intracranial currents that can

excite action potentials and affect specific cortical circuits to reduce seizures, however the evidence for its efficacy is very limited at present.<sup>169</sup> tDCS delivers direct current via scalp electrodes that include an anode and cathode, which are able to suppress seizures via the anode and and interfere with epileptiform discharges.<sup>170</sup> However, there are limited studies available investigating the role of tDCS in patients with drug resistant epilepsy at present. tVNS and TNS have been investigated in small studies, however their clinical use is not supported by high-quality evidence as of yet.<sup>165</sup>

Overall, there is varying evidence for the safety and efficacy for VNS, DBS , RNS, tDCS for drug resistant epilepsy with the aforementioned modalities emerging as alternatives. Non-invasive options for drug resistant epilepsy in the future may include TMS, tVNS, TNS and tDCS. In the future, it appears that all these neurostimulation devices are likely to undergo further refinement to continuously optimise safety and efficacy.

Finally, the ketogenic diet as a non-pharmacological treatment for drug resistant epilepsy has largely been reserved for children.<sup>171</sup> However, it has not been recommended as a long-term solution due to concerns over detrimental effects on childhood development. The lack of RCTs and the small available studies, indicate a need for further research in the future, particularly in adults.

### ***Nature of Work***

This study was a retrospective clinical analysis of 100 patients with intractable epilepsy who were treated with VNS. I collected all data retrospectively using the

patient records database. I completed all statistical analysis in collaboration with Dr Paul White, Associate Professor of Applied Statistics.

### ***Significance of work***

This work was published in the British Journal of Neurosurgery (Impact Factor 1.29) and cited 7 times since publication. The results of this study demonstrated VNS is effective and safe, where the results were in keeping with the previous literature. This was the first large long-term study published from the UK on VNS in intractable epilepsy. As a result of this work, VNS continues to be offered as a treatment at Frenchay and then Southmead Hospital, Bristol, UK. Further retrospective long-term follow up studies have been completed since this work was published, including Chrastina et al. who provided data on patients with VNS for up to 17 years in the Czech Republic.<sup>172</sup> Given the heterogeneity of intractable epilepsy variability to response to VNS it has been important over time to determine whether the effectiveness of VNS is sustained over time and determine what constitutes VNS treatment failure. It appears that the efficacy of VNS plateaus over time, however failure should not be concluded until 2 years of therapy have elapsed with no response. The Commissioning Policy: Vagal Nerve Stimulation for Epilepsy, 2013, Ref.: NHSCB//D04/P/d sets out the criteria for VNS to be funded under the NHS.

The basic scientific and clinical literature review I wrote, gave me a deeper understanding of how neurochemistry can be manipulated with electrical stimulation. This later led me to become interested in brain cancer associated seizures because these particular seizures were known to be very resistant to AEDs with no effective treatment options available. Further, VNS is a form of

electrical stimulation that led me to become interested in other forms of neuro-modulation such as deep brain stimulation, and in particular, cellular electric fields.

### ***Critical appraisal of published paper***

This was an observation study that was undertaken retrospectively, therefore it is of a moderate quality of evidence on the hierarchy of clinical evidence. At the time of publication, randomised controlled trials had already been published on the subject, however these were based outside of the United Kingdom (UK). It is particularly important for surgical interventions to be audited and studied to determine whether the clinical outcomes are similar or deviate significantly to those published elsewhere. In the case of this paper, we reported the clinical outcomes of the largest group of patients at a single centre in the UK implanted with VNS. This provided useful clinical data to support the ongoing use of VNS in similar settings within the UK and potentially elsewhere. Such “real world” data is important, particularly to determine potential adverse events that were not identified in the trials supporting the intervention. Unfortunately, a number of patients were excluded from our study as insufficient clinical data was available. This could lead to systematic bias and skew the data. Since this was not a prospective study, there are a number of forms of bias that this study could be affected by. For example selection and confounding biases would undermine the validity of the data in this study.

Overall, this study provides clinical data to support the ongoing use of VNS in treatment resistant epilepsy in the UK. However, this data should not be used in

isolation when making clinical decisions and the available randomised controlled trial data should be used alongside it.

## **Chapter 2: Glutamate transport in neonatal brain injury**

### ***Introduction***

There are a number of conditions that can lead to brain injury around the time of birth, which include hypoxia-ischaemia, stroke and intracranial haemorrhage, which are important causes of neonatal mortality and long-term morbidities such as cerebral palsy.<sup>173,174</sup> An important precursor of neonatal brain injury is premature birth, defined as less than 37 gestational weeks. In England, it has been shown that neonatal brain injury occurs in 2.91 per 1000 live births among term infants and 24.45 per 1000 live births among pre-term infants.<sup>175</sup> Worldwide, premature births represent 11.1% of all live birth, which is likely to rise in the future as neonatal care continues to advance.<sup>176</sup> The cause of pre-term brain injury is complicated and likely multifactorial, as summarised in figure 20. Given the critical role of glutamate in both epilepsy and multiple forms of brain injury, I sought to determine the role of glutamate transport in neonatal injury. Herein, I summarise the relevant literature pertaining to this subject, summarise the current and emerging therapies relating to preterm brain injury, and give an overview of published paper pertaining to this chapter.



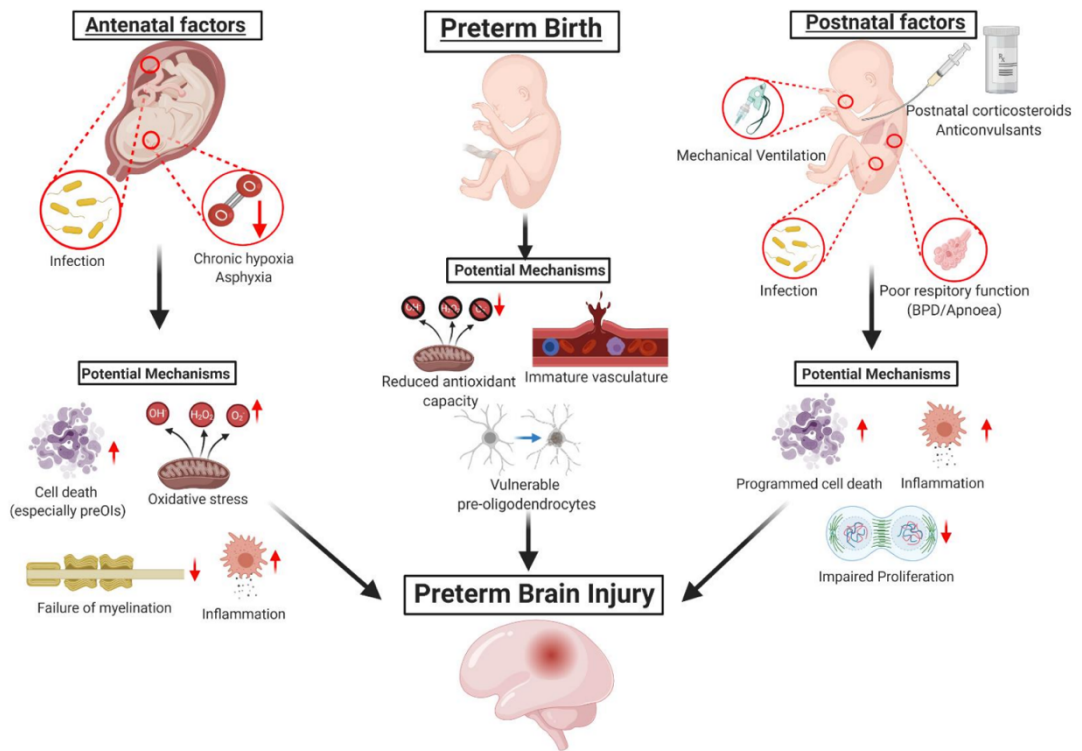


**Figure 20:** Possible factors contributing to pre-term brain injury. Image taken from Yates et al.<sup>176</sup>

### **Aims**

- Review the literature pertaining to preterm brain injury and the neurochemical mechanisms that mediate it
- Summarise the current and emerging treatment modalities for pre-term brain injury
- Summarise the methodology, nature, and significance of this work, and provide a critical appraisal of the published paper pertaining to this chapter

### **Literature review**

Progress in perinatal care over the last three decades has led to greater survival rates in infants born prematurely. In a multicentre cohort study of 3785 infants between 1993 and 1998, survival of infants delivered at 22-26 and 27-32 weeks

of gestation improved from 55 to 61% and 82 to 86% respectively.<sup>177</sup> These results have been corroborated by findings from a single centre cohort study including 496 extremely low birthweight premature infants finding that survival increased from 49 to 68% when comparing infants delivered between 1982-1989 and 1990-1999 respectively.<sup>178</sup> Survival of infants delivered between 2000-2002 was found to be 71% but no statistical significance was found when compared to 1990-1999.<sup>178</sup> More recently, this pattern of improved survival has been determined in the Trent region in the United Kingdom, demonstrating greater rate of survival of 47% over 36% when comparing infants delivered during 2000-2005 and 1994-1999 respectively.<sup>179</sup> In 2005 11,657 infants were born in England and Wales less than 33 weeks of gestational age with over 90% surviving beyond the postpartum period.<sup>180</sup> In the United States of America it has been estimated that 1.5% of live births, accounting for 63,000 infants, are to infants with very low body weights (VLBW), defined as less than 1.5 kilograms.<sup>181</sup> Of the infants surviving with VLBW, 10% will be afflicted by cerebral palsy and about 50% by behavioural and cognitive deficits.<sup>182,183</sup>

The medical significance of improving preterm infant survival is the growing unmet therapeutic need for the neurodevelopmental impairment in the greater number of infants with VLBW. Approximately 35 to 38% of all premature infants delivered before 32 weeks of gestation will have neurodevelopmental impairments at 18-24 months of age, which may include cerebral palsy, cognitive disability and behavioural dysfunction.<sup>177,178</sup> Selective white matter injury underlies these deleterious effects where severity may be predicted by multimodal imaging.<sup>184</sup> Although it is evident from previous studies that the incidence of cerebral palsy and neurodevelopmental impairment has reduced

over time, a need for a treatment modality to prevent these potential complications will heighten as neonatal intensive care advances.<sup>177,178</sup>

The preterm brain is especially susceptible to cerebral white matter injury (WMI) that leads to dysfunction of myelination events in normal development. Preterm infant care advances have led to far less severe focal necrotic brain lesions to a milder diffuse WMI, which is the major form of brain injury in premature birth survivors.<sup>185</sup> The age at which there is the highest risk of WMI is 23-32 weeks post conceptional age. Perinatal WMI, including necrotic lesions of periventricular leukomalacia (PVL), was a common finding in 42.5% of children affected by preterm births.<sup>186</sup> Other pathologies can cause WMI in full term infants, including chronic placental insufficiency and congenital heart disease, where prolonged in utero ischaemia or compromised cerebral oxygenation can be associated with WMI.<sup>187,188</sup> WMI in preterm infants varies in severity, where three major pathological forms have been described, including: 1) Focal cystic necrosis, 2) Focal microscopic necrosis, and 3) Diffuse non-necrotic lesions.<sup>189</sup> Focal cystic necrosis is the most severe type of WMI that is characterised by large foci of necrosis that is pathognomonic of PVL.<sup>190</sup> PVL affects specific cortical areas including the white matter adjacent to the ventricular walls, white matter anterior to the frontal horn and external angles of the lateral ventricles for example. However, the underlying reasons for preferential areas being affected have not been established. Focal microscopic necrosis (microcysts) in contrast, occurs commonly, which are characterised by small cystic lesions less than 1mm in diameter.<sup>182</sup> As such, these lesions are not visible clinically with neuro-imaging modalities, however, their clinical relevance depends on the number and distribution within white matter regions. Microcyst distribution mimics focal cystic

necrosis, indicating a possible common ischaemic origin. Diffuse WMI is currently the most common premature brain injury and characterised widespread punctate, linear or cluster lesions on MRI with no clear boundaries.<sup>191,192</sup> Survivors of diffuse WMI can have significant MRI changes that include enlarged subarachnoid spaces, reduced white matter, ventriculomegaly and gyral deficits.<sup>193</sup>

In recent times, much has been elucidated regarding the pathogenesis and cellular mechanisms of white matter injury in preterm humans. Three significant pathogenic factors have been described: cerebral ischemia, systemic infection/inflammation, and maturation dependent intrinsic vulnerability of pre-myelinating oligodendrocytes (pre-OL).<sup>198</sup> Underlying mechanisms for the lattermost include free radical attack, microglial activation and glutamate mediated excitotoxicity. The role of glutamate will be discussed in more detail, a comprehensive review on the subject has been published by Volpe<sup>198</sup>.

Glutamate is the most abundant neurotransmitter in the mammalian central nervous system and mediates its excitatory physiological effect by binding to ionotropic and metabotropic receptors.<sup>199,200</sup> The main ionotropic receptor subtypes include  $\alpha$ -amino-3-hydroxy-5-methyl-4-isoxazole propionate (AMPA), kainate, and N-methyl-D-Aspartate (NMDAR). Ionotropic receptor function is determined by subunit structure, and while NMDAR is always permeable to calcium ions, AMPA are relatively impermeable because of the presence of GluR2 subunit usually but sparsely expressed in immature neurons.<sup>201</sup>

Normally a fraction of glutamate is maintained in extracellular fluid, where an extremely large concentration gradient is maintained across plasma membranes in a dynamic equilibrium.<sup>200</sup> Glutamate mediates its physiological effects through the aforementioned receptors found extracellularly.<sup>200,201</sup> Extracellular leak of glutamate occurs when cells deplete available energy supplies or if there is a rapid turnover of glutamate.<sup>200</sup> When the preterm brain is subjected to hypoxia-ischemia, trauma, and energy failure, the neurotransmitter glutamate is released into extracellular space causing a rise in concentration above normal.<sup>201,202</sup> The resultant over activation of these receptors through excess extracellular glutamate leads to excitotoxicity, one of the primary underlying mechanisms of PVL.<sup>198</sup>

Glutamate receptor activation leads to a rise in intracellular calcium, which activates numerous enzymes including inducible nitric oxide synthase (iNOS), see figure 21.<sup>203</sup> In glutamate excess, raised nitric oxide levels lead to peroxynitrite formation, an unstable structural isomer of nitrate that causes damage to cellular molecules including mitochondrial DNA. Further, in developing oligodendrocytes, nitric oxide (NO) induces cell death via release of apoptosis inducing factor, see figure 22. Increased extracellular glutamate levels have also been shown to generate free radicals through glutathione depletion resulting from excessive glutamate-cysteine exchange.<sup>204</sup> Addition of free radical scavengers was later shown to completely prevent cell death.<sup>205</sup> In addition, ischaemia/reperfusion causes formation of superoxide anions that are physiologically converted to hydrogen peroxide and then into the harmless constituents water and oxygen by peroxisome catalase and glutathione peroxidase. However, failure of these enzyme and in the presence of iron, the

Fenton reaction occurs resulting in the formation of potent hydroxyl radicals, exacerbating cellular damage.<sup>196</sup> These mechanisms are part of glutamate mediated excitotoxicity.

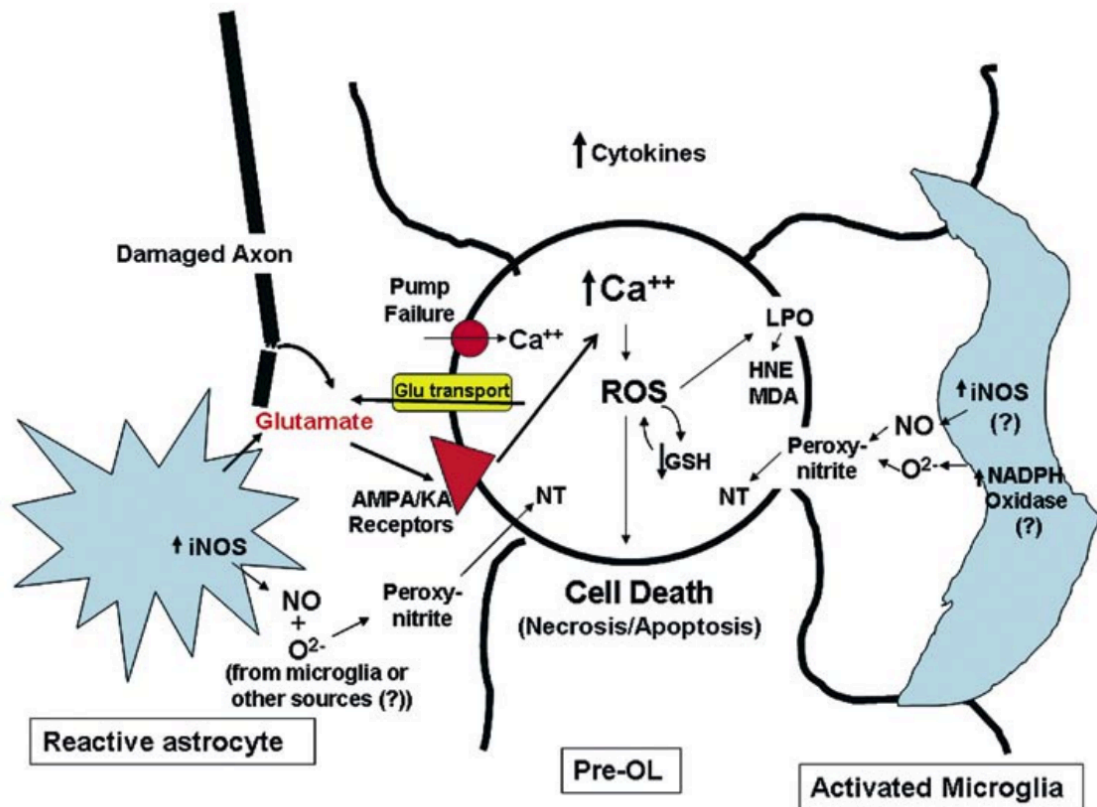


**Figure 21:** Postulated mechanisms of free radical mediated developing-oligodendrocyte injury. The source of oxidative stress is thought to result from 1) ischaemia/reperfusion that leads to pump failure and excitotoxicity, both leading to calcium influx and thus a release of reactive oxygen species (ROS) and reduction in reduced glutathione (GSH), 2) Maternal or foetal infection leading to a reactive astrocytic and microglial inflammatory response in the surrounding white matter, and 3) A combination of 1) and 2). As GSH depletes, the cell shifts to an oxidised environment that results in further ROS accumulation. Cerebral ischaemia leads to oxygen and glucose deprivation, resulting in failure of membrane channels regulating ionic and osmotic homeostasis. Voltage dependent ion channels are subsequently activated, amongst other mechanisms,

that result in activation of lipases, proteases and DNA polymerases that result in further ROS production. If reperfusion subsequently occurs, further ROS is generated where increased oxygen availability that exceeds oxygen consumption creates an even more deleterious environment. ROS release also occurs downstream of ischaemia related excitotoxicity in a similar vein to ischaemia/reperfusion injury. Excitotoxicity is initiated by excessive glutamate concentrations that results from a number of sources including damaged axons, necrosis, glutamate transporter function reversal, and astrocyte generated glutamate. The prolonged depolarisation that occurs secondary to glutamate excess is caused by excessive AMPA and KA receptor binding, resulting in further calcium influx. Nitritative damage occurs through increased expression of inducible nitric oxide synthase (iNOS) by reactive astrocytes and activated microglia, resulting in NO release and subsequent binding with superoxide ( $O_2^-$ ) to form peroxynitrite and subsequent nitrotyrosine formation (NT). LPO – lipid peroxidation, HNE – 4-hydroxy 2-nonenal, MDA - malonaldehyde. HNE and MDA are toxic lipid aldehydes. Image taken from Haynes et al.<sup>206</sup>

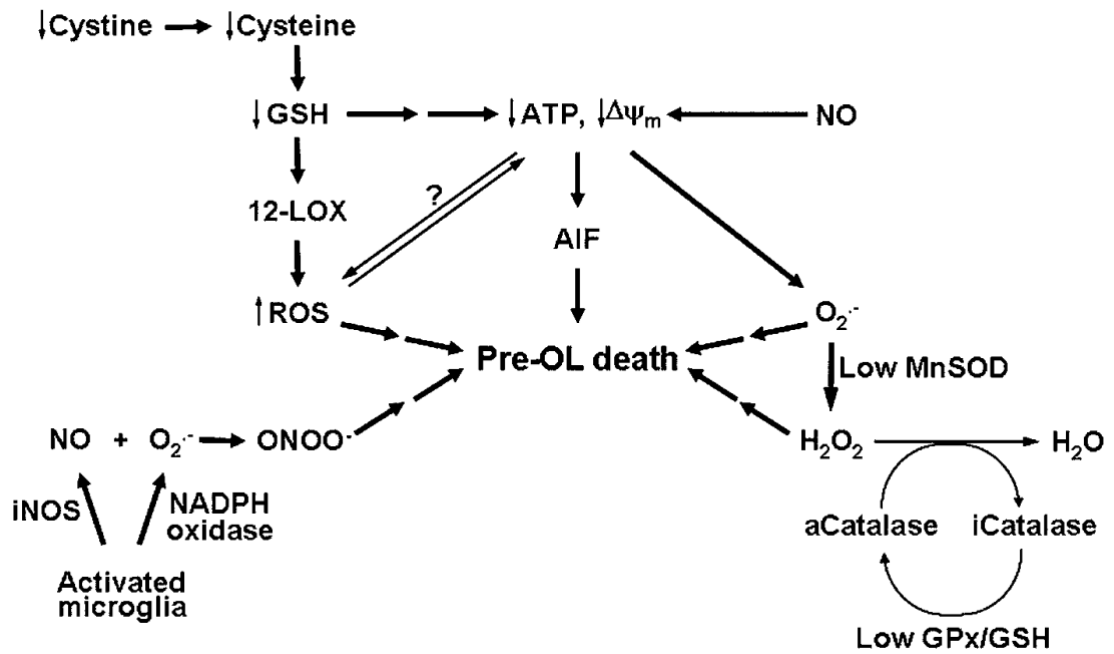


**Figure 22:** Mechanisms of ROS toxicity in developing oligodendrocytes. A reduction in cystine results in a reduction of cysteine and subsequent depletion of glutathione (GSH). ROS generation occurs via LOX-12 (lipoxygenase-type enzyme) activation that causes pre-oligodendrocyte (OL) death. Exogenous nitrous oxide (NO) and GSH depletion can reduce available energy through adenosine triphosphate (ATP) reduction and loss of mitochondrial membrane potential ( $\Delta\Psi_m$ ), leading to mitochondrial release of apoptosis inducing factor, which translocates to the cell nucleus and initiates cell death. Superoxide anions ( $O_2^{\cdot-}$ ) generated from the mitochondrial transport chain undergo conversion to hydrogen peroxide ( $H_2O_2$ ) by superoxide dismutase (SOD), which is toxic to pre-OLs. Catalase converts  $H_2O_2$  to its harmless constituents  $H_2O$  and  $O_2$ . Mitochondrial SOD (MnSOD) expression is lower in pre-OLs than mature OLs, resulting in higher levels of  $H_2O_2$ , which also inhibit catalase activity. Furthermore, pre-OLs have lower glutathione peroxidase (GPx) activity, resulting in less reactivation of catalase. Activated microglia produce NO and  $O_2^{\cdot-}$ , which react to



form peroxynitrite (ONOO<sup>-</sup>), an unstable isomer of nitrate, that is toxic to pre-OLs.

Image taken from Haynes et al.<sup>206</sup>

Physiological means of removing glutamate from extracellular fluid is limited to protein uptake since there is a lack of extracellular enzymes and simple diffusion is only viable across very small distances such as synaptic clefts.<sup>200</sup> Five subtypes of these sodium dependent plasma membrane glutamate transporters have been identified as excitatory amino acid transporter (EAAT) 1-5.<sup>64,207</sup> The astroglial EAAT2 has been shown to be responsible for as much as 90% of all extracellular glutamate in adult specimens.<sup>208</sup> Recently, a highly prevalent polymorphism of the promoter of the EAAT2 gene occurring in of the population has been associated with poorer neurological outcomes compared to the wild type in adult stroke patients.<sup>209</sup> Authors corroborated their findings by transfecting the mutant EAAT2 promoter in the rat model and employing a bio-informatics approach that both supported their hypothesis. To date this phenomenon has not been investigated in preterm infants.

Glutamate transport by EAATs is reversible where the usual inward transport under physiological conditions can be change to outward transport when extracellular Na<sup>+</sup> and intracellular K<sup>+</sup> decrease, and/or intracellular Na<sup>+</sup> and extracellular K<sup>+</sup> increase.<sup>210,211</sup> Since transport of glutamate is electrogenic, membrane depolarisation will result in a reversal of transport direction due to the reduced driving force for uptake in depolarised conditions.<sup>212</sup> In models of stroke, it has been shown that due to energy deprivation, ATP synthesis reduces and later leads to reduced Na<sup>+</sup> and K<sup>+</sup> concentration gradients across the neuronal membrane, usually maintained by Na<sup>+</sup>/K<sup>+</sup> ATPase. Therefore, glutamate

transport direction is reversed due changes in transmembrane potential and Na<sup>+</sup> and K<sup>+</sup> concentration gradient caused by ischaemia.<sup>212,213</sup> As such, reverse glutamate transport can turn EAATs into sources of extracellular glutamate and exacerbate excitotoxic injury. Although, the role of reverse glutamate transport has not been studied in preterm brain injury, the potential for neuroprotection by reverse transport pharmacological blockade has been shown in animal models.<sup>214</sup> Therefore, reverse glutamate transport may be therapeutic target to investigate in the context of preterm brain injury in the future.

The most promising potential therapies for white matter injury in preterm infants mitigate the action of glutamate excess by blocking glutamate receptors. The anticonvulsant topiramate has been shown to prevent white matter injury due to hypoxia-ischaemia in the rat model through AMPA-kainate blockade.<sup>215</sup> Similarly, the NMDA receptor antagonist memantine has been shown to be efficacious against the immature rat model of PVL with better neuromotor outcomes.<sup>216</sup> Recently this has been followed up with promising evidence that memantine does not cause constitutive apoptosis that is associated with other NMDAR antagonists such as ketamine and isoflurane in immature rodents.<sup>217</sup> Another potential target yet to be investigated in preterm infants is upregulation of EAAT2 using peroxisome proliferator-activated receptor PPAR $\gamma$  agonists, which have been shown to mediate neuroprotection by upregulating expression of EAAT2. I pursued this concept in the context of brain tumour seizures as described in Section 3.

### ***Current and emerging therapies for preterm brain injury***

At present the main treatments in current clinical use for preterm infants include systemic steroids, magnesium sulphate and anti-epilepsy drugs (AEDs). Maternal glucocorticoid therapy has been shown to be effective in threatened or preterm labour to accelerate foetal lung development, where a single course of antenatal steroids has been shown to be effective in a Cochrane meta-analysis.<sup>218</sup> The role of postnatal steroids in preterm infants with bronchopulmonary dysplasia is less clear, where the risks may not outweigh the benefits, such as an increased risk of cerebral palsy.<sup>219</sup> Further high quality long-term studies are required to clarify the role of post-natal systemic steroids in preterm infants, particularly as there have been reports of its association with PVL.<sup>220</sup> Magnesium sulphate binds NMDA receptors and prevents ion flux and thus reduces the excitotoxic effects of excessive glutamate.<sup>221</sup> This has led to a number of studies examining its use as a neuroprotective agent for preterm babies. However, the data remains controversial because a meta-analysis of large RCTs administering magnesium sulphate to women in preterm labour showed that the risk of cerebral palsy and motor dysfunction reduces there was no overall benefit to death and disability.<sup>222,223</sup> The most commonly used AEDs for treatment of seizures used by neonatal physicians include the barbiturates phenobarbital and phenytoin, which are GABAergic drugs. A systemic review found that there was no robust evidence available for the routine use of AEDs in the neonatal as 50% of neonates respond to first line therapy, with some reports suggesting AEDs are harmful.<sup>224</sup>

Treatments with known neuroprotective properties that have been used in both pre-clinical and clinical trials include erythropoietin (epo) and induced hypothermia. Epo has been widely used to prevent anaemia in premature infants

and has multiple neuroprotective targets including caspase inhibition, oxidative stress modulation and anti-apoptotic gene activation.<sup>225,226</sup> Phase 1 and 2 trials have shown that epo is a promising neuroprotective treatment for preterm infants, where dosing and therapeutic regimens have yet to be optimised.<sup>227</sup> Mild induced hypothermia has been shown in a meta-analysis to be effective in treating preterm infants with hypoxic ischaemic encephalopathy without undue adverse effects.<sup>228</sup> At present the Preemie Hypothermia for Neonatal Encephalopathy Trial (NCT01793129) that aims to investigate the safety and effectiveness of whole body hypothermia for 3 days in preterm infants with severe neonatal encephalopathy, is no longer recruiting but is still active.

Potential treatments that have preclinical evidence of neuroprotection in preterm infants melatonin, vitamin D, and several cell based therapies. Melatonin is an indolamine secreted by the pineal gland with an important role in generating circadian rhythms and has been shown to have partial neuroprotective effects along with its diluent, ethanol, in preterm sheep.<sup>229</sup> A recent investigation of combined hypothermia and rapid melatonin infusions in piglet infants models of hypoxia-ischaemia, showed significant improvements in neurological function using electrodiagnostics and neuroimaging but also confirmed the unexpected independent neuroprotective effect of ethanol.<sup>230</sup> Vitamin D deficiency is known to be a risk factor for preterm birth and has shown to have a role in important neurodevelopmental cellular processes including neurotransmitter synthesis, calcium signalling, neurotrophic factor expression and anti-oxidant activity.<sup>231</sup> In an animal model of stroke, using middle cerebral artery occlusion followed by reperfusion, pre-treatment with vitamin D has been shown to significantly reduce the infarct volume through reduced expression of inflammatory cytokines such as

interleukin-6 and transforming growth factor- $\beta$ .<sup>232</sup> At present, vitamin D has yet to be investigated in preterm animal models, however, clearly as its deficiency is a risk factor for premature birth and with preclinical evidence of neuroprotection, it may be a promising therapy to investigate in the future. Cell based therapies including stem cells, human amnion epithelial cells (hAECs) and umbilical cord blood (UCB) cells, have shown neuroprotective effects in some animal models. For example, intranasal infusions of hAECs in preterm sheep has been shown to improve brain weight and neural development following asphyxia.<sup>233</sup> Further, UCB treatments in rodent and sheep models of hypoxia have demonstrated neuroprotective effects, where UCB cells have the advantage of being accessible non-invasively.<sup>234,235</sup>

Although it is now clear that EAAT2 dysregulation can contribute to preterm infant brain injury and neurological outcomes, treatments targeting EAAT2 modulation has yet to be established for clinical use. Ceftriaxone is a licensed antibiotic commonly used to treat central nervous system infections in preterm infants, which is known to upregulate EAAT2 expression. Rodent models of preterm brain injury have shown that pre-treatment with ceftriaxone upregulates EAAT2 and provides significant neuroprotection and improved neurological function.<sup>236</sup> The post hoc analysis of the Preventative Antibiotics in Stroke Study (PASS) showed improved neurological outcomes following thrombolysis for stroke with ceftriaxone compared to thrombolysis alone, although there was a trend towards increased symptomatic intracerebral haemorrhage.<sup>237</sup> Since ceftriaxone is currently safe in preterm infants, it may be a treatment that can be explored in the future. Another potential treatment known to upregulate EAAT2 function is guanosine, a nucleotide metabolite that has neurotrophic and neuro-regenerative

properties. Recently, it has been shown in rat models of ischaemic stroke that intranasally administered guanosine 3 hours post-stroke prevented significant neurological dysfunction, notably reducing long-lasting motor function loss.<sup>238</sup> This builds upon the pre-clinical evidence that guanosine is neuroprotective in ischaemic stroke via EAAT2 upregulation.<sup>239</sup> At present it is unknown whether these agents enhance total glutamate uptake or potentially worsen reverse glutamate transport, therefore further work would be required to clarify the clinical use of these agents, particularly in preterm infant brain injury. This will also be important in the context of precision medicine if eventually using EAAT2 mutation status, for example, to select the most suitable therapy for preterm infants. Finally, it may be necessary to investigate the role of combination therapies to optimise clinical outcomes where, for example, combined hypothermia with an EAAT2 enhancer, may be an effective treatment worth exploring in the future when further data validating the latter as a monotherapy has been established.

### ***Methodological overview***

The literature was reviewed by completing searches in Web of Science, PubMed and handpicking the most relevant papers. Important search phrases used included: “pre-term infants”, “brain injury”, “glutamate excitotoxicity”, “excitatory amino acid transporter”, “genetic susceptibility”. Papers describing the epidemiology, pathogenesis, basic science, clinical assessment and clinical treatment were categorised for my own assimilation. I completed this and provided the first draft of the introduction to the paper. I went on to explore the relationship between modulation of neuro-inflammation and stroke in animal models and in human studies, finding that there were potential therapeutic targets

that had not been previously explored in the field of neonatal brain injury, namely PPAR $\gamma$  agonists in the context of neuroprotection.

### ***Nature of work***

The work presented here represents a large clinical neuro-genetics study that was driven by a collaboration between scientists and clinicians. Blood spots of very pre-term infants were used to correlate SNPs to clinical outcomes retrospectively. Primary rat astrocytes were used to demonstrate that these mutations alter glutamate homeostasis in vitro.

### ***Significance of work***

This work was published in *Molecular Neurobiology* (Impact Factor 4.50) and cited 5 times since publication. The results of this study provided the first evidence that SNPs of EAAT2 result in reduced glutamate transport and are associated with worse neuro-developmental outcomes in very pre-term infants. EAAT2 SNPs may therefore be a potential biomarker to identify infants at a higher risk of brain injury and indicate that glutamate transport manipulation may be a novel therapeutic target in these diseases.

While assisting in the writing of this paper, I became interested in how to design an experiment to reduce glutamate mediated excitotoxicity by shunting excessive glutamate through upregulating protein transport. This led to me to review the literature extensively as I will describe in Chapter 3.

### ***Critical Appraisal of published work***

This was a robustly designed clinical study using the blood spots of preterm infants to undertake genetic analysis of genes encoding EAAT2. Sanger sequencing revealed two single nucleotide polymorphisms (g.-200C>A and 181A>C) were associated with an increased risk of cerebral palsy and worse neurodevelopmental outcomes. However, as this was a retrospective study, not all blood spots could be traced from the complete population included in the study, resulting in loss to follow up and potential selection bias. Further, the neurodevelopmental assessment tools used in different hospitals was not homogenous, leading to further potential confounding and skewing of results. Finally, preterm brain injury is very likely to be multifactorial where this study is limited to the study of a single gene, therefore genome-wide studies with comparisons of different preterm brain injuries would be necessary to build a panel of genetic variations that can fully characterise such brain injuries.

In summary, this study provides early evidence that EAAT2 variants may be an important biomarker for prognostication of following preterm brain injury and may have a role in developing future targeted therapeutics that ameliorate lack of EAAT2 function. Further larger, prospective studies would be required to potentially translate these findings into routine clinical practice.



## **Chapter 3: Glutamate transport in brain tumours**

### ***Introduction***

A human study of brain tumour and peritumoural samples revealed that patients with a higher risk of suffering from tumour-associated seizures (TAS) had higher glutamate concentrations and reduced glutamate transporter expression.<sup>240</sup> Therefore, the pathogenesis of TAS was similar to that of pre-term neonatal brain injury, whereby glutamate excess is caused by reduced protein mediated transport (Fig. 23). This led me to investigate whether a novel treatment strategy using an already licensed drug, to increase glutamate transporter expression, was feasible. Previously, sulfasalazine had been shown to prevent release of glutamate from glioma cells and prevent TAS in rodent models.<sup>241</sup> However, raising protein mediated glutamate transport via excitatory amino acid transporter 2 (EAAT2) had not been investigated previously. Since PPAR gamma agonists are known to upregulate functional EAAT2 expression in astrocytes and prevent excitotoxicity caused by glutamate excess<sup>242-246</sup>, I sought to gain a detailed understanding of these drugs by undertaking an extensive literature search. In the course of this, I found that these agents are also known to have antineoplastic activity, including in gliomas.<sup>247-253</sup> I therefore wrote and published a review on the mechanisms of this group of drugs and highlighted a novel potential treatment for TAS.<sup>254</sup> In this chapter I review the literature that cited my paper and summarise them.

### ***Aims***

- Review the papers that cited the published paper relating to this chapter

- Summarise recent developments in the field of tumour epilepsy in terms of animal models, therapeutics and PPAR gamma agonists
- Summarise the methodology, nature, and significance of this work

### ***Literature review***

As my published work pertaining to this chapter is a literature review, I will summarise the papers that have cited it in terms of glutamate modulation in the context of TAS and provide a concise update of what has been published in the field of TAS therapeutics. To date, 3 papers have cited my paper according to PubMed metrics as follows:

Ruda and Soffietti published a review in 2015 that focused on new developments in the treatment of epilepsy in gliomas.<sup>255</sup> They summarise the findings that glutamate plays a central role in epileptogenicity and growth of glial and glioneural tumours. The importance of EAAT1-5 is described, where EAAT2 is responsible for over 90% of active reuptake of glutamate from synaptic clefts. System  $x_c^-$  is described, alluding to equilibrium created with EAAT2 that when disrupted, results in glutamate accumulation and excitotoxicity. The importance of increased extracellular glutamate concentrations and system  $x_c^-$  found in patient samples and pre-clinical models was summarised.<sup>240,241</sup> Attempted modulation of system  $x_c^-$  using sulfasalazine in a phase 1-2 clinical trial, was cited, stating that 5 of the 10 treated patients developed cerebral oedema.<sup>256</sup> They go on to describe the importance of astrocytic glutamate uptake, which may be disrupted by ammonia, which is produced from glutamine deamination to glutamate by glutaminase, an enzyme highly expressed by GBM.<sup>257</sup> This, therefore, is a potential treatment target whereby anti-oxidants that inhibit the ammonia-induced

inhibition of glutamate re-uptake may be beneficial clinically.<sup>258</sup> Another strategy they allude to is my hypothesis that EEAT2 upregulation leading to increased glutamate uptake with drugs such as pioglitazone may be a future treatment target.<sup>254</sup>

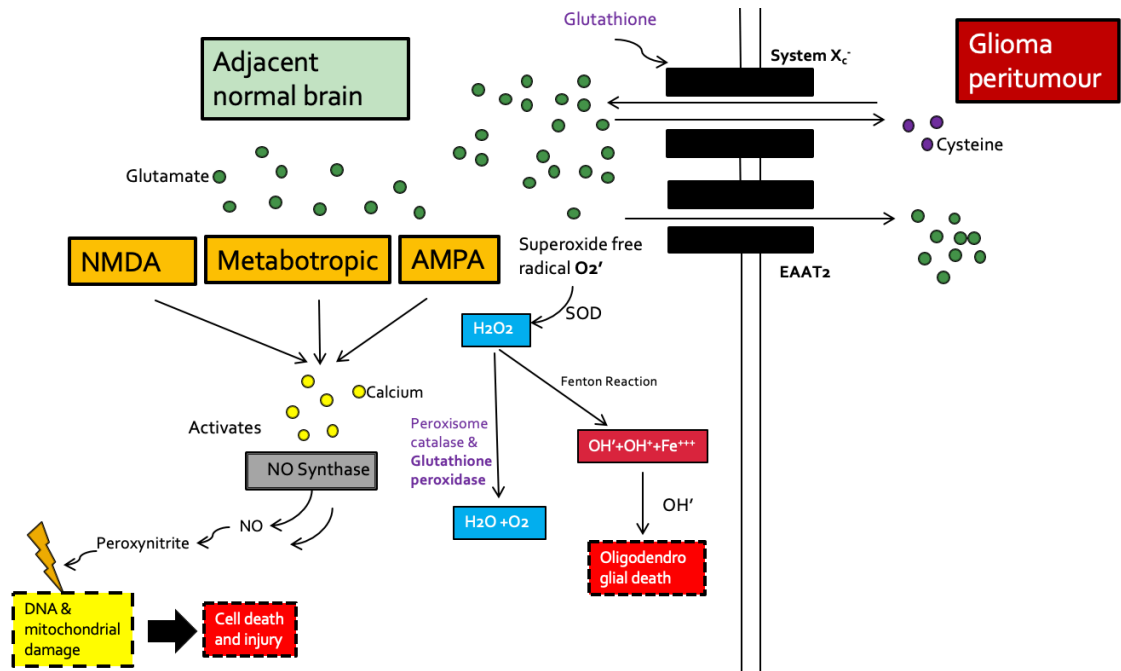


**Figure 23:** Diagram summarising the mechanisms of glutamate excitotoxicity in the context of a brain tumour causing glutamate excess in adjacent normal brain. System  $x_c^-$ , expressed on brain tumour cells, exchanges glutamate (green dots), for cysteine (purple dots). Excitatory amino acid transporter 2 (EAAT2) transports glutamate intracellular, but expression is reduced in brain tumours of patients who are prone to tumour associated epilepsy. This results in excessive extracellular glutamate which causes an increase in intracellular calcium concentration through activation of: 1) the N-methyl d-aspartate (NMDA) receptor with opening of the receptor-linked ionophore, 2) [alpha]-amino-3-hydroxy-5-methylisoxazole-4-propionic acid receptor (AMPA) with voltage-gated calcium channel opening, and 3) the metabotropic receptor, with release of intracellular calcium via inositol triphosphate and diacylglycerol. Raised calcium levels cause

activation or proteases, lipases and endonucleases, as well as nitric oxide (NO) synthase which generates superoxide free radicals. This then leads to peroxynitrite formation, mitochondrial injury and DNA damage. In addition, the Fenton reaction (iron oxidation) exacerbates this by formation of hydroxy radical formation ( $\text{OH}^\cdot$ ), lipid peroxidation and ferroptosis, a form of regulated cell death, in oligodendroglial cells in particular. Figure drawn by J Ching, adapted from Kochanek et al.<sup>203</sup> and Oka et al.<sup>204</sup>

The authors go on to discuss that deficiency of glutamine synthetase has been found in epileptogenic GBMs compared to non-epileptogenic, which results in raised glutamate levels in peritumour fluid.<sup>259,260</sup> Such raised glutamate levels is thought to activate sufficient neuronal glutamate receptors that activates neuronal networks leading to clinical seizures.<sup>261</sup> Ionotropic and metabotropic glutamate receptors have been shown to be highly expressed in glial tumour cells and thought to trigger electrical activity, particularly via AMPA and NMDA, that acts as a precursor to seizure activity.<sup>262,263</sup> However, GBM cells have been shown to have lower AMPA expression levels compared to normal brain, providing a mechanism by which GBM cells can survive glutamate-rich microenvironments and are likely less electrically excitable.<sup>264</sup> The AMPA receptor antagonist, Talampanel, is effective in treating partial seizures and improves the prognosis of newly diagnosed GBM but the effect on TAS is unknown.<sup>265</sup>

Inglesias et al. published a review in 2017 discussing the role of PPARs in potentially modulating the inflammatory and metabolic cascades involved in astrogliosis as a result of neuroischaemia or neurodegenerative diseases.<sup>266</sup> They go on to describe each of the subtypes of PPARs ( $\alpha$ ,  $\beta/\delta$  and  $\gamma$ ) in detail and

their roles in inflammation and diseases of the central nervous system. A rodent model of lithium pilocarpine induced seizures is described, whereby the PPAR $\gamma$  agonist, rosiglitazone, was shown to significantly reduce cognitive impairment caused by seizures and maintained glutathione homeostasis along with significant astrocyte inhibition.<sup>267</sup> My hypothesis that upregulating EAAT2 expression is mentioned, alluding to the potential impact on mitigating excitotoxicity mediated epileptogenesis. The authors complete this aspect of their discussion by referring to Hyperzine A, a drug that has been shown to have anti-inflammatory, activity against demyelination and axonal injury in the spinal cord dependent on PPAR $\gamma$ .<sup>268</sup>

Fernandez et al. carried out a study in 2017 investigating the role of PPAR $\gamma$  in glucose metabolism and reproductive pathways by creating an inducible knockout of PPAR $\gamma$  in astrocytes mouse model.<sup>269</sup> They found that these mice demonstrated dysregulation of glucose tolerance and female reproductive pathways, indicating a dependence on PPAR $\gamma$  in astrocytes to regulate these pathways. My review was cited at the beginning of this paper in reference to prior studies that had described PPAR $\gamma$  mediated energy intake and expenditure.

Four further published works have cited my paper including in the fields of nanoparticle research<sup>270-273</sup>, glioblastoma chemotherapy<sup>274</sup>. In addition, a PhD thesis from the University of Melbourne cited my paper (access: <http://hdl.handle.net/11343/212227>).

## *Update on glutamate and TAS*

### Pre-clinical models

Animal models of TAS have been most reported and validated by the Sontheimer Laboratory in the past.<sup>241,275</sup> In brief, their method uses immunodeficient mice that are implanted in one or both brain hemispheres with human glioblastoma cells and permitted to proliferate over 2-4 weeks. This is followed by invasive electroencephalogram recordings and subsequent sacrifice to perform electrophysiological recordings using layer 2/3 pyramidal cells. To my knowledge, this model has not been recapitulated elsewhere and the Melbourne Brain Tumour Research Group were unable to repeat the experiment successfully. Kirschstein and Kohling later reviewed all animal models of TAS in detail, describing the advantages, disadvantages and unanswered questions in this field.<sup>276</sup>

A more recently described novel animal model of TAS that used clustered regularly interspaced short palindromic repeats (CRISPR) in utero electroporation (IUE) deletions of 3 GBM related genes to induce the formation of brain tumours and associated epilepsy in immunocompetent mice.<sup>277</sup> By deleting phosphatase and tensin homolog (Pten), neurofibromin 1 (nf1), and p53 (Trp53), as previously described<sup>278</sup>, the authors generated glial tumours in vivo without the need for GBM xenografts and demonstrated progressive cortical hyperexcitability and generalized tonic-clonic seizures correlating to tumour proliferation. Peritumoural cortex staining revealed raised  $x_c^-$  expression correlating with generalized seizure activity in older mice (P80) (Fig. 24). Further, confirmation of the anti-epileptic activity of the system  $x_c^-$  inhibitor, sulfasalazine, was confirmed (Fig. 24). This TAS model likely represents a significant

advancement in both our understanding and ability to reliably recapitulate TAS. This would be an ideal in vivo model to examine the effects of PPAR $\gamma$  on glutamate transport and seizure activity as the peritumoural microenvironment in high grade gliomas is accurately recapitulated. Further studies that take advantage of CRISPR and IUE to induce the formation of low grade tumours, will be helpful in dissecting the mechanisms that underlie the pathogenesis of TAS.

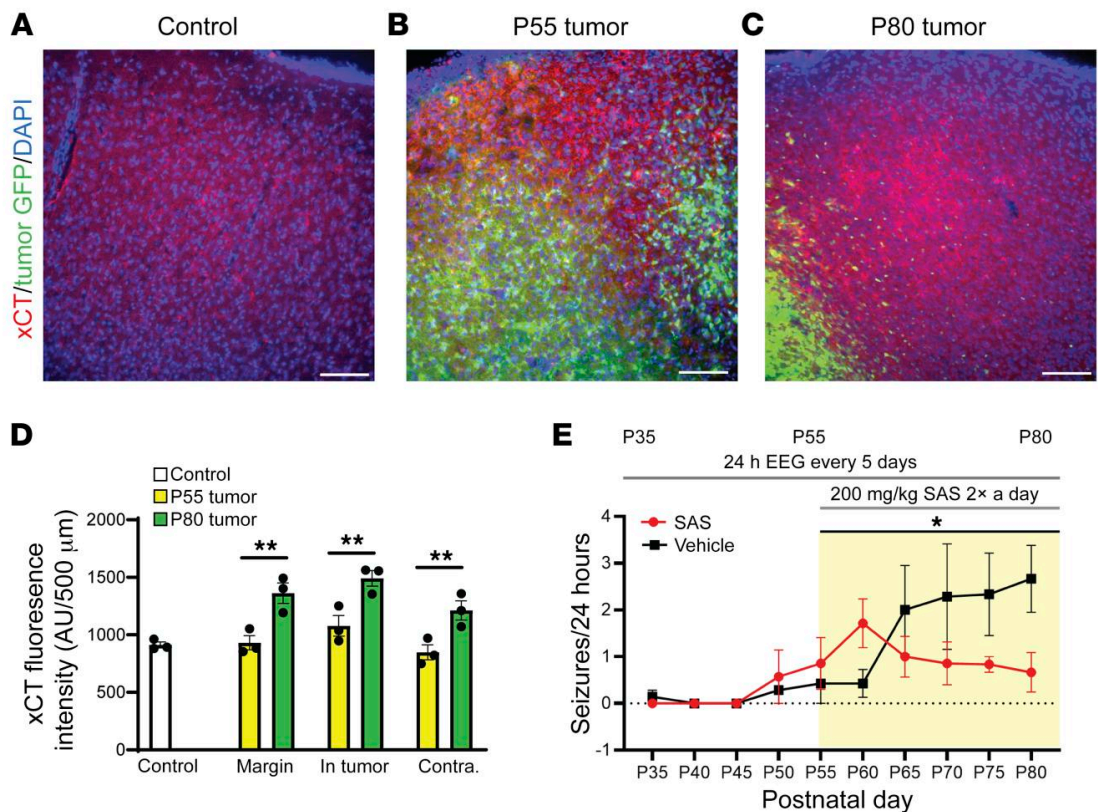


**Figure 24:** Glial tumours established by in utero electroporation of CRISPR constructs showing raised peritumoural system  $x_c^-$  (xCT) antibody staining in older post-natal day (P) 80 mice (C) compared to non-tumour controls (A) and P55 mice (B). Raised system  $x_c^-$  expression was confirmed by comparing fluorescence intensity (D). Sulfasalazine, a system  $x_c^-$  inhibitor, was given 200mg/kg twice a day from P55 to P80, control animals received PBS, gradually reducing seizure frequency (E). Figure taken from Hatcher et al.<sup>277</sup>

An established *ex vivo* model of epilepsy used for drug screening is organotypic hippocampal slice cultures.<sup>279</sup> I investigated augmenting this model by transplanting human GBM cells into organotypic hippocampal slices with the goal of modelling TAS. I describe this in Chapter 4. This attempt was to create an alternative to the previously described animal models from the Sontheimer Laboratory. Recently, the organotypic hippocampal slice model of epilepsy has been further developed by altering culture medium, whereby serum deprivation causes seizure activity and the associated inflammatory events found *in vivo*.<sup>280</sup> To date, there have otherwise been no further published reports on *ex vivo* models of TAS and most likely the model reported by Hatcher et al.<sup>277</sup> will become more widely used as it overcomes the confounding issues associated with using immunodeficient mice and heterogeneity of using human xenografts.

An important consideration when developing models of TAS is to consider whether there are any particular brain regions that are affected more than others by GBM invasion. Clinically, it is known that TAS is multifactorial, where the risk of seizures changes according to histological subtype, genetic factors, tissue hypoxia, changes in neurotransmitters, ionic dysregulation, and importantly tumour location.<sup>281</sup> A recent clinical study found that the majority (60%) of patients with studied with TAS had tumours located in the parenchyma, where generalized seizures were the predominant clinical phenotype.<sup>282</sup> The remaining 40% of patients in this study had focal seizures. These authors found no correlation between the histological subtype of tumour and the type of epilepsy, nor was there any correlation with the location of the lesion in the parenchyma or meninges. However, it was found that lobar distribution had a role in the type of



seizure, where frontal tumours had an association with generalized seizures and temporal or parietal lobe tumours were more likely to cause focal seizures. It has previously been reported that lower grade gliomas are more likely to be associated with seizures<sup>283</sup>, however larger studies are required to elucidate this possible correlation. Future development of TAS models may need to take this into consideration, particularly if developing an ex vivo model.

### Therapeutics

There have been no clinical trials registered specifically aiming to investigate a novel therapy for TAS. A previous trial of the licensed anti-inflammatory drug, sulfasalazine, was terminated early owing to a high rate of adverse events in patients treated for GBM.<sup>256</sup> This was unfortunate, particularly as there has been strong pre-clinical evidence that sulfasalazine inhibits system  $x_c^-$  in GBM<sup>241</sup>, where in theory it may have anti-convulsant activity as an adjuvant therapy for TAS.<sup>284</sup> A pilot, open-label, non-randomized study investigating the effect of sulfasalazine on brain glutamate levels using magnetic resonance spectroscopy was completed in 2016 (ClinicalTrials.gov Identifier: NCT01577966). The authors demonstrated that in these patients with biopsy confirmed  $x_c^-$  expression, sulfasalazine acutely inhibited levels of glutamate.<sup>285</sup>

While there appear to be no trials on the horizon for treating TAS, there is convincing and growing evidence of the importance of glutamate transport dysregulation. Targeting glutamate uptake via EAAT2 modulation has yet to be investigated in a human trial setting. A significant concern with the PPAR $\gamma$  agonist, pioglitazone, has been the association with bladder cancer. A recent meta-analysis demonstrated a small but significant risk of bladder cancer that

appeared to be dose and time dependent.<sup>286</sup> The underlying carcinogenic mechanisms for PPARs have yet to be clarified, however, Lv et al. recently demonstrated that PPAR $\gamma$  agonists, pioglitazone and rosiglitazone, induce cell cycle G2 arrest and apoptosis in Umuc-3 and 5637 bladder cancer cells.<sup>287</sup> There is still, therefore, a strong rationale to continue to investigate PPAR $\gamma$  agonists in the context of its neoplastic and potential seizure averting potential in GBM.

#### Pioglitazone update in neurological disease

Pioglitazone, was previously shown to reduce cognitive impairment in rodents treated with whole brain irradiation.<sup>288</sup> The observed neuroprotective effects were accrued to a reduction in the inflammatory cascade mediated by NF $\kappa$ B. Recently, pioglitazone has been shown by the same group to be safe and well tolerated in a phase 1 trial investigating the radiation-induced cognitive decline (RICD) in patients with primary or secondary brain tumours.<sup>289</sup> There is also emerging evidence that pioglitazone may be a therapeutic target in neurodegenerative diseases such as Alzheimer's and Parkinson's disease. Using a mouse model of Alzheimer's disease. Searcy et al. demonstrated that pioglitazone was neuroprotective, providing further pre-clinical evidence for its use in humans.<sup>290</sup> Later, in 2013-2015 the TOMORROW Phase 3 international trial was started that included an investigation of the role of pioglitazone on the delay of the diagnosis of Alzheimer's disease in high risk patients compared to placebo.<sup>291</sup> Unfortunately, in 2018 the trial failed to delay the onset of cognitive impairment and the rate of change of MRI changes were unaltered by pioglitazone.<sup>292</sup> Several authors of this study believe that this and prior clinical studies were inadequate to definitively assess the neuroprotective potential of pioglitazone fully and thus recommend larger, longer terms clinical studies in the future.<sup>293</sup> In mouse models

of Parkinson's disease, there is evidence that the progression of the disease can be slowed down by pioglitazone treatment.<sup>294</sup> Unfortunately, a Phase 2 clinical trial did not confirm this where it showed there was no difference in the Unified Parkinson's Disease Rating Scale (UPDRS) between the treatment and placebo groups.<sup>295</sup>

In the field of stroke medicine, previous animal model studies indicated that pioglitazone is potentially neuroprotective and a suitable drug candidate for clinical trials in humans.<sup>296,297</sup> Subsequently, the Insulin Resistance Intervention after Stroke (IRIS) Trial, a multicenter double blind controlled trial, demonstrated that pioglitazone was effective in reducing the risk of ischaemic stroke or transient ischemic attack in patients with insulin resistance compared to placebo.<sup>298</sup> Clinically, these findings translate to an estimated 3 patients being prevented from developing a stroke or myocardial infarction out of 100 patients with similar characteristics to the study patients, administered pioglitazone over approximately 5 years. Adverse effects of pioglitazone that were reported included weight gain, oedema, and bone fragility. Heart failure was not found to be more common in the pioglitazone treatment group compared to the placebo group. As such, pioglitazone may have an important therapeutic role in neurological diseases in the future.

### ***Methodological overview***

A search was performed using the search terms "glioma", "seizures", "glutamate" and "peroxisome proliferator agonists" inputted into Embase and Embase Classic (1947 to January 2014) and Ovid Medline In-Process & Other Non-Indexed Citations (1946 to Present). Further relevant articles were handpicked and

included if they alluded to the mechanisms of peroxisome proliferator agonists, brain tumour seizures, central nervous system glutamate dysfunction and glioblastoma drug treatments.

Using these resources, I wrote an extensive review of the potential role of peroxisome proliferator agonists on modulating glutamate transport in brain tumour epilepsy. I conceived this concept as a result of this. All co-authors reviewed my manuscript drafts without any role in conception.

### ***Nature of work***

This work represents my own original concepts derived from my prior work in epilepsy, neonatal brain injury and brain tumours. This literature review represents my independent pursuit of an answer to the question as to whether glutamate transport could be manipulated using an established drug and formed the basis for my research project detailed in Chapter 4.

### ***Significance of work***

This review was published in the Journal of Clinical Neuroscience (Impact Factor 1.59) and has been cited 3 times since publication according to PubMed metrics. A further 4 PubMed indexed papers have cited this paper.

## Chapter 4: Modulating glutamate transport in brain tumours

### *Introduction*

Unexplained seizures may represent the first sign of a primary brain tumour. Such tumour-associated seizures (TAS) can be pharmaco-resistant, adversely affecting the patient's quality of life.<sup>299</sup> Neurobiological research has elucidated that excessive glutamate levels present in glioma tissues are pro-convulsant in the rodent model.<sup>241</sup> Furthermore, blocking the system  $X_c^-$  cysteine-glutamate exchange transporter using sulfasalazine reduces the frequency of seizures in the rodent model.<sup>241</sup> The pro-convulsant properties of glutamate excess have been confirmed in the analysis of human brain tumour and peritumoural tissue, along with reduced EAAT2 expression.<sup>240</sup>

EAAT2 is one of 5 subtypes of sodium dependent plasma membrane glutamate transporters that accounts for up to 90% of extracellular glutamate uptake.<sup>64,207</sup> PPAR $\gamma$  is a ligand-dependent transcription factor that responds to both physiological and chemical stimuli, including the cyclopentanone prostaglandin 15-deoxy $\Delta^{12,14}$  prostaglandin  $J_2$  (15d-PG $J_2$ ) and thiazolidinediones (TDZ) respectively.<sup>300</sup> Expression of PPAR $\gamma$  in the brain has been found in multiple cell types including microglia, astrocytes, oligodendrocytes, and neurons. It has been shown with rat cortical cultures and genetic analysis that agonists of PPAR $\gamma$  increases expression of EAAT2 at both the mRNA and protein levels.<sup>243</sup> The reduction in infarct volume after administration of rosiglitazone, a commercially available TDZ, in rats with middle cerebral artery occlusion demonstrated in this study is supported with clinical evidence of better neurological outcomes found in a small case-matched controlled study investigating stroke recovery with TDZ

drugs.<sup>243,301</sup> The mechanism of PPAR $\gamma$  agonists could potentially be applicable in seizure reduction in gliomas through upregulation of EAAT2 and reduction of glutamate concentration. A literature review on this concept has been published by myself with expert colleagues.<sup>254</sup> I then went on to investigate the role of pioglitazone in EAAT2 expression and extracellular glutamate levels.

In our study, we found that the PPAR $\gamma$  agonist pioglitazone modulates functional EAAT2 expression and reduces extracellular glutamate levels in U251 glioma cells.<sup>302</sup> Further, pioglitazone alters glioblastoma cell lines U87 MG and U251 cell morphology and reduces cell viability of U87 and U251 cells. We confirmed that pioglitazone and other PPAR $\gamma$  agonists may offer a novel treatment paradigm for the treatment of TAS through promotion of extracellular glutamate clearance at both the glioma cell level and surrounding astrocytes. In light of these findings, we attempted to develop a novel model of TAS using organotypic hippocampal slices transplanted with fluorescently labelled GBM cells, however this model failed to demonstrate epileptiform activity. We also attempted to retrospectively identify patients with TAS and concomitant treatment with a PPAR $\gamma$  agonist but there were insufficient numbers to draw any meaningful conclusions. Further work is required to definitively elucidate the mechanisms of this therapeutic strategy but is also limited by the lack of reproducible brain tumour seizure models.

The aims of this chapter are as follows:

- Provide an overview of the methods used in this study and unpublished related work:
  - Clinical retrospective study of TAS and PPAR $\gamma$  agonists

- Cell culture and molecular pathway interrogation methods
- Novel ex vivo model of TAS using organotypic hippocampal slices
- Summarise the current and emerging drug treatment for TAS
- Summarise the methodology, nature, and significance of this work, and provide a critical appraisal of the published paper pertaining to this chapter

### ***Methodological overview***

#### *1. Retrospective clinical study:*

The two patient groups previously recruited by Yuen and colleagues were included in this study.<sup>240</sup> These were glioma patients from either Royal Melbourne Hospital or Melbourne Private Hospital with supratentorial gliomas identified between 1996 and 2006 (group 1) and between 2007 and 2009 (group 2). Clinical details were acquired through patient medical records and telephone interviews of patients and relatives. Neuropathologists graded tumour samples using the WHO criteria. Stored peritumoural samples from these patients were analysed for glutamate levels and expression of several proteins including EAAT1 and 2, and system  $x_c^-$ . Data was entered on to the Australian Cancer Grid Database. All these resources were to be used to identify the following information about patients: Age, sex, past medical history (specifically type II diabetes), preoperative imaging findings, WHO tumour grade, epilepsy risk factors, tumour location, pre-operative TAS presence, TAS frequency/week, number of antiepileptic drugs (AEDs) tried, drug history (specifically if on or previous use of TDZ drugs), duration of seizures pre- and post-operatively and mean seizure free period. It was expected that approximately 15% of glioma patients will have a diagnosis of diabetes, as reported in a previous study.<sup>303</sup> The primary outcome variable for this study was defined as ongoing or previous use of TDZ drugs.

Statistical methods were to be employed to determine any significant association between variables. The aim of this study was to determine whether there is an association between the use of TDZ drugs and development of TAS in glioma patients.

Unfortunately, only 6 patients were found in the database who met these criteria. Whilst, none of these patients had reported TAS, it was decided that this was an insufficient number of patients to draw any meaningful conclusions. This aspect of the investigation was therefore aborted.

## *2. The role of PPAR $\gamma$ agonists on glutamate transport in glioblastoma cells*

In order to investigate the role of PPAR $\gamma$  agonists in vitro, I chose 2 established, widely used immortalised human glioblastoma cell lines U87MG and U251MG. U251MG was chosen in particular as it had been previously been shown to be epileptogenic following intracranial implantation in mice.<sup>241</sup> I chose human primary glioma stem cell (GSC) line #35 from the established library of primary samples in the Department of Neurosurgery, Royal Melbourne Hospital, specifically because this patient had suffered from TAS. This primary GSC line was chosen as the patient had suffered from tumour epilepsy. The fresh tumour sample was dissociated by trypsinisation to form neurospheres that were initially cultured in DMEM/F12 (Gibco) supplemented with 10 ng/L epidermal growth factor (BD Biosciences), 10 ng/L fibroblastic growth factor (BD Biosciences), 1 $\times$  B27 without vitamin A (Gibco) and 1 $\times$  penicillin/streptomycin (Gibco)] in six-well ultra-low adhesion plates (Corning).



I established and maintained cell cultures of these cell lines by using 2 methods:

- 1) U87MG and U251MG were maintained in DMEM supplemented with 5% foetal calf serum (FCS) and penicillin/streptomycin at 37°C in 10% carbon dioxide and
- 2) GSC #35 was cultured in DMEM/F12 supplemented with epidermal growth factor, basic fibroblast growth factor, B27 and penicillin/streptomycin at 37°C in 10% carbon dioxide in ultra-low adhesion 6 well plates in order to form neurospheres.

I then measured the expression of the key glutamate transporters EAAT2 and EAAT1 (glutamate aspartate transporter [GLAST1]) in these cell lines, using rat pup cortex and thalamus as controls, with western blotting, repeated in triplicate (all experiments were repeated at least three times). I found that expression of EAAT1 and EAAT2 was reduced compared to the controls, which was in keeping with previous studies.<sup>304,305</sup> Western blots were carried out, briefly, cell lysates were separated by SDS-PAGE on pre-made gels (Invitrogen), transferred onto a polyvinylidene fluoride membrane and incubated with the primary antibodies of interest. Protein expression was visualised with an ECL chemiluminescence detect kit (GE Healthcare, Rydelmere, N.S.W., Australia) following secondary antibody incubation.

As I planned to determine whether the PPAR $\gamma$  agonist pioglitazone affected the expression of glutamate transporters EAAT2 and EAAT1 in glioblastoma cells, I first undertook a viability assay to determine a dose response curve. I used the CellTiter-Glo® Luminescent Cell Viability Assay (Promega, Madison, WI, USA). I utilised a 96 well plate and seeded a consistent number of glioma cells ( $1 \times 10^4$  cells per well) and incubated for 24, 48 and 72 hours with pioglitazone alone, the

PPAR $\gamma$  antagonist GW9662 alone and a combination of both drugs before measuring luminescence using the GloMax $\text{\textcircled{R}}$  Microplate Luminometer (Madison, WI, USA).

I went on to examine whether the addition of varying concentrations of pioglitazone to the cell culture media of each of the cell lines affected the expression of EAAT2 and EAAT1 by performing further Western blots. My results demonstrated that there was a dose dependent increase in EAAT2 expression but not EAAT1 in U87MG and U251MG cells. There was no change in EAAT2 expression in GSC #35 with pioglitazone. I repeated these experiments with GW9662 to determine if the change in EAAT2 expression was PPAR $\gamma$  dependent, finding that this was the case in U87MG but not U251MG cells.

Having found that pioglitazone can upregulate the expression of glutamate transporters in glioma cell lines, I sought to determine whether extracellular glutamate levels were affected by this. In order to measure this, I designed a set of experiments in collaboration with Andrew Bjorksten, Associate Professor in Pharmacology and Therapeutics who is an expert in high performance liquid chromatography (HPLC). Using the same HPLC techniques he previously used to analyse glutamate levels in human brain tumour samples with previously<sup>240</sup>, we determined how to optimise his protocol to analyse extracellular media samples by first confirming background glutamate levels in media containing FCS. As such, I cultured each cell line in pioglitazone alone, GW9662 alone, and combinations of the two drugs according to the cell viability assay results for 24, 48 and 72 hours and provided 5mL of media of each condition to Dr Bjorksten, who completed the HPLC analysis. We found that extracellular glutamate levels

were significantly reduced by increasing concentrations of pioglitazones at the 72 hour time point in U87MG and U251MG cells, but not GSC #35 cells.

Following these results, I felt it necessary to examine whether these drugs had any effect on cell morphology. I used brightfield microscopy to quantify the cell numbers of U87MG and U251MG in culture with different concentrations of drug in the media. I found that cell numbers reduced with higher concentrations of drug and observed the reduced formation of astrocytic processes in correlation with this. I repeated this for GSC #35, but instead measuring the average neurosphere size, finding that there was no significant difference with the addition of pioglitazone in the culture media.

Finally, in order to further dissect the anti-neoplastic downstream effectors of pioglitazone, I investigated proteins from a number of oncogenic signalling cascades that were either known to be affected by PPAR $\gamma$  agonists or I hypothesised may be affected. I utilised a series of antibodies for western blotting analysis, including: anti-Akt, anti-phospho-Akt (threonine 308), anti-GSK3 $\beta$ , anti-phospho-GSK3 $\alpha/\beta$  (ser219), anti-FAK, anti-phospho-FAK, anti-YAP, anti-phospho-YAP (pSer127). As before, I exposed the glioma cell lines to varying concentrations of pioglitazone and performed Western blot analysis to determine whether expression of these proteins was altered. I found significant changes in Akt and GSK (published<sup>306</sup>).

### *3. The role of PPAR $\gamma$ agonists in tumour associated epilepsy*

In order to examine the functional effects of PPAR $\gamma$  agonists on TAS, I hypothesised that transplanting glioblastoma cells into live organotypic brain

slices may initiate epileptiform activity due to the release of glutamate from the transplanted cells. The role of PPAR $\gamma$  agonists on such epileptiform activity could then be studied using an ex vivo model. As such, I designed and refined a transplantation technique that successfully grows transplanted fluorescently labelled glioblastoma cells in organotypic brain slices but does not elicit epileptiform activity. This technique was eventually abandoned as the electrophysiological measurements from these slices was non-reproducible. The following is a description of the methods I designed and attempted.

#### Organotypic tumour associated seizure model method

##### 1) Organotypic brain slice culture

Using previously established methods, prepare organotypic hippocampal slice cultures (OHSC) and whole brain slices cultures (WBSC).<sup>307,308</sup> OHSC prepared by first anaesthetising 8-12 day old rats with isoflurane before sacrificing by removing the head using a scalpel. The skull is cut with scissors sagittally, removed and the brain scooped out into ice cold cutting solution (625mg glucose dissolved in 100mL Grey's balanced salt solution). From the point of sacrifice to immersing the brain in solution should take no longer than 1 minute. Remove the frontal lobes and cerebellum using coronal cuts. Isolate the hippocampi and immerse in cutting solution (Table 4), then place under a dissecting microscope and cut into 350 $\mu$ m slices. Using P1000 filtered pipette with tip cut off, pipette slices into TC plate with dissecting media. Pipette slices onto Millipore inserts pre-placed and pre-heated in a six well plate. Up to 3 slices can be placed on each membrane (Fig. 25). Add 1mL of culture media (Table 5) to outer wells. Incubate. For WBSC follow the method as above, but separate hemispheres through the corpus callosum and super glue the medial sides to a Teflon sheet

on a McIlwain Tissue Chopper (Campden Instruments Ltd., Loughborough, England).

<b>Chemical</b>	<b>mM</b>	<b>MW</b>	<b>Factor</b>	<b>Weight (g)</b>
<b>Choline Cl</b>	125.0	139.63	X 10	87.300
<b>KCl</b>	2.5	74.55	X 10	0.932
<b>CaCl<sub>2</sub>.2H<sub>2</sub>O</b>	0.4	147.00	X 10	0.244
<b>MgCl<sub>2</sub>.6H<sub>2</sub>O</b>	6.0	203.30	X 10	6.000
<b>NaH<sub>2</sub>PO<sub>4</sub>.H<sub>2</sub>O</b>	1.3	156		0.975
<b>Following must be added fresh</b>				
<b>before use:</b>				
<b>NaHCO<sub>3</sub></b>	26.0	184.01		2.210
<b>D-Glucose</b>	20.0	180.2		3.690
<b>Total solution</b>	500mL in distilled water			

**Table 4:** Cutting solution used for preparation of organotypic brain slice culture

<b>Reagent</b>	<b>Volume</b>
MEM	200mL
Earle's balanced salt solution	100mL
Horse serum (heat inactivated)	100mL
Glucose 32.5% (dissolved in mem)	8mL
B27	8mL

**Table 5:** Culture media for maintaining organotypic brain slice cultures

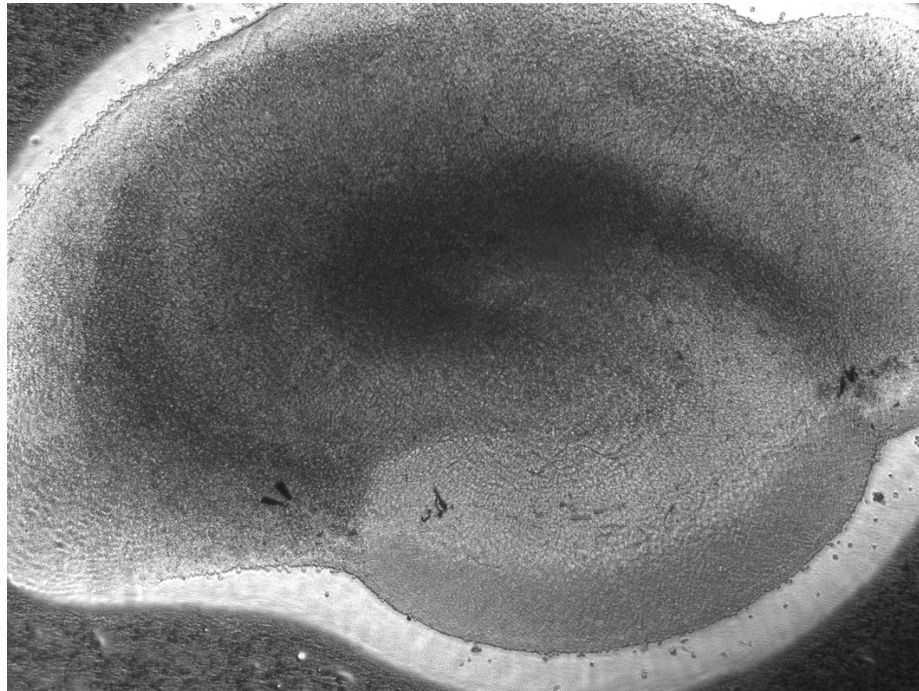


**Figure 25.** Bright field microscopy image (4 x magnification) of an example organotypic hippocampal slice. Brain slice preparation, ex vivo culture and images taken by J Ching.

## 2) Fluorescent labelling of glioblastoma cells using viral transfection

Lucy Paradiso, Research Assistant, University of Melbourne, generated the CMV-driven Td-Tom adenovirus for infection of my glioblastoma cell lines. Briefly, Td-Tomato was cloned from pENTR-Td-Tom in the destination vector pAd/VMC/V5-DEST (Invitrogen) using the restriction enzyme EcoRI to generate pAd.CMV-Td-Tom adenoviral plasmids. This was then amplified as described by Luwor et al.<sup>309</sup> U251MG, U87MG and GSC #35 were infected with Ad.pCMV-td-tomato virus as varying multiplicity of infection (MOI) of 200, 500 or 2500. The lowest MOI was found to have the highest transfection efficiency, particularly in U87MG cells (Fig. 26).

### 3) Transplantation of glioblastoma cells into organotypic brain slices

We infused 0.1 $\mu$ L of a cell suspension of labelled U87MG ( $5 \times 10^4$  cells/ $\mu$ L resuspended in medium for brain slices) over 1.5 minutes into the midpoint of brain slices using a 0.5 $\mu$ L Hamilton Syringe with a 33 gauge, 210 $\mu$ m wide-outer diameter, needle fixed to a micromanipulator and infusion pump (Aladdin single-syringe infusion pump, AL-1000, World Precision Instruments, Sarasota, USA) using a dissecting microscope, adapted from de Bouard et al.<sup>308</sup> Different anatomical regions should be injected as tumour associated seizures have been shown to occur from most intracranial locations. CA3 should initially be targeted on OHSC as this is classically where an electrode is placed for electrophysiological recordings and is the region most likely have abnormal electrophysiology. Repeat infusions with either DMSO or NIH/3T3 murine cells acted as a control (Fig. 27 & 28).

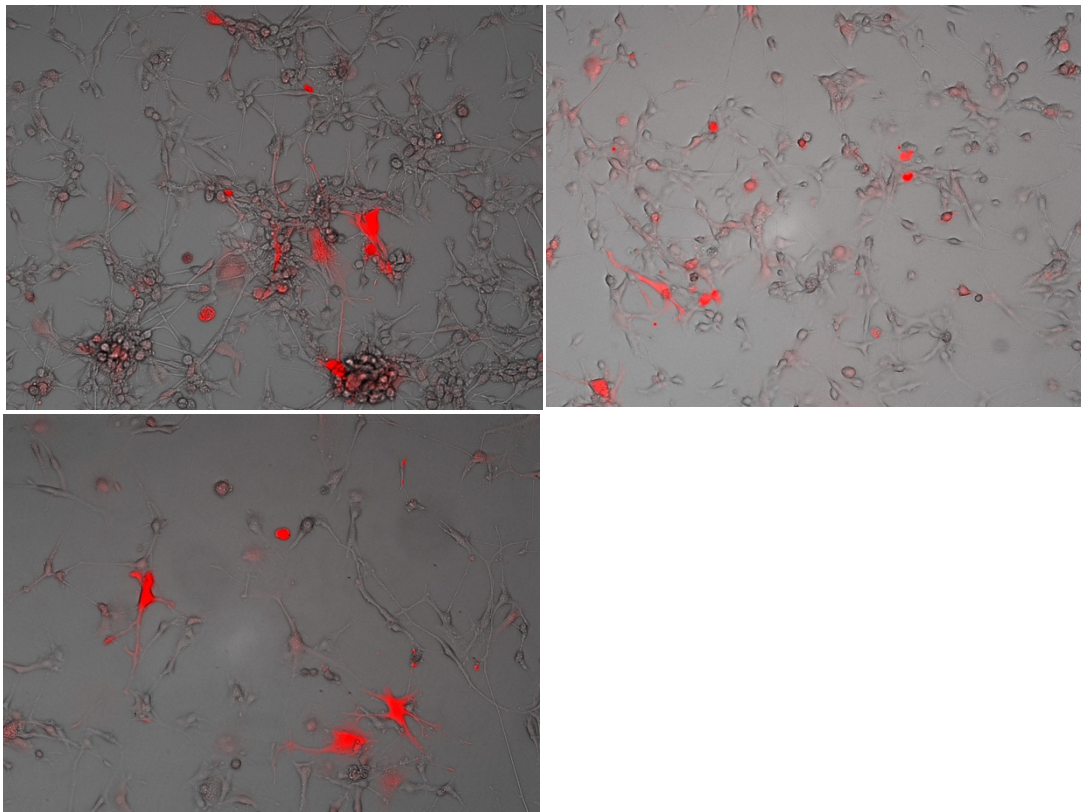


**Figure 26:** Bright field microscopy images (10x magnification) with Td-tomato transfected cells overlay of U87MG cells with multiplicity of infection (MOI) 200 (a), 500 (b), and 2500 (c). Cell culture maintained and images taken by J Ching.

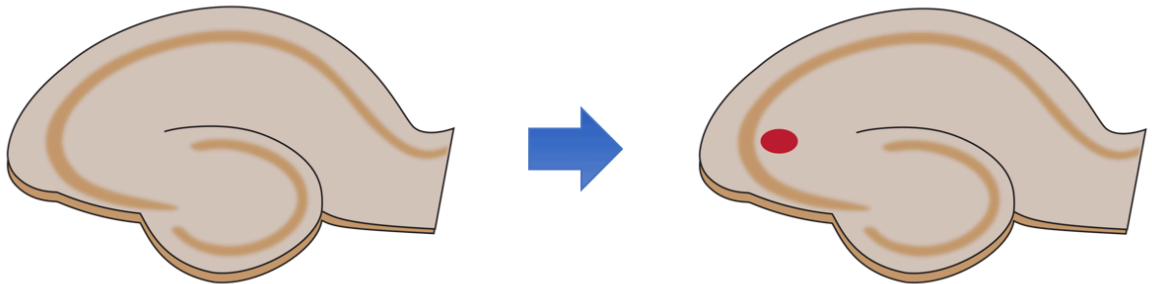


**Figure 27:** Schematic of implantation of fluorescently labelled glioma cells (red) into organotypic brain slices.

Next, we incubated glioma cells with organotypic slice in slice medium as an alternative to the above method.  $5 \times 10^4$  cells/ $\mu\text{L}$  re-suspended in brain slice medium was placed at the slice surface/air interface. This was repeated with either DMSO or NIH/3T3 as a control. Fluorescent microscopy was used to monitor progress of glioma growth and proliferation. Successful transplantation was indicated by proliferation of the fluorescent glioblastoma cells. Electrophysiological recordings were taken at daily time points with slices placed in normal and magnesium free artificial cerebrospinal fluid (ACSF). Once baseline recordings were established, this was compared with magnesium free ACSF. Pioglitazone was added to the ACSF during the experiment to determine whether electrophysiological recordings were modulated. This method was found to be inferior to infusing glioma cells into the brain slices as a foci of tumour cells did form, which would mimic a primary GBM tumour more accurately and



thus secondary epileptiform activity. This technique was therefore abandoned and infusion-based transplantation was used instead.

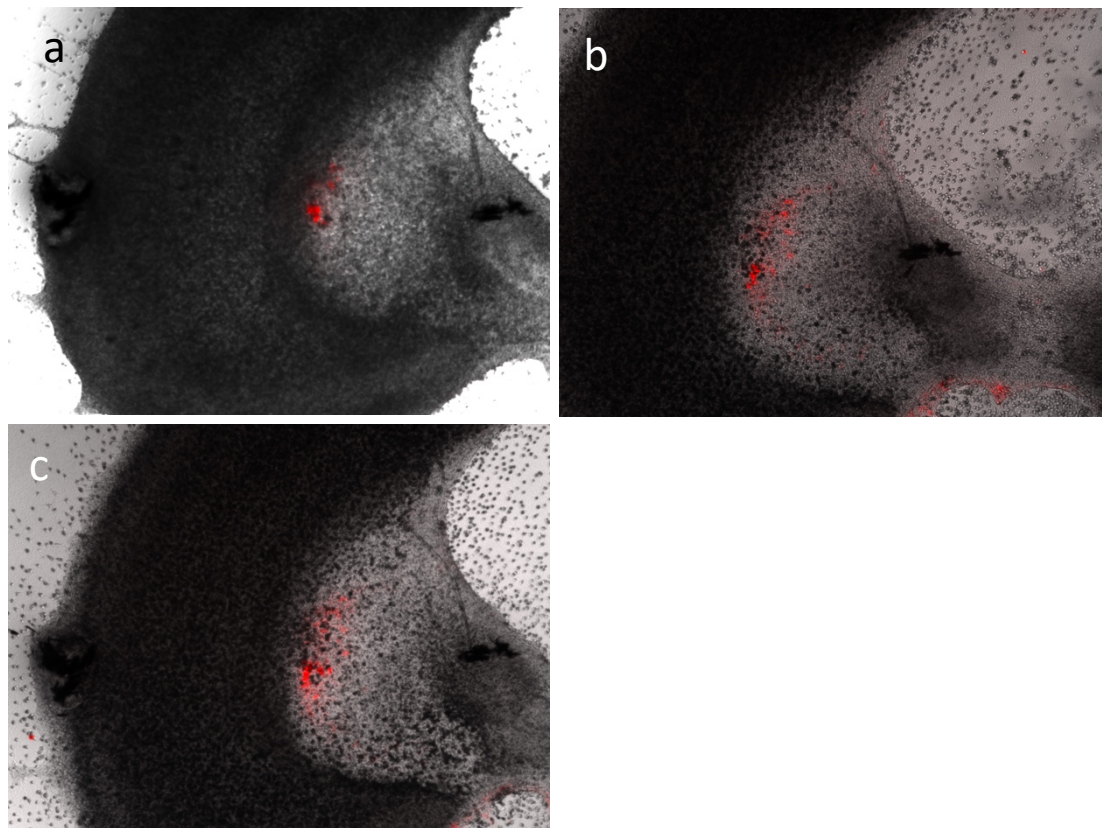


**Figure 28:** Brightfield microscopy images with Td-Tomato overlay, demonstrating an organotypic hippocampal slice with transplanted fluorescent Td-Tomato labelled U87MG cells at day 3 (a), day 6 (b), and day 8 (c) *in vitro*. There is evidence of proliferation and migration from the implantation site. Preparation of organotypic hippocampal slices, implantation of glioblastoma cells, *ex vivo* slice culture and microscopy images by J Ching.

#### 4) Measurement of organotypic brain slices transplanted with glioblastoma cells electrical potentials

Brain slices were transferred to pre-warmed artificial cerebrospinal fluid (Table 6) prepared in an enclosed electrophysiology rig with a dedicated microscope (Olympus BX51). Electrical potentials were measured at baseline and at regular

intervals at key brain slice sites, including within the tumour, peritumour, and normal parenchyma, if these boundaries were clearly identifiable. Brain slices were then incubated with varying concentrations of pioglitazone, with the goal of determining whether this affected epileptiform activity in a dose and time dependent manner. As organotypic slices last 6 weeks, electrophysiological responses were measured throughout this period. Dr Thomas Zheng, Postdoctoral Research Fellow in Neurology, undertook all electrophysiological recordings. The set of results obtained for these experiments was inconclusive.

<b>Chemical</b>	<b>mM</b>	<b>MW</b>	<b>Factor</b>	<b>Weight</b>
NaCl	126.0	58.44	X 10	73.600
KCl	2.5	74.55	X 10	1.860
NaH <sub>2</sub> PO <sub>4</sub> .2H <sub>2</sub> O	1.4	156.01	X 10	2.100
CaCl <sub>2</sub> .2H <sub>2</sub> O	2.0	147.02	X 10	2.940
MgCl <sub>2</sub> .6H <sub>2</sub> O	4.0	203.30	X 10	8.100
Following must be added fresh before use:				
NaHCO <sub>3</sub>	26.0	84.01		2.200
D-Glucose	10.0	180.20		1.800
<b>Total solution</b>	1000mL in distilled water			

**Table 6:** Artificial cerebrospinal fluid used during electrophysiology experiments.

- 5) Measuring the effect of PPAR $\gamma$  agonists on extracellular glutamate levels in an organotypic model of tumour associated seizures

Borate buffer (provided by Andrew Bjorksten) was mixed with organotypic slice media samples for storage before HPLC analysis of glutamate levels. Once organotypic brain slices were harvested, they were placed in culture for 2-4 days before changing media and implanting glioblastoma cells in half the obtained slices. Using half of the tumour bearing slices and half of the slices alone, pioglitazone was added to the slice media at 1 $\mu$ M, 5 $\mu$ M, and 10 $\mu$ M and allowed a further 2-3 days in culture. At the end of this period the slice media was changed. At this point samples for glutamate level analysis was taken at timepoints 0 hours, 0.5 hours, 1 hour, and 2 hours, taking 50 $\mu$ L of media and adding it to 250 $\mu$ L of borate buffer. All samples stored at -20°C prior to HPLC analysis. The results of these experiments were inconclusive.

### ***Current and emerging medical treatment for TAS***

Anti-epileptic drugs (AEDs) are generally recommended as first line treatment for seizures associated with brain tumours, where the newer drugs are recommended initially, such as levetiracetam, lamotrigine, lacosomide, topiramate and pregabalin.<sup>310</sup> These drugs are also known to be associated with fewer interactions with chemotherapies and favourable side effect profiles.<sup>311</sup> Van Breemen et al. found in their single centre study of 140 patients with TAS that a combination of valproic acid and levetiracetam was more effective than valproic acid alone (59% versus 52% response), indicating that combination therapy for TAS may be more effective.<sup>299</sup> A phase II clinical trial comparing monotherapy of levetiracetam and pregabalin for TAS found they were effective in 75% of patients treated.<sup>312</sup> It should be noted that the AED selected will also be dependent on the type of seizure the patient suffers from where more than two AEDs to unresponsive patients should generally not be pursued as it is known to be

ineffective.<sup>7</sup> Prophylaxis for seizures in TAS has been previously reviewed in a Cochrane systematic review that included 5 randomised controlled trials, finding that there was no difference between treatment with phenytoin, phenobarbital or divalproex and control groups.<sup>313</sup> Therefore, starting patients on AEDs for seizure prophylaxis in brain tumours is not recommended, not least because it can cause harm through side-effects.

The non-competitive AMPAR antagonist perampanel has gained significant interest in treating TAS since it was recently found by Venkatesh et al. that glutamate released by gliomas promote tumour progression in addition to activating neurones causing seizures and ecotoxicity.<sup>314</sup> Therefore, it has been hypothesised that perampanel can elicit dual functions as an anti-neoplastic and anti-epileptic agent. Six small studies (n = 8-36) to date have reported a promising responder rate of 75-100% when treating TAS with perampanel.<sup>315</sup> There are two trials actively recruiting that are investigating the effect of perampanel on peritumour hyper-excitability in brain tumours (NCT04497142) and perampanel in combination with AEDs in treating TAS (NCT03636968). Other ongoing trials related to glutamate modulation include sulfasalazine combined with stereotactic radiosurgery in recurrent glioblastoma (NCT04205357) and those using the NMDAR receptor antagonist memantine (NCT03194906 and NCT01430351). Therefore, the results of these and future studies examining glutamate modulation in the context of TAS and glioma treatment will shed light on how to the current armamentarium can potentially be improved.

### ***Nature of Work***

Following the aforementioned literature review (Chapter 3), I subsequently wrote a research proposal, which was accepted by Professor Andrew Kaye and Professor Terence O' Brien at the University of Melbourne. I then pursued this as a clinical and basic science project as a Research Fellow, collaborating with numerous clinicians and scientists. The clinical arm of this project entailed searching through patient medical records retrospectively, attempting to identify patients with brain tumours taking a PPAR $\gamma$  agonist for type 2 diabetes. Unfortunately, insufficient numbers of patients were identified to make any meaningful conclusions and this was abandoned.

The laboratory-based work consisted of two inter-related projects. The first was based in the Brain Tumour Laboratory of Professor Andrew Kaye and focused on cell culture of immortalised glioblastoma cell lines and primary brain tumour stem cells. Pioglitazone and a PPAR $\gamma$  antagonist were used to determine whether extracellular glutamate levels were affected by different concentrations of drugs by using high performance liquid chromatography. Relevant signalling proteins were analysed using western blotting and cellular morphology was analysed using microscopy.

The second project was based in Professor Terence O' Brien's Neurology Laboratory, attempting to establish a novel model of brain tumour epilepsy using rodent organotypic hippocampal slices and implanting fluorescently labelled brain tumour cells. Whilst I was able to develop a protocol to reliably implant brain tumour cells, we were unable to demonstrate seizure activity when measuring extracellular electric fields using an electrophysiology rig. This aspect of the

project was eventually abandoned, particularly as others in the group had attempted to recapitulate a previously published rodent in vivo model of brain tumour seizures with very limited success over a number of years. As such, the main outcomes of this work were based on the in vitro work that was performed.

### ***Significance of work***

This work has been published as an original article in the journal *Oncotarget* (Impact Factor 5.16) and has been cited 9 times since publication. I presented this work at the British Neuro-Oncology Society Meeting as a podium presentation and the conference abstract published in the journal *Neuro-Oncology* (Impact Factor 10.24).

### ***Critical Appraisal of published work***

This study provides robust evidence that EAAT2 expression on glioblastoma cells can be increased with pioglitazone in vitro, suggesting a potential role in treating tumour associated epilepsy. However, this study lacks in vivo experiments to demonstrate the interplay between tumoural and peritumoural normal brain tissue changes in EAAT2 expression on extracellular glutamate levels. Although it is known that pioglitazone can upregulate EAAT2 in astrocytes, it has not been shown in this study to do so, which is important as the peritumour microenvironment may alter astrocyte function. A glutamate uptake assay would have been beneficial in this study to ensure it is truly functional upregulation of EAAT2 responsible for the reduced glutamate levels reported, rather than some other mechanism. Finally, pioglitazone should be trialled in a model of tumour epilepsy. As discussed in this chapter, developing a novel organotypic model of tumour epilepsy was attempted but not successful.

Overall, this study provides robust in vitro evidence of the potential role of pioglitazone in treating tumour epilepsy, however further preclinical studies would be required before moving to human clinical trials.

## **Chapter 5: Metabolic and perfusion changes in brain tumours**

### ***Introduction***

Glioblastoma multiforme (GBM) is the most malignant and frequent primary brain tumour occurring in humans.<sup>316,317</sup> Median survival following diagnosis and optimal therapy is a discouraging 10-14 months, with a minimal 3% - 5% of patients surviving for more than 3 years.<sup>318</sup>

GBM has been shown to invade the surrounding parenchyma, destroying the normal functional architecture of the brain. At present, optimal treatment for GBM utilises the Stupp Protocol, which employs multimodal treatments including resective surgery and chemoradiotherapy. Despite this, tumour recurrence is common, where a renewed aggression manifests. Such reports of relapse and marginal improvements in prognosis prove the poor efficacy and potential limit in the use of these conventional therapies.<sup>319</sup>

Following surgical removal, tumour recurrence tends to localise within the resection cavity or immediately adjacent to the resection margin, since tumour cells have already invaded adjacent normal brain tissue at the time of the surgery.<sup>320,321</sup> It has also been found that disease progression often occurs within areas where high dose radiotherapy is applied to areas of tumour invasion.<sup>322-324</sup> The invasive margin cannot be accurately delineated with conventional neuroimaging including T<sub>1</sub> and T<sub>2</sub>-weighted, and fluid-attenuated inversion recovery (FLAIR) magnetic resonance imaging (MRI) sequences.<sup>325,326</sup>



As such, we sought to better characterise the invasive margin by combining alternative MRI sequences including diffusion tensor magnetic resonance imaging (DTI) and dynamic susceptibility contrast perfusion imaging (DSCI). DTI imaging is sensitive to water diffusion along white matter tracts and can be analysed with two signatures that include isotropic diffusion (p: magnitude of diffusion) and anisotropic diffusion (q: directionality of diffusion). DSCI provides information regarding relative cerebral blood volume (rCBV) that is known to correlate with tumour vascularity and cellular proliferation. Additionally, multi-voxel MR spectroscopy (MRS) provides information on tissue metabolism including measures of glutamate + glutamine (Glx), N-acetylaspartate (NAA), myo-inositol (Ins) and total choline (Cho). In this study, we demonstrated that by combining DTI with rCBV and MRS the invasive region can be identified where increased perfusion, Glx/Cr, Cho/NAA and Cho/Cr was measured compared to unaffected contralateral brain parenchyma.<sup>327</sup> Critically, this work confirmed that there are raised concentrations of glutamate at the invasive margin of GBM, which facilitates cell death and invasion through glutamate mediated excitotoxicity and degradation of extracellular matrix (ECM).<sup>304,328-330</sup>

In the following sections I present my own literature review, methods, results and discussion of the initial study I completed for this project. As the results from my work were promising, further patients were added and my work was amalgamated into the final analysis and published work. Therefore my aims include:

- Provide a literature review of the glioblastoma vasoproliferation and neuro-imaging

- Summarise the current and emerging neuro-imaging innovations in elucidating the glioblastoma invasive margin
- Summarise the methodology, nature, and significance of this work, and provide a critical appraisal of the published paper pertaining to this chapter

### ***Literature review***

Gliomas are highly vascular tumours that require nourishment via arterial perfusion and waste removal via venous outflow from a newly formed blood supply to support increasing metabolic demands as it invades and proliferates into normal brain tissue.<sup>331</sup> Four mechanisms are known to contribute to the formation of such new vessels, including co-option, angiogenesis, vasculogenesis and intussusception (Fig. 29).<sup>332</sup> Co-option is known to occur at the earliest phase of tumour formation, whereby existing brain blood vessels undergo perivascular tumoural invasion that leads to ischaemia and vascular regression, causing cell death and release of angiogenic factors.<sup>333,334</sup> Angiogenesis follows, which is stimulated by the release of growth factors including vascular endothelial growth factor (VEGF)<sup>335</sup>, fibroblast growth factor (FGF) and platelet derived growth factor (PDGF)<sup>336</sup> from the avascular necrotic peri-tumour and hypoxic conditions caused by the failing local vasculature. Vasculogenesis is an incompletely understood process whereby bone marrow derived cells can incorporate directly into the brain tumour vessels.<sup>337</sup> Stromal derived factor-1 has been found to have a role in incorporating marrow derived precursors into tumour endothelium.<sup>338</sup> Intussusception is a mechanism by which tumour vascular remodelling and expansion leading to investment into pre-existing blood vessels and has been shown to occur in bowel and pulmonary cancer metastasis to the brain in mouse models.<sup>339</sup>

All gliomas are vasogenic, however glioblastomas are the most vascular and demonstrate the most malignant potential.<sup>340</sup> The formation of a new vessels permits growth, proliferation and eventually spread to distant sites.<sup>332</sup> Gliomas have been shown to rely on angiogenesis<sup>340</sup>, where quantification studies have demonstrated a positive correlation between tumour grade and vascularity.<sup>341</sup>

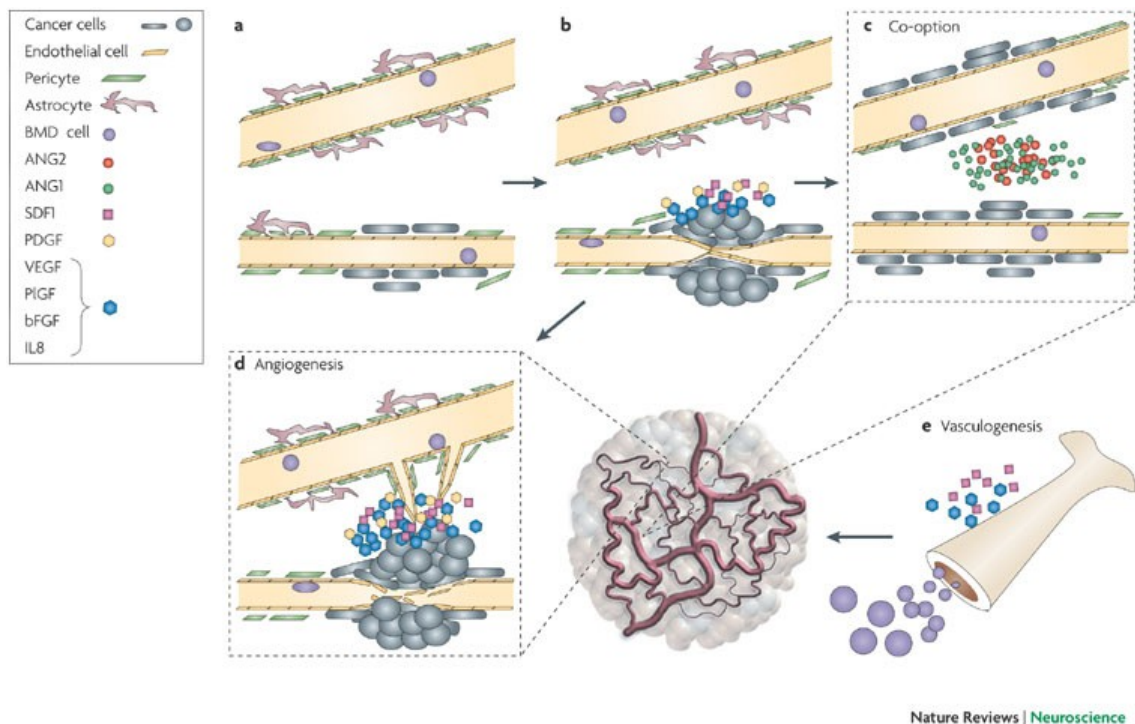


**Figure 29:** Diagram demonstrating mechanisms of tumoural blood vessel formation. Brain blood vessels are normally formed of astrocytes, pericytes and endothelial cells (a). Peritumoural spread and invasion of normal blood vessels occurs as the cancer cells proliferate (b). Co-option of normal brain vessels supports the invading tumour cells by providing nutrients and oxygenation (c). As the tumour grows and invades the normal vasculature, hypoxia and cell death leads to secretion of growth factors including vascular endothelial growth factor (VEGF), basic fibroblast growth factor (bFGF), interleukin 8 (IL8) and stromal-cell-derived factor 1 (SDF1), leading to angiogenesis (d). Furthermore, platelet-

derived growth factor receptor (PDGF) can upregulate VEGF, causing autocrine effects on the perivascular and endothelial cells. These factors can lead to vasculogenesis (e). Key: angiopoietin 1 (ANG1), angiopoietin 2 (ANG2). Diagram taken from Jain et al.<sup>332</sup>

Relative cerebral blood volume (rCBV) is a measure that has been associated with both tumour vascularity<sup>342-345</sup> and VEGF expression.<sup>346</sup> It is measured by dynamic-susceptibility weighted contrast-enhanced perfusion MR imaging (DSC), which measures changes in the  $T_2^*$  signal-intensity caused by differences in magnetic susceptibility induced by passage of paramagnetic contrast.<sup>347</sup> Recently, rCBV has been histologically correlated with MIB-1, a tumour proliferation index, in an image-guided biopsy study (Fig. 30).<sup>348</sup> Increased rCBV was also detected in peritumoural areas beyond regions of enhancement in four out of six patients, indicating that rCBV is sensitive to the invading tumour margin.

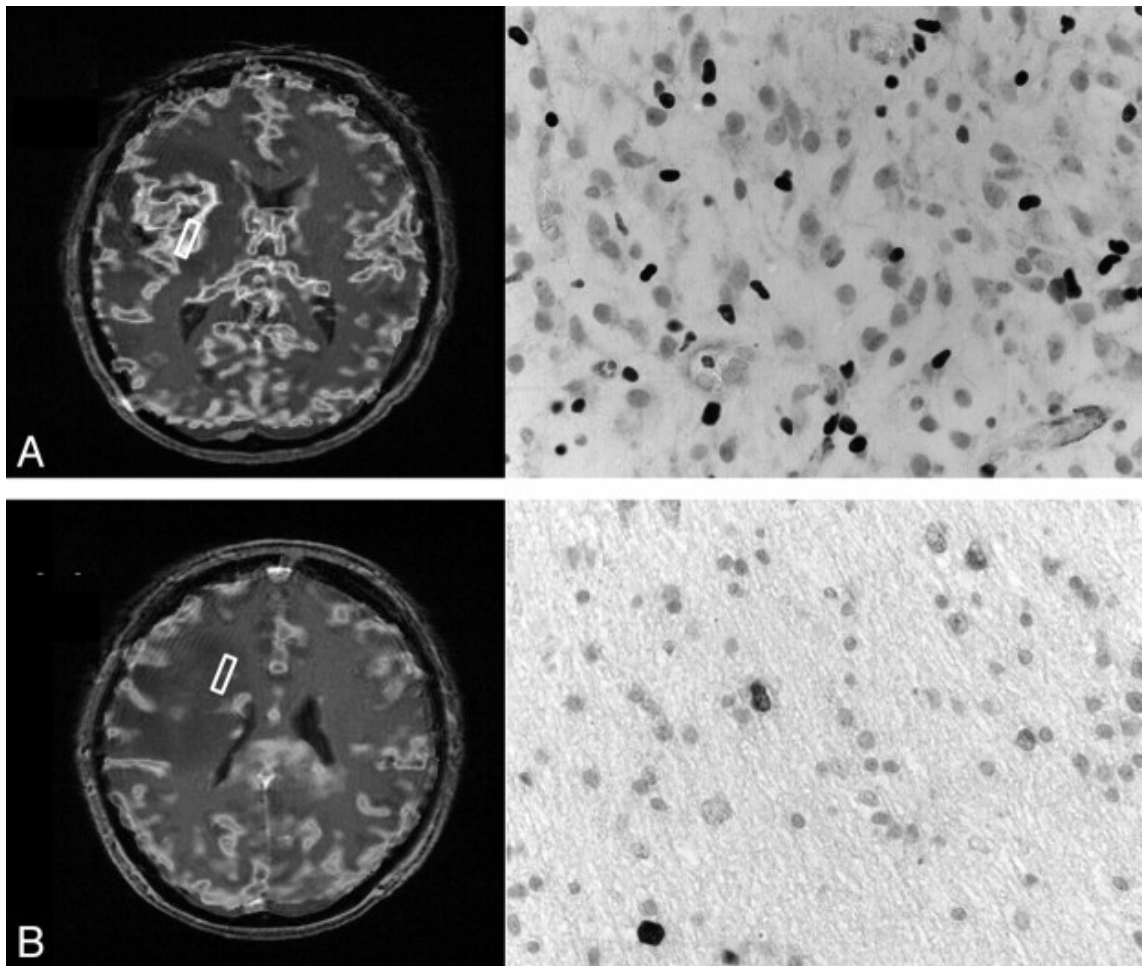


**Figure 30:** Spoiled gradient-recalled (SPGR) images showing region of interest (white rectangle) where biopsy was taken and correlated MIB-1 immunohistochemistry (x40 magnification). A central tumoural biopsy was taken, where mean rCBV was 8.1 and MIB-1 labelling index was 33% (A). In the same patient, a second biopsy was taken 2cm from the contrast-enhanced area, mean rCBV was 2.3 and MIB-1 index 3.5% (B). Image taken from Price et al.<sup>348</sup>

Diffusion weighted imaging (DWI) is a widely used imaging technique that is sensitive to molecular movements of water, where it is assumed that water diffuses equally in all directions. Brain water movement is, however, heterogeneous due to the variations in microstructural environments,<sup>349</sup> where preferential diffusion along white matter tracts occurs, known as anisotropy. Brain water diffusion can be modelled as an ellipse, which can be represented by a

tensor in mathematics. Eigen values and orthogonal eigenvectors can be used to determine the magnitude and principle axis of diffusion. This is the basis for diffusion tensor imaging (DTI), where isotropy and anisotropy can be estimated. It has been shown that by decomposing the p and q components of DTI, diffusion tissue signatures can be calculated, which has been shown to correlate with peritumoural white matter tract disruption.<sup>350</sup> Glial tumours are associated with a loss of anisotropy due vasogenic oedema, increased cellularity and destruction of white matter, causing a reduction in anisotropy (q) and rise in isotropy (p). It has been shown that peritumoural areas with increased p but reduced q accurately correlate with the invading tumour margin identified on histology (Fig. 31).<sup>351</sup>

Previous studies have been unable to utilise conventional imaging to accurately identify tumour margins.<sup>352-356</sup> Advanced MRI techniques have demonstrated potential in grading brain tumours and assessing the proliferating invasive margin. Previous attempts to take advantage of conventional DTI as a means of detecting occult tumour spread have revealed inconsistent results. Some authors have demonstrated increased fractional anisotropy in the peritumoural area beyond enhancing zones,<sup>357-359</sup> while others show increases in diffusivity only.<sup>360,361</sup>

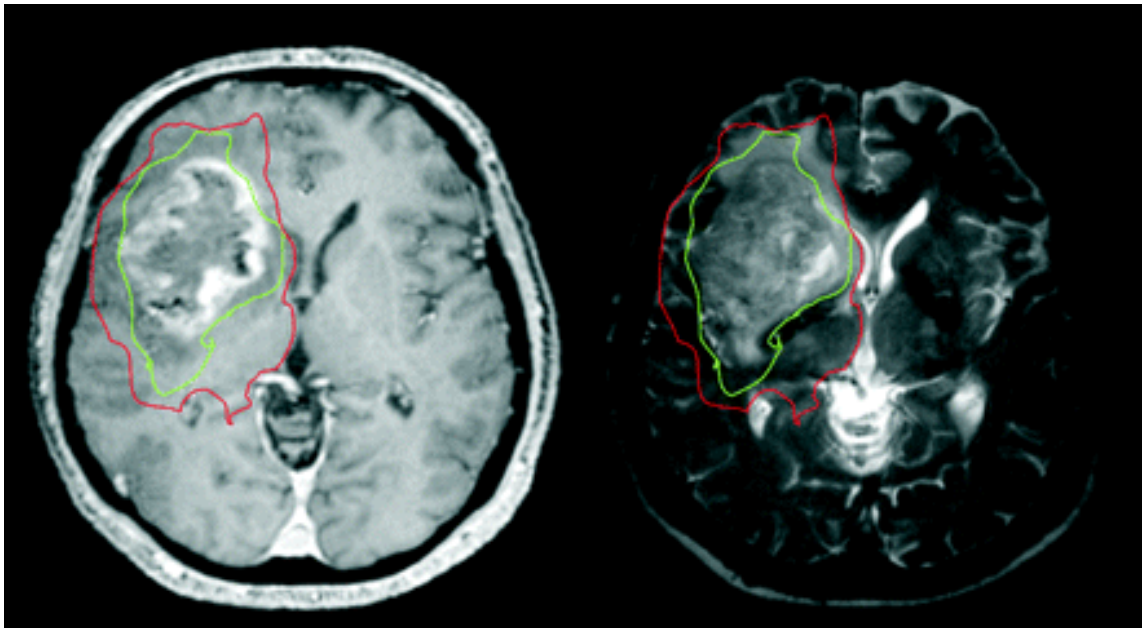


**Figure 31:** Gadolinium contrast enhanced T1 weighted (left) and T2-weighted (right) MRI showing a glioma demarcated with a region with reduced anisotropy (q, green) and a larger surrounding area with normal anisotropy but increased isotropy (p, red) that highlights the infiltrating region of the tumour margin that was confirmed by immunohistochemical analysis of biopsy samples. Image taken from Price et al.<sup>326</sup>

Other methods of analysing DTI data have made discrimination of the invading tumour margin promising, which are sensitive to peritumoural vasogenic oedema, avoiding false positive identification of infiltrating tumour. Lu et al. demonstrated that diffusion tensor magnetic resonance metrics permits differentiation between tumour infiltrating oedema and purely vasogenic oedema in forty patients (n = 40), resulting in their suggestion of a tumour infiltration index.<sup>360</sup> Zhou et al. utilised the regional fibre coherence index to more accurately identify regions of tumour infiltration compared to conventional methods in a small number of patients (n = 4).<sup>362</sup> Morita et al. demonstrated that lambda chart analysis discriminates between infiltrated oedema in high-grade gliomas and pure

vasogenic oedema in low-grade tumours, metastasis and meningiomas (n = 43).<sup>363</sup> The aforementioned studies were not confirmed with histology. However, these results support the existence of a mechanism that differentiates diffusivity in peritumoural vasogenic oedema and infiltrated oedema/region such as the breakdown of the extracellular matrix by metalloproteinase present in high-grade gliomas but not in low grade tumours.<sup>364</sup>

Price et al. suggest decomposing the diffusion tensor into separate p and q components, which has shown to be effective in identifying the infiltrating tumour margin<sup>351</sup> (n = 20) without falsely identifying purely vasogenic regions of oedema. This DTI method has also shown to be useful in predicting patterns of tumour recurrence (n = 26), strengthening the potential for clinical application.<sup>365</sup> This method has been applied in combination with DSC in the present study.

A recently revived theory of how gliomas behave is stem cell theory.<sup>366</sup> In short, self-renewing cancer stem cells (CSCs) may exist as a subpopulation of tumour tissue that are responsible for ongoing proliferation of cancer cells. Although these cancer cells have been shown to be reliant on angiogenesis, an independent phenotype formed through exposure to hypoxia causes the formation of stem cells that rely on anaerobic means of respiration and are able to survive without a vascular supply.<sup>367</sup> This has been shown with xenotransplantation studies.<sup>368</sup> Bevacizumab, a monoclonal antibody against VEGF, has been shown to reduce angiogenesis. However, this has been shown to increase tumour infiltration and proliferation in the mouse model in first generation harvested GBM tissue.<sup>369</sup> Therefore it could be the case that rCBV only detects a subpopulation of angiogenesis-dependent-tumour cells where



such CSCs can be interspersed or even have infiltrated beyond the identified margin. Thus, rCBV may be useful as a marker of vascularity of the invasive margin and provide some information about what type of cancer stem cells are likely to be present. This has both therapeutic and prognostic implications.

In conclusion rCBV values correlate positively with the invasive margin identified by splitting the p and q components of DTI. Larger prospective studies would be required to validate this method into clinical practice. These findings are in keeping with current thinking in the way that malignant glioma cells proliferate and rely on an adequate blood supply. Current models of cancer stem cell forming an angiogenesis-independent phenotype, may indicate a further use of rCBV.

### ***Methodological overview***

#### *Patients*

Thirty patients with high-grade cerebral gliomas (Table 7) were imaged pre-operatively with multiple MRI sequences as part of a larger study between the 30<sup>th</sup> June 2010 and 2<sup>nd</sup> December 2011 at the Wolfson Brain Imaging Centre. Twenty patients were male (66%) and mean age was 58 years old (range 31-69). Twenty-eight patients (93.00%) had WHO grade IV gliomas (28 GBM, 5 with oligodendroglial differentiation and 1 with giant cell GBM) and two patients (6.67%) had WHO grade III gliomas (both anaplastic oligoastrocytomas). Table 1 lists these details for each patient. All studies were approved by the Cambridge Local Research Ethics Committee, and written, informed consent was obtained from all patients.

*Image Studies*

Neuroimaging sequencing

As described in the published work.<sup>327</sup>

				<b>WHO</b>
<b>Patient</b>	<b>Age</b>	<b>Sex</b>	<b>Histology</b>	<b>grade</b>
1	43	M	AO	III
2	55	M	AO	IV
3	60	M	GBM	IV
4	61	M	GBM	IV
5	43	F	GBM	IV
6	62	F	GBM	IV
7	52	F	GBM	IV
8	61	M	GBM	IV
9	67	F	GBM	IV
10	64	M	GBM	IV
11	66	F	GBM	IV
12	62	M	GBM	IV
13	52	M	GBM	IV
14	61	M	GBM	IV
15	67	M	GBM	IV
16	48	M	GBM	IV
17	66	F	GBM	IV
18	69	M	GBM	IV
19	59	F	GBM	IV
20	57	M	GBM	IV

21	31	F	GBM	IV
22	64	M	GBM	IV
23	68	M	GBM	IV
24	54	M	GBM	IV
25	61	M	GBM + O	IV
26	67	M	GBM + O	IV
27	63	M	GBM + O	IV
28	64	F	GBM + O	IV
29	64	M	GBM + O	IV
30	39	F	GC GBM	IV

---

**Table 7.** Patient demographics. AO – Anaplastic oligoastrocytoma, GBM – glioblastoma multiforme, O – Oligodendroglial differentiation, GC – Giant Cell.

#### Co-registration of DTI and DSC image datasets

I transferred DTI and DSC datasets to a remote Linux based workstation and co-registered against respective transverse T<sub>2</sub> turbo spin echo images using a linear image registration tool (FLIRT, developed by Mark Jenkinson, FMRIB Centre, UK).<sup>370</sup> Co-registration was visually checked by drawing an outline of the whole brain and ventricles and superimposed on the target image to ensure accuracy.

#### Image processing

I then processed rCBV mapping using NordiciCE (NordicNeuroLab, Bergen, Norway) with the Perfusion/DCE Module. T<sub>2</sub>\* DSC images were processed

automatically with this software to produce rCBV maps. For each voxel, the eigenvalues ( $\lambda_1$ ,  $\lambda_2$ ,  $\lambda_3$ ) were computed using FDT diffusion toolbox in FSL version 4.1.9 (developed by Mark Jenkinson, FMRIB Centre, UK). These were calculated on a voxel-by-voxel basis to produce maps of both the p and q components according to previously described methods.<sup>326,371</sup> A 3D affine co-registration to T<sub>2</sub> using the FLIRT tool box of FSL (developed by Mark Jenkinson, FMRIB Centre, UK) was performed of DTI, DSCI and T1C datasets.

I went on to draw regions of interest around the area of obviously reduced anisotropy on the q map, and this was superimposed on the p map where another region was drawn around the isotropic abnormality. Regions where p exceeded q were drawn and then superimposed on co-registered rCBV maps. As rCBV values are not absolute, an elliptical region was drawn over the centrum semiovale in the contralateral white matter to normalize rCBV values. Adjacent areas to the region of tumour invasion were drawn on co-registered T<sub>1</sub> with contrast images by superimposing the p and q regions of abnormality (Fig. 32). Values for rCBV were calculated using ImageJ (Version 1.46r, developed by Wayne Rasband, National Institute of Health, Bethesda, Maryland, USA, <http://rsb.info.nih.gov/ij/>).

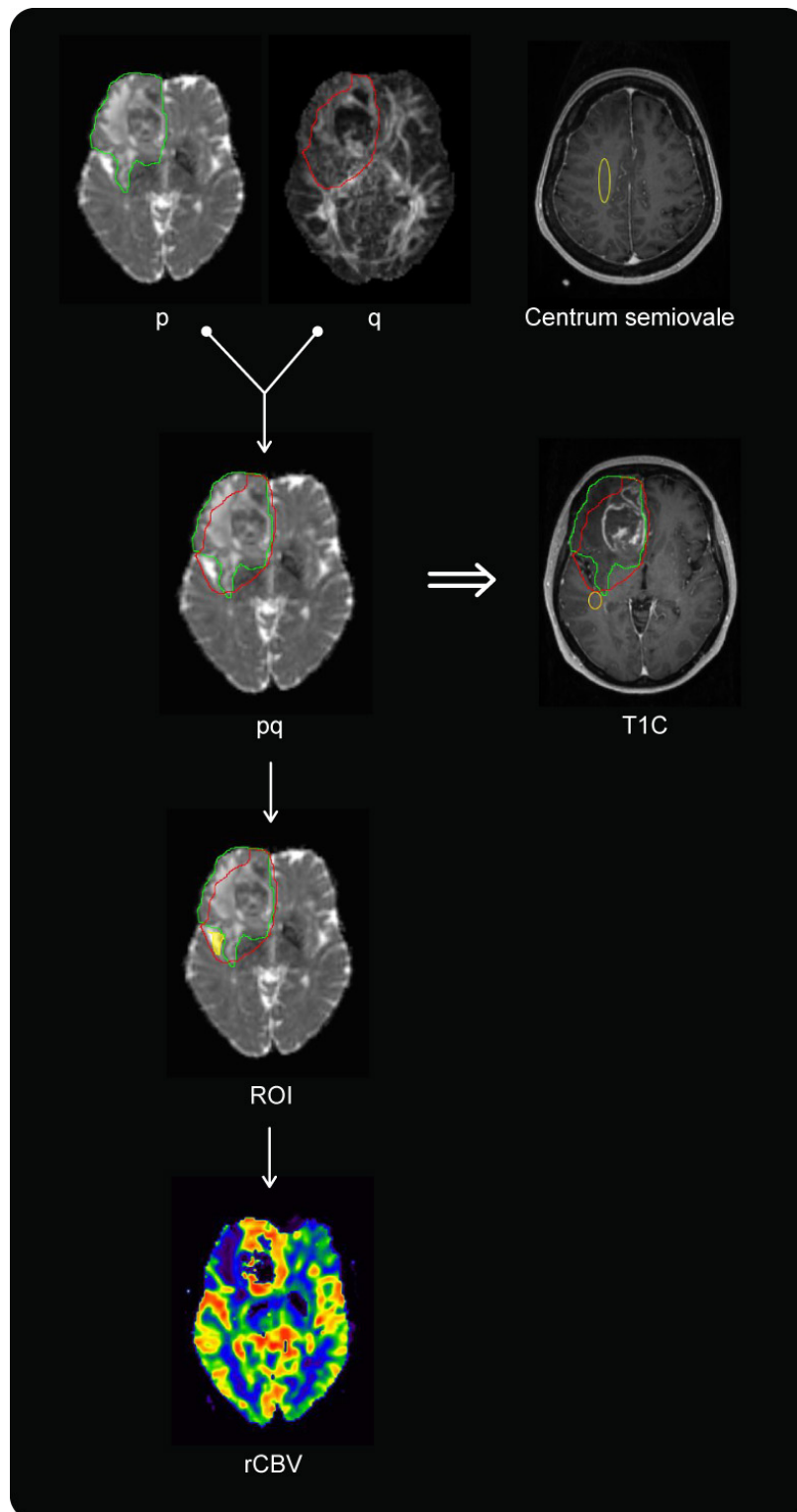


**Figure 32:** Schematic of the method used to obtain regions of interest (ROI). The p, q, T<sub>1</sub> with contrast (T1C), and relative cerebral blood volume map (rCBV) were all co-registered to a T<sub>2</sub> turbo spin image. The p (anisotropic) and q (isotropic) areas of abnormality were drawn (in green and red respectively), along with an elliptical area selected from the contralateral white matter in the centrum

semiovale (in yellow) for standardisation of relative cerebral blood volume (rCBV) values. The q area of abnormality was then transposed on to the p map and a ROI (shaded in yellow) selected defined by areas that extended beyond the p or q areas, this was defined as the invasive margin. Non-invasive regions adjacent to the ROI were selected on the T1C image with the p and q areas superimposed, as white matter tracts were better visualised on T1C. The invasive ROI, adjacent non-invasive region and ellipse on the centrum semiovale were then superimposed on the rCBV, at correlated image slices, and measure using Image J (Version 1.46r, developed by Wayne Rasband, National Institute of Health, Bethesda, Maryland, USA, <http://rsb.info.nih.gov/ij/>).

### Statistical Analysis

Statistical analysis was completed using the Statistical Package for the Social Sciences for Windows (release 19.0.0, IBM, 2012, Chicago, Illinois). rCBV values were tested for normality using the Kolmogorov-Smirnov and Shapiro Wilk test. The sample size was sufficient for a Students Paired Samples t-test ( $n = 30$ ) irrespective of the presence of a normal distribution.

### Results

The mean ( $\pm$  standard deviation) rCBV for the identified invasive and non-invasive regions were  $1.67 \pm 0.87$  and  $1.13 \pm 0.57$  respectively. The mean rCBV difference  $\pm$  SD (percentage difference, range) between the invasive and non-invasive regions was  $0.36 \pm 0.76$  (42.60%, -76.7 to 222.5) where this achieved statistical significance ( $p = .014$ ).

## ***Current and emerging imaging modalities of the invasive margin of glioblastoma***

DTI in recent times has been advanced by Rahmat et al. by utilising automatic segmentation methods to define p and q such that potentially may avoid the interobserver errors borne through manual segmentation.<sup>372</sup> In the future, this may make surgical and radiotherapy treatment planning more accurate and reliable.<sup>373</sup> It is also emerging that in post-operative MRI imaging of glioblastomas previously resected, that p map is a better candidate than the q map for target volume delineation.<sup>374</sup> The recent emergence of immune checkpoint therapies has resulted in significant interest in using these novel therapies for solid tumours, as well as biomarkers in MRI imaging.<sup>375</sup> For example, ferumoxytyl is a superparamagnetic iron oxide that is being investigated as an alternative contrast agent that may be beneficial to determine treatment efficacy.<sup>376</sup> Artificial intelligence (AI) has become of great interest in recent times for medical applications, particularly in the field of medical imaging. Radiomics alongside AI may hold promise in identifying novel biomarkers or means of delineating the invasive margin of brain tumours through the possible creation of “super-voxels” that integrate multimodal MRI imaging.<sup>377</sup> As such, there are a number of novel imaging techniques that could enable more accurate localisation and treatment of the invasive tumour margin and potentially provide sufficient resolution to assess treatment response using automated algorithms and AI.

## ***Nature of work***

This piece of work involved working under the supervision of Mr Stephen Price, Consultant Neurosurgeon, Addenbrookes Hospital, Cambridge. This was a clinically orientated research project that focused on improving detection of the

invasive margin of GBM with novel imaging techniques. I collected and analysed data from patients' MRI images, having been taught the relevant analytic techniques. I also reviewed the literature pertaining to the role of emerging neuro-imaging techniques in mapping out the invasive margin of brain tumours. I gained knowledge in clinical imaging techniques and expanded my understanding of the cell biology of the invasive margin of GBM. Specifically, I co-registered the images for the patients included in my study, completed all imaging processing, including ROI selection) and statistical analysis of all data. The results of my study were promising, and Mr Price and his colleagues decided to add more eligible patients to create a larger study. The culmination of my work and Mr Price's group resulted in the publication of a larger study involving 50 patients, including the 30 patients I had originally analysed. The validity of the ROI selection was strengthened by using a random subsample of 15 patients and having two trained independent readers draw ROIs, which were compared to the ROIs used for the final analysis.

### ***Significance of work***

The original article on delineating the invasive margin of GBM with MRI sequences was published in the Journal of Magnetic Resonance Imaging (Impact Factor 3.95) and cited 15 times since publication. This work was presented at the British Neuro-Oncology Society Meeting as a poster presentation with the conference abstract published in the journal Neuro-Oncology (Impact Factor 10.24). This work demonstrated that modern MRI sequences can be used to enhance detection of the invasive margin of GBM beyond conventional techniques.



### ***Critical appraisal of published work***

This is a study providing early evidence that DTI can identify invasive regions of glioblastoma using multi-modal MRI sequences. Whilst the sample size is significant with 50 patients included, there is no histological correlation with identified invasive region. To definitively define the invasive margin of glioblastoma would require corroboration with tissue analysis, however it would be understandably challenging to justify this since “normal” tissue beyond the identified invasive margin would need to be analysed to confirm the present or lack of tumour cells. Further, clinical outcomes have yet to be clarified by using the DTI defined invasive margin in surgery or radiotherapy. Therefore, while the imaging outcomes of this study are significant, the applicability to clinical practice was limited at the time of publication. It should also be noted that 3T resolution was utilised in this study and higher resolutions may provide further information about the invasive margin.

In summary, this study presents a novel means to define the invasive tumour margin using DTI to define this. Further studies correlating with clinical outcomes would be needed to clarify whether this technique can be beneficial in clinical practice.

## **Chapter 6: Electric fields in neural stem cell migration**

### ***Introduction***

Throughout life, neurogenesis occurs in the mammalian brain in the subgranular zone of the dentate gyrus and the subventricular zone (SVZ). Neural precursor cells reside in these regions, which differentiate into neuroblasts in the SVZ and migrate long distances along the rostral migratory stream to reach the olfactory bulb throughout life. The directed migration of neuroblasts has been shown to be directed by a number of guidance cues, including electric fields. In this chapter I summarise key processes in neurogenesis and guidance cues of neuroblasts, including the role of electric fields that the published paper this chapter refers to.

The aims of this chapter are as follows:

- Provide an overview of neurogenesis and the guidance cues known to be involved in neural stem cell migration
- Summarise the current and emerging therapeutic approaches manipulating neural stem cell migration
- Summarise the methodology, nature, and significance of this work, and provide a critical appraisal of the published paper pertaining to this chapter

### ***Literature review***

The earliest events leading to development of the central nervous system (CNS) are orchestrated by a small number of neural stem cells (NSCs) that line the neural tube<sup>378</sup>. The initial stages of this process involve neurogenesis, whereby the primary progenitor NSCs, radial glial cells (RGCs), divide symmetrically to form more NSCs and asymmetrically to form intermediate progenitors and a number of differentiated cells.<sup>379</sup> The 3 primary cells of the CNS arise from

successive waves of neurogenesis, first forming neurones, followed by astrocytes and later oligodendrocytes.<sup>380,381</sup> RGCs are derived from the neuro-epithelial cells and function to guide migration of its neural progeny.<sup>382</sup> At birth, the process of neurogenesis was previously thought to completely cease. However, the first description of neural multipotent progenitor cells in the adult human brain within the subventricular zone (SVZ) provided definitive evidence that this was not true.<sup>383</sup> Indeed, it is now accepted that neurogenesis continues throughout adult life, primarily in the forebrain SVZ (Fig. 33) and subgranular zone (SGZ) of the hippocampal dentate gyrus.<sup>384,385</sup> These specialised regions have been found to contain neural stem cell niches that contain glial fibrillary acid protein positive cells, or astrocytic NSCs.<sup>386-389</sup> Such NSCs or radial glia-like stem cells in the SGZ generate neurons throughout life and integrate into the circuitry of the dentate gyrus and contribute to functions such as learning, memory and executive functions.<sup>390,391</sup> In adult rodents, neurogenesis in the SVZ has been shown to be important for olfactory function, whereby NSCs migrate along the rostral migratory stream (RMS) before differentiating into granule or periglomerular cells prior to integrating into the olfactory bulb (OB).<sup>392</sup> Diseases of the CNS have been thought to dysregulate neurogenesis, for example, animal models of epilepsy increase neurogenesis but form neurones with aberrant morphologies.<sup>393,394</sup> Other pathologies that are known to affect neurogenesis include stroke, neurodegenerative diseases such as Alzheimers and Parkinsons, and demyelinating disease.<sup>394</sup> There is now emerging evidence that the cell origin for human glioblastomas may be derived from NSCs in the SVZ, where it has been found that in patients with IDH1 wild-type glioblastoma, tissues from their tumour free SVZ harboured classic oncogenic mutations of PTEN and p53 for example.<sup>395</sup>

An important example of NSC migration over long distances are neuroblasts derived from the SVZ traversing the RMS.<sup>384,385,396-398</sup> In humans, neuroblasts in the RMS have been shown to course from the SVZ adjacent to the lateral ventricle, turning caudal and ventral under the caudate nucleus (CN), followed by a rostral turn to enter the anterior olfactory cortex, which gives rise to the olfactory tract that leads to the OB (Fig. 34).<sup>398</sup> Dysfunction of such neural cell migration are associated with diseases including epilepsy, lissencephaly (smooth brain) and learning difficulties.<sup>399,400</sup> In rodent models of stroke, neuroblasts can migrate to sites of injured striatum and differentiate into functional neurones, but this is insufficient for neuro-regeneration.<sup>401,402</sup> The mechanisms of NSC migration are multifaceted and include cytoskeletal changes, diffusible factors as guidance cues, and migration along scaffolds such as neuron chains and astrocytic processes.<sup>403</sup>

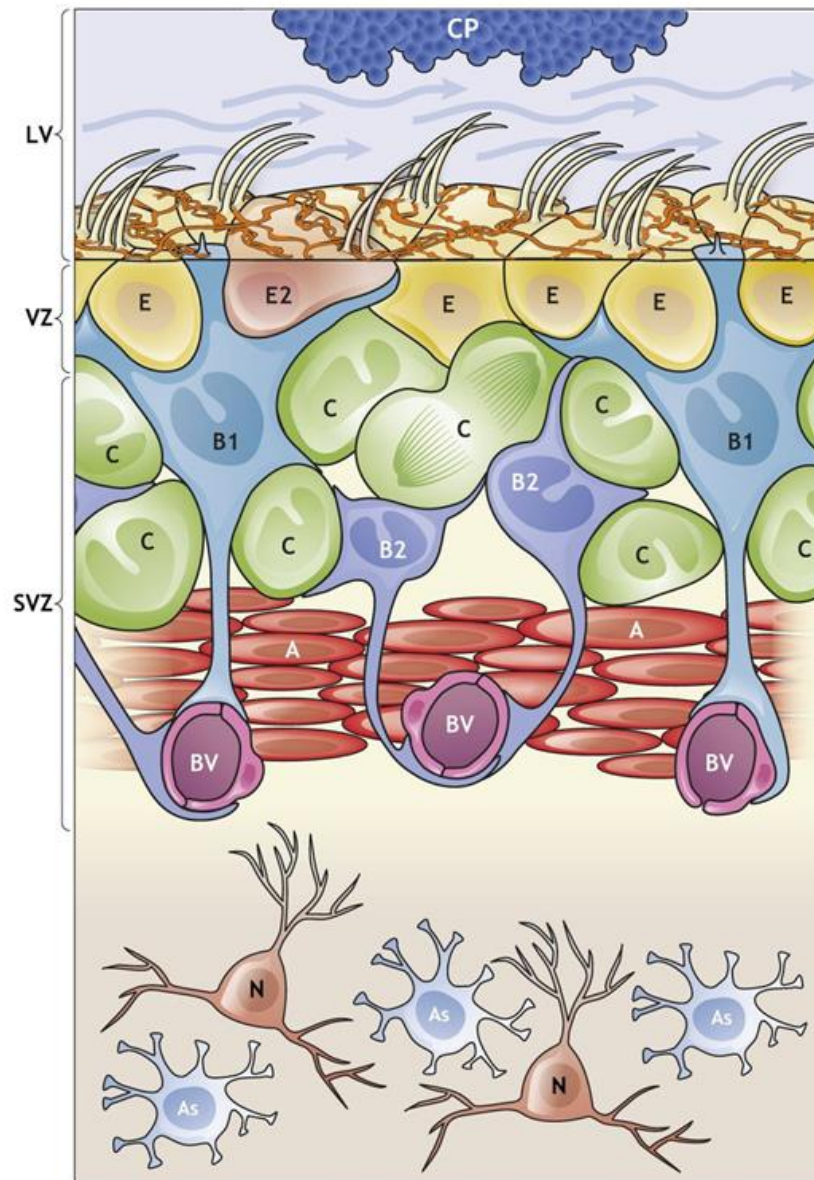


**Figure 33:** Schematic of the subventricular zone (SVZ) organisation and cellular composition in the walls of the lateral ventricles (LV). B1 cells (light blue) have astroglial properties and function as NSCs, giving rise to B2 cells (dark blue) that share astroglial characteristics of B1 cells and make blood vessel (BV) contacts. In addition, B1 cells give rise to C cells (green), which are transiently amplifying cells that generate early neurones (A cells, red). B1 cells are in contact with CSF via apical contacts that have primary cilium. The choroid plexus (CP, blue) secretes factors necessary for B1 cell function. B1 apical endings are surrounded by ependymal cells (E/E2), which are multi-ciliated. Supraependymal axons

(orange) traverse the ventricular wall surface, making contacts with B1 and E cells. B1 cells make contacts with C, A, and B2 cells, as well as BV. Mature neurons, N (orange), and astrocytes, As (pale blue), are found in the striatum. Diagram taken from Obernier and Alvarez-Buylla.<sup>404</sup>

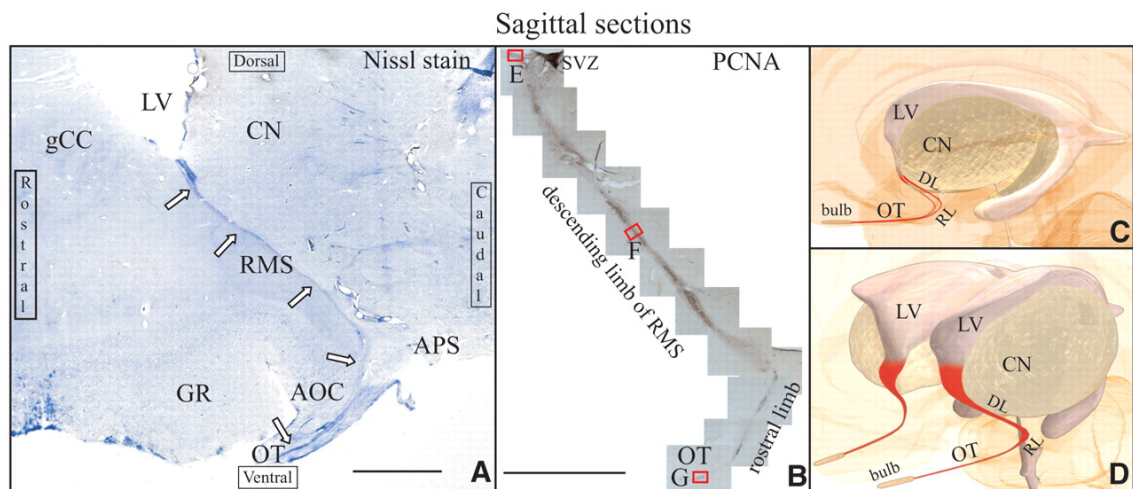


**Figure 34:** Neuroblasts traverse the human rostral migratory stream (RMS) by coursing caudally from the SVZ to olfactory cortex. A, Nissl staining of a human sagittal section of forebrain reveal staining of the RMS tract behind the gyrus rectus (GR) and in front of the caudal nucleus (CN) and anterior perforate substance (APS). Lateral ventricle (LV), genu of corpus callosum (gCC) and olfactory tract (OT) are shown. B, Proliferating cell nuclear antigen (PCNA) staining for proliferating cells is shown in both the descending and rostral limbs of the RMS. C, Schematic diagram showing lateral view of RMS (red tract). D, Frontal-oblique schematic view of wide dorsal descending limb (DL) of RMS descending and narrowing into rostral limb (RL) (red tract). Figure adapted from Curtis et al.<sup>398</sup>

Neuroblasts migrate in a saltatory pattern that involves three stages including leading-process extension, swelling formation and centrosomal migration, and

somal translocation.<sup>405</sup> This permits maintenance of a consistently longer leading process and shorter trailing process that is characteristic of the bipolar morphology associated with migrating neuroblasts. Neuroblasts accumulate filamentous (F)-actin at the leading tips, which is regulated by the Rho-family of small GTPases and downstream F-actin modulators.<sup>406</sup> The extension of this leading tip is also dependent on microtubules, where chemical or genetic disruption of microtubular function leads to shorter neuroblast extending processes.<sup>405,407</sup> Cytosolic swelling in the proximal part of the leading process is activated by RhoA, which is followed by centrosomal migration into the swelling, requiring the Rho effector mammalian homologue of Diaphanous (mDia).<sup>408</sup> Reorientation of the neuroblast is initiated by Slit, which causes the formation of a new leading process and centrosomal reorientation.<sup>409</sup> Finally, somal translocation is regulated by actomyosin dynamics regulated by RhoA signalling, whereby Myosin II activity and F-actin accumulates at the proximal leading process and rear of the cell.<sup>405,406</sup>

The role of neuroblast chemoattractants released by the OB, such as Netrin1, Prokinectin-2 and glial cell line-derived neurotrophic factor, are unclear because surgical removal of the OB does not affect directed migration and Netrin-1 is downregulated in the developing neonatal brain.<sup>410,411</sup> Neuroblasts form migratory chains with each other, a process that relies on the expression of cell-adhesion molecules including N-cadherin and polysialylated neural cell-adhesion molecule.<sup>412,413</sup> The adhesion molecules  $1\beta$  and  $8\beta$  integrins are expressed by neuroblasts and act as adhesion molecules that chain migration relies upon, as previously shown in vitro and in vivo.<sup>414,415</sup> However, in stroke models, neuroblasts have been found to migrate to ischaemic striatum as individual cells

but with weaker directionality in comparison to neuroblast chains.<sup>416</sup> In order to traverse dense meshworks of neural and glial processes, neuroblasts rely on astrocytic tunnels in the RMS that are maintained by Slit-Robo signalling.<sup>417</sup> This process is accompanied by remodelling of the extracellular matrix (ECM) by matrix metalloproteinases (MMP), including MMP3 and MMP9, which are expressed by migrating neuroblasts.<sup>418</sup>

Neuroblasts undergo cytoskeletal remodelling in order to facilitate cell migration through extracellular signals that initiate intracellular signalling pathways.<sup>419</sup> F-actin is formed of polymers in a double helix of actin subunits and are polarised with their plus-end orientated toward the leading end of the cell.<sup>420</sup> The outer layer of the actin network within cells is linked to the cell membrane in a reverse back-to-front gradient, such that the lowest density is found at the front of cells, which allows membrane protrusion due to low membrane-actin attachment.<sup>421</sup> The movement of the actin network relies on actin based motor proteins, such as myosin II, which forms a further network of actomyosin.<sup>422</sup> Actomyosin fibres are anchored to ECM by focal adhesions that produce contractile forces.<sup>423</sup> Myosin II is predominantly controlled by myosin light chain (MLC) phosphorylation, which is mediated by MLC kinase and Rho-kinase. Actomyosin contraction at the rear of the cell creates the driving force necessary to project the nucleus towards the leading process and has a role in detaching cells from extracellular adhesions and retraction of the trailing process.<sup>405,422</sup> Migrating neuroblasts have been shown to accumulate Shootin1B at the leading process of growth cones, which couples F-actin retrograde flow and cell adhesions as a clutch molecule, which generates the driving forces necessary for migration.<sup>424</sup>



Microtubules are a further cytoskeletal component that are composed of hollow filaments made up of  $\alpha$ -tubulin and  $\beta$ -tubulin heterodimers.<sup>425</sup> Microtubules are also polarised with a plus end with exposed  $\beta$ -tubulin and minus end with exposed  $\alpha$ -tubulin. Microtubule associated proteins (MAPS) and the motor proteins kinesin and dynein mediate the functions of microtubules. The interphase centrosome protein AKNA has been shown to have a significant role in centrosomal microtubule organisation in the SVZ and migration of neuroblasts.<sup>426</sup> The polarity of microtubules permits directional movement of molecular motors and cargos needed for cell migration processes.<sup>425</sup> Microtubules are able to disassemble focal adhesions through guanine nucleotide exchange factors to modify Rho-like GTPase Rac to permit cell migration.<sup>427</sup> During cell migration, the mediator of store-operated  $\text{Ca}^{2+}$  influx of endoplasmic reticulum STIM1, is transported to the front of cells via the plus ends of microtubules, to further reduce  $\text{Ca}^{2+}$  at the front of the cells that is important in the phospholipase C- $\text{Ca}^{2+}$ -diacylglycerol-STIM1 signalling system that is important in directed cell migration.<sup>428</sup> Further, microtubules are able to carry mitochondria to the front of the cell via interactions between kinesin and mitochondrial Rho-GTPases1 (MIRO1) to meet the energy demands required for cell migration.<sup>429</sup> Another component of the cytoskeleton are intermediate filaments, which include proteins grouped into subsets such as type III, including vimentin, type V, including the laminin family, and type VI, including nestin.<sup>430</sup> The expression profile of intermediate filaments in neuroblasts is incompletely characterised and therefore the roles of intermediate filaments in neuroblast cell migration have yet to be established.

Neuroblast migration is also influenced by growth factors and neurotransmitters, such as vascular endothelial growth factor (VEGF), which is known to promote

neuroblast migration along the RMS.<sup>431</sup> Brain derived neurotrophic factor (BDNF) is secreted by endothelium of blood vessels within the RMS, which mediates neuroblast migration via the neurotrophin receptor p75NTR expressed on neuroblasts.<sup>432</sup> Inhibition of this pathway can be mediated by neuroblast secretion of GABA that induces Ca<sup>2+</sup> dependent insertion of high affinity tropomyosin receptor kinase B (TrkB) receptors into astrocyte plasma membranes, which causes trapping of BDNF. GABA secretion has also been shown to play a role in reducing neuroblast migration velocity by interfering with Ca<sup>2+</sup> signalling independently of depolarisation.<sup>433</sup> Further, glutamate signalling has been implicated in neuroblast survival during migration across the RMS, whereby functional NMDAR receptor expression is progressively acquired during migration and activated by RMS astrocytic glutamate release.<sup>434</sup> Neuroblasts appear to rely on this glutamate signalling for neurogenesis and survival during migration along the RMS.

Ca<sup>2+</sup> signalling is known to have numerous roles in cell biology, including cell migration. Neuroblasts have been shown to undergo spontaneous and depolarisation-evoked intracellular transients that are regulated by high voltage activated L-type Ca<sup>2+</sup> channels during migrations along the RMS.<sup>435</sup> However, it was found that blocking voltage gated Ca<sup>2+</sup> channels did not affect migration of neuroblasts. Serotonergic axons that innervate the RMS regulate neuroblast migration velocity and directionality through the ionotropic serotonin receptor 5HT3A mediated Ca<sup>2+</sup> influxes.<sup>436</sup> These authors found that in an 5HT3A knock mouse model, injection of a lentivirus expressing a calcium reporter GCaMP6s demonstrated spontaneous spikes of Ca<sup>2+</sup> that were six fold higher in amplitude in control neuroblasts compared to knockout neuroblasts, lasting 2-5 seconds.

Ca<sup>2+</sup> activity was abolished when Cre recombinase was injected with GCaMP6s, indicating that the 5HT3A receptor is a critical mediator of Ca<sup>2+</sup> influx in neuroblasts. Furthermore, migration directedness and velocity was reduced significantly alongside large calcium spike loss in knockout migrating neuroblasts, providing evidence of the importance of serotonergic innervation acting as Ca<sup>2+</sup> gate via 5HT3A receptors.

A further guidance cue for long distance neuroblast migration is the presence of endogenous cellular electric fields (EF), which have been shown to be mediated by the transient expression of P2Y1 receptors.<sup>437</sup> These authors confirmed the presence of a naturally occurring inward and outward electrical current between the SVZ and OB of  $-1.6 \pm 0.4 \mu\text{A}/\text{cm}^2$  and  $-1.5 \pm 0.6 \mu\text{A}/\text{cm}^2$ , respectively. Electrogenic pumps such as Na<sup>+</sup>/K<sup>+</sup>-ATPase were found to be apically distributed in the superficial layers of the OB in high concentrations in relation to the ependymal of the lateral ventricles, which would allow the OB to act as a voltage sink for currents traversing the RMS. Labelled neuroblasts were then transplanted into rodent brain slices and a voltage of 10 or 50mV/mm was applied. It was found that greater directed neuroblast migration occurred in the presence of an EF compared to when no EF was applied (**Fig. 35**). Finally, chemical inhibition or knockdown of P2Y1 resulted in significantly reduced directed neuroblast migration. Overall, these results suggested that a naturally occurring electrical gradient exists along the RMS, where the SVZ acts as an anode and the OB a cathode, and neuroblast directed migration partially relies upon this through P2Y1 expression.

P2Y1 is a receptor for ATP, which has roles as a neurotransmitter and neuromodulator in the central nervous system. ATP is known to increase  $\text{Ca}^{2+}$  levels and neuronal excitation in specific brain regions, such as the hypothalamus.<sup>438</sup> Electrical stimulation of neurones has been shown to cause release of ATP, thus subsequent release of  $\text{Ca}^{2+}$ .<sup>439</sup> Previous work on prostate cancer spheroids demonstrated that EF treatment causes a release of intracellular ATP via anion channels to the extracellular space, which then can activate purinergic receptors to elicit a transient  $\text{Ca}^{2+}$  response that regulates cell migration.<sup>440</sup> These authors reported that following stimulation with a single electrical field pulse of  $750 \text{ Vm}^{-1}$  for 60 second, it took 40 seconds before  $\text{Ca}^{2+}$  was detected. Such calcium waves arise from repeated activation of transient-generating  $\text{Ca}^{2+}$  channels, that cause spread throughout the cytoplasm, occurring in the order of seconds to minutes usually. Previously, it has been found that a natural electric field along the rostral migratory stream of approximately  $2\text{mV/mm}$  exists, where neuroblasts migrate approximately  $40\text{-}80\mu\text{m}$  over 5 hours without an exogenously applied electric field. It can therefore be inferred that  $\text{Ca}^{2+}$  transport with respect to neuroblast migration, occurs over at least seconds to minutes with relation to P2Y1 mediated directed migration. However,  $\text{Ca}^{2+}$  transport time has not specifically been reported in neuroblasts arising from the SVZ. Spontaneous  $\text{Ca}^{2+}$  transients have been detected in neuroblasts arising from the SVZ, which have been shown to have a mean frequency of 8.0 peaks/10 min with a mean duration of 12 seconds.<sup>441</sup> It has been found that larger  $\text{Ca}^{2+}$  transients occur at the front of cells, where  $\text{Ca}^{2+}$  microdomains have a role in both steering directed cell migration and mediated via stretch-activated cation channels (TRPM7).<sup>442-444</sup>  $\text{Ca}^{2+}$  transients also enable translocation of Rac1 to the plasma membrane, which is important in lamellipodia formation.<sup>445</sup> Other

functions of Ca<sup>2+</sup> in neuroblast migration include mobilisation of mitochondria to sites of high energy demand through MIRO1 uncoupling and kinesin.<sup>446</sup>

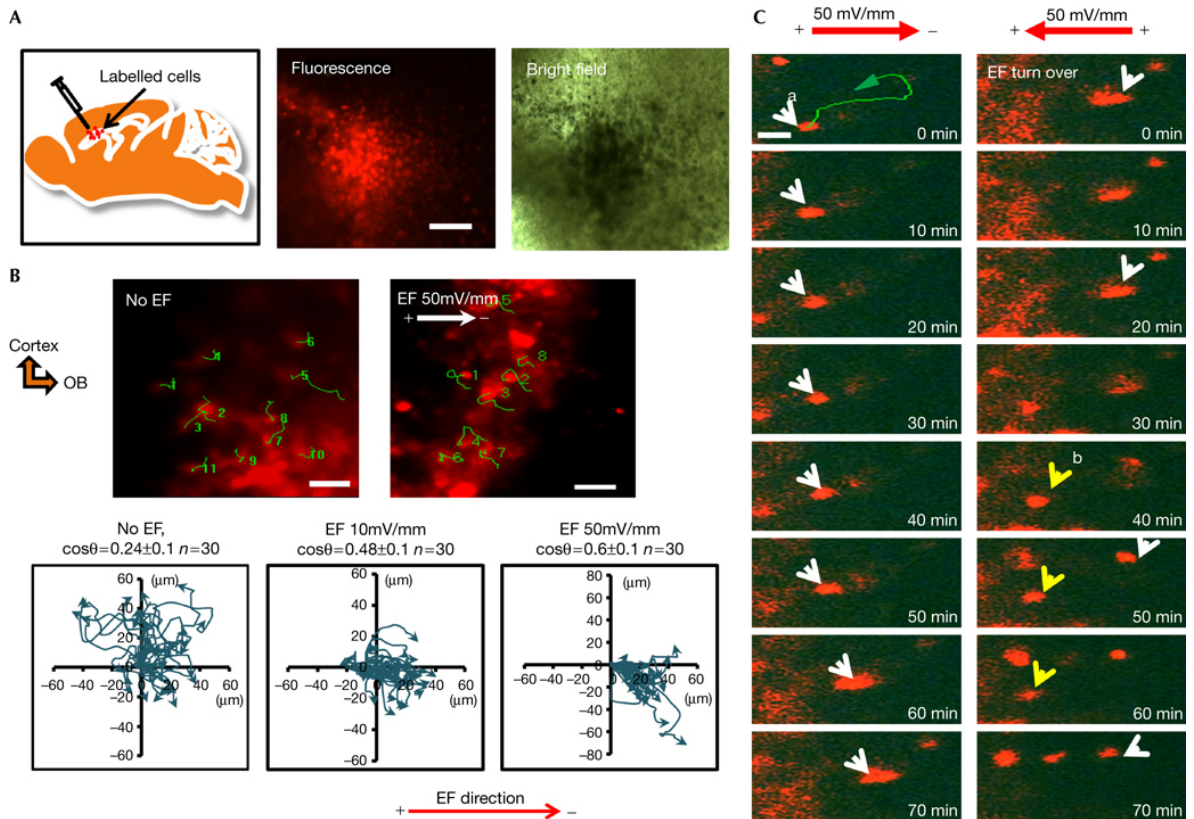


**Figure 35:** A, Neuroblasts stained with Dil, visualised by microscopy and transplanted into the SVZ of neonatal mice (p3-7). B, Neuroblasts directedness was 0.48 and 0.6 under 10 and 50mV/mm of EF, respectively, compared to 0.24 without EF (scale bar 40μm). Directedness (Cosθ) shown as mean±SEM. C, Neuroblasts migrate towards cathode (white arrow) correlating with the applied EF. Neuroblasts reverse their migration with the applied EF is reversed, with another neuroblast appearing in the focal plane over time (yellow arrow). Scale bar 15μm. EF – electric field, SVZ – subventricular zone, OB – olfactory bulb. Images taken from Cao et al.<sup>437</sup>

Following this study, we aimed to investigate the role of endogenous EF on chain migration of NSCs, choosing to use murine neuroblasts and the SH-SY5Y neuroblastoma cell line. We found that EF upregulates P2Y1 to mediate neuroblast chain migration through the expression of N-cadherin,  $\beta$ -catenin and PKC activation.<sup>447</sup> This provided further evidence of the role of naturally occurring EF along the RMS in neuroblast migration.

### ***Current and emerging therapeutic approaches manipulating neural stem cell migration***

Neurogenesis within the SVZ is known to be upregulated following injury to the brain, where neural stem cells can differentiate into neuroblasts and migrate outside of the RMS towards the region of injury.<sup>448-450</sup> This has led to significant interest in understanding the underlying mechanisms of neuroblast migration to identify potential treatment strategies to more efficiently guide them to the site of pathology. The major advantage of targeting neural stem cells in the SVZ is that they are available throughout life without necessarily needing to implant cells. Previously, although neuroblasts had demonstrated a tropism for sites of brain injury, it appeared insufficient to effectively recover neural function to baseline levels.<sup>451,452</sup> Previous, work on potential pharmacological approaches using neurotrophic factors and signalling peptides such as EGF, BDNF, and Ang1 have been shown to increase neurogenesis of neural precursor cells in the SVZ and induce greater migration to injury sites.<sup>453-455</sup> However, more recent pre-clinical data has provided convincing evidence that augmenting neuroblast migration to sites of injury can effectively result in robust functional recovery.<sup>456-460</sup> One promising example is overexpression of neuroblast Slit1 resulted in significantly improved migration to the site of brain injury through disruption of the actin

cytoskeleton in reactive astrocytes, allowing the neuroblasts to mature into striatal neurons and regenerate neural circuits.<sup>456</sup> Another approach that utilised a thin tract of laminin created by injection leading from the RMS to the site of excitotoxic damage within the prefrontal cortex, permitted neuroblasts to migrate and mature into neurones at the site of injury.<sup>459</sup>

An emerging approach that uses fabricated three-dimensional tissue-engineered “living scaffolds” that mimics the RMS glial tube and are implantable to create an artificial conduit between the SVZ and chosen brain region directed neuroblast migration.<sup>461</sup> The tissue engineered RMS in this study was derived from human gingiva mesenchymal stem cells to form astrocyte like cells that can facilitate neuroblast migration in vitro and in vivo. However, further work is needed to determine whether neuroblasts would be able to use this implantable conduit to then integrate, repair and regenerate damaged or lost neurones in sites of injury. The same authors highlight such challenges and others, including that such a technology would rely on the artificial RMS to replicate all functions of the RMS including directing neuronal migration, maturation and priming immature neurons for integration into existing neuronal circuits.<sup>462</sup> A significant draw back of this approach is that it is unlikely to be appropriate for use in the acute setting, such as stroke, when the brain microenvironment is likely to be damaging to the implant. Therefore, it would be best served as a longer-term neural replacement therapy that utilises the brains own source of neurogenesis in the SVZ rather than as a neuroprotective therapy. An alternative approach would be to utilise implantable electrodes that potentially divert neuroblast migration to regions of brain injury. Whilst these studies have yet to be undertaken, such an approach could potentially be less invasive than a “living scaffold”. The results of this study

on the role electric fields on directed neuroblast migration and my colleagues, suggest that this maybe a feasible strategy in the future.<sup>437,447</sup>

Previous clinical trials have attempted to harness the ability of neural stem cells (NSCs) to differentiate into neurones in order to replace those damaged by ischaemic stroke. Human malignant tumour derived NSCs and porcine derived NSCs transplants failed to proceed beyond Phase II and I trials, respectively.<sup>463,464</sup> Human foetal derived cell line CTX0E03 NSCs is currently undergoing Phase II Clinic trials in ischaemic stroke (PISCES clinical trials, ReNeuron, NCT03629275). Due to the COVID-19 Pandemic these trials have been temporarily suspended but are planned to resume in the future. Otherwise there have been no clinical studies investigating the manipulation of endogenous neuroblasts to repairs the injured brain. From the evidence presented in this chapter and the studies highlighted, it is clear that novel approaches may be on the horizon that could include implantable RMS tissues or electric field mediated neuroblast directed migration.

### ***Methodological overview***

My role in this study was to perform electrotaxis experiments using SH-SY5Y cells that share characteristics with sympathetic neuroblasts in culture<sup>465</sup>, perform cellular migration analysis, compare electrotactic responses with the addition of drugs of interest, western blotting of proteins of interest and contribute to preparing the manuscript for this work. I provide an overview of the methods I used for my contribution to the published manuscript:

#### *Cell Culture*



SH-SY5Y (ATCC® CRL-2266™) cells were maintained in a 1:1 mixture of Basal Medium Eagle (Life Technologies) and F12 Medium (Life Technologies), supplemented with 10% foetal bovine serum (Life Technologies) and penicillin-streptomycin mixture (Life Technologies) at 37°C in humidified air containing 5% CO<sub>2</sub>.

### *Electrotaxis assay*

Electrotactic chambers were assembled according to the protocols established by Professor McCaig's Group previously published in Nature Protocols.<sup>466</sup> Briefly, SH-SY5Y cells were seeded onto the 20 mm x 10 mm x 0.3 mm chamber created on a Falcon tissue culture dish (BD Biosciences) that was sealed with a coverglass using silicone grease (Dow Corning Corporation) as shown in Fig. 36. Electric fields (EF) 5-100 mV/mm were applied to the cells with or without 100 μM ATP (Sigma) through agar salt bridges connected to silver/silver chloride (Ag/AgCl) electrodes immersed in beakers containing Steinberg's solution to pools of culture media at either end of the chamber. Time lapse microscopy was performed on a Zeiss Axiovert 100 microscope with stage incubator maintaining a temperature of 37°C. Cells were imaged in regions of interest every 10 minutes and analysed using MetaMorph (Universal Imaging Corp.). Cellular migration was assessed using the following parameters: directedness ( $\cosine \theta$ )<sup>467</sup>, trajectory rate (Tt/T), displacement rate (Td/T), displacement along the x-axis (Dx/T).  $\theta$  was defined as the angle between EF vector and a straight line connecting the start and end position of a cell, such that a cell moving perfectly towards the cathode would have a directedness of 1.0, whereas a cell moving towards the anode would have a directedness value of -1.0. A value close to 0 represents random cellular migration. The total length of trajectory (Tt) a cell migrated divided by time

(T) was used to calculate trajectory rate. The projection of the cell trajectory on the x-axis (Dx) was divided by time (T) to calculate the displacement along the x-axis, which represents the ability of cells to migrate along the EF vector.

#### *Drug treatments*

The P2Y1 receptor was activated using 100  $\mu$ M ATP (Sigma) during electrotactic experiments. Similarly, P2Y1 was inhibited with the specific antagonist 100  $\mu$ M MRS2179 (Sigma) during electrotactic experiments.

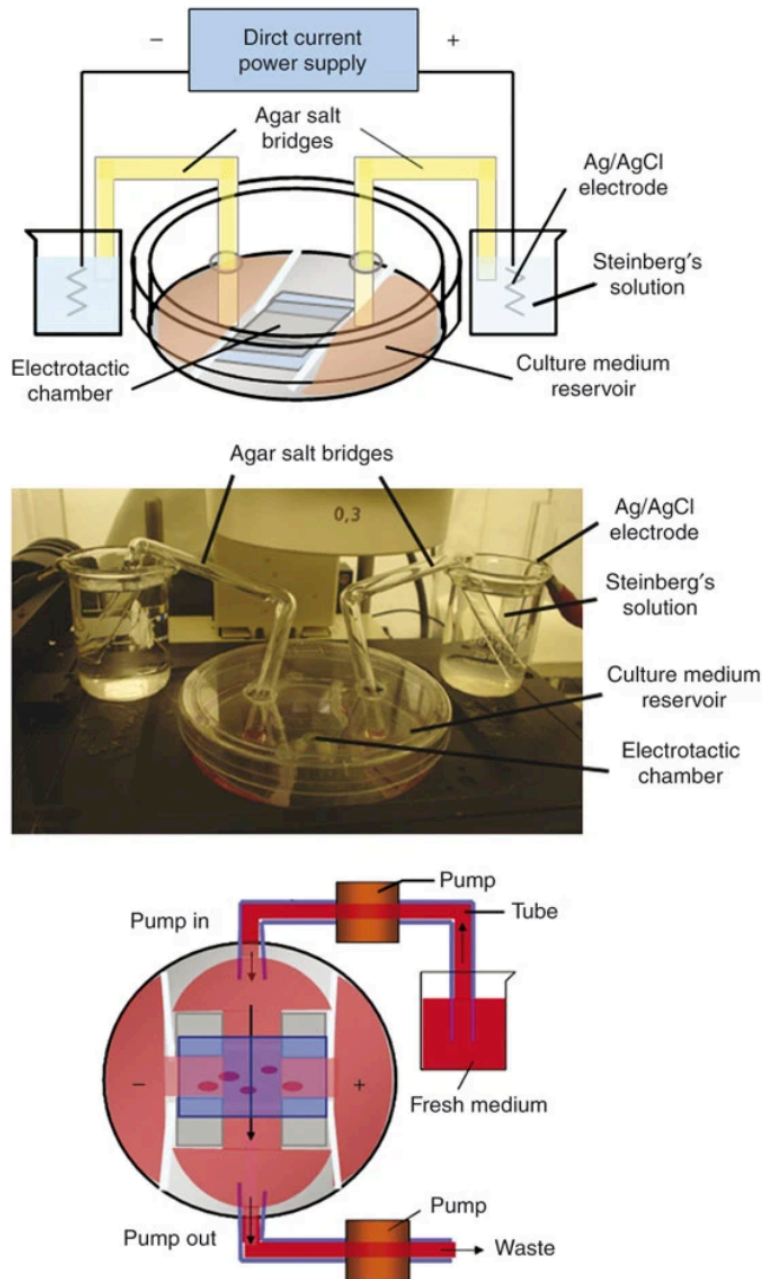


**Figure 36:** Electrotactic chamber assembly. Schematic of electric field application (top). Photograph of the electrotactic chamber assembled on a microscope stage (middle), showing electric current being passed through the Ag/AgCl electrodes, Steinberg's solution and agar salt bridges. Schematic of media flow (agar salt bridges not shown), demonstrating that the electrotactic chamber is connected to a pump that provides continuous flow of fresh media perpendicular to the long axis of the chamber. Images taken from Song et al.<sup>466</sup>

### *Western Blotting*

Lysates from SH-SY5Y cells, having been exposed to an EF of 50mV/mm for 1, 3, 5 and 8 hours, were processed for western blotting as previously described.<sup>468</sup>

Quantification of proteins of interest was carried out using primary antibodies: anti- $\beta$ -catenin (Cell Signalling), anti-N-cadherin (Abcam), anti-P2Y1 (Cell Signalling), anti p-PKC (Cell Signalling) and anti-GAPDH (Santa Cruz). Chemiluminescence was detected by using Liminata Forte Wester HRP substrate (Millipore).

### ***Nature of work***

This project was a basic science project under the supervision of Professor Colin McCaig, Regius Professor of Physiology, Institute of Medical Sciences, University of Aberdeen. I was taught the laboratory-based techniques used to investigate cellular electrotaxis, including: preparation of electrotactic chambers, time lapse microscopy and analytical methods to measure parameters relating to directed cell migration. Alongside this work, I reviewed the literature on cellular electric fields and was involved with the preparation of the manuscript prior to publication.

### ***Significance of work***

The original article on neuroblast chain migration was published in the journal Stem Cell Reviews and Reports (Impact Factor 5.31) and cited 10 times since publication. This work provided evidence for a mechanistic explanation for the role of physiological electric fields in neural stem cell migration in the rostral migratory stream. In addition, the concept of manipulating neural stem cell

migration with electric fields for potential therapeutic use was strengthened and recently demonstrated in vivo by colleagues in the field.<sup>469</sup>

### ***Critical appraisal of published work***

This study provides further evidence of in vitro evidence using neural stem cells and SVZ explants to demonstrate that electric fields play an important role in directed cell migration in the RMS. A strength of this study is the molecular pathway interrogation, where it was found that P2Y1 receptors mediate electric field guided migration. This was confirmed by adding ATP, a ligand of P2Y1, to the culture media of neural stem cells and P2Y1 knockdown to confirm its mechanistic role in electric field mediated migration. The data presented in this work is robust and adequately repeated, providing the basis for which in vivo work can be undertaken. However, further work would be required in disease models before considering whether this could be translated into a therapeutic approach.

In summary, this is paper strengthens prior work in the field and provides the a basis from which to explore electric fields and neural stem cell migration in vivo and in disease models.

## Chapter 7: Electric fields in brain tumour cell migration

### *Introduction*

The aggressive invasion and rapid proliferation rate of neoplastic cells within brain parenchyma is a hallmark of GBM.<sup>470</sup> Such invasion occurs as a result of brain parenchymal cells generating actin-rich membrane protrusions: lamellipodia and invadopodia.<sup>471,472</sup> These membrane protrusions are generally rich in microfilaments and undergo anterior polymerisation and posterior depolymerisation. Migration at any distance, short or long, is stimulated and regulated by diffusible chemicals such as integrins to allow random migration (chemokinesis) or directional migration (chemotaxis).<sup>473</sup> Most guidance signals necessary for migration are transduced into common intracellular regulatory pathways, with major effects exerted by the monomeric GTPase proteins of the Rho family. Specifically, these include cdc42, Rho and Rac which are implicated in the regulation of electrotaxis and chemotaxis.<sup>473</sup>

Electrotaxis is directed cell migration in response to physiological gradients of electrical potential.<sup>474</sup> Electrical gradients generated through ionic differences have been shown to behave as guidance cues in concert with chemical gradient signals.<sup>475</sup> Such extracellular electrical signals are known to regulate neuronal migration, neuronal growth cone guidance, neuronal regeneration and play a critical role in CNS development.<sup>476-482</sup> Furthermore, epileptic seizures are known to induce extracellular electrical signals in the brain.<sup>483</sup> The role of electrotaxis has been investigated in multiple cancer types including prostate and breast cancer cells.<sup>484,485</sup> GBM directed cell migration has been shown to be affected by

externally applied electric fields in both glioma stem cell (GSC) and differentiated GBM states.<sup>486,487</sup>

As it was emerging that the GSC subpopulation attribute many of the malignant characteristics of GBM, including recurrence and invasion, I focused on neural stem cell electrotactic migration in the CNS to understand possible related mechanisms in GSCs.<sup>488-490</sup> The largest persistent neural stem cell (NSC) niche of the CNS is the subventricular zone (SVZ), which harbours neuroblasts that migrate along the rostral migratory stream (RMS) via a chain-like conformation to the olfactory bulb (OB) where they differentiate into interneurons.<sup>491-493</sup> At the SVZ there is a high concentration of Na<sup>+</sup>/K<sup>+</sup>-ATPase on the basal surface of the cells, transferring 3Na<sup>+</sup> from the extracellular space into the brain tissue, and pumping 2K<sup>+</sup> back into the extracellular space. This causes the SVZ to become positively charged. At the OB the opposite occurs; there is a high concentration of Na<sup>+</sup>/K<sup>+</sup>-ATPase on the apical surface, causing the OB to become negatively charged.<sup>437</sup> Therefore the OB acts as a cathode and the SVZ an anode. In order to further identify underlying mechanisms for these previous findings, I collaborated with colleagues to investigate the effect of physiological electric fields on neuroblasts in vitro as described in Chapter 6.

Studies in breast and prostate cancer cells have shown that applied electric fields (EF) induce migration of cells towards the cathode or anode, depending on the metastatic potential of the cell lineage in study.<sup>494</sup> Li and colleagues demonstrated that direct current electric fields can direct migration of U87, C6 and U251 gliomas cell lines with a predominance of cells migrating towards the cathode.<sup>495</sup> They found that migration was related to activation of Akt (protein kinase B) and Erk

1/2 (extracellular signal-regulated kinase) signalling pathways, and a reduction in activation of both correlated with decreased directional migration.

The PI3K/Akt signalling pathway is heavily implicated in cell electrotaxis.<sup>495-500</sup> One such mechanism involves a cathodal redistribution of epidermal growth factor receptors (EGFR), resulting in polarised activation of the PI3K/Akt pathway and subsequent polarised actin remodelling.<sup>497,501</sup> This produces asymmetrical membrane protrusions and consequently migration in the direction of the cathode. This pathway is frequently dysregulated in GBM through EGFR overexpression (65% of GBM), and downregulation of the Akt inhibitor PTEN (78% of GBM).<sup>502</sup> We therefore sought to investigate the effect of an applied EF on the migration of primary GBM cell lines, both differentiated; HROG02-Diff, HROG05-Diff and HROG24-Diff; and de-differentiated, GSC; HROG02-GSC, HROG05-GSC with the aim of providing a greater understanding of the infiltrative behaviour of GBM. We demonstrated for the first time that differentiated GBM cells and GSCs have opposing preferences for anodal and cathodal migration, respectively.<sup>503</sup>

Furthermore, we investigated the potential of PPAR $\gamma$  in modulating the PI3K/Akt pathway. PPAR $\gamma$  activation has been shown to upregulate PTEN, causing downstream inhibition of Akt.<sup>306,504</sup> The potential role of Akt in electrically guided migration of GBM in conjunction with the high frequency of Akt activating mutations led us to investigate the effect of the PPAR $\gamma$  agonist pioglitazone in both differentiated and GSC primary GBM cell lines. We found that pioglitazone treatment significantly decreased the directedness of electrotaxis of primary GBM cell lines in both differentiated and de-differentiated states.<sup>503</sup> This inhibitory



effect was diminished by the PPAR $\gamma$  antagonist GW9662, directly implicating PPAR $\gamma$  activation in suppression of EF guided migration of primary GBM cell lines. PPAR $\gamma$  activation inhibited electrotaxis in both differentiated and de-differentiated phenotypes implies a common migratory pathway downstream of PPAR $\gamma$ , such as the PI3K/Akt pathway. This provides early evidence that inhibition of GBM directed cell migration reliant on electrotaxis may be targeted with drug therapies.

As such the aims for this chapter are as follows:

- Provide an overview of glioblastoma cell migration and the underlying mechanisms
- Summarise the current and emerging therapeutic approaches using electric fields in glioblastoma treatment
- Summarise the methodology, nature, and significance of this work, and provide a critical appraisal of the published paper pertaining to this chapter

### ***Literature review***

GBM has been shown to invade the surrounding parenchyma, destroying the normal functional architecture of the brain and consequentially compromising routine mechanisms. This destruction and functional impairment results in a clinical picture of seizures, nausea, headaches, imbalance and rarely hemiparesis. Current optimal treatment of GBM is a combined approach aimed at eradication of tumour mass, however GBM is highly resistant to these conventional approaches, e.g. chemotherapy and ionizing radiation. At present optimal treatment for GBM utilises the Stupp Protocol, which employs multimodal treatments including respective surgery and chemoradiotherapy. However,

recurrence with tumours is quite common post-treatment, where a renewed aggression manifests even after the use of therapeutic agents for effective GBM cell death. Such reports of relapse and marginal improvements in prognosis prove the poor efficacy and potential limit in the use of these conventional therapies.<sup>319</sup>

GBM remains an extremely challenging disease to manage due to its aggressive behaviour and recurrence. After surgical removal, tumour recurrence tends to occur within the resection cavity or immediately adjacent to the resection margin, since tumour cells have already invaded adjacent normal brain tissue at the time of the surgery.<sup>320,321</sup> Invasiveness and migration is governed by multiple processes. Cancer cells maintain a motile phenotype through transient interactions with the extracellular matrix (ECM) and with adjacent cells, changes in cell morphology, which become polarized and with protrusive activity of the cell membrane, modifications of cell body and reorganization of the actin cytoskeleton, by changes in the interactions between integrins and ECM.<sup>320,505</sup> Modifications also occur within the ECM, becoming a permissive substratum rather than acting as a barrier for cell migration, caused in part by the action of proteolytic enzymes secreted by tumour cells. Many studies focus on the participation of chemotactic migration as a great supportive of active cell movement<sup>321</sup>, however new approaches in understanding cell migration have been discovered, including electrotaxis.

Li et al.<sup>495</sup> demonstrated that DCEF can direct migration of U87, C6 and U251 gliomas cell lines with a predominance of cells migrating towards the cathode. They found that migration was related to activation of Akt (protein kinase B) and

Erk 1/2 (extracellular signal-regulated kinase) signalling pathways, and a reduction in activation of both correlated with decreased directional migration. The importance of these discoveries is grounded in the manipulation of electric fields and the pathways induced that may be applied as new gateways to the establishment of cancer pathogenesis. Importantly, this may lead to the discovery of new treatment modalities. Herein, I review the literature pertaining to the potential role of electrical fields in malignant brain tumour physiology. I allude to how this may be beneficial in terms of the prevention of infiltration and understanding of the underlying pathogenesis.

The existence of a mammalian neural stem cell (NSC) from the adult central nervous system (CNS) has not been investigated until recently. This notion was revived only in the past decade<sup>506,507</sup>, remarkably after the isolation of these cells from human tissue by Uchida et al.<sup>507</sup> The identification and isolation of NSC was performed by targeting cell surface markers such as CD133 and 5E12, which are present on the surface of NSCs. NSCs are found in high-density in the subventricular zone (SVZ) and in the subgranular zone of the dentate gyrus (hippocampus) in the adult mammalian brain.<sup>506</sup> These cells are able to self-renew and capable of multi-lineage differentiation allowing them to give rise to the three prime cell types of the CNS: neurons, astrocytes and oligodendrocytes.<sup>507,508</sup> Transplantation of NSCs into the hippocampus have shown extensive migration towards the olfactory bulb (OB) via the rostral migratory stream (RMS), while transplantation into the SVZ leads to NSC migration into the granular cell layer.<sup>509</sup> Further, neuroblasts, a type of NCS, generated from the SVZ have been shown to differentiate into granule interneurons upon arrival at the OB.<sup>510</sup> While cell-cell interactions with selective

adhesion molecules have been implicated in neuroblast migration within the RMS, how migration is co-ordinated is unclear.<sup>511</sup> In the past it was unclear whether electrotaxis played a role in such migration and this was subsequently investigated.

The  $\beta$ 2-subunit of  $\text{Na}^+/\text{K}^+$ -ATPase (known as the adhesion molecule on glia (AMOG)), normally present in glial cells was found to be absent in most GBM cells. Furthermore, when the AMOG expression was decreased in normal glial cells, an invasive phenotype manifested.<sup>512</sup> If the absence of this particular subunit were to affect the ability of  $\text{Na}^+/\text{K}^+$ -ATPase to transfer  $\text{Na}^+$  and  $\text{K}^+$  against their concentration gradients, this could result in abnormal ionic gradients between the GBM and both local and distal brain parenchyma, thus resulting in abnormal electrical fields. This in turn could explain how the infiltration of GBM cells can be so diffuse and variable.

Another cell membrane molecule shown to be involved with electric field directed neuroblast migration through the RMS is the P2Y1 purigenic receptor, the involvement of which has been demonstrated through pharmacological inhibition.<sup>437</sup> One proposed mechanism for this function is the up regulation of the P2Y1 receptor in response to an electrical field, resulting in increased expression of adhesion molecules such as N-cadherin and  $\beta$ -catenin. These adhesion molecules then provide the framework and structure within the RMS for neuroblast migration, allowing further distribution of immobile cells from the SVZ to the OB.<sup>447</sup> GSC migration and invasiveness has been shown to be regulated by activation of WNT/ $\beta$ -catenin signalling, causing epithelial-to-mesenchymal transition activators induction, which is more active in regions of infiltration close

to healthy tissue.<sup>513</sup> Furthermore N-cadherin has been shown to be up-regulated in response to increased  $\text{Ca}^{2+}$  signalling within astrocytes in regions of brain injury, resulting in astrogliosis, which has numerous functions including, cell polarisation, proliferation and migration.<sup>514</sup> An increase in N-cadherin expression has also been associated with an increase in the invasiveness of GSCs<sup>515</sup> which along with the apparent influence of  $\beta$ -catenin, suggests a role for endogenous electrical fields in the spread of GBMs via P2Y1 up regulation.

In the past 2 decades, research in the field haematological oncology have led to the cancer stem cell (CSC) hypothesis, following observations of a subset of cancer cells demonstrating stem cell properties.<sup>516</sup> A small subset of cells inside a tumour characterised by self-renewal properties and multilineage differentiation have been labelled as CSCs. CSC populations were hypothesised to be responsible for sustaining tumourigenesis and giving rise to all cell lines in the tumour mass.<sup>488,517</sup> Primary GSCs have been previously isolated from human brain tumour samples and previous studies have shown that the morphological and phenotypical diversity of cells comprising a tumour mass may be explained by the existence of GSCs.<sup>518</sup>

The CD133 (prominin-1) glycoprotein has been found to be present on a number of stem cell types and is used as a surface marker for NSCs.<sup>519</sup> The presence of CD133 glycoprotein on glioma stem cells (GSC) is associated with an increase in the aggressiveness of the tumours, and thus an increasingly poor prognosis.<sup>520</sup> However, CD133 negative cells may also act aggressively, indicating that the presence of CD133 is not an absolute requirement in determining the aggressiveness of GBM.<sup>521</sup> A factor to consider with positive and negative

expression of CD133 is the interchangeability of the location of the glycoprotein, be it within the cytoplasm (considered CD133 negative), or expressed on the plasma membrane (CD133 positive).<sup>521</sup> This poses the question of what drives a CD133 negative cell to become CD133 positive, and in particular whether the presence of an electrical field plays a role into this process. It has been hypothesised that whilst CD133 positive cells are more invasive, once migration occurs there is lower CD133 expression<sup>522</sup>, perhaps suggesting a primary role of CD133 in GBM migration. CD133 has been implicated in recurrences of GBMs following treatment. In particular the contrasting CD133 status between local and distant spread, with local CD133 negative and distant CD133 positive. Further, an increase in CD133 positive cells has been associated with a faster distant recurrence time<sup>523</sup> and correlates with a poor survival rate.<sup>524</sup>

There is strong evidence implicating Akt within the PI3K/Akt and Focal Adhesion Kinase (FAK) signalling pathway (Fig. 37).<sup>525</sup> ECM binding and growth factor receptor activation stimulates FAK phosphorylation, consequently mediating phosphatidylinositol-3-kinase (PI3K) mobilization into the membrane and Akt signalling. Moreover, PI3K/Akt signalling leads to an augmentation in actin remodelling and protrusion formation, subsequently influencing Rac proteins, as well as the modulation of cell migration and invasion via p70S6K activation.<sup>470</sup>

The PI3K/Akt pathway is further controlled by tumour suppressor gene PTEN. Through its expression of phosphatase tensin homologue (PTEN)<sup>476</sup> the PTEN gene inhibits the action of PI3K by preventing its activation of Akt (Fig. 37).<sup>497</sup> In isolation, PI3K activates Akt via the phosphorylation of phosphatidylinositol (PI) lipids to form phosphatidylinositol triphosphate (PIP3). By acting as a

phosphatase PTEN halts this conversion, thus preventing the activation of Akt and its subsequent activity<sup>526</sup>, namely its role in cytoskeletal recruitment; a critical component of cell migration.<sup>495</sup>

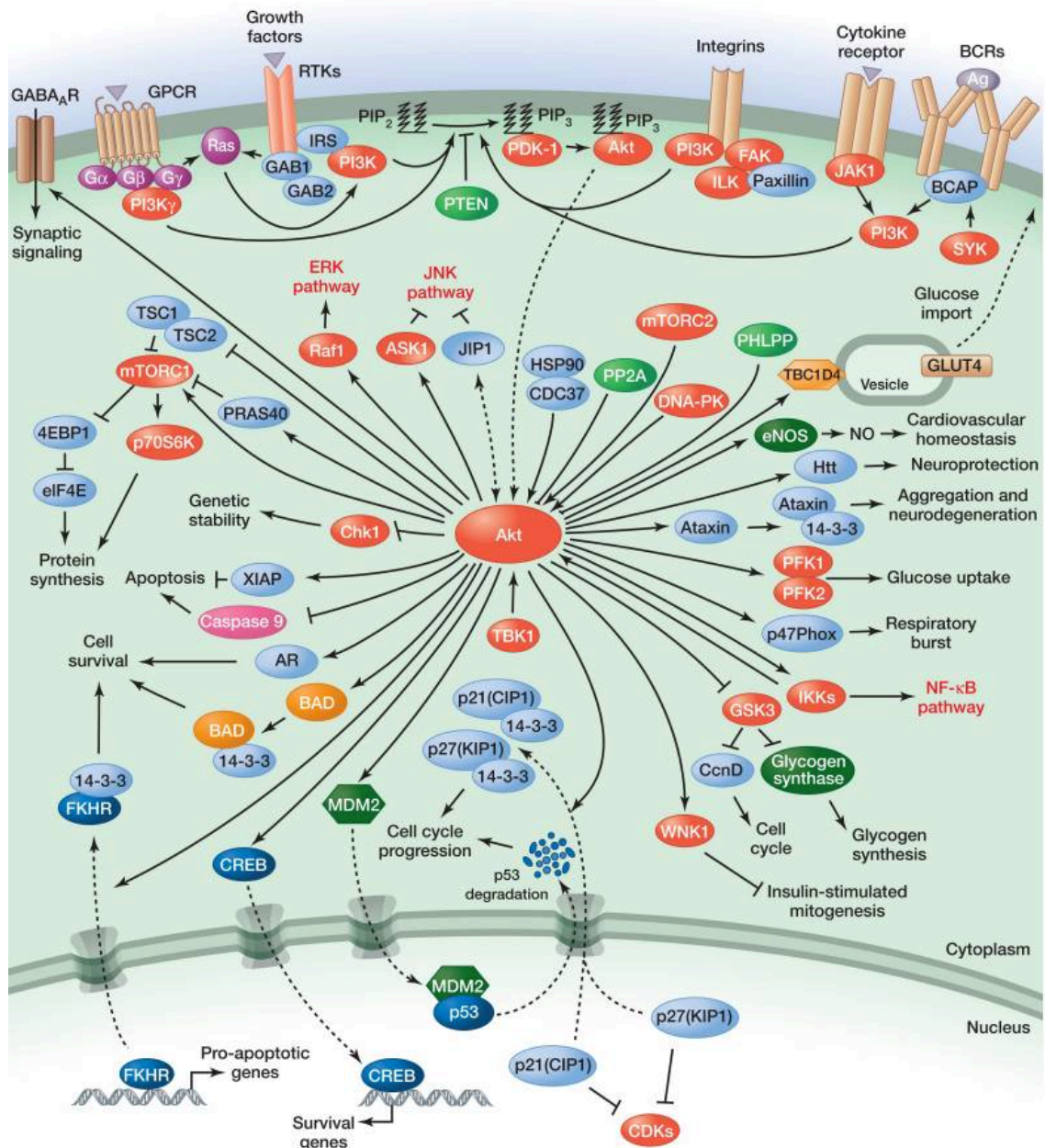


**Figure 37:** Diagram of signalling events of Akt and the cellular functions regulated by it. The protein kinase B (Akt) plays multiple roles in the cell, including proliferation, growth, cell metabolism and proliferation. Its activation is controlled by multiple steps that involve phosphoinositide-3-kinase (PI3K). Following growth

factor activation of receptor tyrosine kinases (RTKs), insulin receptor substrate (IRS) proteins stimulate PI3K to activate its catalytic domain that converts phosphatidylinositol (3,4)-bisphosphate (PIP<sub>2</sub>) lipids to phosphatidylinositol (3,4,5)-triphosphate (PIP<sub>3</sub>). Akt binds to PIP<sub>3</sub> at the plasma membrane and allows PDK1 to phosphorylate T308 in the “activation loop”, leading to partial Akt activation. Phosphorylation of Akt at S473 in the carboxy-terminal hydrophobic motif, either by mammalian target of rapamycin (mTOR) or by DNA-dependent protein kinase (DNA-PK), stimulates full Akt activity. Fully activated Akt leads to substrate-specific phosphorylation events in the cytoplasm and nucleus, including inhibitory phosphorylation of the pro-apoptotic FOXO proteins. Antagonism of Akt is mediated by conversion of PIP<sub>3</sub> to PIP<sub>2</sub> by PTEN, desphosphorylation of T308 by protein phosphatase 2 (PP2A) and S473 by PH-domain leucine-rich-repeat-containing protein phosphatases (PHLPP1/2). Schematic taken from Hemmings and Restuccia.<sup>527</sup>

The PI3K/Akt pathway is believed to be affected by electric fields through an alteration in the distribution and activity of growth factor (GF) receptors in response to an electric field (Fig. 38). In the presence of an electric field, GF receptors are redistributed, and their activity heightened such that there is an increased concentration and activity of GF receptors at the leading edge of the cell in the direction of the cathode.<sup>497</sup> PI3K and consequently Akt are responsive to GFs (in particular epidermal GF (EGF) and basic fibroblast growth factor (FGF-2)) and therefore this localised increase in concentration of GF receptors results in an increase in PI3K/Akt concentration on the cathodal side of the cell resulting cytoskeletal recruitment and subsequent cathodally directed cell migration. The cathodal preference of PI3K and Akt has been further supported by reversing the



electrical field polarity and tagging PI3K and Akt with fluorescent proteins. Upon this reversal the tagged PI3K/Akt concentration swiftly changes so that it is once again higher at the cathodal side of the cell.<sup>528</sup> In addition, it has been shown that GBMs often express increased levels of (EGFR)<sup>502</sup>, recently suggested to be caused by overexpression of the protein mucin 4.<sup>529</sup> This may mean that the activity of the PI3K/Akt pathway may be enhanced in GBMs when compared to normal brain tissue.

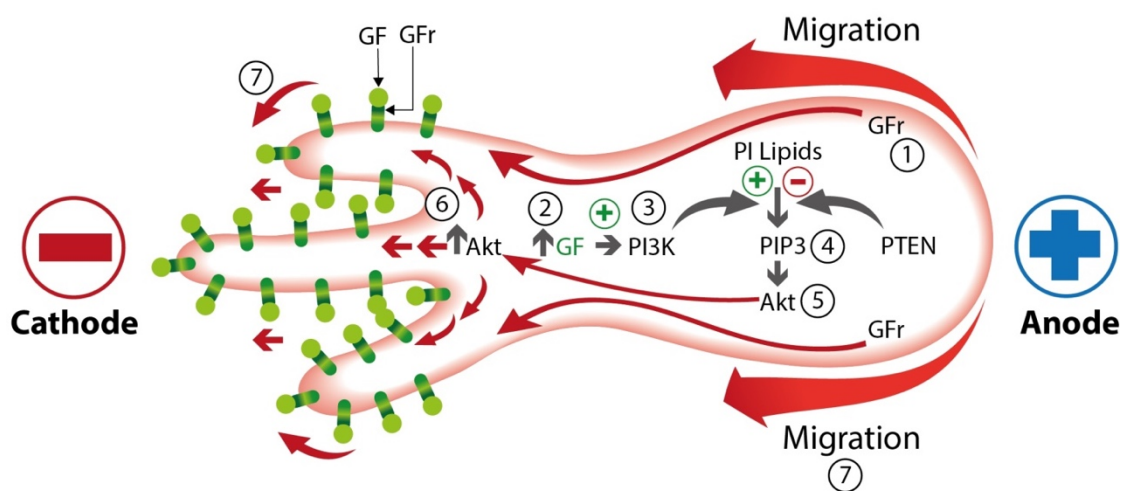


**Figure 38:** Diagram to show the effect of electrical field on cell migration via PI3K/Akt pathway. 1) In the presence of an electrical field, GFr (epidermal growth factor receptor) is redistributed to the cathodal facing edge of the cell, and the receptor activity increased. 2) This results in an increase in growth factor (GF) concentration at the cathodal side of the cell. 3) Raised GF concentration leads to increased PI3K activity. 4) PI3K stimulates phosphorylation of PIP lipids to form PIP3. 5) PIP3 in turn activates Akt. 6) This results in an increase Akt concentration at the cathodal side of the cell. 7) The resulting cytoskeletal alterations (namely microvilli formation) from increased Akt activity results in cathodally directed cell migration. Illustration by WL Sung (Department of Medical Illustration, Polwarth Building, Foresterhill), concept by H Clancy and J Ching.

The PI3K/Akt pathway has been previously elucidated in primary human GBM cells, whereby loss of the tumour suppressor protein PTEN leads to Akt activation and expression of mutant EGFR vIII is associated with phosphorylation of the Akt effectors, including mammalian target of rapamycin (mTOR).<sup>530</sup> This confirms the possible importance of PTEN expression in the potentially electrically guided migration GSCs, especially when combined with the observation of frequent PTEN mutations and decreased PTEN expression in GBMs.<sup>502</sup> Moreover, cell lines with mutations in PTEN have been shown to have increased cell membrane folds, including long dendritic protrusions. Such cell membrane morphologies are believed to have an association with functions required for invasion and infiltration<sup>531</sup> further suggesting a role for PTEN/PI3K/Akt pathway in the migration and invasion of GBM in response to electrical fields.

### ***Current and emerging therapeutic approaches using electric fields in glioblastoma treatment***

To date, the only electric field-based treatment with pre-clinical and clinical trial evidence for efficacy in glioblastoma are Tumour Treating Fields (TTF) that was first approved by the US Food and Drug Administration (FDA) in 2011 for recurrent glioblastoma.<sup>532-534</sup> In 2015 it was FDA approved for the treatment of newly diagnosed GBM. TTF is a non-invasive anticancer treatment that delivers low intensity (1-3v/cm), intermediate frequency (100-300kHz), alternating electric fields that exert their effect on dipoles. Several parameters have been shown to influence the efficacy of treatment, including treatment duration of more than 18 hours daily improves survival, greater electric field intensity correlates with a greater reduction in cell proliferation, and electric field frequency of 200kHz is

optimal for glioblastoma cells.<sup>533,535</sup> Low frequency alternating current of less than 1kHz is known to increase neuronal firing, while high frequency fields of greater than 500kHz are known to cause vibration of charged and polar molecules that creates heat through the creation of thermal energy from friction.<sup>536</sup> Intermediate frequencies of 100-300kHz that do not initiate action potentials or cause a temperature increase, were shown to inhibit cancer cell growth in vitro and in vivo by interfering with microtubule polymerisation during mitosis.<sup>532</sup> This paved the way for the development of TTF as a cancer treatment strategy following the first pilot study (EF-07) in GBM patients.<sup>533</sup> Subsequently clinical trials demonstrated that overall survival increased by a median of 4.9 months where no significant adverse events were reported.<sup>537,538</sup>

The most widely used clinical TTF delivery system called Optune (Novocure™) consists of 4 transducer arrays, a field generator, and a power source. For patients with GBM, the transducer array is attached in pairs and orientated orthogonally to the patient's scalp. Localisation of the arrays in relation to the tumour location is planned using NovoTAL™ (Novocure Ltd., Haifa, Israel) simulation software that uses the dimensions of the patient's head and tumour location to optimise treatment. The field generator delivers alternating electric fields through the transducer arrays across the brain and to the tumour site.

Given the success of TTF on GBM, a range of other cancers are under investigation in clinical trials including non-small cell lung cancer (Phase III, NCT02973789), pancreatic cancer (Phase III, NCT03377491), ovarian cancer (Phase III, NCT03940196), hepatocellular carcinoma (Phase II, NCT03606590), and gastric cancer (Phase II, NCT04281576). It therefore seems likely that more

widespread use of TTF in cancer treatment is on the horizon. However, to date there have been no licensed therapies using direct current to manipulate cancer cell migration. As we have demonstrated in this study, a surgical approach using implantable electrodes or chemical approach with a drug such as pioglitazone, can be used in theory to manipulate electrotaxis of GBM cells. Such approaches would require careful voltage adjustment in animal models before considering human use. Further, the effect of a resection cavity on brain electric fields would need to be investigated thoroughly, as a cavity may act as a voltage sink and therefore as a cathode, permitting differentiated GBM cells to migrate away. While there is still further work to be undertaken before direct current electric fields can be considered for human use in GBM, it may be a promising target in the future as a monotherapy or as a further adjunct in combination treatment regimens.

### ***Methodological overview***

In order to avoid utilising immortalised GBM cell lines, my goal was to source fresh primary brain tumour samples. To this end, I completed an ethics application to the Local Research Ethics Committee and completed an application to the Integrated Research Application System (IRAS). As such, I developed all the study materials including the research proposal, clinical research protocol, participant information sheet, study consent form and protocols for isolating primary GBM cells as follows:

## Study Protocol Version 7.0

Dr Jared Ching, Professor Colin McCaig, Mr Pragnesh Bhatt

**Study Title:** The role of Electrical Currents and Cell Signalling in Brain Tumours and Brain Tumour Stem Cells

### **Research outline:**

The most common type of brain tumour is glioblastoma multiforme (GBM). GBM is one of the most deadly diseases known to mankind and almost three decades of research has helped to increase survival by only several months. As we are still not entirely sure what causes this disease or where it comes from, many research groups have sought to understand this better in order to develop new treatment methods. Removing these tumours with surgery has temporary benefits, and together with radiotherapy and chemotherapy can maximise survival, although only by a number of months. This combination of treatments is known as the "Stupp Protocol", which is the most commonly used protocol worldwide. A patient under this treatment regimen would be expected to survive for approximately 14 months from the time of the brain tumour being diagnosed. Part of the reason that such brain tumours are so difficult to treat is their ability to regenerate and resist these treatments. Until recently the reasons for this have been largely unknown.

A relatively new explanation for the difficulty in treating this disease is the cancer stem cell theory. In 2004 brain tumour "stem cells" were first discovered from brain tumour samples. These "stem cells" were found to be very resistant to radiotherapy and chemotherapy in laboratory experiments and form a small population within mature brain tumour cells. This has provided a new way of studying brain tumours and several new theories about where these tumours come from. By investigating these "stem cells" we are more likely to find new treatments that can further improve patient survival.

Stem cells are defined as early cells that can self-renew and grow into other types of cell. There are also different types of stem cells, for example neural stem cells, which can grow into the three main types of neural cell. What makes brain tumour stem cells different to normal neural stem cells is their ability to form malignant tumours. In comparison to the rest of a brain tumour, brain tumour stem cells grow relatively slowly and this is thought to be part of the reason why they are not as sensitive to treatment. In addition, these stem cells replicate themselves so that not only do they cause the growth of the tumour, but form more stem cells to continue this process.

One theory that has not been explored in great depth is that brain tumours start from "stem cells" that develop very early in life. Clearly it is not feasible to study these cells in foetuses or neonates, making it necessary to study these cells in the laboratory from samples that we can obtain safely. The mechanism by which these "stem cells" travel around the brain may provide insight as to where these tumours come from and how they form. We already know from basic scientific research that a number of migrating cell types including normal neural stem cells and brain tumour cells, show directed

## Study Protocol Version 7.0

Dr Jared Ching, Professor Colin McCaig, Mr Pragnesh Bhatt

migration in response to electrical signals.<sup>1</sup> Cell signalling processes are modulated by these voltage gradients within the extracellular spaces, allowing cells to migrate in a particular direction and rate. Until now, the role of these processes in glioma stem cells has not been investigated.

A potentially new method of treating brain tumours first described in 2000, is the use of normal neural stem cells. Such stem cells have been shown to target and prevent brain tumours from spreading and growing. Surprisingly, when neural stem cells are injected into rats blood circulation, they are able to target and prevent growth and spread of the tumour.<sup>2</sup> How these cells “find” the tumour cells is largely unknown. One way such neural stem cells may track down brain tumours is by using extracellular electrical signals. Furthermore, this special property has not been explored in brain tumour stem cells. Endogenous electric cues may play a role in such targeted migration.

By investigating the role of electrical signals in directing the migration of glioblastoma cells, we hope to find a target for which we can prevent these tumour stem cells from growing, migrating, and self-renewing. This would also be beneficial in gaining a better understanding of how these cells behave and how their migration may be stopped. The results of this study would also be used towards developing a new treatment device that has not yet been investigated.

We plan to answer the following questions:

1. Can manipulating electrical signals and/or related cell signalling cascades in brain tumours lead to the development of new treatments?
2. Do glioma stem cells respond to electrical fields with directed cell migration and do these electrical signals regulate glioma cell division?
3. Are glioma stem cells guided by endogenous electrical gradients to particular parts of the brain?
4. In what ways do electrical fields influence glioma stem cell signalling?
5. Do brain tumour stem cells create intrinsic electrical gradients in surrounding tissue?
6. Does migration of neural stem cells to brain tumour cells rely on endogenous electrical currents?

### **Sponsor:**

Co-sponsorship between NHS Grampian and University of Aberdeen has been agreed.

### **Funding Source:**

## Study Protocol Version 7.0

Dr Jared Ching, Professor Colin McCaig, Mr Pragnesh Bhatt

No specific funding has been applied for or secured yet. Our intention is to apply for small grants from various funding sources including Tenovus Scotland, NHS Grampian Endowments and other charitable sources.

### Study Contacts:

Mr Pragnesh Bhatt MBBS, MS, FRCS (SN)  
Consultant Neurosurgeon  
Department of Neurosurgery  
Aberdeen Royal Infirmary  
Aberdeen AB25 2ZD  
Tel: (01224 553453)  
Email: Pragnesh.bhatt@nhs.net

Professor Colin McCaig Bsc (Hons), PhD,  
FRSE (Chief Investigator)  
Regius Professor of Physiology  
Head of School of Medical Sciences  
Institute of Medical Sciences  
Aberdeen AB25 2ZD  
Tel: (01224 437394)  
Email: c.mccaig@abdn.ac.uk

Dr Jared Ching MB, ChB, MPharm, MRPharmS  
(Research Co-ordinator)  
Academic Foundation Doctor  
Honorary Clinical Fellow  
Aberdeen Royal Infirmary  
Aberdeen AB25 2ZD  
Tel: (01224 553453)  
Email: jared.ching@nhs.net

### Phases of Research:

#### 1. Establishment of glioma stem cell and differentiated cell lines from primary tumour resections.

Tumour samples and tumour surgical aspirate waste will be processed using published methods to grow tumour cells in culture dishes.

#### 2. Field potentials in brain tumours

Fresh tumour samples will be cut into very thin slices and kept "alive" using special conditions that allow access to air and support tissue metabolism. These slices will then be probed to determine what level of electrical activity exists at different regions within the tumour. This will give us data on what electrical activity exists in live brain tumour tissue. This can then be compared to the results of the electrotaxis experiments.

### **3. The role of electrical fields in the migration and spread of glioma stem cells and glioma cell lines**

The established cell lines will be used in electrotaxis experiments where the effect of the electric field in directing cell migration is measured. These experiments involve applying varying strength of electrical field across growing cells. Time-lapse video microscopy will allow us to determine if electrical fields of varying strength affect directional migration, rate of growth, frequency and orientation of cell division.

### **4. The role of cell signalling cascades activated by electric fields in glioma stem cells and glioma cell lines**

If it is found that electric fields have a clear role in directing the migration of glioma stem cells and cell lines, the aim would be to test known pathways that affect migration. Knockdown experiments, where the signalling cascade of interest is removed by an engineered virus, will be used to identify the signalling molecules that regulate electrically-directed cell migration.

### **5. Migratory potential between neural stem cells and glioma stem cells**

Currently it is known that neural stem cells migrate to brain tumour cells when grown in the same culture plate. This results in a reduction in spread of the brain tumour cells and prevents further growth. Interestingly, when rats are injected with neural stem cells, these cells migrate to the sites of the brain tumour and prevent further growth. However, it is not clear what mechanisms allow the stem cells to target the brain tumour cells. The established role of endogenous electrical fields in neural stem cell movements, indicates their likely involvement. We will use special culture methods to determine if this is the case.

### **6. Drug testing to identify new targets that influence electrically-directed migration**

Identified signalling targets that are regulated by electrical currents will be tested with drugs that enhance or reduce the effects of such signalling cascades. Commercially available drugs will be used to identify potentially new ways of treating this disease.

### **7. The potential role of electric fields in glioma stem cell migration as a developmental disease model**

In order to find out more about where brain tumour stem cells may come from, implanting brain tumour stem cells in rat brains and applying an electric field may give insights into the manner in which these cells spread. Implanting brain tumour cells in this way will also allow us to determine whether electrical signals differ between the tumour itself and adjacent normal brain.

## **Experimental Design**



## Study Protocol Version 7.0

Dr Jared Ching, Professor Colin McCaig, Mr Pragnesh Bhatt

Patients 18 years old and above will be recruited from the Neurosurgical Unit, Aberdeen Royal Infirmary. Patients who have an MRI scan that shows a mass that appears most likely to be a tumour and/or have had a minimally-invasive biopsy, will be given information about this study at the time of follow up. When patients are consented for a craniotomy, awake or anaesthetised, for resection of a brain tumour, consent for tumour samples to be used for research will be taken.

The methods for each phase of this study are summarised as follows:

### **1. Establishment of glioma stem cell and differentiated cell lines from primary tumour resections.**

Fresh tumour resection will be processed initially by using an enzyme cocktail (Accutase) to break the tissue into single cells. Initially, glioma surgical aspirate (obtained from sterile traps connected to Cavitation Ultrasonic Surgical Aspirator) will be obtained also, as recent evidence suggests this is a reliable source of glioma cells for culture. Aspirate samples will be spun down to obtain the cellular fraction and suspended in growth media to form a single cell suspension. Single cells from both sources are then grown in stem cell growth media that permits survival of stem cells. We will grow these stem cells as a flat layer using laminin as a growth promoting substrate as this has been shown to be the most effective method of propagating these cells. Commonly, neuronal stem cells are grown as "spheres", which is also possible for brain tumour stem cells but less desirable for our purposes. Depending on the yield of stem and mature glioma cells from each source, one source will be chosen for the remainder of the project. Surgical aspirates have been shown to be a more reliable source in this respect, but evidence for this has not yet been fully established.

In order to confirm that the "stem cells" isolated are truly stem-like, we will use commercially available antibodies to identify known markers of neural stem cells on small populations of these cells after growing them in sufficient numbers. First, using immunohistochemistry and fluorescent labels to ensure usual markers of stem cells are present (nestin, SOX 2, CD44). Then by adding serum to the growth media and withdrawing stem cell growth factors, brain tumour stem cells will mature/differentiate into different types of brain tumour cell. Again, markers specific for this will be identified by using specific antibodies (Olig 2, beta III tubulin, GFAP). These experiments will ensure the isolated cells have stem cell properties, including multipotency (ability to differentiate into differentiate) and self-renewal.

Finally, in order to "enrich" for a subset of "true" glioma stem cells, we will sort cells into CD133 positive and negative cell populations. Recently it has been determined that CD133 is essential for glioma stem cell survival and a potential target for novel therapies. We will use fluorescence activated cell

sorting (FACS) and the CD133 antibody to isolate and propagate this small proportion of glioma stem cells.

## **2. Field potentials in brain tumours**

Using established culture techniques we will keep brain tumour tissue “healthy” in order to measure electrical activity. In brief, freshly resected brain tumour will be thinly sliced using a tissue chopper (McIlwain) and then placed onto a membrane (Millipore) that is immersed in warmed media that maintains tissue viability. These organotypic slices will be incubated until stable and tested using micromanipulators to place electrodes to measure field potentials. Field potentials from slices made from tissue samples obtained from the tumour periphery (near the peritumoural edge), a region between the core and periphery, and from the core of the tumour will be measured.

## **3. The role of electrical fields in the migration and spread of glioma stem cells and glioma cell lines**

Using published methods established in The Institute of Medical Sciences, Aberdeen, electrotaxis assays will be used to determine how application of an electric field affects directional movement of brain tumour cells. In addition, a scratch wound healing assay with and without applied electric currents will be carried out in order to further characterise cell migration.

In brief, glass electrotactic chambers made from cover slips set up in a water tight environment within a petri dish will be used to grow cell lines and apply an electric field. Agar salt bridges will be used as cathode/anode and for media renewal (Please refer to Figure 1). Time-lapse video microscopy will be used to measure migration of the cell lines. The control experiment will be no application of an electric field.

Scratch wound healing assays will be carried out whereby brain tumour cells grown flat and to confluence in culture will be “wounded” by using a sterile pipette. A “line” and/or small “circle” will be made on the plate, damaging the cells in these areas. This will then allow us to observe, microscopically how the cells heal by growing into the gap. This control wound healing will be compared to conditions where we apply electrical fields to the wounded cells, as described above.

## **4. The role of cell signalling cascades activated by electric fields in glioma stem cells and glioma cell lines**

If it is found that glioma stem cells respond to electric fields with directed migration, signalling cascades will be investigated by using sufficiently large electrotactic chambers to harvest responding cells in sufficient numbers for immunoblotting experiments. Primary antibodies of interest will be used to quantify protein expression of modulators of motility and oncogenesis.

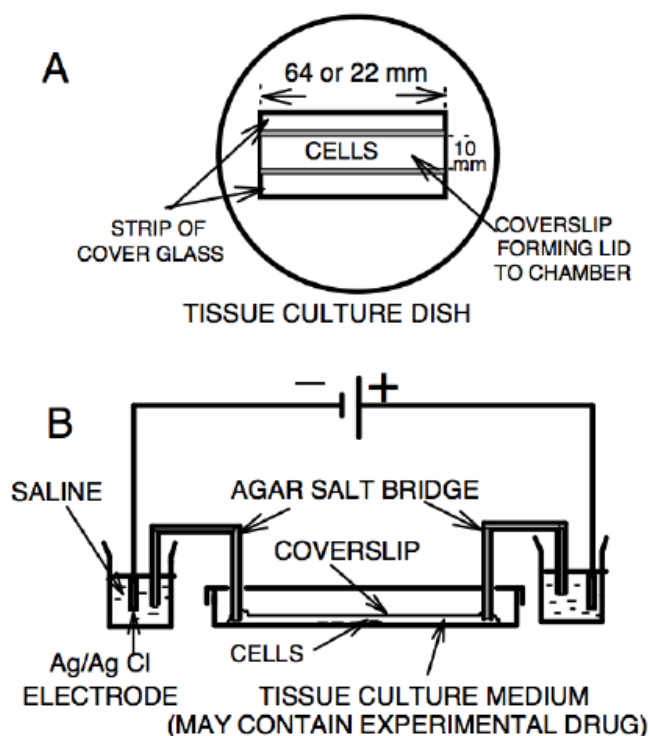


**Figure 1.** Schematic of a glass electrostatic chamber made using cover slips in a petri dish.<sup>3</sup> (A) Above view of electrostatic chamber design. (B) Side-on view of electrostatic chamber connected to agar salt bridges with DC power supply. Ag = Silver, Cl = Chlorine.

### 5. Migratory potential between neural stem cells and glioma stem cells

A migration assay will be used (Boyden chamber) to determine whether neural stem cells are attracted to glioma stem cells or *vice versa*. If results are positive, removing specific genes through genetic knockdown will then be commenced in order to determine what signalling cascades associated with electrotaxis this process relies upon.

### 6. Drug testing to identify new targets that influence electrical current directed migration

Depending on which signalling targets are identified, suitable drugs will be selected for cell culture testing. This will entail treating cells with different concentrations with the drug of interest and determining the effect on cell viability, cell migration and protein expression. This process will permit identification of novel therapeutic targets

### **The potential role of electric fields in glioma stem cell migration as a developmental disease model**

Methods previously described by Aberdeen researchers will be used. In brief, one hemisphere obtained from a rodent brain will be immobilised in artificial cerebrospinal fluid. Labelled human glioma stem cells will then be implanted into the subventricular zone and dentate gyrus. Migration of the stem cells will be assessed with and without an applied electrical field.

### **Experimental work conducted in other research groups**

We have working collaborations with other groups who have similar interests in the role of electric signals, cellular motility and brain tumour stem cells. Where collaboration will be beneficial in advancing this area of research, fully anonymised samples will be sent securely domestically or internationally. Prior to samples being sent, a material transfer agreement (MTA) will be instigated whereby both Aberdeen University and the recipient institute will agree on specific terms of use. This would include the type of experimental work permitted, ownership rights, publication rights, and plans for disposal or return of the samples. Patient consent will be requested for this and information provided in the participant information leaflet.

### **Tissue Bank and future work**

No future work will be carried after the duration of this project. All patient samples and anonymised identifiers will be discarded safely and securely. All electronically stored data matching the samples to patients will be kept securely for a total of 5 years as detailed in the Data Management section.

### **Safety Considerations**

As the research will not affect routine care, no further safety considerations are needed.

### **Data Management**

Patients will be asked specifically to provide consent for access and storage of personal data. Imaging and histology results will be accessed and stored when available on a password protected (128 bit encryption) Excel 2007 spread sheets. For each patient only a unique study identifier and relevant clinical details will be stored on the spread sheet, without a name or any other identifiable information. A separate password protected spreadsheet that contains identifiable information linking the unique study numbers to the patient will only be accessible to the Data Custodian (Mr Pragnesh Bhatt). The former spreadsheets with no identifiable information will only be accessible to the researchers.

We will hold this information for 5 years for the purposes of future studies where a link to clinical data would prove useful. On completion of this study, all secured data will be returned to Mr Bhatt, who

## **Study Protocol Version 7.0**

Dr Jared Ching, Professor Colin McCaig, Mr Pragnesh Bhatt

will maintain secure storage on an NHS Grampian password protected computer. Mr Bhatt will be sole guardian of this data thereafter.

Patient personal data linking samples back to the patient will be important in this study to measure whether correlations between the scientific properties investigated and clinical progression and outcomes. This will be valuable data as it would provide an indication of how clinically useful electric currents may be.

We will hold this information for 5 years for the purposes of future studies where a link to clinical data would prove useful. On completion of this study, all secured data will be returned to Mr Bhatt, who will maintain secure storage on an NHS Grampian password protected computer. Mr Bhatt will be sole guardian of this data onwards.

### **Adverse Events**

There are a number of adverse events that may result from surgery. The following may occur as a result of any routine brain tumour resection requiring a craniotomy: Nausea, vomiting, weakness, visual changes including double vision and loss of peripheral vision, headache, seizures, personality changes, changes in the sensation of balance and reduced co-ordination. These events will not be collected and treated as routine practice.

Serious adverse events (SAEs) may include: Hydrocephalus (build-up of fluid in the brain), stroke, coma, infection, brain swelling, clot in the blood vessels, bleeding, coning (brainstem pushed against skull opening resulting in death). Expected or unexpected SAEs where the level of severity is unexpected will be recorded and reported to the sponsor.

All patients requiring a craniotomy would be expected to stay as an inpatient in hospital after the operation. The need for hospital stay will therefore not be recorded as an event in any of the participants.

### **Expected Outcomes of Study**

It is expected that this project will generate data about the ability of physiological electrical fields to direct glioma stem cell migration. This will provide insight into the pathophysiology of this disease and thus provide potentially new therapeutic targets. We envisage developing a novel treatment modality as a result of this research.

### **Dissemination of Results and Publication Policy**

## Study Protocol Version 7.0

Dr Jared Ching, Professor Colin McCaig, Mr Pragnesh Bhatt

The results of this project will be published in international, peer-reviewed medical and scientific journals. Presentation of this data by members of the research group at national and international conferences would be envisaged.

### **Other Research Activities of the investigators**

Mr Pragnesh Bhatt

Main areas of research

- STITCH II Randomised Controlled Trial
- Neuro-oncology
- Clinical Neurosurgery
- Education in Neurosurgery

Research expertise: Clinical Trials, Observational Studies, Clinical Case Studies.

Professor Colin McCaig

Main areas of research

- The Role of Electrical Currents in Cell Motility
- Electrical current mediated wound healing in cornea and skin
- Spinal cord injury repair using electrical currents
- Electrical currents and cell signalling in breast carcinoma
- Genetic rodent models of Schizophrenia
- Colorectal cancer
- Neurodevelopmental biology
- Electrophysiology

Research expertise and skills: Professor McCaig has published extensively in his areas of interest.

Dr Jared Ching

Main areas of research

- The role of glutamate in gliomas and tumour associated seizures
- Molecular cell biology of gliomas and glioma stem cells
- Brain tumour heterogeneity in Magnetic Resonance Imaging
- Vagal Nerve Stimulation for pharmaco-resistant/multifocal epilepsy

Research skills: Cancer cell biology, Medicinal Chemistry and Observational Clinical Studies.

### **References**

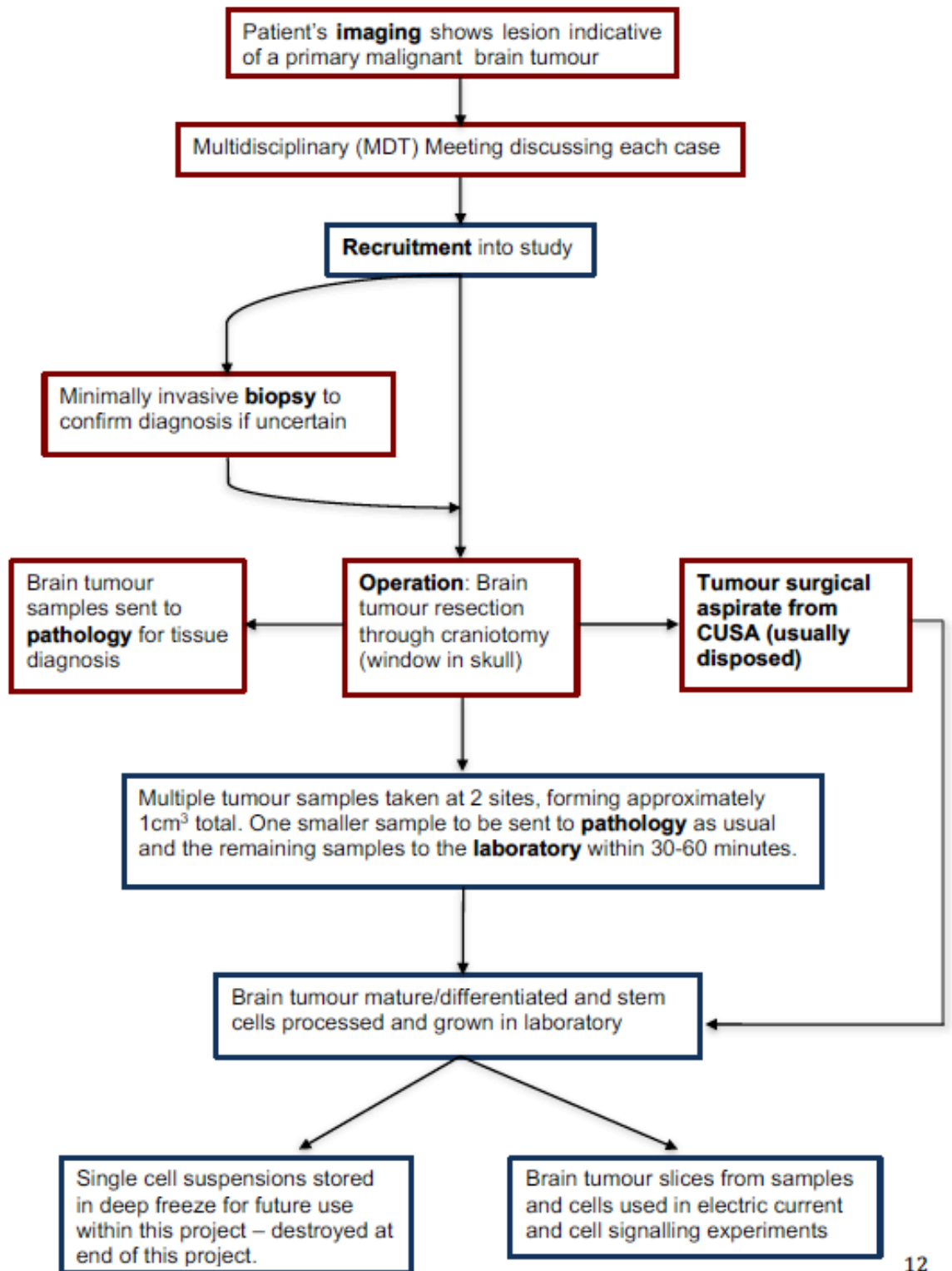
## Study Protocol Version 7.0

Dr Jared Ching, Professor Colin McCaig, Mr Pragnesh Bhatt

1. McCaig CD, Song B, Rajnicek AM. Electrical dimensions in cell science. *Journal of Cell Science*; 2009. p. 4267-76
2. Aboody KS, Brown A, Rainov NG, et al. Neural stem cells display extensive tropism for pathology in adult brain: evidence from intracranial gliomas. *ProcNatlAcadSciUSA* 2000; 97(23): 12846-51.
3. Zhao M, Agius-Fernandez A, Forrester JV, McCaig CD. Orientation and directed migration of cultured corneal epithelial cells in small electric fields are serum dependent. *Journal of Cell Science*; 1996. p. 1405-14.

**Study Protocol Flow Chart**

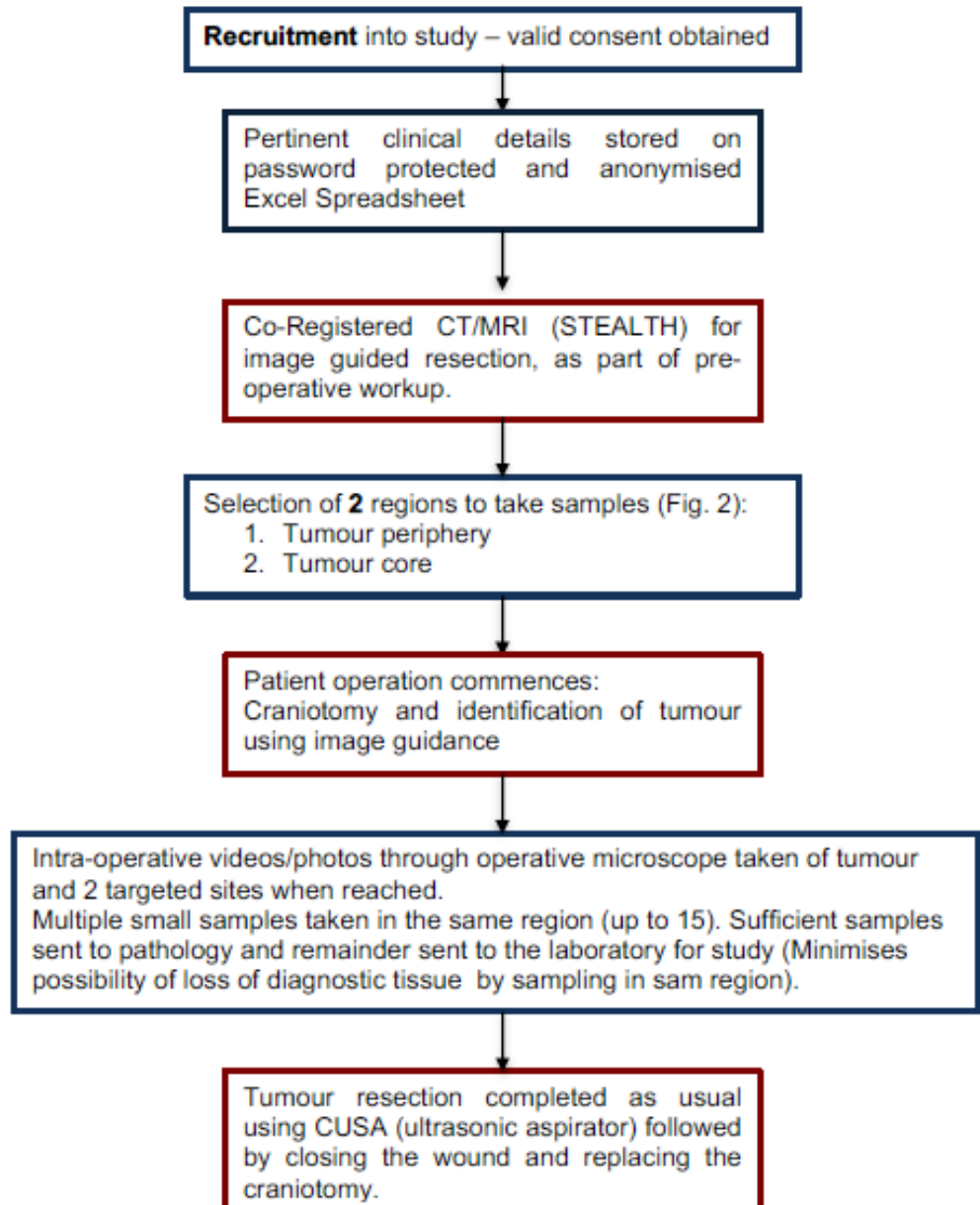
— Study protocol  
 — Usual care





**Surgical Protocol Flow Chart**

— Study protocol  
— Usual care



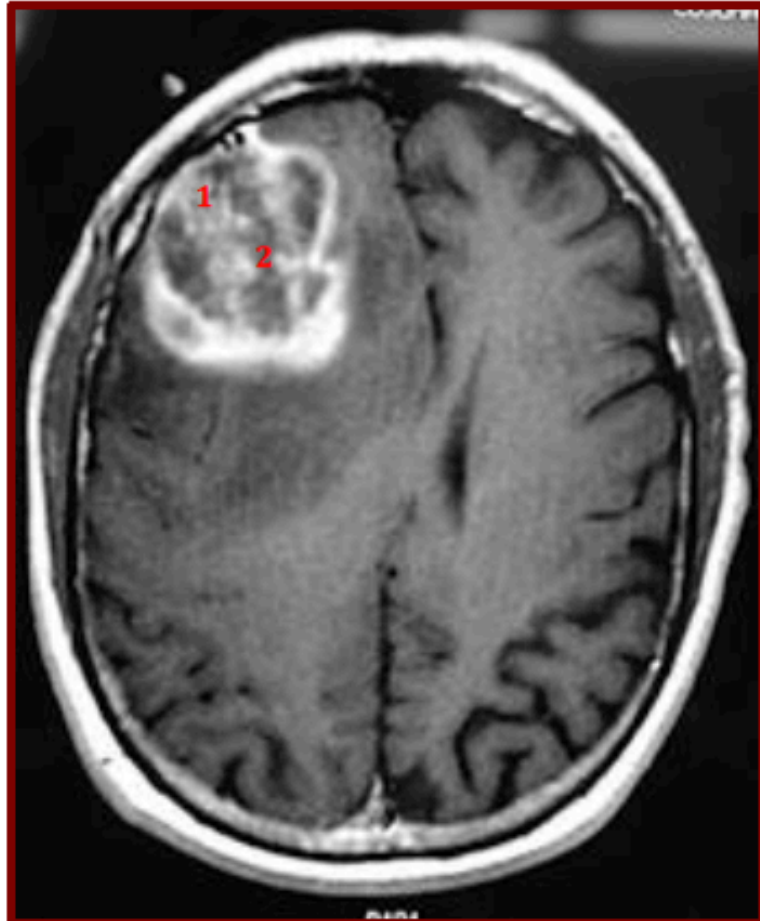


**Figure 2:** Example MRI demonstrating contrast enhancing lesion, a glioblastoma multiforme located in the right frontal region. Numbers are representative of regions for sample resections to be taken. Image downloaded from Google Images.



## PARTICIPANT INFORMATION SHEET

**Study Title:** The Role of Electric Currents and Cell Signalling in Brain Tumours

We are delighted to be able to invite you to take part in this new research project that we hope will help us understand how to treat brain tumours and develop a new way of treating this disease. Please find information about this in the following pages. Please do not hesitate to contact the Department of Neurosurgery if you have any questions regarding this research prior to your operation.

### What is the purpose of the research?

To help us treat brain tumours better, it is important to obtain samples from patients that we may then grow and test in the laboratory. We plan to use these samples to test how electrical currents affect movement of cells and growth of this disease. Another part of this research will be to test drugs that may be used in the future to treat this disease.

We are also interested in how these tumour cells behave in relation to symptoms patients may or may not experience before surgery.

### Do I have to take part?

No – this is entirely your decision. If you decide to take part, you will be guided through a consent form stating that you understand what is involved in participating in the study before being asked to sign it. If taking part, you are free to withdraw from the study at any time without giving a reason.

### What will taking part involve?

We would like to take small samples of your tumour during your operation. We will only take samples that we know are safe to remove. As the aim of the surgery will be to remove as much of the tumour as possible, taking samples does not prolong or change your operation.

In addition we will use the “waste” generated from removing your tumour using ultrasound. This will not affect or change your surgery in any way.

### Is taking samples safe and will it affect my surgery?

Taking samples is always performed to obtain a formal tissue diagnosis. Brain tumours are always removed in a way that avoids removing normal brain. In no way will taking samples affect or change your surgery whatsoever.

### Will you need other samples?

No, we will not need any other samples such as blood or genetic tests.

### Will my samples be stored and used in the future?

No – your samples will only be used for the duration of this study. We will not store your samples for other projects in the future.

### What are the possible benefits of taking part?

There will be no direct personal benefit by agreeing to provide samples for this research project. However, this may benefit others in the future with the same condition as you.

### Will my participation in the study be kept confidential?

All information that we collect will be kept according to confidentiality requirements. Your personal information will not be used for any purpose other than research. In addition, we will anonymise samples so that those working with them will have no means to identify you. **Mr Bhatt, Prof. McCaig and Dr. Ching** will electronically store personal information in the neurosciences ward and laboratory using secure passwords. All



tumour samples will be placed in storage with unique codes that do not contain your name and cannot be linked back to yourself.

In some cases it is useful to send samples to other research groups within the UK or internationally. If we were to send samples in this way, these would be anonymised and would be in no way traceable to yourself. If these samples were not completely used, they would be returned to us or safely discarded.

After our study is complete, we will discard any remaining samples, and require our collaborators to do the same at the end of the study period.

#### **Why does my personal data need to be stored?**

In order to gain an understanding of why different patients with brain tumours show differences in the way they respond to treatments and how we can improve treatments for the individual. As stated earlier, your information will be kept confidential and safe. We will only use data relevant to the study such as your scan results and histology results and ensure that it is not traceable by removing all identifiers including your name and address.

#### **Who is organising and funding the research?**

The research is being organised by Mr Bhatt (Consultant Neurosurgeon), Professor McCaig (Regius Professor of Physiology and Head of School of Medical Sciences), and Dr Jared Ching (Academic Foundation Doctor) who are based at both the Aberdeen Royal Infirmary and University of Aberdeen. Funding will be sought from NHS Grampian and charitable organisations.

#### **Who has reviewed this study?**

The study has been reviewed by the NRES Committees – North of Scotland.

#### **How to complain**

If you have any concerns or complaints you would like to raise about this study, a complaints procedure is available. We recommend first speaking to one of the researchers listed below first and then follow the NHS complaints procedure if the problem is not resolved.

#### **What next?**

If you are interested in participating in the study, a member of the research team will discuss this in more detail when you have arrived in the Department of Neurosurgery before your operation. We will ask you to sign a consent form if you are happy to take part.

**Thank you very much for taking the time to read this information sheet and considering taking part in this study.**

Mr Pragnesh Bhatt  
Consultant Neurosurgeon  
Department of Neurosurgery  
Aberdeen Royal Infirmary  
Aberdeen AB25 2ZD  
Tel: (01224 553453)  
Email: Pragnesh.bhatt@nhs.net

Professor Colin McCaig  
Regius Professor Physiology  
Head of School of Medical Sciences  
Institute of Medical Sciences  
Aberdeen AB25 2ZD  
Tel: (01224 437394)  
Email: c.mccaig@abdn.ac.uk

Dr Jared Ching  
Academic Foundation Doctor  
Honorary Clinical Fellow  
Aberdeen Royal Infirmary, AB25 2ZD  
Tel: (01224 553453)  
Email: jared.ching@nhs.net



## Study Title: Controlling Brain Tumours Electrically (CTBE)

### Protocol: Establishing in vitro cultures from fresh specimens

#### Summary

1. Tissue Culture Hood Preparation
2. Operating Theatre
3. Processing Fresh Tumour Samples in the Laboratory
4. Cell counting, Seeding, Passaging

#### Protocol

##### 1. Tissue Culture Hood Preparation

- a. Start of day when surgery scheduled
  - i. UV Light on for 30 minutes at start of the day before using TC hood
  - ii. While waiting switch on water bath and incubate required media/reagents (Complete DMEM, 0.25% trypsin, PBS)
  - iii. Make sure liquid nitrogen available (Dr. Pu) and sterile Eppendorf tubes
- b. Prior to samples being delivered to laboratory or at the time when samples arrive from operating theatre
  - i. Open hood glass cover, switch on fan, wait for purging process to complete (light switches on)
  - ii. Spray inner surfaces with Presept first and wipe down with blue towel, then immediately spray down inner surfaces with 70% ethanol and wipe down with fresh blue towels.
  - iii. Remove reagents from water bath and spray with ethanol before placing side by side at the back of the tissue culture (TC) hood in the order of use.
  - iv. Spray all equipment prior to placing in TC hood – waste bottle with Presept added to bottom, electric pipette filler, 5 and 10mL pipettes, sterile 1mL Pasteur pipettes, T75 flasks, white topped 25mL tubes, 50mL blue topped tubes, tube rack, autoclaved beaker with forceps, packaged no. 10 scalpel blade, 10cm petri dish (if solid tumour sample being used), cryotubes (from level 6 remember to keep sealed and spray whole packet with ethanol, remove 5 tubes, reseal packet then place outside hood), DMSO (needed to freeze suspensions of cells), spray Gilson P200 and P20 pipette and box of sterile yellow pipette tips.

##### 2. Operating Theatre

- a. Set up

- i. Theatre staff usually take the CUSA trap to send to pathology, make sure to explain we are able to take samples from these traps if a patient has consented.
    - ii. Two ice boxes needed: one to place beneath CUSA trap to maintain a low temperature as tumour aspirate is collected, and the other icebox to keep white topped tubes for solid samples
    - iii. In terms of timing – solid samples should be available first and then CUSA aspirate taken towards the end. If no solid samples are taken, just aim to take aspirate.
  - b. Solid tumour sample
    - i. Solid samples to be taken from central and peripheral regions if feasible – two white topped 25mL tubes with a C and P labelled should be filled with 10-15mL of HBSS and left on ice.
    - ii. One piece of tumour about 1-3cm in diameter placed in HBSS filled 25mL white topped tube on ice. Solid tumour should be taken to the laboratory as soon as possible unless next solid piece can be obtained within 60 minutes, then waiting until second sample can be taken. If there is considerable tumour aspirate available, take all the samples to the laboratory – there is no need to wait for surgery to finish (NB when we start preparing brain tumour stem cells, we will only have a maximum of 60 minutes to return to the laboratory when specimens are given to us).
    - iii. If surgery is prolonged, return back to operating theatre and await for CUSA aspirate sample to be ready.
  - c. CUSA aspirate
    - i. Ensure throughout surgery the CUSA trap is immersed in ice (use ice box placed on a small chair or whatever can elevate it to the level of the CUSA trap).
    - ii. Before the end of surgery ask theatre staff to remove trap and close with sterile technique, as much is feasible, with the solid lid.
    - iii. Carry sample on ice to laboratory
3. Processing Fresh Tumour Samples in the Laboratory
  - a. Solid Surgical Tumour Specimens
    - GBM tumour is then placed in appropriately sized falcon tube containing DMEM containing 10-15% penicillin/streptomycin.
    - Tube is placed on ice and taken to Laboratory 2.47 at the IMS and sprayed with ethanol before being placed under a sterile hood.
    - Ensure 0.25% Trypsin-EDTA is prewarmed at 37°C in water bath for 2.5 minutes.
    - Place GBM tumour tissue in sterile Petri Dish using forceps.

- Divide sample into half and use forceps to place in sterile Eppendorf and snap freeze in liquid nitrogen (If not available immediately, place half specimen in original trap with HBSS and leave on ice until arrives).
  - Wash tissue sample 3 times using 5ml of HBSS to remove blood and debris (use sterile 10mL pipette to transfer HBSS onto specimen without touching it, if in doubt use new sterile 10mL pipette for each wash).
  - Using a No. 10 scalpel blade to cut GBM tumour tissue into tiny pieces. Mince in both the horizontal and vertical planes for 2-3 minutes.
  - Transfer minced tissue into a 50mL falcon tube then add 3-5ml (depending on amount of tissue available – aim to immerse the tissue in trypsin) of pre-warmed trypsin 0.25% and incubate for 2-3 minutes – flick vigorously every 30 seconds to disperse tissue.
  - Enzymatic Trypsin reaction is halted by addition of an equivalent volume of complete DMEM.
  - The suspension is then triturated using 10mL pipette (up and down until milky suspension forms, at this step 6 times as for cell culture will not be sufficient) to ensure trypsin inactivation.
  - The suspension is centrifuged at 800rpm (110g) for 5 minutes until pellet is formed.
  - Discard supernatant fluid and resuspend tissue pieces in 1ml of sterile DMEM.
  - Triturate about 6 times (but triturate more if needed) until a smooth milky single cell suspension is achieved.
  - Undissociated pieces and debris are removed by adding 10-15ml of DMEM to the tube and filtering the resulting suspension through a 40-micron cell strainer into a 50ml tube. Ensure to pipette underside of filter to capture any lost cells.
  - Centrifuge at 800rpm (110g) for 5 minutes and discard supernatant fluid.
  - Re-suspend pellet in 1-2ml of complete DMEM. Continue to cell counting.
- b. CUSA Aspirate
- Sterilise outside of CUSA trap with ethanol then place in TC hood
  - Pipette 20 mL of complete DMEM to the inside of the trap. Use sterile forceps break apart and scrap any hard cells. Add the resultant HBSS to a 50mL falcon tube.
  - Centrifuge at 200g for 10 min at room temperature (Gomez & Kruse, 2004). Discard the supernatant.
  - Add 2-3 mL trypsin to the pellet and triturate until milky suspension. Incubate for 2 min in the water bath. Tap vigorously every 30 seconds.
  - Add 15 mL of DMEM to quench trypsin activity.



- Re-suspend the pellet in 10 mL of complete medium and filter this cell suspension through a 40-micron cell strainer into a 50ml tube (Fael Al Mayahani et al., 2009; Mullins et al., 2013).
- The filtered suspension is centrifuged at 800rpm (110g) for 5min. The supernatant is discarded (Azari, Millette, Ansari, Rahman, Deleyrolle, & Reynolds, 2011).

#### 4. Cryofreezing, Cell counting, Seeding, Passaging glioma cells

##### a. Cryofreezing

Cells suspended in growth medium DMEM are mixed with an equal volume of ice-cold, heat-inactivated foetal calf serum (1.5 mL) containing 15% of DMSO. For highly confluent T75 flask, re-suspend in 2ml and then aliquot 0.5ml into four cryotubes (Pollard, et al., 2009). Freeze in cryogenic vials using a Cryomatic Cellevator (L.A.O Enterprises, Gaithersburg, MD) suspended above the liquid nitrogen (Gomez & Kruse, 2004).

##### b. Cell counting

- Pipette 50 $\mu$ L of Trypan blue in a 1ml Eppendorf tube.
- Add 50 $\mu$ L of the cell suspension (mix the original suspension by trituration) to the 1ml Eppendorf tube.
- Triturate suspension for adequate mixing.
- Transfer 10 $\mu$ L of cell/Trypan blue mixture to haemocytometer for cell counting – cells that take up the dye are dead, do not include this in your count.
- Equation:
  - Average of four outer quadrants  $\times 2 \times 10^4 =$  no. of cells / mL
- After counting, add required volume of cells to T75 flask and make total volume up to 20mL.
- Flask should then be placed at 37°C in 5% CO<sub>2</sub> incubator, DO NO spray flask as the lid has a vented lid – ethanol can get into the cells.

##### c. Passaging

When cells become about 70-75% confluent, rinse the attached cells with PBS (previously warmed in water bath for 30-60 min), aspirate and discard (Pollard, et al., 2009). Then add 2-4 mL of 0.025% trypsin-EDTA in PBS (previously warmed in water bath for 30-60 min) and return the flask to the incubator for at least 2 minutes (no longer than 5 mins), until the cells detach. Tap the side of the flask against a bench to assure the cells will dislodge (Pollard, et al., 2009).

When the cells are detached from the flask, add 10 mL of cell culture medium (previously warmed in water bath for 30-60 min) to suppress the trypsin activity and pipette

up and down, washing against the culture surface. Transfer the content to a centrifuge tube and centrifuge the cells for 3 mins at 300g. Discard the supernatant and replace with 10 mL of fresh culture medium to re-suspend for cell counting in haemocytometer (Gomez & Kruse, 2004; Pollard, et al., 2009).

Transfer the cell suspension equally to several flasks (4-5 flasks) (Di Tomaso et al., 2000) at a density of  $1.5-2 \times 10^6$  cells per flask. Culture cells in fresh culture medium.

## References

Azari, H., Millette, S., Ansari, S., Rahman, M., Deleyrolle, L. P., & Reynolds, B. A. (2011). Isolation and Expansion of Human Glioblastoma Multiforme Tumor Cells Using the Neurosphere Assay. *Journal of Visualized Experiments* .

Di Tomaso, E., Pang, J. C., Ng, H. K., Lam, P. Y., Tian, X. X., Suen, K. W., et al. (2000). Establishment and characterization of a human cell line from paediatric cerebellar glioblastoma multiforme. *Neuropathology and Applied Neurobiology* , 26, 22-30.

Fael Al Mayahani, T. M., Ball, S. L., Zhao, J., Fawcett, J., Ichimura, K., Collins, P. V., et al. (2009). An efficient method for derivation and propagation of glioblastoma cell lines that conserves the molecular profile of their original tumours. *Journal of Neuroscience Methods* , 176, 192-199.

Gomez, G. G., & Kruse, C. A. (2004). Isolation and Culture of Human Brain Tumor Cells. In: S. P. Langdon (Ed.), *Cancer Cell Culture - Methods and Protocols* (pp. 101 - 109). Totowa, NJ: Human Press Inc.

Mullins, C. S., Schneider, B., Stockhammer, F., Krohn, M., Classen, C. F., & Linnebacher, M. (2013). Establishment and Characterization of Primary Glioblastoma Cell Lines from Fresh and Frozen Material: A Detailed Comparison. *PLOS ONE* , 8 (8).

Pollard, S. M., Yoshikawa, K., Clarke, I. D., Danovi, D., Stricker, S., Russell, R., et al. (2009). Glioma Stem Cell Lines Expanded in Adherent Culture Have Tumor-Specific Phenotypes and Are Suitable for Chemical and Genetic Screens. *Cell Stem Cell* , 4, 568-580.

Once ethical approvals were in place, I submitted an application to NHS Endowments and was successful in obtaining £7,300 as Co-Investigator with Professor Colin McCaig. Alongside this, I established a collaboration with Professor Michael Linnebacher, University of Rostock, Germany, who kindly gifted a number of primary cell lines that were established in his laboratory and published.<sup>539</sup>

Once I had sourced all necessary reagents, I established protocols for culturing both primary and frozen cell lines (from the University of Rostock). I subsequently taught these techniques to medical students who worked on this project and supervised them in collaboration Professor McCaig's Group in collecting data. I was awarded a "Science Without Borders" bursary to supervise an international Medical Student from Brazil, Natalia Curcio, who completed a short project under my supervision. I supervised a final year medical student at the time, Dr. Hannah Clancy, who took this project further by spending her elective time and beyond collecting data alongside Postdoctoral Fellow Dr. Michal Pruski. Dr Clancy and Dr Pruski are the first and second named authors on the paper we have submitted, where the methods I established are described. The electroaxis assays were set up as described in Chapter 6. My plan to isolate primary GBM cells from local patients was unsuccessful. Although I was able to recruit 6 patients, cell growth in culture proved to be very unreliable. As such we focused on using the cell lines from the University of Rostock.

### ***Nature of Work***

This project was based on my own research proposal that I had prepared based on my accumulated knowledge at the time. I completed an ethics application via

the IRAS, gaining approvals to obtain primary brain tumour samples from patients to use in electrotaxis experiments. I was subsequently awarded a competitive grant from NHS Endowments of £7,300 as Co-Investigator with Professor Colin McCaig. I established local protocols for brain tumour tissue collection from the Department of Neurosurgery, Aberdeen Royal Infirmary and laboratory protocols to isolate primary GBM cells from this tissue. I subsequently supervised a number of students, teaching them the necessary techniques including: cell culture, electrotaxis chamber preparation, time lapse microscopy, fluorescent microscopy and analytical techniques. Under my supervision, Hannah Clancy has recently completed preparation of the manuscript pertaining to this work as first author, having presented the preliminary data as a poster presentation at the British Neuro-Oncology Society Meeting.

### ***Significance of work***

The original article has been accepted by the journal *Experimental Cell Research* (3.90). The preliminary data was presented at the British Neuro-Oncology Society Meeting as a poster presentation with the conference abstract published in the journal *Neuro-Oncology* (Impact Factor 10.24). This work provided the first evidence that differentiated and stem like GBM cells derived from the same primary cell lines have opposing electric field biases. These findings have possible clinicopathological implications for tumour recurrence and may be targeted in the future as a therapeutic strategy to prevent tumour invasion, migration and recurrence. Recently, our collaborators at Rostock University confirmed our findings using similar cell lines and inhibitors of EGF and Akt, showing a reduction in directed cell migration. This has provided further validation

of our findings, indicating the need to study electrotaxis in preclinical models of glioblastoma for future potential therapeutic use.<sup>540</sup>

### ***Critical appraisal of published work***

This study provides robust evidence of electrotactic responses of glioblastoma cells in the differentiated and glioma stem cell transition state, derived from the same primary cancer cell lines. The key data presented in this paper are from in vitro experiments of electrotaxis and do not include ex vivo or in vivo data. To critically confirm the results of this work, it would be necessary to investigate the role of electric fields in animal models of glioblastoma. Until such preclinical work is undertaken, it would not be feasible to consider human trials for novel treatments that chemically or surgically manipulate glioblastoma cell electric field migration. The results of this work have been independently validated by Lange et al., however their data is confirmed to in vitro experiments.<sup>540</sup>

## **Chapter 8: General Discussion and Conclusions**

The range of topics in this thesis include a number of neurological diseases that are interrelated in different ways but highlight the need for cross pollination between fields in order to develop promising new therapeutic targets. Refractory epilepsies, for example, share some characteristics with tumour associated seizures, although the underlying pathologies may differ, their pharmacotherapy strategies can be similar at present. Preterm infant brain injuries involve neurotransmitter and inflammatory cascade dysfunction, as does stroke and malignant brain tumours, indicating that certain common pathways may be targetable. Thus, combinatorial treatment that is tailored to each disease state that targets multiple specific features of a disease may result in more effective or even definitive therapies in the future. Further, neural stem cells are known to have a distinct tropism for glioblastoma cells, making neural stem cell and glioma stem cell migration a potentially promising field to gain an understanding of how migration can be exploited for therapeutic purposes for example. Neuroblasts arising from the subventricular zone (SVZ) are also known to have a tropism for sites of brain injury, which has been manipulated in preclinical models to induce functional repair of injured sites in the mature and neonatal brains, making this a further promising therapeutic strategy for stroke and neonatal brain injury. Electric fields have been found to play an important role in neuroblast directed migration, where it has been shown applied exogenous electric fields can manipulate their migration, and in theory to sites of injury in both stroke and preterm brain injuries. As such the aims of this chapter are as follows:

- Integrate the therapeutic concepts between each chapter to highlight potential and emerging therapeutic targets
- Discuss the future directions of therapeutic approaches in the neurological diseases presented in this thesis

### ***Thesis integration***

#### *Vagal nerve stimulation (VNS)*

VNS has become an important treatment for medically refractory epilepsy that has undergone refinements over the years and continues to be optimised as discussed in Chapter 1. Although the mechanisms of action of VNS remain incompletely understood, there is evidence that VNS elicits anti-convulsant effects via afferent stimulation that leads to noradrenaline (NA) and 5-hydroxytryptamine (5-HT) firing via the locus coeruleus, both of which are known to have anticonvulsant activity. Tumour associated seizures (TAS) are thought to be predominantly driven by glutamate excess in the peritumoural region, resulting in excitotoxicity and abnormal neuronal firing. As TAS is commonly drug resistant, it may be advantageous to consider VNS, which is indicated in drug resistant forms of epilepsy, as an adjunctive treatment prior to more invasive options such as resective surgery or repeat surgery. This concept has been examined in a small retrospective study including 16 patients with TAS, finding a mean 41.7% reduction in seizure frequency.<sup>541</sup> These authors reported no significant adverse effects from VNS treatment in patients with TAS, which is highly beneficial to optimising the quality of life of patients with high grade gliomas who have a very poor prognosis of approximately 1.5-2.0 years. However, as alluded to previously, lower grade gliomas are more commonly associated with TAS and therefore would enjoy a better quality of life with years of seizure freedom or

reduction of frequency with VNS. Further, pharmacological treatments commonly have a side effect profile that may be avoided by either considering VNS as a primary treatment or if VNS is used initially, and anti-epileptic therapies can then be tapered over time. It has also been shown that low grade gliomas are associated with neurocognitive decline, which has been shown to be associated with depression.<sup>542,543</sup> As VNS has been FDA approved for depression since 2005, it would not be inconceivable that this may also benefit patients with TAS who also suffer from neurocognitive decline and depression, which more likely would occur in low grade gliomas, but can be present in high grade cases too. Therefore, in the future, optimal glioma treatment may incorporate multiple interventions that address numerous aspects of the disease, not restricted to cytoreduction through chemotherapy, radiotherapy and surgery, but also implantable devices such as VNS that can augment the complications of gliomas including seizures and neurocognitive sequelae.

Whilst VNS has not been utilised for preterm brain injury, it has been used for complications associated with preterm birth and there is emerging data for its use in cerebral palsy, a common clinical manifestation later in life of preterm brain injury. Preterm neonates who may also have suffered from brain injury, have a higher incidence of oral feeding dysfunction that requires placement of a gastric tube for feeding.<sup>544</sup> Preterm infants that reach 40 weeks gestational age and fail feeding rehabilitation will need surgical implantation of a gastric tube, which can also result in further motor developmental delay.<sup>545</sup> A recent open label study investigating the role of transcutaneous auricular VNS (taVNS), non-invasive form of VNS, with bottle feeding rehabilitation found a significant improvement in feeding volume trajectories with possible improvements in oromotor



dyscoordination and fewer implanted gastric tubes on hospital discharge.<sup>546</sup> Further, there is a growing body of evidence that indicates VNS may have a beneficial role for cerebral palsy.<sup>547</sup> Paediatric patients implanted with VNS for epilepsy secondary to tuberous sclerosis, also exhibited greater improvements in cognitive and neuropsychologic domains. As cerebral palsy is known to disrupt sleep, VNS may have further benefits in regulating cognitive function, including language, resulting in an improved quality of life as was previously shown when treating paediatric patients with drug resistant epilepsy.<sup>548</sup> Again, these therapeutic effects may be mediated by NA and 5-HT, and although are known to promote the wake pathway, VNS dosing can be adjusted accordingly.<sup>549</sup> In the future, the role of VNS in the sequelae of preterm brain injury may become more widespread, particularly as taVNS has emerged as a minimally invasive alternative but will need further studies to elucidate its mechanisms of action optimal dosing.<sup>550</sup>

In the field of stroke medicine, VNS has been shown in a randomised controlled trial (NCT03131960) to have significant improvements in impairment and function of the upper limb when combined with rehabilitation compared to sham treatment.<sup>551</sup> This trial was carried out on the basis of preclinical work carried out on rodent models of stroke. Notably, Khodaparast et al found that upper limb strength could be recovered to baseline levels when VNS was delivered during rehabilitation training.<sup>552</sup> The same authors had demonstrated previously that VNS drives efficient plasticity of the motor cortex when combined with motor training.<sup>553</sup> The underlying mechanism of this may be related to the established role of NA to promote neural plasticity, which is known to work synergistically with acetylcholine, for which VNS is almost known to engage.<sup>554</sup>

### *Glutamate transporter mutations*

The role of genetic screening for mutations in glutamate transporters to stratify preterm infant risk for brain injury has yet to be established. Whilst common genetic variations in EAAT2 expression are associated with cerebral palsy and neurodevelopmental delay<sup>555</sup>, replication in larger sample with genome-wide designs and comparisons between preterm and term brain injuries would be required before validating this a biomarker for poorer neurological outcome. Further, prospective studies with a complete recruitment that included non-survivors, would be needed to make these results widely applicable. The existence of such genetic variations in glutamate transporters raises the possibility of treating preterm infants prone to poorer neurological outcomes, treatment that can mitigate glutamate mediated excitotoxicity. While there are no new promising drug candidates to improve glutamate uptake in the preterm population, a current licensed medication known to enhance glutamate transporter expression is the antibiotic ceftriaxone, which is safe for use in preterm infants.<sup>556</sup>

In the field of stroke medicine, from which Rajatileka et al. were inspired<sup>555</sup>, Mallolas et al. identified novel polymorphisms in the EAAT2 promotor region and found higher plasma glutamate levels with worse neurological outcomes post-stroke.<sup>209</sup> However, since these findings, there have been no further studies examining or validating it as a biomarker for neurological outcomes. The potential clinical benefit of undertaking such testing is that it could inform clinicians and

patients about the prognosis following their stroke and help inform rehabilitation efforts.

As glutamate is the predominant excitatory neurotransmitter in the brain, glutamate transporter function can incite or augment epileptiform activity.<sup>557</sup> EAAT2 expression is known to prevent epilepsy, where knockout and overexpression experiments have shown increased seizure activity and reduced chronic seizure frequency, respectively.<sup>558</sup> However, there have been no studies to date examining the correlation between epilepsy and genetic mutations in EAATs in humans. Therefore, it is unknown whether polymorphisms that have been found in stroke patients and preterm infants, have any correlation to epilepsy susceptibility. Practically, it may be difficult to undertake such a study as the variety of epilepsies are large with numerous underlying causes. Epilepsy caused by ion channel mutations, for example, may be further augmented if EAAT polymorphisms are present, causing raised glutamate mediated firing that results in worsening seizure severity.

To date, mutations of EAATs in glioblastoma cells have yet to be identified, which is in stark contrast to the 55 mutations detected in ion channels that were found to affect 90% of samples studied in a genomic analysis by Parsons et al.<sup>559</sup> However, as it is known that human glioblastoma cells have reduced EAAT2 expression and increased systemic  $x_c^-$ , there would be a limited role in screening for EAAT mutations as this would not help guide prognostication or further treatment.

*Manipulating glutamate transport*

Since glutamate plays a pivotal role in excitatory neurotransmission and in excess causes excitotoxicity, there has been significant interest in mitigating its damaging effects through increasing transport. Glutamate transport dysfunction has been implicated in all the diseases examined in this thesis, including epilepsy, neonatal brain injury, stroke, malignant brain tumours and tumour associated seizures. In addition, glutamate transport dysfunction has been correlated with numerous other CNS conditions including Alzheimer's disease, Parkinson's disease, Huntingdon's disease, multiple sclerosis, amyotrophic lateral sclerosis, and spinocerebellar ataxia.<sup>560</sup> As it is known that the majority of neuronal glutamate uptake is elicited by EAAT2, the majority of pharmacotherapies have targeted this subtype rather than EAAT1 or EAAT3-5. Such drug treatments that increase expression of EAAT2 include dexamethasone, corticosterone, retinol, valproate, minocycline, amitriptyline, tamoxifen and ceftriaxone.<sup>561</sup> Valproate, an established anti-epileptic drug, has been in use for around 60 years and is known to have multiple possible mechanisms of action, including increasing GABA levels and inhibition of voltage gated ion channels.<sup>562</sup> Valproate has also been found to increase the expression of EAAT2 and enhance glutamate levels, such that it has neuroprotective properties and mitigates excitotoxic damage.<sup>563,564</sup> As mentioned earlier, the antibiotic ceftriaxone is known to upregulate glutamate transporters through transcriptional activation and afford neuroprotection.<sup>556,565</sup> Dexamethasone is a potent steroid commonly used in the treatment of cerebral oedema associated with glioblastoma where secondary seizures may be controlled with this drug.<sup>566</sup> Dexamethasone is also known to induced EAAT2 protein expression and be neuroprotective in hypoxic-ischaemic injury in the neonatal rat brain.<sup>567</sup> These examples demonstrate the possibility of taking advantage of multiple targets

elicited by single drug molecules. In a similar vein, part of my goal of investigating pioglitazone was to take advantage of its numerous downstream effects including as an anti-inflammatory, anti-neoplastic agent and effect on upregulating EAAT2 expression such that multiple pathways of glioblastoma could be targeted in addition to its potential to mitigate tumour associated seizures caused by glutamate excess at the peritumoural region. Such a multi-target approach with a single drug molecule can be exploited as a powerful treatment that also limits the number of potential side effects compared to a polypharmacy approach. However, translating these treatments into promising drug candidates is not without numerous challenges as altering EAAT2 expression levels can be inadvertently widespread and be an intrinsic risk for complications.<sup>568</sup> Furthermore, a number of the targeted mechanisms underlie the expression of other genes, such that transcriptional or translational modulators can induce off-target effects beyond the glutamate system. Finally, treatments that target EAAT2 expression may not be suitable for acute conditions such as ischaemic stroke, but rather prophylactic therapies or where a condition such as tumour epilepsy is being treated.

There have been a number of compounds that have been identified that can modulate the transporter activity of EAAT2, as opposed to its expression, including riluzole, guanosine, nicergoline, MS-153, parawixin1 and GT949/GT951.<sup>561</sup> Riluzole is a sodium channel blocking benzothiazole anti-epileptic drug that has also been shown to reduce excitotoxicity and neurodegeneration via a number of mechanisms, including enhancing glutamate transport.<sup>569</sup> In both cortical and striatal astrocytes, riluzole has been shown to increase glutamate uptake and further shown to be neuroprotective when

excitotoxicity is induced in vivo.<sup>570-572</sup> Presently, riluzole is FDA approved for the treatment of amyotrophic lateral sclerosis and may be a possible drug candidate for treating pathologies involving an underlying mechanism of excitotoxicity. A further glutamate transporter enhancer is guanosine, that has been shown to be effective in rodent models of cortical ischemia.<sup>239</sup> These and the aforementioned compounds are not highly specific in their mechanism of actions, such that they induce off target effects that can lead to unwanted side-effects and thus limit their widespread use. An important goal of any novel therapy is to aim for a single mechanistic target with the least or no side effects associated and maximal efficacy for the targeted indication. However, using novel drug molecules or even altered moieties based on an established drug backbone, can lead to long and protracted drug development delays before reaching the market (usually at least a decade) because they have to be treated as a completely new drug. Therefore, investigating established drugs with licenses for other indications could lead to shorter approval times as the side-effect profile will have already been established.

Targeting the system  $x_c^-$  has also drawn interest in recent times, where Nehser et al. developed structural analogues of sulfasalazine.<sup>573</sup> These authors found that novel aryl-substituted amino-naphthylsulfonate analogues inhibit system  $x_c^-$  more potently than sulfasalazine in vitro, with evidence to suggest that these molecules interact with the same or proximal inhibitory binding sites. For the aforementioned reasons, studying an established drug, such as sulfasalazine with a long-term track record of safety in treating ulcerative colitis, Crohn's disease and rheumatoid arthritis, reduces the risk of developing novel drugs that could have significant adverse effects. As sulfasalazine has been FDA approved

for a number of years and is an established inhibitor of system  $x_c^-$ , it is a highly relevant drug from which to develop novel treatments.

Recently, a novel strategy to reduce neural glutamate levels has been described whereby mesenchymal stem cells (MSCs) were transfected with EAAT2-encoding cDNA and shown to subsequently express functional EAAT2.<sup>574</sup> These MSCs were then shown to uptake glutamate in vitro and when administered to rodents with induced neural ischaemia, indicating a possible new therapeutic strategy for modulating glutamate transport. This recent development is an example of applying EAAT2 expression in a cell based therapy, such that the glutamate transport is carried out in cells that are transported through the central nervous system (CNS), rather than by altering EAAT2 expressions within the CNS cells. This potentially overcomes some of the disadvantages described earlier with systemic drug treatment, including widespread changes in EAAT2 expression and off-target drug effects. Other avenues that can be explored within this include the application of induced pluripotent stem cells (iPSCs) that may be transfected with EAAT2 for example. Depending on the condition being treated, for example if tumour associated seizures where acute treatment is not as important as stroke, iPSCs can be derived from the patient and prepared in the laboratory before administration. This may afford the advantages of autograft as opposed to allograft transplantation.

#### *Advanced neuro-imaging*

Since the first CT and MRI images in the 1970's, neuroimaging has continued to advance at a rapid rate.<sup>575</sup> The development of different MRI sequences has led to multi-model imaging and the refinement of identifying histological correlates

from imaging in order to optimise radiotherapy and surgical treatments. Characterising malignant brain tumours with neuroimaging has seen significant advancements in enabling surgical and radiotherapy planning and even guiding intraoperative resections using 3-dimensional reconstructions of CT and MRI brain scans (StealthStation surgical navigation system, Medtronic). In contrast to brain tumours, epilepsy disorders often do not have a physical abnormality that is causative. In the case of tumour associated epilepsy, part of the tumour is the nidus for epileptogenesis and as described earlier, NMR spectroscopy can be used measure glutamate levels, however it is now emerging that radiotracers used in positron emission tomography (PET) can potentially identify the epileptogenic component of a brain tumour.<sup>576</sup> For example increased  $\alpha$ -[<sup>11</sup>C]methyl-L-tryptophan (AMT) uptake detected by amino acid PET imaging in tuberous sclerosis and cortical developmental malformations have been highly correlated with electroencephalogram (EEG) data, indicating that amino acid PET can detect epileptogenic foci without any additional investigations necessary. However, there is little imaging available on tumour associated seizures, it would could be a powerful imaging modality, particularly if combined with multi-modal MRI. The technique of proton magnetic resonance spectroscopy (<sup>1</sup>H-MRS) using chemical exchange saturation technique (CEST) at 7 Tesla (7T) can measure glutamate levels accurately and has been quite recently shown to lateralise epileptic foci in patients with temporal lobe epilepsy.<sup>577</sup> Whilst the number of patients studied to date is small, this is an emerging area of research in high resolution MRI at the 7T level, where glutamate CEST quantification may be invaluable in elucidating the epileptogenic areas of the peritumour to optimise treatment.



Patients with drug resistant epilepsy currently undergo multimodal structural and function imaging for surgical planning. Conventional 3 Tesla (3T) MRI, 18-fluorodeoxyglucose positron emission tomography (FDG-PET), single photon emission computed tomography (SPECT) and magnetoencephalography (MEG) are all undertaken as standard neuroimaging. In combination with EEG, it is not possible to localise the seizure focus in a large proportion of patients and despite this, 87% of patients will have abnormally histology following surgical resection.<sup>578</sup> Furthermore, the ILAE published official recommendations for MRI sequences in epilepsy, including 3D millimetric T1-weighted images, fluid-attenuated inversion recovery (FLAIR) images, and 2D submillimetric coronal T2-weighted images.<sup>579</sup> Despite this standardisation, there are still patients who have completely normal MRI images despite presenting with epilepsy, indicating a further need for more advanced neuroimaging to understand any structural defect that can be targeted. One newer structural MRI sequence that has shown some promise is double inversion recovery (DIR) for detecting temporal lobe and extratemporal focal epilepsies.<sup>580</sup> Advanced diffusion imaging is an emerging field that has provided new insights into neurological and psychiatric disease, including epilepsy. Multi-shell protocols of diffusion MRI include diffusion kurtosis imaging (DKI), q-space imaging (QSI), restriction spectrum imaging (RSI), and neurite orientation dispersion and density imaging (NODDI), which have all provided brain microstructural details.<sup>580,581</sup> NODDI has been shown to demonstrate reduced neurite density in temporal lobe epilepsy foci.<sup>580</sup> Multimodal imaging by combining MRI and FDG-PET has been shown to improve visual detection of epileptic foci, indicating that combining advanced modalities such as NODDI with conventional imaging can enhance the diagnostic yield in treatment resistant epilepsy and potentially tumour associated epilepsy.<sup>582</sup> The highest resolution

MRI available is 10,5 Tesla (10,5T) at present, however the role of 7T has yet to be firmly established as the diagnostic gains over conventional 3T or 1.5.T have been variable and not proven in epilepsy.<sup>583</sup> Although some of the aforementioned imaging modalities and sequences show promise of providing more detailed diagnostic information that could guide more accurate treatment, little is known about the long term efficacy of these methods and caution should be practiced until more robust long term data is available to verify these findings on improving long term outcomes for patients with treatment resistant epilepsy.

Neuroimaging in the preterm infant plays an important role in the diagnosis, monitoring and treatment of brain injuries including cystic white matter injury and germinal matrix-intraventricular haemorrhage. The American Academy of Pediatrics (AAP) recommends cranial ultrasound is used first line in screening pre-term infants and subsequently detection of brain injury in the neonatal intensive care unit.<sup>584</sup> However, the AAP has taken into account the emerging role of MRI in preterm infants to characterise more subtle brain injury that cannot be elucidated by ultrasound, where this can have a role in neurodevelopmental prognostication for the patient's family over the next 2 decades. As discussed in Chapter 5, DWI can detect water movements in the brain and it has also been shown to effectively image white matter and grey matter maturation by assessing water diffusion properties in voxel reflecting brain microstructures.<sup>585</sup> Developmental milestones can be characterised by DWI, for example, the early cortical plate is initially anisotropic due to the radial orientation of glia and apical dendrites, however, becomes isotropic at term age due to dendritic arborisation.<sup>585</sup> It is also possible to detect damage of grey matter and white matter tracts with DWI in preterm infants, for example in a prospective study

examining very low birthweight preterm infants with high grade brain injury, altered fractional anisotropy was found in the internal capsule, cingulum, and corpus collosum.<sup>586</sup> In the future it may be possible to fully characterise the microstructural changes of brain injury in preterm infants, which can have implications for prognostication and emerging treatments that may be individualised to the extent of pathology.

### *Neural stem cells*

As described earlier, there are currently a variety of treatments for the different forms of epilepsy that range from medications to invasive surgery. In recent times the possibility of cell-based replacement therapies has emerged given the growing evidence that neurogenesis is affected in animal models of epilepsy, resulting in depletion of the neural stem cell niche.<sup>587,588</sup> Of the two neural stem cell niches in the brain, the subgranular zone (SGZ) of the hippocampal dentate gyrus is frequently affected by epilepsy.<sup>589</sup> Neurogenesis of the subventricular zone (SVZ), however, has also been shown to be altered in prolonged seizures in rodent models, such that there is increased neurogenesis within the SVZ, increased migration of neuroblasts along the RMS and diversion of neuroblasts outside the RMS.<sup>590</sup> As previously discussed, the potential to divert neuroblasts to sites of brain injury, such as stroke, emerged as a potential novel therapeutic target. However, as the brain lesions in epilepsy are less well circumscribed and tend to affect the hippocampus more commonly, neural precursor cells in the SGZ have attracted more interest for cell-based therapies in epilepsy. For example, medial ganglionic eminence (MGE) precursor cell engraftment into the hippocampus derived from human-induced pluripotent stem cells have been shown to reduce the frequency of spontaneous seizures through a reduction in

interneuron loss and abnormal neurogenesis.<sup>591</sup> Other approaches include the use of microRNAs that modulate aberrant neurogenesis to reduce seizures and extracellular vesicles derived from MSCs that are delivered intranasally and reach the hippocampus to elicit anti-epileptic effects.<sup>592</sup> While these approaches show promise in animal models, they have yet to be translated into therapies for human use. However, it is clear that manipulation of stem cell niches or transplantation of neural stem cells may be on the horizon as either a primary or adjunct treatment in epilepsy and in particular, drug-resistant epilepsies.

In a similar vein to the potential role of neuroblasts derived from the SVZ in treating stroke, neuroblasts may have a potential therapeutic role in neonatal brain injury. Recently, it has been shown that radial glia persist in the injured postnatal brain and act as a scaffold for SVZ derived neuroblasts to migrate to the site of injury.<sup>460</sup> Critically, it was found that neural cadherin (N-cadherin) cell adhesion was pre-requisite for guided migration and subsequent artificial scaffolds were designed containing N-cadherin, which promoted neuroblast migration to injury sites and incited functional recovery. Since the neonatal brain is highly neurogenic, such a therapeutic approach that guides neuroblasts to sites of brain injury could be a very promising therapeutic approach in the future.<sup>593</sup>

Altering neural glutamate transport has been approached using non-neural stem cells, including mesenchymal stem cells (MSCs), which have been shown to migrate preferentially to areas of injury and inflammation.<sup>594</sup> Further, MSCs have been utilised as vehicles to delivery gene therapy and growth factors.<sup>595</sup> Lee et al. demonstrated that MSCs can deliver microRNAs (miRNAs) to neural stem cells and astrocytes where they found delivery of miR-124 increased expression

of both EAAT1 and EAAT2.<sup>596</sup> More recently, MSCs expressing EAAT2 administered to ischaemic animal models, showed reduced blood glutamate levels and reduction in infarct sizes on MRI imaging, indicating the clinical potential of combined MSC treatment with enhancing glutamate transport.<sup>574</sup> This approach avoids the need to target EAAT2 expression directly and therefore the deleterious effects associated with potentially enhancing global EAAT2 expression are avoided. Such a novel therapeutic approach may have further applications in preterm brain injury, brain tumour seizures, some forms of epilepsy and other neuro-pathologies affected by excitotoxicity.

Neural stem cells have also been shown to have a distinct tropism for glioma cells when implanted intracranially or extracranially.<sup>597</sup> In animal models it has been found that neural stem cells can “chase down” infiltrating tumour cells and “surround” the invading tumour border. This approach has been further developed by engineering neural stem cells to carry a v-myc gene and a gene for cytosine deaminase so that the prodrug 5-fluorocytosine can be converted to the toxic 5-fluorouracil directly and around the tumour.<sup>598</sup> This has since been approved by the FDA for use in human clinical trials. Although neural stem cells may afford a novel therapeutic approach for glioblastoma, SVZ derived neural stem cells may be the source of glioblastoma. It has been shown that glioblastoma may arise from the acquisition of several gene mutations, for example glial fibrillary acidic protein-expressing SVZ derived neural stem cells or the TERT promoter mutation can result in gliomagenesis.<sup>599</sup> However, generally the distance between the SVZ and glioblastoma tumours are significant and there is only early evidence to suggest that gliomagenesis occurs within the SVZ. Nevertheless, the therapeutic potential of neural stem cells is promising but it will be critical to gain an understanding of

the underlying pathogenesis of glioma cells to optimise future therapeutic approaches.

#### *Electrical control of cells*

There is strong evidence for the role of physiological electric fields in directed cell migration of neural stem cells in the rostral migratory stream (RMS) as shown by the paper I present in Chapter 6 and others. The feasibility of harnessing this as a potential therapy to overcome the challenges in delivering a sufficient quantity of neural stem cells to sites of injury or lesions has been investigated by Feng et al.<sup>469</sup> These authors show that transplanted neural stem cells in the rodent RMS, can be reversed by an applied electric field, such that these cells enter the SVZ and can traverse as far as the corpus collosum. This provides early evidence that electric fields may provide a therapeutic means to guide neural stem cells to sites of interest. To date, it is unknown whether such an approach would permit neural stem cells to traverse all areas of the brain and in particular, sites of injury or target lesions, where the microenvironment may differ considerably to the RMS, which is very permissible to cellular migration. Further investigation of neural stem cell migration in animal models of brain disease will be required before considering electric field-based treatments for human clinical trials.

It should be noted that electrotaxis has yet to be investigated in the context of epilepsy, where seizure activity may disrupt an applied electric field. Another possibility is that an applied electric field could be deleterious for seizure activity. However, since electrostimulation with VNS or DBS has been shown to be effective against seizure activity, it would not be inconceivable to adjust applied electric fields in a targeted manner to manipulate cellular migration. For example,

if targeting neurogenesis in the SGZ, electrotaxing neural stem cells to this niche to treat epilepsy could be a possibility therapeutic approach.

The neonatal brain, as discussed earlier, has significant neurogenesis potential but naturally occurring electrical gradients have not been characterised. Therefore, investigating whether manipulation of neural stem cells in the neonatal brain with electric currents could lead to a novel means to enhance neuroregeneration in preterm brain injuries in the future. For example, targeted electric fields may be utilised to divert neural stem cells from the SVZ to sites of brain injury to enhance neural repair, neuro-protection and cellular replacement. How neural stem cells interact with the neonatal brain microenvironment and sites of brain injury would need to be carefully studied.

As demonstrated in Chapter 7, glioblastoma cells have opposing migration preferences according to their transition state as a cancer stem cell or differentiated cancer cell. Lange et al. recently confirmed our findings, in the same primary glioblastoma cell lines, that differentiated glioblastoma cells have a migratory preference for the anode. Further, they confirmed that the EGFR inhibitor afatinib and Akt inhibitor capivasertib inhibited electrotaxis weakly and strongly, respectively. This provides further evidence that targeting signalling pathways involved in electrotaxis can be chemically targeted, as we demonstrated with pioglitazone.<sup>600</sup> Although NovoTTF has provided clinical evidence that externally placed electrode arrays can improve the prognosis of glioblastoma, albeit by a relative short period of time, this suggests that internally implanted electrodes may have a more significant effect. In the future, a multi-mechanism approach to manipulated electrotaxis may become a potential

therapeutic strategy in the future, where for example, targeted chemical inhibition, internally and externally implanted electrodes are utilised to treat post-resection glioblastoma patients to prevent cancer recurrence and improve prognosis. Further research using animal models of glioblastoma would be first required before human clinical trials can be pursued.

### *Conclusions*

Electrostimulation therapies such as vagal nerve stimulation can be used to manipulate neurotransmitters to treat intractable epilepsies, enhance neuroplasticity for motor function lost secondary to ischaemic stroke or preterm brain injury. In the future, VNS may become an adjunct in tumour associated epilepsy and has already been licensed for depression and is currently under investigation for other neuropsychiatric conditions and inflammatory conditions such as inflammatory bowel disease. Manipulating glutamate transport through altering EAAT expression or function may have future potential as a clinical therapy for preterm brain injury, stroke, glioblastoma, tumour associated epilepsy and potentially certain forms of epilepsy, either by using established licensed medications such as ceftriaxone or novel drugs that target EAAT. Novel strategies to mitigate glutamate mediated excitotoxicity include EAAT2 expression stem cell therapy that “grab” excess glutamate. Multimodal imaging approaches to improve the treatment, treatment planning and prognostication epilepsy, brain tumours, tumour associated seizures, preterm brain injury and stroke may permit improved clinical outcomes in the future. Diagnostic approaches using advanced imaging can identify the extent and nature of the disease such that targeted therapies or more conservative or extensive surgery can be offered, such that it is optimised for the individual patient. Cell based



therapies that harness and manipulate the neural stem cell niches may improve neurological outcomes in stroke in the future. Given the highly neurogenic state of the neonatal brain, this may also be a feasible therapeutic approach in preterm brain injury in the future. Since chronic epilepsy is known to affect the SGZ in the hippocampus, neural stem cell treatment derived from the SVZ or iPSCs could be a potential therapy in the future. Neural stem cell tropism for glioma cells is currently a promising treatment modality as targeted prodrug metaboliser. Electric field manipulation of cells to direct preferential migration may be a promising therapeutic target either chemically or surgically with the placement of electrode arrays. In brain tumours, this may be used to prevent tumour recurrence by migrating glioma stem cells towards the resection cavity for example. Neural stem cells can be potentially migrated to sites of injury or interest using electric fields.

In summary, the neurological diseases examined in this thesis are inter-related with varying degrees of similarity in their underlying pathogenesis. Therefore, they share some common potential therapeutic targets, which have been discussed. In particular, I have identified novel therapeutic strategies for epilepsy, brain tumour seizures and brain tumours that manipulate glutamate and electric fields that may be translatable into clinical practice in the future.

## Evidence of Contribution



**Professor Terence J. O'Brien, MB, BS, MD, FRACP, FRCPE, FAHMS, FAES**  
Professor of Medicine (Neurology)  
Head, The Central Clinical School, Monash University  
Program Director, Alfred Brain and Deputy Director of Research, Alfred Health  
Professorial Fellow, The Department of Medicine, The Royal Melbourne Hospital, The University of Melbourne.

19<sup>th</sup> June 2021

To whom it may concern,

**RE: Jared Ching MB ChB, MPharm, MRPharmS, AFHEA, FRCOphth**

I confirm that Dr. Jared Ching made significant contributions when he was working in the Department of Surgery, The Royal Melbourne Hospital, The University of Melbourne. During his time in Melbourne, he proposed and carried out a significant amount of work in the following research outputs, in which I supervised and acted as a senior author:

1) Ching J, Amiridis S, Stylli SS, Morokoff AP, O'Brien TJ, Kaye AH. A novel treatment strategy for glioblastoma multiforme and glioma associated seizures: increasing glutamate uptake with PPAR $\gamma$  agonists. *J Clin Neurosci*. Jan 2015;22(1):21-8. doi:10.1016/j.jocn.2014.09.001

2) Ching J, Amiridis S, Stylli SS, Bjorksten AR, Kountouri N, Zheng T, Paradiso L, Luwor RB, Morokoff AP, O'Brien TJ, Kaye AH. The peroxisome proliferator activated receptor gamma agonist pioglitazone increases functional expression of the glutamate transporter excitatory amino acid transporter 2 (EAAT2) in human glioblastoma cells. *Oncotarget*. Aug 2015;6(25):21301-14. doi:10.18632/oncotarget.4019

Yours sincerely,

A handwritten signature in purple ink, appearing to read "T. O'Brien".

**Professor Terence J. O'Brien**

**Central Clinical School**  
Faculty of Medicine, Nursing and Health Sciences  
The Alfred Centre  
Level 6, 99 Commercial Rd  
Melbourne Victoria 3004, Australia  
Telephone +61 418 370 566 Facsimile +61 3 9903 0843  
e-mail: Terence.O'Brien@monash.edu  
www.med.monash.edu.au  
ABN 12 377 614 012 CRICOS Provider #00008C

**Mr David R. Sandeman FRCS(Edin)**  
Consultant Neurosurgeon and Spinal Surgeon  
Department of Neurosurgery  
North Bristol NHS Trust  
Brunel Building, Southmead Hospital  
Bristol. BS10 5NB

Personal Assistant  
Jenny Williams  
Tel: 07896 367106  
E-Mail: [jennywilliams0@googlemail.com](mailto:jennywilliams0@googlemail.com)

Postal Address  
Harcombe Farm Barn  
Tormarton Road  
Marshfield. SN14 8JG

20/1/15

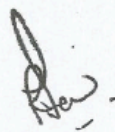
**TO WHOM IT MAY CONCERN**

Re: Mr Jared Ching

I understand that Mr Ching is applying for a training number in neurosurgery. In support of his application I would like to confirm that, while on a medical student elective attachment to my firm, Mr Ching completed the following

1. An audit on vagal nerve stimulation (VNS) for epilepsy in August 2011 which was presented at a Southwest regional neuroscience meeting.
2. Collected sufficient VNS data to prepare an original article on the efficacy and tolerability of VNS, published in the British Journal of Neurosurgery - *Ching J, Sandeman D et al. Long-term effectiveness and tolerability of vagal nerve stimulation (VNS) in adults with intractable epilepsy: A retrospective analysis of 100 patients. Brit J Neurosurgery; 2012.*
3. This was subsequently presented at the Royal College of Surgeons of Edinburgh where he won the "Best Poster Award".
4. During his elective he observed and assisted in a total of 28 operations as validated in his eLogbook.
5. Helped in the first use of the Renishaw Robot for the placement of depth electrodes to assess extratemporal epilepsy in the UK.

Yours Sincerely



David R Sandeman  
Consultant Neurosurgeon  
Southmead Hospital  
Bristol

Gregory Baer, Associate Editor  
Springer Nature

1 New York Plaza, Suite 4600  
New York, NY 10004-1562  
USA

T +1 212 620 8420

gregory.baer@springer.com  
www.springernature.com

Jared Ching MB ChB, MPharm, MRPharmS, AFHEA, FRCOphth  
NIHR Academic Clinical Fellow in Ophthalmology  
John Van Geest Centre for Brain Repair, University of Cambridge, CB2 0PY  
Telephone: (+44) 7453 291 481  
Email: jcc90@cam.ac.uk/jared.ching@nhs.net

17 May 2020

**Publication in Molecular Neurobiology**

To whom it may concern,

I confirm that Jared Ching has had a manuscript published in the journal *Molecular Neurobiology*.

The manuscript is:

Rajatleka, S., Odd, D., Robinson, M.T. et al. Variants of the EAAT2 Glutamate Transporter Gene Promoter Are Associated with Cerebral Palsy in Preterm Infants. *Mol Neurobiol* 55, 2013–2024 (2018).

<https://doi.org/10.1007/s12035-017-0462-1>

Sincerely,

Gregory Baer

Publishing Editor, Molecular Neurobiology

**SPRINGER NATURE**

Discover. Learn. Achieve.

 Springer

nature research

 BMC

 J.B. METZLER

palgrave  
macmillan

apress

SCIENTIFIC  
AMERICAN

macmillan  
education

 Springer Healthcare

 Springer Medizin

 Adis

15<sup>th</sup> February 2021

To Whom It May Concern:

**RE: Elective research project by JARED CHING**

\_\_\_\_\_ This letter is to confirm that Jared Ching worked as an elective student in my lab in July - August 2012. He analysed multimodal MR imaging data of patients with glioblastomas to investigate if there was an increase in rCBV (a marker of angiogenesis and vascular density) in the invasive margin as defined by diffusion tensor methods developed by our group. His findings of increased rCBV in these regions have added to our understanding of these regions as tumour containing despite appearing normal on conventional imaging. A subsequent student added more patient data to this study. This was presented in abstract format at the British Neuro-oncology Society meeting. With additional data derived from spectroscopic imaging, it was published with Dr Ching as one of the authors:

SJ Price, Young AM, Scotton WJ, J Ching, LA Mohsen, NR Boonzaier, VC Lupson, JR Griffiths, MA McLean and TJ Larkin (2016) Multimodal MRI can identify perfusion and metabolic changes in the invasive margin of glioblastomas. *Journal of magnetic resonance imaging* 43(2): 487–494.

MR image analysis is a difficult area that often takes students some time to get used to. Jared picked it up quickly and worked hard during his elective. He also had plenty of time to observe the management of neuro-oncology patients and, as part of his elective, wrote an excellent case review of a patient he followed from pre-operative visit to post-operative results.

Kind regards



**Mr Stephen J Price PhD FRCS(Neuro.Surg)**  
**Hon. Consultant Neurosurgeon and Principal Research Associate**

Neurosurgery Division,  
Box 167,  
Addenbrooke's Hospital,  
Cambridge CB2 0QQ.

Tel: +44 (0) 1223 746455

Fax: +44 (0) 1223 216926

Email: [sjp58@cam.ac.uk](mailto:sjp58@cam.ac.uk)

<https://www.neurosurg.cam.ac.uk/research-groups/brain-tumour-imaging-lab/>



School of Medicine, Medical Sciences & Nutrition  
College of Life Sciences and Medicine  
Institute of Medical Sciences  
Foresterhill  
Aberdeen  
AB25 2ZD  
Scotland United Kingdom  
Tel: +44 (0) 1224 437300  
<http://www.abdn.ac.uk/smmns/>

12/02/21

Reference for Dr Jared Ching

Dear Sir/Madam,

I write to confirm that Dr Jared Ching previously worked in my laboratory, performing research on projects in the field of cellular electrotaxis at the Institute of Medical Sciences, University of Aberdeen, Aberdeen. Whilst working as an Honorary Research Fellow Jared carried out work on two projects:

**1. Neural stem cell electrotaxis**

This project was led by Dr Lin Cao. Dr Ching performed a number of tissue culture experiments that contributed key information crucial to the quality of their subsequent publication. The *in vitro* experiments he carried out entailed establishing the neural stem cell cultures, preparation of electrotactic chambers, detailed time lapse microscopy to track the behaviours of individual cells over many hours, drug treatment of cells and computerized analysis of cell migration patterns.

The combined results of this work were published in the fine paper referenced below and Dr Ching also contributed to drafting, writing, reviewing and editing the final manuscript prior to publication.

Cao, L, Pu, J, Scott, R, Ching, J & McCaig, CD (2015). Physiological electrical signals promote chain migration of neuroblasts by up-regulating P2Y1 purinergic receptors and enhancing cell adhesion. *Stem Cell Reviews and Reports* **11**, 75 - 86.

## 2. Brain tumour electrotaxis

After working on the above project, Dr Ching proposed that he investigate the role of electric fields in primary brain tumours. This was an area of great interest to him and one in which he had much greater experience than I had. He therefore led this project, prepared a competitive grant proposal and was successful with his application for funding. He obtained the necessary ethical approvals to obtain human brain tumour tissue from local patients and formed a collaboration with the University of Rostock to exchange primary tissue.

Following this, he also led the experimental work of the project. He established primary differentiated and de-differentiated brain tumour cultures, performed the electrotaxis experiments and designed drug treatment protocols which uncovered the mechanisms underpinning the different electric field-directed behaviours of different cell types.

He went on to supervise a number of students to complete this work and currently he is responding to reviewer comments following favourable peer review of his excellent studies in the journal *Cellular and Molecular Neurobiology*. The manuscript pre-print is available online:

Hannah Clancy, Michal Pruski, Natalia Curcio Fedrizzi, Bing Lang, Jared Ching, Colin McCaig. Glioblastoma Cell Migration is Directed by Electrical Signals. (2021)

DOI: <https://doi.org/10.1101/2020.09.09.290254>

URL: <https://www.biorxiv.org/content/10.1101/2020.09.09.290254v1>

In short, Jared is a gifted experimental Clinician Scientist well capable of leading his own laboratory and establishing an international reputation for his research programme.

I give him my highest recommendation, without any reservation.

Yours Sincerely,



Professor Colin D McCaig, FRSE,  
Regius Professor of Physiology  
University of Aberdeen, AB25 2ZD,  
Scotland.

## References

1. Fisher RS, van Emde Boas W, Blume W, et al. Epileptic seizures and epilepsy: definitions proposed by the International League Against Epilepsy (ILAE) and the International Bureau for Epilepsy (IBE). *Epilepsia*. Apr 2005;46(4):470-2. doi:10.1111/j.0013-9580.2005.66104.x
2. Fisher RS, Cross JH, French JA, et al. Operational classification of seizure types by the International League Against Epilepsy: Position Paper of the ILAE Commission for Classification and Terminology. *Epilepsia*. 04 2017;58(4):522-530. doi:10.1111/epi.13670
3. Fisher RS, Acevedo C, Arzimanoglou A, et al. ILAE official report: a practical clinical definition of epilepsy. *Epilepsia*. Apr 2014;55(4):475-82. doi:10.1111/epi.12550
4. Lindsay K, Bone I, Fuller G. Neurology and Neurosurgery Illustrated. 2010.
5. Meisler MH, Kearney JA. Sodium channel mutations in epilepsy and other neurological disorders. *Journal of Clinical Investigation*. Aug 2005;115(8):2010-2017. doi:10.1172/jci25466
6. Olney JW. Brain lesions, obesity, and other disturbances in mice treated with monosodium glutamate. *Science*. May 09 1969;164(3880):719-21. doi:10.1126/science.164.3880.719
7. Kwan P, Brodie MJ. Early identification of refractory epilepsy. *New England Journal of Medicine*. 2000;342(5):314-319.
8. Spencer S, Huh L. Outcomes of epilepsy surgery in adults and children. *The Lancet Neurology*. 2008;7(6):525-537. doi:10.1016/s1474-4422(08)70109-1
9. Schuele SU, Lüders HO. Intractable epilepsy: management and therapeutic alternatives. *The Lancet Neurology*. 2008;7(6):514-524. doi:10.1016/s1474-4422(08)70108-x
10. Amar AP, Apuzzo MLJ, Liu CY. Vagus nerve stimulation therapy after failed cranial surgery for intractable epilepsy: Results from the vagus nerve stimulation therapy patient outcome registry (Reprinted from Neurosurgery, vol 55, pg 1086-1093, 2004). *Neurosurgery*. 2008;62(2):506-512. doi:10.1227/01.neu.0000141073.08427.76
11. Makady A, de Boer A, Hillege H, Klungel O, Goettsch W, 1) oboGWP. What Is Real-World Data? A Review of Definitions Based on Literature and Stakeholder Interviews. *Value Health*. 2017 Jul - Aug 2017;20(7):858-865. doi:10.1016/j.jval.2017.03.008
12. Faria R, Hernandez Alava M, Manca A, Wailoo AJ. NICE DSU Technical Support Document 17: The use of observational data to inform estimates of treatment effectiveness for Technology Appraisal: Methods for comparative individual patient data. 2015.
13. Agency EM. European Medicines Agency post-authorisation procedural advice for users of the centralised procedure. 2021.
14. Ching J, Khan S, White P, et al. Long-term effectiveness and tolerability of vagal nerve stimulation in adults with intractable epilepsy: a retrospective analysis of 100 patients. *Br J Neurosurg*. Apr 2013;27(2):228-34. doi:10.3109/02688697.2012.732716
15. Englot DJ, Chang EF, Auguste KI. Vagus nerve stimulation for epilepsy: a meta-analysis of efficacy and predictors of response. *J Neurosurg*. 2011/12/01 2011;115(6):1248-1255. doi:10.3171/2011.7.jns11977



16. Bottomley JM, LeReun C, Diamantopoulos A, Mitchell S, Gaynes BN. Vagus nerve stimulation (VNS) therapy in patients with treatment resistant depression: A systematic review and meta-analysis. *Compr Psychiatry*. Dec 2019;98:152156. doi:10.1016/j.comppsy.2019.152156
17. Kuba R, Brazdil M, Kalina M, et al. Vagus nerve stimulation: Longitudinal follow-up of patients treated for 5 years. *Seizure-European Journal of Epilepsy*. 2009;18(4):269-274. doi:10.1016/j.seizure.2008.10.012
18. Ardesch JJ, Buschman HPJ, Wagener-Schimmel L, van der Aa HE, Hageman G. Vagus nerve stimulation for medically refractory epilepsy: A long-term follow-up study. *Seizure-European Journal of Epilepsy*. 2007;16:579-585. doi:10.1016/j.seizure.2007.04.005
19. Spanaki MV, Allen LS, Mueller WM, Morris GL. Vagus nerve stimulation therapy: 5-year or greater outcome at a university-based epilepsy center. *Seizure-European Journal of Epilepsy*. 2004;13(8):587-590. doi:10.1016/j.seizure.2004.01.009
20. DeGiorgio CM, Schachter SC, Handforth A, et al. Prospective long-term study of vagus nerve stimulation for the treatment of refractory seizures. *Epilepsia*. 2000;41(9):1195-1200.
21. Morris GL, Mueller WM, Vagus Nerve Stimulation Study G. Long-term treatment with vague nerve stimulation in patients with refractory epilepsy. Article. *Neurology*. Nov 1999;53(8):1731-1735.
22. Handforth A, DeGiorgio CM, Schachter SC, et al. Vagus nerve stimulation therapy for partial-onset seizures - A randomized active-control trial. Article. *Neurology*. Jul 1998;51(1):48-55.
23. George R, Salinsky M, Kuzniecky R, et al. VAGUS NERVE-STIMULATION FOR TREATMENT OF PARTIAL SEIZURES .3. LONG-TERM FOLLOW-UP ON FIRST 67 PATIENTS EXITING A CONTROLLED-STUDY. *Epilepsia*. 1994;35(3):637-643.
24. Jiang SH, Hu LP, Wang X, Li J, Zhang ZG. Neurotransmitters: emerging targets in cancer. *Oncogene*. 01 2020;39(3):503-515. doi:10.1038/s41388-019-1006-0
25. Kandimalla R, Reddy PH. Therapeutics of Neurotransmitters in Alzheimer's Disease. *J Alzheimers Dis*. 2017;57(4):1049-1069. doi:10.3233/JAD-161118
26. Lascano AM, Korff CM, Picard F. Seizures and Epilepsies due to Channelopathies and Neurotransmitter Receptor Dysfunction: A Parallel between Genetic and Immune Aspects. *Mol Syndromol*. Sep 2016;7(4):197-209. doi:10.1159/000447707
27. Akyuz E, Polat AK, Eroglu E, Kullu I, Angelopoulou E, Paudel YN. Revisiting the role of neurotransmitters in epilepsy: An updated review. *Life Sci*. Jan 15 2021;265:118826. doi:10.1016/j.lfs.2020.118826
28. Charpak S, Gähwiler BH, Do KQ, Knöpfel T. Potassium conductances in hippocampal neurons blocked by excitatory amino-acid transmitters. *Nature*. Oct 25 1990;347(6295):765-7. doi:10.1038/347765a0
29. Cohen AS, Coussens CM, Raymond CR, Abraham WC. Long-lasting increase in cellular excitability associated with the priming of LTP induction in rat hippocampus. *J Neurophysiol*. Dec 1999;82(6):3139-48. doi:10.1152/jn.1999.82.6.3139
30. Danbolt NC, Furness DN, Zhou Y. Neuronal vs glial glutamate uptake: Resolving the conundrum. *Neurochem Int*. 09 2016;98:29-45. doi:10.1016/j.neuint.2016.05.009
31. Meldrum BS. Glutamate as a neurotransmitter in the brain: review of physiology and pathology. *J Nutr*. 04 2000;130(4S Suppl):1007S-15S. doi:10.1093/jn/130.4.1007S
32. Zamalloa T, Bailey CP, Pineda J. Glutamate-induced post-activation inhibition of locus coeruleus neurons is mediated by AMPA/kainate receptors and sodium-

- dependent potassium currents. *Br J Pharmacol*. Feb 2009;156(4):649-61. doi:10.1111/j.1476-5381.2008.00004.x
33. Lodge D. The history of the pharmacology and cloning of ionotropic glutamate receptors and the development of idiosyncratic nomenclature. *Neuropharmacology*. Jan 2009;56(1):6-21. doi:10.1016/j.neuropharm.2008.08.006
34. Sibarov DA, Antonov SM. Calcium-Dependent Desensitization of NMDA Receptors. *Biochemistry (Mosc)*. Oct 2018;83(10):1173-1183. doi:10.1134/S0006297918100036
35. Hollmann M, Hartley M, Heinemann S. Ca<sup>2+</sup> permeability of KA-AMPA-gated glutamate receptor channels depends on subunit composition. *Science*. May 10 1991;252(5007):851-3. doi:10.1126/science.1709304
36. Gabriel L, Lvov A, Orthodoxou D, Rittenhouse AR, Kobertz WR, Melikian HE. The acid-sensitive, anesthetic-activated potassium leak channel, KCNK3, is regulated by 14-3-3 $\beta$ -dependent, protein kinase C (PKC)-mediated endocytic trafficking. *J Biol Chem*. Sep 21 2012;287(39):32354-66. doi:10.1074/jbc.M112.391458
37. Zhang H, Ciliz NI, Yang C, Hu B, Dong H, Lei S. Depression of neuronal excitability and epileptic activities by group II metabotropic glutamate receptors in the medial entorhinal cortex. *Hippocampus*. Nov 2015;25(11):1299-313. doi:10.1002/hipo.22437
38. Hunt DL, Castillo PE. Synaptic plasticity of NMDA receptors: mechanisms and functional implications. *Curr Opin Neurobiol*. Jun 2012;22(3):496-508. doi:10.1016/j.conb.2012.01.007
39. Johnson JW, Ascher P. Glycine potentiates the NMDA response in cultured mouse brain neurons. *Nature*. 1987 Feb 5-11 1987;325(6104):529-31. doi:10.1038/325529a0
40. Paoletti P, Bellone C, Zhou Q. NMDA receptor subunit diversity: impact on receptor properties, synaptic plasticity and disease. *Nat Rev Neurosci*. Jun 2013;14(6):383-400. doi:10.1038/nrn3504
41. Wyllie DJ, Livesey MR, Hardingham GE. Influence of GluN2 subunit identity on NMDA receptor function. *Neuropharmacology*. Nov 2013;74:4-17. doi:10.1016/j.neuropharm.2013.01.016
42. Stephen D. M, Erika E. F. Chapter 11 - Ionotropic Receptors. Academic Press; 2019. p. 215-243.
43. Nowak L, Bregestovski P, Ascher P, Herbet A, Prochiantz A. Magnesium gates glutamate-activated channels in mouse central neurones. *Nature*. 1984 Feb 2-8 1984;307(5950):462-5. doi:10.1038/307462a0
44. Meriney SD, Fanselow EE. Chapter 11 - Ionotropic Receptors. Academic Press; 2019. p. 215-243.
45. Tian M, Stroebel D, Piot L, David M, Ye S, Paoletti P. GluN2A and GluN2B NMDA receptors use distinct allosteric routes. *Nat Commun*. 08 05 2021;12(1):4709. doi:10.1038/s41467-021-25058-9
46. Martel MA, Ryan TJ, Bell KF, et al. The subtype of GluN2 C-terminal domain determines the response to excitotoxic insults. *Neuron*. May 10 2012;74(3):543-56. doi:10.1016/j.neuron.2012.03.021
47. Parsons MP, Raymond LA. Extrasynaptic NMDA receptor involvement in central nervous system disorders. *Neuron*. Apr 16 2014;82(2):279-93. doi:10.1016/j.neuron.2014.03.030
48. XiangWei W, Jiang Y, Yuan H. Mutations and Rare Variants Occurring in NMDA Receptors. *Curr Opin Physiol*. Apr 2018;2:27-35. doi:10.1016/j.cophys.2017.12.013

49. Lemke JR, Geider K, Helbig KL, et al. Delineating the GRIN1 phenotypic spectrum: A distinct genetic NMDA receptor encephalopathy. *Neurology*. 06 07 2016;86(23):2171-8. doi:10.1212/WNL.0000000000002740
50. Xu XX, Luo JH. Mutations of N-Methyl-D-Aspartate Receptor Subunits in Epilepsy. *Neurosci Bull*. Jun 2018;34(3):549-565. doi:10.1007/s12264-017-0191-5
51. Plattner F, Hernández A, Kistler TM, et al. Memory enhancement by targeting Cdk5 regulation of NR2B. *Neuron*. Mar 05 2014;81(5):1070-1083. doi:10.1016/j.neuron.2014.01.022
52. Bien CG, Urbach H, Schramm J, et al. Limbic encephalitis as a precipitating event in adult-onset temporal lobe epilepsy. *Neurology*. Sep 18 2007;69(12):1236-44. doi:10.1212/01.wnl.0000276946.08412.ef
53. Vincent A, Bien CG. Anti-NMDA-receptor encephalitis: a cause of psychiatric, seizure, and movement disorders in young adults. *Lancet Neurol*. Dec 2008;7(12):1074-5. doi:10.1016/S1474-4422(08)70225-4
54. Vezzani A, French J, Bartfai T, Baram TZ. The role of inflammation in epilepsy. *Nat Rev Neurol*. Jan 2011;7(1):31-40. doi:10.1038/nrneurol.2010.178
55. Viviani B, Bartesaghi S, Gardoni F, et al. Interleukin-1beta enhances NMDA receptor-mediated intracellular calcium increase through activation of the Src family of kinases. *J Neurosci*. Sep 24 2003;23(25):8692-700.
56. Ichiyama T, Nishikawa M, Yoshitomi T, Hayashi T, Furukawa S. Tumor necrosis factor-alpha, interleukin-1 beta, and interleukin-6 in cerebrospinal fluid from children with prolonged febrile seizures. Comparison with acute encephalitis/encephalopathy. *Neurology*. Feb 1998;50(2):407-11. doi:10.1212/wnl.50.2.407
57. Vezzani A, Balosso S, Ravizza T. The role of cytokines in the pathophysiology of epilepsy. *Brain Behav Immun*. Aug 2008;22(6):797-803. doi:10.1016/j.bbi.2008.03.009
58. Uludag IF, Duksal T, Tiftikcioglu BI, Zorlu Y, Ozkaya F, Kirkali G. IL-1 $\beta$ , IL-6 and IL1Ra levels in temporal lobe epilepsy. *Seizure*. Mar 2015;26:22-5. doi:10.1016/j.seizure.2015.01.009
59. Bezzi P, Domercq M, Brambilla L, et al. CXCR4-activated astrocyte glutamate release via TNFalpha: amplification by microglia triggers neurotoxicity. *Nat Neurosci*. Jul 2001;4(7):702-10. doi:10.1038/89490
60. Hu S, Sheng WS, Ehrlich LC, Peterson PK, Chao CC. Cytokine effects on glutamate uptake by human astrocytes. *Neuroimmunomodulation*. 2000;7(3):153-9. doi:10.1159/000026433
61. Stellwagen D, Beattie EC, Seo JY, Malenka RC. Differential regulation of AMPA receptor and GABA receptor trafficking by tumor necrosis factor-alpha. *J Neurosci*. Mar 23 2005;25(12):3219-28. doi:10.1523/JNEUROSCI.4486-04.2005
62. Vezzani A, Aronica E, Mazarati A, Pittman QJ. Epilepsy and brain inflammation. *Exp Neurol*. Jun 2013;244:11-21. doi:10.1016/j.expneurol.2011.09.033
63. Mahmoud S, Gharagozloo M, Simard C, Gris D. Astrocytes Maintain Glutamate Homeostasis in the CNS by Controlling the Balance between Glutamate Uptake and Release. *Cells*. 02 20 2019;8(2)doi:10.3390/cells8020184
64. Anderson CM, Swanson RA. Astrocyte glutamate transport: Review of properties, regulation, and physiological functions. 10.1002/1098-1136(200010)32:1<1::AID-GLIA10>3.0.CO;2-W. *Glia*. 2000;32(1):1-14.
65. Cho Y, Bannai S. Uptake of glutamate and cysteine in C-6 glioma cells and in cultured astrocytes. *J Neurochem*. Dec 1990;55(6):2091-7. doi:10.1111/j.1471-4159.1990.tb05800.x

66. Rose CR, Ziemens D, Untiet V, Fahlke C. Molecular and cellular physiology of sodium-dependent glutamate transporters. *Brain Res Bull.* 01 2018;136:3-16. doi:10.1016/j.brainresbull.2016.12.013
67. Piani D, Fontana A. Involvement of the cystine transport system xc- in the macrophage-induced glutamate-dependent cytotoxicity to neurons. *J Immunol.* Apr 01 1994;152(7):3578-85.
68. Kato S, Ishita S, Sugawara K, Mawatari K. Cystine/glutamate antiporter expression in retinal Müller glial cells: implications for DL-alpha-amino acid toxicity. *Neuroscience.* Nov 1993;57(2):473-82. doi:10.1016/0306-4522(93)90080-y
69. Ye ZC, Rothstein JD, Sontheimer H. Compromised glutamate transport in human glioma cells: reduction-mislocalization of sodium-dependent glutamate transporters and enhanced activity of cystine-glutamate exchange. *J Neurosci.* Dec 15 1999;19(24):10767-77.
70. OXENDER DL, CHRISTENSEN HN. Evidence for two types of mediation of neutral and amino-acid transport in Ehrlich cells. *Nature.* Feb 23 1963;197:765-7. doi:10.1038/197765a0
71. Bannai S. Exchange of cystine and glutamate across plasma membrane of human fibroblasts. *J Biol Chem.* Feb 15 1986;261(5):2256-63.
72. Sato H, Tamba M, Okuno S, et al. Distribution of cystine/glutamate exchange transporter, system x(c)-, in the mouse brain. *J Neurosci.* Sep 15 2002;22(18):8028-33.
73. Waniewski RA, Martin DL. Characterization of L-glutamic acid transport by glioma cells in culture: evidence for sodium-independent, chloride-dependent high affinity influx. *J Neurosci.* Sep 1984;4(9):2237-46.
74. Bannai S, Christensen HN, Vadgama JV, et al. Amino acid transport systems. *Nature.* 1984 Sep 27-Oct 3 1984;311(5984):308. doi:10.1038/311308b0
75. Shih AY, Erb H, Sun X, Toda S, Kalivas PW, Murphy TH. Cystine/glutamate exchange modulates glutathione supply for neuroprotection from oxidative stress and cell proliferation. *J Neurosci.* Oct 11 2006;26(41):10514-23. doi:10.1523/JNEUROSCI.3178-06.2006
76. Lewerenz J, Hewett SJ, Huang Y, et al. The cystine/glutamate antiporter system x(c)- in health and disease: from molecular mechanisms to novel therapeutic opportunities. *Antioxid Redox Signal.* Feb 10 2013;18(5):522-55. doi:10.1089/ars.2011.4391
77. Bassi MT, Gasol E, Manzoni M, et al. Identification and characterisation of human xCT that co-expresses, with 4F2 heavy chain, the amino acid transport activity system xc-. *Pflugers Arch.* May 2001;442(2):286-96. doi:10.1007/s004240100537
78. Sato H, Tamba M, Ishii T, Bannai S. Cloning and expression of a plasma membrane cystine/glutamate exchange transporter composed of two distinct proteins. *J Biol Chem.* Apr 23 1999;274(17):11455-8. doi:10.1074/jbc.274.17.11455
79. Gasol E, Jiménez-Vidal M, Chillarón J, Zorzano A, Palacín M. Membrane topology of system xc- light subunit reveals a re-entrant loop with substrate-restricted accessibility. *J Biol Chem.* Jul 23 2004;279(30):31228-36. doi:10.1074/jbc.M402428200
80. Mandal PK, Seiler A, Perisic T, et al. System x(c)- and thioredoxin reductase 1 cooperatively rescue glutathione deficiency. *J Biol Chem.* Jul 16 2010;285(29):22244-53. doi:10.1074/jbc.M110.121327
81. Gaucher C, Boudier A, Bonetti J, Clarot I, Leroy P, Parent M. Glutathione: Antioxidant Properties Dedicated to Nanotechnologies. *Antioxidants (Basel).* Apr 27 2018;7(5)doi:10.3390/antiox7050062

82. Dringen R, Pfeiffer B, Hamprecht B. Synthesis of the antioxidant glutathione in neurons: supply by astrocytes of CysGly as precursor for neuronal glutathione. *J Neurosci*. Jan 15 1999;19(2):562-9.
83. Hsieh CH, Lin YJ, Chen WL, et al. HIF-1 $\alpha$  triggers long-lasting glutamate excitotoxicity via system x. *J Pathol*. Feb 2017;241(3):337-349. doi:10.1002/path.4838
84. Sasaki H, Sato H, Kuriyama-Matsumura K, et al. Electrophile response element-mediated induction of the cystine/glutamate exchange transporter gene expression. *J Biol Chem*. Nov 22 2002;277(47):44765-71. doi:10.1074/jbc.M208704200
85. Habib E, Linher-Melville K, Lin HX, Singh G. Expression of xCT and activity of system xc(-) are regulated by NRF2 in human breast cancer cells in response to oxidative stress. *Redox Biol*. Aug 2015;5:33-42. doi:10.1016/j.redox.2015.03.003
86. Makowske M, Christensen HN. Contrasts in transport systems for anionic amino acids in hepatocytes and a hepatoma cell line HTC. *J Biol Chem*. May 25 1982;257(10):5663-70.
87. Gallagher M. The System xc- Cystine/Glutamate Antiporter: An Exciting Target for Antiepileptogenic Therapy? *Epilepsy Curr*. 2020 Jan-Feb 2020;20(1):39-42. doi:10.1177/1535759719891983
88. Leclercq K, Lieffering JV, Albertini G, et al. Anticonvulsant and antiepileptogenic effects of system. *Epilepsia*. 07 2019;60(7):1412-1423. doi:10.1111/epi.16055
89. Sears SMS, Hewett JA, Hewett SJ. Decreased epileptogenesis in mice lacking the System x. *Epilepsia Open*. Mar 2019;4(1):133-143. doi:10.1002/epi4.12307
90. Ye Z-C, Rothstein JD, Sontheimer H. Compromised Glutamate Transport in Human Glioma Cells: Reduction–Mislocalization of Sodium-Dependent Glutamate Transporters and Enhanced Activity of Cystine–Glutamate Exchange. *Journal of Neuroscience*; 2000. p. 10767–10777.
91. Fairman WA, Sonders MS, Murdoch GH, Amara SG. Arachidonic acid elicits a substrate-gated proton current associated with the glutamate transporter EAAT4. *Nat Neurosci*. Jun 1998;1(2):105-13. doi:10.1038/355
92. Magi S, Piccirillo S, Amoroso S, Lariccia V. Excitatory Amino Acid Transporters (EAATs): Glutamate Transport and Beyond. *Int J Mol Sci*. Nov 13 2019;20(22)doi:10.3390/ijms20225674
93. Arbas EA, Weidner MH. Transneuronal induction of muscle atrophy in grasshoppers. *J Neurobiol*. Jul 1991;22(5):536-46. doi:10.1002/neu.480220509
94. Zerangue N, Kavanaugh MP. Flux coupling in a neuronal glutamate transporter. *Nature*. Oct 17 1996;383(6601):634-7. doi:10.1038/383634a0
95. Fairman WA, Vandenberg RJ, Arriza JL, Kavanaugh MP, Amara SG. An excitatory amino-acid transporter with properties of a ligand-gated chloride channel. *Nature*. Jun 15 1995;375(6532):599-603. doi:10.1038/375599a0
96. Wadiche JI, Amara SG, Kavanaugh MP. Ion fluxes associated with excitatory amino acid transport. *Neuron*. Sep 1995;15(3):721-8. doi:10.1016/0896-6273(95)90159-0
97. Vandenberg RJ, Ryan RM. Mechanisms of glutamate transport. *Physiol Rev*. Oct 2013;93(4):1621-57. doi:10.1152/physrev.00007.2013
98. Brew H, Attwell D. Electrogenic glutamate uptake is a major current carrier in the membrane of axolotl retinal glial cells. *Nature*. 1987 Jun 25-Jul 1 1987;327(6124):707-9. doi:10.1038/327707a0

99. Watzke N, Rauen T, Bamberg E, Grewer C. On the mechanism of proton transport by the neuronal excitatory amino acid carrier 1. *J Gen Physiol.* Nov 2000;116(5):609-22. doi:10.1085/jgp.116.5.609
100. Zhang Z, Tao Z, Gameiro A, et al. Transport direction determines the kinetics of substrate transport by the glutamate transporter EAAC1. *Proc Natl Acad Sci U S A.* Nov 13 2007;104(46):18025-30. doi:10.1073/pnas.0704570104
101. Grewer C, Zhang Z, Mwaura J, Albers T, Schwartz A, Gameiro A. Charge compensation mechanism of a Na<sup>+</sup>-coupled, secondary active glutamate transporter. *J Biol Chem.* Aug 03 2012;287(32):26921-31. doi:10.1074/jbc.M112.364059
102. Divito CB, Underhill SM. Excitatory amino acid transporters: roles in glutamatergic neurotransmission. *Neurochem Int.* Jul 2014;73:172-80. doi:10.1016/j.neuint.2013.12.008
103. Lerche H, Shah M, Beck H, Noebels J, Johnston D, Vincent A. Ion channels in genetic and acquired forms of epilepsy. *J Physiol.* Feb 15 2013;591(4):753-64. doi:10.1113/jphysiol.2012.240606
104. Oyryer J, Maljevic S, Scheffer IE, Berkovic SF, Petrou S, Reid CA. Ion Channels in Genetic Epilepsy: From Genes and Mechanisms to Disease-Targeted Therapies. *Pharmacol Rev.* 01 2018;70(1):142-173. doi:10.1124/pr.117.014456
105. Lenaeus MJ, Gamal El-Din TM, Ing C, et al. Structures of closed and open states of a voltage-gated sodium channel. *Proc Natl Acad Sci U S A.* 04 11 2017;114(15):E3051-E3060. doi:10.1073/pnas.1700761114
106. Podell M. Epilepsy and seizure classification: a lesson from Leonardo. *J Vet Intern Med.* 1999 Jan-Feb 1999;13(1):3-4.
107. George AL. Inherited disorders of voltage-gated sodium channels. *J Clin Invest.* Aug 2005;115(8):1990-9. doi:10.1172/JCI25505
108. Goldin AL. Mechanisms of sodium channel inactivation. *Curr Opin Neurobiol.* Jun 2003;13(3):284-90. doi:10.1016/s0959-4388(03)00065-5
109. Pal R, Kumar B, Akhtar MJ, Chawla PA. Voltage gated sodium channel inhibitors as anticonvulsant drugs: A systematic review on recent developments and structure activity relationship studies. *Bioorg Chem.* 10 2021;115:105230. doi:10.1016/j.bioorg.2021.105230
110. de Lera Ruiz M, Kraus RL. Voltage-Gated Sodium Channels: Structure, Function, Pharmacology, and Clinical Indications. *J Med Chem.* Sep 24 2015;58(18):7093-118. doi:10.1021/jm501981g
111. Brodie MJ. Sodium Channel Blockers in the Treatment of Epilepsy. *CNS Drugs.* Jul 2017;31(7):527-534. doi:10.1007/s40263-017-0441-0
112. Rogawski MA, Löscher W. The neurobiology of antiepileptic drugs. *Nat Rev Neurosci.* Jul 2004;5(7):553-64. doi:10.1038/nrn1430
113. Ragsdale DS, Scheuer T, Catterall WA. Frequency and voltage-dependent inhibition of type IIA Na<sup>+</sup> channels, expressed in a mammalian cell line, by local anesthetic, antiarrhythmic, and anticonvulsant drugs. *Mol Pharmacol.* Nov 1991;40(5):756-65.
114. Mantegazza M, Curia G, Biagini G, Ragsdale DS, Avoli M. Voltage-gated sodium channels as therapeutic targets in epilepsy and other neurological disorders. *Lancet Neurol.* Apr 2010;9(4):413-24. doi:10.1016/S1474-4422(10)70059-4
115. Lanska DJ. J.L. Corning and vagal nerve stimulation for seizures in the 1880s. *Neurology.* 2002;58(3):452-459.

116. Bailey P, Bremer F. A sensory cortical representation of the vagus nerve - With a note on the effects of low blood pressure on the cortical electrogram. *Journal of Neurophysiology*. 1938;1(5):405-412.
117. Landy HJ, Ramsay RE, Slater J, Casiano RR, Morgan R. Vagus nerve-stimulation for complex partial seizures - surgical technique, safety, and efficacy. Article. *J Neurosurg*. Jan 1993;78(1):26-31.
118. Penry JK, Dean JC. PREVENTION OF INTRACTABLE PARTIAL SEIZURES BY INTERMITTENT VAGAL-STIMULATION IN HUMANS - PRELIMINARY-RESULTS. Proceedings Paper. *Epilepsia*. 1990;31:S40-S43.
119. Reid SA. SURGICAL TECHNIQUE FOR IMPLANTATION OF THE NEUROCYBERNETIC PROSTHESIS. Proceedings Paper. *Epilepsia*. 1990;31:S38-S39.
120. Schachter SC, Saper CB. Vagus nerve stimulation. *Epilepsia*. 1998;39(7):677-686.
121. Nemeroff CB, Mayberg HS, Krahl SE, et al. VNS Therapy in Treatment-Resistant Depression: Clinical Evidence and Putative Neurobiological Mechanisms. *Neuropsychopharmacology*. 2006;31(7):1345-1355.
122. Foley JO, DuBois F. Quantitative studies of the vagus nerve in the cat - I. The ratio of sensory to motor fibers. *Journal of Comparative Neurology*. Jun 1937;67(1):49-67. doi:10.1002/cne.900670104
123. Hammer N, Löffler S, Cakmak YO, et al. Cervical vagus nerve morphometry and vascularity in the context of nerve stimulation - A cadaveric study. *Sci Rep*. 05 2018;8(1):7997. doi:10.1038/s41598-018-26135-8
124. Crossman A, Neary D. *Neuroanatomy: An Illustrated Colour Text*. Third Edition. 2005.
125. Ben-Menachem E. Vagus-nerve stimulation for the treatment of epilepsy. *Lancet Neurology*. Dec 2002;1(8):477-482. doi:10.1016/s1474-4422(02)00220-x
126. Aalbers M, Vles J, Klinkenberg S, Hoogland G, Majoie M, Rijkers K. Animal models for vagus nerve stimulation in epilepsy. *Experimental Neurology*. 2011;230(2):167-175. doi:10.1016/j.expneurol.2011.04.014
127. Rutecki P. Anatomical, Physiological, and Theoretical Basis for the Antiepileptic Effect of Vagus Nerve Stimulation. 10.1111/j.1528-1157.1990.tb05843.x. *Epilepsia*. 1990;31:S1-S6.
128. Randall WC, Ardell JL. *DIFFERENTIAL INNERVATION OF THE HEART*. Zipes, D P and J Jalife. 1985:137-144.
129. Saper CB, Kibbe MR, Hurley KM, et al. Brain natriuretic peptide-like immunoreactive innervation of the cardiovascular and cerebrovascular systems in the rat. *Circulation Research*. 1990;67(6):1345-1354.
130. Henry TR, Bakay RAE, Pennell PB, Epstein CM, Votaw TR. Brain blood-flow alterations induced by therapeutic vagus nerve stimulation in partial epilepsy: II. Prolonged effects at high and low levels of stimulation. *Epilepsia*. 2004;45(9):1064-1070.
131. Zanchetti A, Wang S, Moruzzi G. The effect of vagal afferent stimulation on the EEG of the cat. *Electroencephalogr.Clin.Neurophysiol*; 1952. p. 357-361.
132. Ben-Menachem E, Hamberger A, Hedner T, et al. Effects of vagus nerve stimulation on amino acids and other metabolites in the CSF of patients with partial seizures. *Epilepsy Research*. 1995;20(3):221-227. doi:10.1016/0920-1211(94)00083-9
133. Krahl SE, Senanayake SS, Handforth A. Destruction of Peripheral C-Fibers Does Not Alter Subsequent Vagus Nerve Stimulation-Induced Seizure Suppression in Rats. 10.1046/j.1528-1157.2001.09700.x. *Epilepsia*. 2001;42(5):586-589.

134. Ruffoli R, Giorgi FS, Pizzanelli C, Murri L, Paparelli A, Fornai F. The chemical neuroanatomy of vagus nerve stimulation. *Journal of Chemical Neuroanatomy*. In Press, Corrected Proof doi:10.1016/j.jchemneu.2010.12.002
135. Krahl SE, Senanayake SS, Pekary AE, Sattin A. Vagus nerve stimulation (VNS) is effective in a rat model of antidepressant action. Article. *J Psychiatr Res*. May-Jun 2004;38(3):237-240. doi:10.1016/j.jpsychires.2003.11.005
136. Dorr AE, Debonnel G. Effect of vagus nerve stimulation on serotonergic and noradrenergic transmission. Article; Proceedings Paper. *J Pharmacol Exp Ther*. Aug 2006;318(2):890-898. doi:10.1124/jpet.106.104166
137. Mazarati AM, Baldwin RA, Shinmei S, Sankar R. In vivo interaction between serotonin and galanin receptors types 1 and 2 in the dorsal raphe: implication for limbic seizures. *Journal of Neurochemistry*. Dec 2005;95(5):1495-1503. doi:10.1111/j.1471-4159.2005.03498.x
138. Prendiville S, Gale K. Anticonvulsant effect of fluoxetine on focally evoked limbic motor seizures in rats. *Epilepsia*. 1993 Mar-Apr 1993;34(2):381-4. doi:10.1111/j.1528-1157.1993.tb02425.x
139. Yan QS, Jobe PC, Cheong JH, Ko KH, Dailey JW. Role of serotonin in the anticonvulsant effect of fluoxetine in genetically epilepsy-prone rats. *Naunyn Schmiedeberg's Arch Pharmacol*. Aug 1994;350(2):149-52. doi:10.1007/BF00241089
140. Browning RA, Hoffmann WE, Simonton RL. Changes in seizure susceptibility after intracerebral treatment with 5,7-dihydroxytryptamine: role of serotonergic neurons. *Ann N Y Acad Sci*. Jun 1978;305:437-56. doi:10.1111/j.1749-6632.1978.tb31540.x
141. Statnick M, Dailey J, Jobe P, Browning R. Neither intranigral fluoxetine nor 5,7-dihydroxytryptamine alter audiogenic seizures in genetically epilepsy-prone rats. *Eur J Pharmacol*. Mar 1996;299(1-3):93-102. doi:10.1016/0014-2999(95)00839-x
142. Bagdy G, Kecskemeti V, Riba P, Jakus R. Serotonin and epilepsy. doi:10.1111/j.1471-4159.2006.04277.x. *Journal of Neurochemistry*. 2007;100(4):857-873.
143. Ruggiero DA, Underwood MD, Mann JJ, Anwar M, Arango V. The human nucleus of the solitary tract: visceral pathways revealed with an "in vitro" postmortem tracing method. Review. *J Auton Nerv Syst*. Mar 2000;79(2-3):181-190. doi:10.1016/s0165-1838(99)00097-1
144. Giorgi FS, Pizzanelli C, Biagioni F, Murri L, Fornai F. The role of norepinephrine in epilepsy: from the bench to the bedside. Review. *Neuroscience and Biobehavioral Reviews*. Sep 2004;28(5):507-524. doi:10.1016/j.neubiorev.2004.06.008
145. Fornai F, Ruffoli R, Giorgi FS, Paparelli A. The role of locus coeruleus in the antiepileptic activity induced by vagus nerve stimulation. *European Journal of Neuroscience*. Jun 2011;33(12):2169-2178. doi:10.1111/j.1460-9568.2011.07707.x
146. George R, Salinsky M, Kuzniecky R, et al. Vagus nerve-stimulation for the treatment of partial seizures. 3. Long-term follow-up on first 67 patients exiting a controlled study. *Epilepsia*. 1994;35(3):637-643.
147. Picot MC, Baldy-Moulinier M, Daurès JP, Dujols P, Crespel A. The prevalence of epilepsy and pharmaco-resistant epilepsy in adults: a population-based study in a Western European country. *Epilepsia*. Jul 2008;49(7):1230-8. doi:10.1111/j.1528-1167.2008.01579.x
148. Brodie MJ, Barry SJ, Bamagous GA, Norrie JD, Kwan P. Patterns of treatment response in newly diagnosed epilepsy. *Neurology*. May 15 2012;78(20):1548-54. doi:10.1212/WNL.0b013e3182563b19



149. Brodie MJ, Yuen AW. Lamotrigine substitution study: evidence for synergism with sodium valproate? 105 Study Group. *Epilepsy Res.* Mar 1997;26(3):423-32. doi:10.1016/s0920-1211(96)01007-8
150. Kinirons P, McCarthy M, Doherty CP, Delanty N. Predicting drug-resistant patients who respond to add-on therapy with levetiracetam. *Seizure.* Sep 2006;15(6):387-92. doi:10.1016/j.seizure.2006.05.001
151. Chung S, Ben-Menachem E, Sperling MR, et al. Examining the clinical utility of lacosamide: pooled analyses of three phase II/III clinical trials. *CNS Drugs.* Dec 2010;24(12):1041-54. doi:10.2165/11586830-000000000-00000
152. Brigo F, Ausserer H, Tezzon F, Nardone R. When one plus one makes three: the quest for rational antiepileptic polytherapy with supraadditive anticonvulsant efficacy. *Epilepsy Behav.* Jun 2013;27(3):439-42. doi:10.1016/j.yebeh.2013.03.010
153. French JA, Krauss GL, Biton V, et al. Adjunctive perampanel for refractory partial-onset seizures: randomized phase III study 304. *Neurology.* Aug 07 2012;79(6):589-96. doi:10.1212/WNL.0b013e3182635735
154. Lattanzi S, Cagnetti C, Foschi N, Provinciali L, Silvestrini M. Brivaracetam add-on for refractory focal epilepsy: A systematic review and meta-analysis. *Neurology.* Apr 05 2016;86(14):1344-1352. doi:10.1212/WNL.0000000000002545
155. Thiele EA, Marsh ED, French JA, et al. Cannabidiol in patients with seizures associated with Lennox-Gastaut syndrome (GWPCARE4): a randomised, double-blind, placebo-controlled phase 3 trial. *Lancet.* 03 17 2018;391(10125):1085-1096. doi:10.1016/S0140-6736(18)30136-3
156. Balagura G, Cacciatore M, Grasso EA, Striano P, Verrotti A. Fenfluramine for the Treatment of Dravet Syndrome and Lennox-Gastaut Syndrome. *CNS Drugs.* 10 2020;34(10):1001-1007. doi:10.1007/s40263-020-00755-z
157. Nabbout R, Mistry A, Zuberi S, et al. Fenfluramine for Treatment-Resistant Seizures in Patients With Dravet Syndrome Receiving Stiripentol-Inclusive Regimens: A Randomized Clinical Trial. *JAMA Neurol.* 03 01 2020;77(3):300-308. doi:10.1001/jamaneurol.2019.4113
158. Afra P, Adamolekun B, Aydemir S, Watson GDR. Evolution of the Vagus Nerve Stimulation (VNS) Therapy System Technology for Drug-Resistant Epilepsy. *Front Med Technol.* 2021;3:696543. doi:10.3389/fmedt.2021.696543
159. Fisher B, DesMarteau JA, Koontz EH, Wilks SJ, Melamed SE. Responsive Vagus Nerve Stimulation for Drug Resistant Epilepsy: A Review of New Features and Practical Guidance for Advanced Practice Providers. *Front Neurol.* 2020;11:610379. doi:10.3389/fneur.2020.610379
160. Bajbouj M, Merkl A, Schlaepfer TE, et al. Two-Year Outcome of Vagus Nerve Stimulation in Treatment-Resistant Depression. Article. *Journal of Clinical Psychopharmacology.* Jun 2010;30(3):273-281. doi:10.1097/JCP.0b013e3181db8831
161. Johnson RL, Murray ST, Camacho DK, Wilson CG. Vagal nerve stimulation attenuates IL-6 and TNF $\alpha$  expression in respiratory regions of the developing rat brainstem. *Respir Physiol Neurobiol.* 07 15 2016;229:1-4. doi:10.1016/j.resp.2016.03.014
162. Lange G, Janal MN, Maniker A, et al. Safety and efficacy of vagus nerve stimulation in fibromyalgia: a phase I/II proof of concept trial. *Pain Med.* Sep 2011;12(9):1406-13. doi:10.1111/j.1526-4637.2011.01203.x
163. Silberstein SD, Mechtler LL, Kudrow DB, et al. Non-Invasive Vagus Nerve Stimulation for the ACute Treatment of Cluster Headache: Findings From the

- Randomized, Double-Blind, Sham-Controlled ACT1 Study. *Headache*. Sep 2016;56(8):1317-32. doi:10.1111/head.12896
164. Johnson RL, Wilson CG. A review of vagus nerve stimulation as a therapeutic intervention. *J Inflamm Res*. 2018;11:203-213. doi:10.2147/JIR.S163248
165. Boon P, De Cock E, Mertens A, Trinka E. Neurostimulation for drug-resistant epilepsy: a systematic review of clinical evidence for efficacy, safety, contraindications and predictors for response. *Curr Opin Neurol*. 04 2018;31(2):198-210. doi:10.1097/WCO.0000000000000534
166. Salanova V, Witt T, Worth R, et al. Long-term efficacy and safety of thalamic stimulation for drug-resistant partial epilepsy. *Neurology*. Mar 10 2015;84(10):1017-25. doi:10.1212/WNL.0000000000001334
167. Bergey GK, Morrell MJ, Mizrahi EM, et al. Long-term treatment with responsive brain stimulation in adults with refractory partial seizures. *Neurology*. Feb 24 2015;84(8):810-7. doi:10.1212/WNL.0000000000001280
168. Lundstrom BN, Worrell GA, Stead M, Van Gompel JJ. Chronic subthreshold cortical stimulation: a therapeutic and potentially restorative therapy for focal epilepsy. *Expert Rev Neurother*. Jul 2017;17(7):661-666. doi:10.1080/14737175.2017.1331129
169. Lefaucheur JP, André-Obadia N, Antal A, et al. Evidence-based guidelines on the therapeutic use of repetitive transcranial magnetic stimulation (rTMS). *Clin Neurophysiol*. Nov 2014;125(11):2150-2206. doi:10.1016/j.clinph.2014.05.021
170. Fregni F, El-Hagrassy MM, Pacheco-Barrios K, et al. Evidence-Based Guidelines and Secondary Meta-Analysis for the Use of Transcranial Direct Current Stimulation in Neurological and Psychiatric Disorders. *Int J Neuropsychopharmacol*. 04 21 2021;24(4):256-313. doi:10.1093/ijnp/pyaa051
171. Martin-McGill KJ, Bresnahan R, Levy RG, Cooper PN. Ketogenic diets for drug-resistant epilepsy. *Cochrane Database Syst Rev*. 06 24 2020;6:CD001903. doi:10.1002/14651858.CD001903.pub5
172. Chrastina J, Novák Z, Zeman T, et al. Single-center long-term results of vagus nerve stimulation for epilepsy: A 10-17 year follow-up study. *Seizure*. Jul 2018;59:41-47. doi:10.1016/j.seizure.2018.04.022
173. Ferriero DM. Neonatal brain injury. *N Engl J Med*. Nov 04 2004;351(19):1985-95. doi:10.1056/NEJMr041996
174. Liu L, Oza S, Hogan D, et al. Global, regional, and national causes of under-5 mortality in 2000-15: an updated systematic analysis with implications for the Sustainable Development Goals. *Lancet*. 12 17 2016;388(10063):3027-3035. doi:10.1016/S0140-6736(16)31593-8
175. Gale C, Statnikov Y, Jawad S, Uthaya SN, Modi N, group Blew. Neonatal brain injuries in England: population-based incidence derived from routinely recorded clinical data held in the National Neonatal Research Database. *Arch Dis Child Fetal Neonatal Ed*. Jul 2018;103(4):F301-F306. doi:10.1136/archdischild-2017-313707
176. Yates N, Gunn AJ, Bennet L, Dhillon SK, Davidson JO. Preventing Brain Injury in the Preterm Infant-Current Controversies and Potential Therapies. *Int J Mol Sci*. Feb 07 2021;22(4)doi:10.3390/ijms22041671
177. Vohr BR, Wright LL, Dusick AM, et al. Neurodevelopmental and Functional Outcomes of Extremely Low Birth Weight Infants in the National Institute of Child Health and Human Development Neonatal Research Network, 1993–1994. *Pediatrics*. 2000;105(6):1216-1226.

178. Wilson-Costello D, Friedman H, Minich N, et al. Improved Neurodevelopmental Outcomes for Extremely Low Birth Weight Infants in 2000–2002. *Pediatrics*. 2007;119(1):37-45.
179. David JF, Jon SD, Bradley NM, Elizabeth SD. Survival of extremely premature babies in a geographically defined population: prospective cohort study of 1994-9 compared with 2000-5. *BMJ*. 2008;336
180. Moser K, Macfarlane A, Chow YH, Hilder L, N. D. Introducing new data on gestation-specific infant mortality among babies born in 2005 in England and Wales.: *Health Stat Q*.; 2007. p. 13-27.
181. Martin JA, Kung H-C, Mathews TJ, et al. Annual Summary of Vital Statistics: 2006. *Pediatrics*. 2008;121(4):788-801.
182. Peterson BS, Vohr B, Staib LH, et al. Regional Brain Volume Abnormalities and Long-term Cognitive Outcome in Preterm Infants. *JAMA: The Journal of the American Medical Association*. 2000;284(15):1939-1947.
183. Hack M, Wilson-Costello D, Friedman H, Taylor GH, Schluchter M, Fanaroff AA. Neurodevelopment and Predictors of Outcomes of Children With Birth Weights of Less Than 1000 g: 1992-1995. *Archives of Pediatrics Adolescent Medicine*. 2000;154(7):725-731.
184. Woodward LJ, Anderson PJ, Austin NC, Howard K, Inder TE. Neonatal MRI to Predict Neurodevelopmental Outcomes in Preterm Infants. *New England Journal of Medicine*. 2006/08/17 2006;355(7):685-694. doi:10.1056/NEJMoa053792
185. Joseph J V. Brain injury in premature infants: a complex amalgam of destructive and developmental disturbances. *The Lancet Neurology*. 2009;8(1):110-124. doi:10.1016/s1474-4422(08)70294-1
186. Bax M, Tydeman C, Flodmark O. Clinical and MRI correlates of cerebral palsy: the European Cerebral Palsy Study. *JAMA*. Oct 04 2006;296(13):1602-8. doi:10.1001/jama.296.13.1602
187. Mallard EC, Rees S, Stringer M, Cock ML, Harding R. Effects of chronic placental insufficiency on brain development in fetal sheep. *Pediatr Res*. Feb 1998;43(2):262-70. doi:10.1203/00006450-199802000-00018
188. Sun L, Macgowan CK, Sled JG, et al. Reduced fetal cerebral oxygen consumption is associated with smaller brain size in fetuses with congenital heart disease. *Circulation*. Apr 14 2015;131(15):1313-23. doi:10.1161/CIRCULATIONAHA.114.013051
189. Back SA. White matter injury in the preterm infant: pathology and mechanisms. *Acta Neuropathol*. Sep 2017;134(3):331-349. doi:10.1007/s00401-017-1718-6
190. Pierson CR, Folkerth RD, Billiards SS, et al. Gray matter injury associated with periventricular leukomalacia in the premature infant. *Acta Neuropathol*. Dec 2007;114(6):619-31. doi:10.1007/s00401-007-0295-5
191. Buser JR, Maire J, Riddle A, et al. Arrested preoligodendrocyte maturation contributes to myelination failure in premature infants. *Ann Neurol*. Jan 2012;71(1):93-109. doi:10.1002/ana.22627
192. Kersbergen KJ, Benders MJ, Groenendaal F, et al. Different patterns of punctate white matter lesions in serially scanned preterm infants. *PLoS One*. 2014;9(10):e108904. doi:10.1371/journal.pone.0108904
193. Engelhardt E, Inder TE, Alexopoulos D, et al. Regional impairments of cortical folding in premature infants. *Ann Neurol*. Jan 2015;77(1):154-62. doi:10.1002/ana.24313
194. Volpe JJ. *Neurology of the Newborn*. 2008.

195. Pierrat V, Duquennoy C, van Haastert IC, Ernst M, Guilley N, de Vries LS. Ultrasound diagnosis and neurodevelopmental outcome of localised and extensive cystic periventricular leucomalacia. *Archives of Disease in Childhood - Fetal and Neonatal Edition*. 2001;84(3):F151-F156.
196. Joseph J V. Brain injury in the premature infant – from pathogenesis to prevention. *Brain and Development*. 1997;19(8):519-534. doi:10.1016/s0387-7604(97)00078-8
197. Gould SJ, Howard S, Hope PL, Reynolds EOR. Periventricular intraparenchymal cerebral haemorrhage in preterm infants: The role of venous infarction. 10.1002/path.1711510307. *The Journal of Pathology*. 1987;151(3):197-202.
198. Volpe JJ, Kinney HC, Jensen FE, Rosenberg PA. The developing oligodendrocyte: key cellular target in brain injury in the premature infant. *International Journal of Developmental Neuroscience*. 2011;29(4):423-440. doi:10.1016/j.ijdevneu.2011.02.012
199. Curtis D, Johnston G. Amino acid transmitters in the mammalian central nervous system. *Ergebnisse der Physiologie, biologischen Chemie und experimentellen Pharmakologie*. 1974;69(-1):97-188. doi:10.1007/3-540-06498-2\_3
200. Niels C D. Glutamate uptake. *Progress in Neurobiology*. 2001;65(1):1-105. doi:10.1016/s0301-0082(00)00067-8
201. Jensen FE. Role of Glutamate Receptors in Periventricular Leukomalacia. *Journal of Child Neurology*. 2005;20(12):950-959.
202. Hara MR, Snyder SH. Cell Signaling and Neuronal Death. *Annual Review of Pharmacology and Toxicology*. 2007/02/01 2007;47(1):117-141. doi:10.1146/annurev.pharmtox.47.120505.105311
203. Kochanek PM, Clark RSB, Ruppel RA, et al. Biochemical, cellular, and molecular mechanisms in the evolution of secondary damage after severe traumatic brain injury in infants and children: Lessons learned from the bedside. *Pediatric Critical Care Medicine*. 2000;1(1)
204. Oka A, Belliveau MJ, Rosenberg PA, Volpe JJ. Vulnerability of oligodendroglia to glutamate - Pharmacology, mechanisms, and prevention. *Journal of Neuroscience*. Apr 1993;13(4):1441-1453.
205. Yonezawa M, Back SA, Gan X, Rosenberg PA, Volpe JJ. Cystine Deprivation Induces Oligodendroglial Death: Rescue by Free Radical Scavengers and by a Diffusible Glial Factor. 10.1046/j.1471-4159.1996.67020566.x. *Journal of Neurochemistry*. 1996;67(2):566-573.
206. Haynes RL, Baud O, Li J, Kinney HC, Volpe JJ, Folkerth RD. Oxidative and Nitrate Injury in Periventricular Leukomalacia: A Review. 10.1111/j.1750-3639.2005.tb00525.x. *Brain Pathology*. 2005;15(3):225-233.
207. Seal RP, Amara SG. EXCITATORY AMINO ACID TRANSPORTERS: A Family in Flux. *Annual Review of Pharmacology and Toxicology*. 1999/04/01 1999;39(1):431-456. doi:10.1146/annurev.pharmtox.39.1.431
208. M.B R. Review Article The family of sodium-dependent glutamate transporters: a focus on the GLT-1/EAAT2 subtype. *Neurochemistry International*. 1998;33(6):479-491. doi:10.1016/s0197-0186(98)00055-2
209. Mallolas J, Hurtado O, Castellanos M, et al. A polymorphism in the EAAT2 promoter is associated with higher glutamate concentrations and higher frequency of progressing stroke. *The Journal of Experimental Medicine*. 2006;203(3):711-717.
210. Szatkowski M, Barbour B, Attwell D. Non-vesicular release of glutamate from glial cells by reversed electrogenic glutamate uptake. *Nature*. Nov 29 1990;348(6300):443-6. doi:10.1038/348443a0

211. Szatkowski M, Attwell D. Triggering and execution of neuronal death in brain ischaemia: two phases of glutamate release by different mechanisms. *Trends Neurosci.* Sep 1994;17(9):359-65. doi:10.1016/0166-2236(94)90040-x
212. Grewer C, Gameiro A, Zhang Z, Tao Z, Braams S, Rauen T. Glutamate forward and reverse transport: from molecular mechanism to transporter-mediated release after ischemia. *IUBMB Life.* Sep 2008;60(9):609-19. doi:10.1002/iub.98
213. Rossi DJ, Oshima T, Attwell D. Glutamate release in severe brain ischaemia is mainly by reversed uptake. *Nature.* Jan 20 2000;403(6767):316-21. doi:10.1038/35002090
214. Seki Y, Feustel PJ, Keller RW, Tranmer BI, Kimelberg HK. Inhibition of ischemia-induced glutamate release in rat striatum by dihydrokinate and an anion channel blocker. *Stroke.* Feb 1999;30(2):433-40. doi:10.1161/01.str.30.2.433
215. Follett PL, Deng W, Dai W, et al. Glutamate Receptor-Mediated Oligodendrocyte Toxicity in Periventricular Leukomalacia: A Protective Role for Topiramate. *The Journal of Neuroscience.* 2004;24(18):4412-4420.
216. Manning SM, Talos DM, Zhou C, et al. NMDA Receptor Blockade with Memantine Attenuates White Matter Injury in a Rat Model of Periventricular Leukomalacia. *The Journal of Neuroscience.* 2008;28(26):6670-6678.
217. Manning SM, Boll G, Fitzgerald E, Selip DB, Volpe JJ, Jensen FE. The clinically available NMDA receptor antagonist, memantine, exhibits relative safety in the developing rat brain. *International Journal of Developmental Neuroscience.* 2011;29(7):767-773. doi:10.1016/j.ijdevneu.2011.05.005
218. Roberts D, Brown J, Medley N, Dalziel SR. Antenatal corticosteroids for accelerating fetal lung maturation for women at risk of preterm birth. *Cochrane Database Syst Rev.* 03 21 2017;3:CD004454. doi:10.1002/14651858.CD004454.pub3
219. Doyle LW, Cheong JL, Ehrenkranz RA, Halliday HL. Early (< 8 days) systemic postnatal corticosteroids for prevention of bronchopulmonary dysplasia in preterm infants. *Cochrane Database Syst Rev.* 10 24 2017;10:CD001146. doi:10.1002/14651858.CD001146.pub5
220. Baud O, Foix-L'Helias L, Kaminski M, et al. Antenatal glucocorticoid treatment and cystic periventricular leukomalacia in very premature infants. *N Engl J Med.* Oct 14 1999;341(16):1190-6. doi:10.1056/NEJM199910143411604
221. Galinsky R, Bennet L, Groenendaal F, et al. Magnesium is not consistently neuroprotective for perinatal hypoxia-ischemia in term-equivalent models in preclinical studies: a systematic review. *Dev Neurosci.* 2014;36(2):73-82. doi:10.1159/000362206
222. Doyle LW. Antenatal magnesium sulfate and neuroprotection. *Curr Opin Pediatr.* Apr 2012;24(2):154-9. doi:10.1097/MOP.0b013e3283504da1
223. Doyle LW, Crowther CA, Middleton P, Marret S. Antenatal magnesium sulfate and neurologic outcome in preterm infants: a systematic review. *Obstet Gynecol.* Jun 2009;113(6):1327-1333. doi:10.1097/AOG.0b013e3181a60495
224. Booth D, Evans DJ. Anticonvulsants for neonates with seizures. *Cochrane Database Syst Rev.* Oct 18 2004;(4):CD004218. doi:10.1002/14651858.CD004218.pub2
225. Ohlsson A, Aher SM. Early erythropoietin for preventing red blood cell transfusion in preterm and/or low birth weight infants. *Cochrane Database Syst Rev.* Jul 19 2006;(3):CD004863. doi:10.1002/14651858.CD004863.pub2
226. Juul SE, Comstock BA, Heagerty PJ, et al. High-Dose Erythropoietin for Asphyxia and Encephalopathy (HEAL): A Randomized Controlled Trial - Background, Aims, and Study Protocol. *Neonatology.* 2018;113(4):331-338. doi:10.1159/000486820

227. Fischer HS, Reibel NJ, Bühner C, Dame C. Prophylactic Early Erythropoietin for Neuroprotection in Preterm Infants: A Meta-analysis. *Pediatrics*. May 2017;139(5)doi:10.1542/peds.2016-4317
228. Jacobs SE, Berg M, Hunt R, Tarnow-Mordi WO, Inder TE, Davis PG. Cooling for newborns with hypoxic ischaemic encephalopathy. *Cochrane Database Syst Rev*. Jan 31 2013;(1):CD003311. doi:10.1002/14651858.CD003311.pub3
229. Drury PP, Davidson JO, Bennet L, et al. Partial neural protection with prophylactic low-dose melatonin after asphyxia in preterm fetal sheep. *J Cereb Blood Flow Metab*. Jan 2014;34(1):126-35. doi:10.1038/jcbfm.2013.174
230. Robertson NJ, Lingam I, Meehan C, et al. High-Dose Melatonin and Ethanol Excipient Combined with Therapeutic Hypothermia in a Newborn Piglet Asphyxia Model. *Sci Rep*. 03 03 2020;10(1):3898. doi:10.1038/s41598-020-60858-x
231. Eyles D, Burne T, McGrath J. Vitamin D in fetal brain development. *Semin Cell Dev Biol*. Aug 2011;22(6):629-36. doi:10.1016/j.semcd.2011.05.004
232. Evans MA, Kim HA, Ling YH, et al. Vitamin D. *Neuromolecular Med*. 03 2018;20(1):147-159. doi:10.1007/s12017-018-8484-z
233. van den Heuvel LG, Fraser M, Miller SL, et al. Delayed intranasal infusion of human amnion epithelial cells improves white matter maturation after asphyxia in preterm fetal sheep. *J Cereb Blood Flow Metab*. 02 2019;39(2):223-239. doi:10.1177/0271678X17729954
234. Wang XL, Zhao YS, Hu MY, Sun YQ, Chen YX, Bi XH. Umbilical cord blood cells regulate endogenous neural stem cell proliferation via hedgehog signaling in hypoxic ischemic neonatal rats. *Brain Res*. Jun 26 2013;1518:26-35. doi:10.1016/j.brainres.2013.04.038
235. Li J, Yawno T, Sutherland A, et al. Preterm white matter brain injury is prevented by early administration of umbilical cord blood cells. *Exp Neurol*. 09 2016;283(Pt A):179-87. doi:10.1016/j.expneurol.2016.06.017
236. Lai PC, Huang YT, Wu CC, Lai CJ, Wang PJ, Chiu TH. Ceftriaxone attenuates hypoxic-ischemic brain injury in neonatal rats. *J Biomed Sci*. Sep 21 2011;18:69. doi:10.1186/1423-0127-18-69
237. Vermeij JD, Westendorp WF, Roos YB, et al. Preventive Ceftriaxone in Patients with Stroke Treated with Intravenous Thrombolysis: Post Hoc Analysis of the Preventive Antibiotics in Stroke Study. *Cerebrovasc Dis*. 2016;42(5-6):361-369. doi:10.1159/000446160
238. Müller GC, Loureiro SO, Pettenuzzo LF, et al. Effects of intranasal guanosine administration on brain function in a rat model of ischemic stroke. *Purinergic Signal*. 06 2021;17(2):255-271. doi:10.1007/s11302-021-09766-x
239. Moretto MB, Boff B, Lavinsky D, et al. Importance of schedule of administration in the therapeutic efficacy of guanosine: early intervention after injury enhances glutamate uptake in model of hypoxia-ischemia. *J Mol Neurosci*. Jun 2009;38(2):216-9. doi:10.1007/s12031-008-9154-7
240. Yuen TI, Morokoff AP, Bjorksten A, et al. Glutamate is associated with a higher risk of seizures in patients with gliomas. *Neurology*. Aug 2012;79(9)doi:10.1212/WNL.0b013e318266fa89
241. Buckingham SC, Campbell SL, Haas BR, et al. Glutamate release by primary brain tumors induces epileptic activity. *Nature Medicine*. Oct 2011;17(10)doi:10.1038/nm.2453
242. Romera C, Hurtado O, Botella SH, et al. In vitro ischemic tolerance involves upregulation of glutamate transport partly mediated by the TACE/ADAM17-tumor

- necrosis factor-alpha pathway. *Journal of Neuroscience*. Feb 11 2004;24(6):1350-1357. doi:10.1523/jneurosci.1596-03.2004
243. Romera C, Hurtado O, Mallolas J, et al. Ischemic preconditioning reveals that GLT1//EAAT2 glutamate transporter is a novel PPAR[gamma] target gene involved in neuroprotection. *J Cereb Blood Flow Metab*. 2007;27(7):1327-1338.
244. Harvey BK, Airavaara M, Hinzman J, et al. Targeted Over-Expression of Glutamate Transporter 1 (GLT-1) Reduces Ischemic Brain Injury in a Rat Model of Stroke. *PLoS ONE*. 2011;6(8):e22135. doi:10.1371/journal.pone.0022135
245. Chu K, Lee S-T, Sinn D-I, et al. Pharmacological induction of ischemic tolerance by glutamate transporter-1 (EAAT2) upregulation. *Stroke*. Jan 2007;38(1):177-182. doi:10.1161/01.str.0000252091.36912.65
246. Verma R, Mishra V, Sasmal D, Raghurir R. Pharmacological evaluation of glutamate transporter 1 (GLT-1) mediated neuroprotection following cerebral ischemia/reperfusion injury. *European Journal of Pharmacology*. 2010;638(1-3):65-71. doi:10.1016/j.ejphar.2010.04.021
247. Elstner E, Williamson EA, Zang C, et al. Novel therapeutic approach: ligands for PPAR gamma and retinoid receptors induce apoptosis in bcl-2-positive human breast cancer cells. *Breast Cancer Research and Treatment*. Jul 2002;74(2):155-165. doi:10.1023/a:1016114026769
248. Sarraf P, Mueller E, Jones D, et al. Differentiation and reversal of malignant changes in colon cancer through PPAR gamma. *Nature Medicine*. Sep 1998;4(9):1046-1052. doi:10.1038/2030
249. Lee MW, Kim DS, Kim HR, et al. Cell death is induced by ciglitazone, a peroxisome proliferator-activated receptor gamma (PPAR gamma) agonist, independently of PPAR gamma in human glioma cells. *Biochemical and Biophysical Research Communications*. Jan 6 2012;417(1):552-557. doi:10.1016/j.bbrc.2011.12.001
250. Grommes C, Landreth GE, Heneka MT. Antineoplastic effects of peroxisome proliferator-activated receptor gamma agonists. Review. *Lancet Oncology*. Jul 2004;5(7):419-429. doi:10.1016/s1470-2045(04)01509-8
251. Tatenhorst L, Hahnen E, Heneka MT. Peroxisome Proliferator-Activated Receptors (PPARs) as Potential Inducers of Antineoplastic Effects in CNS Tumors. *Ppar Research*. 2008 2008;204514. doi:10.1155/2008/204514
252. Wang P, Yu J, Yin Q, Li W, Ren X, Hao X. Rosiglitazone Suppresses Glioma Cell Growth and Cell Cycle by Blocking the Transforming Growth Factor-Beta Mediated Pathway. *Neurochemical Research*. Oct 2012;37(10):2076-2084. doi:10.1007/s11064-012-0828-8
253. Wan Z, Shi W, Shao B, et al. Peroxisome proliferator-activated receptor gamma agonist pioglitazone inhibits beta-catenin-mediated glioma cell growth and invasion. *Molecular and Cellular Biochemistry*. Mar 2011;349(1-2):1-10. doi:10.1007/s11010-010-0637-9
254. Ching J, Amiridis S, Stylli SS, Morokoff AP, O'Brien TJ, Kaye AH. A novel treatment strategy for glioblastoma multiforme and glioma associated seizures: increasing glutamate uptake with PPAR $\gamma$  agonists. *J Clin Neurosci*. Jan 2015;22(1):21-8. doi:10.1016/j.jocn.2014.09.001
255. Rudà R, Soffietti R. What is New in the Management of Epilepsy in Gliomas? *Curr Treat Options Neurol*. Jun 2015;17(6):351. doi:10.1007/s11940-015-0351-8
256. Robe PA, Martin DH, Nguyen-Khac MT, et al. Early termination of ISRCTN45828668, a phase 1/2 prospective, randomized study of Sulfasalazine for the

- treatment of progressing malignant gliomas in adults. *Bmc Cancer*. Oct 19 2009;9372. doi:10.1186/1471-2407-9-372
257. Seltzer MJ, Bennett BD, Joshi AD, et al. Inhibition of glutaminase preferentially slows growth of glioma cells with mutant IDH1. *Cancer Res*. Nov 2010;70(22):8981-7. doi:10.1158/0008-5472.CAN-10-1666
258. Yao PS, Kang DZ, Lin RY, Ye B, Wang W, Ye ZC. Glutamate/glutamine metabolism coupling between astrocytes and glioma cells: neuroprotection and inhibition of glioma growth. *Biochem Biophys Res Commun*. Jul 2014;450(1):295-9. doi:10.1016/j.bbrc.2014.05.120
259. Rosati A, Poliani PL, Todeschini A, et al. Glutamine synthetase expression as a valuable marker of epilepsy and longer survival in newly diagnosed glioblastoma multiforme. *Neuro Oncol*. May 2013;15(5):618-25. doi:10.1093/neuonc/nos338
260. Prakash O, Lukiw WJ, Peruzzi F, Reiss K, Musto AE. Gliomas and seizures. *Med Hypotheses*. Nov 2012;79(5):622-6. doi:10.1016/j.mehy.2012.07.037
261. Morimoto K, Fahnstock M, Racine RJ. Kindling and status epilepticus models of epilepsy: rewiring the brain. *Prog Neurobiol*. May 2004;73(1):1-60. doi:10.1016/j.pneurobio.2004.03.009
262. Aronica E, Yankaya B, Jansen GH, et al. Ionotropic and metabotropic glutamate receptor protein expression in glioneuronal tumours from patients with intractable epilepsy. *Neuropathol Appl Neurobiol*. Jun 2001;27(3):223-37. doi:10.1046/j.0305-1846.2001.00314.x
263. Aronica E, Gorter JA, Ijst-Keizers H, et al. Expression and functional role of mGluR3 and mGluR5 in human astrocytes and glioma cells: opposite regulation of glutamate transporter proteins. *Eur J Neurosci*. May 2003;17(10):2106-18. doi:10.1046/j.1460-9568.2003.02657.x
264. van Vuurden DG, Yazdani M, Bosma I, et al. Attenuated AMPA receptor expression allows glioblastoma cell survival in glutamate-rich environment. *PLoS One*. Jun 2009;4(6):e5953. doi:10.1371/journal.pone.0005953
265. Grossman SA, Ye X, Chamberlain M, et al. Talampanel with standard radiation and temozolomide in patients with newly diagnosed glioblastoma: a multicenter phase II trial. *J Clin Oncol*. Sep 2009;27(25):4155-61. doi:10.1200/JCO.2008.21.6895
266. Iglesias J, Morales L, Barreto GE. Metabolic and Inflammatory Adaptation of Reactive Astrocytes: Role of PPARs. *Mol Neurobiol*. 05 2017;54(4):2518-2538. doi:10.1007/s12035-016-9833-2
267. Hong S, Xin Y, HaiQin W, et al. The PPAR $\gamma$  agonist rosiglitazone prevents cognitive impairment by inhibiting astrocyte activation and oxidative stress following pilocarpine-induced status epilepticus. *Neurol Sci*. Jun 2012;33(3):559-66. doi:10.1007/s10072-011-0774-2
268. Tian GX, Zhu XQ, Chen Y, Wu GC, Wang J. Huperzine A inhibits CCL2 production in experimental autoimmune encephalomyelitis mice and in cultured astrocyte. *Int J Immunopathol Pharmacol*. 2013 Jul-Sep 2013;26(3):757-64. doi:10.1177/039463201302600320
269. Fernandez MO, Hsueh K, Park HT, et al. Astrocyte-Specific Deletion of Peroxisome-Proliferator Activated Receptor-. *J Endocr Soc*. Nov 2017;1(11):1332-1350. doi:10.1210/js.2017-00242
270. Pourgholi F, Hajivalili M, Farhad JN, Kafil HS, Yousefi M. Nanoparticles: Novel vehicles in treatment of Glioblastoma. *Biomed Pharmacother*. Feb 2016;77:98-107. doi:10.1016/j.biopha.2015.12.014



271. Taghizadehghalehjoughi A, Hacimuftuoglu A, Cetin M, et al. Effect of metformin/irinotecan-loaded poly-lactic-co-glycolic acid nanoparticles on glioblastoma: in vitro and in vivo studies. *Nanomedicine (Lond)*. 07 2018;13(13):1595-1606. doi:10.2217/nnm-2017-0386
272. Silva J, Mendes M, Cova T, Sousa J, Pais A, Vitorino C. Unstructured Formulation Data Analysis for the Optimization of Lipid Nanoparticle Drug Delivery Vehicles. *AAPS PharmSciTech*. Jul 2018;19(5):2383-2394. doi:10.1208/s12249-018-1078-0
273. Steffens L, Dias M, Arantes P, Henn G, Nugent M, Moura D. Chapter 12 - Nanopolymeric systems to improve brain cancer treatment outcomes. *Advances and Challenges in Pharmaceutical Technology*; 2021. p. 355-394.
274. Han S, Lv X, Wang Y, et al. Effect and mechanism of peroxisome proliferator-activated receptor- $\gamma$  on the drug resistance of the U-87 MG/CDDP human malignant glioma cell line. *Mol Med Rep*. Aug 2015;12(2):2239-46. doi:10.3892/mmr.2015.3625
275. Campbell SL, Robel S, Cuddapah VA, et al. GABAergic disinhibition and impaired KCC2 cotransporter activity underlie tumor-associated epilepsy. *Glia*. Jan 2015;63(1):23-36. doi:10.1002/glia.22730
276. Kirschstein T, Köhling R. Animal models of tumour-associated epilepsy. *J Neurosci Methods*. Feb 2016;260:109-17. doi:10.1016/j.jneumeth.2015.06.008
277. Hatcher A, Yu K, Meyer J, Aiba I, Deneen B, Noebels JL. Pathogenesis of peritumoral hyperexcitability in an immunocompetent CRISPR-based glioblastoma model. *J Clin Invest*. 05 2020;130(5):2286-2300. doi:10.1172/JCI133316
278. John Lin CC, Yu K, Hatcher A, et al. Identification of diverse astrocyte populations and their malignant analogs. *Nat Neurosci*. Mar 2017;20(3):396-405. doi:10.1038/nn.4493
279. Sundstrom L, Morrison B, Bradley M, Pringle A. Organotypic cultures as tools for functional screening in the CNS. *Drug Discov Today*. Jul 2005;10(14):993-1000. doi:10.1016/S1359-6446(05)03502-6
280. Magalhães DM, Pereira N, Rombo DM, Beltrão-Cavacas C, Sebastião AM, Valente CA. Ex vivo model of epilepsy in organotypic slices-a new tool for drug screening. *J Neuroinflammation*. Jul 2018;15(1):203. doi:10.1186/s12974-018-1225-2
281. Giulioni M, Marucci G, Martinoni M, et al. Epilepsy associated tumors: Review article. *World J Clin Cases*. Nov 16 2014;2(11):623-41. doi:10.12998/wjcc.v2.i11.623
282. Zhang X, Zheng L, Duan J, Li Z, Tang Y. Clinical characteristics of brain tumor-related epilepsy and factors influencing the identification of epilepsy-associated tumors. *Acta Epileptologica* 2020.
283. Rudà R, Trevisan E, Soffietti R. Epilepsy and brain tumors. *Curr Opin Oncol*. Nov 2010;22(6):611-20. doi:10.1097/CCO.0b013e32833de99d
284. Sontheimer H, Bridges RJ. Sulfasalazine for brain cancer fits. *Expert Opin Investig Drugs*. May 2012;21(5):575-8. doi:10.1517/13543784.2012.670634
285. Robert SM, Buckingham SC, Campbell SL, et al. SLC7A11 expression is associated with seizures and predicts poor survival in patients with malignant glioma. *Sci Transl Med*. May 2015;7(289):289ra86. doi:10.1126/scitranslmed.aaa8103
286. Tang H, Shi W, Fu S, et al. Pioglitazone and bladder cancer risk: a systematic review and meta-analysis. *Cancer Med*. 04 2018;7(4):1070-1080. doi:10.1002/cam4.1354
287. Lv S, Wang W, Wang H, Zhu Y, Lei C. PPAR $\gamma$  activation serves as therapeutic strategy against bladder cancer via inhibiting PI3K-Akt signaling pathway. *BMC Cancer*. Mar 2019;19(1):204. doi:10.1186/s12885-019-5426-6

288. Zhao W, Payne V, Tommasi E, Diz DI, Hsu FC, Robbins ME. Administration of the peroxisomal proliferator-activated receptor gamma agonist pioglitazone during fractionated brain irradiation prevents radiation-induced cognitive impairment. *Int J Radiat Oncol Biol Phys*. Jan 01 2007;67(1):6-9. doi:10.1016/j.ijrobp.2006.09.036
289. Cramer CK, Alphonse-Sullivan N, Isom S, et al. Safety of pioglitazone during and after radiation therapy in patients with brain tumors: a phase I clinical trial. *J Cancer Res Clin Oncol*. Feb 2019;145(2):337-344. doi:10.1007/s00432-018-2791-5
290. Searcy JL, Phelps JT, Pancani T, et al. Long-term pioglitazone treatment improves learning and attenuates pathological markers in a mouse model of Alzheimer's disease. *J Alzheimers Dis*. 2012;30(4):943-61. doi:10.3233/JAD-2012-111661
291. Moon JH, Kim HJ, Yang AH, et al. The effect of rosiglitazone on LRP1 expression and amyloid  $\beta$  uptake in human brain microvascular endothelial cells: a possible role of a low-dose thiazolidinedione for dementia treatment. *Int J Neuropsychopharmacol*. Feb 2012;15(1):135-42. doi:10.1017/S1461145711001611
292. Burns DK, Alexander RC, Welsh-Bohmer KA, et al. Safety and efficacy of pioglitazone for the delay of cognitive impairment in people at risk of Alzheimer's disease (TOMMORROW): a prognostic biomarker study and a phase 3, randomised, double-blind, placebo-controlled trial. *Lancet Neurol*. 07 2021;20(7):537-547. doi:10.1016/S1474-4422(21)00043-0
293. Saunders AM, Burns DK, Gottschalk WK. Reassessment of Pioglitazone for Alzheimer's Disease. *Front Neurosci*. 2021;15:666958. doi:10.3389/fnins.2021.666958
294. Dehmer T, Heneka MT, Sastre M, Dichgans J, Schulz JB. Protection by pioglitazone in the MPTP model of Parkinson's disease correlates with I kappa B alpha induction and block of NF kappa B and iNOS activation. *J Neurochem*. Jan 2004;88(2):494-501. doi:10.1046/j.1471-4159.2003.02210.x
295. Investigators NETiPDN-PF-Z. Pioglitazone in early Parkinson's disease: a phase 2, multicentre, double-blind, randomised trial. *Lancet Neurol*. Aug 2015;14(8):795-803. doi:10.1016/S1474-4422(15)00144-1
296. Zhao Y, Patzer A, Gohlke P, Herdegen T, Culman J. The intracerebral application of the PPARgamma-ligand pioglitazone confers neuroprotection against focal ischaemia in the rat brain. *Eur J Neurosci*. Jul 2005;22(1):278-82. doi:10.1111/j.1460-9568.2005.04200.x
297. Culman J, Nguyen-Ngoc M, Glatz T, Gohlke P, Herdegen T, Zhao Y. Treatment of rats with pioglitazone in the reperfusion phase of focal cerebral ischemia: a preclinical stroke trial. *Exp Neurol*. Dec 2012;238(2):243-53. doi:10.1016/j.expneurol.2012.09.003
298. Kernan WN, Viscoli CM, Furie KL, et al. Pioglitazone after Ischemic Stroke or Transient Ischemic Attack. *N Engl J Med*. Apr 07 2016;374(14):1321-31. doi:10.1056/NEJMoa1506930
299. van Breemen MSM, Rijsman RM, Taphoorn MJB, Walchenbach R, Zwinkels H, Vecht CJ. Efficacy of anti-epileptic drugs in patients with gliomas and seizures. *Journal of Neurology*. Sep 2009;256(9)doi:10.1007/s00415-009-5156-9
300. Bernardo A, Minghetti L. Regulation of Glial Cell Functions by PPAR-gamma Natural and Synthetic Agonists. *PPAR research*. 2008 2008;2008:864140.
301. Lee J, Reding M. Effects of Thiazolidinediones on Stroke Recovery: A Case-Matched Controlled Study. *Neurochemical Research*. 2007;32(4):635-638. doi:10.1007/s11064-006-9138-3
302. Ching J, Amiridis S, Stylli SS, et al. The peroxisome proliferator activated receptor gamma agonist pioglitazone increases functional expression of the glutamate

- transporter excitatory amino acid transporter 2 (EAAT2) in human glioblastoma cells. *Oncotarget*. Aug 2015;6(25):21301-14. doi:10.18632/oncotarget.4019
303. Grommes C, Conway DS, Alsheklee A, Barnholtz-Sloan JS. Inverse association of PPAR gamma agonists use and high grade glioma development. *Journal of Neuro-Oncology*. Nov 2010;100(2):233-239. doi:10.1007/s11060-010-0185-x
304. Ye ZC, Sontheimer H. Glioma cells release excitotoxic concentrations of glutamate. Article. *Cancer Research*. Sep 1999;59(17):4383-4391.
305. de Groot JF, Liu TJ, Fuller GWK, Yung A. The Excitatory Amino Acid Transporter-2 Induces Apoptosis and Decreases Glioma Growth In vitro and In vivo. 2005. p. 1934-1940.
306. Ching J, Amiridis S, Stylli SS, et al. The peroxisome proliferator activated receptor gamma agonist pioglitazone increases functional expression of the glutamate transporter excitatory amino acid transporter 2 (EAAT2) in human glioblastoma cells. *Oncotarget*. 2015:1-14.
307. Stoppini L, Buchs PA, Muller D. A SIMPLE METHOD FOR ORGANOTYPIC CULTURES OF NERVOUS-TISSUE. *Journal of Neuroscience Methods*. Apr 1991;37(2):173-182. doi:10.1016/0165-0270(91)90128-m
308. de Bouard S, Christov C, Guillermo JS, et al. Invasion of human glioma biopsy specimens in cultures of rodent brain slices: a quantitative analysis. *J Neurosurg*. Jul 2002;97(1):169-176.
309. Luwor RB, Hakmana D, Iaria J, Nheu TV, Simpson RJ, Zhu HJ. Single live cell TGF- $\beta$  signalling imaging: breast cancer cell motility and migration is driven by sub-populations of cells with dynamic TGF- $\beta$ -Smad3 activity. *Mol Cancer*. Feb 2015;14:50. doi:10.1186/s12943-015-0309-1
310. Klinger NV, Shah AK, Mittal S. Management of brain tumor-related epilepsy. *Neurol India*. 2017 2017;65(Supplement):S60-S70. doi:10.4103/neuroindia.NI\_1076\_16
311. Yap KY, Chui WK, Chan A. Drug interactions between chemotherapeutic regimens and antiepileptics. *Clin Ther*. Aug 2008;30(8):1385-407. doi:10.1016/j.clinthera.2008.08.011
312. Rossetti AO, Jeckelmann S, Novy J, Roth P, Weller M, Stupp R. Levetiracetam and pregabalin for antiepileptic monotherapy in patients with primary brain tumors. A phase II randomized study. *Neuro Oncol*. Apr 2014;16(4):584-8. doi:10.1093/neuonc/not170
313. Tremont-Lukats IW, Ratilal BO, Armstrong T, Gilbert MR. Antiepileptic drugs for preventing seizures in people with brain tumors. *Cochrane Database Syst Rev*. Apr 16 2008;(2):CD004424. doi:10.1002/14651858.CD004424.pub2
314. Venkatesh HS, Morishita W, Geraghty AC, et al. Electrical and synaptic integration of glioma into neural circuits. *Nature*. 09 2019;573(7775):539-545. doi:10.1038/s41586-019-1563-y
315. Lange F, Hörnschemeyer J, Kirschstein T. Glutamatergic Mechanisms in Glioblastoma and Tumor-Associated Epilepsy. *Cells*. 05 17 2021;10(5)doi:10.3390/cells10051226
316. Schwartzbaum JA, Fisher JL, Aldape KD, Wrensch M. Epidemiology and molecular pathology of glioma. 10.1038/ncpneuro0289. *Nat Clin Pract Neuro*. 2006;2(9):494-503.
317. Adamson C, Kanu OO, Mehta AI, et al. Glioblastoma multiforme: a review of where we have been and where we are going. *Expert Opinion on Investigational Drugs*. 2009;18(8):1061-1083. doi:10.1517/13543780903052764

318. Rulseh AM, Keller J, Klener J, et al. Long-term survival of patients suffering from glioblastoma multiforme treated with tumor-treating fields. *World J Surg Oncol*. Oct 2012;10:220. doi:10.1186/1477-7819-10-220
319. Denysenko T, Gennero L, Roos MA, et al. Glioblastoma cancer stem cells: heterogeneity, microenvironment and related therapeutic strategies. *Cell Biochem Funct*. Jul 2010;28(5):343-51. doi:10.1002/cbf.1666
320. Lefranc F, Brotchi J, Kiss R. Possible Future Issues in the Treatment of Glioblastomas: Special Emphasis on Cell Migration and the Resistance of Migrating Glioblastoma Cells to Apoptosis. *J Clin Oncol*. ; 2005. p. 2411-22.
321. Demuth T, Berens ME. Molecular mechanisms of glioma cell migration and invasion.: *J Neurooncol*; 2004. p. 217-28.
322. Oppitz U, Maessen D, Zunterer H, Richter S, Flentje M. 3D-recurrence-patterns of glioblastomas after CT-planned postoperative irradiation. *Radiotherapy and Oncology*. 1999;53(1):53-57. IN FILE.
323. Lee SW, Fraass BA, Marsh LH, et al. Patterns of failure following high-dose 3-D conformal radiotherapy for high-grade astrocytomas: a quantitative dosimetric study. *International Journal of Radiation Oncology, Biology, Physics*. 1999;43(1):79-88. IN FILE.
324. Brandes AA, Tosoni A, Franceschi E, et al. Recurrence Pattern After Temozolomide Concomitant With and Adjuvant to Radiotherapy in Newly Diagnosed Patients With Glioblastoma: Correlation With MGMT Promoter Methylation Status. *Journal of Clinical Oncology*. 2009;27(8):1275-1279. IN FILE.
325. Kelly PJ, Daumas-Duport C, Kispert DB, Kall BA, Scheithauer BW, Illig JJ. Imaging-based stereotaxic serial biopsies in untreated intracranial glial neoplasms. To determine whether CT or MR identifies the histological limits of glioma in individual patients best. *J Neurosurg*. 1987;66(6):865-874. IN FILE.
326. Price S, Jena R, Burnet N, et al. Improved delineation of glioma margins and regions of infiltration with the use of diffusion tensor imaging: An image-guided biopsy study. *American Journal of Neuroradiology*. OCT 2006 2006;27(9):1969-1974.
327. Price SJ, Young AM, Scotton WJ, et al. Multimodal MRI can identify perfusion and metabolic changes in the invasive margin of glioblastomas. *J Magn Reson Imaging*. Feb 2016;43(2):487-94. doi:10.1002/jmri.24996
328. Marcus HJ, Carpenter KLH, Price SJ, Hutchinson PJ. In vivo assessment of high-grade glioma biochemistry using microdialysis: a study of energy-related molecules, growth factors and cytokines. *Journal of Neuro-Oncology*. Mar 2010;97(1):11-23. doi:10.1007/s11060-009-9990-5
329. Chawla S, Zhang Y, Wang S, et al. Proton magnetic resonance spectroscopy in differentiating glioblastomas from primary cerebral lymphomas and brain metastases. *J Comput Assist Tomogr*. 2010 Nov-Dec 2010;34(6):836-41. doi:10.1097/RCT.0b013e3181ec554e
330. Ramadan S, Andronesi OC, Stanwell P, Lin AP, Sorensen AG, Mountford CE. Use of in vivo two-dimensional MR spectroscopy to compare the biochemistry of the human brain to that of glioblastoma. *Radiology*. May 2011;259(2):540-9. doi:10.1148/radiol.11101123
331. Jain RK, di Tomaso E, Duda DG, Loeffler JS, Sorensen AG, Batchelor TT. Angiogenesis in brain tumours. *Nat Rev Neurosci*. Aug 2007;8(8):610-22. doi:10.1038/nrn2175

332. Jain RK, Di Tomaso E, Duda DG, Loeffler JS, Sorensen AG, Batchelor TT. Angiogenesis in brain tumours. *Nature Reviews Neuroscience*. Aug 2007;8(8):610-622. doi:10.1038/nrn2175
333. Holash J, Maisonpierre PC, Compton D, et al. Vessel cooption, regression, and growth in tumors mediated by angiopoietins and VEGF. *Science*. Jun 1999;284(5422):1994-8. doi:10.1126/science.284.5422.1994
334. Padera TP, Stoll BR, Tooredman JB, Capen D, di Tomaso E, Jain RK. Pathology: cancer cells compress intratumour vessels. *Nature*. Feb 2004;427(6976):695. doi:10.1038/427695a
335. Plate KH, Breier G, Weich HA, Risau W. Vascular endothelial growth factor is a potential tumour angiogenesis factor in human gliomas in vivo. *Nature*. 1992;359(6398):845-848. IN FILE.
336. Auguste P, Gürsel DB, Lemièrè S, et al. Inhibition of fibroblast growth factor/fibroblast growth factor receptor activity in glioma cells impedes tumor growth by both angiogenesis-dependent and -independent mechanisms. *Cancer Res*. Feb 2001;61(4):1717-26.
337. Duda DG, Cohen KS, Kozin SV, et al. Evidence for incorporation of bone marrow-derived endothelial cells into perfused blood vessels in tumors. *Blood*. Apr 2006;107(7):2774-6. doi:10.1182/blood-2005-08-3210
338. Aghi M, Cohen KS, Klein RJ, Scadden DT, Chiocca EA. Tumor stromal-derived factor-1 recruits vascular progenitors to mitotic neovasculature, where microenvironment influences their differentiated phenotypes. *Cancer Res*. Sep 2006;66(18):9054-64. doi:10.1158/0008-5472.CAN-05-3759
339. Yano S, Shinohara H, Herbst RS, et al. Production of experimental malignant pleural effusions is dependent on invasion of the pleura and expression of vascular endothelial growth factor/vascular permeability factor by human lung cancer cells. *Am J Pathol*. Dec 2000;157(6):1893-903. doi:10.1016/S0002-9440(10)64828-6
340. Brem S. The role of vascular proliferation in the growth of brain tumors. *Clinical neurosurgery*. 1976 1976;23:440-53.
341. Brem S, Cotran R, Folkman J. Tumor angiogenesis: a quantitative method for histologic grading. To devise a quantitative method of evaluating the degree of tumour vascularity using histological features. Aim was to provide an objective way of assessing neovascularisation for further work in anti-angiogenesis therapies. *Journal of the National Cancer Institute*. 1972;48:347-356. IN FILE.
342. Sugahara T, Korogi Y, Kochi M, et al. Correlation of MR imaging-determined cerebral blood volume maps with histologic and angiographic determination of vascularity of gliomas. *AJRAmerican Journal of Roentgenology*. 1998;171(6):1479-1486. IN FILE.
343. Knopp EA, Cha S, Johnson G, et al. Glial neoplasms: Dynamic contrast-enhanced T2\*-weighted MR imaging. *Radiology*. Jun 1999;211(3):791-798.
344. Aronen HJ, Perkio J. Dynamic susceptibility contrast MRI of gliomas. *Neuroimaging Clin N Am*. 2002;12(4):501-523. IN FILE.
345. Lev MH, Rosen BR. Clinical applications of intracranial perfusion MR imaging. *Neuroimaging Clin N Am*. 1999;9(2):309-331. NOT IN FILE.
346. Maia AC, Malheiros SM, da Rocha AJ, et al. MR Cerebral Blood Volume Maps Correlated with Vascular Endothelial Growth Factor Expression and Tumor Grade in Nonenhancing Gliomas. *American Journal of Neuroradiology*. 2005;26(4):777-783. IN FILE.

347. Cha S, Knopp EA, Johnson G, Wetzel SG, Litt AW, Zagzag D. Intracranial mass lesions: dynamic contrast-enhanced susceptibility-weighted echo-planar perfusion MR imaging. *Radiology*. 2002;223(1):11-29. IN FILE.
348. Price SJ, Green HA, Dean AF, Joseph J, Hutchinson PJ, Gillard JH. Correlation of MR relative cerebral blood volume measurements with cellular density and proliferation in high-grade gliomas: an image-guided biopsy study. *AJNR Am J Neuroradiol*. Mar 2011;32(3):501-6. doi:10.3174/ajnr.A2312
349. Basser PJ, Mattiello J, Lebihan D. ESTIMATION OF THE EFFECTIVE SELF-DIFFUSION TENSOR FROM THE NMR SPIN-ECHO. *Journal of Magnetic Resonance Series B*. Mar 1994;103(3):247-254. doi:10.1006/jmrb.1994.1037
350. Price SJ, Pena A, Burnet NG, et al. Tissue signature characterisation of diffusion tensor abnormalities in cerebral gliomas. *EurRadiol*. 2004;14(10 ):1909-1917. IN FILE.
351. Price SJ, Jena R, Burnet NG, et al. Improved delineation of glioma margins and regions of infiltration with the use of diffusion tensor imaging: An image-guided biopsy study. *American Journal of Neuroradiology*. Oct 2006;27(9):1969-1974.
352. Lunsford LD, Martinez AJ, Latchaw RE. Magnetic resonance imaging does not define tumor boundaries. Assess if MR accurately detects histologic tumou. *Acta RadiolSuppl*. 1986;369:154-156. IN FILE.
353. Sinha S, Bastin ME, Whittle IR, Wardlaw JM. Diffusion tensor MR imaging of high-grade cerebral gliomas. *AJNR American Journal of Neuroradiology*. 2002;23(4):520-527. IN FILE.
354. Kono K, Inoue Y, Nakayama K, et al. The role of diffusion-weighted imaging in patients with brain tumors. *AJNR American Journal of Neuroradiology*. 2001;22(6):1081-1088. IN FILE.
355. Watanabe M, Tanaka R, Takeda N. MAGNETIC-RESONANCE-IMAGING AND HISTOPATHOLOGY OF CEREBRAL GLIOMAS. *Neuroradiology*. Nov 1992;34(6):463-469.
356. Johnson PC, Hunt SJ, Drayer BP. Human cerebral gliomas: correlation of postmortem MR imaging and neuropathologic findings. CT does not show tumour cells infiltrating normal brain tissue. Aims to understand better the limitations of MR imaging of human astrocytic tumors by correlating findings to neuropathology of whole-brain sections. *Radiology*. 1989;170(1):211-217. IN FILE.
357. Price SJ, Burnet NG, Donovan T, et al. Diffusion tensor Imaging of brain tumours at 3 T: A potential tool for assessing white matter tract invasion? *Clinical Radiology*. Jun 2003;58(6):455-462. doi:10.1016/s0009-9260(03)00115-6
358. Provenzale JM, McGraw P, Mhatre P, Guo AC, Delong D. Peritumoral brain regions in gliomas and meningiomas: investigation with isotropic diffusion-weighted MR imaging and diffusion-tensor MR imaging. *Radiology*. 2004;232(2):451-460. IN FILE.
359. Tropine A, Vucurevic G, Delani P, et al. Contribution of diffusion tensor imaging to delineation of gliomas and glioblastomas. *Journal of Magnetic Resonance Imaging*. 2004;20(6):905-912. IN FILE.
360. Lu S, Ahn D, Johnson G, Law M, Zagzag D, Grossman RI. Diffusion-Tensor MR Imaging of Intracranial Neoplasia and Associated Peritumoral Edema: Introduction of the Tumor Infiltration Index. *Radiology*. 2004;232(1):221-228. IN FILE.
361. van Westen D, Lñtt J, Englund E, Brockstedt S, Larsson EM. Tumor extension in high-grade gliomas assessed with diffusion magnetic resonance imaging: values and lesion-to-brain ratios of apparent diffusion coefficient and fractional anisotropy. *Acta Radiologica*. 2006;47(3):311-319. IN FILE.

362. Zhou XJ, Leeds NE. Assessing glioma cell infiltration using a fiber coherence index: a DTI study. *Proceedings of the International Society for Magnetic Resonance in Medicine*. 2005;13:365. IN FILE.
363. Morita K, Matsuzawa H, Fujii Y, Tanaka R, Kwee IL, Nakada T. Diffusion tensor analysis of peritumoral edema using lambda chart analysis indicative of the heterogeneity of the microstructure within edema. *J Neurosurg*. 2005;102(2):336-341. IN FILE.
364. Fillmore HL, VanMeter TE, Broaddus WC. Membrane-type matrix metalloproteinases (MT-MMPs): expression and function during glioma invasion. *Journal of Neuro-Oncology*. 2001;53(2):187-202. IN FILE.
365. Price SJ, Jena R, Burnet NG, Carpenter TA, Pickard JD, Gillard JH. Predicting patterns of glioma recurrence using diffusion tensor imaging. Article. *European Radiology*. Jul 2007;17(7):1675-1684. doi:10.1007/s00330-006-0561-2
366. Louis DN. Molecular Pathology of Malignant Gliomas. *Annual Review of Pathology: Mechanisms of Disease*. 2006/02/01 2006;1(1):97-117. doi:10.1146/annurev.pathol.1.110304.100043
367. Bjerkvig R, Johansson M, Miletic H, Niclou SP. Cancer stem cells and angiogenesis. *Seminars in Cancer Biology*. Oct 2009;19(5):279-284. doi:10.1016/j.semcancer.2009.09.001
368. Sakariassen PO, Prestegarden L, Wang J, et al. Angiogenesis-independent tumor growth mediated by stem-like cancer cells. *Proc Natl Acad Sci U S A*. Oct 31 2006;103(44):16466-16471. doi:10.1073/pnas.0607668103
369. Keunen O, Johansson M, Oudin AØ, et al. Anti-VEGF treatment reduces blood supply and increases tumor cell invasion in glioblastoma. *Proceedings of the National Academy of Sciences*. 2011;108(9):3749-3754. IN FILE.
370. Jenkinson M, Beckmann CF, Behrens TEJ, Woolrich MW, Smith SM. Fsl. *NeuroImage*. 2012-Aug-15 2012;62(2):782-90.
371. Pena A, Green H, Carpenter T, Price S, Pickard J, Gillard J. Enhanced visualization and quantification of magnetic resonance diffusion tensor imaging using the p : q tensor decomposition. *British Journal of Radiology*. FEB 2006 2006;79(938):101-109. doi:10.1259/bjr/24908512
372. Rahmat R, Brochu F, Li C, Sinha R, Price SJ, Jena R. Semi-automated construction of patient individualised clinical target volumes for radiotherapy treatment of glioblastoma utilising diffusion tensor decomposition maps. *Br J Radiol*. Apr 2020;93(1108):20190441. doi:10.1259/bjr.20190441
373. Rahmat R, Saednia K, Haji Hosseini Khani MR, Rahmati M, Jena R, Price SJ. Multi-scale segmentation in GBM treatment using diffusion tensor imaging. *Comput Biol Med*. 08 2020;123:103815. doi:10.1016/j.combiomed.2020.103815
374. Beigi M, Safari M, Ameri A, et al. Findings of DTI-p maps in comparison with T. *Cancer Imaging*. Sep 18 2018;18(1):33. doi:10.1186/s40644-018-0166-4
375. Sinigaglia M, Assi T, Besson FL, et al. Imaging-guided precision medicine in glioblastoma patients treated with immune checkpoint modulators: research trend and future directions in the field of imaging biomarkers and artificial intelligence. *EJNMMI Res*. Aug 20 2019;9(1):78. doi:10.1186/s13550-019-0542-5
376. Toth GB, Varallyay CG, Horvath A, et al. Current and potential imaging applications of ferumoxytol for magnetic resonance imaging. *Kidney Int*. 07 2017;92(1):47-66. doi:10.1016/j.kint.2016.12.037

377. Limkin EJ, Sun R, Dercle L, et al. Promises and challenges for the implementation of computational medical imaging (radiomics) in oncology. *Ann Oncol*. Jun 01 2017;28(6):1191-1206. doi:10.1093/annonc/mdx034
378. Kriegstein A, Alvarez-Buylla A. The glial nature of embryonic and adult neural stem cells. *Annu Rev Neurosci*. 2009;32:149-84. doi:10.1146/annurev.neuro.051508.135600
379. Zhao X, Moore DL. Neural stem cells: developmental mechanisms and disease modeling. *Cell Tissue Res*. 01 2018;371(1):1-6. doi:10.1007/s00441-017-2738-1
380. Rowitch DH, Kriegstein AR. Developmental genetics of vertebrate glial-cell specification. *Nature*. Nov 2010;468(7321):214-22. doi:10.1038/nature09611
381. Okano H, Temple S. Cell types to order: temporal specification of CNS stem cells. *Curr Opin Neurobiol*. Apr 2009;19(2):112-9. doi:10.1016/j.conb.2009.04.003
382. Noctor SC, Flint AC, Weissman TA, Dammerman RS, Kriegstein AR. Neurons derived from radial glial cells establish radial units in neocortex. *Nature*. Feb 2001;409(6821):714-20. doi:10.1038/35055553
383. Sanai N, Alvarez-Buylla A, Berger M. Neural stem cells and the origin of gliomas. *New England Journal of Medicine*; 2005. p. 811-22.
384. Luskin MB. Restricted proliferation and migration of postnatally generated neurons derived from the forebrain subventricular zone. *Neuron*. Jul 1993;11(1):173-89. doi:10.1016/0896-6273(93)90281-u
385. Lois C, Alvarez-Buylla A. Long-distance neuronal migration in the adult mammalian brain. *Science*; 1994. p. 1145-8.
386. Garcia AD, Doan NB, Imura T, Bush TG, Sofroniew MV. GFAP-expressing progenitors are the principal source of constitutive neurogenesis in adult mouse forebrain. *Nat Neurosci*. Nov 2004;7(11):1233-41. doi:10.1038/nn1340
387. Morshead CM, Garcia AD, Sofroniew MV, van Der Kooy D. The ablation of glial fibrillary acidic protein-positive cells from the adult central nervous system results in the loss of forebrain neural stem cells but not retinal stem cells. *Eur J Neurosci*. Jul 2003;18(1):76-84. doi:10.1046/j.1460-9568.2003.02727.x
388. Imura T, Kornblum HI, Sofroniew MV. The predominant neural stem cell isolated from postnatal and adult forebrain but not early embryonic forebrain expresses GFAP. *J Neurosci*. Apr 2003;23(7):2824-32.
389. Laywell ED, Rakic P, Kukekov VG, Holland EC, Steindler DA. Identification of a multipotent astrocytic stem cell in the immature and adult mouse brain. *Proc Natl Acad Sci U S A*. Dec 2000;97(25):13883-8. doi:10.1073/pnas.250471697
390. Göritz C, Frisén J. Neural stem cells and neurogenesis in the adult. *Cell Stem Cell*. Jun 2012;10(6):657-659. doi:10.1016/j.stem.2012.04.005
391. Kempermann G, Song H, Gage FH. Neurogenesis in the Adult Hippocampus. *Cold Spring Harb Perspect Biol*. Sep 2015;7(9):a018812. doi:10.1101/cshperspect.a018812
392. Carleton A, Petreanu LT, Lansford R, Alvarez-Buylla A, Lledo PM. Becoming a new neuron in the adult olfactory bulb. *Nat Neurosci*. May 2003;6(5):507-18. doi:10.1038/nn1048
393. Kokaia M. Seizure-induced neurogenesis in the adult brain. *Eur J Neurosci*. Mar 2011;33(6):1133-8. doi:10.1111/j.1460-9568.2011.07612.x
394. Balu DT, Lucki I. Adult hippocampal neurogenesis: regulation, functional implications, and contribution to disease pathology. *Neurosci Biobehav Rev*. Mar 2009;33(3):232-52. doi:10.1016/j.neubiorev.2008.08.007



395. Lee JH, Lee JE, Kahng JY, et al. Human glioblastoma arises from subventricular zone cells with low-level driver mutations. *Nature*. 08 2018;560(7717):243-247. doi:10.1038/s41586-018-0389-3
396. Alvarez-Buylla A, Lim DA. For the long run: maintaining germinal niches in the adult brain. *Neuron*. Mar 2004;41(5):683-6. doi:10.1016/s0896-6273(04)00111-4
397. Sanai N, Tramontin AD, Quiñones-Hinojosa A, et al. Unique astrocyte ribbon in adult human brain contains neural stem cells but lacks chain migration. *Nature*. Feb 2004;427(6976):740-4. doi:10.1038/nature02301
398. Curtis MA, Kam M, Nannmark U, et al. Human neuroblasts migrate to the olfactory bulb via a lateral ventricular extension. *Science*. Mar 2007;315(5816):1243-9. doi:10.1126/science.1136281
399. Wynshaw-Boris A, Gambello MJ. LIS1 and dynein motor function in neuronal migration and development. *Genes Dev*. Mar 2001;15(6):639-51. doi:10.1101/gad.886801
400. Dobyns WB, Andermann E, Andermann F, et al. X-linked malformations of neuronal migration. *Neurology*. Aug 1996;47(2):331-9. doi:10.1212/wnl.47.2.331
401. Arvidsson A, Collin T, Kirik D, Kokaia Z, Lindvall O. Neuronal replacement from endogenous precursors in the adult brain after stroke. *Nat Med*. Sep 2002;8(9):963-70. doi:10.1038/nm747
402. Yamashita T, Ninomiya M, Hernández Acosta P, et al. Subventricular zone-derived neuroblasts migrate and differentiate into mature neurons in the post-stroke adult striatum. *J Neurosci*. Jun 2006;26(24):6627-36. doi:10.1523/JNEUROSCI.0149-06.2006
403. Kaneko N, Sawada M, Sawamoto K. Mechanisms of neuronal migration in the adult brain. *J Neurochem*. 06 2017;141(6):835-847. doi:10.1111/jnc.14002
404. Obernier K, Alvarez-Buylla A. Neural stem cells: origin, heterogeneity and regulation in the adult mammalian brain. *Development*. 02 2019;146(4)doi:10.1242/dev.156059
405. Schaar BT, McConnell SK. Cytoskeletal coordination during neuronal migration. *Proc Natl Acad Sci U S A*. Sep 2005;102(38):13652-7. doi:10.1073/pnas.0506008102
406. Shinohara R, Thumkeo D, Kamijo H, et al. A role for mDia, a Rho-regulated actin nucleator, in tangential migration of interneuron precursors. *Nat Neurosci*. Jan 2012;15(3):373-80, S1-2. doi:10.1038/nn.3020
407. Koizumi H, Higginbotham H, Poon T, Tanaka T, Brinkman BC, Gleeson JG. Doublecortin maintains bipolar shape and nuclear translocation during migration in the adult forebrain. *Nat Neurosci*. Jun 2006;9(6):779-86. doi:10.1038/nn1704
408. Ota H, Hikita T, Sawada M, et al. Speed control for neuronal migration in the postnatal brain by Gmp-mediated local inactivation of RhoA. *Nat Commun*. Jul 2014;5:4532. doi:10.1038/ncomms5532
409. Higginbotham H, Tanaka T, Brinkman BC, Gleeson JG. GSK3beta and PKCzeta function in centrosome localization and process stabilization during Slit-mediated neuronal repolarization. *Mol Cell Neurosci*. 2006 May-Jun 2006;32(1-2):118-32. doi:10.1016/j.mcn.2006.03.003
410. Murase S, Horwitz AF. Deleted in colorectal carcinoma and differentially expressed integrins mediate the directional migration of neural precursors in the rostral migratory stream. *J Neurosci*. May 2002;22(9):3568-79. doi:20026349
411. Astic L, Pellier-Monnin V, Saucier D, Charrier C, Mehlen P. Expression of netrin-1 and netrin-1 receptor, DCC, in the rat olfactory nerve pathway during development

- and axonal regeneration. *Neuroscience*. 2002;109(4):643-56. doi:10.1016/s0306-4522(01)00535-8
412. Yagita Y, Sakurai T, Tanaka H, Kitagawa K, Colman DR, Shan W. N-cadherin mediates interaction between precursor cells in the subventricular zone and regulates further differentiation. *J Neurosci Res*. Nov 2009;87(15):3331-42. doi:10.1002/jnr.22044
413. Chazal G, Durbec P, Jankovski A, Rougon G, Cremer H. Consequences of neural cell adhesion molecule deficiency on cell migration in the rostral migratory stream of the mouse. *J Neurosci*. Feb 2000;20(4):1446-57.
414. Belvindrah R, Hankel S, Walker J, Patton BL, Müller U. Beta1 integrins control the formation of cell chains in the adult rostral migratory stream. *J Neurosci*. Mar 2007;27(10):2704-17. doi:10.1523/JNEUROSCI.2991-06.2007
415. Mobley AK, McCarty JH.  $\beta$ 8 integrin is essential for neuroblast migration in the rostral migratory stream. *Glia*. Nov 2011;59(11):1579-87. doi:10.1002/glia.21199
416. Zhang RL, Chopp M, Gregg SR, et al. Patterns and dynamics of subventricular zone neuroblast migration in the ischemic striatum of the adult mouse. *J Cereb Blood Flow Metab*. Jul 2009;29(7):1240-50. doi:10.1038/jcbfm.2009.55
417. Kaneko N, Marín O, Koike M, et al. New neurons clear the path of astrocytic processes for their rapid migration in the adult brain. *Neuron*. Jul 2010;67(2):213-23. doi:10.1016/j.neuron.2010.06.018
418. Barkho BZ, Munoz AE, Li X, Li L, Cunningham LA, Zhao X. Endogenous matrix metalloproteinase (MMP)-3 and MMP-9 promote the differentiation and migration of adult neural progenitor cells in response to chemokines. *Stem Cells*. Dec 2008;26(12):3139-49. doi:10.1634/stemcells.2008-0519
419. Ayala R, Shu T, Tsai LH. Trekking across the brain: the journey of neuronal migration. *Cell*. Jan 12 2007;128(1):29-43. doi:10.1016/j.cell.2006.12.021
420. Lehtimäki J, Hakala M, Lappalainen P. Actin Filament Structures in Migrating Cells. *Handb Exp Pharmacol*. 2017;235:123-152. doi:10.1007/164\_2016\_28
421. Bisaria A, Hayer A, Garbett D, Cohen D, Meyer T. Membrane-proximal F-actin restricts local membrane protrusions and directs cell migration. *Science*. 06 12 2020;368(6496):1205-1210. doi:10.1126/science.aay7794
422. Bellion A, Baudoin JP, Alvarez C, Bornens M, Métin C. Nucleokinesis in tangentially migrating neurons comprises two alternating phases: forward migration of the Golgi/centrosome associated with centrosome splitting and myosin contraction at the rear. *J Neurosci*. Jun 15 2005;25(24):5691-9. doi:10.1523/JNEUROSCI.1030-05.2005
423. Naumanen P, Lappalainen P, Hotulainen P. Mechanisms of actin stress fibre assembly. *J Microsc*. Sep 2008;231(3):446-54. doi:10.1111/j.1365-2818.2008.02057.x
424. Minegishi T, Uesugi Y, Kaneko N, Yoshida W, Sawamoto K, Inagaki N. Shootin1b Mediates a Mechanical Clutch to Produce Force for Neuronal Migration. *Cell Rep*. 10 16 2018;25(3):624-639.e6. doi:10.1016/j.celrep.2018.09.068
425. Garcin C, Straube A. Microtubules in cell migration. *Essays Biochem*. 10 31 2019;63(5):509-520. doi:10.1042/EBC20190016
426. Camargo Ortega G, Falk S, Johansson PA, et al. The centrosome protein AKNA regulates neurogenesis via microtubule organization. *Nature*. 03 2019;567(7746):113-117. doi:10.1038/s41586-019-0962-4
427. Rooney C, White G, Nazgiewicz A, et al. The Rac activator STEF (Tiam2) regulates cell migration by microtubule-mediated focal adhesion disassembly. *EMBO Rep*. Apr 2010;11(4):292-8. doi:10.1038/embor.2010.10

428. Tsai FC, Seki A, Yang HW, et al. A polarized Ca<sup>2+</sup>, diacylglycerol and STIM1 signalling system regulates directed cell migration. *Nat Cell Biol.* Feb 2014;16(2):133-44. doi:10.1038/ncb2906
429. Schuler MH, Lewandowska A, Caprio GD, et al. Miro1-mediated mitochondrial positioning shapes intracellular energy gradients required for cell migration. *Mol Biol Cell.* Aug 01 2017;28(16):2159-2169. doi:10.1091/mbc.E16-10-0741
430. Bott CJ, Winckler B. Intermediate filaments in developing neurons: Beyond structure. *Cytoskeleton (Hoboken).* 03 2020;77(3-4):110-128. doi:10.1002/cm.21597
431. Wittko IM, Schänzer A, Kuzmichev A, et al. VEGFR-1 regulates adult olfactory bulb neurogenesis and migration of neural progenitors in the rostral migratory stream in vivo. *J Neurosci.* Jul 08 2009;29(27):8704-14. doi:10.1523/JNEUROSCI.5527-08.2009
432. Snapyan M, Lemasson M, Brill MS, et al. Vasculature guides migrating neuronal precursors in the adult mammalian forebrain via brain-derived neurotrophic factor signaling. *J Neurosci.* Apr 01 2009;29(13):4172-88. doi:10.1523/JNEUROSCI.4956-08.2009
433. Bolteus AJ, Bordey A. GABA release and uptake regulate neuronal precursor migration in the postnatal subventricular zone. *J Neurosci.* Sep 01 2004;24(35):7623-31. doi:10.1523/JNEUROSCI.1999-04.2004
434. Platel JC, Dave KA, Gordon V, Lacar B, Rubio ME, Bordey A. NMDA receptors activated by subventricular zone astrocytic glutamate are critical for neuroblast survival prior to entering a synaptic network. *Neuron.* Mar 25 2010;65(6):859-72. doi:10.1016/j.neuron.2010.03.009
435. Darcy DP, Isaacson JS. L-type calcium channels govern calcium signaling in migrating newborn neurons in the postnatal olfactory bulb. *J Neurosci.* Feb 25 2009;29(8):2510-8. doi:10.1523/JNEUROSCI.5333-08.2009
436. García-González D, Khodosevich K, Watanabe Y, Rollenhagen A, Lübke JHR, Monyer H. Serotonergic Projections Govern Postnatal Neuroblast Migration. *Neuron.* May 03 2017;94(3):534-549.e9. doi:10.1016/j.neuron.2017.04.013
437. Cao L, Wei D, Reid B, et al. Endogenous electric currents might guide rostral migration of neuroblasts. Article. *Embo Reports.* FEB 2013 2013;14(2):184-190. doi:10.1038/embor.2012.215
438. Chen ZP, Levy A, Lightman SL. Activation of specific ATP receptors induces a rapid increase in intracellular calcium ions in rat hypothalamic neurons. *Brain Res.* Apr 04 1994;641(2):249-56. doi:10.1016/0006-8993(94)90151-1
439. Edwards FA, Gibb AJ, Colquhoun D. ATP receptor-mediated synaptic currents in the central nervous system. *Nature.* Sep 10 1992;359(6391):144-7. doi:10.1038/359144a0
440. Sauer H, Stanelle R, Hescheler J, Wartenberg M. The DC electrical-field-induced Ca(2+) response and growth stimulation of multicellular tumor spheroids are mediated by ATP release and purinergic receptor stimulation. *J Cell Sci.* Aug 15 2002;115(Pt 16):3265-73. doi:10.1242/jcs.115.16.3265
441. Liu X, Hashimoto-Torii K, Torii M, Haydar TF, Rakic P. The role of ATP signaling in the migration of intermediate neuronal progenitors to the neocortical subventricular zone. *Proc Natl Acad Sci U S A.* Aug 19 2008;105(33):11802-7. doi:10.1073/pnas.0805180105
442. Blaser H, Reichman-Fried M, Castanon I, et al. Migration of zebrafish primordial germ cells: a role for myosin contraction and cytoplasmic flow. *Dev Cell.* Nov 2006;11(5):613-27. doi:10.1016/j.devcel.2006.09.023

443. Wei C, Wang X, Chen M, Ouyang K, Song LS, Cheng H. Calcium flickers steer cell migration. *Nature*. Feb 12 2009;457(7231):901-5. doi:10.1038/nature07577
444. Wei C, Wang X, Zheng M, Cheng H. Calcium gradients underlying cell migration. *Curr Opin Cell Biol*. Apr 2012;24(2):254-61. doi:10.1016/j.ceb.2011.12.002
445. Price LS, Langeslag M, ten Klooster JP, Hordijk PL, Jalink K, Collard JG. Calcium signaling regulates translocation and activation of Rac. *J Biol Chem*. Oct 10 2003;278(41):39413-21. doi:10.1074/jbc.M302083200
446. Saotome M, Safiulina D, Szabadkai G, et al. Bidirectional Ca<sup>2+</sup>-dependent control of mitochondrial dynamics by the Miro GTPase. *Proc Natl Acad Sci U S A*. Dec 30 2008;105(52):20728-33. doi:10.1073/pnas.0808953105
447. Cao L, Pu J, Scott RH, Ching J, McCaig CD. Physiological electrical signals promote chain migration of neuroblasts by up-regulating P2Y1 purinergic receptors and enhancing cell adhesion. *Stem Cell Rev Rep*. Feb 2015;11(1):75-86. doi:10.1007/s12015-014-9524-1
448. Chang EH, Adorjan I, Mundim MV, Sun B, Dizon ML, Szele FG. Traumatic Brain Injury Activation of the Adult Subventricular Zone Neurogenic Niche. *Front Neurosci*. 2016;10:332. doi:10.3389/fnins.2016.00332
449. Young CC, Brooks KJ, Buchan AM, Szele FG. Cellular and molecular determinants of stroke-induced changes in subventricular zone cell migration. *Antioxid Redox Signal*. May 15 2011;14(10):1877-88. doi:10.1089/ars.2010.3435
450. Addington CP, Roussas A, Dutta D, Stabenfeldt SE. Endogenous repair signaling after brain injury and complementary bioengineering approaches to enhance neural regeneration. *Biomark Insights*. 2015;10(Suppl 1):43-60. doi:10.4137/BMI.S20062
451. Kernie SG, Parent JM. Forebrain neurogenesis after focal Ischemic and traumatic brain injury. *Neurobiol Dis*. Feb 2010;37(2):267-74. doi:10.1016/j.nbd.2009.11.002
452. Hayashi Y, Jinnou H, Sawamoto K, Hitoshi S. Adult neurogenesis and its role in brain injury and psychiatric diseases. *J Neurochem*. 12 2018;147(5):584-594. doi:10.1111/jnc.14557
453. Craig CG, Tropepe V, Morshead CM, Reynolds BA, Weiss S, van der Kooy D. In vivo growth factor expansion of endogenous subependymal neural precursor cell populations in the adult mouse brain. *J Neurosci*. Apr 15 1996;16(8):2649-58.
454. Ohab JJ, Fleming S, Blesch A, Carmichael ST. A neurovascular niche for neurogenesis after stroke. *J Neurosci*. Dec 13 2006;26(50):13007-16. doi:10.1523/JNEUROSCI.4323-06.2006
455. Schäbitz WR, Steigleder T, Cooper-Kuhn CM, et al. Intravenous brain-derived neurotrophic factor enhances poststroke sensorimotor recovery and stimulates neurogenesis. *Stroke*. Jul 2007;38(7):2165-72. doi:10.1161/STROKEAHA.106.477331
456. Kaneko N, Herranz-Pérez V, Otsuka T, et al. New neurons use Slit-Robo signaling to migrate through the glial meshwork and approach a lesion for functional regeneration. *Sci Adv*. 12 2018;4(12):eaav0618. doi:10.1126/sciadv.aav0618
457. Wang Z, Zheng Y, Zheng M, et al. Neurogenic Niche Conversion Strategy Induces Migration and Functional Neuronal Differentiation of Neural Precursor Cells Following Brain Injury. *Stem Cells Dev*. 02 15 2020;29(4):235-248. doi:10.1089/scd.2019.0147
458. Ma M, Ma Y, Yi X, et al. Intranasal delivery of transforming growth factor-beta1 in mice after stroke reduces infarct volume and increases neurogenesis in the subventricular zone. *BMC Neurosci*. Dec 10 2008;9:117. doi:10.1186/1471-2202-9-117

459. Gundelach J, Koch M. Redirection of neuroblast migration from the rostral migratory stream into a lesion in the prefrontal cortex of adult rats. *Exp Brain Res*. 04 2018;236(4):1181-1191. doi:10.1007/s00221-018-5209-3
460. Jinnou H, Sawada M, Kawase K, et al. Radial Glial Fibers Promote Neuronal Migration and Functional Recovery after Neonatal Brain Injury. *Cell Stem Cell*. 01 04 2018;22(1):128-137.e9. doi:10.1016/j.stem.2017.11.005
461. O'Donnell JC, Purvis EM, Helm KVT, et al. An implantable human stem cell-derived tissue-engineered rostral migratory stream for directed neuronal replacement. *Commun Biol*. 07 15 2021;4(1):879. doi:10.1038/s42003-021-02392-8
462. Purvis EM, O'Donnell JC, Chen HI, Cullen DK. Tissue Engineering and Biomaterial Strategies to Elicit Endogenous Neuronal Replacement in the Brain. *Front Neurol*. 2020;11:344. doi:10.3389/fneur.2020.00344
463. Kondziolka D, Steinberg GK, Wechsler L, et al. Neurotransplantation for patients with subcortical motor stroke: a phase 2 randomized trial. *J Neurosurg*. Jul 2005;103(1):38-45. doi:10.3171/jns.2005.103.1.0038
464. Savitz SI, Dinsmore J, Wu J, Henderson GV, Stieg P, Caplan LR. Neurotransplantation of fetal porcine cells in patients with basal ganglia infarcts: a preliminary safety and feasibility study. *Cerebrovasc Dis*. 2005;20(2):101-7. doi:10.1159/000086518
465. Biedler JL, Roffler-Tarlov S, Schachner M, Freedman LS. Multiple neurotransmitter synthesis by human neuroblastoma cell lines and clones. *Cancer Res*. Nov 1978;38(11 Pt 1):3751-7.
466. Song B, Gu Y, Pu J, Reid B, Zhao Z, Zhao M. Application of direct current electric fields to cells and tissues in vitro and modulation of wound electric field in vivo Nature Protocol; 2007. p. 1479-1489.
467. Zhao M, Song B, Pu J, et al. Electrical signals control wound healing through phosphatidylinositol-3-OH kinase-gamma and PTEN. Article. *Nature*. JUL 27 2006 2006;442(7101):457-460. doi:10.1038/nature04925
468. Pu J, Zhao M. Golgi polarization in a strong electric field. *J Cell Sci*. Mar 2005;118(Pt 6):1117-28. doi:10.1242/jcs.01646
469. Feng JF, Liu J, Zhang L, et al. Electrical Guidance of Human Stem Cells in the Rat Brain. *Stem Cell Reports*. 07 2017;9(1):177-189. doi:10.1016/j.stemcr.2017.05.035
470. Kwiatkowska A, Kijewska M, Lipko M, Hibner U, Kaminska B. Downregulation of Akt and FAK phosphorylation reduces invasion of glioblastoma cells by impairment of MT1-MMP shuttling to lamellipodia and downregulates MMPs expression. *Biochim Biophys Acta*. May 2011;1813(5):655-67. doi:10.1016/j.bbamcr.2011.01.020
471. Wu C, Asokan SB, Berginski ME, et al. Arp2/3 is critical for lamellipodia and response to extracellular matrix cues but is dispensable for chemotaxis. *Cell*. Mar 2012;148(5):973-87. doi:10.1016/j.cell.2011.12.034
472. Moshfegh Y, Bravo-Cordero JJ, Miskolci V, Condeelis J, Hodgson L. A Trio-Rac1-Pak1 signalling axis drives invadopodia disassembly. *Nat Cell Biol*. Jun 2014;16(6):574-86. doi:10.1038/ncb2972
473. Becchetti A, Arcangeli A. Integrins and ion channels in cell migration: implications for neuronal development, wound healing and metastatic spread. *Adv Exp Med Biol*. 2010;674:107-23. doi:10.1007/978-1-4419-6066-5\_10
474. Robinson KR. The responses of cells to electrical fields: a review. *J Cell Biol*. Dec 1985;101(6):2023-7. doi:10.1083/jcb.101.6.2023

475. McCaig C, Rajniecek A, Song B, Zhao M. Controlling cell behavior electrically: Current views and future potential. Review. *Physiological Reviews*. JUL 2005 2005;85(3):943-978. doi:10.1152/physrev.00020.2004
476. McCaig CD, Song B, Rajniecek AM. Electrical dimensions in cell science. *Journal of Cell Science*; 2009. p. 4267-4276
477. McCaig CD, Rajniecek AM, Song B, Zhao M. Has electrical growth cone guidance found its potential? *Trends Neurosci*. Jul 2002;25(7):354-9. doi:10.1016/s0166-2236(02)02174-4
478. Hotary KB, Robinson KR. Endogenous electrical currents and the resultant voltage gradients in the chick embryo. *Dev Biol*. Jul 1990;140(1):149-60. doi:10.1016/0012-1606(90)90062-n
479. Hotary KB, Robinson KR. The neural tube of the *Xenopus* embryo maintains a potential difference across itself. *Brain Res Dev Brain Res*. Mar 1991;59(1):65-73. doi:10.1016/0165-3806(91)90030-m
480. Shi R, Borgens RB. Three-dimensional gradients of voltage during development of the nervous system as invisible coordinates for the establishment of embryonic pattern. *Dev Dyn*. Feb 1995;202(2):101-14. doi:10.1002/aja.1002020202
481. Shi R, Borgens RB. Embryonic neuroepithelial sodium transport, the resulting physiological potential, and cranial development. *Dev Biol*. Sep 1994;165(1):105-16. doi:10.1006/dbio.1994.1238
482. Borgens RB, Jaffe LF, Cohen MJ. Large and persistent electrical currents enter the transected lamprey spinal cord. *Proc Natl Acad Sci U S A*. Feb 1980;77(2):1209-13. doi:10.1073/pnas.77.2.1209
483. Jefferys JG. Influence of electric fields on the excitability of granule cells in guinea-pig hippocampal slices. *J Physiol*. 1981;319:143-52. doi:10.1113/jphysiol.1981.sp013897
484. Pu J, McCaig CD, Cao L, Zhao Z, Segall JE, Zhao M. EGF receptor signalling is essential for electric-field-directed migration of breast cancer cells. *J Cell Sci*. Oct 2007;120(Pt 19):3395-403. doi:10.1242/jcs.002774
485. Djamgoz MBA, Mycielska M, Madeja Z, Fraser SP, Korohoda W. Directional movement of rat prostate cancer cells in direct-current electric field: involvement of voltage-gated Na<sup>+</sup> channel activity. *J Cell Sci*. Jul 2001;114(Pt 14):2697-705.
486. Li F, Chen T, Hu S, Lin J, Hu R, Feng H. Superoxide Mediates Direct Current Electric Field- Induced Directional Migration of Glioma Cells through the Activation of AKT and ERK PLoS ONE; 2013. p. e61195.
487. Huang YJ, Hoffmann G, Wheeler B, Schiapparelli P, Quinones-Hinojosa A, Searson P. Cellular microenvironment modulates the galvanotaxis of brain tumor initiating cells. *Sci Rep*. Feb 2016;6:21583. doi:10.1038/srep21583
488. Singh SK, D. CI, Terasaki M, et al. Identification of a Cancer Stem Cell in Human Brain Tumors. *Cancer Research*; 2003. p. 5821–5828.
489. Galli R, Binda E, Orfanelli U, et al. Isolation and Characterization of Tumorigenic, Stem-like Neural Precursors from Human Glioblastoma. *Cancer Research*. 2004;64(19):7011-7021. IN FILE.
490. Ignatova TN, Kukekov VG, Laywell ED, Suslov ON, Vrionis FD, Steindler DA. Human cortical glial tumors contain neural stem-like cells expressing astroglial and neuronal markers in vitro. *Glia*. Sep 2002;39(3):193-206. doi:10.1002/glia.10094
491. Alvarez-Buylla A, Garcia-Verdugo JM. Neurogenesis in adult subventricular zone. *J Neurosci*. Feb 2002;22(3):629-34.

492. Lois C, García-Verdugo JM, Alvarez-Buylla A. Chain migration of neuronal precursors. *Science*. Feb 1996;271(5251):978-81. doi:10.1126/science.271.5251.978
493. O'Rourke NA, Chenn A, McConnell SK. Postmitotic neurons migrate tangentially in the cortical ventricular zone. *Development*. Mar 1997;124(5):997-1005.
494. Mycielska ME, Djamgoz MB. Cellular mechanisms of direct-current electric field effects: galvanotaxis and metastatic disease. *J Cell Sci*. Apr 2004;117(Pt 9):1631-9. doi:10.1242/jcs.01125
495. Li F, Chen T, Hu S, Lin J, Hu R, Feng H. Superoxide Mediates Direct Current Electric Field-Induced Directional Migration of Glioma Cells through the Activation of AKT and ERK. *PLOS ONE*. 2013;8(4):1-11.
496. Arocena M, Zhao M, Collinson JM, Song B. A Time-Lapse and Quantitative Modelling Analysis of Neural Stem Cell Motion in the Absence of Directional Cues and in Electric Fields. *Journal of Neuroscience Research*. 2010;88:3267-3274.
497. Meng X, Arocena M, Penninger J, Gage FH, Zhao M, Song B. PI3K mediated electrotaxis of embryonic and adult neural progenitor cells in the presence of growth factors. *Experimental Neurology*. 2011;227:210-217.
498. Pu J, McCaig CD, Cao L, Zhao Z, Segall JE, Zhao M. EGF receptor signalling is essential for electric-field directed migration of breast cancer cells. *Journal of Cell Science*. 2007;120:3395-3403.
499. Yao L, Shanley L, McCaig C, Zhao M. Small Applied Electric Fields Guide Migration of Hippocampal Neurons. *Journal of Cellular Physiology* 2008;216:527-535.
500. Zhao M, Song B, Pu J, et al. Electrical signals control wound healing through phosphatidylinositol-3-OH kinase- $\gamma$  and PTEN. *Nature*. 2006;442:457-460.
501. Zhao M, Pu J, Forrester JV, McCaig CD. Zhao, M., Pu, Membrane lipids, EGF receptors and intracellular signals co-localize and are polarized in epithelial cells moving directionally in a physiological electric field. *Federation of American Societies for Experimental Biology*. 2002;16(8):857-859.
502. Mezey G, Treszl A, Schally AV, et al. Prognosis in human glioblastoma based on expression of ligand growth hormone-releasing hormone, pituitary-type growth hormone-releasing hormone receptor, its splicing variant receptors, EGF receptor and PTEN genes. *Journal of Cancer Research and Clinical Oncology*. 2014;140:1641-1649.
503. Clancy H, Pruski M, Fedrizzi NC, Lang B, McCaig C, Ching J. PP46. THE PEROXISOME PROLIFERATOR ACTIVATED RECEPTOR GAMMA AGONIST PIOGLITAZONE REDUCES ELECTRICALLY DIRECTED GLIOBLASTOMA MULTIFORME CELL MIGRATION. *Neuro-Oncology*; 2017. p. i13.
504. Patel L, Pass I, Coxen P, Downes CP, Smith SA, Macphee CH. Tumor suppressor and anti-inflammatory actions of PPAR $\gamma$  agonists are mediated via upregulation of PTEN. *Current Biology*. 2001;11(10):765-768.
505. Ray-Chaudhury A. Glioblastoma: Molecular Mechanisms of Pathogenesis and Current Therapeutic Strategies. In: Ray SK, Editor, editor. 2010. p. 76-84.
506. Gage FH. Mammalian neural stem cells. *Science*. Feb 2000;287(5457):1433-8. doi:10.1126/science.287.5457.1433
507. Uchida N, Buck DW, He D, et al. Direct isolation of human central nervous system stem cells. *Proc Natl Acad Sci U S A*. Dec 2000;97(26):14720-5. doi:10.1073/pnas.97.26.14720
508. Kennea NL, Mehmet H. Neural stem cells. *J Pathol*. Jul 2002;197(4):536-50. doi:10.1002/path.1189
509. Englund U, Björklund A, Wictorin K. Migration patterns and phenotypic differentiation of long-term expanded human neural progenitor cells after

- transplantation into the adult rat brain. *Brain Res Dev Brain Res*. Mar 2002;134(1-2):123-41. doi:10.1016/s0165-3806(01)00330-3
510. Kornack DR, Rakic P. The generation, migration, and differentiation of olfactory neurons in the adult primate brain. *Proc Natl Acad Sci U S A*. Apr 2001;98(8):4752-7. doi:10.1073/pnas.081074998
511. Wang Y, Kaneko N, Asai N, et al. Girdin is an intrinsic regulator of neuroblast chain migration in the rostral migratory stream of the postnatal brain. *J Neurosci*. Jun 2011;31(22):8109-22. doi:10.1523/JNEUROSCI.1130-11.2011
512. Sun MZ, Kim JM, Oh MC, et al. Na<sup>+</sup>/K<sup>+</sup>-ATPase  $\beta$ 2-subunit (AMOG) expression abrogates invasion of glioblastoma-derived brain tumor-initiating cells. *Neuro Oncol*. Nov 2013;15(11):1518-31. doi:10.1093/neuonc/not099
513. Kahlert UD, Maciaczyk D, Doostkam S, et al. Activation of canonical WNT/ $\beta$ -catenin signaling enhances in vitro motility of glioblastoma cells by activation of ZEB1 and other activators of epithelial-to-mesenchymal transition. *Cancer Lett*. Dec 2012;325(1):42-53. doi:10.1016/j.canlet.2012.05.024
514. Kanemaru K, Kubota J, Sekiya H, Hirose K, Okubo Y, Iino M. Calcium-dependent N-cadherin up-regulation mediates reactive astrogliosis and neuroprotection after brain injury. *Proc Natl Acad Sci U S A*. Jul 2013;110(28):11612-7. doi:10.1073/pnas.1300378110
515. Velpula KK, Rehman AA, Chelluboina B, et al. Glioma stem cell invasion through regulation of the interconnected ERK, integrin  $\alpha$ 6 and N-cadherin signaling pathway. *Cell Signal*. Nov 2012;24(11):2076-84. doi:10.1016/j.cellsig.2012.07.002
516. Singh SK, Hawkins C, Clarke ID, et al. Identification of human brain tumour initiating cells. *Nature*. 2004;432(7015):396-401. IN FILE.
517. Visvader J, Lindeman G. Cancer stem cells in solid tumours: accumulating evidence and unresolved questions. *Nature Reviews Cancer*; 2008. p. 755-68.
518. Sutter R, Yadirgi G, Marino S. Neural stem cells, tumour stem cells and brain tumours: dangerous relationships? *Biochim Biophys Acta*. Dec 2007;1776(2):125-37. doi:10.1016/j.bbcan.2007.07.006
519. Kania G, Corbeil D, Fuchs J, et al. Somatic stem cell marker prominin-1/CD133 is expressed in embryonic stem cell-derived progenitors. *Stem Cells*. 2005 Jun-Jul 2005;23(6):791-804. doi:10.1634/stemcells.2004-0232
520. Zeppernick F, Ahmadi R, Campos B, et al. Stem cell marker CD133 affects clinical outcome in glioma patients. *Clin Cancer Res*. 2008;14(1):123-129. IN FILE.
521. Brescia P, Ortensi B, Fornasari L, Levi D, Broggi G, Pelicci G. CD133 Is Essential for Glioblastoma Stem Cell Maintenance. Article. *Stem Cells*. MAY 2013 2013;31(5):857-869. doi:10.1002/stem.1317
522. Yang XJ, Cui W, Gu A, et al. A novel zebrafish xenotransplantation model for study of glioma stem cell invasion. *PLoS One*. 2013;8(4):e61801. doi:10.1371/journal.pone.0061801
523. Shibahara I, Sonoda Y, Saito R, et al. The expression status of CD133 is associated with the pattern and timing of primary glioblastoma recurrence. *Neuro Oncol*. Sep 2013;15(9):1151-9. doi:10.1093/neuonc/not066
524. Shin JH, Lee YS, Hong YK, Kang CS. Correlation between the prognostic value and the expression of the stem cell marker CD133 and isocitrate dehydrogenase1 in glioblastomas. *J Neurooncol*. Dec 2013;115(3):333-41. doi:10.1007/s11060-013-1234-z
525. Schlaepfer DD, Mitra SK. Multiple connections link FAK to cell motility and invasion. *Curr Opin Genet Dev*. Feb 2004;14(1):92-101. doi:10.1016/j.gde.2003.12.002



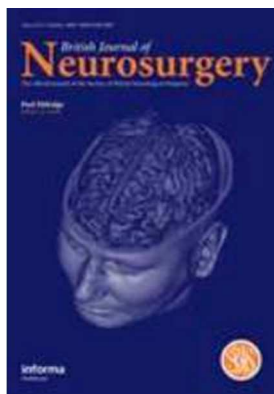
526. Cao L, Graue-Hernandez EO, Tran V, et al. Downregulation of PTEN at corneal wound sites accelerates wound healing through increased cell migration. *Invest Ophthalmol Vis Sci*. Apr 2011;52(5):2272-8. doi:10.1167/iovs.10-5972
527. Hemmings BA, Restuccia DF. PI3K-PKB/Akt pathway. *Cold Spring Harb Perspect Biol*. Sep 01 2012;4(9):a011189. doi:10.1101/cshperspect.a011189
528. Zhao M. Electrical fields in wound healing-An overriding signal that directs cell migration. *Semin Cell Dev Biol*. Aug 2009;20(6):674-82. doi:10.1016/j.semcdb.2008.12.009
529. Li W, Wu C, Yao Y, et al. MUC4 modulates human glioblastoma cell proliferation and invasion by upregulating EGFR expression. *Neurosci Lett*. Apr 2014;566:82-7. doi:10.1016/j.neulet.2014.02.033
530. Choe G, Horvath S, Cloughesy TF, et al. Analysis of the phosphatidylinositol 3'-kinase signaling pathway in glioblastoma patients in vivo. *Cancer Res*. Jun 2003;63(11):2742-6.
531. Memmel S, Sukhorukov VL, Höring M, et al. Cell surface area and membrane folding in glioblastoma cell lines differing in PTEN and p53 status. *PLoS One*. 2014;9(1):e87052. doi:10.1371/journal.pone.0087052
532. Kirson E, Gurchikov Z, Schneiderman R, et al. Disruption of cancer cell replication by alternating electric fields. Article. *Cancer Research*. MAY 1 2004 2004;64(9):3288-3295. doi:10.1158/0008-5472.CAN-04-0083
533. Kirson E, Dbaly V, Tovarys F, et al. Alternating electric fields arrest cell proliferation in animal tumor models and human brain tumors. Article. *Proceedings of the National Academy of Sciences of the United States of America*. JUN 12 2007 2007;104(24):10152-10157. doi:10.1073/pnas.0702916104
534. Stupp R, Wong E, Kanner A, et al. NovoTTF-100A versus physician's choice chemotherapy in recurrent glioblastoma: A randomised phase III trial of a novel treatment modality. Article. *European Journal of Cancer*. SEP 2012 2012;48(14):2192-2202. doi:10.1016/j.ejca.2012.04.011
535. Toms SA, Kim CY, Nicholas G, Ram Z. Increased compliance with tumor treating fields therapy is prognostic for improved survival in the treatment of glioblastoma: a subgroup analysis of the EF-14 phase III trial. *J Neurooncol*. Jan 2019;141(2):467-473. doi:10.1007/s11060-018-03057-z
536. Cheung AY, Neyzari A. Deep local hyperthermia for cancer therapy: external electromagnetic and ultrasound techniques. *Cancer Res*. Oct 1984;44(10 Suppl):4736s-4744s.
537. Stupp R, Taillibert S, Kanner AA, et al. Maintenance Therapy With Tumor-Treating Fields Plus Temozolomide vs Temozolomide Alone for Glioblastoma: A Randomized Clinical Trial. *JAMA*. Dec 15 2015;314(23):2535-43. doi:10.1001/jama.2015.16669
538. Stupp R, Taillibert S, Kanner A, et al. Effect of Tumor-Treating Fields Plus Maintenance Temozolomide vs Maintenance Temozolomide Alone on Survival in Patients With Glioblastoma: A Randomized Clinical Trial. *JAMA*. 12 19 2017;318(23):2306-2316. doi:10.1001/jama.2017.18718
539. Mullins CS, Schneider B, Stockhammer F, Krohn M, Classen CF, Linnebacher M. Establishment and characterization of primary glioblastoma cell lines from fresh and frozen material: a detailed comparison. *PLoS One*. 2013;8(8):e71070. doi:10.1371/journal.pone.0071070

540. Lange F, Venus J, Shams Esfand Abady D, et al. Galvanotactic Migration of Glioblastoma and Brain Metastases Cells. *Life (Basel)*. Apr 14 2022;12(4)doi:10.3390/life12040580
541. Patel KS, Moussazadeh N, Doyle WK, Labar DR, Schwartz TH. Efficacy of vagus nerve stimulation in brain tumor-associated intractable epilepsy and the importance of tumor stability. *J Neurosurg*. Aug 2013;119(2):520-5. doi:10.3171/2013.3.JNS121890
542. Taphoorn MJ. Neurocognitive sequelae in the treatment of low-grade gliomas. *Semin Oncol*. Dec 2003;30(6 Suppl 19):45-8. doi:10.1053/j.seminoncol.2003.11.023
543. Perini G, Cotta Ramusino M, Sinforiani E, Bernini S, Petrachi R, Costa A. Cognitive impairment in depression: recent advances and novel treatments. *Neuropsychiatr Dis Treat*. 2019;15:1249-1258. doi:10.2147/NDT.S199746
544. Huang X, Stodieck SK, Goetze B, et al. Progressive maturation of silent synapses governs the duration of a critical period. *Proc Natl Acad Sci U S A*. Jun 16 2015;112(24):E3131-40. doi:10.1073/pnas.1506488112
545. Anderson E, Gregoski MJ, Gehle D, et al. Severity of respiratory disease is correlated with time of first oral feeding and need for a gastrostomy tube at discharge in premature infants born at <30 weeks of gestation. *Pediatr Pulmonol*. 01 2022;57(1):193-199. doi:10.1002/ppul.25713
546. Badran BW, Jenkins DD, Cook D, et al. Transcutaneous Auricular Vagus Nerve Stimulation-Paired Rehabilitation for Oromotor Feeding Problems in Newborns: An Open-Label Pilot Study. *Front Hum Neurosci*. 2020;14:77. doi:10.3389/fnhum.2020.00077
547. Jaseja H. Efficacy of vagal nerve stimulation in patients with cerebral palsy: emerging corroborative evidence. *Clin Neurol Neurosurg*. Sep 2011;113(7):603. doi:10.1016/j.clineuro.2011.02.020
548. Hallbook T, Lundgren J, Kohler S, Blennow G, Stromblad LG, Rosen I. Beneficial effects on sleep of vagus nerve stimulation for refractory epilepsy in children with therapy resistant epilepsy. *Eur J Paediatr Neurol*; 2005. p. 399 - 407
549. Mitchell HA, Weinshenker D. Good night and good luck: norepinephrine in sleep pharmacology. *Biochem Pharmacol*. Mar 15 2010;79(6):801-9. doi:10.1016/j.bcp.2009.10.004
550. Yap JYY, Keatch C, Lambert E, Woods W, Stoddart PR, Kameneva T. Critical Review of Transcutaneous Vagus Nerve Stimulation: Challenges for Translation to Clinical Practice. *Front Neurosci*. 2020;14:284. doi:10.3389/fnins.2020.00284
551. Dawson J, Liu CY, Francisco GE, et al. Vagus nerve stimulation paired with rehabilitation for upper limb motor function after ischaemic stroke (VNS-REHAB): a randomised, blinded, pivotal, device trial. *Lancet*. 04 24 2021;397(10284):1545-1553. doi:10.1016/S0140-6736(21)00475-X
552. Khodaparast N, Hays SA, Sloan AM, et al. Vagus nerve stimulation during rehabilitative training improves forelimb strength following ischemic stroke. *Neurobiol Dis*. Dec 2013;60:80-8. doi:10.1016/j.nbd.2013.08.002
553. Porter BA, Khodaparast N, Fayyaz T, et al. Repeatedly pairing vagus nerve stimulation with a movement reorganizes primary motor cortex. *Cereb Cortex*. Oct 2012;22(10):2365-74. doi:10.1093/cercor/bhr316
554. Bear MF, Singer W. Modulation of visual cortical plasticity by acetylcholine and noradrenaline. *Nature*. 1986 Mar 13-19 1986;320(6058):172-6. doi:10.1038/320172a0
555. Rajatileka S, Odd D, Robinson MT, et al. Variants of the EAAT2 Glutamate Transporter Gene Promoter Are Associated with Cerebral Palsy in Preterm Infants. *Mol Neurobiol*. 03 2018;55(3):2013-2024. doi:10.1007/s12035-017-0462-1

556. Rothstein JD, Patel S, Regan MR, et al. Beta-lactam antibiotics offer neuroprotection by increasing glutamate transporter expression. *Nature*. Jan 06 2005;433(7021):73-7. doi:10.1038/nature03180
557. Barker-Haliski M, White HS. Glutamatergic Mechanisms Associated with Seizures and Epilepsy. *Cold Spring Harb Perspect Med*. Jun 22 2015;5(8):a022863. doi:10.1101/cshperspect.a022863
558. Petr GT, Sun Y, Frederick NM, et al. Conditional deletion of the glutamate transporter GLT-1 reveals that astrocytic GLT-1 protects against fatal epilepsy while neuronal GLT-1 contributes significantly to glutamate uptake into synaptosomes. *J Neurosci*. Apr 01 2015;35(13):5187-201. doi:10.1523/JNEUROSCI.4255-14.2015
559. Parsons DW, Jones S, Zhang X, et al. An integrated genomic analysis of human glioblastoma multiforme. *Science*. Sep 26 2008;321(5897):1807-12. doi:10.1126/science.1164382
560. Malik AR, Willnow TE. Excitatory Amino Acid Transporters in Physiology and Disorders of the Central Nervous System. *Int J Mol Sci*. Nov 12 2019;20(22)doi:10.3390/ijms20225671
561. Fontana AC. Current approaches to enhance glutamate transporter function and expression. *J Neurochem*. Sep 2015;134(6):982-1007. doi:10.1111/jnc.13200
562. Owens MJ, Nemeroff CB. Pharmacology of valproate. *Psychopharmacol Bull*. 2003;37 Suppl 2:17-24.
563. Kimura A, Guo X, Noro T, et al. Valproic acid prevents retinal degeneration in a murine model of normal tension glaucoma. *Neurosci Lett*. Feb 19 2015;588:108-13. doi:10.1016/j.neulet.2014.12.054
564. Hassel B, Iversen EG, Gjerstad L, Taubøll E. Up-regulation of hippocampal glutamate transport during chronic treatment with sodium valproate. *J Neurochem*. Jun 2001;77(5):1285-92. doi:10.1046/j.1471-4159.2001.00349.x
565. Hu YY, Xu J, Zhang M, Wang D, Li L, Li WB. Ceftriaxone modulates uptake activity of glial glutamate transporter-1 against global brain ischemia in rats. *J Neurochem*. Jan 2015;132(2):194-205. doi:10.1111/jnc.12958
566. Cenciarini M, Valentino M, Belia S, et al. Dexamethasone in Glioblastoma Multiforme Therapy: Mechanisms and Controversies. *Front Mol Neurosci*. 2019;12:65. doi:10.3389/fnmol.2019.00065
567. Zschocke J, Bayatti N, Clement AM, et al. Differential promotion of glutamate transporter expression and function by glucocorticoids in astrocytes from various brain regions. *J Biol Chem*. Oct 14 2005;280(41):34924-32. doi:10.1074/jbc.M502581200
568. Matos-Ocasio F, Hernández-López A, Thompson KJ. Ceftriaxone, a GLT-1 transporter activator, disrupts hippocampal learning in rats. *Pharmacol Biochem Behav*. Jul 2014;122:118-21. doi:10.1016/j.pbb.2014.03.011
569. Brothers HM, Bardou I, Hopp SC, et al. Riluzole partially rescues age-associated, but not LPS-induced, loss of glutamate transporters and spatial memory. *J Neuroimmune Pharmacol*. Dec 2013;8(5):1098-105. doi:10.1007/s11481-013-9476-2
570. Frizzo ME, Dall'Onder LP, Dalcin KB, Souza DO. Riluzole enhances glutamate uptake in rat astrocyte cultures. *Cell Mol Neurobiol*. Feb 2004;24(1):123-8. doi:10.1023/b:cemn.0000012717.37839.07
571. Carbone M, Duty S, Rattray M. Riluzole elevates GLT-1 activity and levels in striatal astrocytes. *Neurochem Int*. Jan 2012;60(1):31-8. doi:10.1016/j.neuint.2011.10.017

572. Dagi T, Yilmaz O, Taskiran D, Peker G. Neuroprotective agents: is effective on toxicity in glial cells? *Cell Mol Neurobiol*. Mar 2007;27(2):171-7. doi:10.1007/s10571-006-9082-4
573. Nehser M, Dark J, Schweitzer D, et al. System X. *Neurochem Res*. Jun 2020;45(6):1375-1386. doi:10.1007/s11064-019-02901-6
574. Pérez-Mato M, Iglesias-Rey R, Vieites-Prado A, et al. Blood glutamate EAAT. *EBioMedicine*. Jan 2019;39:118-131. doi:10.1016/j.ebiom.2018.11.024
575. Edelman RR. The history of MR imaging as seen through the pages of radiology. *Radiology*. Nov 2014;273(2 Suppl):S181-200. doi:10.1148/radiol.14140706
576. Juhász C, Mittal S. Molecular Imaging of Brain Tumor-Associated Epilepsy. *Diagnostics (Basel)*. Dec 05 2020;10(12)doi:10.3390/diagnostics10121049
577. Davis KA, Nanga RP, Das S, et al. Glutamate imaging (GluCEST) lateralizes epileptic foci in nonlesional temporal lobe epilepsy. *Sci Transl Med*. Oct 14 2015;7(309):309ra161. doi:10.1126/scitranslmed.aaa7095
578. Cohen-Gadol AA, Wilhelmi BG, Collignon F, et al. Long-term outcome of epilepsy surgery among 399 patients with nonlesional seizure foci including mesial temporal lobe sclerosis. *J Neurosurg*. Apr 2006;104(4):513-24. doi:10.3171/jns.2006.104.4.513
579. Bernasconi N, Wang I. Emerging Trends in Neuroimaging of Epilepsy. *Epilepsy Curr*. Mar 2021;21(2):79-82. doi:10.1177/1535759721991161
580. Sone D, Sato N, Ota M, Maikusa N, Kimura Y, Matsuda H. Abnormal neurite density and orientation dispersion in unilateral temporal lobe epilepsy detected by advanced diffusion imaging. *Neuroimage Clin*. 2018;20:772-782. doi:10.1016/j.nicl.2018.09.017
581. White NS, Leergaard TB, D'Arceuil H, Bjaalie JG, Dale AM. Probing tissue microstructure with restriction spectrum imaging: Histological and theoretical validation. *Hum Brain Mapp*. Feb 2013;34(2):327-46. doi:10.1002/hbm.21454
582. Salamon N, Kung J, Shaw SJ, et al. FDG-PET/MRI coregistration improves detection of cortical dysplasia in patients with epilepsy. *Neurology*. Nov 11 2008;71(20):1594-601. doi:10.1212/01.wnl.0000334752.41807.2f
583. Park JE, Cheong EN, Jung DE, Shim WH, Lee JS. Utility of 7 Tesla Magnetic Resonance Imaging in Patients With Epilepsy: A Systematic Review and Meta-Analysis. *Front Neurol*. 2021;12:621936. doi:10.3389/fneur.2021.621936
584. Inder TE, de Vries LS, Ferriero DM, et al. Neuroimaging of the Preterm Brain: Review and Recommendations. *J Pediatr*. 10 2021;237:276-287.e4. doi:10.1016/j.jpeds.2021.06.014
585. Dubois J, Alison M, Counsell SJ, Hertz-Pannier L, Hüppi PS, Benders MJNL. MRI of the Neonatal Brain: A Review of Methodological Challenges and Neuroscientific Advances. *J Magn Reson Imaging*. 05 2021;53(5):1318-1343. doi:10.1002/jmri.27192
586. Lean RE, Han RH, Smyser TA, et al. Altered neonatal white and gray matter microstructure is associated with neurodevelopmental impairments in very preterm infants with high-grade brain injury. *Pediatr Res*. 09 2019;86(3):365-374. doi:10.1038/s41390-019-0461-1
587. Devinsky O, Vezzani A, O'Brien TJ, et al. Epilepsy. *Nat Rev Dis Primers*. 05 03 2018;4:18024. doi:10.1038/nrdp.2018.24
588. Toda T, Parylak SL, Linker SB, Gage FH. The role of adult hippocampal neurogenesis in brain health and disease. *Mol Psychiatry*. 01 2019;24(1):67-87. doi:10.1038/s41380-018-0036-2

589. Rodrigues RS, Lourenço DM, Paulo SL, et al. Cannabinoid Actions on Neural Stem Cells: Implications for Pathophysiology. *Molecules*. Apr 05 2019;24(7)doi:10.3390/molecules24071350
590. Parent JM, Valentin VV, Lowenstein DH. Prolonged seizures increase proliferating neuroblasts in the adult rat subventricular zone-olfactory bulb pathway. *J Neurosci*. Apr 15 2002;22(8):3174-88. doi:20026296
591. Upadhyia D, Hattiangady B, Castro OW, et al. Human induced pluripotent stem cell-derived MGE cell grafting after status epilepticus attenuates chronic epilepsy and comorbidities via synaptic integration. *Proc Natl Acad Sci U S A*. 01 02 2019;116(1):287-296. doi:10.1073/pnas.1814185115
592. Lourenço DM, Ribeiro-Rodrigues L, Sebastião AM, Diógenes MJ, Xapelli S. Neural Stem Cells and Cannabinoids in the Spotlight as Potential Therapy for Epilepsy. *Int J Mol Sci*. Oct 03 2020;21(19)doi:10.3390/ijms21197309
593. Jinnou H. Regeneration using endogenous neural stem cells following neonatal brain injury. *Pediatr Int*. Jan 2021;63(1):13-21. doi:10.1111/ped.14368
594. Spaeth E, Klopp A, Dembinski J, Andreeff M, Marini F. Inflammation and tumor microenvironments: defining the migratory itinerary of mesenchymal stem cells. *Gene Ther*. May 2008;15(10):730-8. doi:10.1038/gt.2008.39
595. Danielyan L, Schäfer R, von Ameln-Mayerhofer A, et al. Therapeutic efficacy of intranasally delivered mesenchymal stem cells in a rat model of Parkinson disease. *Rejuvenation Res*. Feb 2011;14(1):3-16. doi:10.1089/rej.2010.1130
596. Lee HK, Finniss S, Cazacu S, Xiang C, Brodie C. Mesenchymal stem cells deliver exogenous miRNAs to neural cells and induce their differentiation and glutamate transporter expression. *Stem Cells Dev*. Dec 01 2014;23(23):2851-61. doi:10.1089/scd.2014.0146
597. Aboody KS, Brown A, Rainov NG, et al. Neural stem cells display extensive tropism for pathology in adult brain: evidence from intracranial gliomas. *Proc Natl Acad Sci USA*. 2000;97(23):12846-12851. IN FILE.
598. Aboody KS, Najbauer J, Metz MZ, D'Apuzzo MG, M. Neural Stem Cell-Mediated Enzyme/Prodrug Therapy for Glioma: Preclinical Studies. *Science*; 2013. p. 184ra59.
599. Zhang GL, Wang CF, Qian C, Ji YX, Wang YZ. Role and mechanism of neural stem cells of the subventricular zone in glioblastoma. *World J Stem Cells*. Jul 26 2021;13(7):877-893. doi:10.4252/wjsc.v13.i7.877
600. Clancy H, Pruski M, Lang BVOP, Ching J, McCaig C. Glioblastoma Cell Migration is Directed by Electrical Signals. bioRxiv; 2020.



**Long-term effectiveness and tolerability of vagal nerve stimulation (VNS) in adults with intractable epilepsy: A retrospective analysis of 100 patients**

Journal:	<i>British Journal of Neurosurgery</i>
Manuscript ID:	CBJN-2012-0262.R1
Manuscript Type:	Original Article
Date Submitted by the Author:	n/a
Complete List of Authors:	Ching, Jared; Institute of Neurosciences, Khan, Sadaquate; Institute of Neurosciences, White, Paul; Department of Mathematics and Statistics, University of the West of England Reed, Judith; Institute of Neurosciences, Frenchay Hospital Ramnarine, Devindra; Institute of Neurosciences, Frenchay Hospital Sieradzan, Kasia; Institute of Neurosciences, Sandeman, David; Frenchay Hospital, Neurosurgery; Institute of Neurosciences, Frenchay Hospital
Keywords:	Vagal Nerve Stimulation, Epilepsy, Long term followup, Quality of life

SCHOLARONE™  
Manuscripts

**Title: Long-term effectiveness and tolerability of vagal nerve stimulation (VNS) in adults with intractable epilepsy:**

**A retrospective analysis of 100 patients**

**Authors:** Jared Ching<sup>1</sup>, Sadaquate Khan<sup>1</sup>, Paul White<sup>2</sup>, Judith Reed<sup>1</sup>, Devindra Ramnarine<sup>1</sup>, Kasia Sieradzan<sup>1</sup>, David Sandeman\*<sup>1</sup>

<sup>1</sup>Institute of Neurosciences, Frenchay Hospital, Bristol

<sup>2</sup>Applied Statistics Group, University of the West of England, Bristol.

\*Corresponding author

David Sandeman, Consultant Neurosurgeon

Institute of Neurosciences, Frenchay Hospital, Bristol BS16 1LE

Tel: (44)117 9701212

Fax: (44)117 9701161

Email: [david.sandeman@nbt.nhs.uk](mailto:david.sandeman@nbt.nhs.uk)

**Key Words:** Vagal Nerve Stimulation – Epilepsy – Long term followup – Quality of life.

Running Title: VNS in resistant Epilepsy

Number of text pages: 10

Number of Tables: 9

Number of Figures: 2, 1 in colour

1  
2  
3 **Abstract:** Data for 100 VNS patients was collected and analysed retrospectively. The mean seizure reduction was  
4  
5 17.86% (n=67) at 6 months, 26.21% (n=63) at 1 year, 30.43% (n=53) at 2 years, 48.10% (n=40) at 3 years, 49.44%  
6  
7 (n=32) at 4 years, 50.52% (n=35) at 5 years, 45.85% (n=31) at 6 years, 62.68% (n=25) at 8 years, 76.41% (n=9) at 10  
8  
9 years, 82.90% (n=4) at 12 years. Evidence of statistical significance for mean seizure reduction over time was strong  
10  
11 with all p values less than 0.05 except at 12 years (p=.125) where the sample size was small (n = 4). Mean seizure  
12  
13 reduction was 49.04% and 51 (51%) patients were considered responders, defined as a 50% or more reduction in  
14  
15 seizure frequency. Twenty one (21%) patients suffered surgical complications. Of these 15 were self-limiting and 6  
16  
17 were irreversible or required a device revision. Fifty patients (50%) suffered from side-effects while vagal stimulation  
18  
19 cycled on (VNS on) post-operatively. However, of these, only 1 patient suffered from intolerable side effects  
20  
21 requiring the device to be switched off temporarily. This study demonstrates long-term efficacy in seizure reduction  
22  
23 with the use of VNS. Complication rates and tolerability did not deviate greatly from that previously reported,  
24  
25 indicating VNS is a safe and effective treatment for seizure reduction in intractable epilepsy.  
26  
27  
28  
29

### 30 **Introduction**

31  
32 Vagal Nerve Stimulation (VNS) is considered an adjunctive treatment for intractable epilepsy where patients are not  
33  
34 suitable for resective surgery or express a preference for an alternative to surgery requiring a craniotomy. Response  
35  
36 to anti-epileptic drugs (AEDs), and likewise VNS, is defined by a reduction in seizure frequency of 50% or more after  
37  
38 treatment.<sup>1</sup>  
39  
40  
41  
42

43  
44 Approximately 50 million people around the world are estimated to have epilepsy, of whom about one third will be  
45  
46 resistant to treatment with AEDs and therefore may be considered for surgical intervention.<sup>2,3</sup> Where resective  
47  
48 surgery is not viable, for example if no discernible seizure focus can be identified or where epilepsy is multifocal in  
49  
50 nature, alternative surgical options can be considered. These include VNS, corpus callosotomy and multiple subpial  
51  
52 resections, the least invasive of which is VNS.<sup>3-5</sup>  
53  
54  
55

56  
57 Here we present the first case series based in the United Kingdom (UK). While efficacy of VNS has been proven with  
58  
59 randomised controlled trials (RCTs), identifying individuals for whom VNS will benefit most remains challenging as  
60  
only a proportion benefit and in a variable fashion. However, a recent meta-analysis and systematic review  
URL: <http://mc.manuscriptcentral.com/cbjn>



1 determined that tuberous sclerosis and post-traumatic epilepsy were positive predictive factors for a favourable  
2 response to VNS.<sup>4</sup>  
3  
4  
5

## 6 **Methods**

7  
8  
9 100 patients were implanted with a vagal nerve simulator (Cyberonics, Houston, Texas) between November 1995  
10 and July 2010 by one surgeon (D.R.S.) at Frenchay Hospital, Bristol, United Kingdom. Collected data included  
11 demographic information, associated past medical history, epilepsy risk factors, seizure frequency per month at  
12 baseline (prior to VNS implantation) and at future intervals (6 months, 1, 2, 3, 4, 5, 6, 8, 10, and 12 years), the total  
13 number of AEDs tried in the past, AEDs prescribed prior to and after VNS implantation, neuropsychiatric results,  
14 presurgical evaluation findings, diagnosis(es), VNS device models, complications resulting from surgery, VNS on time,  
15 and AEDs, VNS battery replacements, VNS removal, last VNS settings, number of admissions, days spent in hospital  
16 as an inpatient and total outpatient appointments attended. Seizure frequency data was not available beyond 12  
17 years post-implantation.  
18  
19

20 A number of patients underwent a full epilepsy surgery work-up including EEG, video telemetry, MRI, Wada test and  
21 a neuropsychiatric assessment when necessary. Cases were discussed at an epilepsy multi-disciplinary team meeting  
22 (MDT) prior to implantation. At each operation the current VNS model at the time was used at first implant or when  
23 replacing the battery, which may have been model 100, 101, 102, 102R (Duo), 103 or 104 (Duo). Lead models that  
24 were used include the 300, 302 and 304. Surgical technique was consistent with known published methods.<sup>6</sup>  
25  
26

27 Patient clinical and operative notes were reviewed retrospectively. Seizure diaries were not always available. In such  
28 cases the monthly seizure frequency, estimated by the patient or their carers, and recorded in follow-up letters was  
29 used. **Responders were considered patients who experienced a 50% or greater reduction in seizure frequency.**  
30  
31

32 Approval from the local Research and Audit Department permitted access to patient medical notes.  
33  
34

35 *Outcome measures:* The primary outcome measure was total seizure frequency per month which included simple  
36 partial seizures (SPS), complex partial seizures with or without secondary generalisation (SG), generalised tonic clonic  
37 seizures (GTC) and any seizure subtypes. The ILAE 1981 classification was utilised and each seizure subclassification  
38 recorded before and after treatment with VNS to determine subtle benefits that may have arisen. However, the  
39 recently revised criteria invalidates certain terms including SG, and as such this has been kept in mind for the final  
40  
41  
42  
43  
44  
45  
46  
47  
48  
49  
50  
51  
52  
53  
54  
55  
56  
57  
58  
59  
60

1  
2  
3  
4  
5  
6  
7  
8  
9  
10  
11  
12  
13  
14  
15  
16  
17  
18  
19  
20  
21  
22  
23  
24  
25  
26  
27  
28  
29  
30  
31  
32  
33  
34  
35  
36  
37  
38  
39  
40  
41  
42  
43  
44  
45  
46  
47  
48  
49  
50  
51  
52  
53  
54  
55  
56  
57  
58  
59  
60

analyses.<sup>7</sup> Seizure diaries were analysed in detail if available and baseline seizure frequency was often available from the Epilepsy Surgery Program assessments prior to surgery. Adverse effects of a surgical nature, while VNS was on and due to antiepileptic drug (AEDs) were recorded, along with the number of AEDs taken pre- and post-operatively. Epilepsy aetiology, related medical history (including nature of birth, previous trauma), risk factors and pre-surgical evaluation results (including video telemetry/EEG, MRI and PET scans) were recorded. The diagnosis pre- and post-operatively at last follow-up were recorded to determine if the nature of seizures had changed.

**Statistical analysis:** A non-parametric Wilcoxon Signed Rank Test was used to assess changes in seizure frequency statistically for each follow-up time point against baseline. The strength of the relationship between percentage change in seizure frequency and independent variables using Pearson's correlation coefficient. Responders and non-responders form two independent groups and differences between these groups on potentially important factors (Age and Age at onset of epilepsy) were compared using the independent samples t-test. Assessment of association between categorical variables (Sex, Intra-cranial surgery) and responder status was performed using the chi-squared test of association. All statistical analysis was performed in SPSS version 19.0.

## Results

**Patient demographics:** for the 100 patients sampled are summarised in Table I. Mean age at implant was 35.80 years (range: 17-75 years). Mean duration of epilepsy prior to implantation was 28 years (range: 7-59), mean age of onset of epilepsy was 7.28 years. Causes of epilepsy are detailed in table II, with an unknown aetiology being most common. Mean length of treatment with VNS was 4.10 years.

**Effectiveness:** Mean seizure reduction was 17.86% (n=67) at 6 months, 26.21% (n=63) at 1 year, 30.43% (n=53) at 2 years, 48.10% (n=40) at 3 years, 49.44% (n=32) at 4 years, 50.52% (n=35) at 5 years, 45.85% (n=31) at 6 years, 62.68% (n=25) at 8 years, 76.41% (n=9) at 10 years, 82.90% (n=4) at 12 years (Table III and Figure I). Post-VNS implantation, three patients were seizure free for at least 1 year before seizures returned at last follow up. Last follow-up seizure reduction is included in the discussion.

1 Univariate analysis to elucidate any statistical correlation on seizure frequency change in relation to important  
2 independent variables, including age of onset of epilepsy, duration of epilepsy prior to VNS implantation, previous  
3 intracranial surgery, cause of epilepsy, EEG findings number of AEDs pre-and post-VNS revealed no statistical  
4 evidence of a difference/no statistically significant difference (Tables IV, V and text). The mean number of AEDs  
5 prescribed reduced from 3.29 to 3.12, however no statistical significance was found ( $p > .05$  at all time periods)  
6 (Table V). There was no statistical evidence for a difference between responders and non-responders with respect to  
7 age at onset of epilepsy, age at operation and duration of seizures up to the point of treatment (all  $p$  values  $> .05$ )  
8 (Table IV). 30 out of 61 males (49.20%) were responders compared with 19 out of 39 females (48.70%). This gender  
9 difference did not achieve statistical significance ( $\chi^2 = 0.002$ ,  $df = 1$ ,  $p = .964$ ). 9 out of 12 (75.00%) with a history of  
10 failed intracranial surgery were responders compared with 42 out of 88 (47.70%) without a history of intracranial  
11 surgery. Failed intracranial surgery did not achieve statistical significance ( $\chi^2 = 3.143$ ,  $df = 1$ ,  $p = .076$ ). Four patients  
12 were seizure free at last follow-up

13  
14  
15  
16  
17  
18  
19  
20  
21  
22  
23  
24  
25  
26  
27 **Device removal and battery replacements:** Six patients (6%) had their devices removed and 35 (35%) had battery  
28 replacements, although 11 patient's date of original implant or replacement was not available at the time of writing.  
29 Reasons for device removal included failure to improve ( $n=3$ ), unknown ( $n=2$ ), and investigation for other pathology  
30 using magnetic resonance imaging ( $n=1$ ). Average battery life was 6.29 years. Patients received Cyberonics VNS  
31 Model 100 ( $n=16$ ), 101 ( $n=20$ ), 102 ( $n=35$ ), 102R ( $n=3$ ), 103 ( $n=7$ ), and 104 ( $n=5$ ). Mean battery life was 6.68 years  
32 ( $n=9$ , Model 100), 7.80 years ( $n=9$ , Model 101), 4.64 years (Model 102,  $n=6$ ), and Models 103 and 104 had not been  
33 replaced at the time of writing.

34  
35  
36  
37  
38  
39  
40  
41  
42  
43 **Complications:** No patients died as a direct result of VNS surgery, although one patient died following a collapse 2.86  
44 years post-operatively. The post-mortem in this case was inconclusive and the responsible neurologist could not rule  
45 out sudden unexplained death in epilepsy (SUDEP). 20 (20%) patients suffered from surgical complications. Five had  
46 temporary dysphonia due to unilateral vocal cord paresis, three of which required ENT intervention and two were  
47 self limiting. 11 patients had discomfort at the site of the implant, including three early cases where the larger device  
48 batteries migrated from the implant site and two cases where the wires were placed superficially and deemed  
49 unsightly. One patient suffered from a left-sided Horner's Syndrome, another transient dysphagia, and in two  
50 patients the lead was damaged at implantation. 13 out of the 20 were self-limiting and 7 were irreversible. 6  
51  
52  
53  
54  
55  
56  
57  
58  
59  
60

1 required a device revision. In this series there were no cases of infection or cases of cardiac complications. However  
2 we acknowledge that there is a 2-3% risk of infection in routine implant surgery.  
3  
4

5 50 (50%) patients suffered from some discomfort while the vagal nerve stimulator was on. Only 1 (1%) patient  
6 suffered from intolerable chest pain requiring the device to be switched off temporarily after 6 months of treatment.  
7

8 Otherwise stimulator was generally well tolerated and discomfort self-limiting over time. On occasion frequency  
9 settings were reduced to alleviate symptoms including discomfort and coughing. Table VI summarises this.  
10  
11

12 36 (36%) patients suffered from AED adverse effects either before or after VNS (data not shown).  
13  
14

15 **Other outcomes:** Relevant past medical history included learning difficulties (26%), psychotic episodes (7%), spina  
16 bifida (4%), West Syndrome (2%), neurofibromatosis type I (1%), depression (1%), and pseudoseizures (1%) were  
17 present in this patient group. Last follow-up VNS generator and magnet settings were recorded (Table VII).  
18  
19  
20  
21  
22  
23  
24  
25  
26  
27

## 28 Discussion

29  
30 **Previous studies:** Only two short-term, double blinded, randomised controlled-trials have been undertaken assessing  
31 the efficacy of VNS in Epilepsy, the E03 and E05 Trials respectively, comparing low and high stimulation VNS (refer to  
32 Table VIII for a summary of results).<sup>8 9</sup> Since then, studies have been retrospective follow-ups, prospective  
33 observational and registry designed studies in order to elucidate long term efficacy of VNS and to determine factors  
34 that contribute to efficacy, including AED changes, age, co-morbidities, previous intra-cranial surgery, and VNS  
35 settings. Table VIII summarises the results of salient studies to date. Two paediatric studies are included to highlight  
36 the difference in response rate, however studies that determine VNS efficacy in specific patient groups were not  
37 included, such as adults and children with learning difficulties.<sup>10</sup>  
38  
39  
40  
41  
42  
43  
44  
45  
46  
47  
48

49 To date, this is the first retrospective study on the efficacy of VNS based in the United Kingdom.  
50  
51

52 **Effectiveness:** Responders were considered patients who experienced a  $\geq 50\%$  reduction in seizures, which has been  
53 a criteria used throughout the literature. At last follow-up 51% of patients would be considered responders.  
54 Responder rates reduced as the lower limit of seizure reduction is raised, where 26%, 8% and 3% patients benefited  
55 from a  $\geq 75\%$ ,  $\geq 90\%$  and 100% (seizure freedom) seizure reduction (refer to Table IX). This compares well with  
56 previous studies. Fifteen (15%) patients had no change in monthly seizure frequency at last follow up and 13 (13%)  
57  
58  
59  
60

1 patients had worsening of seizure frequency. Mean seizure frequency reduction at 1 year and beyond was greater in  
2 the present study compared to the findings of two similar long-term studies (Table IX and Figure II).<sup>11 12</sup> However,  
3 mean seizure reduction was less favourable compared to findings in the most recent retrospective long term study.<sup>13</sup>  
4 Elliot and colleagues<sup>13</sup> utilised a multi-centre patient population and unlike the present study, did not report that any  
5 patients had worsened in outcome. Although in the larger cohort (n=436), Elliot and colleagues did report that  
6 12.25% experienced no seizure reduction and 2.5% had worsened seizure frequency.<sup>14</sup>  
7  
8  
9  
10  
11  
12

13 Responder rates (as listed in Table VIII) of the present study demonstrated comparable seizure frequency reduction  
14 to related studies, and exceeded results of several papers. However, this does not hold true when compared to the  
15 most recent comparable long-term study where a significant difference exists between those experiencing  $\geq 50\%$   
16 (51.0% vs. 90.80%)  $\geq 75\%$  (26.73% vs 58.80%),  $\geq 90\%$  (8.91 vs 36.90) and 100% (3.96 vs 15.40) mean seizure reduction.  
17  
18  
19  
20  
21  
22

23 Last follow-up seizure reduction was not included in the main results, however, as this has been previously reported  
24 in similar studies, a brief description from our cohort follows.<sup>12 13 15</sup> At last follow-up 15 (15.00%) patients had no  
25 change in seizure frequency and 14 (14.00%) had an increase. Last follow-up mean seizure reduction was calculated  
26 to include all patients, **(Mean  $\pm$  SD (Range), 33.86  $\pm$  61.30 (-380 to 100))** and then to include only patients who did  
27 not have an increase in seizure frequency **(48.70  $\pm$  35.39 (0-100))**. Mean seizure reduction per month increase from  
28 33.86% to 48.70% when excluding the 14 patients with a worsened outcome at last follow up. This indicates a  
29 detectable difference in efficacy that may account for differences in seizure reduction between the present and  
30 other studies.  
31  
32  
33  
34  
35  
36  
37  
38  
39  
40

41 Total trialed AEDs was reported as 6.6 in the present study compared to 5.6 in the largest retrospective follow-up to  
42 date.<sup>14</sup> It is noteworthy that this study included children in contrast to our entirely adult cohort.  
43  
44  
45

46 This study demonstrates that a minority of patients may worsen after VNS, but no predisposing or causative factors  
47 were identified in these individuals. Elliot et al. found that none of their patients of the 400 eligible for outcome  
48 analysis demonstrated a worsening of seizure frequency (range reported as 0-100% vs. -380-100% in the present  
49 study at last follow up).<sup>13 14</sup> However, studies that found similar levels of efficacy reported that some patients  
50 worsened including Ardesch et al. who reported 2 (10.53%) patients experienced a mild increase in seizure  
51 frequency post-VNS and Uthman et al. who reported 8 (16.67%) of their patients had an increase or no change in  
52 seizure frequency.<sup>11 12</sup>  
53  
54  
55  
56  
57  
58  
59  
60

1  
2  
3  
4  
5  
6  
7  
8  
9  
10  
11  
12  
13  
14  
15  
16  
17  
18  
19  
20  
21  
22  
23  
24  
25  
26  
27  
28  
29  
30  
31  
32  
33  
34  
35  
36  
37  
38  
39  
40  
41  
42  
43  
44  
45  
46  
47  
48  
49  
50  
51  
52  
53  
54  
55  
56  
57  
58  
59  
60

It is apparent from the accumulated data that individuals appear to respond variably, but the common consensus is that seizure reduction improves over time. Our findings support this, along with the recent meta-analysis that corroborate these findings, demonstrating a mean seizure reduction of 45%.<sup>4</sup>

**Complications:** The majority of surgical complications were minor and did not require further surgery. Side-effects from VNS cycling on occurred in almost half the patients, but in only one patient did this require the device to be switched off temporarily. None of the complications were life threatening. This is consistent with current literature.

**Device settings:** VNS device settings were recorded at last follow-up to determine if there was any correlation between efficacy and tolerability. Pulse width and/or output current was reduced or kept low when vocal changes were not well tolerated. Output currents were also not stepped up if patients felt apprehensive. This has previously been investigated in the XE5 study (n=154), where it was found that device settings were not associated with a change in effectiveness, including rapid cycle settings (reduced off time).<sup>16</sup> Here we report that no statistically significant correlation between VNS generator and magnet settings were found.

**Limitations:** Records of seizure frequency will vary in accuracy from patient to patient, making reports open to prior responder bias. It is well documented in the literature that seizures may not be witnessed, for example if nocturnal, and accuracy is dependent on how meticulous and able the patient or carer is at keeping a diary and recognising seizure types as they occur. However, the diaries were on occasion either unavailable in the notes, or a diary was not kept, despite instructions given to maintain one. For this reason retrospective studies on the effectiveness of VNS continue to include this as a discussion point, explaining that the reliability of such results is questionable.

**Patient selection for VNS therapy is unlikely to have remained consistent over the study period due to changing medical practices over time. This may have been contributory in the variability of patient response to VNS.**

Natural disease regression not affected by therapies should be considered, particularly in the long-term follow up, as a contributing factor to overall seizure reduction. Without a control group it is difficult to be certain that seizure reduction was completely due to VNS.

Changes in drug regimens were not accounted for in our analysis. Indeed, a number of patients' improved response was associated with the addition of or substitution with a new AED. **The introduction and widespread use of new AEDs onto the market over the study period may have also had an effect in some patients.**

## Conclusion

The results of this study are in keeping with the results of past literature and a recent systematic review and meta-analysis, where seizure reduction demonstrated time dependence. This provides reconfirmation that VNS is safe and effective for treatment resistant epilepsy in a proportion of individuals. Complications were generally well tolerated. However, no predisposing factors were found to be associated with a better or worse outcome.

## Acknowledgements:

A special thanks to Anita Summerfield and Beverley Curtis, Secretaries to the Department of Neurosurgery, for acquiring patient notes.

## Declaration of Interest

The authors report no conflicts of interest.

## References

1. Marson AG, Kadir ZA, Hutton JL, Chadwick DW. The New Antiepileptic Drugs: A Systematic Review of Their Efficacy and Tolerability. *Epilepsia* 1997;38(8):859-80.
2. Kwan P, Brodie MJ. Early identification of refractory epilepsy. *New England Journal of Medicine* 2000;342(5):314-19.
3. Spencer S, Huh L. Outcomes of epilepsy surgery in adults and children. *The Lancet Neurology* 2008;7(6):525-37.
4. Englot DJ, Chang EF, Auguste KI. Vagus nerve stimulation for epilepsy: a meta-analysis of efficacy and predictors of response. *Journal of Neurosurgery* 2011;115(6):1248-55.
5. Schuele SU, Lüders HO. Intractable epilepsy: management and therapeutic alternatives. *The Lancet Neurology* 2008;7(6):514-24.
6. Santos PM. Surgical placement of the vagus nerve stimulator. *Operative Techniques in Otolaryngology-Head and Neck Surgery* 2004;15(3):201-09.
7. Berg A, Berkovic S, Brodie M, Buchhalter J, Cross H, Boas W, et al. Revised terminology and concepts for organization of the epilepsies: Report of the Commission on Classification and Terminology: International League Against Epilepsy, 2009.
8. Ben-Menachem E, et al. Vagus Nerve-stimulation for treatment of partial seizures. 1. A controlled-study of effect on seizures: *Epilepsia*, 1994:616-26.
9. Handforth A, DeGiorgio CM, Schachter SC, Uthman BM, Naritoku DK, Tecoma ES, et al. Vagus nerve stimulation therapy for partial-onset seizures - A randomized active-control trial. *Neurology* 1998;51(1):48-55.
10. Lund C, et al. Efficacy and tolerability of long-term treatment with vagus nerve stimulation in adolescents and adults with refractory epilepsy and learning disabilities: *Seizure: Eur J Epilepsy*, 2010.
11. Ardesch JJ, Buschman HPJ, Wagener-Schimmel L, van der Aa HE, Hageman G. Vagus nerve stimulation for medically refractory epilepsy: A long-term follow-up study. *Seizure-European Journal of Epilepsy* 2007;16:579-85.
12. Uthman BM, Reichl AM, Dean JC, Eisenschenk S, Gilmore R, Reid S, et al. Effectiveness of vagus nerve stimulation in epilepsy patients - A 12-year observation. *Neurology* 2004;63(6):1124-26.

13. Elliott RE, Morsi A, Tanweer O, Grobelny B, Geller E, Carlson C, et al. Efficacy of vagus nerve stimulation over time: Review of 65 consecutive patients with treatment-resistant epilepsy treated with VNS > 10 years. *Epilepsy & Behavior* 2011;20(3):478-83.
14. Elliott R, et al. Vagus nerve stimulation in 436 consecutive patients with treatment-resistant epilepsy: Long-term outcomes and predictors of response: *Epilepsy and Behavior*, 2011:57-63.
15. Kuba R, Brazdil M, Kalina M, Prochazka T, Hovorka J, Nezadal T, et al. Vagus nerve stimulation: Longitudinal follow-up of patients treated for 5 years. *Seizure-European Journal of Epilepsy* 2009;18(4):269-74.
16. DeGiorgio CM, Thompson J, Lewis P, Arrambide S, Naritoku D, Handforth A, et al. Vagus Nerve Stimulation: Analysis of Device Parameters in 154 Patients during the Long-Term XE5 Study. *Epilepsia* 2001;42(8):1017-20.
17. George R, Salinsky M, Kuzniecky R, Rosenfeld W, Bergen D, Tarver WB, et al. Vagus nerve-stimulation for the treatment of partial seizures. 3. Long-term follow-up on first 67 patients exiting a controlled study. *Epilepsia* 1994;35(3):637-43.
18. Morris GL, Mueller WM, Vagus Nerve Stimulation Study G. Long-term treatment with vague nerve stimulation in patients with refractory epilepsy. *Neurology* 1999;53(8):1731-35.
19. Vonck K, Boon P, D'Have N, Vandekerckhove T, O'Connor S, de Reuck J. Long-term results of vagus nerve stimulation in refractory epilepsy. *Seizure-European Journal of Epilepsy* 1999;8(6):328-34.
20. Murphy JV. Left vagal nerve stimulation in children with medically refractory epilepsy. The Pediatric VNS Study Group. *J Pediatr* 1999;134(5):563-6.
21. Helmers SL, Wheless JW, Frost M, Gates J, Levisohn P, Tardo C, et al. Vagus nerve stimulation therapy in pediatric patients with refractory epilepsy: Retrospective study. *Journal of Child Neurology* 2001;16(11):843-48.
22. Spanaki MV, Allen LS, Mueller WM, Morris GL. Vagus nerve stimulation therapy: 5-year or greater outcome at a university-based epilepsy center. *Seizure-European Journal of Epilepsy* 2004;13(8):587-90.
23. Amar AP, Apuzzo MLJ, Liu CY. Vagus nerve stimulation therapy after failed cranial surgery for intractable epilepsy: Results from the vagus nerve stimulation therapy patient outcome registry (Reprinted from *Neurosurgery*, vol 55, pg 1086-1093, 2004). *Neurosurgery* 2008;62(2):506-12.
24. Labar D. Vagus nerve stimulation for 1 year in 269 patients on unchanged antiepileptic drugs. *Seizure-European Journal of Epilepsy* 2004;13(6):392-98.



**Author Contributions**

- 1
- 2 Jared Ching – Literature review, study design, data collection, data analysis, manuscript drafts and revisions
- 3
- 4 Sadaquate Khan – Study design, data collection, manuscript revisions
- 5
- 6 Paul White – Statistical analysis, manuscript revisions
- 7
- 8 Judith Reed – Study design, data collection
- 9
- 10 Devindra Ramnarine – Data collection, final manuscript revision
- 11
- 12 Kasia Sieradzan – Provided patient group, neurology input, manuscript revisions
- 13
- 14 David Sandeman – Conception of study, provided patient group, final manuscript revisions and appraisal
- 15
- 16
- 17
- 18
- 19
- 20
- 21
- 22
- 23
- 24
- 25
- 26
- 27
- 28
- 29
- 30
- 31
- 32
- 33
- 34
- 35
- 36
- 37
- 38
- 39
- 40
- 41
- 42
- 43
- 44
- 45
- 46
- 47
- 48
- 49
- 50
- 51
- 52
- 53
- 54
- 55
- 56
- 57
- 58
- 59
- 60

For Peer Review Only

## TABLES

**Table I:** Demographic parameters for the 101 patients included in this study.

Demographic parameter	Mean $\pm$ SD (Range) or Number (%)
<b>Sex</b>	M: 61 (61) F: 39 (39)
<b>Age (years)</b>	44.21 $\pm$ 12.46 (20-81)
<b>Age onset (years)</b>	5.10 $\pm$ 7.42 (Birth-36)
<b>Duration Epilepsy pre-VNS (years)</b>	28.00 $\pm$ 11.52 (7-59)
<b>Age at VNS insertion (years)</b>	35.80 $\pm$ 12.41 (17-75)
<b>Mean No. of seizure/month</b>	Baseline: 42.85 $\pm$ 58.58 (1-280) Post-VNS (at last follow up): 26.73 $\pm$ 55.10 (0-280)
<b>Mean No. of AEDs</b>	Trialed: 6.64 $\pm$ 2.81 (2-13) Baseline: 3.29 $\pm$ 1.02 (1-6) Post-VNS: 3.15 $\pm$ 1.42 (1-9)
<b>Previous intra-cranial surgery</b>	12 (12.00)

**Table II:** Aetiology of epilepsy identified from the 100 patients. LGS – Lennox Gastaut Syndrome, AVM – Arteriovenous malformation.

Cause	No. (n)	Cause	No. (n)
Unknown	67	Cortical migration disorder	2
Trauma	7	Vaccination	2
Tuberous sclerosis	5	Viral encephalitis	2
Cerebral Palsy	4	Tumour	2
Infection	3	AVM	2
LGS	3	Other	1

**Table III:** Mean seizure reduction at important time points in VNS treatment and One-Sample Test of the change in seizure frequency per month

Time	n.	Mean	SD	t	p.	95% Confidence Interval of the Difference	
						Lower	Upper
6 months	67	17.86	61.141	2.391	0.020	2.95	32.77
1 year	63	26.21	70.522	2.950	0.004	8.45	43.97
2 years	53	30.44	70.260	3.154	0.003	11.07	49.80
3 years	40	48.10	35.599	8.545	<0.001	36.71	59.48
4 years	32	49.44	43.682	6.402	<0.001	33.69	65.19
5 years	31	50.52	34.536	8.145	<0.001	37.86	63.19
6 years	31	45.85	37.568	6.795	<0.001	32.07	59.63
8 years	25	62.68	34.557	9.070	<0.001	48.42	76.95
10 years	9	76.41	24.409	9.392	<0.001	57.65	95.17
12 years	4	82.90	15.532	10.674	0.002	58.18	107.61

**Tables IV:** Age, age at admission and years of epilepsy pre-VNS, age at operation and number of years prior to VNS

implantation

	Responders (n=51)		Non-responders (n=49)		t	p
	Mean	SD	Mean	SD		
Age	44.04	11.76	43.78	14.273	0.094	0.925
Age at admission	36.21	11.35	38.32	14.817	-0.769	0.444
Years of epilepsy pre-VNS	27.34	10.92	29.69	13.129	-0.754	0.453

**Table V:** Correlation analysis (using Pearson's correlation coefficient) comparing age of onset of seizures, number of years of epilepsy pre-VNS, and number of AEDs prescribed pre- and post-VNS with mean changes in seizure frequency.

Time	Age at onset	Years of epilepsy pre-VNS	No. AEDS	
			Pre-VNS	Post-VNS
6 months	-.04	-.006	-.130	-.020
1 year	.158	-.132	-.016	-.240
2 years	.069	-.052	-.161	-.267
3 years	.360	-.300	-.072	-.025
4 years	.089	.152	-.160	.075
5 years	.194	-.248	-.012	-.134
6 years	.413*	.277	-.133	.185
8 years	.213	.219	.045	.339
10 years	.588	.186	-.513	.170
12 years	-.580	.848	-.771	.449

\*Statistically significant  $p < 0.05$ , \*\*Correlation is significant at the 0.01 level (2-tailed).

**Table VI:** Complications of VNS surgery and during vagal stimulation (VNS on) separated into minor and severe according to the complication being self-limiting or requiring removal or replacement, or being intolerable to the patient. Total indicated in bold.

Complications		Total (%)	Self-limiting (%)	Required revision or removal (%)
<b>Surgical</b>	Implant site discomfort	5 (4.00)	4 (4.00)	1 (1.00)
	Device migration	3 (3.00)	1 (1.00)	2 (2.00)
	Laryngeal palsy	3 (3.00)	1 (1.00)	0 (0.00)
	Lead damage	2 (2.00)	0 (0.00)	2 (2.00)
	Electrode wires visible on neck	2 (2.00)	2 (2.00)	0 (0.00)
	Dysphonia/vocal cord paralysis	2 (2.00)	1 (1.00)	1 (1.00)
	Dysphagia	1 (1.00)	1 (1.00)	0 (0.00)
	Neck swelling	1 (1.00)	1 (1.00)	0 (0.00)
	Horner's Syndrome	1 (1.00)	1 (1.00)	0 (0.00)
		<b>20 (20.00)</b>	<b>14 (14.00)</b>	<b>6 (6.00)</b>
<b>VNS on</b>	Cough	16 (16.00)	16 (16.00)	0 (0.00)
	Discomfort	8 (8.00)	8 (8.00)	0 (0.00)
	Hoarseness/vocal change	7 (7.00)	7 (7.00)	0 (0.00)
	Chest pain	3 (3.00)	2 (2.00)	1 (1.00)
	Jaw discomfort/pain	3 (3.00)	3 (3.00)	0 (0.00)
	Shortness of breath	2 (2.00)	2 (2.00)	0 (0.00)
	Nausea vomiting	2 (2.00)	2 (2.00)	0 (0.00)
	Choking	2 (2.00)	2 (2.00)	0 (0.00)
	Arm spasm (new)	2 (2.00)	2 (2.00)	0 (0.00)
	Tugging sensation	1 (1.00)	1 (1.00)	0 (0.00)
	Palpitations	1 (1.00)	1 (1.00)	0 (0.00)
	Sensation of lump	1 (1.00)	1 (1.00)	0 (0.00)
		<b>48 (48.00)</b>	<b>47 (47.00)</b>	<b>1 (1.00)</b>

**Table VII:** Last follow up device and magnet settings.

VNS settings	
<b>Generator</b>	Mean $\pm$ SD (Range)
Current	2.04 $\pm$ 0.66 (0.5-3.25)
Frequency	25.00 $\pm$ 4.5 (20-30)
Pulse Width	307.22 $\pm$ 142.96 (30-500)
On time	28.94 $\pm$ 6.95 (1.80-60)
Off time	3.95 $\pm$ 3.91 (1-30)
<b>Magnet</b>	
Output current	2.40 $\pm$ 0.59 (0.75-3.50)
Pulse width	403.85 $\pm$ 126.59 (250-500)
On time	60.00 $\pm$ 0.00 (60-60)

**Table VIII:** Related published studies to date in chronological order of publication.  $\geq 50\%$ ,  $\geq 75\%$ ,  $\geq 90\%$  and  $100\%$  indicate seizure reduction limits where percentages in the corresponding columns indicate the percentage of patients who benefited from that level of seizure reduction. DBRCT – Double blinded randomised controlled trial, Int – International (included Sweden, USA, and Germany), PO – Prospective observational, CZ – Czech Republic, RFU – Retrospective follow-up, ICS – Intracranial surgery (Group A had failed epilepsy surgery whereas group B had no history of cranial surgery). Table adapted.<sup>13 14</sup>

Year, Authors	Design	Patient's country	Sample size	Patient group	Treatment period	Mean seizure reduction	$\geq 50\%$	$\geq 75\%$	$\geq 90\%$	100%
1994, Ben-Menachem et al.(E03) <sup>8</sup>	DBRCT	Int	67	All	3.5	30.90%	38.70%	-	-	-
1995, George <sup>17</sup>	DBRCT	Int	114	All	3.5	24.50%	31%	-	-	-
1998, Handforth (E05) <sup>9</sup>	DBRCT	USA	198	All	3	38.00%	23.4%	10.6%	-	-
1999, Morris <sup>18</sup>	PO	USA	450	All	3	-	36.8%	-	-	-
1999, Vonck et al. <sup>19</sup>	PO	CZ	118	All	48	55%	51%	-	2.5%	-
1999, Murphy et al. <sup>20</sup>	Registry	USA	60	Children	18	23.00%	-	-	-	-
2000, DeGeorgio et al.(XE5) <sup>16</sup>	PO	USA	195	All	12	40%	35%	20%	-	-
2001, Helmers et al. <sup>21</sup>	RFU	USA	125	Children	6	-	52.60%	28.40%	-	2.10%
2004, Spanaki <sup>22</sup>	RFU	USA	26	All	60-84	-	28.46%	-	-	-
2004, Uthman et al. <sup>12</sup>	RFU	USA	48	All	144	48%	60%	42%	-	-
2004, Amars et al. (A) <sup>23</sup>	Registry	USA	921	ICS	24	-	55.10%	31.40%	17.30%	5.10%
2004, Amars et al. (B) <sup>23</sup>	Registry	USA	3822	Non-ICS	24	-	62.20%	43.70%	26.8%	8.30%
2004, Labar et al. <sup>24</sup>	Registry	USA	269	AED-controlled	12	58%~	-	-	-	-
2007, Ardesch et al. <sup>11</sup>	RFU	Netherlands	19	All	72	31.67%^	-	-	-	-
2009, Kuba et al. <sup>15</sup>	RFU	CZ	90	All	60	55.90%	48.90%	-	10.00%	5.50%
2011, Elliot et al. <sup>13</sup>	RFU	USA	65	All	>120	-	90.80%	58.50%	36.90%	15.40%
2011, Elliot et al. <sup>14</sup>	RFU	USA	436	All	132	59.20%	63.75%	40.50%	22.50%	8.25%
Present study	RFU	UK	100	All*	175§	49.04%¥	51.00%	26.00%	8.00%	3.00%

\*Some patients were implanted during childhood and subsequently had revision surgery as an adult under D.R.S.

~Median seizure reduction reported at 12 months.

^Calculated as an average from published results, not a figure calculated by authors.

§One patient was implanted with VNS in November 1995, remaining patients were implanted between September 1998 and July 2010.

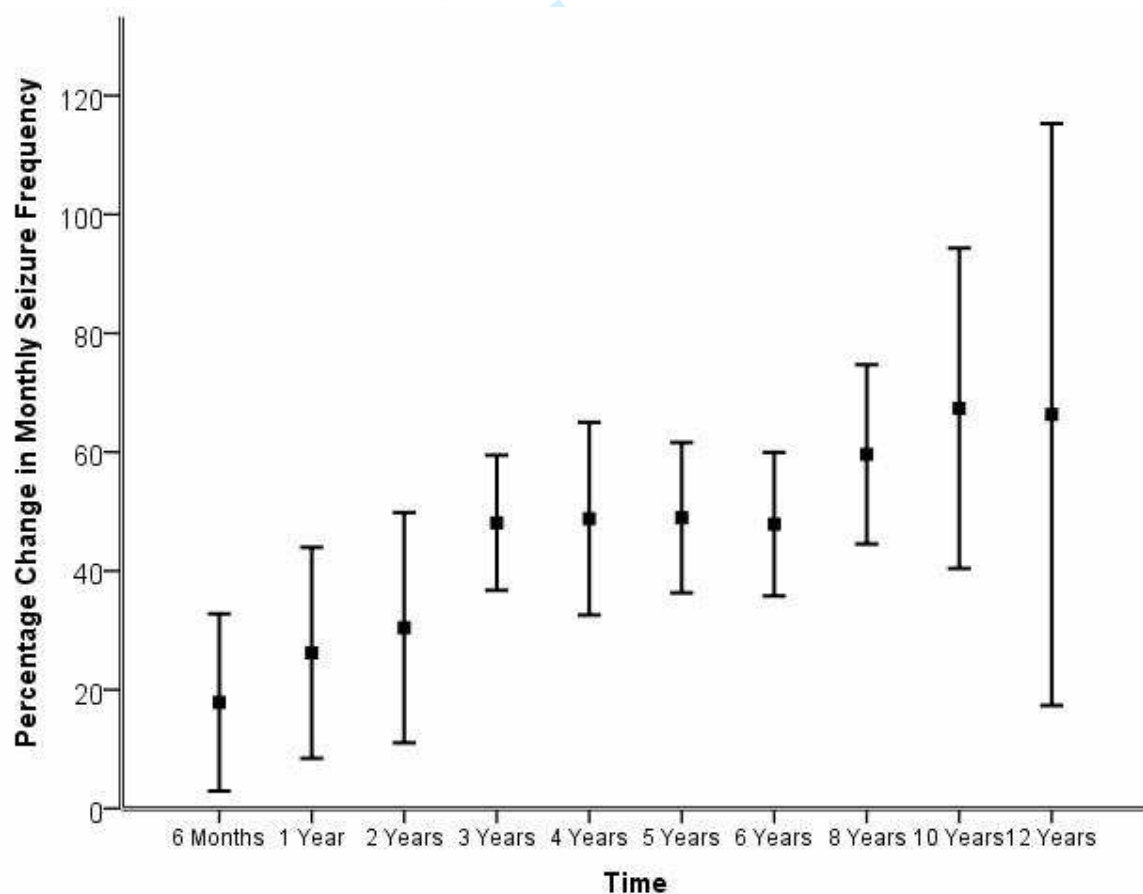
¥Mean seizure reduction of all time points (NB: mean seizure reduction at last follow-up in this study was 33.86%).

**Table IX:** A selection of long term follow-up studies compared to the present study. Seizure reduction from last visit carried forward included in this table from Uthman et al.<sup>12</sup>

Year, Authors	Mean seizure reduction (%)									
	6 months	1 year	2 years	3 years	4 years	5 years	6 years	8 years	10 years	12 years
2004 Uthman et al. <sup>12</sup>	22	26	28	25	-	30	-	-	49	52
2007, Ardesch et al. <sup>11</sup>	-	14	25	29	29	43	50	-	-	-
2011, Elliot et al. <sup>13</sup>	35.7	52.1	58.3	-	60.5	-	65.7	75.5	75.5	
Present study	17.86	26.2	30.43	48.1	49.44	50.52	45.85	62.8	76.41	82.9

## Figures

**Figure I:** Figure 3: 95% error bar chart showing mean reduction in seizure frequency over time with continued VNS.



1  
2  
3  
4  
5  
6  
7  
8  
9  
10  
11  
12  
13  
14  
15  
16  
17  
18  
19  
20  
21  
22  
23  
24  
25  
26  
27  
28  
29  
30  
31  
32  
33  
34  
35  
36  
37  
38  
39  
40  
41  
42  
43  
44  
45  
46  
47  
48  
49  
50  
51  
52  
53  
54  
55  
56  
57  
58  
59  
60

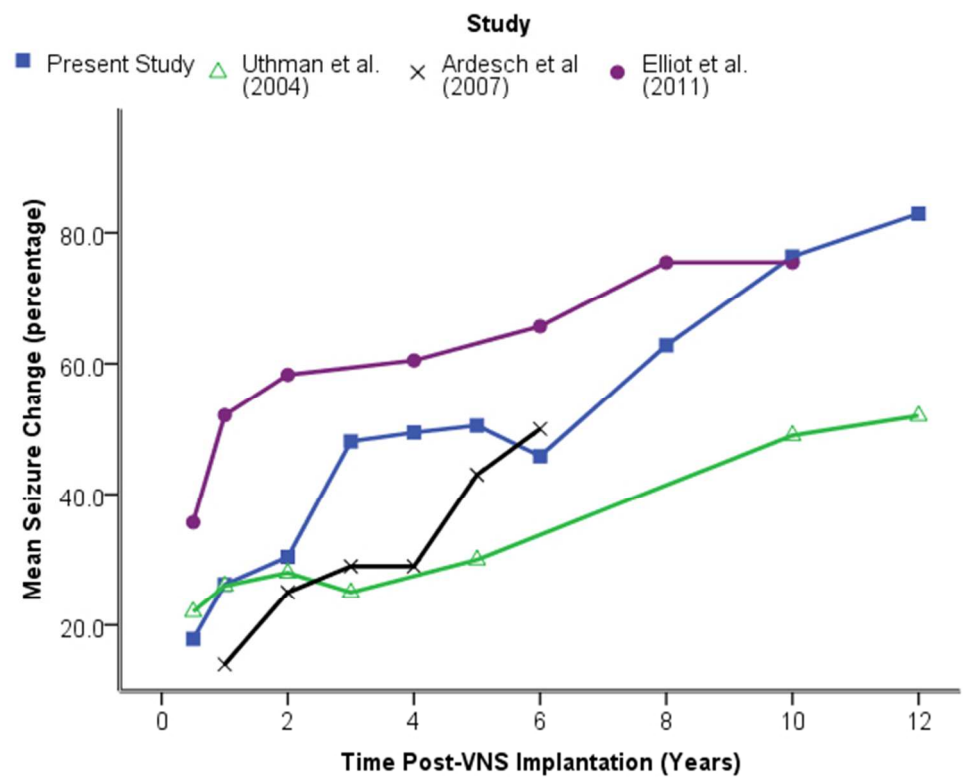


Figure II: Comparison of other long term studies  
220x176mm (72 x 72 DPI)

ew Only

# Variants of the *EAAT2* Glutamate Transporter Gene Promoter Are Associated with Cerebral Palsy in Preterm Infants

Shavanthi Rajatileka<sup>1</sup> · David Odd<sup>2,3</sup> · Matthew T. Robinson<sup>4</sup> · Alexandra C. Spittle<sup>5</sup> · Louis Dwomoh<sup>1</sup> · Maggie Williams<sup>6</sup> · David Harding<sup>7</sup> · Miles Wagstaff<sup>8</sup> · Marie Owen<sup>8</sup> · Charlene Crosby<sup>6</sup> · Jared Ching<sup>2</sup> · Elek Molnár<sup>5</sup> · Karen Luyt<sup>2,7</sup> · Anikó Váradi<sup>1</sup> 

Received: 8 July 2016 / Accepted: 16 February 2017 / Published online: 7 March 2017  
© The Author(s) 2017. This article is published with open access at Springerlink.com

**Abstract** Preterm delivery is associated with neurodevelopmental impairment caused by environmental and genetic factors. Dysfunction of the excitatory amino acid transporter 2 (*EAAT2*) and the resultant impaired glutamate uptake can lead to neurological disorders. In this study, we investigated the role of single nucleotide polymorphisms (SNPs; g.-200C>A and g.-181A>C) in the *EAAT2* promoter in susceptibility to brain injury and neurodisability in very preterm infants born at or before 32-week gestation. DNA isolated from newborns' dried blood spots were used for pyrosequencing to detect both SNPs. Association between *EAAT2* genotypes and cerebral palsy, cystic periventricular leukomalacia and a low developmental score was then assessed. The two SNPs were concordant in 89.4% of infants resulting in three common genotypes all carrying two C and two A alleles in different combinations. However, in 10.6% of cases, non-

concordance was found, generating six additional rare genotypes. The A alleles at both loci appeared to be detrimental and consequently, the risk of developing cerebral palsy increased four- and sixfold for each additional detrimental allele at -200 and -181 bp, respectively. The two SNPs altered the regulation of the *EAAT2* promoter activity and glutamate homeostasis. This study highlights the significance of glutamate in the pathogenesis of preterm brain injury and subsequent development of cerebral palsy and neurodevelopmental disabilities. Furthermore, the described *EAAT2* SNPs may be an early biomarker of vulnerability to neurodisability and may aid the development of targeted treatment strategies.

**Keywords** Brain injury · Cerebral palsy · Excitatory amino acid transporter 2 (*EAAT2*) · Glutamate · Glutamate transporter · Neurodevelopmental disorder · Periventricular

Shavanthi Rajatileka and David Odd are joint first authors.

EM, KL and AV contributed equally to this paper.

**Electronic supplementary material** The online version of this article (doi:10.1007/s12035-017-0462-1) contains supplementary material, which is available to authorized users.

✉ Anikó Váradi  
Aniko.Varadi@uwe.ac.uk

<sup>1</sup> Centre for Research in Biosciences, Department of Applied Sciences, Faculty of Health and Applied Sciences, University of the West of England, Bristol BS16 1QY, UK

<sup>2</sup> Neonatal Neuroscience, School of Clinical Sciences, University of Bristol, St Michael's Hospital, Southwell Street, Bristol BS2 8EG, UK

<sup>3</sup> Neonatal Intensive Care Unit, Southmead Hospital, North Bristol NHS Trust, Bristol BS10 5NB, UK

<sup>4</sup> College of Life & Environmental Sciences, University of Exeter, Stocker Road, Exeter EX4 4QD, UK

<sup>5</sup> Centre for Synaptic Plasticity, School of Physiology, Pharmacology and Neuroscience, University of Bristol, Biomedical Sciences Building, University Walk, Bristol BS8 1TD, UK

<sup>6</sup> Bristol Genetics Laboratory, Pathology Sciences, Blood Sciences and Bristol Genetics, Southmead Hospital, Bristol BS10 5NB, UK

<sup>7</sup> Regional Neonatal Intensive Care Unit, St Michael's Hospital, University Hospital NHS Trust, Bristol BS2 8EG, UK

<sup>8</sup> Neonatal Intensive Care Unit, Gloucestershire Royal Hospital, Gloucestershire NHS Trust, Gloucester GL1 3NN, UK



leukomalacia · Preterm infant · Promoter activity · Pyrosequencing · Single nucleotide polymorphism

## Introduction

Progress in perinatal care over the last three decades has led to greater survival rates in infants born prematurely [1, 2]. The incidence of premature birth in developed countries varies from 7.6–12% of all births [3]. While 90% of very preterm infants (below 32-week gestation) now survive beyond the postpartum period, ~35% have neurodisabilities [4]. These disabilities include cerebral palsy, cognitive- and behavioural problems [5]. The estimated cost of preterm birth throughout childhood in England and Wales with a birth rate of 700,000/year is around £3 billion per annum [6]. Susceptibility of a preterm infant to neurodisability is difficult to predict, shows considerable variation between individuals [7] and is likely to be modulated by genetic factors [8]. Better diagnostic approaches for the early identification of infants with higher risk of neurodisability are important to facilitate the development and application of appropriate treatment strategies.

Much of the neurodisability seen in very preterm infants is caused by white matter injury, known as periventricular leukomalacia (PVL) and the subsequent disruption of normal neural connectivity [9]. While the pathogenesis of PVL remains to be established, *in vitro* and *in vivo* animal studies have identified important roles for oxidative stress, cytokine-mediated injury and glutamate-induced excitotoxicity [10, 11]. Following hypoxia-ischaemia, the excitatory neurotransmitter glutamate is released into the extracellular space, causing over-activation of ionotropic glutamate receptors present in pre-myelinating oligodendrocytes [12], which induces their excitotoxic cell death and subsequent white matter lesions [10].

In the brain, neuronal and glial excitatory amino acid transporters (EAATs) play a key role in maintaining extracellular glutamate below neurotoxic levels. The activity of the predominantly astroglial high-affinity glutamate transporter EAAT2 (also known as solute carrier family 1 member 2-*SLC1A2* or the rodent ortholog glutamate transporter 1-*GLT-1*) is responsible for 90% of total glutamate uptake [13, 14]. Furthermore, EAAT2 has been implicated in the pathology of cerebral ischemia [15]. While ischaemic brain injury was exacerbated in transgenic mice lacking the EAAT2 protein in the brain [16], upregulation of EAAT2 provides neuroprotection [15]. EAAT2 is widely expressed in the white matter of the developing human brain [17] and upregulated in reactive astrocytes in post-mortem brain tissue of preterm infants with PVL, which may indicate a response to either hypoxic-ischemic injury or inflammation [18]. Collectively, these findings suggest that dysregulated EAAT2 activity may contribute to white matter damage.

A functional single nucleotide polymorphism (SNP) in the promoter region of the *EAAT2* gene has been associated with higher serum glutamate levels in adults and consequently a worse neurological outcome after stroke [19] and also with relapsing multiple sclerosis [20]. These studies raised the intriguing possibility that similar genetic differences may enhance predisposition to neurodevelopmental impairment after preterm birth. The aim of this study was to establish the role of two closely linked functional SNPs in the *EAAT2* gene promoter [19, 21] in susceptibility to brain injury and neurodisability in very preterm infants.

## Materials and Methods

### Patient Selection

The risk of CP in infants born <33 weeks of gestation is 30 times higher than among those born at term [22]. Therefore, our study included infants born at this vulnerable period. Newborns' dried blood spots and clinical data were obtained from all infants born ≤32 weeks of gestation and survived to discharge in the South West of England recruited to the Avon Premature Infant Project (APIP; 1990–1993, *n* = 329 [23]) or received care within the neonatal unit of Gloucestershire Royal Hospital (2002–2008; *n* = 127); Southmead Hospital, North Bristol NHS Trust (2005–2010; *n* = 169) or St Michael's Hospital, University Hospitals Bristol NHS Trust (2002–2008; *n* = 196). Infants with major congenital anomalies of the central nervous system and genetic syndromes that may cause neurodevelopmental impairment or cerebral palsy were excluded. The archived blood spots were fully anonymised according to the Human Tissue Act and Medical Research Council (UK) Guidance and used for research without individual informed consent as permitted by the UK newborn screening programme Code of Practice for the retention and Storage of Residual Spots (April 2005, ISBN 0955013801). From the total (*n* = 821 infants), 208 blood spots were not traceable, 1 was excluded with a chromosomal abnormality, ten DNA samples failed all pyrosequencing assays and 61 infants had no outcome data, leaving a total of 541 infants for the analyses (Table 1).

### Sample Collection and DNA Isolation

Blood was collected from heel prick blood sampling on blood spot screening cards prepared routinely within 5–8 days of birth as part of the UK Newborn Screening Programme [<http://newbornbloodspot.screening.nhs.uk>]. DNA was isolated as described previously [24].

**Table 1** Birth-related information and neurodevelopmental outcomes ( $n = 541$ ). Values are numbers with % or means  $\pm$  standard deviation, as appropriate. All measures were analysed independently so denominator may vary

Measure	Avon Premature Infant Project (APIP; $n = 228$ )	Gloucestershire Royal Hospital ( $n = 90$ )	Southmead Hospital ( $n = 81$ )	St Michael's Hospital ( $n = 142$ )
Gestational age (week)	29.9 ( $\pm 2.0$ )	27.8 ( $\pm 2.2$ )	26.8 ( $\pm 1.8$ )	27.4 ( $\pm 1.7$ )
Birth weight (g)	1435 ( $\pm 384$ )	1130 ( $\pm 347$ )	916 ( $\pm 278$ )	992 ( $\pm 404$ )
Male	131 (57.5%)	44 (49.4%)	42 (52.5%)	69 (50.4%)
Multiple birth	48 (21.1%)	27 (30.0%)	29 (36.3%)	35 (25.6%)
White ethnicity	209 (92.1%)	80 (90.9%)	–	44 (81.5%)
Apgar score				
1 min	6.3 ( $\pm 2.2$ )	6.2 ( $\pm 2.1$ )	5.7 ( $\pm 2.1$ )	6.3 ( $\pm 2.1$ )
5 min	8.5 ( $\pm 1.6$ )	8.4 ( $\pm 1.5$ )	7.6 ( $\pm 2.1$ )	8.4 ( $\pm 1.4$ )
Cerebral palsy	19 (8.3%)	12 (14.0%)	–	10 (8.4%)
Cystic PVL	18 (8.1%)	6 (6.9%)	7 (8.6%)	6 (4.4%)
Low developmental score	16 (8.0%)	9 (10.2%)	–	17 (16.4%)

### Generation of Biotinylated PCR Products for Pyrosequencing

Two sequence-specific primers (EAAT2PyroF-BIO and EAAT2PyroR; Table 2) were designed to amplify a 166 bp region of the *EAAT2* promoter which included the two SNPs rs111885243:C>A or g.-200C>A (at positions -200 bp) and rs4354668:a>c or g.-181A>C (at position -181 bp) using the software provided by Qiagen Pyrosequencing. The 5' end of the forward primer was modified with biotin. PCR reactions contained 4–6 ng of genomic DNA, 1 $\times$  PCR buffer (100 mM Tris-HCl, 500 mM KCl pH 8.3), 1.5 mM MgCl<sub>2</sub>, 200  $\mu$ M of each dNTP, 100 pmol of each oligonucleotide and 1 unit of high-fidelity Taq polymerase (FastStart High Fidelity Taq Polymerase, Roche Diagnostics Limited, West Sussex, UK) per reaction. Amplification was performed as follows: 95 °C for 5 min, 50 cycles of 94 °C for 30 s, 60 °C for 30 s, 72 °C for 30 s and final extension 72 °C for 10 min. Two additional

SNPs, rs116392274 in *EAAT2* and rs1835740 [21], which are involved in glutamate homeostasis, were also analysed in the cohort and data are shown as [Supplementary materials](#).

### Pyrosequencing and Sanger Sequencing

All steps were carried out as previously described (Table 2) [21, 24]. Genotypes of randomly selected samples ( $n = 51$ ) from pyrosequencing were confirmed by Sanger sequencing (using ABI 3730x1 96 capillary DNA Analyzers) at Eurofins MWG Operon (Ebesberg, Germany).

### Primary Astrocyte Cultures and Preparation of the *EAAT2* Promoter Constructs

Primary rat astrocytes were separated from mixed glial cultures of embryonic (E20) Sprague-Dawley rat brains (Harlan, UK) using the previously described selective detachment

**Table 2** Pyrosequencing primers and reaction conditions used in the study

Oligonucleotide	Sequence 5'-3'	Product (bp)	Annealing T (°C)	Modifications
EAAT2PyroF-BIO	GGGGCTAAACCTTGCAATC	166	60	5' Biotin
EAAT2PyroR	GAGTGGCGGGAGCAGAGA			None
EAAT2PyroSeq	GGGTGTGTGCGCGCC	N/A		None
Target sequence for pyrosequencing		<b>T</b> /GGGGAGGCGGTGGAGGCCG/TCTG		
Nucleotide dispensation order		<u>CGTG</u> <u>C</u> AGCGTGAGCGT <u>G</u> C		

Primer pair EAAT2PyroF-BIO/EAAT2PyroR were used to generate biotinylated PCR products flanking SNPs g.-200C>A and g.-181A>C. Primer EAAT2PyroSeq was used for pyrosequencing. The target sequence and the order of nucleotide dispensation for the pyrosequencing assay are listed. In the dispensation order the nucleotides used as negative controls are underlined. In optimal pyrosequencing conditions, these nucleotides are not incorporated into the target DNA sequence and therefore their addition do not generate peaks on the pyrogram (Fig. 1). The nucleotide change in the target sequence for pyrosequencing is indicated in bold

N/A not available

(shaking) method [25]. Following separation at day 10 in vitro, astrocytes were maintained in T75 cell culture flasks (Corning Incorporated, New York, USA) at 37 °C in a humidified 5% CO<sub>2</sub>: 95% air atmosphere. Cells were cultured in Dulbecco's modified Eagle's medium (Sigma Aldrich, MO, USA) containing 4.5 g/l glucose, 29 mM sodium bicarbonate, 50 U/ml penicillin, 50 µg/ml streptomycin (Sigma Aldrich, MO, USA) and 10% (v/v) foetal bovine serum (Life Technologies Ltd., Paisley, UK). Glial fibrillary acidic protein immuno-labelling and trypan blue staining [26, 27] were used to confirm the purity and viability of the astrocyte cultures. Previously described oligonucleotides were used to amplify a 773 bp fragment of the *EAAT2* promoter [19]. Genomic DNA of genotype 1 and genotype 3 was amplified in 25 µl reactions containing 2 µl genomic DNA, 1X High Fidelity PCR buffer (100 mM Tris-HCl, 500 mM KCl pH 8.3), 1.5 mM MgCl<sub>2</sub>, 200 µM of each dNTP, 100 pmol of each oligonucleotide and 1 unit of high-fidelity Taq polymerase (FastStart High Fidelity Taq Polymerase, Roche Diagnostics Limited, West Sussex, UK). Amplification was performed as follows: 1 cycle at 95 °C for 5 min, 35 cycles of 94 °C for 30 s, 65 °C for 30 s, 72 °C for 1 min and final extension at 72 °C for 10 min. Following enzyme digestion and fragment purification, the promoter fragment was inserted upstream of the firefly luciferase reporter in the pGL3-basic luciferase reporter vector.

### Transfection of Astrocytes and Luciferase Reporter Gene Assay

Cells were seeded at a density of  $1 \times 10^5$  per well in 1 ml of complete growth medium in a 12 well plate (Corning Incorporated, New York, USA) 24 h prior to transfection. At >80% confluency, the cells were transfected using 1 µg of *EAAT2* promoter construct (EAAT2PrWT -200 bp C/C -181 bp A/A or EAAT2PrMT -200 bp A/A -181 bp C/C) and 10 µl of TransIT®-Neural Transfection Reagent (Mirus Bio, Madison, WI 5371, USA) in Opti-MEM® I Reduced Serum

Media (Life Technologies Ltd., Paisley, UK). One hundred nanograms of pRL-thymidine kinase plasmid (Promega, WI, USA) containing the *Renilla* luciferase gene was co-transfected with each construct and used as an internal control. Forty-eight-hour post-transfection, the cells were washed and harvested for the promoter activity assay. All transfections were carried out in triplicates and all experiments were repeated three times. *EAAT2* promoter activity was determined using the Dual-Luciferase Reporter (DLR) Assay System (Promega, WI, USA) following the manufacturer's guidelines.

### Patient Outcome Measures

The primary outcome measure was the diagnosis of cerebral palsy. Cerebral palsy was diagnosed when a disorder of movement and posture causing activity limitation were present at clinical examination performed at 2 years of age [28]. The secondary outcome measures were (i) cystic PVL diagnosed on a cerebral ultrasound scan during the neonatal stay and (ii) a low developmental score using standardised developmental assessment tools at 2 years of age. Cerebral ultrasound scans were performed as part of routine clinical monitoring by the clinicians in all four groups of infants. Cystic PVL was diagnosed as standard [29] (i.e. when any cystic changes were visible in the periventricular white matter on ultrasound).

Standardised developmental assessment data was available for three of the four infant groups (Table 3). The Griffith Mental Developmental Scale [30] was used for the APIP and the Gloucestershire Royal Hospital group, while the Bayley Scales of Infant Development (BSID) score (initially version II to 2006, version III after 2006 to-date) [31, 32] for the St Michael's Hospital group. BSID-II is divided into two subscales (i) cognitive (Mental Developmental Index; MDI) and (ii) motor (Psychomotor Developmental Index; PDI). The updated BSID-III has three subscales: cognitive, language and motor PDI. Infants falling in the lowest 10th centile for either the main score (Griffith) or any of the subscales (BSID) in

**Table 3** Summary neurodevelopmental scores and standardised assessment used. Results are median (interquartile range-IQR). The standardised neurodevelopmental assessment scales used were: Griffith Mental Developmental Scale [30], Bayley Scales of infant development 2nd edition (BSID-II) [31] and 3rd edition (BSID-III) [32]. (For details, see the "Materials and Methods" section)

Developmental assessment used	Median (IQR)	'Low developmental score'—10th percentile cut-off
APIP		
Griffith Mental Developmental Scale	96 (90–105)	<82
Gloucestershire Royal Hospital		
Griffith Mental Developmental Scale	101 (90–111)	<64
St Michael's Hospital		
BSID-II-Mental Developmental Index	94 (70–108)	<51
BSID-II-Psychomotor Developmental Index	87 (71–100)	<53
BSID-III-Cognitive Developmental Index	100 (85–110)	<76
BSID-III-Language Developmental Index	96 (85–103)	<76
BSID-III-Psychomotor Developmental Index	96 (89–107)	<84

each infant group were defined a priori as having a low developmental score. Birth weight, gestational age at birth and physiological condition during the first 5 min after birth (Apgar scores at 1 and 5 min) were considered a priori possible confounders.

### Statistical Analysis

Initially, the perinatal/intrapartum characteristics (gestation, birth weight, gender, multiple births, ethnicity and Apgar score) of the population were assessed, split by their genotype. Then, univariable associations were assessed, between the two *EAAT2* genotypes and the primary and secondary outcome measures (see previous section). Due to the data coming from multiple infant groups with different developmental tools, multi-level logistic regression models were derived using the Stata 10 (Stata Corp, TX, USA) “xtlogit” command, to investigate the association of the odds of each additional polymorphic allele and the outcome measures. Adjustment for possible confounders was performed by adding the perinatal/intrapartum variables described above to the logistic regression models as continuous variables. Two sensitivity analyses were performed: (i) the analysis was repeated using single-level (rather than multi-level) modelling, and (ii) the missing covariates were imputed to allow the adjusted analysis to

contain the same number of individuals as the unadjusted. Genotypes or outcome data was not imputed. Imputation was performed using multiple imputation with chained equations [33]. Details of imputation technique are available on request. All analyses were conducted with Stata 10 (Stata Corp, TX, USA) or Excel (Microsoft Corp, WA, US). All data are presented as odds ratio (OR) (95% confidence interval (CI)), mean (SD) or number (percent (%)).

### Results

#### Simultaneous Pyrosequencing of Two SNPs in the *EAAT2* Promoter

A functional SNP was reported previously in the *EAAT2* promoter at -181 bp (rs4354668) [19]. Our detailed investigation of the *EAAT2* promoter using Sanger sequencing revealed another SNP, 19 bp upstream of rs4354668, at position -200 bp (rs111885243) [21]. These two SNPs cannot be distinguished by single-strand conformational polymorphism used in the previous study [19]; therefore, a pyrosequencing assay was developed (Fig. 1). All traceable blood spots were analysed ( $n = 613$ ) by pyrosequencing and 521 produced clear pyrograms. Ten percent of these samples ( $n = 51$ ) were

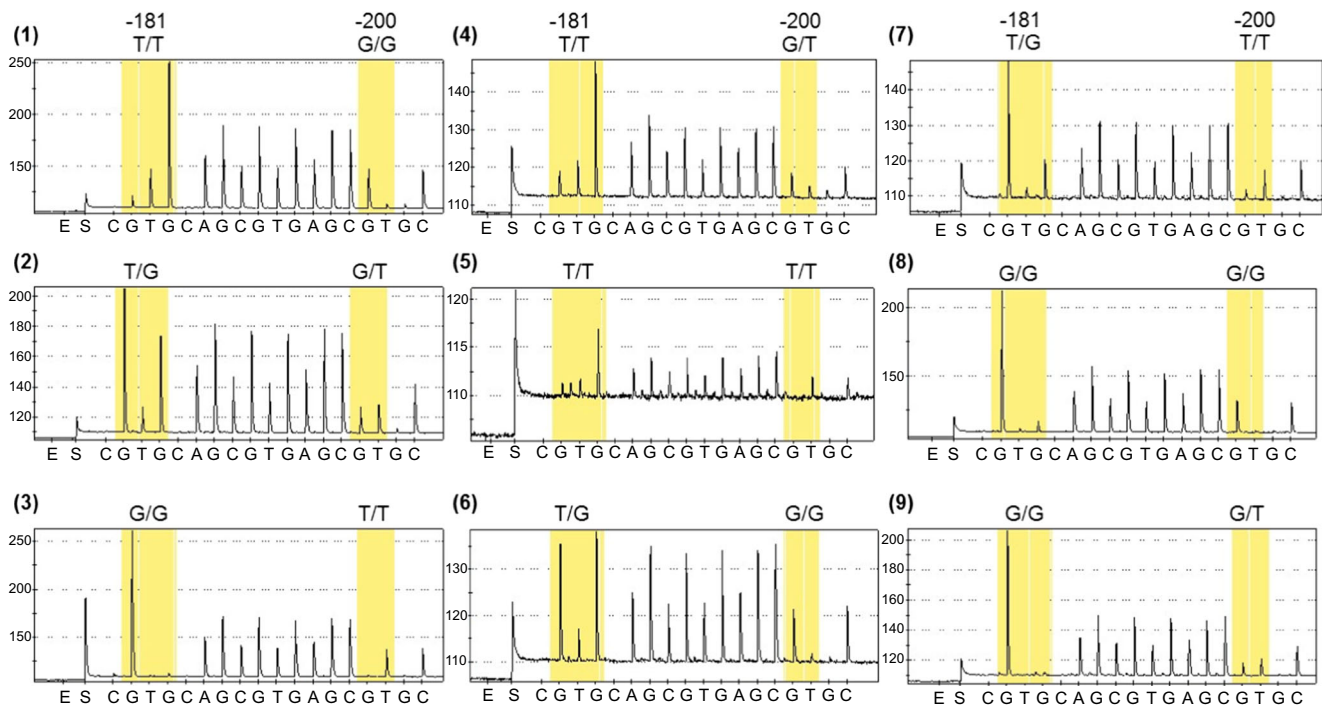


**Fig. 1** Pyrograms of the *EAAT2* promoter SNPs. The position of the SNPs is highlighted in yellow boxes, the *x*-axis of each pyrogram indicates the order of reagent addition (E-enzyme, S-substrate and nucleotide A, G, T or C); the *y*-axis shows the light intensity generated. The numbering of pyrograms corresponds to the genotype numbers in

Table 2. Due to the high GC content of the target sequence and the four C repeats before the SNP at position -181 bp, the pyrosequencing was carried out on the reverse strand. Thus, note that the sequence is in reverse orientation

sequenced and the concordance with pyrosequencing was 100%. In total, 471 of the infants had clinical outcome available for the analysis of rs4354668 and rs4354668.

### Distribution of Different Alleles in the Study Population

Nine genotype combinations were identified (Table 4 and Fig. 1). In 419 samples (88.9%), the two SNPs were in linkage disequilibrium ( $p < 0.001$ ). Linkage disequilibrium was not complete and hence the nine different genotypes (Table 4). The majority of alleles demonstrated high levels of concordance, such that if the -200 locus was homozygous (C/C or A/A), the -181 locus was also homozygous (A/A or C/C) and if -200 locus was heterozygous, the -181 locus was heterozygous as well (Table 4; genotypes 1–3). In the rarer genotypes (11.0% of the cases, Table 4; genotypes 4–9), the alleles were non-concordant between the two polymorphic loci. We investigated rs116392274 (g.-168C>T) in the *EAAT2* promoter in the cohort but apart from one infant, who was a heterozygote, all others carried C/C alleles. Allele distribution of rs1835740 is shown in Supplementary materials.

### EAAT2 Promoter Activity

To analyse the functional effects of the -200 C>A; -181A>C SNPs on transcriptional activity in vitro, genotype 1 (-200 C/C; -181 A/A) or genotype 3 (-200 A/A; -181 C/C) reporter constructs were transiently transfected into primary astrocytes, together with the pRL-TK vector as an internal control that constitutively expresses the *Renilla* luciferase. The genotype 1 promoter construct displayed between 4- and 4.7-fold greater activity compared with the genotype 3 construct ( $p < 0.0015$ ; Fig. 2).

Several attempts were made to measure the promoter activity of genotypes 5 and 8 using initially the three clinical

**Table 4** Distribution of genotypes in the sample cohort. Genotypes were identified by pyrosequencing and confirmed by Sanger sequencing ( $n = 51$ )

Genotype	Genotype	-200C>A	-181A>C	Number and proportion
1	C/C	A/A		95 (20.2%)
2	C/A	A/C		261 (55.4%)
3	A/A	C/C		63 (13.4%)
4	C/A	A/A		9 (1.9%)
5	A/A	A/A		2 (0.4%)
6	C/C	A/C		19 (4.0%)
7	A/A	A/C		8 (1.7%)
8	C/C	C/C		1 (0.2%)
9	C/A	C/C		13 (2.8%)
Allele frequency		C = 0.56 A = 0.44	A = 0.53 C = 0.47	$n = 471$

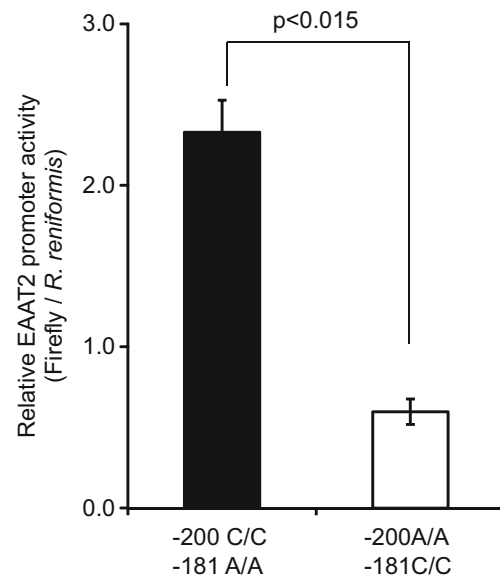


**Fig. 2** Promoter activity of *EAAT2*. Astrocytes were transiently transfected with sequences corresponding to genotype 1 (-200 C/C; -181 A/A) and 3 (-200 A/A; -181 C/C) reporter constructs. Firefly and *R. reniformis* luciferase activities were measured as detailed in the “Materials and Methods” section and the relative firefly/*Renilla* luciferase values are shown. Bars represent relative luciferase values from three independent experiments with standard deviation

samples that carried these genotypes (Table 4). These blood samples were 15–20 years old and the isolated gDNA and the resulting PCR products were of insufficient quality [24] for successful ligation to produce the required promoter constructs. In an alternative approach, we attempted to generate these variants using site directed mutagenesis of genotypes 1 and 3. However, due to the very high GC content of the promoter amplicon (over 70%; [34]), no correct mutants were obtained.

### Characteristics of the Cohort

The intrapartum/perinatal characteristics of the eligible infants split by groups or genotypes are shown in Tables 1 and 5. Importantly, the patient outcome measures (e.g.: the rate of cerebral palsy ( $p = 0.284$ ), cystic PVL ( $p = 0.553$ ) and low developmental scores ( $p = 0.084$ )) did not differ between the four groups investigated (Table 1) and thus were combined for subsequent analysis. An association between ethnicity and genotype was observed ( $p < 0.001$ ) when the whole cohort was investigated (Table 5). To better understand the nature of the association between ethnicity and the two SNPs, the cohort was investigated in more details. While there was no difference in the individual frequencies at the two SNPs by ethnicity (-181,  $p = 0.206$  and -200,  $p = 0.854$ ), white infants were more likely to show the concordance discussed above than non-white infants (94.6 vs. 76.1%,  $p < 0.001$ ). Data on ethnicity was available for three of the four infant groups (Table 1) and within this population of preterm infants, there

**Table 5** Intrapartum/perinatal characteristics of the cohort

Perinatal measure	<i>n</i>	-200C>A			-181A>C			<i>p</i>
		CC	AC	AA	AA	AC	CC	
Gestation (week)	466	28.5 (±2.3)	28.4 (±2.4)	29.0 (±2.3)	28.6 (±2.4)	28.4 (±2.3)	28.7 (±2.5)	0.673
Birth weight (g)	466	1217 (±402)	1182 (±437)	1267 (±466)	1218 (±403)	1185 (±438)	1254 (±462)	0.690
Male	465	63 (56.8%)	147 (52.7%)	40 (54.8%)	59 (56.2%)	149 (52.7%)	42 (54.6%)	0.525
Multiple birth	466	28 (24.6%)	68 (24.4%)	22 (30.1%)	24 (22.9%)	75 (26.4%)	19 (24.7%)	0.268
White ethnicity	333	78 (91.8%)	183 (90.2%)	40 (88.9%)	77 (93.9%)	180 (90.5%)	44 (84.6%)	<0.001
Apgar score								
1 min	452	6.1 (±1.9)	6.3 (±2.2)	6.1 (±2.1)	6.1 (±2.0)	6.3 (±2.1)	6.0 (±2.2)	0.526
5 min	451	8.3 (±1.5)	8.3 (±1.7)	8.3 (±1.6)	8.3 (±1.5)	8.4 (±1.6)	8.2 (±1.7)	0.769

*n*-number of infants with data available. Values are numbers with % or means ± standard deviation, as appropriate

was strong evidence of deviation from the Hardy-Weinberg equilibrium ( $p < 0.001$ ).

### Outcome Measures

In the univariable analyses (in which associations were assessed between each of the *EAAT2* SNP and the primary and secondary outcome measures independently), there was no clear evidence for an association between different alleles with cerebral palsy, cystic PVL or a low developmental score (Table 6). However, when adding both polymorphisms into the multivariable analysis, the presence of A alleles at -181 and -200 bp appeared to increase the likelihood of a low developmental score with OR of 4.56(1.53–13.60) and 3.73(1.29–10.80), respectively (Table 7; unadjusted (1)). This association persisted in the analysis adjusted for gestation, birth weight, gender and physiological condition at birth (Table 7; adjusted (2)). In contrast, there was less evidence for any association between either allele and cerebral palsy or cystic PVL. Due to the association seen with ethnicity (Table 5), this covariate was added to the model in a final adjusted analysis (Table 7; adjusted (3)). In this final model,

the association with cerebral palsy strengthened with each additional A allele (locus -200 bp OR 4.34 (1.12–16.77) and locus -181 bp OR 6.64(1.76–25.07)), although there was less evidence that the polymorphism at locus -200 bp remained associated with an increased risk of a low developmental score (OR 2.84 (0.71–11.44)). Repeating the analysis using a model where the missing covariate data was imputed, the results were compatible with the main analysis. The single infant who was a heterozygote for rs116392274 had no CP or a low developmental score. Similarly, no association was observed between rs1835740 and CP or a low developmental score (Supplementary Materials).

### Discussion

#### SNPs in *EAAT2* Promoter Are Associated with Neurodevelopmental Impairment After Preterm Birth

To our knowledge, this is the first study that demonstrates association between genetic variants of *EAAT2* involved in

**Table 6** Univariable associations between genotype and outcome measures

Outcome measure	<i>n</i>	Homozygote	Heterozygote	Homozygote	<i>p</i>
-200C>A		CC	AC	AA	
Cerebral palsy <sup>a</sup>	385	9 (9.6%)	23 (9.7%)	3 (5.6%)	0.621
Cystic PVL	458	7 (6.3%)	21 (7.6%)	3 (4.2%)	0.566
Low developmental score <sup>a</sup>	349	7 (7.7%)	26 (12.4%)	3 (6.3%)	0.286
-181A>C		AA	AC	CC	
Cerebral palsy <sup>a</sup>	385	10 (11.4%)	23 (9.5%)	2 (3.9%)	0.263
Cystic PVL	458	7 (6.7%)	20 (7.3%)	4 (5.2%)	0.817
Low developmental score <sup>a</sup>	349	11 (12.9%)	22 (10.3%)	3 (5.9%)	0.424

*n*-number of infants with data available. Values are numbers with %

<sup>a</sup> Cerebral palsy and low developmental score data were only available from three cohorts (for details, see Table 1)

maintaining glutamate homeostasis and neurodevelopmental impairment in very preterm infants. We identified that SNP g.-200C>A in the *EAAT2* promoter is strongly linked to the previously described functional SNP g.-181A>C [19], which has not been reported in earlier studies [19, 20, 35]. The A alleles at both loci appear to increase the risk of cerebral palsy and low developmental scores (Table 7). In the common concordant inheritance pattern (Table 4, genotypes 1–3), the protective C and detrimental A alleles are usually inherited together whereas in the rare non-concordant genotypes, only detrimental alleles (Tables 4 and 8, genotypes 4/5/7) or just protective alleles (Tables 4 and 8, genotypes 6/8/9) were found at both loci. This concordance was more likely with white ethnicity. Due to the strong linkage between the two SNPs, it was appropriate to enter both into the multi-level regression analysis to assess the impact of increasing detrimental A alleles. In the multi-level regression analysis (Table 7), adjustment for gestation, birth weight, gender, multiple births and Apgar scores made no significant difference to the odds of any of the outcome measures. However, the addition of ethnicity into the regression analysis strengthened the effect seen on cerebral palsy at both loci. In addition, the odds of a low developmental score were also significantly increased with each A allele at -181 bp. To put this in context, for each additional A allele at -181 or -200, the odds of cerebral palsy increased by about four- and sixfold and the odds of a low developmental score increased fourfold. The prevalence of cerebral palsy or a low developmental score was as high as 28 and 44% for genotypes 7 and 4 with three detrimental alleles, respectively (Table 8). In contrast, no association was observed between rs116392274 or rs1835740 and CP or a low developmental score in the cohort indicating that these SNPs are unlikely to play important roles in the injury of the developing brain (Supplementary materials).

## Regulation of *EAAT2* Promoter Activity

These two SNPs significantly affect *EAAT2* promoter activity in vitro. The promoter fragment -742/+31 [19] containing -200A/A -181C/C sequence (genotype 3) showed a 70–80% reduction in basal *EAAT2* promoter activity compared to -200C/C -181A/A (genotype 1; Fig. 2). This is a larger impact than the previously reported ~30% reduction [19]; however, in that study, the SNP at position -200 bp was not identified and it is not clear which nucleotide was present in their promoter construct. The change from A to C at -181 bp abolishes the binding site for transcription factor AP-2 (activating enhancer binding protein 2) and creates a site for GC-binding factor 2 (GCF2) which represses *EAAT2* expression (Fig. 3; [19]). Reduced *EAAT2* expression alters extracellular glutamate levels [13]. Despite the large difference in *EAAT2* promoter activity between genotypes 3 and 1, there was no clear association with low developmental score or cerebral palsy in any of the main three genotypes (Table 8; genotypes 1–3). Similar observations were made in patients with multiple sclerosis [20] and migraine [36] where the allele and genotype frequencies for the *EAAT2* promoter polymorphism were similar in patients and controls. However, the polymorphism at -181 bp was associated with higher plasma glutamate concentrations during relapsing multiple sclerosis [20].

Gene expression in the nervous system is not only controlled by the transcriptional machinery, but it is also subject to modulation by epigenetic mechanisms such as DNA methylation [36, 37]. Dynamic DNA methylation is observed during brain development [38, 39] and the levels of DNA methylation are increased upon ischemic injury [40]. Recent studies revealed that the basal transcriptional activity of the *EAAT2* gene is controlled by DNA methylation of cytosine residues in the region of -1010 to -1 bp of the *EAAT2* promoter [41, 42]. Hypermethylation of the

**Table 7** Multi-level regression analysis for presence of each increasing -200 or -181 A allele and outcomes

Outcome measure	Unadjusted (1)			Adjusted (2)			Adjusted (3)		
	<i>n</i>	OR (95% CI)	<i>p</i>	<i>n</i>	OR (95% CI)	<i>p</i>	<i>n</i>	OR (95% CI)	<i>p</i>
<b>-200C&gt;A</b>									
Cerebral palsy	385	1.70 (0.62–4.66)	0.299	365	1.68 (0.57–4.94)	0.346	314	4.34 (1.12–16.77)	0.033
Cystic PVL	458	0.88 (0.30–2.58)	0.812	444	0.82 (0.26–2.60)	0.740	317	0.68 (0.13–3.50)	0.641
Low developmental score	349	3.73 (1.29–10.80)	0.015	329	3.23 (1.04–10.02)	0.042	282	2.84 (0.71–11.44)	0.142
<b>-181A&gt;C</b>									
Cerebral palsy	385	2.44 (0.87–6.79)	0.089	365	2.72 (0.90–8.22)	0.083	314	6.64 (1.76–25.07)	0.005
Cystic PVL	458	1.00 (0.32–3.13)	0.812	444	0.99 (0.31–3.10)	0.980	317	0.88 (0.18–4.31)	0.870
Low developmental score	349	4.56 (1.53–13.60)	0.007	329	3.93 (1.23–12.57)	0.013	282	4.15 (1.05–16.38)	0.042

(1) Multi-level for neonatal unit of care and developmental tool used. (2) Adjusted for gender, birth weight, gestation and Apgar scores at 1 and 5 min. (3) Additionally adjusted for ethnicity. *n*—number of infants with data available. Values are odds ratio (95% confidence interval)

**Table 8** EAAT2 genotypes and outcomes

Genotype				Low developmental score		Cerebral palsy		Low developmental score OR cerebral palsy	
A alleles	Genotype code	SNP -200 bp	SNP -181 bp	Number with outcomes	%	Number with outcomes	%	Number with at least one outcome	%
0	8	C/C	C/C	0	–	0	–	0	–
1	9	C/A	C/C	10	1 (10.0%)	10	0 (0.0%)	10	1 (10.0%)
1	6	C/C	A/C	14	0 (0.0%)	16	1 (6.3%)	16	1 (6.3%)
2	3	A/A	C/C	41	2 (4.9%)	46	2 (4.4%)	46	4 (8.7%)
2	2	C/A	A/C	192	21 (10.9%)	218	21 (9.6%)	220	32 (14.6%)
2	1	C/C	A/A	77	7 (9.1%)	78	8 (10.3%)	80	10 (12.5%)
3	7	A/A	A/C	7	1 (14.3%)	7	1 (14.3%)	7	2 (28.6%)
3	4	C/A	A/A	8	4 (50.0%)	9	2 (22.2%)	9	4 (44.4%)
4	5	A/A	A/A	0	–	1	0 (0.0%)	1	0 (0.0%)

*EAAT2* promoter is involved in repression of *EAAT2* activation [42]. Furthermore, a recent study revealed significant differences in the methylation of ten genes involved in neuronal and glial signalling, neurotransmission, apoptosis and cellular energetics between preterm and term infants [43]. Importantly, among these genes was *EAAT2*, which promoter was differentially methylated at multiple CpG sites. Additionally, significant variation of *EAAT2*

promoter activity was observed in different brain regions and even between neighbouring cells [44]. These findings indicate that *EAAT2* promoter is dynamically regulated under physiological conditions. In genotypes 4/5/7, the C alleles at both -200 and -181 bp are replaced partially or fully by A alleles (Table 8), which might interfere with the normal methylation process and the binding of GCF2 transcription factor to the *EAAT2* promoter [19] (Fig. 3).

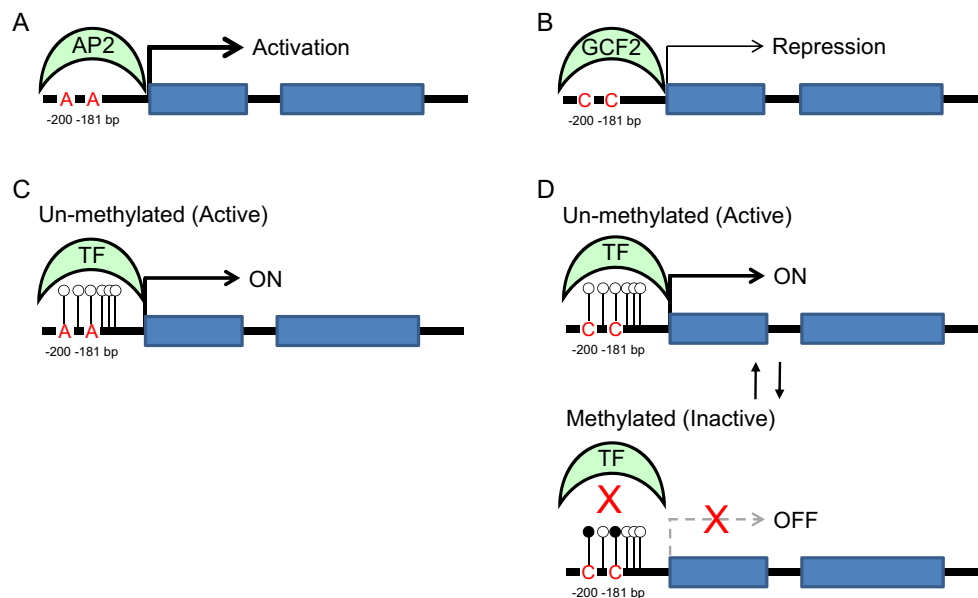


**Fig. 3** Proposed model of the SNPs impact on *EAAT2* gene regulation. **a** *EAAT2* promoter contains a consensus binding site for transcription factor activating enhancer binding protein 2 (AP-2), which is an activator of transcription in the developing brain [53]. **b** Nucleotide change from A to C at -181 bp abolishes this AP-2 consensus sequence and creates a binding site for transcription factor GC-binding factor 2 (GCF2) which represses *EAAT2* gene expression [19]. **c, d** *EAAT2* promoter is not only controlled by the transcriptional machinery, but is also subject to

modulation by epigenetic mechanism such as DNA methylation at CpG dinucleotides that inhibits gene expression [38, 39, 41, 42]. DNA methylation is reversible and subject to dynamic regulation throughout embryogenesis. Nucleotide changes from C to A might interfere with the normal DNA methylation process of *EAAT2* at both -200 and -181 bp, affecting gene expression. The ability to downregulate *EAAT2* in the developing brain seems beneficial since infants with three C alleles have better outcomes than those with only one



## Regulation of Glutamate Level by EAAT2 in the Developing Brain

One major pathology associated with cerebral palsy is PVL [10]. Oligodendrocyte cell death is particularly prominent following hypoxia-ischemia, which leads to hypomyelination [9]. Although the causes of PVL are not completely understood, cerebral ischemia is likely to play an important role [9, 10] implicating glutamate excitotoxicity, and excessive activation of ionotropic glutamate receptors [12]. The regulation of glutamate concentration in the extracellular space by EAAT2 is therefore essential for normal synaptic function [13] as well as neuronal survival by preventing excitotoxicity [16]. However, when there is a dissipation of electrochemical gradients across the plasma membrane as occurs during hypoxia-ischemia, EAAT2 operates in reverse to release glutamate, thereby promoting excitotoxicity [45]. In a rat model, glutamate was reduced in oligodendrocytes and axons following hypoxia-ischemia suggesting that these are the main sources of glutamate in developing white matter [46]. Furthermore, EAAT2 deficient mice are more vulnerable to neuronal loss in the hippocampus following a short episode of ischemia, while the wild-type mice are more vulnerable to neuronal death following prolonged ischaemia [47]. These findings suggest that in prolonged ischaemia, EAAT2 becomes the major contributor to abnormal concentrations of extracellular glutamate. EAAT2 expression is limited primarily to oligodendrocytes early in development and is increased during the period when the premature infant is most vulnerable to PVL [17]. Furthermore, the EAAT2 protein level was found to increase substantially in some cases of PVL compared to age-related controls [18]. Similarly, a recent study showed that EAAT2 is selectively expressed in cortical layer V neurons that are damaged in premature infants with PVL [48] and hypothesised that the reversal of glutamate transport by EAAT2 together with hyperactivation of ionotropic glutamate receptors contribute to excess ambient glutamate and consequently cell death specifically in these neurons [49]. Taking together, these data indicate that in the developing white matter, it is advantageous to have the ability to dynamically downregulate EAAT2 expression during ischaemia. Our genetic data supports this hypothesis; C alleles at -200 and/or -181 bp allow for dynamic alteration of EAAT2 expression via methylation and by the binding of GCF2 transcription factor (Fig. 3). In contrast, in infants who carry mainly A alleles, regulation of EAAT2 via these mechanisms is impaired, which increases ischaemic vulnerability and subsequent impaired neurodevelopment and cerebral palsy.

### Study Design Benefits and Limitations

This study included all infants of 32-week gestation or less, including multiples who survived the first 5–8 days of life.

Consequently, preterm infants with severe brain injury due to hypoxia-ischaemia or intraventricular haemorrhage, who often die in the first few days of life, were not included which may explain the deviation from the Hardy-Weinberg equilibrium. Participants originated from four different infant groups/neonatal centres in the South West of England and included all ethnic groups and therefore the findings are applicable to the whole UK population of preterm infants. However, due to the retrospective design of the study, not all bloodspots could be traced from the complete population. The use of different neurodevelopmental assessment tools for the different groups precluded the use of raw cognitive or motor scores as continuous variables. The pragmatic solution was to classify those in the lowest 10th percentile of each group for each subscale/score as having a low developmental score. The lowest 10th percentile for each score translated as two standard deviations below the normal population mean, which is widely accepted as the cut-off for moderate/severe developmental impairment when using a single developmental assessment tool in clinical studies [50]. Cystic PVL was diagnosed on routine clinically directed cerebral ultrasound and white matter injury was reported and coded if it was severe and cystic in nature. We included an extra group with cystic PVL data (Table 1; Southmead Hospital) but despite increasing the power of the analysis, there was no evidence for an association between the SNPs tested and the measurable ultrasound changes. The overall proportion of cystic PVL in this work was 6.7%, which is not statistically different from the population rate in the UK Vermont Oxford dataset at the time (4.8%;  $p = 0.117$ ). These data suggest that milder (non-cystic) white matter injury may not have been detected on clinical cerebral ultrasound in these groups and consequently an association with EAAT2 genotype and white matter damage was not found. Magnetic resonance imaging, which is more sensitive in detecting milder grades of white matter injury [51], is not used routinely in the UK to screen the preterm brain. These neuroimaging approaches performed in the first weeks of life are imprecise surrogate markers of neurological function. Therefore, structured functional neurological assessment at 2 years for cerebral palsy and neurodevelopmental impairment (used in this study) is considered to be the gold standard measure of neurological outcome in preterm infants [52].

### Conclusions

In this study, we have found that g.-200C>A and 181A>C SNPs are associated with both clinical neurodevelopmental outcomes and measurable in vitro effects on glutamate homeostasis. These findings indicate that glutamate is likely to be involved in the pathogenesis of brain injury and subsequent development of cerebral palsy and neurodevelopmental impairments in the human infant. It is

plausible that g.-200C>A SNP may also have a major effect on the development of neurological diseases in the adult population as this SNP is so closely linked to the g.-181A>C SNP, which was reported to affect neurological function after adult stroke [19], multiple sclerosis [20] and in schizophrenia [35]. The described EAAT2 SNPs may have utility as a viable early biomarker of cerebral palsy and long-term neurodisability in high-risk preterm infants. These results warrant a prospective study with complete recruitment (including non-survivors) to confirm the utility as early biomarker of neurological outcome. Our results also validate the notion that glutamate plays a pivotal role in preterm brain injury and opens the debate around exploration of glutamate uptake manipulation as potential pharmacological intervention for the prevention of preterm brain injury in infants with this genetic vulnerability. Better understanding of the dynamic transcriptional regulation of EAAT2 during the perinatal period may be key to the future development of effective clinical interventions.

**Acknowledgements** We would like to thank Dr. Helena Kemp for assisting with tracing the dried blood spots from the screening archive, Professor Neil Marlow for providing data on the Avon Premature Infant Project (APIP) infants, Dr. Sam O'Hare and Dr. Manal el Bokle for performing data collection on the Southmead Hospital infants and Dr. Sally Jary for performing neurodevelopmental assessments on the St Michael's Hospital infants.

**Author Contributions** SR: study design, sample preparation for experiments, pyrosequencing, data interpretation, manuscript preparation. DO: patient data collection and analysis, statistical analysis, preparation of manuscript. MTR: Promoter construct generation. ACS and LD: primary astrocyte generation and transfection for promoter assay. MW and CC: pyrosequencing assay optimisation. DH, MW and MO: clinical sample and data collection. JC: manuscript preparation. EM, KL and AV: conception, design of the study, manuscript preparation, supervision of the experimental work, funding.

**Compliance with Ethical Standards** The study received ethical approval in April 2010 from the National Research Ethics Service, UK (REC reference number 10/H0106/10).

**Conflict of Interest** EM is member of the Scientific Advisory Board of Hello Bio [www.hellobio.com].

**Funding** This work was supported by the University of the West of England, Bristol, UK (AV). EM is supported by the Biotechnology and Biological Sciences Research Council, UK (grants BB/F011326/1 and BB/J015938/1). The blood spot retrieval was funded by the David Telling Charitable Trust (KL).

**Open Access** This article is distributed under the terms of the Creative Commons Attribution 4.0 International License (<http://creativecommons.org/licenses/by/4.0/>), which permits unrestricted use, distribution, and reproduction in any medium, provided you give appropriate credit to the original author(s) and the source, provide a link to the Creative Commons license, and indicate if changes were made.

## References

- Field DJ, Dorling JS, Manktelow BN, Draper ES (2008) Survival of extremely premature babies in a geographically defined population: prospective cohort study of 1994–9 compared with 2000–5. *Br Med J* 336:1221–1223. doi:10.1136/bmj.39555.670718.BE
- Costeloe KL, Hennessy EM, Haider S, Stacey F, Marlow N, Draper ES (2012) Short term outcomes after extreme preterm birth in England: comparison of two birth cohorts in 1995 and 2006 (the EPICure studies). *Br Med J* 345:e7976. doi:10.1136/bmj.e7976
- Galinsky R, Polglase GR, Hooper SB, Black MJ, Moss TJ (2013) The consequences of chorioamnionitis: preterm birth and effects on development. *J Pregnancy* 2013:412831. doi:10.1155/2013/412831
- Moser K, Macfarlane A, Chow YH, Hilder L, Dattani N (2007) Introducing new data on gestation-specific infant mortality among babies born in 2005 in England and Wales. *Health Stat Q* 2007 Autumn:13–27.
- Wilson-Costello D, Friedman H, Minich N, Siner B, Taylor G, Schluchter M, Hack M (2007) Improved neurodevelopmental outcomes for extremely low birth weight infants in 2000–2002. *Pediatrics* 119:37–45. doi:10.1542/peds.2006-1416
- Mangham LJ, Petrou S, Doyle LW, Draper ES, Marlow N (2009) The cost of preterm birth throughout childhood in England and Wales. *Pediatrics* 123:e312–e327. doi:10.1542/peds.2008-1827
- Marret S, Marchand-Martin L, Picaud J-C, Mascoët J-M, Arnaud C, Rozé JC, Truffert P, Larroque B et al, EPIPAGE Study Group (2013) Brain injury in very preterm children and neurosensory and cognitive disabilities during childhood: the EPIPAGE cohort study. *PLoS One* 8:e62683. doi:10.1371/journal.pone.0062683
- Boardman JP, Waley A, Ball G, Takousis P, Krishnan ML, Hughes-Carre L, Aljabar P, Serag A et al (2014) Common genetic variants and risk of brain injury after preterm birth. *Pediatrics* 133:e1655–e1663. doi:10.1542/peds.2013-3011
- Volpe JJ (2009) The encephalopathy of prematurity-brain injury and impaired brain development inextricably intertwined. *Semin. Pediatr Neurol* 16:167–178. doi:10.1016/j.spen.2009.09.005
- Volpe JJ, Kinney HC, Jensen FE, Rosenberg PA (2011) The developing oligodendrocyte: key cellular target in brain injury in the premature infant. *Int J Devl Neurosci* 29:423–440. doi:10.1016/j.ijdevneu.2011.02.012
- Elitt CM, Rosenberg PA (2014) The challenge of understanding cerebral white matter injury in the premature infant. *Neuroscience* 276:216–238. doi:10.1016/j.neuroscience.2014.04.038
- Jensen FE (2005) Role of glutamate receptors in periventricular leukomalacia. *J Child Neurol* 20:950–959
- Danbolt NC (2001) Glutamate uptake. *Prog Neurobiol* 65:1–105
- Maragakis NJ, Rothstein JD (2004) Glutamate transporters: animal models to neurologic disease. *Neurobiol Dis* 15:461–473. doi:10.1016/j.nbd.2003.12.007
- Chao X-D, Fei F, Fei Z (2010) The role of excitatory amino acid transporters in cerebral ischemia. *Neurochem Res* 35:1224–1230. doi:10.1007/s11064-010-0178-3
- Tanaka K, Watase K, Manabe T, Yamada K, Watanabe M, Takahashi K, Iwama H, Nishikawa T et al (1997) Epilepsy and exacerbation of brain injury in mice lacking the glutamate transporter GLT-1. *Science* 276:1699–1702
- DeSilva TM, Kinney HC, Borenstein NS, Trachtenberg FL, Irwin N, Volpe JJ, Rosenberg PA (2007) The glutamate transporter EAAT2 is transiently expressed in developing human cerebral white matter. *J Comp Neurol* 501:879–890. doi:10.1002/cne.21289
- DeSilva TM, Billiards SS, Borenstein NS, Trachtenberg FL, Volpe JJ, Kinney HC, Rosenberg PA (2008) Glutamate transporter EAAT2 expression is up-regulated in reactive astrocytes in human

- periventricular leukomalacia. *J Comp Neurol* 508:238–248. doi:10.1002/cne.21667
19. Mallolas J, Hurtado O, Castellanos M, Blanco M, Sobrino T, Serena J, Vivancos J, Castillo J et al (2006) A polymorphism in the EAAT2 promoter is associated with higher glutamate concentrations and higher frequency of progressing stroke. *J Exp Med* 203:711–717. doi:10.1084/jem.20051979
  20. Pampliega O, Domercq M, Villoslada P, Sepulcre J, Rodríguez-Antigüedad A, Matute C (2008) Association of an EAAT2 polymorphism with higher glutamate concentration in relapsing multiple sclerosis. *J Neuroimmunol* 195:194–198. doi:10.1016/j.jneuroim.2008.01.011
  21. Rajatleka S, Luyt K, Williams M, Harding D, Odd D, Molnár E, Váradi A (2014) Detection of three closely located single nucleotide polymorphisms in the EAAT2 promoter: comparison of single-strand conformational polymorphism (SSCP), pyrosequencing and Sanger sequencing. *BMC Genet* 15:80. doi:10.1186/1471-2156-15-80
  22. MacLennan AH, Thompson SC, Gez J (2015) Cerebral palsy: causes, pathways, and the role of genetic variants. *Am J Obstet Gynaecol* 213:779–788. doi:10.1016/j.ajog.2015.05.034
  23. Avon Premature Infant Project (1998) Randomised trial of parental support for families with very preterm children. *Arch Dis Child Fetal Neonatal Ed* 79:F4–11. doi:10.1136/fn.79.1.F4
  24. Rajatleka S, Luyt K, El-Bokle M, Williams M, Kemp H, Molnár E, Váradi A (2013) Isolation of human genomic DNA for genetic analysis from premature neonates: a comparison between newborn dried blood spots, whole blood and umbilical cord tissue. *BMC Genet* 14:105. doi:10.1186/1471-2156-14-105
  25. McCarthy KD, de Vellis J (1980) Preparation of separate astroglial and oligodendroglial cell cultures from rat cerebral tissue. *J Cell Biol* 85:890–902
  26. Luyt K, Váradi A, Molnár E (2003) Functional metabotropic glutamate receptors are expressed in oligodendrocyte progenitor cells. *J Neurochem* 84:1452–1464. doi:10.1046/j.1471-4159.2003.01661.x
  27. Luyt K, Slade TP, Dorward JJ, Durant CF, Wu Y, Shigemoto R, Mundell SJ, Váradi A et al (2007) Developing oligodendrocytes express functional GABA<sub>B</sub> receptors that stimulate cell proliferation and migration. *J Neurochem* 100:822–840. doi:10.1111/j.1471-4159.2006.04255.x
  28. Bax M, Goldstein M, Rosenbaum P, Leviton A, Paneth N, Dan B, Jacobsson B, Damiano D et al, Executive Committee for the Definition of Cerebral Palsy (2005) Proposed definition and classification of cerebral palsy, April 2005. *Dev Med Child Neurol* 47:571–576
  29. de Vries LS, Eken P, Dubowitz LM (1992) The spectrum of leukomalacia using cranial ultrasound. *Behav Brain Res* 49:1–6
  30. Huntley M (1996) The Griffiths Mental Development Scales: from birth to 2 years. Association for Research in Infant and Child Development (ARICD). Oxford, UK: The Test Agency 1996:5–39.
  31. Bayley N (1993) Manual for the Bayley scales of infant development, 2nd edition edn. Psychological Corporation, San Antonio, Texas
  32. Bayley N (2006) Bayley scales of infant development, 3rd edition edn. Harcourt Assessment, San Antonio, Texas
  33. Odd DE, Lewis G, Whitelaw A, Gunnell D (2009) Resuscitation at birth and cognition at 8 years of age: a cohort study. *Lancet* 373:1615–1622. doi:10.1016/S0140-6736(09)60244-0
  34. Sun D, Ostermaier MK, Heydenreich FM, Mayer D, Jaussi R, Standfuss J, Veprintsev DB (2013) AAscan, PCRdesign and MutantChecker: a suite of programs for primer design and sequence analysis for high-throughput scanning mutagenesis. *PLoS One* 8:e78878. doi:10.1371/journal.pone.0078878
  35. Spangaro M, Bosia M, Zanoletti A, Bechi M, Cocchi F, Pirovano A, Lorenzi C, Bramanti P et al (2012) Cognitive dysfunction and glutamate reuptake: effect of EAAT2 polymorphism in schizophrenia. *Neurosci Lett* 522:151–155. doi:10.1016/j.neulet.2012.06.030
  36. Shin HE, Han SJ, Lee KS, Park JW (2011) Polymorphism of the glutamate transporter protein EAAT2 and migraine transformation into chronic daily headache. *J Clin Neurol* 7:143–147. doi:10.3988/jcn.2011.7.3.143
  37. Feng J, Fouse S, Fan G (2007) Epigenetic regulation of neural gene expression and neuronal function. *Pediatr Res* 61:58R–63R. doi:10.1203/pdr.0b013e3180457635
  38. Lister R, Mukamel EA, Nery JR, Urich M, Puddifoot CA, Johnson ND, Lucero J, Huang Y et al (2013) Global epigenomic reconfiguration during mammalian brain development. *Science* 341:1237905. doi:10.1126/science.1237905
  39. Spiers H, Hannon E, Schalkwyk LC, Smith R, Wong CC, O'Donovan MC, Bray NJ, Mill J (2015) Methylomic trajectories across human fetal brain development. *Genome Res* 25:338–352. doi:10.1101/gr.180273.114
  40. Endres M, Meisel A, Biniszkiwicz D, Namura S, Prass K, Ruscher K, Lipski A, Jaenisch R et al (2000) DNA methyltransferase contributes to delayed ischemic brain injury. *J Neurosci* 20:3175–3181
  41. Zschocke J, Allritz C, Engele J, Rein T (2007) DNA methylation dependent silencing of the human glutamate transporter EAAT2 gene in glial cells. *Glia* 55:663–674. doi:10.1002/glia.20497
  42. Yang Y, Gozen O, Vidensky S, Robinson MB, Rothstein JD (2010) Epigenetic regulation of neuron-dependent induction of astroglial synaptic protein GLT1. *Glia* 58:277–286. doi:10.1002/glia.20922
  43. Sparrow S, Manning JR, Cartier J, Anlagan D, Bastin ME, Piyasena C, Pataky R, Moore EJ et al (2016) Epigenomic profiling of preterm infants reveals DNA methylation differences at sites associated with neural function. *Transl Psychiatry* 6:e716. doi:10.1038/tp.2015.210
  44. de Vivo L, Melone M, Rothstein JD, Conti F (2010) GLT-1 promoter activity in astrocytes and neurons of mouse hippocampus and somatic sensory cortex. *Front Neuroanat* 3:31. doi:10.3389/neuro.05.031.2009
  45. Fern R, Möller T (2000) Rapid ischemic cell death in immature oligodendrocytes: a fatal glutamate release feedback loop. *J Neurosci* 20:34–42
  46. Back SA, Craig A, Kayton RJ, Luo NL, Meshul CK, Allcock N, Fern R (2007) Hypoxia-ischemia preferentially triggers glutamate depletion from oligodendroglia and axons in perinatal cerebral white matter. *J Cereb Blood Flow Metab* 27:334–347. doi:10.1038/sj.cjcbfm.9600344
  47. Mitani A, Tanaka K (2003) Functional changes of glial glutamate transporter GLT-1 during ischemia: an in vivo study in the hippocampal CA1 of normal mice and mutant mice lacking GLT-1. *J Neurosci* 23:7176–7182
  48. Andiman SE, Haynes RL, Trachtenberg FL, Billiards SS, Folkerth RD, Volpe JJ, Kinney HC (2010) The cerebral cortex overlying periventricular leukomalacia: analysis of pyramidal neurons. *Brain Pathol* 20:803–814. doi:10.1111/j.1750-3639.2010.00380.x
  49. DeSilva TM, Borenstein NS, Volpe JJ, Kinney HC, Rosenberg PA (2012) Expression of EAAT2 in neurons and protoplasmic astrocytes during human cortical development. *J Comp Neurol* 520:3912–3932. doi:10.1002/cne.23130
  50. Wood NS, Marlow N, Costeloe K, Gibson AT, Wilkinson AR (2000) Neurologic and developmental disability after extremely preterm birth. EPICure study group. *N Engl J Med* 343:378–384. doi:10.1056/NEJM200008103430601
  51. Miller SP, Cozzio CC, Goldstein RB, Ferriero DM, Partridge JC, Vigneron DB, Barkovich AJ (2003) Comparing the diagnosis of white matter injury in premature newborns with serial MR imaging and transfontanel ultrasonography findings. *AJNR Am J Neuroradiol* 24:1661–1669
  52. Marlow N (2004) Neurocognitive outcome after very preterm birth. *Arch Dis Child Fetal Neonatal Ed* 89:F224–F228
  53. Mitchell PJ, Timmons PM, Hébert JM, Rigby PW, Tjian R (1991) Transcription factor AP-2 is expressed in neural crest cell lineages during mouse embryogenesis. *Genes Dev* 5:105–119

**D-14-00706**

**Review**

**A novel treatment strategy for glioblastoma multiforme and glioma associated seizures:**

**Increasing glutamate uptake with PPAR $\gamma$  agonists**

Jared Ching<sup>a,c,d,\*</sup>, Stephanie Amiridis<sup>a,c</sup>, Stanley S. Stylli<sup>a,b</sup>, Andrew P. Morokoff<sup>a,b</sup>, Terence J.

O'Brien<sup>c</sup>, Andrew H. Kaye<sup>a,b</sup>

<sup>a</sup> Department of Surgery, The University of Melbourne, Royal Melbourne Hospital, VIC, Australia

<sup>b</sup> Department of Neurosurgery, The Royal Melbourne Hospital, Parkville, VIC, Australia

<sup>c</sup> Department of Medicine, The University of Melbourne, Royal Melbourne Hospital, VIC, Australia

 <sup>d</sup> Institute of Medical Sciences, Foresterhill, University of Aberdeen, Aberdeen, AB25 2ZD, UK

\*Corresponding author. Tel.: +44 1224 551 815.

*E-mail address:* jared.ching@nhs.net (J. Ching).

**Conflicts of Interest/Disclosures**

The authors declare that they have no financial or other conflicts of interest in relation to this research and its publication.

## **Abstract**

The established role of glutamate in the pathogenesis of glioma-associated seizures (GAS) lead us to investigate a novel treatment method using an established drug class, peroxisome proliferator activated receptor (PPAR) gamma agonists. Previously, sulfasalazine has been shown to prevent release of glutamate from glioma cells and prevent GAS in rodent models. However, raising protein mediated glutamate transport via excitatory amino acid transporter 2 (EAAT2) has not been investigated previously to our knowledge. PPAR gamma agonists are known to upregulate functional EAAT2 expression in astrocytes and prevent excitotoxicity caused by glutamate excess. These agents are also known to have anti-neoplastic mechanisms. Herein we discuss and review the potential mechanisms of these drugs and highlight a novel method of potentially treating GAS.

*Keywords:* Glioma; Glutamate; PPAR gamma; Seizures

## 1. Introduction

Glioblastoma multiforme accounts for 77% of malignant brain tumours and despite medical advances improvements in prognosis have been limited.<sup>1,2</sup> Recent identification of therapy resistant stem-like glioma cells has provided a possible explanation for the great difficulties in treating this disease.<sup>3</sup> Identification of novel indications for currently marketed medications may permit swifter additions to the present armamentarium. The unexplored mechanisms of action of these drugs may be beneficial in other disease states, in particular cancer and epilepsy as multimodal action is desirable and potentially effective. One such class of compounds are the peroxisome proliferator activated receptor gamma (PPAR $\gamma$ ) agonists, which influence numerous signalling, inflammatory and transcriptional cascades.

Unexplained seizures may represent the first sign of a primary brain tumour. Glioma associated seizures (GAS) can be pharmaco-resistant to anti-epileptic medications, adversely affecting patients' quality of life, necessitating the need for further research<sup>4</sup>. Excessive glutamate levels present in glioma tissues have been shown to be pro-convulsant.<sup>5</sup> Furthermore, blocking the system X<sub>c</sub><sup>-</sup> cysteine-glutamate exchange transporter using sulfasalazine was observed to reduce the frequency of seizures in this model.<sup>5</sup> A recent study also confirmed an association between glutamate levels in human glioma tissue and the associated seizures in patients.<sup>6</sup> In addition, significantly reduced expression of the excitatory amino acid transporter 2 (EAAT2) in the GAS tumour samples was also reported.

EAAT2 is one of five subtypes of sodium dependent plasma membrane glutamate transporters that accounts for up to 90% of extracellular glutamate uptake.<sup>7,8</sup> PPAR $\gamma$  is a ligand-dependent transcription factor that responds to both physiological and chemical stimuli, including the cyclopentenone prostaglandin, 15-deoxy $\Delta^{12,14}$  prostaglandin J<sub>2</sub> (15d-PGJ<sub>2</sub>) and thiazolidinediones (TDZ) respectively.<sup>9</sup> Expression of PPAR $\gamma$  in the brain has been found in multiple cell types

including microglia, astrocytes, oligodendrocytes and neurons. It has been shown that agonists of PPAR $\gamma$  increases expression of EAAT2 at both the mRNA and protein levels in rat cortical cultures.<sup>10</sup> Reductions in infarct volume after administration of rosiglitazone (a commercially available TDZ) in rats with middle cerebral artery occlusion is supported with the clinical evidence of improved neurological outcomes in a small case-matched controlled study investigating stroke recovery post TDZ drug administration.<sup>10,11</sup> These observations suggest that PPAR $\gamma$  agonists could potentially be utilised for seizure reduction in glioma patients through the upregulation of EAAT2 and subsequent reduction of glutamate concentration.

Herein we review the current literature examining the role of glutamate transporters in glioma biology and GAS. We also describe how this pertains to a potentially novel role for PPAR $\gamma$  agonists in the treatment of GAS with reference to our ongoing laboratory study, which has demonstrated that pioglitazone modulates EAAT2 expression and significantly reduces glutamate levels in glioma cell lines.

## **2. Review of the literature**

### *2.1. PPAR structure, mechanisms and current indications*

Peroxisome proliferator activated receptors (PPAR) form a superfamily of ligand-activated transcription factors that regulate glucose and lipid metabolism. Specific ligands, usually small lipophilic molecules, bind PPAR, causing conformational changes of the receptor that activates transcription of target genes.<sup>12,13</sup> Endogenous and chemical ligands include 15d-PGJ<sub>2</sub> and the TDZ. PPAR are known to regulate gene expression by binding to retinoid X receptors (RXR) as a heterodimeric partner to specific DNA sequences called PPAR response elements. Three subtypes of

PPAR have been characterised:  $\alpha$ ,  $\beta/\delta$  and  $\gamma$ , located on chromosomal regions 22q12-q13.1, 3p25, and 6p21.1-21.1 respectively.<sup>14-16</sup> Two PPAR isotypes PPAR $\gamma$ 1 and PPAR $\gamma$ 2 have also been identified with alternative splicing and promoter usage. PPAR $\gamma$ 1 and PPAR $\gamma$ 3 mRNA encode PPAR $\gamma$ 1 proteins, which are expressed throughout the majority of tissues in the body. Alternatively, PPAR $\gamma$ 2 mRNA encode the PPAR $\gamma$ 2 protein, which is specific only to adipocytes.<sup>17</sup> PPAR $\gamma$  is most concentrated in the large intestines and adipose tissue, with moderate amounts detected in the liver, small intestine and kidneys, and lesser amounts observed in muscle tissue.<sup>18</sup> All PPAR subtypes share the known modular arrangement of nuclear receptors whereas the N-terminal regulatory domain has been shown to possess ligand independent transactivation.<sup>19</sup> PPAR isotype  $\alpha$  and  $\gamma$  expression can be also be modulated in this region by mitogen activated kinase phosphorylation.<sup>20</sup> The highly conserved DNA binding region has two zinc-fingers that bind hormone response elements.<sup>19</sup> The ligand binding domain (LBD) has a ligand-dependent trans-activation function, (AF)-2, which interacts with transcriptional co-activators including steroid receptor co-activator and the cAMP binding response element binding-protein (CREB) binding protein.<sup>18,21-24</sup>

Elucidation of the crystal structure of PPAR $\gamma$ -RXR $\alpha$  has revealed the structural basis of heterodimer conformational changes upon ligand binding. C2 asymmetry of this complex is evident whereby the PPAR $\gamma$  LBD is rotated approximately 10° to its RXR partner.<sup>25</sup> This contrasts with the symmetrical PPAR $\gamma$  - ligand free (apo) RXR complexes and ultimately may be related to functional differences between nuclear hormone receptors<sup>25,26</sup> (Fig. 1). PPAR bind numerous naturally-occurring endogenous ligands, however some specificity exists for each isoform, although some ligands are able to activate all subtypes. PPAR $\gamma$  responds to endogenous prostanoids synthesised through the lipoxygenase route including 15d-PGJ<sub>2</sub> and 12- and 15-hydroxy-eicosatetraenoic acid (12- and 15-HETE), as well as the modified lipids 9- and 13-hydroxyoctadecadienoic acid (9- and 13-HODE).<sup>17</sup> In



addition, it has been shown that 15d-PGJ<sub>2</sub> is the most potent and abundant naturally occurring ligand for PPAR $\gamma$ .<sup>27</sup>

TDZ are PPAR $\gamma$  agonists which have been widely used in the treatment of non-insulin dependent diabetes mellitus. Troglitazone was the first TDZ introduced into the market but was withdrawn in 2000 when hepatotoxicity was reported as an evident adverse reaction. This was attributed to the possibility of quinone epoxide toxicity.<sup>28</sup> Rosiglitazone was approved in the USA in 1999, however, the emergence of significant cardiovascular side-effects has made its use controversial. In contrast, the European Medicines Agency (EMA) withdrew the use of rosiglitazone in 2010.<sup>29,30</sup> The USA Food and Drug Administration have since restricted the use of rosiglitazone, although it arguably remains available. However, fluid retention resulting in the worsening of congestive heart failure and peripheral oedema relates to class effect of TDZ, which have been shown to be mediated through the abundant PPAR $\gamma$  receptors expressed in renal collecting ducts.<sup>31,32</sup> Pioglitazone has been shown to have far less significant cardiovascular side-effects in a recent meta-analysis.<sup>33</sup> However, the primary concern of recent times regarding the use of pioglitazone is its association with the increased incidence of bladder cancer.<sup>34,35</sup> Meta-analyses have revealed a small probability of this link, but it has generally been agreed that the benefits outweigh the risks and the EMA have supported the use of pioglitazone in suitable patients with non-insulin dependent diabetes mellitus.

## 2.2. PPAR in the brain

All three PPAR isotypes ( $\alpha$ ,  $\beta/\delta$ ,  $\gamma$ ) are co-expressed in the nervous system. However, PPAR $\alpha$  and PPAR $\gamma$  have transient peaks in expression in late rodent embryogenesis, which declines in the third trimester and post-natally. This is in contrast to the constantly high expression levels of PPAR $\beta/\delta$ .<sup>36</sup> Heterogeneous patterns of distribution exist between PPAR subtypes in different regions in the brain

although the frontal cortex, basal ganglia, reticular formation, deep cerebellar nuclei, cerebellar golgi cells, and several cranial nerve nuclei including the oculomotor, trigeminal, vagus, and lateral vestibular nuclei exhibit high concentrations of all subtypes.<sup>37</sup> PPAR $\beta/\delta$  is widespread, whereas  $\alpha$  and  $\gamma$  subtypes are more localised in specific areas.<sup>37,38</sup> PPAR $\gamma$  is completely absent in the olfactory bulb, and expressed variably throughout the rodent brain but it is mostly concentrated in the piriform cortex, olfactory tubercle, caudate putamen, ventral pallidum, rhomboid nucleus, centromedial nucleus, parafascicular nucleus, stellate cells in the cerebellum, and parvicellular and gigantocellular nuclei in the reticular formation.<sup>37</sup> PPAR $\gamma$  is predominantly expressed in microglial cells, whereas all subtypes are present in astroglial cells.<sup>39,40</sup>

Numerous signalling cascades can be repressed or upregulated by the downstream effects of PPAR $\gamma$ , for example the inflammatory mediators interleukin (IL) 1 $\beta$ , IL-6 and tumour necrosis factor  $\alpha$  are known to be suppressed by PPAR $\gamma$  agonists and have been linked to the onset of temporal lobe epilepsy<sup>41 42</sup>. The therapeutic role of PPAR $\gamma$  in neurological diseases has a growing body of evidence of efficacy, particularly in Alzheimer's disease, multiple sclerosis and Parkinson's disease.<sup>43-46</sup> Of pertinence to this review are its roles in ischaemia, tumours and seizures.

### *2.3. Neuronal ischaemia*

#### *2.3.1. Inflammation*

It has been demonstrated that exposure to rosiglitazone, a PPAR $\gamma$  agonist, results in a reduction of infarct volumes in rats induced with a cardiac ischaemia reperfusion injury compared to non-exposure.<sup>47</sup> Authors of this study credited this protective effect to the cumulative anti-inflammatory

properties of rosiglitazone, as macrophage and neutrophil infiltration was significantly reduced preventing the release of proposed cytotoxic substances such as reactive oxygen species. Together with previous evidence that PPAR $\gamma$  agonists reduce the expression of inducible nitric oxide synthase, cyclo-oxygenase 2 and pro-inflammatory markers, the anti-inflammatory effects of rosiglitazone are the most likely mechanism by which the therapeutic benefits were conferred in this study.<sup>41,48,49</sup> In addition, as stroke is known to be associated with a strong inflammatory response, PPAR $\gamma$  agonists have also been trialled in pre-clinical stroke models.<sup>50-53</sup> Protective effects as a result of PPAR $\gamma$  agonist treatment were observed in the stroke models with a reduction in both infarct volumes and inflammatory markers.<sup>50-52</sup> The dependence of the PPAR $\gamma$  interaction was demonstrated with a loss of neuroprotection coupled with the concomitant treatment of the PPAR $\gamma$  antagonising agent T0070907<sup>54</sup>. The neuroprotective effects of PPAR $\gamma$  have also been shown to rely on the promotion of increased binding to intracerebral receptors by intracerebroventricular infusions of pioglitazone.<sup>55</sup> Although ischaemia induces upregulation of PPAR $\gamma$  mRNA, it is primarily associated with reduced PPAR $\gamma$  DNA binding, as it has been demonstrated that DNA binding is promoted by exposure to a TDZ or the natural ligand 15d-PGJ<sub>2</sub>.<sup>54,56</sup>

### 2.3.2. Role of glutamate

In addition to the inflammatory processes associated with neuronal ischaemia, glutamate mediated excitotoxicity has been extensively studied and shown to play an important role in the pathogenesis of neuronal cell death. Glutamate is the most abundant neurotransmitter in the mammalian central nervous system and mediates its excitatory physiological effect by binding to ionotropic and metabotropic receptors.<sup>57,58</sup> The main ionotropic receptor subtypes include  $\alpha$ -amino-3-hydroxy-5-methyl-4-isoxazole propionate (AMPA), kainate, and N-methyl-D-aspartate (NMDAR). Ionotropic receptor function is determined by receptor subunit structure, and while NMDAR is always permeable

to calcium ions, AMPA are usually relatively impermeable because of the presence of GluR2 subunit on this receptor.<sup>58,59</sup> Normally, minimal levels of glutamate are maintained in the extracellular fluid, whereas a significant concentration gradient is maintained across plasma membranes through a dynamic equilibrium mediated via the aforementioned cell surface receptors.<sup>58</sup>

In ischaemic brain tissue, hypoxia leads to a reduction in oxidative phosphorylation which causes a reduction in the generation of adenosine triphosphate (ATP).<sup>60</sup> This leads to a decreased amount of energy available to ionic transporters such as  $\text{Ca}^{2+}$  ATPase, which assist in maintaining a low intracellular concentration of calcium.<sup>60</sup> As the level of  $\text{Ca}^{2+}$  and  $\text{Na}^+$  increases, depolarisation of the presynaptic neurones results in the release of excessive glutamate. This results in the activation of glutamate receptors causing the excessive intracellular influx of  $\text{Ca}^{2+}$ . An increase in intracellular  $\text{Ca}^{2+}$  can lead to free radical formation and the induction of apoptosis and is mitochondrially mediated through either intrinsic or extrinsic pathways.<sup>61,62</sup> These pathways are reviewed in detail elsewhere.<sup>63</sup> In brief, the intrinsic pathway involves activation of calpains from the raised  $\text{Ca}^{2+}$  levels, which cleave Bid into truncated Bid which leads to the formation of an apoptosome which results in the activation of caspase-3, subsequently cleaving nuclear DNA repair enzymes and ultimately leading to cell death. The extrinsic pathway also follows a caspase-mediated apoptosis pathway but is preceded by binding of the extracellular Fas ligands to Fas death receptors, leading to the formation of a death inducing signalling complex that activates caspase 8. In addition, the formation of reactive oxygen species mediated by the over-activation of neuronal nitric oxide synthetase as a result of increased concentrations of  $\text{Ca}^{2+}$  exacerbates the damage caused by excitotoxicity.<sup>64</sup> Formation of peroxynitrite, an unstable structural isomer of nitrate, also causes damage to DNA along with the activation of apoptic pathways mediating further neuronal damage as part of the process of excitotoxicity.

These damaging downstream effects can be mitigated in theory by reducing the amount of extracellular glutamate. Antagonists of glutamate target receptors NMDA and AMPA have been shown to protect against the damaging effects of cerebral ischaemia by preventing glutamate binding.<sup>65,66</sup> Despite promising results in rodent ischaemic models, all clinical trials to our knowledge have yielded no beneficial effects of NMDA antagonism.<sup>67</sup> Recently, a more promising approach has been elicited mediated by increasing glutamate clearance through the upregulation of EAAT2 with PPAR $\gamma$  agonists, which has shown some pre-clinical evidence of efficacy.<sup>10,11</sup> Addition of the PPAR $\gamma$  inhibitor T0070907 reversed glutamate uptake in rat cortical cultures exposed to the PPAR $\gamma$  agonist rosiglitazone.<sup>10</sup> T0070907 also prevented the increased EAAT2 expression associated with ischaemic pre-conditioning in rodent models, as well as astrocytic [<sup>3</sup>H] glutamate uptake, indicating that EAAT2 can be functionally modulated to avoid glutamate mediated excitotoxicity. Neuroprotection using this strategy has been supported by the findings of Harvey and colleagues who demonstrated that overexpression of GLT-1/EAAT2 using an adenoviral vector expressing the GLT-1 rat cDNA was effective in reducing glutamate levels and improving post-stroke behavioural outcome.<sup>68</sup> Similarly, intraperitoneally administered ceftriaxone (a known PPAR $\gamma$  agonist) exhibited prophylactic benefits in a pre-clinical rodent stroke model.<sup>69,70</sup> However, Verma and colleagues have reported conflicting results involving the expression levels of EAAT2 by PPAR $\gamma$  agonists. They did not observe an increase in EAAT2 mRNA levels when rosiglitazone was administered to ischaemic rodents, despite improved functional outcomes.<sup>71</sup> However, Sattler and colleagues have recently demonstrated that the non-PPAR $\gamma$  agonist thiamphenicol upregulates peritumoural EAAT2 expression *in vivo* and prevents tumour progression, indicating a PPAR $\gamma$  independent EAAT upregulation.<sup>72</sup> Yuen and colleagues have recently confirmed that reduced EAAT2 expression and raised glutamate levels in human tumour specimens are associated with GAS.<sup>6</sup> This provides a strong rationale for trialling functional upregulators of PPAR $\gamma$  in order to clear excessive glutamate, which could offer a novel treatment for pharmaco-resistant GAS as summarised in Figure 2.

## *2.4. Anti-neoplastic activity in gliomas*

### *2.4.1. Oncogenic signalling pathways*

The human glioblastoma cell line Lipari (Ll) has been shown to express PPAR $\gamma$ , which is increased in the presence of the peroxisome proliferator perfluorodecanoic acid with or without exposure to retinoic acid.<sup>73</sup> Raised PPAR $\gamma$  expression has been associated with beneficial effects in other tumours including breast and colon,<sup>74,75</sup> and relative to other cancer cell lines glioma cells express lower levels of PPAR $\gamma$ .<sup>76</sup> A broader review of the antineoplastic effects of PPAR $\gamma$  agonists is available elsewhere.<sup>77</sup>

Numerous signalling pathways have been implicated in the antineoplastic effects of TDZ. Most notably, favourable modulations occur in the expression levels of cyclin D1, MMP-9, caspase 3, and N-cadherin, which are known to participate in the processes of cell cycle arrest, reduced invasion, induction of apoptosis and re-differentiation, respectively. These and additional mechanisms involved including reduced angiogenesis, production of reactive oxygen species, and inhibition of transforming growth factor beta (TGF $\beta$ ) are reviewed elsewhere.<sup>78</sup> Importantly, rosiglitazone has recently been shown to suppress expression of TGF $\beta$  and its receptor resulting in a reduction of glioma cell proliferative activity, indicating an additional pathway that can be targeted by PPAR $\gamma$  agonists.<sup>79</sup>

PPAR $\gamma$  agonists have been shown to reduce the expression of  $\beta$ -catenin, which is an important intracellular signalling protein involved in carcinogenesis.<sup>80</sup> PPAR $\gamma$ -independent pathways were implicated as the efficacy of pioglitazone in the aforementioned study was dose dependent and partially reversed by the potent PPAR $\gamma$  inhibitor, GW9662. Furthermore, it has also been

demonstrated that the PPAR $\gamma$  agonist citaglitazone mediates glioma cell apoptosis independently of PPAR $\gamma$  through the downregulation of Akt and induction of mitochondrial membrane potential loss.<sup>76</sup> Interestingly, increased cell death was observed during pre-treatment with GW9662 or downregulation of PPAR $\gamma$  expression with siRNA in the T98G glioma cell line. Table 1 summarises the antineoplastic mechanisms found to be elicited by PPAR $\gamma$  agonists at the time of writing.

Glycogen synthase kinase 3 (GSK3) is a serine/threonine protein kinase that inactivates glycogen synthase through phosphorylation.<sup>81</sup> GSK-3 $\alpha$  and GSK-3 $\beta$  are the two known isoforms, and GSK-3 $\beta$  has been shown to be abundant in the central nervous system with neuronal specificity.<sup>82</sup> PPAR $\gamma$  agonists are known to be non-ATP competitive GSK3 inhibitors with a neuroprotective role in stroke models through promotion of cell survival in addition to the aforementioned modulation of EAAT2 expression.<sup>83,84</sup> Although active GSK3 has been shown to negatively regulate survival pathways, GSK3 inhibition has been paradoxically shown to be effective against several neoplasms.<sup>85,86</sup> GSK3 inhibition in glioma stem cells has been shown to induce differentiation and regulate proliferation.<sup>87</sup> Atkins and colleagues demonstrated that Akt mediated GSK-3 $\beta$  regulation may occur through the inhibition of Akt.<sup>88</sup> Recently our studies have shown that PPAR $\gamma$  agonists may inactivate GSK-3 $\beta$  activity in glioma cells (unpublished data). As GSK-3 $\beta$  is part of the Wnt/ $\beta$ -catenin pathway, direct GSK-3 $\beta$  inhibition may account for the reduction in  $\beta$ -catenin.<sup>80</sup>

#### 2.4.2. *Glutamate transport*

The role of the system x<sub>c</sub><sup>-</sup> transporter in cancer cell lines has been validated in hepatoma, lymphoma, breast, pancreatic, and glioma cells.<sup>89</sup> The x<sub>c</sub><sup>-</sup> transporter is important in the exchange of extracellular glutamate for extracellular cysteine.<sup>90</sup> Cysteine is an essential precursor to glutathione, which has a role in preventing cellular damage by reactive oxygen species. Hence, intracellular uptake of cysteine

through system  $x_c^-$  permits glioma cell survival by increasing intracellular glutamate concentrations. However, the release of glutamate from glioma cells exacerbates excitotoxic conditions, causing necrosis of adjacent parenchyma and facilitating the invasion and growth of glioma cells.<sup>91</sup> Migration of glioma cells can occur through glutamate-mediated autocrine signalling through AMPA receptors located on the surface of glioma cells.<sup>92</sup> A valid inference from this data would be to block system  $x_c^-$  pharmacologically to potentially prevent the proliferation of glioma cells. Sulfasalazine (a potent system  $x_c^-$  inhibitor) has been observed to reduce glioma cell proliferation by targeting the system  $x_c^-$  transporter.<sup>93</sup> This effect on glioma cell proliferation has also been witnessed in a rodent glioma model, although a clinical trial involving the treatment of glioma patients with sulfasalazine was unfortunately ceased early due to a lack of efficacy and adverse effects.<sup>94</sup> However, sulfasalazine has yet to be investigated specifically for the treatment of GAS in a clinical setting. Finally, glioma cells are known to lack expression of the glutamate transporters EAAT1 and 2, which can intensify the rising extracellular concentrations of glutamate.<sup>90,95</sup> However, overexpression of EAAT in glioma cells has been shown to reduce viability and cell proliferation.<sup>96</sup>

#### *2.4.3. Glioma stem cells*

Recently, the PPAR $\gamma$  agonist citagliptone and 15d-PGJ<sub>2</sub> have been shown to inhibit the proliferation of brain tumour stem cells and reduce expression of stemness genes in glioma cells.<sup>97,98</sup> These results provide some promising therapeutic potential since self-renewing glioma stem cells are proposed to form a treatment resistant subpopulation of glioma cells.<sup>3,99,100</sup> However, there is some controversy over dedifferentiating established glioma cell lines, since the origin of these cells is unclear.<sup>101</sup>

The role of glutamate transport in glioma stem cells has yet to be investigated to our knowledge. Interestingly, Gilley and colleagues noted that neural stem cells derived from the hippocampal dentate



gyrus demonstrated increased EAAT2 expression in hypoxic-ischaemic and traumatic brain injury rodent models.<sup>102</sup> Furthermore, these authors also showed that knockdown of EAAT1 and EAAT2 expression resulted in increased neurosphere formation and cellular proliferation, whereas overexpression had the converse effect.

### *2.5. Anti-convulsant activity*

There is evidence that PPAR $\gamma$  agonists have anticonvulsant activity in epilepsy models. However, these mechanisms are unexplored in the context of GAS. Okada and colleagues demonstrated a delay in the age of onset of seizures in genetically susceptible mice when administered pioglitazone.<sup>103</sup> This group observed a reduction in mRNA expression of IL-1 $\beta$ , IL-6, and tumour necrosis factor  $\alpha$  in the brains of mice treated with pioglitazone but no definitive mechanism was identified. Mohazeb and colleagues sought to investigate this by investigating the effect of a PPAR $\gamma$  antagonist on anti-convulsant activity in mice given GABA antagonist pentylenetetrazole (PTZ). Their results showed that the specific PPAR $\gamma$  inhibitor GW9662 prevented anti-convulsant activity and proposed a role for nitric oxide in this process.<sup>104</sup> A similar study involving the intraperitoneal administration of PTZ further supported the role of nitric oxide in the anti-convulsant effect of pioglitazone.<sup>105</sup> A mechanism involving nitric oxide may therefore have a role in the treatment of GAS, in addition to the PPAR $\gamma$  mediated upregulation of EAAT2.

### *2.6. Rationale*

The literature reviewed here show that PPAR $\gamma$  agonists are a very promising class of agents to be utilised for the treatment of gliomas and GAS, since numerous beneficial targets may be targeted

concomitantly. Reduction in extracellular glutamate through EAAT2 upregulation prevents proliferation through excitotoxic destruction and induces cell death by overcoming protective mechanisms such as glutamate/cysteine exchange.

PPAR $\gamma$  mediated anti-inflammatory effects have roles in neuroprotection from stroke and epileptogenesis. In addition, PPAR agonists have been shown to upregulate EAAT2 expression in normal astrocytes and are thus most pertinent at the peritumoural interface between normal brain and the tumour.

### **3. Future investigation**

Targeting PPAR $\gamma$  in diabetes has an established role, where current research goals are towards developing ligands that avoid initiating the unwanted side-effects associated with TDZ drugs. The benzyl indole MRL24 has been shown to modulate gene expression akin to rosiglitazone through cyclin dependent kinase 5 (cdk-5) inhibition without acting as a full agonist at the LBD of PPAR $\gamma$ .<sup>106</sup> A novel non-agonist of PPAR $\gamma$  SR1664 inhibits cdk-5 phosphorylation and has been found to mediate anti-diabetic effects without *in vitro* reduction in bone formation or *in vivo* fluid retention, which are both common side-effects of TDZ treatment.<sup>107</sup> These findings have validated the possibility of generating novel, tissue specific PPAR $\gamma$  modulators without the unwanted side-effects associated with TDZ for the treatment of type two diabetes.<sup>108</sup> This recent work has been based on models of diabetes and further work would therefore be required in order to understand how the phosphorylation status of PPAR at different sites including Ser<sup>112</sup> and Ser<sup>273</sup> affects expression levels in glioma cells and astrocytes. Further post-translational regulations through the acetylation, ubiquitination and sumoylation of PPAR may also provide relevant novel targets allowing for the development of drugs with greater specificity.

Targeting glutamate transport in glioma therapeutics is attractive and the potential for adjunctive therapy with currently utilised protocols should be considered.<sup>109</sup> Novel agents that promote glutamate transport are currently being developed with high throughput screening and advanced drug design technologies that potentially expedite drug discovery.<sup>110</sup> It is also possible to investigate genome-wide transcriptional regulation with new sequencing methodologies, providing data on gene expression, epigenetic status, chromatin structure, and small molecule mediators.<sup>111</sup> This has permitted an extensive expansion of our current understanding of PPAR $\gamma$  DNA binding and transcript sites. Cell specific genomic binding sites for PPAR $\gamma$  have been elucidated in adipocytes and macrophages, using chromatin immunoprecipitation and high throughput screening (ChIP-seq).<sup>112</sup> Furthermore, the numerous downstream effects of PPAR $\gamma$  activation have been found to elicit may be in part due to the many DNA binding sites implicated in adipogenesis.<sup>113</sup> However, such techniques have not yet been applied to cells of the central nervous system or gliomas to our knowledge. Acquiring such genome-wide data in glioma would provide a better understanding of genetic dysregulation and allow for identification of specific DNA targets that could be exploited for more targeted therapies.

In general, the time-course of new drugs developed from novel “hits” to pre-clinical studies to clinical trials is often at least a decade. As such, current clinically approved drugs such as sulfasalazine and pioglitazone could be considered for new indications to expedite this process. In an attempt to take advantage of existing drugs a new adjuvant treatment approach using existing drugs such as disulfiram and ketoconazole has recently been proposed.<sup>114</sup> It is common practice to use “backbones” of existing drugs to screen for structural variants which are selective in their action and avoid unwanted effects. Since there are a limited number of known molecules that modulate EAAT2 expression, including thiamphenicol and ceftriaxone, further drug development would be desirable for the treatment of a wide range of pathologies.<sup>69,72</sup>

We have recently completed a preliminary laboratory study demonstrating that the PPAR $\gamma$  agonist pioglitazone upregulates functional expression of EAAT2 in glioma cell lines. The theoretical implications of this are that glutamate transport may be improved via astrocytes and viable glioma cells at the peritumoural edge. Further investigation with xenograft studies should also be conducted in pre-clinical trials to conclusively validate glutamate uptake as a viable therapeutic target. The role of this class of drugs should also be investigated in GAS models. Transcriptional targets of PPAR $\gamma$  activation in glioma cells should be examined to identify how these drugs work and elucidate new therapeutic targets. PPAR $\gamma$  agonists elicit a wide and diverse range of effects that impart benefits for a number of neurological diseases. The evidence reviewed here provides a strong foundation for utilising this class of agents as adjunct therapies in glioma management and in particular GAS mediated through glutamate and anti-inflammatory processes. Novel drugs acting through this mechanism may provide potential additions to the armamentarium for GAS.

## References

1. Schwartzbaum JA, Fisher JL, Aldape KD, Wrensch M. Epidemiology and molecular pathology of glioma. *Nat Clin Pract Neuro* 2006; **2**(9): 494-503.
2. Adamson C, Kanu OO, Mehta AI, et al. Glioblastoma multiforme: a review of where we have been and where we are going. *Expert Opinion on Investigational Drugs* 2009; **18**(8): 1061-83.
3. Singh SK, Hawkins C, Clarke ID, et al. Identification of human brain tumour initiating cells. *Nature* 2004; **432**(7015): 396-401.
4. van Breemen MSM, Rijsman RM, Taphoorn MJB, Walchenbach R, Zwinkels H, Vecht CJ. Efficacy of anti-epileptic drugs in patients with gliomas and seizures. *Journal of Neurology* 2009; **256**(9).

5. Buckingham SC, Campbell SL, Haas BR, et al. Glutamate release by primary brain tumors induces epileptic activity. *Nature Medicine* 2011; **17**(10).
6. Yuen TI, Morokoff AP, Bjorksten A, et al. Glutamate is associated with a higher risk of seizures in patients with gliomas. *Neurology* 2012; **79**(9).
7. Seal RP, Amara SG. Excitatory Amino Acid Transporters: A Family in Flux. *Annual Review of Pharmacology and Toxicology* 1999; **39**(1): 431-56.
8. Anderson CM, Swanson RA. Astrocyte glutamate transport: Review of properties, regulation, and physiological functions. *Glia* 2000; **32**(1): 1-14.
9. Bernardo A, Minghetti L. Regulation of Glial Cell Functions by PPAR-gamma Natural and Synthetic Agonists. *PPAR research* 2008; **2008**: 864140.
10. Romera C, Hurtado O, Mallolas J, et al. Ischemic preconditioning reveals that GLT1//EAAT2 glutamate transporter is a novel PPAR[gamma] target gene involved in neuroprotection. *J Cereb Blood Flow Metab* 2007; **27**(7): 1327-38.
11. Lee J, Reding M. Effects of Thiazolidinediones on Stroke Recovery: A Case-Matched Controlled Study. *Neurochemical Research* 2007; **32**(4): 635-8.
12. Kliewer SA. Fatty acids and eicosanoids regulate gene expression through direct interactions with peroxisome proliferator-activated receptors [alpha] and [gamma].
13. Nagy L, Schwabe JWR. Mechanism of the nuclear receptor molecular switch.
14. Greene ME, Blumberg B, McBride OW, et al. Isolation of the human peroxisome proliferator activated receptor gamma cDNA: Expression in hematopoietic cells and chromosomal mapping. *Gene Expression* 1995; **4**(4-5): 281-99.
15. Sher T, Yi HF, McBride OW, Gonzalez FJ. CDNA Cloning, Chromosomal Mapping, and Functional-characterization of the human Peroxisome Proliferator Activated Receptor. *Biochemistry* 1993; **32**(21): 5598-604.

16. Yoshikawa T, Brkanac Z, Dupont BR, Xing GQ, Leach RJ, DeteraWadleigh SD. Assignment of the human nuclear hormone receptor, NUC1 (PPARD), to chromosome 6p21.1-p21.2. *Genomics* 1996; **35**(3): 637-8.
17. Collino M, Patel NSA, Thiemermann C. PPAR as new therapeutic targets for the treatment of cerebral ischemia/reperfusion injury. *Therapeutic advances in cardiovascular disease* 2008; **2**(3): 179-97.
18. Fajas L, Auboeuf D, Raspe E, et al. The organization, promoter analysis, and expression of the human PPAR gamma gene. *Journal of Biological Chemistry* 1997; **272**(30): 18779-89.
19. Kumar R, Thompson EB. The structure of the nuclear hormone receptors. *Steroids* 1999; **64**(5): 310-9.
20. Juge-Aubry CE, Hammar E, Siegrist-Kaiser C, et al. Regulation of the transcriptional activity of the peroxisome proliferator-activated receptor alpha by phosphorylation of a dependent trans-activating domain. *Journal of Biological Chemistry* 1999; **274**(15): 10505-10.
21. Krey G, Braissant O, Lhorset F, et al. Fatty acids, eicosanoids, and hypolipidemic agents identified as ligands of peroxisome proliferator-activated receptors by coactivator-dependent receptor ligand assay. *Molecular Endocrinology* 1997; **11**(6): 779-91.
22. Kalkhoven E, Valentine JE, Heery DM, Parker MG. Isoforms of steroid receptor co-activator 1 differ in their ability to potentiate transcription by the oestrogen receptor. *Embo Journal* 1998; **17**(1): 232-43.
23. Onate SA, Tsai SY, Tsai MJ, Omalley BW. Sequence and Characterization of a Coactivator for the Steroid-hormone Receptor Superfamily. *Science* 1995; **270**(5240): 1354-7.
24. Dowell P, Ishmael JE, Avram D, Peterson VJ, Nevriy DJ, Leid M. p300 functions as a coactivator for the peroxisome proliferator-activated receptor alpha. *Journal of Biological Chemistry* 1997; **272**(52): 33435-43.

25. Gampe J, Robert T., Montana VG, Lambert MH, et al. Asymmetry in the PPAR. *Molecular Cell*; 2000. p. 545–55.
26. Bourguet W, Vivat V, Wurtz JM, Chambon P, Gronemeyer H, Moras D. Crystal structure of a heterodimeric complex of RAR and RXR ligand-binding domains.
27. Forman BM, Tontonoz P, Chen J, Brun RP, Spiegelman BM, Evans RM. 15-deoxy-delta(12,14)-prostaglandin j(2) is a Ligand for the Adipocyte Determination Factor PPAR-gamma. *Cell* 1995; **83**(5): 803-12.
28. Yamamoto Y, Yamazaki H, Ikeda T, et al. Formation of a novel quinone epoxide metabolite of troglitazone with cytotoxic to HepG2 cells. *Drug Metabolism and Disposition* 2002; **30**(2): 155-60.
29. Nissen SE, Wolski K. Effect of rosiglitazone on the risk of myocardial infarction and death from cardiovascular causes (vol 356, pg 2457, 2007). *New England Journal of Medicine* 2007; **357**(1): 100-.
30. Patel C, Wyne KL, McGuire DK. Thiazolidinediones, peripheral oedema and congestive heart failure: what is the evidence? *Diabetes & vascular disease research : official journal of the International Society of Diabetes and Vascular Disease* 2005; **2**(2): 61-6.
31. Zhang H, Zhang AH, Kohan DE, Nelson RD, Gonzalez FJ, Yang TX. Collecting duct-specific deletion of peroxisome proliferator-activated receptor gamma blocks thiazolidinedione-induced fluid retention. *Proceedings of the National Academy of Sciences of the United States of America* 2005; **102**(26): 9406-11.
32. Guan YF, Hao CM, Cha DR, et al. Thiazolidinediones expand body fluid volume through PPAR gamma stimulation of ENaC-mediated renal salt absorption. *Nature Medicine* 2005; **11**(8): 861-6.
33. Lincoff AM, Wolski K, Nicholls SJ, Nissen SE. Pioglitazone and risk of cardiovascular events in patients with type 2 diabetes mellitus - A meta-analysis of randomized trials. *Jama-Journal of the American Medical Association* 2007; **298**(10): 1180-8.

34. Lewis JD, Ferrara A, Peng T, et al. Risk of Bladder Cancer Among Diabetic Patients Treated With Pioglitazone Interim report of a longitudinal cohort study. *Diabetes Care* 2011; **34**(4): 916-22.
35. Colmers IN, Bowker SL, Majumdar SR, Johnson JA. Use of thiazolidinediones and the risk of bladder cancer among people with type 2 diabetes: a meta-analysis. *Canadian Medical Association Journal* 2012; **184**(12): E675-E83.
36. Braissant O, Wahli W. Differential expression of peroxisome proliferator-activated receptor- $\alpha$ , - $\beta$ , and - $\gamma$  during rat embryonic development. *Endocrinology* 1998; **139**(6): 2748-54.
37. Moreno S, Farioli-Vecchioli S, Ceru MP. Immunolocalization of peroxisome proliferator-activated receptors and retinoid X receptors in the adult rat CNS. *Neuroscience* 2004; **123**(1): 131-45.
38. Woods JW, Tanen M, Figueroa DJ, et al. Localization of PPAR delta in murine central nervous system: expression in oligodendrocytes and neurons. *Brain Research* 2003; **975**(1-2): 10-21.
39. Cristiano L, Bernardo A, Ceru MP. Peroxisome proliferator-activated receptors (PPAR) and peroxisomes in rat cortical and cerebellar astrocytes. *Journal of Neurocytology* 2001; **30**(8): 671-83.
40. Cullingford TE, Bhakoo K, Peuchen S, Dolphin CT, Patel R, Clark JB. Distribution of mRNAs encoding the peroxisome proliferator-activated receptor  $\alpha$ ,  $\beta$  and  $\gamma$  and the retinoid X receptor  $\alpha$ ,  $\beta$  and  $\gamma$  rat central nervous system. *Journal of Neurochemistry* 1998; **70**(4): 1366-75.
41. Jiang CY, Ting AT, Seed B. PPAR- $\gamma$  agonists inhibit production of monocyte inflammatory cytokines. *Nature* 1998; **391**(6662): 82-6.
42. Abdelrahman M, Sivarajah A, Thiemermann C. Beneficial effects of PPAR- $\gamma$  ligands in ischemia-reperfusion injury, inflammation and shock. *Cardiovascular Research* 2005; **65**(4): 772-81.
43. Sato T, Hanyu H, Hirao K, Kanetaka H, Sakurai H, Iwamoto T. Efficacy of PPAR- $\gamma$  agonist pioglitazone in mild Alzheimer disease. *Neurobiology of Aging* 2011; **32**(9): 1626-33.



44. Landreth G. Therapeutic use of agonists of the nuclear receptor PPAR gamma in Alzheimer's disease. *Current Alzheimer Research* 2007; **4**(2): 159-64.
45. Racke MK, Gocke AR, Muir M, Diab A, Drew PD, Lovett-Racke AE. Nuclear receptors and autoimmune disease: The potential of PPAR agonists to treat multiple sclerosis. *Journal of Nutrition* 2006; **136**(3): 700-3.
46. Chaturvedi RK, Beal MF. PPAR: a therapeutic target in Parkinson's disease. *Journal of Neurochemistry* 2008; **106**(2): 506-18.
47. Yue TL, Chen J, Bao WK, et al. In vivo myocardial protection from ischemia/reperfusion injury by the peroxisome proliferator-activated receptor-gamma agonist rosiglitazone. *Circulation* 2001; **104**(21): 2588-94.
48. Subbaramaiah K, Lin DT, Hart JC, Dannenberg AJ. Peroxisome proliferator-activated receptor gamma ligands suppress the transcriptional activation of cyclooxygenase-2 - Evidence for involvement of activator protein-1 and CREB-binding protein/p300. *Journal of Biological Chemistry* 2001; **276**(15): 12440-8.
49. Heneka MT, Feinstein DL, Galea E, Gleichmann M, Wullner U, Klockgether T. Peroxisome proliferator-activated receptor gamma agonists protect cerebellar granule cells from cytokine-induced apoptotic cell death by inhibition of inducible nitric oxide synthase. *Journal of Neuroimmunology* 1999; **100**(1-2): 156-68.
50. Shimazu T, Inoue I, Araki N, et al. A peroxisome proliferator-activated receptor-gamma agonist reduces infarct size in transient but not in permanent ischemia. *Stroke* 2005; **36**(2): 353-9.
51. Sundararajan S, Gamboa JL, Victor NA, Wanderi EW, Lust WD, Landreth GE. Peroxisome proliferator-activated receptor-gamma ligands reduce inflammation and infarction size in transient focal ischemia. *Neuroscience* 2005; **130**(3): 685-96.
52. Allahtavakoli M, Shabanzadeh A, Roohbakhsh A, Pourshanazari A. Combination therapy of rosiglitazone, a peroxisome proliferator-activated receptor-gamma ligand, and NMDA receptor

antagonist (MK-801) on experimental embolic stroke in rats. *Basic & Clinical Pharmacology & Toxicology* 2007; **101**(5): 309-14.

53. Barone FC, Feuerstein GZ. Inflammatory mediators and stroke: New opportunities for novel therapeutics. *Journal of Cerebral Blood Flow and Metabolism* 1999; **19**(8): 819-34.

54. Victor NA, Wanderi EW, Gamboa J, et al. Altered PPAR gamma expression and activation after transient focal ischemia in rats. *European Journal of Neuroscience* 2006; **24**(6): 1653-63.

55. Zhao Y, Patzer A, Gohlke P, Herdegen T, Culman J. The intracerebral application of the PPAR gamma-ligand pioglitazone confers neuroprotection against focal ischaemia in the rat brain. *European Journal of Neuroscience* 2005; **22**(1): 278-82.

56. Ou Z, Zhao X, Labiche LA, et al. Neuronal expression of peroxisome proliferator-activated receptor-gamma (PPAR gamma) and 15d-prostaglandin J(2) - Mediated protection of brain after experimental cerebral ischemia in rat. *Brain Research* 2006; **1096**: 196-203.

57. Curtis D, Johnston G. Amino acid transmitters in the mammalian central nervous system. *Ergebnisse der Physiologie, biologischen Chemie und experimentellen Pharmakologie* 1974; **69**(-1): 97-188.

58. Niels C D. Glutamate uptake. *Progress in Neurobiology* 2001; **65**(1): 1-105.

59. Sattler R, Tymianski M. Molecular mechanisms of calcium-dependent excitotoxicity. *Journal of Molecular Medicine-Jmm* 2000; **78**(1): 3-13.

60. Doyle KP, Simon RP, Stenzel-Poore MP. Mechanisms of ischemic brain damage. *Neuropharmacology* 2008; **55**(3): 310-8.

61. Culmsee C, Zhu CL, Landshamer S, et al. Apoptosis-inducing factor triggered by poly(ADP-ribose) polymerase and bid mediates neuronal cell death after oxygen-glucose deprivation and focal cerebral ischemia. *Journal of Neuroscience* 2005; **25**(44): 10262-72.

62. Broughton BRS, Reutens DC, Sobey CG. Apoptotic Mechanisms After Cerebral Ischemia. *Stroke* 2009; **40**(5): E331-E9.

63. Love S. Apoptosis and brain ischaemia. *Progress in Neuro-Psychopharmacology & Biological Psychiatry* 2003; **27**(2): 267-82.
64. Samdani AF, Dawson TM, Dawson VL. Nitric oxide synthase in models of focal ischemia. *Stroke* 1997; **28**(6): 1283-8.
65. Sheardown MJ, Nielsen EO, Hansen AJ, Jacobsen P, Honore T. 2,3-dihydroxy-6-nitro-7-sulfamoyl-benzo(f)quinoxaline - a Neuroprotectant for Cerebral-Ischemia. *Science* 1990; **247**(4942): 571-4.
66. Shen H, Chen GJ, Harvey BK, Bickford PC, Wang Y. Inosine reduces ischemic brain injury in rats. *Stroke* 2005; **36**(3): 654-9.
67. Villmann C, Becker C-M. On the hypes and falls in neuroprotection: Targeting the NMDA receptor. *Neuroscientist* 2007; **13**(6): 594-615.
68. Harvey BK, Airavaara M, Hinzman J, et al. Targeted Over-Expression of Glutamate Transporter 1 (GLT-1) Reduces Ischemic Brain Injury in a Rat Model of Stroke. *Plos One* 2011; **6**(8).
69. Chu K, Lee ST, Jung KH, Kim M, Roh JK. Upregulation of glutamate transporter-1 by ceftriaxone induces prolonged ischemic tolerance. *Stroke* 2006; **37**(2): 730-.
70. Chu K, Lee S-T, Sinn D-I, et al. Pharmacological induction of ischemic tolerance by glutamate transporter-1 (EAAT2) upregulation. *Stroke* 2007; **38**(1): 177-82.
71. Verma R, Mishra V, Sasmal D, Raghurir R. Pharmacological evaluation of glutamate transporter 1 (GLT-1) mediated neuroprotection following cerebral ischemia/reperfusion injury. *European Journal of Pharmacology* 2010; **638**(1-3): 65-71.
72. Sattler R, Tyler BB, Hoover B, et al. Increased expression of glutamate transporter GLT-1 in peritumoral tissue associated with prolonged survival and decreases in tumor growth in a rat model of experimental malignant glioma *Journal of Neurosurgery*; 2013. p. 1-9.

73. Cimini A, Cristiano L, Bernardo A, Farioli-Vecchioli S, Stefanini S, Ceru MP. Presence and inducibility of peroxisomes in a human glioblastoma cell line. *Biochimica Et Biophysica Acta-General Subjects* 2000; **1474**(3): 397-409.
74. Elstner E, Williamson EA, Zang C, et al. Novel therapeutic approach: ligands for PPAR gamma and retinoid receptors induce apoptosis in bcl-2-positive human breast cancer cells. *Breast Cancer Research and Treatment* 2002; **74**(2): 155-65.
75. Sarraf P, Mueller E, Jones D, et al. Differentiation and reversal of malignant changes in colon cancer through PPAR gamma. *Nature Medicine* 1998; **4**(9): 1046-52.
76. Lee MW, Kim DS, Kim HR, et al. Cell death is induced by ciglitazone, a peroxisome proliferator-activated receptor gamma (PPAR gamma) agonist, independently of PPAR gamma in human glioma cells. *Biochemical and Biophysical Research Communications* 2012; **417**(1): 552-7.
77. Grommes C, Landreth GE, Heneka MT. Antineoplastic effects of peroxisome proliferator-activated receptor gamma agonists. *Lancet Oncology* 2004; **5**(7): 419-29.
78. Tatenhorst L, Hahnen E, Heneka MT. Peroxisome Proliferator-Activated Receptors (PPAR) as Potential Inducers of Antineoplastic Effects in CNS Tumors. *Ppar Research* 2008.
79. Wang P, Yu J, Yin Q, Li W, Ren X, Hao X. Rosiglitazone Suppresses Glioma Cell Growth and Cell Cycle by Blocking the Transforming Growth Factor-Beta Mediated Pathway. *Neurochemical Research* 2012; **37**(10): 2076-84.
80. Wan Z, Shi W, Shao B, et al. Peroxisome proliferator-activated receptor gamma agonist pioglitazone inhibits beta-catenin-mediated glioma cell growth and invasion. *Molecular and Cellular Biochemistry* 2011; **349**(1-2): 1-10.
81. Embi N, Rylatt D, Cohen P. Glycogen synthase kinase-3 from rabbit skeletal muscle. Separation from cyclic-AMP-dependent protein kinase and phosphorylase kinase. *European Journal of Biochemistry*. p. 519-27.

82. Leroy K, Brion J-P. Developmental expression and localization of glycogen synthase kinase-3 $\beta$  in rat brain. 1999. p. 279-93.
83. Kelly S, Zhao H, Sun GH, et al. Glycogen synthase kinase 3h inhibitor Chir025 reduces neuronal death resulting from oxygen-glucose deprivation, glutamate excitotoxicity, and cerebral ischemia *Experimental Neurology*; 2004. p. 378–86
84. Martinez A, Alonso M, Castro A, Perez C, Moreno FJ. First Non-ATP Competitive Glycogen Synthase Kinase 3 *Journal of Medicinal Chemistry*; 2002. p. 1292-9
85. Wang Z, Smith KS, Murphy M, Piloto O, Somerville TCP, Cleary ML. Glycogen synthase kinase 3 in *MLL* leukaemia maintenance and targeted therapy. 2008. p. 1205-9.
86. Jing TL, Zhuang Hui-Sun, LeongN. Gopalakrishna, IyerEdison T. Lu Qiang Yu. Pharmacologic Modulation of Glycogen Synthase Kinase-3 $\beta$  Promotes p53-Dependent Apoptosis through a Direct Bax-Mediated Mitochondrial Pathway in Colorectal Cancer Cells. 2005. p. 9012-20.
87. Korur S, Huber RM, Sivasankaran B, et al. GSK3b Regulates Differentiation and Growth Arrest in Glioblastoma *PlosONE*; 2009.
88. Atkins RJ, Dimou J, Paradiso L, et al. Regulation of glycogen synthase kinase-3 beta (GSK-3b) by the Akt pathway in gliomas. *Journal of Clinical Neuroscience*; 2012. p. 1558-63.
89. Lo M, Wang YZ, Gout PW. The x(c)(-) cystine/glutamate antiporter: A potential target for therapy of cancer and other diseases. *Journal of Cellular Physiology* 2008; **215**(3): 593-602.
90. Ye ZC, Sontheimer H. Glioma cells release excitotoxic concentrations of glutamate. *Cancer Research* 1999; **59**(17): 4383-91.
91. Chung WJ, Lyons SA, Nelson GM, et al. Inhibition of cystine uptake disrupts the growth of primary brain tumors. *Journal of Neuroscience* 2005; **25**(31).
92. Lyons SA, Chung WJ, Weaver AK, Ogunrinu T, Sontheimer H. Autocrine glutamate signaling promotes glioma cell invasion. *Cancer Research* 2007; **67**(19): 9463-71.

93. Chung J, Sontheimer H. Sulfasalazine inhibits the growth of primary brain tumors independent of nuclear factor- $\kappa$ B. *J Neurochem*; 2009. p. 182–93.
94. Robe PA, Martin DH, Nguyen-Khac MT, et al. Early termination of ISRCTN45828668, a phase 1/2 prospective, randomized study of Sulfasalazine for the treatment of progressing malignant gliomas in adults. *Bmc Cancer* 2009; **9**.
95. Ye Z-C, Rothstein JD, Sontheimer H. Compromised Glutamate Transport in Human Glioma Cells: Reduction–Mislocalization of Sodium-Dependent Glutamate Transporters and Enhanced Activity of Cystine–Glutamate Exchange. *Journal of Neuroscience*; 2000. p. 10767–77.
96. de Groot JF, Liu TJ, Fuller GWK, Yung A. The Excitatory Amino Acid Transporter-2 Induces Apoptosis and Decreases Glioma Growth In vitro and In vivo. 2005. p. 1934-40.
97. Pestereva E, Kanakasabai S, Bright JJ. PPAR gamma agonists regulate the expression of stemness and differentiation genes in brain tumour stem cells. *British Journal of Cancer* 2012; **106**(10).
98. Chearwae W, Bright JJ. PPAR gamma agonists inhibit growth and expansion of CD133+brain tumour stem cells. *British Journal of Cancer* 2008; **99**(12): 2044-53.
99. Kurian KM. The impact of neural stem cell biology on CNS carcinogenesis and tumor types. *Pathology research international* 2011; **2011**: 685271.
100. Louis DN. Molecular Pathology of Malignant Gliomas. *Annual Review of Pathology: Mechanisms of Disease* 2006; **1**(1): 97-117.
101. Stiles C, Rowitch D. Glioma stem cells: a midterm exam. 2008. p. 832-46.
102. Gilley J, Kernie S. Excitatory amino acid transporter 2 and excitatory amino acid transporter 1 negatively regulate calcium-dependent proliferation of hippocampal neural progenitor cells and are persistently upregulated after injury. *European Journal of Neuroscience*; 2011. p. 1712–23.
103. Okada K, Yamashita U, Tsuji S. Ameliorative effect of pioglitazone on seizure responses in genetically epilepsy-susceptible EL mice. *Brain Research* 2006; **1102**: 175-8.

104. Mohazab RA, Javadi-Paydar M, Delfan B, Dehpour AR. Possible involvement of PPAR-gamma receptor and nitric oxide pathway in the anticonvulsant effect of acute pioglitazone on pentylenetetrazole-induced seizures in mice. *Epilepsy Research* 2012; **101**(1-2): 28-35.
105. Shafaroodi H, Moezi L, Ghorbani H, et al. Sub-chronic treatment with pioglitazone exerts anti-convulsant effects in pentylenetetrazole-induced seizures of mice: The role of nitric oxide. *Brain Research Bulletin* 2012; **87**(6): 544-50.
106. Choi JH, Banks AS, Estall JL, et al. Anti-diabetic drugs inhibit obesity-linked phosphorylation of PPARc by Cdk5 Nature; 2010. p. 451-7.
107. Choi JHB, Alexander S. Kamenecka, Theodore M. Busby, Scott A. Chalmers, Michael J. Kumar, Naresh Kuruvilla, Dana S. Shin, Youseung He, Yuanjun Bruning, John B. Marciano, David P. Cameron, Michael D. Laznik, Dina Jurczak, Michael J. Schurer, Stephan C. Vidovic, Dusica Shulman, Gerald I. Spiegelman, Bruce M. Griffin, Patrick R. Antidiabetic actions of a non-agonist PPAR gamma ligand blocking Cdk5-mediated phosphorylation. *Nature*; 2011. p. 477-81.
108. Ahmadian M, Suh JM, Hah N, et al. PPAR gamma signaling and metabolism: the good, the bad and the future. *Nature Medicine*; 2013. p. 557-66.
109. Stupp R, Hegi ME, Mason WP, et al. Effects of radiotherapy with concomitant and adjuvant temozolomide versus radiotherapy alone on survival in glioblastoma in a randomised phase III study: 5-year analysis of the EORTC-NCIC trial. *The Lancet Oncology* 2009; **10**(5): 459-66.
110. Colton CK, Kong Q, Lai L, et al. Identification of Translational Activators of Glial Glutamate Transporter EAAT2 through Cell-Based High-Throughput Screening. *Journal of Biomolecular Screening* 2010; **15**(6): 653-62.
111. Hawkins RD, Hon GC, Ren B. Next-Generation Genomics: an Integrative Approach *Nature Reviews Genetics*; 2010. p. 476–86.
112. Lefterova MI, Steger DJ, Zhuo D, et al.: *Molecular and Cellular Biology*; 2010. p. 2078–89.

113. Hamza MS, Pott S, Vega VB, et al. De-Novo Identification of PPARc/RXR Binding Sites and Direct Targets during Adipogenesis. *PLoS ONE*; 2009. p. e4907.
114. Kast RE et al. A conceptually new treatment approach for relapsed glioblastoma: Coordinated undermining of survival paths with nine repurposed drugs (CUSP9) by the International Initiative for Accelerated Improvement of Glioblastoma Care Oncotarget; 2013. p. 502-30.
115. Grommes C, Karlo JC, Andrew C, D'Arbra B, Anne D, E. LG. The PPAR $\gamma$  agonist pioglitazone crosses the blood-brain barrier and reduces tumor growth in a human xenograft model. *Cancer Chemotherapy and Pharmacology*; 2013. p. 929-36.
116. Chearwae WB, J J. PPAR gamma agonists inhibit growth and expansion of CD133+ brain tumour stem cells. *British Journal of Cancer*; 2008. p. 2044-53
117. Coras R, Holsken A, Seufert S, et al. The peroxisome proliferator-activated receptor- $\gamma$  agonist troglitazone inhibits transforming growth factor- $\beta$ -mediated glioma cell migration and brain invasion. *Molecular Cancer Therapeutics*; 2007. p. 1745-54.
118. Spagnolo A, Glick RP, Lin H, Cohen EP, Feinstein DL, Lichtor T. Prolonged survival of mice with established intracerebral glioma receiving combined treatment with peroxisome proliferator-activated receptor-gamma thiazolidinedione agonists and interleukin-2-secreting syngeneic/allogeneic fibroblasts. *Journal of Neurosurgery* 2007; **106**(2): 299-305.
119. Grommes C, Landreth GE, Sastre M, et al. Inhibition of in vivo glioma growth and invasion by peroxisome proliferator-activated receptor gamma agonist treatment. *Molecular Pharmacology* 2006; **70**(5): 1524-33.
120. Grommes C, Landreth GE, Schlegel U, Heneka MT. The nonthiazolidinedione tyrosine-based peroxisome proliferator-activated receptor gamma ligand GW7845 induces apoptosis and limits migration and invasion of rat and human glioma cells. *Journal of Pharmacology and Experimental Therapeutics* 2005; **313**(2): 806-13.



121. Liu DC, Zang CB, Liu HY, Possinger K, Fan SG, Elstner E. A novel PPAR alpha/gamma dual agonist inhibits cell growth and induces apoptosis in human glioblastoma T98G cells. *Acta Pharmacologica Sinica* 2004; **25**(10): 1312-9.
122. Chandra V, Huang P, Hamuro Y, et al. Structure of the intact PPAR-gamma-RXR- nuclear receptor complex on DNA.

### **Table and figure legend**

Table 1. Summary of research at the time of writing demonstrating antineoplastic efficacy of peroxisome proliferator activated receptor gamma (PPAR $\gamma$ ) agonists against gliomas. The dual PPAR $\alpha/\gamma$  agonist thiazolidinediones 18 (TDZ18) has shown efficacy but has not been included in this review as it not a pure PPAR $\gamma$  agonist.<sup>121</sup>

Fig. 1. Peroxisome proliferator activated receptor gamma (PPAR $\gamma$ ) – retinoid X receptors heterodimer complex with synthetic PPAR $\gamma$  agonist rosiglitazone and 9-cis-retinoic acid in place, bound to the PPAR response elements DNA binding site with two zinc fingers. Adapted from Protein Data Bank Entry 3DZY using University of California San Francisco Chimera.<sup>122</sup>

Fig. 2. Schematic of a glioma cell exchanging glutamate for cysteine through system Xc- and peroxisome proliferator activated receptor gamma (PPAR $\gamma$ ) mediated upregulation of excitatory amino acid transporter 2 (EAAT2) and subsequent uptake of glutamate. The adjacent cell (astrocyte or neuron) is undergoing glutamate mediated excitotoxicity. Cystein is advantageous since it forms glutathione which acts as electron donor to free radicals, being reduced to glutathione disulphide (or

L-(-)-glutathione. PPAR $\gamma$  – retinoid X receptors heterodimer binding at the peroxisome proliferator response element (PPRE). Illustration by Suankaew Chueysai.

AMPA =  $\alpha$ -amino-3-hydroxy-5-methyl-4-isox-azole propionate, NMDA = N-methyl-D-aspartate.



# The peroxisome proliferator activated receptor gamma agonist pioglitazone increases functional expression of the glutamate transporter excitatory amino acid transporter 2 (EAAT2) in human glioblastoma cells

Jared Ching<sup>1,2</sup>, Stephanie Amiridis<sup>1,2</sup>, Stanley S. Stylli<sup>1,4</sup>, Andrew R. Bjorksten<sup>3</sup>, Nicole Kountouri<sup>1</sup>, Thomas Zheng<sup>2</sup>, Lucy Paradiso<sup>1</sup>, Rodney B. Luwor<sup>1</sup>, Andrew P. Morokoff<sup>1,4</sup>, Terence J. O'Brien<sup>2</sup>, Andrew H. Kaye<sup>1,4</sup>

<sup>1</sup>Department of Surgery, The University of Melbourne, The Royal Melbourne Hospital, Victoria, Australia

<sup>2</sup>Department of Medicine, The University of Melbourne, The Royal Melbourne Hospital, Victoria, Australia

<sup>3</sup>Department of Anaesthesia and Pain Management, The Royal Melbourne Hospital, Victoria, Australia

<sup>4</sup>Department of Neurosurgery, The Royal Melbourne Hospital, Victoria, Australia

## Correspondence to:

Andrew H. Kaye, e-mail: a.kaye@unimelb.edu.au

Keywords: glutamate, pioglitazone, PPAR gamma, glioblastoma multiforme, EAAT2

Received: March 19, 2015

Accepted: May 21, 2015

Published: June 03, 2015

## ABSTRACT

**Glioma cells release glutamate through expression of system  $x_c^-$ , which exchanges intracellular glutamate for extracellular cysteine. Lack of the excitatory amino acid transporter 2 (EAAT2) expression maintains high extracellular glutamate levels in the glioma microenvironment, causing excitotoxicity to surrounding parenchyma. Not only does this contribute to the survival and proliferation of glioma cells, but is involved in the pathophysiology of tumour-associated epilepsy (TAE). We investigated the role of the peroxisome proliferator activated receptor gamma (PPAR $\gamma$ ) agonist pioglitazone in modulating EAAT2 expression in glioma cells. We found that EAAT2 expression was increased in a dose dependent manner in both U87MG and U251MG glioma cells. Extracellular glutamate levels were reduced with the addition of pioglitazone, where statistical significance was reached in both U87MG and U251MG cells at a concentration of  $\geq 30 \mu\text{M}$  pioglitazone ( $p < 0.05$ ). The PPAR $\gamma$  antagonist GW9662 inhibited the effect of pioglitazone on extracellular glutamate levels, indicating PPAR $\gamma$  dependence. In addition, pioglitazone significantly reduced cell viability of U87MG and U251MG cells at  $\geq 30 \mu\text{M}$  and  $100 \mu\text{M}$  ( $p < 0.05$ ) respectively. GW9662 also significantly reduced viability of U87MG and U251MG cells with  $10 \mu\text{M}$  and  $30 \mu\text{M}$  ( $p < 0.05$ ) respectively. The effect on viability was partially dependent on PPAR $\gamma$  activation in U87MG cells but not U251MG cells, whereby PPAR $\gamma$  blockade with GW9662 had a synergistic effect. We conclude that PPAR $\gamma$  agonists may be therapeutically beneficial in the treatment of gliomas and furthermore suggest a novel role for these agents in the treatment of tumour associated seizures through the reduction in extracellular glutamate.**

## INTRODUCTION

Glutamate is the most abundant neurotransmitter in the mammalian central nervous system and mediates its excitatory physiological effect by binding to ionotropic and metabotropic receptors. [1, 2] Glioma cells release glutamate through expression of the  $x_c^-$  exchanger, which exchanges intracellular glutamate for extracellular

cysteine. [3] Intracellular uptake of cysteine via system  $x_c^-$  permits glioma cell survival through glutathione formation. Excitatory amino acid transporter 2 (EAAT2) is one of 5 subtypes of sodium dependent plasma membrane glutamate transporters that accounts for up to 90% of extracellular glutamate uptake, with Glutamate Aspartate Transporter (GLAST-1) accounting for the largest remaining proportion. [4, 5] Glioma cell lines

lack expression of both EAAT2 and GLAST-1, which is associated with impaired glutamate uptake. [3, 6] Together, these features result in abnormally high extracellular glutamate concentrations resulting in excitotoxicity, causing necrosis of the adjacent parenchyma, which creates space permitting proliferation. [7, 8] Additionally, cysteine uptake provides a precursor for the formation of glutathione, which is protective against endogenous reactive oxygen species and further promotes glioma growth. [7] Furthermore, deranged glutamate transport has been associated with the pathogenesis of glial tumour associated epilepsy (TAE). [9, 10]

PPAR $\gamma$  is a ligand-dependent transcription factor that responds to both physiological and chemical stimuli, including the cyclopentanone prostaglandin, 15-deoxy $\Delta^{12,14}$  prostaglandin J<sub>2</sub> (15d-PGJ<sub>2</sub>) and thiazolidinediones (TDZ) respectively. [11] Expression of PPAR $\gamma$  in the brain has been found in multiple cell types including microglia, astrocytes, oligodendrocytes, and neurons. It has been shown in rat cortical cultures incubated with the commercially available PPAR $\gamma$  agonist rosiglitazone, that this drug increases the expression levels of EAAT2 at both the protein and mRNA levels. [12] Furthermore, reduction in the infarct volume after administration of rosiglitazone in rats with middle cerebral artery occlusion demonstrated in this study strongly supports the clinical evidence of better neurological outcomes found in a small case-matched controlled study investigating stroke recovery with TDZ drugs. [12, 13]

Increased PPAR $\gamma$  expression has been associated with beneficial effects in cancers including breast and colon, including a reduction in cell proliferation and improved patient prognoses. [14–17] In comparison to other cancer cell lines, it has been observed that glioma cells express lower endogenous levels of PPAR $\gamma$ . [18] Nevertheless, there is a growing body of evidence that demonstrates several mechanisms by which PPAR $\gamma$  agonists elicit anti-neoplastic effects in gliomas. Pioglitazone has been shown to reduce the expression of  $\beta$ -catenin independently of PPAR $\gamma$ . [19] Others have observed that the PPAR $\gamma$  agonist citaglitazone mediates glioma cell apoptosis independently of PPAR $\gamma$  through the reduction of Akt and induction of mitochondrial membrane potential loss. [18] Citaglitazone has also been shown to inhibit proliferation of brain tumour stem cells and expression of stemness genes in de-differentiated glioma cell lines. [20] Most recently, Grommes and colleagues demonstrated the efficacy of pioglitazone in reducing tumour growth with a human glioma xenograft model, highlighting the ability of pioglitazone to cross the blood brain barrier. [21]

Glycogen Synthase Kinase 3 (GSK3) is a serine/threonine protein kinase, which was first characterised in 1980 and is inactivated by phosphorylation at serine 21 in GSK-3 $\alpha$  or serine 9 in GSK-3 $\beta$ . [22, 23] PPAR $\gamma$  agonists are known to be GSK3 inhibitors, which has been shown

to have a neuroprotective role in stroke models through the promotion of cell survival. [24, 25] Although active GSK3 has been known to inhibit survival pathways, the inhibition of GSK3 has been paradoxically shown to be effective against several neoplasms. [26, 27] GSK3 inhibition in glioma stem cells has also been observed to induce differentiation and regulate proliferation by Korur and colleagues. [28]

As glioma cells express some PPAR $\gamma$ , we were interested in the potential of PPAR $\gamma$  agonists in increasing the expression of the glutamate transporter EAAT2. Herein, we describe a novel mechanism of the PPAR $\gamma$  agonist, pioglitazone, in which we demonstrate its ability to increase EAAT2 expression and consequently extracellular glutamate levels in glioma cells. In addition we show that this agent alters cellular morphology, whilst also reducing the viability of human glioblastoma cell lines. These results warrant further investigation into the potential role of this class of agents in both anti-neoplastic and anti-convulsant therapy in gliomas.

## RESULTS

### Human glioblastoma multiforme (GBM) cell lines express low levels of the glutamate transporters EAAT2 and GLAST-1

We established the baseline expression of the glutamate transporters EAAT2 and GLAST-1 (EAAT1) in a number of glioma cell lines (U87MG, U251MG and GSC #35) relative to rodent normal brain tissue as a control. EAAT2 and GLAST-1 were expressed in low levels in these cell lines in comparison to the rat brain cortex and thalamus control tissues (Figure 1). This was in keeping with previous literature results with respect to EAAT2 and GLAST-1 basal expression levels observed in U251MG and U87MG cells respectively. [6, 29] Interestingly, we detected higher basal levels of PPAR $\gamma$  in the glioma cells compared to the normal brain tissue controls (Figure 1).

### Pioglitazone increases expression of EAAT2 and PPAR $\gamma$ but not GLAST-1 in U87MG and U251MG cells

To determine whether glutamate transporters in glioma cells could be modulated with PPAR $\gamma$  agonists as with astrocytes, we treated glioma cells with increasing concentrations of pioglitazone. Incubating U87MG and U251MG cell lines with pioglitazone resulted in a dose dependent activation of EAAT2 and PPAR $\gamma$  but not GLAST-1 protein expression (Figure 2). PPAR $\gamma$  protein expression was also increased in this manner. We confirmed that EAAT2 expression is unchanged in GSC #35 by pioglitazone (Figure 3).

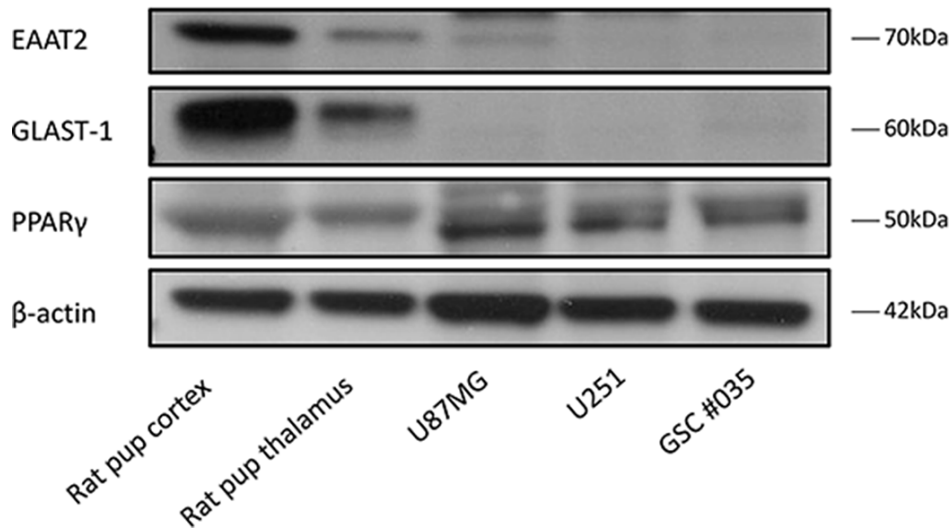


**Figure 1: Representative blots showing EAAT2, GLAST-1, PPAR $\gamma$  and  $\beta$ -actin expression in rat cortex, thalamus and glioma cells. EAAT2 and GLAST-1 are expressed in low levels in glioblastoma cell lines and glioma stem cells.**

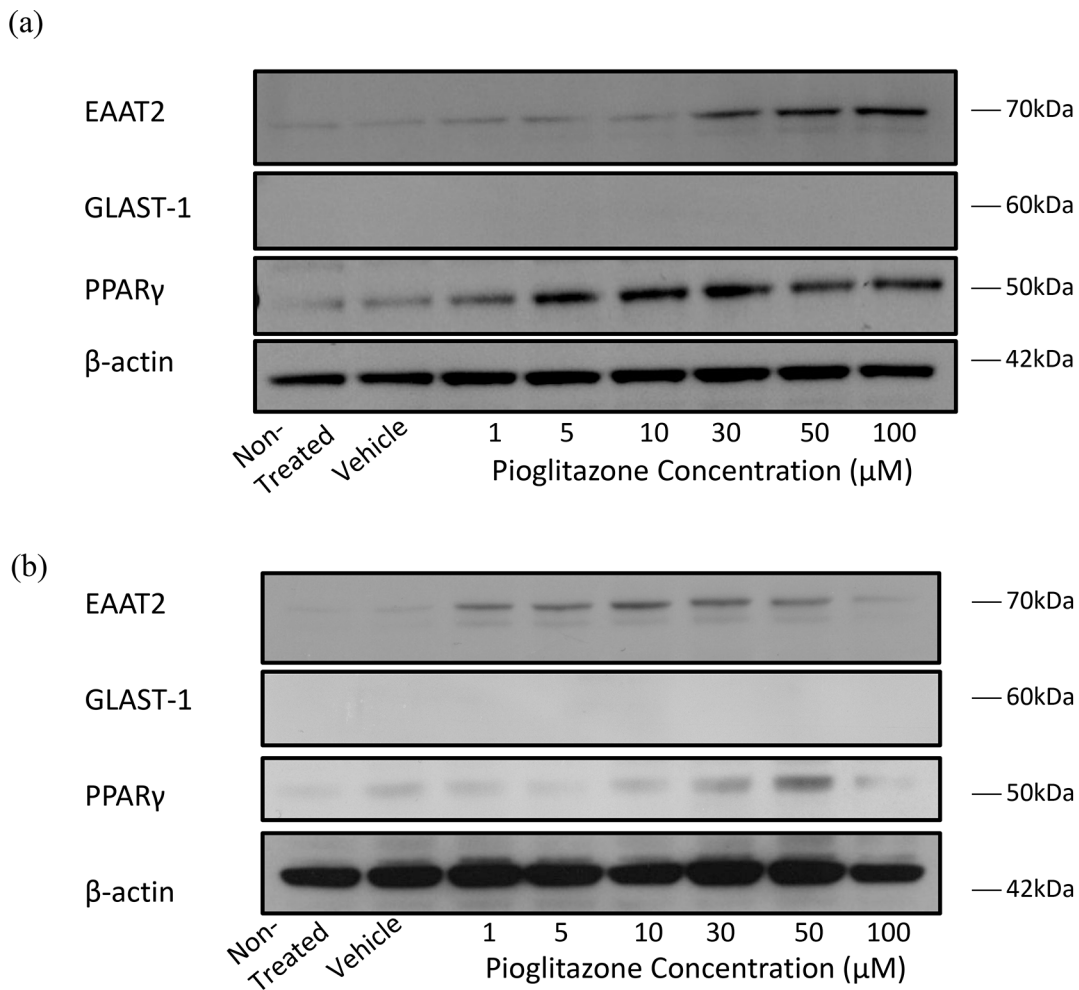


**Figure 2: Representative blots showing EAAT2, GLAST-1, PPAR $\gamma$  and  $\beta$ -actin expression in glioma cells treated with increasing concentrations of pioglitazone for 48 hours. Representative blots showing EAAT2, GLAST-1, PPAR $\gamma$  and  $\beta$ -actin expression in (a) U87MG and (b) U251MG glioma cells treated with increasing concentrations of pioglitazone for 48 hours.**

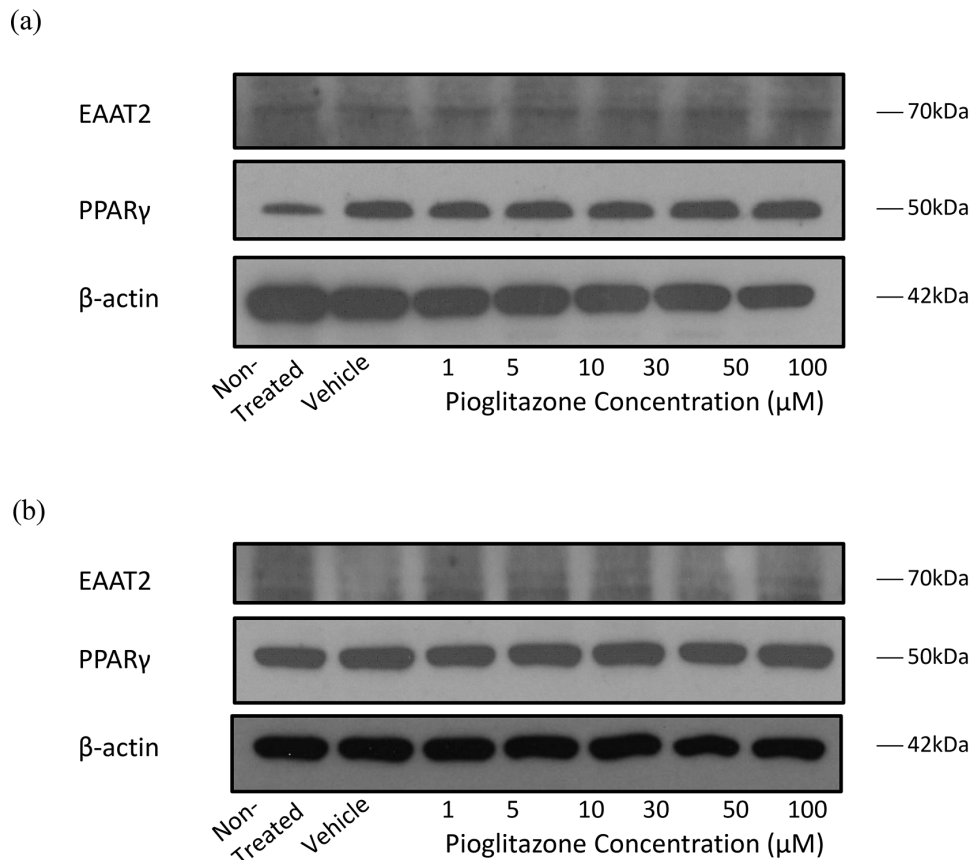


**Figure 3: Representative blots showing EAAT2, PPAR $\gamma$  and  $\beta$ -actin expression in GSC #035 cells treated with increasing concentrations of pioglitazone for 72 hours alone (a) and with 5  $\mu$ M GW9662 (b).**

### Pioglitazone reduces the cell viability of GBM cell lines

Concentrations of pioglitazone of 30  $\mu$ M or above resulted in a significant reduction in cell viability of U87MG cells (Figure 4(a)). In U251MG glioma cells, a significant reduction in cell viability was only observed at a pioglitazone concentration of 100  $\mu$ M (Figure 4(b)). However, pioglitazone was not found to elicit cytotoxicity in GSC #35 (Figure 6(a-h)).

### GW9662 reduces viability of GBM cell lines

U87MG cell viability was reduced significantly when exposed to 10  $\mu$ M or above of the PPAR $\gamma$  blocker GW9662 (Figure 4(c)), whereas a reduction in U251MG cell viability was observed at concentrations of 30  $\mu$ M or above (Figure 4(d)). GSC #35 did not demonstrate such sensitivity to GW9662 (Figure 6(b-d)).

### Pioglitazone efficacy is partially dependent on PPAR $\gamma$ activation in U87MG but not in U251MG cells

The loss in cell viability caused by a cytostatic concentration of pioglitazone in U87MG cells was

diminished when co-incubated with GW9662 at a concentration of 10  $\mu$ M or above (Figure 5(a)). Earlier we showed that GW9662 alone significantly reduced U87MG cell viability at the same concentrations, but in combination with pioglitazone there was a reduced effect compared to pioglitazone alone. U251MG cells demonstrated an opposing phenomenon whereby increasing doses of GW9662 resulted in a significant dose dependent reduction in cellular viability (Figure 5(b)).

### Pioglitazone reduces extracellular glutamate release from glioma cells

In order to elucidate whether glutamate uptake in glioma cells is increased by any potential reduction in glutamate transporters, we measured glutamate levels in the glioma culture media. As the glioma cell lines U87MG and U251MG were cultured in media containing 5% FCS, a high glutamate background was expected as has been previously reported. [30] We determined the background glutamate concentration in culture medium was  $34.16 \mu\text{M} \pm 12.08$  (data not shown). In U87MG cells we observed a significant dose-dependent reduction in extracellular glutamate levels with increasing concentrations of pioglitazone  $\geq 30 \mu\text{M}$  at 72 hours (Figure 7(a)). A similar observation was made with

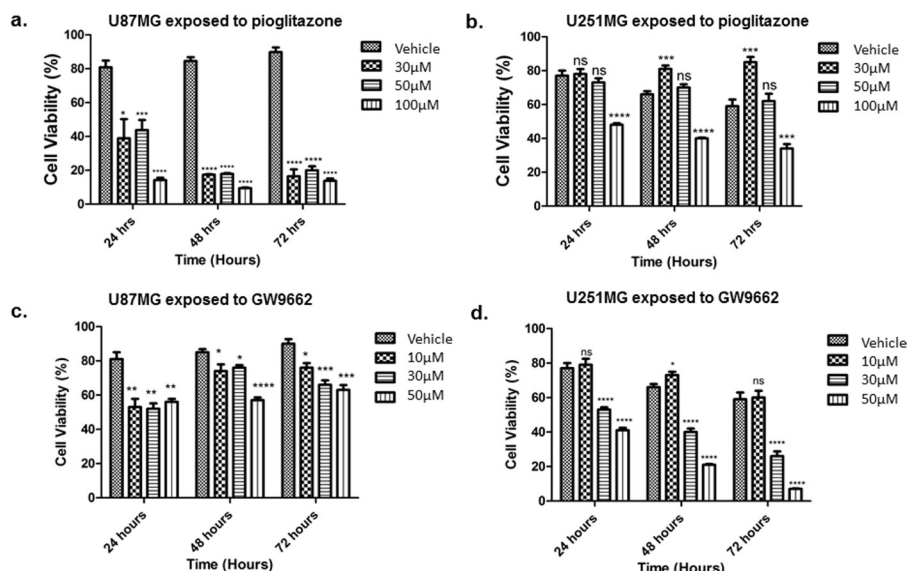


**Figure 4: Effect of increasing concentrations of pioglitazone on U87MG (a) and U251 (b) glioma cells.** Pio concentrations of 30  $\mu\text{M}$  U87MG cells (a) and a concentration of 100  $\mu\text{M}$  in U251MG (b) results in a significant reduction in cell viability. Effect of increasing concentrations of GW9662 on U87MG (c) and U251 (d) Cell lines. (c) GW9662 concentration of 10  $\mu\text{M}$  or above resulted in a significant reduction of cell viability in U87MG glioma cells. (d) GW9662 concentration of 10  $\mu\text{M}$  and above were required for a significant reduction in cell viability of U251MG cells. Bars show mean with SEM, ns refers to non-significance, and asterisks indicate statistical significance where  $*p = 0.01$  to 0.05,  $**p = 0.001$  to 0.01,  $***p < 0.001$ , and  $****p < 0.0001$ . Student's *t*-test,  $n = 4$  (a),  $n = 6$  (b).

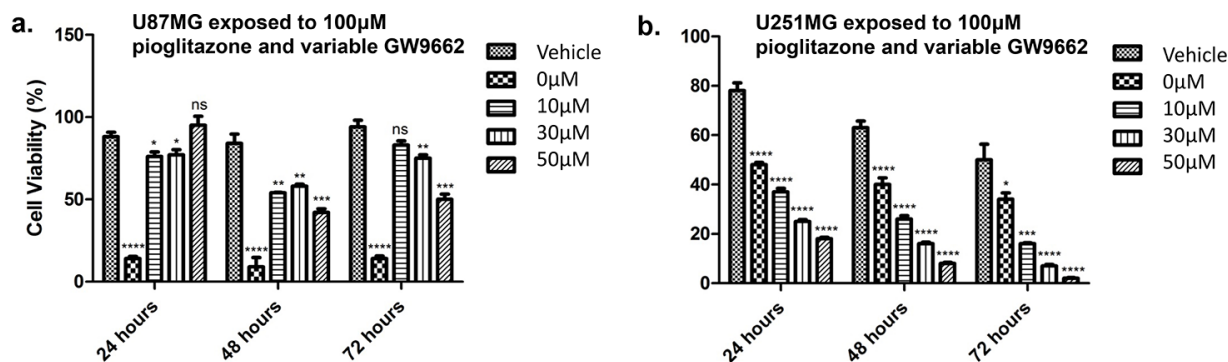


**Figure 5: Effect of increasing concentrations of GW9662 with co-treatment of high dose (100  $\mu\text{M}$ ) pioglitazone on U87MG (a) and U251MG (b) glioma cell lines.** (a) Inhibition of PPAR with GW9662 reduced the fall in cell viability that was caused by a high concentration of pioglitazone alone. (b) Pioglitazone and GW9662 co-treatment result in synergistic decrease cell viability of U251MG cells. Bars show mean with SEM, ns refers to non-significance, and asterisks indicate statistical significance where  $*p = 0.01$  to 0.05,  $**p = 0.001$  to 0.01,  $***p < 0.001$ , and  $****p < 0.0001$ . Student's *t*-test,  $n = 4$  (a),  $n = 6$  (b).

U251MG (Figure 8(a)). This correlated with the change in protein expression, where increased EAAT2 expression was highest at pioglitazone concentrations of 30  $\mu\text{M}$  and 10  $\mu\text{M}$  in U87MG and U251MG respectively (Figure 2(a) & (b)). These results suggest that pioglitazone-induced upregulation of EAAT2 leads to increased uptake of extracellular glutamate. These results were not corroborated in GSC #35, where no significant change in extracellular glutamate was elucidated (Figure 9(a)). Although GW9662 was associated with a significant reduction in glutamate in U87MG and U251MG cells at

$\geq 30 \mu\text{M}$  and 50  $\mu\text{M}$  respectively (Figure 7(b) & 8(b)), these concentrations were associated with a significant reduction in cell viability (Figure 4(c) & (d)).

### Pioglitazone mediated reduction in extracellular glutamate is PPAR $\gamma$ dependent

To confirm whether EAAT2 modulation in glioma cells using pioglitazone was PPAR $\gamma$  dependent, the U87MG and U251MG glioma cell lines were treated with GW9662 alone and co-administration of pioglitazone and GW9662.

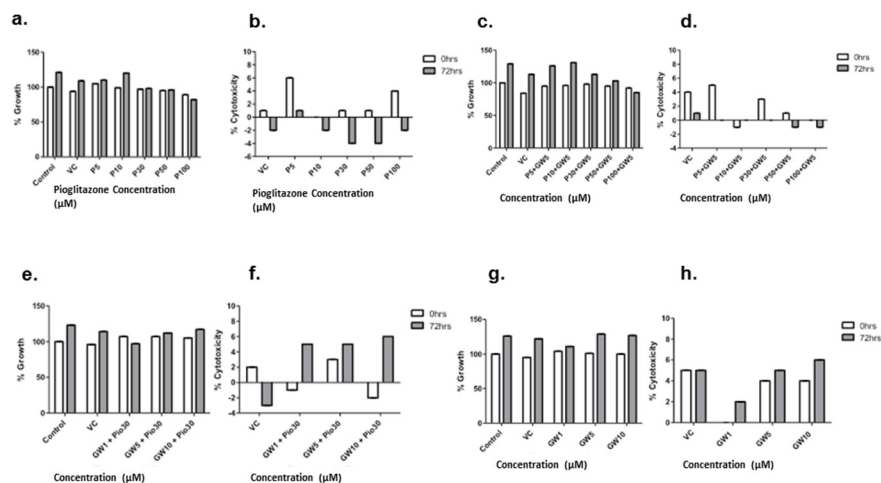


**Figure 6: Effect of increasing concentrations of Pioglitazone and/or GW9662 treatment on glioma stem cell line #035.** Cell growth and cell death was detected using the LDH assay at 0 hour and 72 hours. Addition of 30  $\mu\text{M}$  or more of Pioglitazone reduces cell growth at 72 hours (a) however this reduction is lessened by the addition of GW9662 (c & e) GW alone does not promote cell growth compared to the control (g) Treatment with increasing concentrations of GW9662 and 30  $\mu\text{M}$  of Pioglitazone causes reduction of growth compared to GW 9662 alone. No treatments caused significant cytotoxicity further supporting Pioglitazone as a cytostatic agent (b, d, f & h) Bars show means with SEM, ns refers to non-significance. Student *t* test,  $n = 3$  (a–d). All results were non-significant,  $p$  value  $> 0.05$ .

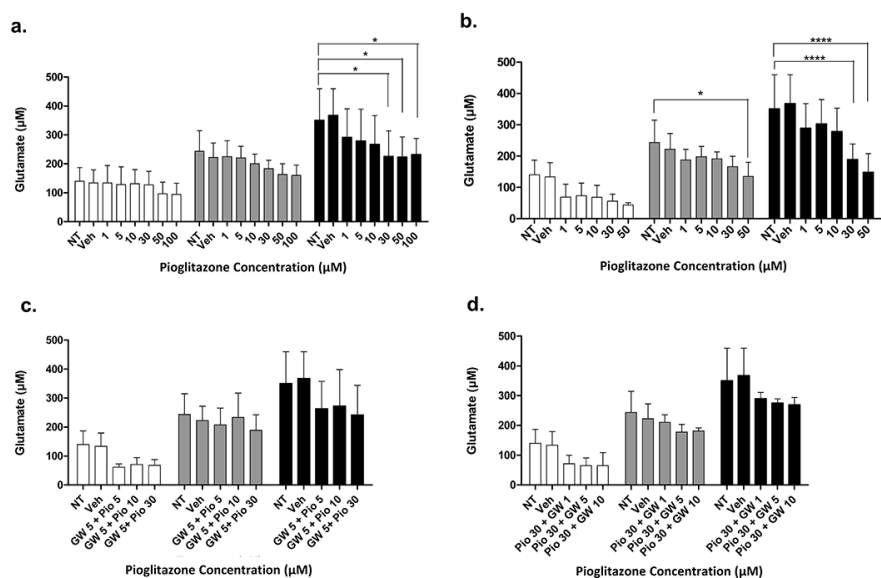


**Figure 7: Extracellular glutamate levels measured with HPLC in U87MG cells incubated with varying concentrations of pioglitazone. (a) GW9662 (b) GW9662 + pioglitazone (c & d) for 24, 48 and 72 hours ( $n = 6$ ).** A significant reduction in glutamate release was elicited at a concentration of  $\geq 30$   $\mu\text{M}$  of pioglitazone at 72 hours (a). GW9662 at was associated with a significant reduction of glutamate at 48 and 72 hours using 50  $\mu\text{M}$  and  $\geq 30$   $\mu\text{M}$  respectively (b). There was no significant difference in glutamate release with co-administration of pioglitazone and GW9662 (c & d). Bars show mean with SEM and asterisks indicate statistical significance where  $*p = 0.01$  to  $0.05$ ,  $**p = 0.001$  to  $0.01$ ,  $***p < 0.001$ , and  $****p < 0.0001$ . ANOVA with Bonferroni Post hoc test,  $n = 6$ . Abbreviations: NT: non-treated, Veh: Vehicle control, Pio: Pioglitazone, GW: GW9662.

We demonstrated that the lowest effective concentration of pioglitazone of 30  $\mu\text{M}$  in both cell lines is inhibited by concentrations of GW9662 as low as 1  $\mu\text{M}$  (Figures 7(c) & (d) & 8(c) & (d)). Therefore, the capacity for pioglitazone to reduce extracellular glutamate is highly dependent on

PPAR $\gamma$  in cell lines. In GSC #35, the converse is true, whereby GW9662 is associated with significantly reduced extracellular glutamate levels at 72 hours exposure alone (Figure 9(b)) or in combination with pioglitazone (Figure 9(c)–(d)).



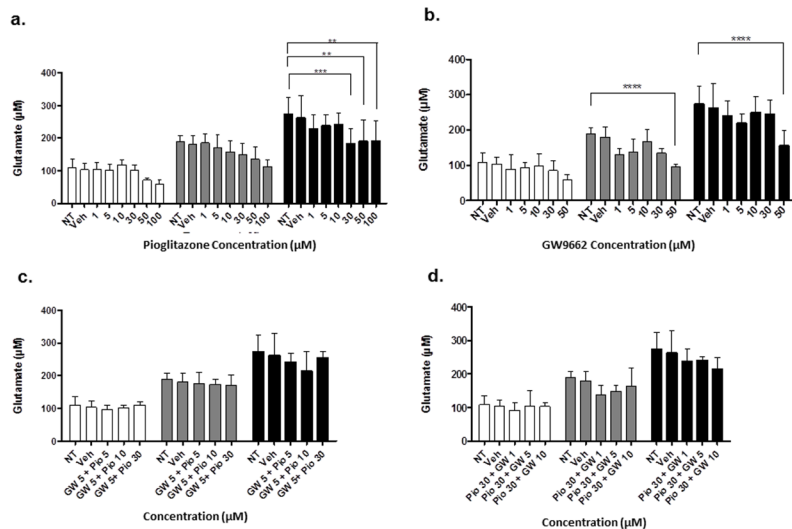


**Figure 8: Extracellular glutamate levels measured with HPLC in U251MG cells incubated with varying concentrations of pioglitazone (a) GW9662 (b) GW9662 + pioglitazone (c & d) for 24, 48 and 72 hours ( $n = 6$ ).** A significant reduction in glutamate release was elicited at a concentration of  $\geq 30 \mu\text{M}$  of pioglitazone at 72 hours (a). GW9662 at was associated with a significant reduction of glutamate at 48 and 72 hours using  $50 \mu\text{M}$  (b). There was no significant difference in glutamate release with co-administration of pioglitazone and GW9662 (c & d). Bars show mean with SEM and asterisks indicate statistical significance where  $*p = 0.01$  to  $0.05$ ,  $**p = 0.001$  to  $0.01$ ,  $***p < 0.001$ , and  $****p < 0.0001$ . ANOVA with Bonferroni Post hoc test,  $n = 6$ . NT: non-treated, Veh: Vehicle control, Pio: Pioglitazone, GW: GW9662.

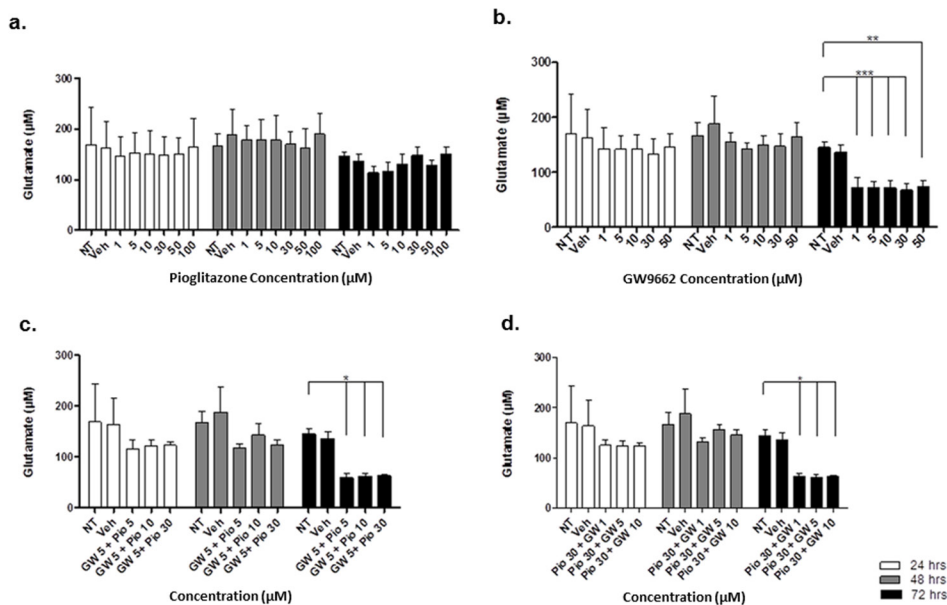


**Figure 9: Extracellular glutamate levels measured with HPLC in GSC #035 cells incubated with varying concentrations of pioglitazone (a) GW9662 (b) GW9662 + pioglitazone (c & d) for 24, 48 and 72 hours ( $n = 6$ ).** A significant reduction in glutamate release was elicited at a concentration of  $\geq 1 \mu\text{M}$  of GW9662 at 72 hours (b–d). There was no significant difference in glutamate release administration of pioglitazone alone (a). Bars show mean with SEM and asterisks indicate statistical significance where  $*p = 0.01$  to  $0.05$ ,  $**p = 0.001$  to  $0.01$ ,  $***p < 0.001$ , and  $****p < 0.0001$ . ANOVA with Bonferroni Post hoc test,  $n = 6$ . NT: non-treated, Veh: Vehicle control, Pio: Pioglitazone, GW: GW9662.

### Pioglitazone alters GBM cell line morphology and reduces glioma sphere formation

As it has previously been established that PPAR $\gamma$  agonists have cytotoxic and cytostatic activity, we sought to

determine if pioglitazone can alter glioma cellular morphology. [19, 31] In U87MG glioma cells, we observed that cellular morphology was transformed at a pioglitazone concentration of  $100 \mu\text{M}$  with a reduction in cellularity, coupled with a compromised ability to form astrocytic processes (Figure 10).

A similar observation was made in U251MG glioma cells at a pioglitazone concentration of 100  $\mu\text{M}$  (Figure 10). Glioma sphere formation, as assessed in the GSC #35 line, was reduced with the pioglitazone treatment but sphere size was not significantly reduced (Figure 11). Quantification of these observations correlates well with viability results (Figure 12).

### Pioglitazone may alter Akt and GSK-3 $\beta$ activity

In order to understand how pioglitazone may reduce cell viability in glioblastoma cell lines, we sought to measure the expression of pertinent oncogenic signalling cascades. Lee and colleagues have previously demonstrated

that ciglitazone treatment results in reduced phosphorylation of Akt (Thr<sup>308</sup>), which is not altered by the presence of the PPAR $\gamma$  inhibitor, GW9662. [18] We observed that in U87MG cells treated with pioglitazone there was increased expression of both phosphorylated Akt and phosphorylated GSK-3 $\beta$  with no change in the levels of total Akt or GSK-3 $\beta$  (Figure 13(a)). In contrast, when treating U251MG cells with pioglitazone, we did not detect a significant change in the phosphorylation status of GSK-3 $\beta$ , although total Akt protein levels were marginally reduced with 100  $\mu\text{M}$  pioglitazone (Figure 13(b)). This suggests that pioglitazone operates through a different mechanism of apoptotic cell death in glioma cells compared to ciglitazone.

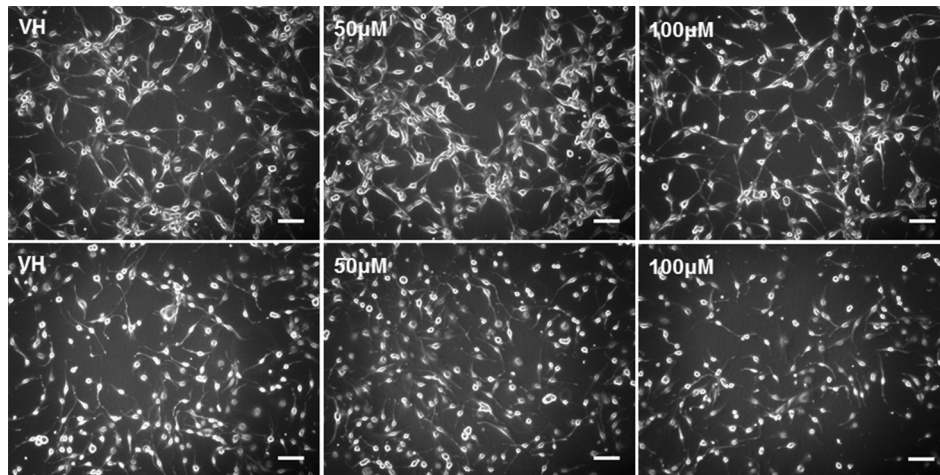


**Figure 10: Top row: U87MG treated with increasing doses of pioglitazone for 48 hours.** Cellularity and formation of spreading astrocytic process formation were reduced with 100 M pioglitazone compared with vehicle control (VH). Cells were smaller and numerous detached cells were present but quantity and length of astrocytic processes were unchanged at 10X objective. Bottom row: U251 cells cultured for 48 hours treated with increasing concentrations of pioglitazone. Cellularity and formation of astrocytic processes decreased at concentrations above 10  $\mu\text{M}$  at 10X objective. Scale bars = 100  $\mu\text{m}$ .

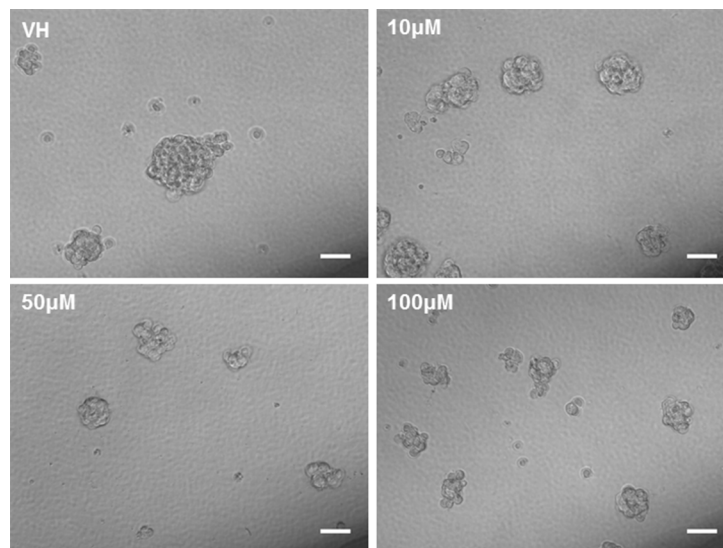


**Figure 11: Phase contrast photos at 20X objective of glioma stem cell line #035 incubated with vehicle control (VH) and increasing concentrations of pioglitazone for 48 hours.** Pioglitazone reduces the quantitative formation and size of neurosphere formation. Scale bars = 50  $\mu\text{m}$ .

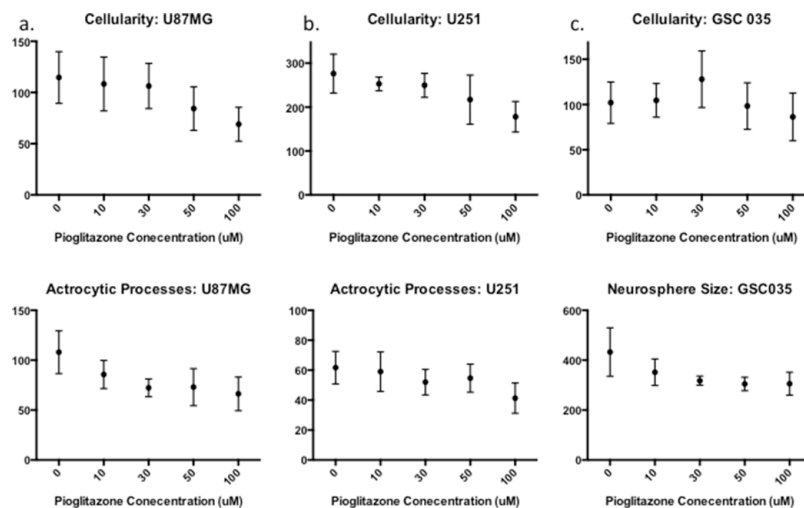


**Figure 12: Quantification of photomicrograph cellularity and morphological change.** Increasing concentrations of Pioglitazone 30 μM or above significantly reduces cellularity and astrocytic process formation in U87MG (a) but not in U251MG (b) Glioma stem cell neurosphere formation (cellularity) reduces significantly with a concentration of 100 μM of Pioglitazone (c) however, the average area of neurospheres reduces but does not change significantly in these conditions. For all experiments  $n = 3$ .

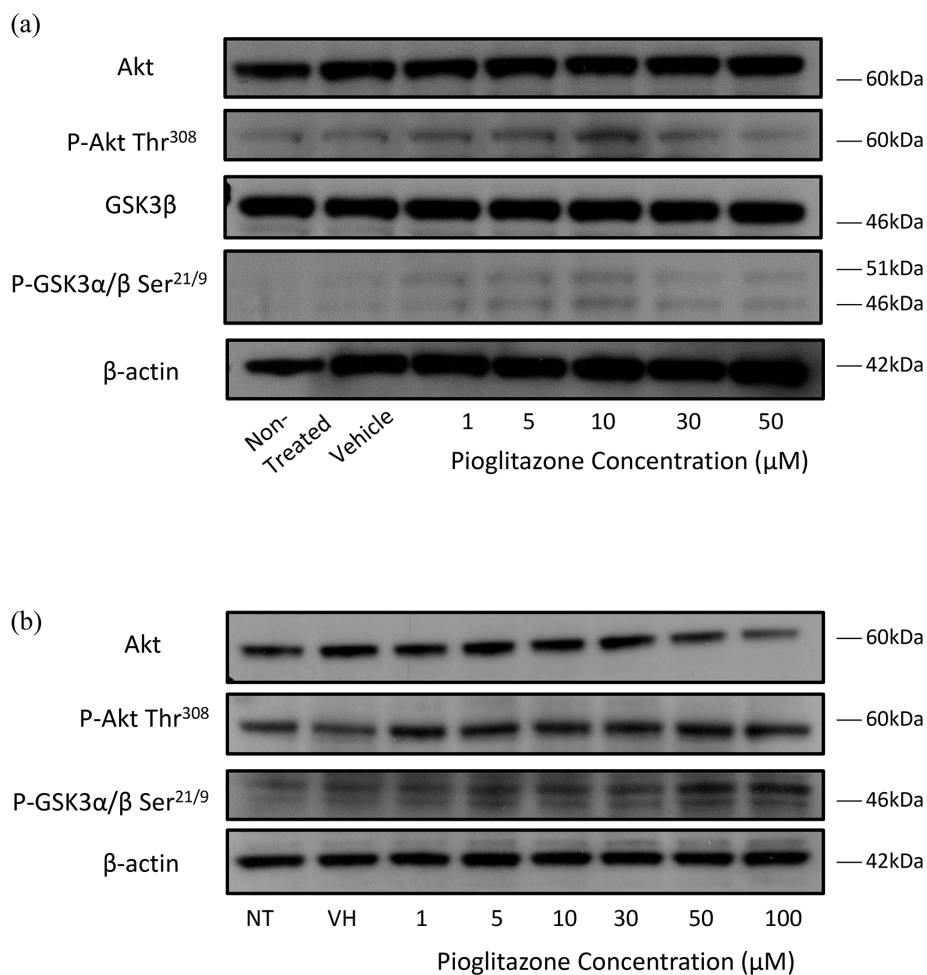


**Figure 13: (a) Representative blots showing Akt, p-Akt, GSK-3β and p-GSK-3α/β and β-actin expression in U87 glioma cells treated with increasing concentrations of pioglitazone for 72 hours. (b) Representative blots showing Akt, p-Akt, p-GSK-3β and β-actin expression in U251MG glioma cells treated with increasing concentrations of pioglitazone for 48 hours.**

## DISCUSSION

Our study provides evidence that the PPAR $\gamma$  agonist pioglitazone increases the functional expression of the glutamate transporter EAAT2 in glioma cells. This represents a potential novel mechanism for treatment of glioma associated seizures, whereby excess extracellular glutamate is transported back into glioma cells and also by normal astrocytes at the peritumoural edge. This is a potentially therapeutic approach by preventing glutamate mediated seizures and excitotoxic damage. In light of the findings by Romera and colleagues that PPAR $\gamma$  agonists increase astrocytic EAAT2 and subsequently reduce extracellular glutamate, which we show that PPAR $\gamma$ -mediated EAAT2 modulation is also applicable to glioma cells. [32] We did not carry out a glutamate uptake assay, which would be important to confirm true functional upregulation. [6] However, cell viability was not significantly reduced at the effective concentration of 30  $\mu$ M of pioglitazone in U251MG glioma cells reported here, providing a surrogate for EAAT2 function. Whether pioglitazone also affects glutamate release, glutamate uptake or both requires further investigation.

De Groot and colleagues previously demonstrated that overexpression of EAAT2 in glioma cell lines, including U87MG and U251MG glioma cells, resulted in a reduced ability to form tumours and also caused *in vivo* and *in vitro* apoptosis. [29] Pioglitazone induced EAAT2 upregulation may play a role in reducing glioma cell viability via multiple mechanisms, particularly through the activation of caspase-3, which has been shown in both overexpression studies and cellular apoptosis assays. [29, 33]

Deactivation of oncogenic mediators such as Akt and  $\beta$ -catenin has been implicated as possible PPAR $\gamma$  independent mechanisms for PPAR $\gamma$  agonists. [18, 19] We observed a reduction in total Akt protein expression levels in U251MG glioma cells following treatment with 50 and 100  $\mu$ M of pioglitazone. This was in contrast to the increase in Akt protein expression detected in U87MG cells, where Akt phosphorylation at the threonine 473 (thr<sup>308</sup>) residue was unchanged in U251MG cells but increased in U87MG cells (Figure 13). Lee and colleagues observed that a concentration of 30  $\mu$ M pioglitazone effectively reduced total Akt activity and phosphorylation at threonine 308 (thr<sup>308</sup>) residue, but not ser<sup>473</sup> in T98G cells after 48 hours. [18] The increased phosphorylation of Akt thr<sup>308</sup> was not seen to significantly reduce cell viability when cells were incubated with pioglitazone. Reduction in Akt activity is desirable to counteract mutations in RTK/PTEN/PI3K in gliomas that lead to increased Akt activity downstream, resulting in uncontrolled proliferation.

We discovered that GSK-3 $\beta$  expression levels were decreased with a corresponding increase in GSK-3 $\alpha$  and GSK-3 $\beta$  phosphorylation on ser<sup>21</sup> and ser<sup>9</sup> residues, respectively, in U87MG cells treated with pioglitazone (Figure 13) but not in U251MG after 72 hours (data not

shown), indicating inactivation of GSK-3 $\beta$ . However, we did not observe a correlation between Akt mediated GSK-3 $\beta$  inactivating phosphorylation as reported by Atkins and colleagues. [34] This implies that PPAR $\gamma$  agonists may inactivate GSK-3 $\beta$  through other upstream mediators alongside or independently through direct inhibition. [25] The more noticeable reduction in astrocytic processes formation in U251MG over U87MG cells may not implicate GSK-3 $\beta$  inhibition as a downstream target of PPAR $\gamma$  agonists, which has been previously shown with lithium chloride of U87MG cells. [35] We also did not detect an association of pioglitazone mediated EAAT2 expression or the activation state of GSK-3 $\beta$ . In addition GSK3 inhibition by pioglitazone may also prevent the formation of neurospheres (Figures 11 & 12), corroborating previous findings by Korur and colleagues. [28] Wan and colleagues previously demonstrated that pioglitazone significantly reduces viability of U87MG and U251MG cells at concentrations of 100  $\mu$ M and 200  $\mu$ M beyond 72 hours. [19] Our results demonstrate that pioglitazone may be more potent in this role as we observed a significant reduction in cell viability at concentrations of  $\geq$  30  $\mu$ M in U87MG and 100  $\mu$ M in U251MG as early as 24 hours.

In order to determine whether the observed effects on viability and EAAT2 modulation relied on PPAR $\gamma$  activation, the inhibitor GW9662 was used as previously described in studies utilising breast tumours and glioma cell lines. [18, 36] In our current study, GW9662 alone reduced cell viability of U87MG and U251MG cells at concentrations of at least 10 and 30  $\mu$ M, respectively. A potential anti-neoplastic pathway for GW9662 is through the reduced expression of Fatty Acid Binding Protein 7 (FABP7), which has been implicated as a target gene for PPAR. [37] Authors of this study demonstrated a reduction in cellular migration after siRNA knockdown of FABP7 and the PPAR antagonist treatment of GSCs with and without irradiation. This potentially contradicts previous findings that PPAR $\gamma$  agonists induce apoptosis in GSCs, however the effect of PPAR $\gamma$  agonists on FABP7 has yet to be thoroughly investigated. [38] Furthermore, these two studies differ in the use of primary and enriched long-term GSC lines, which may explain the differences to previous studies.

We observed no change in EAAT2 expression in glioma stem cell line #035 with pioglitazone exposure, which may be in keeping with a lineage specific GSC as shown by Pollard and Colleagues. [39] Extracellular glutamate levels were not raised in the culture medium from GSC #35 and pioglitazone treatment did not augment this (Figure 9). Interestingly, Gilley and colleagues found that neural stem cells derived from the hippocampal dentate gyrus exhibited raised EAAT2 expression in hypoxic-ischaemic and traumatic brain injury rodent models. [40] Furthermore, these authors showed that siRNA knockdown of EAAT1 and EAAT2 resulted in an increase in neurosphere formation and proliferation,

whereas overexpression had the converse effect. This mirrors our findings, which showed that GSC #035 does not express EAAT1 or 2 and there was reduced formation of glioma stem-like neurospheres with increasing concentrations of pioglitazone. This raises important questions about how GSCs survive in a microenvironment that is rich in glutamate. It could be the case that this alters their proliferative ability, which may ultimately be involved in selecting a subpopulation of GSCs. Our data from one GSC line suggests that such cells can release low levels of glutamate around 10  $\mu\text{M}$  (data not shown).

The morphological effects of pioglitazone on glioma cells has not been previously reported. Herein we have shown that pioglitazone treatment alters the morphology of U87MG, U251MG glioma cells and a primary GSC line in a concentration dependent manner. However, the observed changes in cell morphology did not correlate with cell viability. U87MG morphology notably changed in the presence of 100  $\mu\text{M}$  pioglitazone but cell viability was significantly reduced at concentrations of 30  $\mu\text{M}$  and above. GW9662, an inhibitor of PPAR $\gamma$  demonstrated opposing effects in combination with a cytostatic dose of pioglitazone, which may be due to PPAR $\gamma$  independent effects of the two drugs working synergistically as reported elsewhere. [13].

Bright and colleagues previously demonstrated the efficacy of the more potent PPAR $\gamma$  agonist ciglitazone on CD133<sup>+</sup> U87MG and T98G neurospheres. [38] A cytotoxicity assay on our GSC line #35 with increasing concentrations of pioglitazone did not corroborate these findings (Figure 6(a)–6(h)). However, our GSC line was not de-differentiated from established cell lines, rather isolated from a primary resection. Furthermore, there may be unexplored PPAR $\gamma$ -independent mechanistic differences between pioglitazone and ciglitazone that are not accounted for by the class effect of these drugs.

Owing to the established association between glutamate and tumour associated epilepsy, there may also exist a novel role for PPAR $\gamma$  agonists. [9, 10] Notably, we chose the U251MG cell line since Buckingham and colleagues previously utilised this in establishing a tumour associated epilepsy model in rodents. [10] Although pioglitazone is associated with a minor risk of bladder cancer, it is otherwise a relatively safe drug that could be considered for clinical trials. [41] Alternatively, 293 agents that upregulate EAAT2 protein expression in primary astrocytes have been identified with high throughput screening, providing a new family of candidate drugs that are available to be tested for this treatment strategy. [42]

Currently, the only promising drug candidate for tumour associated epilepsy has been sulfasalazine. [10] Extensive clinical trials have yet to follow, but a previous clinical trial suggests potential challenges with this agent. [43] Sattler and colleagues have recently demonstrated that thiamphenicol, through its upregulation of EAAT2 in peritumoural tissue, may be similarly beneficial. [44] PPAR $\gamma$  agonists may constitute an additional agent that

activates glutamate transport within tumour cells and peritumourally. These agents could be considered for adjunct treatment in current regimens and in combination therapy for dual mechanistic efficacy in sub therapeutic doses to avoid associated adverse effects.

## MATERIALS AND METHODS

### Reagents

Dulbecco's Modified Eagle's Medium (Invitrogen, Camarillo, CA, USA) heat inactivated foetal calf serum (Bovogen, Victoria, Australia) and penicillin/streptomycin (Invitrogen, Camarillo, CA, USA) were source listed. Pioglitazone hydrochloride was obtained from Sigma Aldrich (St. Louis, MO, USA) and GW9662 from Santa Cruz Biotechnology Inc. (Santa Cruz, CA, USA). Primary antibodies for EAAT 2 (rabbit polyclonal IgG, sc-15317) and PPAR $\gamma$  (mouse monoclonal IgG, sc-7273) were purchased from Santa Cruz Biotechnology Inc. (Santa Cruz, CA, USA) and EAAT1/GLAST1 (rabbit polyclonal, cat. #42–8100) from Invitrogen (Camarillo, CA, USA). Primary antibodies for Akt (polyclonal rabbit, cat. #9272), phosphorylated-Akt (ser 473) (polyclonal rabbit, cat. #9271), glycogen synthase kinase 3 beta (GSK3 $\beta$ ) (polyclonal rabbit, cat. #9315) and phosphorylated-GSK3 $\alpha/\beta$  (Serine 21/9) (cat. #9331) were purchased from Cell Signalling Technology Inc. (Danvers, MA, USA).  $\beta$ -actin primary antibody (mouse monoclonal, cat. #A2228) was purchased from Sigma Aldrich (St. Louis, MO, USA). Goat anti-rabbit antibody conjugated with horse raddish peroxidase (cat. #170–6515) and goat anti-mouse antibody conjugated with horse raddish peroxidase (cat. #170–6516) was purchased from Bio-Rad (Hercules, CA USA). Cell Titer Glo Cell Luminescent Viability Assay was purchased from Promega (Madison, WI, USA). Protein estimation of whole cell lysates was carried out using the BCA Protein Assay Reagent (bicinchoninic acid) from Thermo Scientific Rockford, IL, USA). Western Blot reagents, apparatus, and 4–12% Bis-Tris pre-cast gels were purchased from Invitrogen (Camarillo, CA, USA).

### Cell culture

Glioma cell lines U87MG and U251MG cells were obtained from the American Type Culture Collection, Manassas, VA, USA were maintained in DMEM supplemented with 5% foetal bovine serum and penicillin/streptomycin at 37°C and 10% carbon dioxide.

A human glioblastoma stem cell line (GSC #35) was previously generated in our laboratory from a brain tumour tissue specimen (Melbourne Health Research Ethics 2009.016). Neurospheres produced from GSC #35 maintained in DMEM F12 supplemented with epidermal growth factor (1:1000), basic fibroblast growth factor (1:1000), B27 (1:50) and penicillin/streptomycin at 37°C

and 10% CO<sub>2</sub> using ultra low adhesion 6 well plates, as previously described by Singec et al. [45].

### Preparation of rodent brain samples

Non-epileptic control Wistar rats were used for control samples and were obtained from our own breeding colony (Biological Resource Facility, RMH Academic Centre). All procedures were approved by the University of Melbourne Animal Ethics Committee (AEC #1111944) and performed in accordance with the guidelines published by the Australian NHMRC for use of animals in research.

Seven day old Wistar rat pups were culled and samples of cortex and thalamus were stored on dry ice. Whole cell lysates were prepared in erythrocyte lysis buffer (ELB) (500 mM NaCl, 100 mM HEPES, and 10 mM EDTA, 0.2% Triton X100, 20 mM NaF, 2 mM NaV, 2 µg/mL aprotinin). The whole cell lysates were clarified by centrifugation at 13,000 rpm at 4°C for 10 minutes.

### Photomicroscopy and quantification of cell morphology

ImageJ (ver. 1. 48, NIH, Bethesda, Maryland) was utilised to measure cellularity, formation of astrocytic processes, and neurosphere formation and size. Cellularity was measured by converting images to a binary format and using processing tools to demarcate cells for automated counting. Average area of neurospheres was used to estimate the size of neurosphere formation. Astrocytic processes were measured manually using binary processes in ImageJ.

### Drug treatment of cell lines

Pioglitazone hydrochloride (Sigma Aldrich, St. Louis, MO, USA) and GW9662 (Santa Cruz, CA, USA) were dissolved in dimethyl sulfoxide (DMSO) and stored at -20°C until use. Glioma cells were treated at a number of drug concentrations and times as indicated in the results section.

### Cell viability assay

1 × 10<sup>4</sup> glioma cells were seeded in each well of a 96 well plate and at various time points (24, 48 and 72 hours), the culture medium was aspirated and 50 µL of Cell Titre Glo (Promega, Madison, WI, USA) viability solution was added. The plate was incubated at 4°C with gentle rocking for 20 minutes and 40 µL of the viability solution from each well was then transferred to an opaque 96 well plate and luminescence measured with using a GloMax<sup>®</sup> Microplate Luminometer (Madison, WI, USA). Viability was compared with untreated cells at 24, 48 and 72 hours).

### Western blotting

Adherent cells were washed with PBS and lysed with ELB over ice. Proteins were then separated by SDS-PAGE

on 4–12% Bis-Tris gels (Invitrogen), transferred onto polyvinylidene fluoride membrane and probed with the indicated primary antibodies. The signal was visualised using the ECL chemilluminescence detection kit (GE Healthcare, Rydelmere, N.S.W., Australia) following incubation with appropriate secondary antibodies.

### High performance liquid chromatography

Glutamate analysis in cell culture media was performed using the isocratic HPLC method which utilises naphthalene-2, 3-dicarboxyaldehyde derivatisation (NDA) and subsequent fluorescence detection as previously described. [46]

### Statistics

All statistical analysis and graph generation was performed using the software package GraphPad Prism 5.0, La Jolla, CA, USA. The unpaired Student's *t*-test was used to compare groups and statistical significance was considered to be  $p \leq 0.05$ .

## CONCLUSIONS

The PPAR $\gamma$  agonist pioglitazone increases functional EAAT2 expression and reduces extracellular glutamate levels in both U87MG and U251MG glioma cells. Pioglitazone alters the cell morphology and reduces cell viability of the glioma cell lines, U87MG and U251MG. Pioglitazone and other PPAR $\gamma$  agonists may offer a novel treatment paradigm for the treatment of TAE through the promotion of extracellular glutamate clearance at both the glioma cell level and surrounding astrocytes. Further work is required to definitively elucidate the mechanisms of this therapeutic strategy.

## ACKNOWLEDGMENTS

The authors thank the staff in the Hong-Jian Zhu Cancer Signalling Research Laboratory, the Melbourne Brain Centre and the Walter and Eliza-Hall Institute of Medical Research.

## CONFLICTS OF INTEREST

The authors have no conflicts of interest to disclose.

## GRANT SUPPORT

This study was supported by The Royal Melbourne Hospital Neuroscience Foundation and National Health Institutes.

## Authors contributions

Conception: JC APM. Data acquisition: JC SA NK. Viability assays: JC SA RBL NK. Western Blots: JC SA NK SSS. Stem cell culture: SA NK. Rodent brain

preparation: TZ JC. HPLC: ARB. Analysis: JC SA NK. Manuscript preparation: JC SA. Manuscript revisions: JC SA TZ SSS RL APM TJO AHK.

## REFERENCES

1. Curtis D, Johnston G. Amino acid transmitters in the mammalian central nervous system. *Ergebnisse der Physiologie, biologischen Chemie und experimentellen Pharmakologie*. 1974; 69:97–188.
2. Niels C D. Glutamate uptake. *Progress in Neurobiology*. 2001; 65:1–105.
3. Ye ZC, Sontheimer H. Glioma cells release excitotoxic concentrations of glutamate. *Cancer Research*. 1999; 59:4383–4391.
4. Seal RP, Amara SG. Excitatory Amino Acid Transporters: A Family in Flux. *Annual Review of Pharmacology and Toxicology*. 1999; 39:431–456.
5. Anderson CM, Swanson RA. Astrocyte glutamate transport: Review of properties, regulation, and physiological functions. *Glia*. 2000; 32:1–14.
6. Ye Z-C, Rothstein JD and Sontheimer H. (2000). Compromised Glutamate Transport in Human Glioma Cells: Reduction–Mislocalization of Sodium-Dependent Glutamate Transporters and Enhanced Activity of Cystine–Glutamate Exchange. *Journal of Neuroscience*, pp. 10767–10777.
7. Chung WJ, Lyons SA, Nelson GM, Hamza H, Gladson CL, Gillespie GY, Sontheimer H. Inhibition of cystine uptake disrupts the growth of primary brain tumors. *Journal of Neuroscience*. 2005; 25:7101–7110.
8. Takano T, Lin JH, Arcuino G, Gao Q, Yang J, Nedergaard M. Glutamate release promotes growth of malignant gliomas. *Nature Medicine*. 2001; 7:1010–1015.
9. Yuen TI, Morokoff AP, Bjorksten A, D’Abaco G, Paradiso L, Finch S, Wong D, Reid CA, Powell KL, Drummond KJ, Rosenthal MA, Kaye AH, O’Brien TJ. Glutamate is associated with a higher risk of seizures in patients with gliomas. *Neurology*. 2012; 79:883–889.
10. Buckingham SC, Campbell SL, Haas BR, Montana V, Robel S, Ogunrinu T, Sontheimer H. Glutamate release by primary brain tumors induces epileptic activity. *Nature Medicine*. 2011; 17:1269–1274.
11. Bernardo A, Minghetti L. Regulation of Glial Cell Functions by PPAR-gamma Natural and Synthetic Agonists. *PPAR research*. 2008; 2008: 1–10.
12. Romera C, Hurtado O, Mallolas J, Pereira MP, Morales JR, Romera A, Serena J, Vivancos J, Nombela F, Lorenzo P, Lizasoain I, Moro MA. Ischemic preconditioning reveals that GLT1/EAAT2 glutamate transporter is a novel PPAR target gene involved in neuroprotection. *J Cereb Blood Flow Metab*. 2007; 27:1327–1338.
13. Lee J, Reding M. Effects of Thiazolidinediones on Stroke Recovery: A Case-Matched Controlled Study. *Neurochemical Research*. 2007; 32:635–638.
14. Elstner E, Williamson EA, Zang C, Fritz J, Heber D, Fenner M, Possinger K, Koeffler HP. Novel therapeutic approach: ligands for PPAR gamma and retinoid receptors induce apoptosis in bcl-2-positive human breast cancer cells. *Breast Cancer Research and Treatment*. 2002; 74:155–165.
15. Sarraf P, Mueller E, Jones D, King FJ, DeAngelo DJ, Partridge JB, Holden SA, Chen LB, Singer S, Fletcher C, Spiegelman BM. Differentiation and reversal of malignant changes in colon cancer through PPAR gamma. *Nature Medicine*. 1998; 4:1046–1052.
16. Tsukahara T, Haniu H. Peroxisome proliferator-activated receptor gamma overexpression suppresses proliferation of human colon cancer cells. *Biochemical and Biophysical Research Communications*. 2012; 424:524–529.
17. Ogino S, Shima K, Baba Y, Noshio K, Irahara N, Kure S, Chen L, Toyoda S, Kirkner G, Wang L, Govannucci E, Fuchs C. Colorectal Cancer Expression of Peroxisome Proliferator-Activated Receptor gamma (PPARG, PPARgamma) Is Associated With Good Prognosis. *Gastroenterology*. 2009; 136:1242–1250.
18. Lee MW, Kim DS, Kim HR, Kim HJ, Yang JM, Ryu S, Noh YH, Lee SH, Son MH, Jung HL, Yoo KH, Koo HH, Sung KW. Cell death is induced by ciglitazone, a peroxisome proliferator-activated receptor gamma (PPAR gamma) agonist, independently of PPAR gamma in human glioma cells. *Biochemical and Biophysical Research Communications*. 2012; 417:552–557.
19. Wan Z, Shi W, Shao B, Shi J, Shen A, Ma Y, Chen J, Lan Q. Peroxisome proliferator-activated receptor gamma agonist pioglitazone inhibits beta-catenin-mediated glioma cell growth and invasion. *Molecular and Cellular Biochemistry*. 2011; 349:1–10.
20. Pestereva E, Kanakasabai S, Bright JJ. PPAR gamma agonists regulate the expression of stemness and differentiation genes in brain tumour stem cells. *British Journal of Cancer*. 2012; 106.
21. Grommes C, Karlo JC, Andrew C, D’Arbra B, Anne D. The PPARγ agonist pioglitazone crosses the blood-brain barrier and reduces tumor growth in a human xenograft model. *Cancer Chemotherapy and Pharmacology*. 2013; 71:929–936.
22. Embi N, Rylatt D, Cohen P. Glycogen synthase kinase-3 from rabbit skeletal muscle. Separation from cyclic-AMP-dependent protein kinase and phosphorylase kinase. *European Journal of Biochemistry*, pp 519–527.
23. Cross D, Alessi D, Vandenhede J, Mcdowell H, Hundal H, Cohen P. The inhibition of glycogen-synthase kinase-3 by insulin or insulin-like growth-factor-1 in the rat skeletal-muscle cell-line-l6 is blocked by wortmannin, but not by rapamycin - evidence that wortmannin blocks activation of the mitogen-activated protein-kinase pathway in l6-cells between RAS and RAF. *Biochemical Journal*. 1994; 303:21–26.
24. Kelly S, Zhao H, Sun GH, Cheng D, Qiao Y, Luo J, Martin K, Steinberg GK, Harrison SD, Yenari MA.

- Glycogen synthase kinase 3beta inhibitor Chir025 reduces neuronal death resulting from oxygen-glucose deprivation, glutamate excitotoxicity, and cerebral ischemia *Experimental Neurology*. 2004; 188:378–386.
25. Martinez A, Alonso M, Castro A, Perez C, Moreno FJ. First non-ATP competitive glycogen synthase kinase 3 beta (GSK-3beta) inhibitors: thiadiazolidinones (TDZD) as potential drugs for the treatment of Alzheimer's disease. *Journal of Medicinal Chemistry*. 2002; 45:1292–1299.
  26. Wang Z, Smith KS, Murphy M, Piloto O, Somervaille TCP, Cleary ML. Glycogen synthase kinase 3 in MLL leukaemia maintenance and targeted therapy. *Nature*. 2008; 455:1205–1209.
  27. Jing TL, Zhuang Hui-Sun, LeongN. Gopalakrishna, Iyer Edison T. Lu Qiang Yu.. Pharmacologic Modulation of Glycogen Synthase Kinase-3 $\beta$  Promotes p53-Dependent Apoptosis through a Direct Bax-Mediated Mitochondrial Pathway in Colorectal Cancer Cells. 2005; 65:9012–9020.
  28. Korur S, Huber RM, Sivasankaran B, Petrich M, Morin P Jr, Hemmings BA, Merlo A, Lino MM. GSK3b Regulates Differentiation and Growth Arrest in Glioblastoma *PlosONE*. 2009; 4:1–12.
  29. de Groot JF, Liu TJ, Fuller GWK, Yung A. The Excitatory Amino Acid Transporter-2 Induces Apoptosis and Decreases Glioma Growth *In vitro* and *In vivo*. 2005; :1934–1940.
  30. Ye Z-C, Sontheimer H. (1998). Astrocytes Protect Neurons From Neurotoxic Injury by Serum Glutamate. (Glia).
  31. Wang P, Yu J, Yin Q, Li W, Ren X, Hao X. Rosiglitazone Suppresses Glioma Cell Growth and Cell Cycle by Blocking the Transforming Growth Factor-Beta Mediated Pathway. *Neurochemical Research*. 2012; 37:2076–2084.
  32. Romera C, Hurtado O, Botella SH, Lizasoain I, Cardenas A, Fernandez-Tome P, Leza JC, Lorenzo P, Moro MA. *In vitro* ischemic tolerance involves upregulation of glutamate transport partly mediated by the TACE/ADAM17-tumor necrosis factor-alpha pathway. *Journal of Neuroscience*. 2004; 24:1350–1357.
  33. Grommes C, Landreth GE, Sastre M, Beck M, Feinstein DL, Jacobs AH, Schlegel U, Heneka MT. Inhibition of *in vivo* glioma growth and invasion by peroxisome proliferator-activated receptor gamma agonist treatment. *Molecular Pharmacology*. 2006; 70:1524–1533.
  34. Atkins RJ, Dimou J, Paradiso L, Morokoff AP, Kaye AH, Drummond KJ, Hovens CM. Regulation of glycogen synthase kinase-3 beta (GSK-3b) by the Akt pathway in gliomas. *Journal of Clinical Neuroscience*. 2012; 19:1558–1563.
  35. Nowicki MO, Dmitrieva N, Stein AM, Cutter JL, Godlewski J, Saeki Y, Nita M, Berens ME, Sander LM, Newton HB, Chiocca EA, Lawler S. Lithium inhibits invasion of glioma cells; possible involvement of glycogen synthase kinase-3. *Neuro-Oncology*. 2008; 10:690–699.
  36. Seargent JM, Yates EA, Gill JH. GW9662, a potent antagonist of PPAR $\gamma$ , inhibits growth of breast tumour cells and promotes the anticancer effects of the PPAR $\gamma$  agonist rosiglitazone, independently of PPAR $\gamma$  activation. *British Journal of Pharmacology*. 2004; 143:933–937.
  37. De Rosa A, Pellegatta S, Rossi M, Tunici P, Magnoni L, Speranza MC, Malusa F, Miragliotta V, Mori E, Finocchiaro G, Bakker A. A Radial Glia Gene Marker, Fatty Acid Binding Protein 7 (FABP7), Is Involved in Proliferation and Invasion of Glioblastoma Cells. 2012; 7:1–12.
  38. Chearwae W, Bright JJ. PPAR gamma agonists inhibit growth and expansion of CD133+brain tumour stem cells. *British Journal of Cancer*. 2008; 99:2044–2053.
  39. Pollard SM, Yoshikawa K, Clarke ID, Danovi D, Stricker S, Russell R, Bayani J, Renee Head ML, 3 Mark Bernstein,5 Jeremy A. Squire,6 Austin Smith,1 and Peter Dirks2,\* (2009). Glioma Stem Cell Lines Expanded in Adherent Culture Have Tumor-Specific Phenotypes and Are Suitable for Chemical and Genetic Screens *Cell Stem Cell*, pp. 568–580.
  40. Gilley J, Kerner S. Excitatory amino acid transporter 2 and excitatory amino acid transporter 1 negatively regulate calcium-dependent proliferation of hippocampal neural progenitor cells and are persistently upregulated after injury *European Journal of Neuroscience*. 2011; 34:1712–1723.
  41. Colmers IN, Bowker SL, Majumdar SR, Johnson JA. Use of thiazolidinediones and the risk of bladder cancer among people with type 2 diabetes: a meta-analysis. *Canadian Medical Association Journal*. 2012; 184:E675–E683.
  42. Colton CK, Kong Q, Lai L, Zhu MX, Seyb KI, Cuny GD, Xian J, Glicksman MA. Identification of Translational Activators of Glial Glutamate Transporter EAAT2 through Cell-Based High-Throughput Screening. *Journal of Biomolecular Screening*. 2010; 15:653–662.
  43. Robe PA, Martin DH, Nguyen-Khac MT, Artesi M, Deprez M, Albert A, Vanbelle S, Califice S, Bredel M, Bours V. Early termination of ISRCTN45828668, a phase 1/2 prospective, randomized study of Sulfasalazine for the treatment of progressing malignant gliomas in adults. *BMC Cancer*. 2009; 9:1–8.
  44. Sattler, Tyler B, Hoover B, Conddington LT, Recinos V, Hwang L, Brem H, Rothstein JD. Increased expression of glutamate transporter GLT-1 in peritumoral tissue associated with prolonged survival and decreases in tumor growth in a rat model of experimental malignant glioma. *Journal of Neurosurgery*. 2013; 119:1–9.
  45. Singec I, Knoth R, Meyer R, Maciaczyk J, Volk B, Nikkha G, Frotscher M, Snyder E. Defining the actual sensitivity and specificity of the neurosphere assay in stem cell biology. *Nature Methods*. 2006; 3:801–806.
  46. Clarke G, Mahony S, Malone G, Dinan TG. An isocratic high performance liquid chromatography method for the determination of GABA and glutamate in discrete regions of the rodent brain. *Journal of Neuroscience Methods*. 2007; 160:223–230.



# Multimodal MRI Can Identify Perfusion and Metabolic Changes in the Invasive Margin of Glioblastomas

Stephen J. Price, PhD FRCS (Neuro.Surg),<sup>1,2\*</sup> Adam M.H. Young, MRCS,<sup>1</sup>  
William J. Scotton, MRCS,<sup>1</sup> Jared Ching, MB ChB,<sup>1</sup> Laila A. Mohsen, MD,<sup>3</sup>  
Natalie R. Boonzaier, MSc,<sup>1,2</sup> Victoria C. Lupson, BSc,<sup>2</sup>  
John R. Griffiths, DPhil FRCP,<sup>4</sup> Mary A. McLean, PhD,<sup>4</sup>  
and Timothy J. Larkin, PhD<sup>1,2</sup>

**Purpose:** To use perfusion and magnetic resonance (MR) spectroscopy to compare the diffusion tensor imaging (DTI)-defined invasive and noninvasive regions. Invasion of normal brain is a cardinal feature of glioblastomas (GBM) and a major cause of treatment failure. DTI can identify invasive regions.

**Materials and Methods:** In all, 50 GBM patients were imaged preoperatively at 3T with anatomic sequences, DTI, dynamic susceptibility perfusion MR (DSCI), and multivoxel spectroscopy. The DTI and DSCI data were coregistered to the spectroscopy data and regions of interest (ROIs) were made in the invasive (determined by DTI), noninvasive regions, and normal brain. Values of relative cerebral blood volume (rCBV), N-acetyl aspartate (NAA), myoinositol (ml), total choline (Cho), and glutamate + glutamine (Glx) normalized to creatine (Cr) and Cho/NAA were measured at each ROI.

**Results:** Invasive regions showed significant increases in rCBV, suggesting angiogenesis (invasive rCBV 1.64 [95% confidence interval, CI: 1.5–1.76] vs. noninvasive 1.14 [1.09–1.18];  $P < 0.001$ ), Cho/Cr (invasive 0.42 [0.38–0.46] vs. noninvasive 0.35 [0.31–0.38];  $P = 0.02$ ) and Cho/NAA (invasive 0.54 [0.41–0.68] vs. noninvasive 0.37 [0.29–0.45];  $P < 0.03$ ), suggesting proliferation, and Glx/Cr (invasive 1.54 [1.27–1.82] vs. noninvasive 1.3 [1.13–1.47];  $P = 0.028$ ), suggesting glutamate release; and a significantly reduced NAA/Cr (invasive 0.95 [0.85–1.05] vs. noninvasive 1.19 [1.06–1.31];  $P = 0.008$ ). The ml/Cr was not different between the three ROIs (invasive 1.2 [0.99–1.41] vs. noninvasive 1.3 [1.14–1.46];  $P = 0.68$ ). In the noninvasive regions, the values were not different from normal brain.

**Conclusion:** Combining DTI to identify the invasive region with perfusion and spectroscopy, we can identify changes in invasive regions not seen in noninvasive regions.

J. MAGN. RESON. IMAGING 2016;43:487–494.

Despite our improved knowledge and understanding of glioblastomas (GBM), they still carry a dismal prognosis. Survival can be improved by more aggressive surgical resections<sup>1</sup> and the combination of radiotherapy and chemotherapy, yet virtually all patients will die from progressive disease. This disease

progression is usually within the high dose area of radiotherapy<sup>2–5</sup> in an area of tumor invasion. This invasive margin is a cardinal feature of GBM and is one of the major causes of treatment failure.<sup>6</sup> As the invasive margin cannot be accurately identified with clinical, anatomical imaging ( $T_1$ -weighted,

View this article online at [wileyonlinelibrary.com](http://wileyonlinelibrary.com). DOI: 10.1002/jmri.24996

Received Feb 20, 2015, Accepted for publication Jun 23, 2015.

\*Address reprint requests to: S.J.P., Neurosurgery Division, Department of Clinical Neurosciences, University of Cambridge, Box 167, Cambridge Biomedical Campus, Cambridge CB2 0QQ, UK. E-mail: [sjp58@cam.ac.uk](mailto:sjp58@cam.ac.uk)

The copyright line for this article was changed on 20 October 2015 after original online publication.

From the <sup>1</sup>Neurosurgery Division, Department of Clinical Neurosciences, University of Cambridge, Cambridge Biomedical Campus, Cambridge, UK;

<sup>2</sup>Wolfson Brain Imaging Centre, Department of Clinical Neurosciences, University of Cambridge, Cambridge Biomedical Campus, Cambridge, UK;

<sup>3</sup>University Department of Radiology, University of Cambridge, Cambridge Biomedical Campus, Cambridge, UK; and <sup>4</sup>Cancer Research UK Cambridge Institute, University of Cambridge, Li Ka Shing Centre, Cambridge, UK.

This is an open access article under the terms of the Creative Commons Attribution-NonCommercial-NoDerivs License, which permits use and distribution in any medium, provided the original work is properly cited, the use is non-commercial and no modifications or adaptations are made.

$T_2$ -weighted, and fluid-attenuated inversion recovery [FLAIR] imaging),<sup>7,8</sup> new imaging methods are required to delineate it and to facilitate study of its biology.

Our understanding of what happens in the invasive margin is less well developed than for the center of the tumor. It is known that invading cells have a different phenotype and are more motile and less proliferative.<sup>9</sup> The release of enzymes (such as metalloproteases) breaks down the extracellular matrix and the release of glutamate (secondary to disruption of the glial matrix) destroys glia and neuronal processes to provide space for tumor cells to invade.<sup>10,11</sup> As cell numbers increase the tumor cells become hypoxic, providing an important trigger for changes both in brain metabolism and angiogenesis that will lead to further tumor cell invasion.<sup>12</sup> Invasion is therefore a multistage, multicellular process that cannot be completely studied using a single method.

As invasion primarily involves white matter tracts, imaging disruption of the architecture of the white matter will be vital in identifying tumor invasion. Diffusion tensor magnetic resonance imaging (DTI) is a technique sensitive to the ordered diffusion of water along white matter tracts, and it can detect subtle disruption. Studies have shown that it can identify changes in white matter on the periphery of an invasive GBM that are not seen in noninvasive metastases<sup>13,14</sup> or meningiomas,<sup>15</sup> suggesting that these changes in the peritumoral area are due to invasion. Diffusion tensor tissue signatures can split the tensor information into isotropic diffusion ( $p$ : magnitude of diffusion) and anisotropic diffusion ( $q$ : measure of the directionality of diffusion).<sup>16</sup> This procedure can differentiate regions of pure tumor (reduced  $q$  and increased  $p$ ) from invaded white matter (increased  $p$  alone)<sup>17</sup> and is more sensitive than conventional DTI measures such as fractional anisotropy (FA).<sup>8,18</sup> Image-guided biopsies of these regions have confirmed invasive tumor with a high degree of accuracy in both high-grade gliomas<sup>8</sup> and low-grade gliomas.<sup>19</sup> Follow-up studies have shown that these regions predate the development of contrast enhancement at progression, and can predict the time to tumor progression<sup>20</sup> and its pattern.<sup>21,22</sup> This provides a valuable method of identifying the invasive tumor margin.

Dynamic susceptibility contrast perfusion imaging (DSCI) provides information on the relative cerebral blood volume (rCBV) that correlates with tumor vascularity<sup>23,24</sup> and cellular proliferation.<sup>25</sup> Multivoxel MR spectroscopy (MRS), or chemical shift imaging (CSI), reveals changes in tissue metabolism within the invasive region. In this study we aimed to understand the local environment of GBM by exploring the perfusion and metabolic changes seen in the DTI-defined invasive margin of GBMs and compare this to regions defined as noninvasive by DTI. From our knowledge of the biology of the invasive margin we would expect that multimodal imaging methods will show that these DTI-defined invasive regions will appear similar to the main tumor bulk.

## Materials and Methods

### Patients Recruited

Fifty patients (mean age 58.2, range 31.4–71.6 years; 33 males, 17 female) were recruited preoperatively for this prospective MRI study. All patients had imaging appearances of a GBM and histological confirmation was subsequently obtained. All patients provided signed informed consent for this study that was approved by the local Research Ethics Committee.

All patients underwent resection of these tumors using 5-ALA (5-aminolevulinic) fluorescence guidance with an aim of resecting the entire contrast-enhancing tumor as defined by the surgical RANO criteria.<sup>26</sup> Postoperative imaging within 72 hours of surgery showed that this was achieved in 39 patients (78%).

### Imaging Studies

All patients were imaged within a week prior to surgery on a 3T Magnetom Trio MR scanner (Siemens Healthcare, Erlangen, Germany), using a standard 8-channel receive head coil and transmission on the body coil. Conventional anatomical imaging sequences, diffusion tensor imaging, DSCI, and <sup>1</sup>H MR multivoxel spectroscopic imaging (CSI) were performed on all patients. The anatomical sequences included: an axial precontrast  $T_1$ -weighted sequence (relaxation time / echo time [TR/TE]: 500/8.6 msec, number of excitations [NEX]: 1, slice thickness/interslice gap: 4/1 mm, in-plane resolution: 0.74 mm, field of view [FOV]: 24 × 24 cm, 4 min 22 sec); an axial FLAIR sequence (TR/TE/TI: 7840/95/2500 msec, NEX: 1, slice thickness/interslice gap: 4/1 mm, in-plane resolution: 0.7 mm, FOV: 22.4 × 16.8 cm, 4 min 28 sec). Diffusion tensor imaging (DTI) was performed with a single-shot SE-EPI sequence (TR/TE: 8300/98 msec, slice thickness: 2 mm, no gap, in-plane resolution: 2 mm, 12 directions, 5 b-values: 350/650/1000/1300/1600 s/mm<sup>2</sup>, FOV: 19.2 × 19.2 cm, 9 min 26 sec). DSCI was performed (TR/TE: 1500/30 msec, slice thickness: 5 mm, in-plane resolution: 2 mm, FOV 19.2 × 19.2 cm; 90 volumes acquired, 2 min 21 sec) with 9 mL of gadobutrol (Gadovist 1.0 mmol/mL) followed by a 20-mL saline flush given via a power injector at a rate of 5 mL per second after the tenth volume. Following contrast injection a postcontrast 3D  $T_1$ -weighted inversion recovery sequence was performed (MPRAGE; TR/TE/TI: 2300/2.98/900 msec, NEX: 1, slice thickness: 1 mm, no gap, in-plane resolution: 1 mm, FOV: 25.6 × 24.1 cm, 9 min 14 sec). To plan the subsequent spectroscopy, an axial  $T_2$ -weighted acquisition was performed (TR/TE: 4840/114 msec, NEX: 1, slice thickness/interslice gap: 4/1 mm, in-plane resolution: 1 mm, FOV: 22 × 16.5 cm, 1 min 33 sec). 2D multivoxel <sup>1</sup>H MRS was performed using the semi-LASER sequence,<sup>27</sup> with (NEX: 3) water suppression (TR/TE: 2000/35 msec, slice thickness: 20 mm, FOV: 16 × 16 cm, 16 × 16 grid with Hamming acquisition filter, 8 min 6 sec).

### Postprocessing of Imaging Data

All data processing was performed offline. The DTI data were processed using the FDT toolbox in FSL (FMRIB, Oxford, UK). For each voxel, the eigenvalues ( $\lambda_1$ ,  $\lambda_2$ ,  $\lambda_3$ ) were calculated and were used to construct the  $p$  and  $q$  maps using the methodology and terminology described previously.<sup>16</sup>

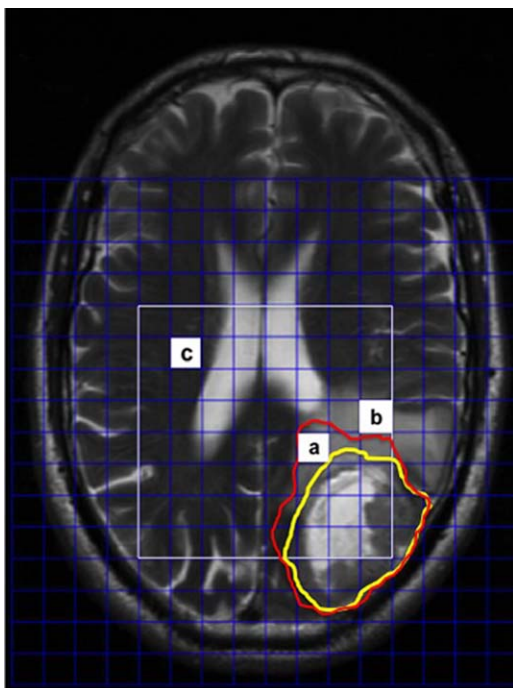


**FIGURE 1:** An example of the placement of ROIs. The DTI and DSCI data were coregistered to the  $T_2$ -weighted sequence used to plan the spectroscopy grid (shown in white). The  $p$  abnormality (red line) and  $q$  (yellow line) is outlined to identify the invasive margin. Regions of interest were taken from (a) the invasive region, (b) the noninvasive region, and (c) contralateral normal brain. Measures of rCBV and MRS were made from each region.

The DSCI data were processed using NordiICE (Nordic-NeuroLab, Bergen, Norway) and maps of rCBV were generated following contrast agent leakage correction.

The MRS data were processed using LC Model.<sup>28</sup> All spectra from the selected voxels were assessed visually for artifacts according to the criteria described by Kreis.<sup>29</sup> The values of the Cramer–Rao lower bounds indicated by the program were used to evaluate the quality and reliability of the  $^1\text{H}$  spectra and values greater than 20% were discarded. The metabolites were expressed as a ratio to creatine to avoid the dilutional effects associated with varying amounts of peritumoral edema<sup>30</sup>

### Regions of Interest (ROIs)

For each patient the contrast-enhanced  $T_1$ -weighted sequence, DTI, and DSCI parametric maps were individually coregistered to the  $T_2$ -weighted images used to plan the grid for the MRS for that patient using the FLIRT toolbox in FSL (affine transformation with 12 degrees of freedom). For the DTI images the  $p$  images (that had improved anatomical details) were coregistered and the transformation matrix applied to the  $q$  images. Coregistered images were inspected visually by S.J.P. (with 15 years neuroimaging experience) to ensure good quality of registration by outlining anatomical structures (eg, ventricles) and assessing the accuracy. The registered images were discarded and coregistration repeated if there were errors of registration greater than 2 mm. This allowed the DTI, perfusion, spectroscopy, and anatomical information to be in the same imaging space.

For each of the  $p$  and  $q$  maps, ROIs were drawn around the visible abnormality on every slice by two reviewers—a neurosurgeon with 15 years of advanced imaging experience who was

involved in developing the methodology, and a radiologist with 11 years experience, using ImageJ software (National Institutes of Health, Bethesda, MD). In a random subsample of 15 patients two trained readers independently drew the ROIs twice at different timepoints to determine both the inter- and intrarater agreement.

### Statistical Analysis

Three regions of interest were determined based on the spectroscopy grid, as shown in Fig. 1:

1. *Invasive*: in the DTI-defined invasive region (ie, within the area of increased  $p$  and outside the area of reduced  $q$  regions);
2. *Noninvasive*: in an area outside of the DTI-defined area (ie, outside the  $p$  abnormality) but in an area similar to the invasive ROI according to anatomical imaging (ie,  $T_2$ -weighted and contrast-enhanced  $T_1$ -weighted areas);
3. *Normal white matter*: in the white matter of the contralateral hemisphere, avoiding any visible pathology (as assessed by S.J.P.).

ROIs were identified where all of the MRS voxels fitted within the regions described above to avoid the issue of partial volume effects. The rCBV was calculated for each of the ROIs as a ratio to normal white matter taken from the contralateral centrum semiovale. Spectroscopic measures of N-acetylaspartate (NAA), myo-inositol (Ins), total choline (Cho) including phosphocholine and glycerylphosphorylcholine, and glutamate + glutamine (Glx) were expressed as a ratio to the total creatine (including phosphocreatine) for each ROI. We felt that it is preferable quantifying metabolites to total creatine (which varies across the tumor) to the water resonance due to problems with dilution in regions of edematous brain.<sup>31</sup> Similarly, the NAA/Cho ratio was determined for each ROI. All values are quoted as mean with 95% confidence interval (CI) unless otherwise stated.

Data were analyzed using IBM SPSS v. 21 (Armonk, NY) and significance was taken at the  $P < 0.05$  level. Differences between the three groups were explored with analysis of variance (ANOVA), with post-hoc analysis using the Tukey-Kramer honestly significant difference (HSD) test. The receiver operator characteristic (ROC) was calculated for each of the parameters to determine which provided the best predictor of the DTI-invasive regions. This was performed by taking the values from 129 ROIs (47 invasive, 40 noninvasive, and 42 normal white matter) and used the binary classification system as invasive or not invasive (which included both the noninvasive and normal white matter ROIs) based on the DTI data. The agreement was quantified using two methods: Dice scores, which are a measure of the extent of overlap between the ROIs, and the edge Hausdorff distance<sup>32</sup> between the ROIs, which is a measure of the maximal distance between the edges of the ROIs being compared. As the Hausdorff distance can be sensitive to outliers, the 95th percentile of the distance was used instead. Classification of the pattern of invasion was made according to previously published criteria.<sup>22</sup>

## Results

### DTI Studies

Regions of abnormal  $p$  and  $q$  from the DTI data could be identified in all patients. Overall, 34 (68%) had a diffuse invasive pattern, 12 (24%) had a localized pattern, and 4 (8%) were minimally invasive. Thirty datasets were randomly assigned to two independent raters. There was agreement in 27 cases (90%),

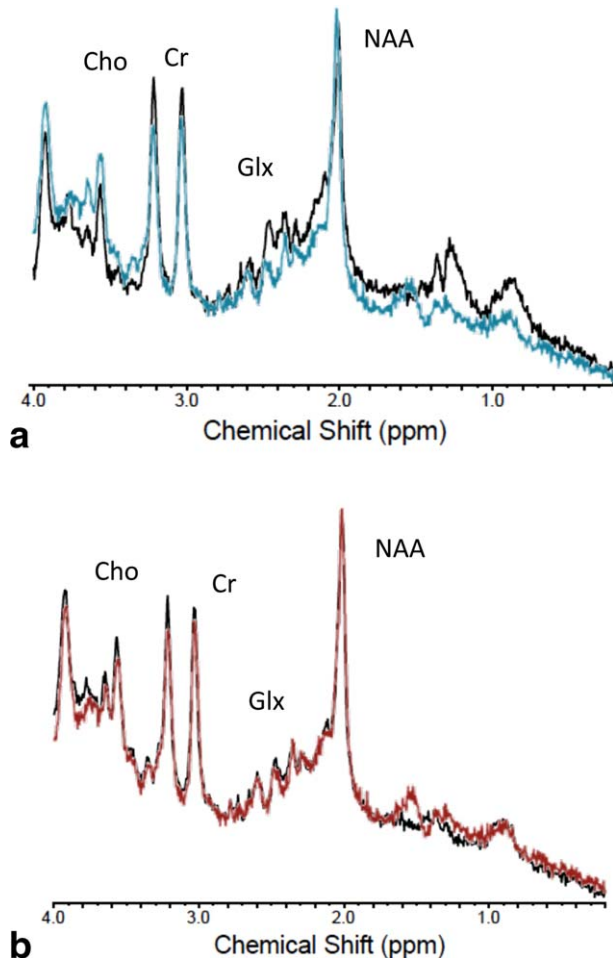


**FIGURE 2:** An example of MR spectra from different ROIs in a glioblastoma patient. **a:** The invasive region (in black) compared with the normal brain (blue). The invasive region demonstrates increased Cho and significantly reduced NAA with increased Glx. **b:** The noninvasive region (in black) compared with the normal brain (red). There is no significant differences between metabolites in these regions.

providing a Cohen’s kappa statistic of 0.81, suggesting very good interrater agreement for the classification of the invasive phenotype. A consensus opinion was used where there was disagreement.

Interrater variability of the ROIs showed good agreement between the two raters. There was excellent agreement for the *p* regions, with mean Dice scores of 0.86 (SD 0.11) and the mean 95th centile of the edge Hausdorff distance was 8.2 mm (SD 4.7 mm). The *q* region agreement between the two raters was also good, but was not as robust as the *p* region (mean Dice scores 0.76, SD 0.16; mean 95th centile of the edge Hausdorff distance 15.7 mm, SD 9.9 mm). There was excellent intrarater agreement for both *p* (mean Dice scores 0.88, SD 0.09; mean 95th centile of the edge Hausdorff distance 7.0 mm, SD 4.9 mm) and *q* ROIs (mean Dice scores 0.85, SD 0.1; mean 95th centile of the edge Hausdorff distance 8.6 mm, SD 7.3 mm).

**Perfusion Imaging**

Values of rCBV could be calculated in all 50 patients. The rCBV was increased in invasive regions (mean 1.64, 95%

CI 1.5–1.78;  $P < 0.001$ ) compared to the noninvasive regions (1.14; 95% CI 1.09–1.18) and normal white matter (1.06, 95% CI 1.02–1.10;  $P < 0.001$ ). There was no difference between rCBV values in the noninvasive and normal white matter regions ( $P = 0.36$ ).

**MRS**

An example of the MR spectra in the ROIs is shown in Fig. 2. The results for the spectroscopy data are summarized in Fig. 3. Useable spectroscopic data were obtained in 41 patients (82%), dropping to 35 patients (70%) for Glx.

The NAA/Cr was significantly reduced in invasive regions (0.95, 95% CI 0.85–1.05) compared to either noninvasive (1.19, 95% CI 1.06–1.31;  $P = 0.008$ ) or normal white matter (1.26, 95% CI 1.15–1.36;  $P < 0.001$ ). There was no difference between noninvasive and normal white matter ( $P = 1.0$ ).

The total choline/creatine (Cho/Cr) ratio was significantly increased in the invasive area (0.42, 95% CI 0.38–0.46) compared to both the noninvasive region (0.35, 95% CI 0.31–0.38;  $P = 0.02$ ) and normal white matter (0.35, 95% CI 0.31–0.39;  $P = 0.019$ ). There was no difference between these two regions ( $P = 1.0$ ).

The glutamate + glutamine to creatine ratio (Glx/Cr) was significantly increased in the invasive region (1.54, 95% CI 1.27–1.82) compared to both the noninvasive region (1.3, 95% CI 1.13–1.47;  $P = 0.028$ ) and to normal white matter (1.15, 95% CI 0.99–1.31;  $P = 0.034$ ). There was no difference between the noninvasive and normal regions ( $P = 0.59$ ).

The choline/NAA ratio, a marker of cellular proliferation,<sup>33</sup> was increased in the invasive region (0.54, 95% CI 0.41–0.68) compared to both the noninvasive region (0.37, 95% CI 0.29–0.45;  $P = 0.032$ ) and the normal white matter (0.32, 95% CI 0.25–0.39;  $P = 0.004$ ). The latter two groups did not differ ( $P = 0.78$ ).

The myoinositol/creatine (mI/Cr) ratio was not significantly different in either the invasive (1.2, 95% CI 0.99–1.41;  $P = 0.35$ ) or the noninvasive regions (1.3, 95% CI 1.14–1.46;  $P = 0.68$ ) compared to the normal white matter (1.37, 95% CI 1.24–1.5).

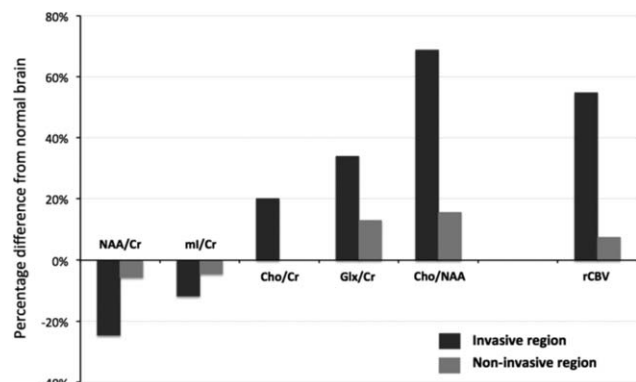


**FIGURE 3:** Percentage change from normal white matter.

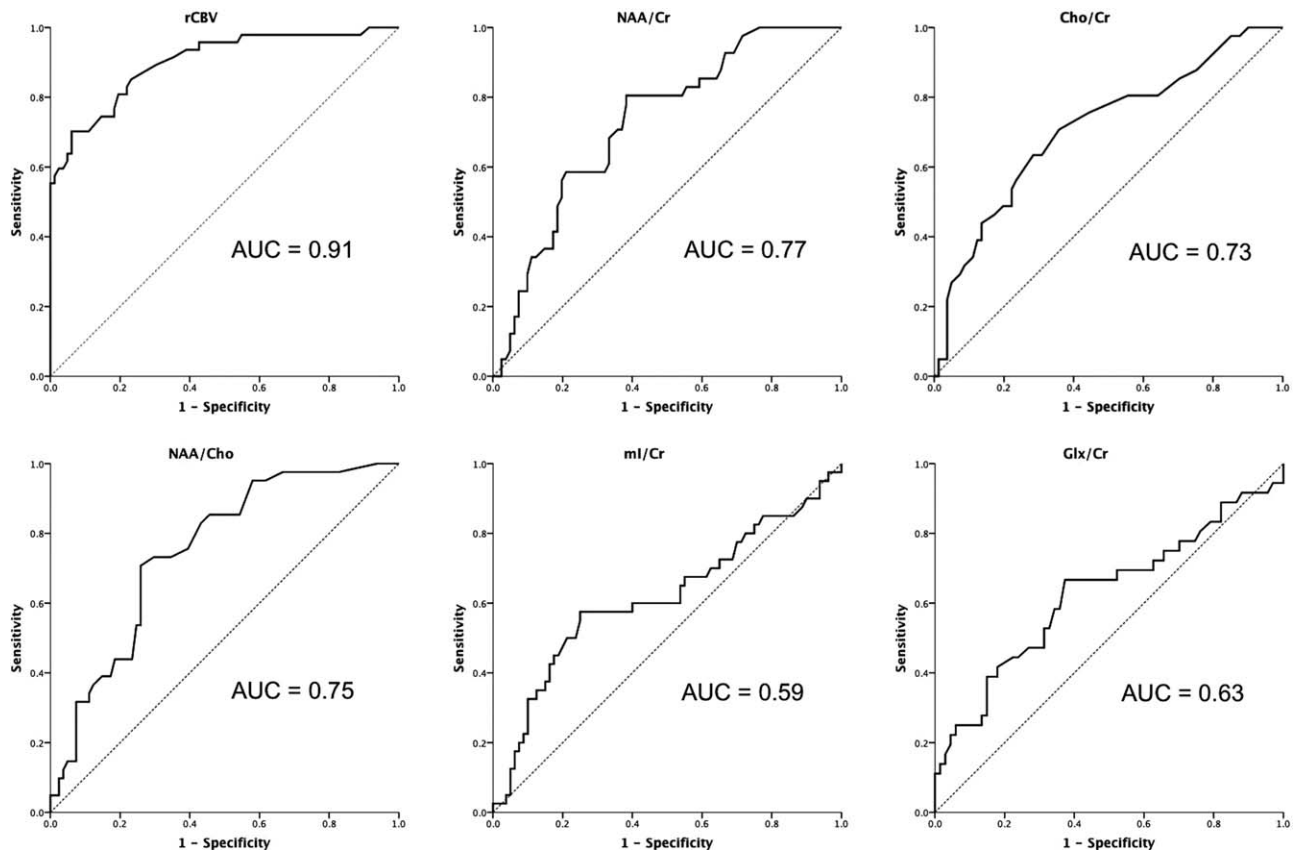


FIGURE 4: The ROC curves for the imaging parameters performance at differentiating invasive region vs. noninvasive (which includes both the noninvasive and normal ROIs). The curve for rCBV suggests that this may be the best discriminator.

### Predicting Invasive Regions

The ROC showed that the rCBV data provided a better predictor of the DTI-defined invasive regions than the spectroscopic measures (data shown in Fig. 4). Using a cutoff for the rCBV of 1.25 provides a predictor with a sensitivity and specificity of 82% for identifying invasive tumor.

### Discussion

Attempts to study the peritumoral region of GBMs, usually defined as the peripheral nonenhancing or edematous region, have shown that there is an increase in total choline and the Cho/NAA ratio with a reduction in total NAA.<sup>31,34–38</sup> Histological studies suggest that total choline and Cho/NAA increase with the degree of invasion of surrounding brain.<sup>36</sup> These changes are not seen in the peritumoral region of noninvasive meningiomas and metastases.<sup>31</sup> Similarly, areas of increased perfusion have been found in the peritumoral region of GBMs.<sup>39–41</sup> In this study we were able to improve the characterization of the peritumoral region using DTI, and have shown that the DTI-defined invasive region has a different local environment compared to either noninvasive or normal contralateral brain using multimodal MRI. Outlining these invasive regions showed high interrater agreement, suggesting a robust methodology. There was an increase in rCBV, Cho/Cr, Cho/NAA, and

Glx/Cr, with a decrease in NAA/Cr in the invasive regions. The noninvasive regions, although showing similar appearances on conventional imaging to the invasive regions, had a similar local environment to the normal-appearing brain from the contralateral hemisphere on multimodal MRI.

In this study we defined the invasive region of the brain based purely on the DTI. Previous studies have justified this and shown that image-guided biopsies of the DTI-defined invasive region can indeed identify invasive tumor with a high degree of accuracy.<sup>8,19</sup> A number of studies have now shown that these DTI-defined invasive regions also predict the site of tumor progression as defined by the site where new contrast enhancement develops.<sup>19,21,22</sup> Our imaging methods are only sensitive enough to detect tumor cells outside of the main contrast-enhancing tumor when they are present in large numbers. As alluded to previously, it is clear that the noninvasive region will still contain tumor cells. As virtually all tumors will recur adjacent to the resection cavity,<sup>2–5</sup> it has been suggested that detecting the site of likely tumor progression (ie, the area with the largest number of tumor cells outside the target of surgical resection) is more important than identifying the true extent of invasion.<sup>5</sup>

These findings provide information on the local environment of the invasive region that correlates with our

understanding of the multiple processes that occur during invasion. As mentioned previously, the invasive cells have a different phenotype, in that they are less proliferative than enhancing tumor. The Cho/NAA ratio has been shown in some studies to correlate well with the proliferation of tumor cells:<sup>33,42</sup> although Cho/NAA increased in the invasive regions in the current study, it was still much lower than in other studies that looked at the enhancing tumor.<sup>43</sup> Others have found choline content to correlate more closely with cell density than proliferation index.<sup>44,45</sup> As the cell density increases, angiogenesis is stimulated by the resultant hypoxia, resulting in increased rCBV. The increase in rCBV appears to be the best measure to identify these invasive regions and has been suggested as a marker that precedes the development of contrast-enhanced tumor.<sup>41</sup> The release of enzymes to degrade the extracellular matrix is accompanied by glutamate release in excitotoxic concentrations.<sup>10,46</sup> This is consistent with the increase in Glx/Cr in these invasive areas seen in our study and reported by other groups looking at GBMs.<sup>47–49</sup> The net effect of these processes is the loss of neurons (measured by decrease in NAA).

In our study we failed to identify a significant change in myoinositol in the invasive region compared to normal brain. Myoinositol is thought to be involved with astrocytic integrity and regulation of brain osmosis.<sup>50</sup> Astrocytic proliferation is associated with an increase in myoinositol and has been reported in the peritumoral region.<sup>31,47</sup> As the grade of tumor increases, however, myoinositol levels decrease, so that in GBMs they are similar to normal brain.<sup>51,52</sup> Our data certainly show a nonsignificant trend of reduced myoinositol in DTI-defined invasive regions where previous histological studies have shown extensive invasion with high glioma cells<sup>8</sup> replacing other normal cell populations (including astrocytes).

The local environment of a tumor has a major influence on how that tumor will behave and respond to therapy.<sup>53</sup> Most imaging studies that aim to predict prognosis or response to therapy have derived measures from the contrast-enhancing tumor alone. Recent publications suggest that studying the nonenhancing component of the tumor also provides prognostic information.<sup>54</sup> Advances in modern neurosurgery now mean that complete resection of the contrast-enhancing tumor is achieved more often; in our series, a complete resection of the contrast-enhancing tumor was achieved in 78% of cases. The result is that nonenhancing tumor margin will be the site of progressive tumor. Studying these regions may be more relevant to prognostication and response to therapies performed after surgical treatments.

One major limitation of our work is the difference in resolution, slice thickness, and gaps between the anatomical imaging, DTI imaging ( $2 \times 2 \times 2$  mm voxel size providing whole brain coverage), DSC imaging ( $2 \times 2 \times 5$  mm voxel

size providing whole brain coverage), and our single-slice multivoxel spectroscopic imaging ( $10 \times 10 \times 20$  mm voxel size). This will lead to issues with the coregistration and lead to partial volume errors. The difference in voxel size is particularly critical for the MRS data and means that the spectral pattern will be dependent on the relative amount of tumor to normal brain in these invasive regions. But these limitations will be the same for each of the three ROIs we compared for each patient. Our findings would suggest that in the DTI-defined invasive regions there is a high proportion of tumor cells, whereas in noninvasive regions there is more normal brain. Other groups have published their experience of 3D spectroscopy—but even then only managed a voxel size of  $10 \times 10 \times 10$  mm.<sup>55</sup> They described changes in NAA and Cho in normal-appearing white matter surrounding gliomas. This study used a longer echo time (70 msec) and as a result was not able to analyze metabolites with smaller concentrations (eg, myoinositol and glutamate + glutamine). Newer sequences providing 3D short echo spectroscopy have been developed and shown to be reproducible<sup>56</sup> but still suffer from poor resolution compared to DTI and DSCI and long acquisition times that make it difficult to use for multimodal imaging in this population. It is likely, however, that these methods will be utilized in the future.

In conclusion, by using DTI to define the limits of invasion we see changes in the local environment in invasive regions that are not seen in noninvasive brain and which fit with our understanding of glioma invasion.

---

## Acknowledgment

Contract grant sponsor: National Institutes of Health Research Clinician Scientist Fellowship.

## Conflict of Interest

The authors declare no conflicts of interest.

---

## References

1. Stummer W, Meinel T, Ewelt C, et al. Prospective cohort study of radiotherapy with concomitant and adjuvant temozolomide chemotherapy for glioblastoma patients with no or minimal residual enhancing tumor load after surgery. *J Neurooncol* 2012;1–9.
2. Oppitz U, Maessen D, Zunterer H, Richter S, Flentje M. 3D-recurrence-patterns of glioblastomas after CT-planned postoperative irradiation. *Radiother Oncol* 1999;53:53–57.
3. Lee SW, Fraass BA, Marsh LH, et al. Patterns of failure following high-dose 3-D conformal radiotherapy for high-grade astrocytomas: a quantitative dosimetric study. *Int J Radiat Oncol Biol Phys* 1999;43:79–88.
4. Brandes AA, Tosoni A, Franceschi E, et al. Recurrence pattern after temozolomide concomitant with and adjuvant to radiotherapy in newly diagnosed patients with glioblastoma: correlation with MGMT promoter methylation status. *J Clin Oncol* 2009;27:1275–1279.

5. Chang EL, Akyurek S, Avalos T, et al. Evaluation of peritumoral edema in the delineation of radiotherapy clinical target volumes for glioblastoma. *Int J Radiat Oncol Biol Phys* 2007;68:144–150.
6. Berens ME, Giese A. "... those left behind." Biology and oncology of invasive glioma cells. *Neoplasia* 1999;1:208–219.
7. Kelly PJ, Dumas-Duport C, Kispert DB, Kall BA, Scheithauer BW, Illig JJ. Imaging-based stereotaxic serial biopsies in untreated intracranial glial neoplasms. *J Neurosurg* 1987;66:865–874.
8. Price SJ, Jena R, Burnet NG, et al. Improved delineation of glioma margins and regions of infiltration with the use of diffusion tensor imaging: an image-guided biopsy study. *Am J Neuroradiol* 2006;27:1969–1974.
9. Giese A, Loo MA, Tran N, Haskett D, Coons SW, Berens ME. Dichotomy of astrocytoma migration and proliferation. *Int J Cancer* 1996;67:275–282.
10. Ye ZC, Sontheimer H. Glioma cells release excitotoxic concentrations of glutamate. *Cancer Res* 1999;59:4383–4391.
11. Deryugina EI, Bourdon MA, Luo GX, Reisfeld RA, Strongin A. Matrix metalloproteinase-2 activation modulates glioma cell migration. *J Cell Sci* 1997;110(Pt 19):2473–2482.
12. Zuniga RM, Torcuator R, Jain R, et al. Efficacy, safety and patterns of response and recurrence in patients with recurrent high-grade gliomas treated with bevacizumab plus irinotecan. *J Neurooncol* 2009;91:329–336.
13. Price S, Burnet N, Donovan T, et al. Diffusion tensor Imaging of brain tumours at 3 T: a potential tool for assessing white matter tract invasion? *Clin Radiol* 2003;58:455–462.
14. Wang S, Kim SJ, Poptani H, et al. Diagnostic utility of diffusion tensor imaging in differentiating glioblastomas from brain metastases. *AJNR Am J Neuroradiol* 2014;35:928–934.
15. Provenzale JM, McGraw P, Mhatre P, Guo AC, Delong D. Peritumoral brain regions in gliomas and meningiomas: investigation with isotropic diffusion-weighted MR imaging and diffusion-tensor MR imaging. *Radiology* 2004;232:451–460.
16. Pena A, Green H, Carpenter T, Price S, Pickard J, Gillard J. Enhanced visualization and quantification of magnetic resonance diffusion tensor imaging using the  $p : q$  tensor decomposition. *Br J Radiol* 2006;79:101–109.
17. Price S, Pena A, Burnet N, et al. Tissue signature characterisation of diffusion tensor abnormalities in cerebral gliomas. *Eur Radiol* 2004;14:1909–1917.
18. Wang W, Steward CE, Desmond PM. Diffusion tensor imaging in glioblastoma multiforme and brain metastases: the role of  $p$ ,  $q$ ,  $L$ , and fractional anisotropy. *AJNR Am J Neuroradiol* 2009;30:203–208.
19. Castellano A, Donativi M, Bello L, et al. Evaluation of changes in gliomas structural features after chemotherapy using DTI-based functional diffusion maps (fDMs): a preliminary study with intraoperative correlation. In: *Proc 19th Annual Meeting ISMRM, Montreal*; 2011. p 2411.
20. Mohsen LA, Shi V, Jena R, Gillard JH, Price SJ. Diffusion tensor invasive phenotypes can predict progression-free survival in glioblastomas. *Br J Neurosurg* 2013;27:419–424.
21. Price S, Pena A, Burnet N, Pickard J, Gillard J. Detecting glioma invasion of the corpus callosum using diffusion tensor imaging. *Br J Neurosurg* 2004;18:391–395.
22. Price S, Jena R, Burnet N, Carpenter T, Pickard J, Gillard J. Predicting patterns of glioma recurrence using diffusion tensor imaging. *Eur Radiol* 2007;17:1675–1684.
23. Sugahara T, Korogi Y, Kochi M, et al. Correlation of MR imaging-determined cerebral blood volume maps with histologic and angiographic determination of vascularity of gliomas. *AJR Am J Roentgenol* 1998;171:1479–1486.
24. Aronen HJ, Pardo FS, Kennedy DN, et al. High microvascular blood volume is associated with high glucose uptake and tumor angiogenesis in human gliomas. *Clin Cancer Res* 2000;6:2189–2200.
25. Price SJ, Green HA, Dean AF, Joseph J, Hutchinson PJ, Gillard JH. Correlation of MR relative cerebral blood volume measurements with cellular density and proliferation in high-grade gliomas: an image-guided biopsy study. *AJNR Am J Neuroradiol* 2011;32:501–506.
26. Vogelbaum MA, Jost S, Aghi MK, et al. Application of novel response/progression measures for surgically delivered therapies for gliomas. *Neurosurgery* 2012;70:234–244.
27. Scheenen TW, Klomp DW, Wijnen JP, Heerschap A. Short echo time 1H-MRSI of the human brain at 3T with minimal chemical shift displacement errors using adiabatic refocusing pulses. *Magn Reson Med* 2008;59:1–6.
28. Provencher SW. Estimation of metabolite concentrations from localized in vivo proton NMR spectra. *Magn Reson Med* 1993;30:672–679.
29. Kreis R. Issues of spectral quality in clinical 1H-magnetic resonance spectroscopy and a gallery of artifacts. *NMR Biomed* 2004;17:361–381.
30. Kamada K, Houkin K, Hida K, et al. Localized proton spectroscopy of focal brain pathology in humans: significant effects of edema on spin-spin relaxation time. *Magn Reson Med* 1994;31:537–540.
31. Wijnen JP, Idema AJ, Stawicki M, et al. Quantitative short echo time 1H MRSI of the peripheral edematous region of human brain tumors in the differentiation between glioblastoma, metastasis, and meningioma. *J Magn Reson Imaging JMIR* 2012;36:1072–1082.
32. Mostayed A, Garlapati RR, Joldes GR, et al. Biomechanical model as a registration tool for image-guided neurosurgery: evaluation against BSpline registration. *Ann Biomed Eng* 2013;41:2409–2425.
33. McKnight TR, Lamborn KR, Love TD, et al. Correlation of magnetic resonance spectroscopic and growth characteristics within Grades II and III gliomas. *J Neurosurg* 2007;106:660–666.
34. Sijens PE, Oudkerk M. 1H chemical shift imaging characterization of human brain tumor and edema. *Eur Radiol* 2002;12:2056–2061.
35. Di Costanzo A, Scarabino T, Trojsi F, et al. Multiparametric 3T MR approach to the assessment of cerebral gliomas: tumor extent and malignancy. *Neuroradiology* 2006;48:622–631.
36. Croteau D, Scarpace L, Hearshen D, et al. Correlation between magnetic resonance spectroscopy imaging and image-guided biopsies: semiquantitative and qualitative histopathological analyses of patients with untreated glioma. *Neurosurgery* 2001;49:823–829.
37. Pirzkall A, Li X, Oh J, et al. 3D MRSI for resected high-grade gliomas before RT: tumor extent according to metabolic activity in relation to MRI. *Int J Radiat Oncol Biol Phys* 2004;59:126–137.
38. Bieza A, Krumin G. Magnetic resonance study on fractional anisotropy and neuronal metabolite ratios in peritumoral area of cerebral gliomas. *Medicina* 2012;48:497–506.
39. Price SJ, Green HAL, Dean AF, Joseph J, Hutchinson PJ, Gillard JH. Correlation of MR relative cerebral blood volume measurements with cellular density and proliferation in high-grade gliomas: an image-guided biopsy study. *Am J Neuroradiol* 2011;32:501–506.
40. Lehmann P, Vallee JN, Saliou G, et al. Dynamic contrast-enhanced T2\*-weighted MR imaging: a peritumoral brain oedema study. *J Neuroradiol* 2009;36:88–92.
41. Blasel S, Franz K, Ackermann H, Weidauer S, Zanella F, Hattingen E. Stripe-like increase of rCBV beyond the visible border of glioblastomas: site of tumor infiltration growing after neurosurgery. *J Neurooncol* 2011;103:575–584.
42. Guo J, Yao C, Chen H, et al. The relationship between Cho/NAA and glioma metabolism: implementation for margin delineation of cerebral gliomas. *Acta Neurochir (Wien)* 2012;154:1361–1370; discussion 1370.
43. Laprie A, Catalaa I, Cassol E, et al. Proton magnetic resonance spectroscopic imaging in newly diagnosed glioblastoma: predictive value for the site of postradiotherapy relapse in a prospective longitudinal study. *Int J Radiat Oncol Biol Phys* 2008;70:773–781.

44. Gupta RK, Cloughesy TF, Sinha U, et al. Relationships between choline magnetic resonance spectroscopy, apparent diffusion coefficient and quantitative histopathology in human glioma. *J Neurooncol* 2000;50:215–226.
45. Nafe R, Herminghaus S, Raab P, et al. Preoperative proton-MR spectroscopy of gliomas—correlation with quantitative nuclear morphology in surgical specimen. *J Neurooncol* 2003;63:233–245.
46. Marcus HJ, Carpenter KL, Price SJ, Hutchinson PJ. In vivo assessment of high-grade glioma biochemistry using microdialysis: a study of energy-related molecules, growth factors and cytokines. *J Neurooncol* 2010;97:11–23.
47. Kallenberg K, Bock HC, Helms G, et al. Untreated glioblastoma multiforme: increased myo-inositol and glutamine levels in the contralateral cerebral hemisphere at proton MR spectroscopy. *Radiology* 2009;253:805–812.
48. Chawla S, Zhang Y, Wang S, et al. Proton magnetic resonance spectroscopy in differentiating glioblastomas from primary cerebral lymphomas and brain metastases. *J Comput Assist Tomogr* 2010;34:836–841.
49. Ramadan S, Andronesi OC, Stanwell P, Lin AP, Sorensen AG, Mountford CE. Use of in vivo two-dimensional MR spectroscopy to compare the biochemistry of the human brain to that of glioblastoma. *Radiology* 2011;259:540–549.
50. Brand A, Richter-Landsberg C, Leibfritz D. Multinuclear NMR studies on the energy metabolism of glial and neuronal cells. *Dev Neurosci* 1993;15:289–298.
51. Castillo M, Smith JK, Kwock L. Correlation of myo-inositol levels and grading of cerebral astrocytomas. *AJNR Am J Neuroradiol* 2000;21:1645–1649.
52. Candiota AP, Majos C, Julia-Sape M, et al. Non-invasive grading of astrocytic tumours from the relative contents of myo-inositol and glycine measured by in vivo MRS. *JBR-BTR* 2011;94:319–329.
53. Persano L, Rampazzo E, Basso G, Viola G. Glioblastoma cancer stem cells: role of the microenvironment and therapeutic targeting. *Biochem Pharmacol* 2013;85:612–622.
54. Jain R, Polsson LM, Gutman D, et al. Outcome prediction in patients with glioblastoma by using imaging, clinical, and genomic biomarkers: focus on the nonenhancing component of the tumor. *Radiology* 2014;272:484–493.
55. Maudsley AA, Roy B, Gupta RK, et al. Association of metabolite concentrations and water diffusivity in normal appearing brain tissue with glioma grade. *J Neuroimaging* 2014;24:585–589.
56. Ding XQ, Maudsley AA, Sabati M, Sheriff S, Dellani PR, Lanfermann H. Reproducibility and reliability of short-TE whole-brain MR spectroscopic imaging of human brain at 3T. *Magn Reson Med* 2015;73:521–528.



# Physiological Electrical Signals Promote Chain Migration of Neuroblasts by Up-Regulating P2Y1 Purinergic Receptors and Enhancing Cell Adhesion

Lin Cao · Jin Pu · Roderick H. Scott · Jared Ching · Colin D. McCaig

Published online: 7 August 2014

© The Author(s) 2014. This article is published with open access at Springerlink.com

**Abstract** Neuroblasts migrate as directed chains of cells during development and following brain damage. A fuller understanding of the mechanisms driving this will help define its developmental significance and in the refinement of strategies for brain repair using transplanted stem cells. Recently, we reported that in adult mouse there are ionic gradients within the extracellular spaces that create an electrical field (EF) within the rostral migratory stream (RMS), and that this acts as a guidance cue for neuroblast migration. Here, we demonstrate an endogenous EF in brain slices and show that mimicking this by applying an EF of physiological strength, switches on chain migration in mouse neurospheres and in the SH-SY5Y neuroblastoma cell line. Firstly, we detected a substantial endogenous EF of  $31.8 \pm 4.5$  mV/mm using microelectrode recordings from explants of the subventricular zone (SVZ). Pharmacological inhibition of this EF, effectively blocked chain migration in 3D cultures of SVZ explants. To mimic this EF, we applied a physiological EF and found that this increased the expression of N-cadherin and  $\beta$ -catenin, both of which promote cell-cell adhesion. Intriguingly, we found that the EF up-regulated P2Y purinoceptor 1 (P2Y1) to contribute to chain migration of neuroblasts through regulating the expression of N-cadherin,  $\beta$ -catenin and the

activation of PKC. Our results indicate that the naturally occurring EF in brain serves as a novel stimulant and directional guidance cue for neuronal chain migration, via up-regulation of P2Y1.

**Keywords** Neuroblasts · Chain migration · P2Y1 ·  $\beta$ -catenin · Extracellular electrical gradients

## Abbreviations

EF	Electrical field
SVZ	Subventricular zone
P2Y1	P2Y purinoceptor 1
RMS	Rostral migratory stream
OB	Olfactory bulb
CNS	Central nervous system
CSF	Cerebro-spinal fluid
miR-9	Brain-specific microRNA-9
PKC	Protein kinase C

## Introduction

The migration of neuronal precursor cells is essential in CNS development and repair. In postnatal mammalian brain, neuroblasts from the subventricular zone (SVZ) migrate within the rostral migratory stream (RMS) in intimate cell-cell contact with one another, forming a chain-like organization without a glial scaffold [1–3].

The persistence of chain migration depends on the interplay of directional cell movement and biased cell to cell contact [4]. For example, cell–cell interactions mediated via selective adhesion molecules establish and maintain chain migration. N-cadherin is expressed abundantly in chain migrating cells in the SVZ and RMS, but is down-regulated after cells exit these regions [5]. Another cell adhesion molecule,

---

Lin Cao and Jin Pu contributed equally

**Electronic supplementary material** The online version of this article (doi:10.1007/s12015-014-9524-1) contains supplementary material, which is available to authorized users.

---

L. Cao (✉) · J. Pu · R. H. Scott · C. D. McCaig (✉)  
School of Medical Sciences, Institute of Medical Sciences,  
University of Aberdeen, Aberdeen AB25 2ZD, UK  
e-mail: l.cao@abdn.ac.uk  
e-mail: c.mccaig@abdn.ac.uk

J. Ching  
Department of Neurosurgery, Aberdeen Royal Infirmary,  
Aberdeen AB25 2ZD, UK

NCAM, is expressed at high levels on neuronal precursor cells migrating towards the olfactory bulb (OB) [6, 7] and girdin,  $\alpha 6 \beta 1$  integrin and miR-9 (brain-specific microRNA-9) are additional intrinsic factors regulating chain migration along the RMS [8–10]. However, it remains poorly understood how neuroblasts use locally acting extracellular cues and intrinsic molecular machinery to coordinate their behaviour during chain migration within the RMS [8].

Extracellular electrical signals also regulate neuronal migration, nerve growth cone guidance, nerve sprouting and nerve regeneration and are widespread in developing and regenerating tissues, including brain and spinal cord [11, 12]. They are present during neurulation, are expressed continuously across the wall of the differentiating neural tube and disrupting them, by chemical, physical, or electrical means causes major developmental abnormalities in the formation of the nervous system [13–18]. In addition, epileptic seizure, stroke, ischaemia, migraine and acute damage to the hippocampus all induce extracellular electrical signals in brain that persist for hours to days [19–23]. Recently, we measured directly an electrical gradient of  $5.7 \pm 1.2$  mV/mm within the extracellular spaces along the RMS *ex vivo* [24]. Using an applied EF of similar strength ( $\sim 5$  mV/mm), directional migration of epithelial cells, neonatal neurones and neuroblasts is induced *in vitro* and *in vivo* [24–28].

Neuronal chain migration involves coordinated cell migrations. Collective migration keeps tissues intact during remodelling, allows mobile cells to carry immobile cells along with them and allows migrating cells to influence each other to ensure appropriate cell distribution and shaping of a tissue [29]. Neuroblasts from the SVZ and newly divided neurons are recruited to the striatum following a stroke [30] and neurogenesis and neuronal stem cell migrations occur in the cortex and the hippocampus after ischaemic insults [31] which cause local EFs. Here, we found that the extracellular EF contributes to chain migration of neuroblasts. This new perspective indicates that the development of new therapeutic strategies involving electrical guidance may be useful to treat brain injury and disease.

## Methods and Materials

### Cell Culture

Adult mice (C57BL/6j, 6–8 weeks, male or female), purchased from Charles River Laboratories, were euthanized in a CO<sub>2</sub> chamber. The method for culturing neurospheres has been described previously [32, 33]. In brief, blocks of SVZ tissue were dissected from mouse brain and digested to release cells. Then a density gradient (OptiPrep density 1.32, Sigma) was used to purify the cells and cultures were suspended in Neurobasal medium (Life technology), supplemented with

2 mM l-glutamine, 2 % B-27 (without Retinyl acetate, Life technology), 20 ng/ml EGF (Life technology), 20 ng/ml FGF-2 (Life technology) and penicillin-streptomycin mixture (Life technologies) at 37 °C in humidified air containing 5 % CO<sub>2</sub>.

### Electrotaxis Detection With/Without Extracellular ATP Treatment

Methods of exposing cells to an applied electric field in an electrotaxis detection chamber have been described [34]. The SVZ neuroblasts were seeded in an electrotaxis chamber created in Falcon tissue culture dishes (BD Biosciences) which had been coated with 2 % Matrigel (BD Biosciences) [35, 36]. The cells were allowed to settle and adhere on the base of the chamber for 1 h. A roof of coverglass was applied and sealed with high vacuum silicone grease (Dow Corning Corporation) to the side walls of the chamber [37]. The final dimensions of the shallow chamber, through which the electric current was passed, were 20 mm  $\times$  10 mm  $\times$  0.3 mm. We applied EFs 10 mV/mm to neurospheres and 5–100 mV/mm to SH-SY5Y cells with/without 100  $\mu$ M ATP (Sigma) treatment through agar-salt bridges that connected silver/silver chloride electrodes in beakers containing Steinberg's solution to pools of culture medium at either side of the chamber. The dish was placed on a Zeiss Axiovert 100 microscope with a stage incubator controlling temperature at 37 °C. Images of cells were recorded every 10 min and analyzed with Digital Pixel and MetaMorph imaging systems (Zeiss Axiovert 100 microscope) [18, 37]. Assessment of migration directedness (cosine  $\theta$ ) was used to quantify how directionally a cell migrated in the field, where  $\theta$  is the angle between the EF vector and a straight line connecting the start and end positions of a cell [23]. Migration rate was analyzed using the following two parameters. Trajectory rate (Tt/T) is the total length of the migration trajectory of a cell (Tt) divided by the given period of time (T). Displacement rate (Td/T) is the straight-line distance between the start and end positions of a cell (Td) divided by the time (T).

### Western Blotting

Cell lysates were collected for Western blot experiments. Western blotting was performed as described previously [38]. Primary antibodies used included anti- $\beta$ -Catenin (Cell Signalling), anti-N-cadherin (Abcam), anti-P2Y1 (Cell Signalling), anti-p-PKC (Cell Signalling) and anti-GAPDH (Santa Cruz). Immunoblots were detected by Luminata Forte Western HRP substrate (Millipore).

### RNA-Interference

To knock-down P2Y1 in mouse derived neurospheres and SH-SY5Y cells, we used 100 nM of siRNA SMARTpools (a mixture of four siRNA duplexes each) using Dharmafect 1

(Thermo Scientific) according to the manufacturer's specifications. siRNA<sup>p2y1</sup> was comprised of: 5'-CUAUUGGUUU UAAUCUGUU-3', 5'-GUUGAAACUUGUAAAUCUC-3', 5'-GUAUUUAUUGAAGAGGUUU-3', 5'-GUACUAGU GUAAAUUCUAU-3'. Under these conditions, 70–90 % of transfection efficiency was achieved, as judged by siGloGreen control (Thermo Scientific). After 72 h transfection, cells were exposed to the EF (no EF application as a control) and cell lysates were collected to confirm the final knock-down effect by Western blotting.

#### Immunofluorescent Staining

Cultured neurospheres were fixed with 4 % paraformaldehyde in PBS for 20 min. After incubation with blocking solution for 90 min at 37 °C, cells or tissue sections were incubated overnight with primary antibodies at 4 °C. Primary antibody dilutions used were as follows: Anti-N-Cadherin, 1:200 (Millipore), anti- $\beta$ -Catenin 1:200 (BD Biosciences) and anti-P2Y1 1:200 (cell signalling). Samples then were incubated for 2 h with a secondary antibody. After washing, counterstaining with DAPI and mounting in anti-fading medium, they were visualized using a Zeiss LSM 510 Meta confocal microscope (Zeiss).

#### Brain Slice Culture

SVZ explants were prepared from P7 neonatal mice as described previously [39]. Briefly, brains taken from mice were sliced using a tissue chopper (Mickle Laboratory Engineering) or with a blade under dissecting microscope at 300–500  $\mu$ m thickness. Then, SVZ tissue was dissected and cut into small pieces under the stereomicroscope to be collected in cold Hanks' balanced salt solution (Life technology). These pieces were embedded on glass-bottom dishes (Matsunami Glass) in a 3:1 mixture of Matrigel (BD Bioscience) and Neurobasal medium (Life technology) supplemented with 2 mM l-glutamine, 2 % B-27 (Life technology), and penicillin-streptomycin mixture (Life technology) at 37 °C in humidified air containing 5 % CO<sub>2</sub> [39]. For inhibition experiments, drugs were added to the medium at the beginning of culture and used at the following concentrations: 10  $\mu$ M digoxin (Calbiochem) and 10  $\mu$ M ouabain (Calbiochem).

#### Microelectrode Measurement

Electrophysiological experiments to measure the electrical field in brain explants were conducted using sharp borosilicate glass microelectrodes. Electrodes were filled with artificial cerebrospinal fluid (ACSF) and had resistances of 2–20 M $\Omega$ . All recordings were made at room temperature (20–25 °C) with an Axoclamp 2A switching

amplifier. After balancing the amplifier with respect to ground (0 mV), a pipette was inserted into a 2 $\times$ 1 $\times$ 0.4 mm brain slice using a Narishige 3D micro-manipulator (Fig. 4b). The brain explants were bathed in ACSF at pH 7.4. The potential difference distribution in the brain slice was determined consistently at 15 s after the electrode was positioned in the tissue and recorded continually for at least 2 min by Scope v3.6-10. At least 4 slices in control and in each treatment group were measured and all experiments were repeated four times. For inhibitor experiments, cells were pre-incubated with 10  $\mu$ M ouabain or 10  $\mu$ M digoxin (both are Na<sup>+</sup>/K<sup>+</sup>-ATPase inhibitors, Sigma), for the time indicated and then exposed to the EF.

#### Statistical Analysis

A minimum of three replicates was analysed for each experiment presented. Data are presented as the mean  $\pm$  s.e.m. Student's *t* test was used to assess the significant difference. Differences were considered as statistically significant with a *p* value <0.05.

## Results

#### Extracellular EFs regulate chain migration in explants from the SVZ of mice

Neuroblasts migrate as chains in SVZ explants cultured in 3D Matrigel [40]. In addition, endogenous voltage gradients were measured in cultured rat hippocampal slices, with extracellular EFs ranging from 6 to 31 mV/mm, (mean = 17  $\pm$  2.9 mV/mm) [41]. Here we used the glass microelectrode method and measured directly an electrical gradient (EF) of  $-31.8 \pm 4.5$  mV/mm in cultured SVZ slices in Matrigel (Fig. 1a and b). The concentration of ions in the extracellular space, for example K<sup>+</sup>, Na<sup>+</sup>, Cl<sup>-</sup> and Ca<sup>2+</sup>, determine the strength of the EF [11]. When the SVZ slices were cultured in low sodium ACSF (data not shown), or exposed to either 10  $\mu$ M ouabain or 10  $\mu$ M digoxin (both inhibitors of Na<sup>+</sup>/K<sup>+</sup>-ATPase), the endogenous EF was reduced significantly, by around 50 % (Fig. 1c). This demonstrates that the formation of the EF in brain tissue explants is dependent at least in part on the function of the Na<sup>+</sup>/K<sup>+</sup> ATPase pump which regulates the distribution of sodium and potassium between the intracellular and extracellular spaces. Meanwhile, we found that chain migration in cultured SVZ explants was suppressed when the endogenous EF was inhibited by Na<sup>+</sup>/K<sup>+</sup>-ATPase inhibitors (Fig. 1d). This highlights that the endogenous EF may be one element capable of regulating neuronal migration in chains within SVZ explants.

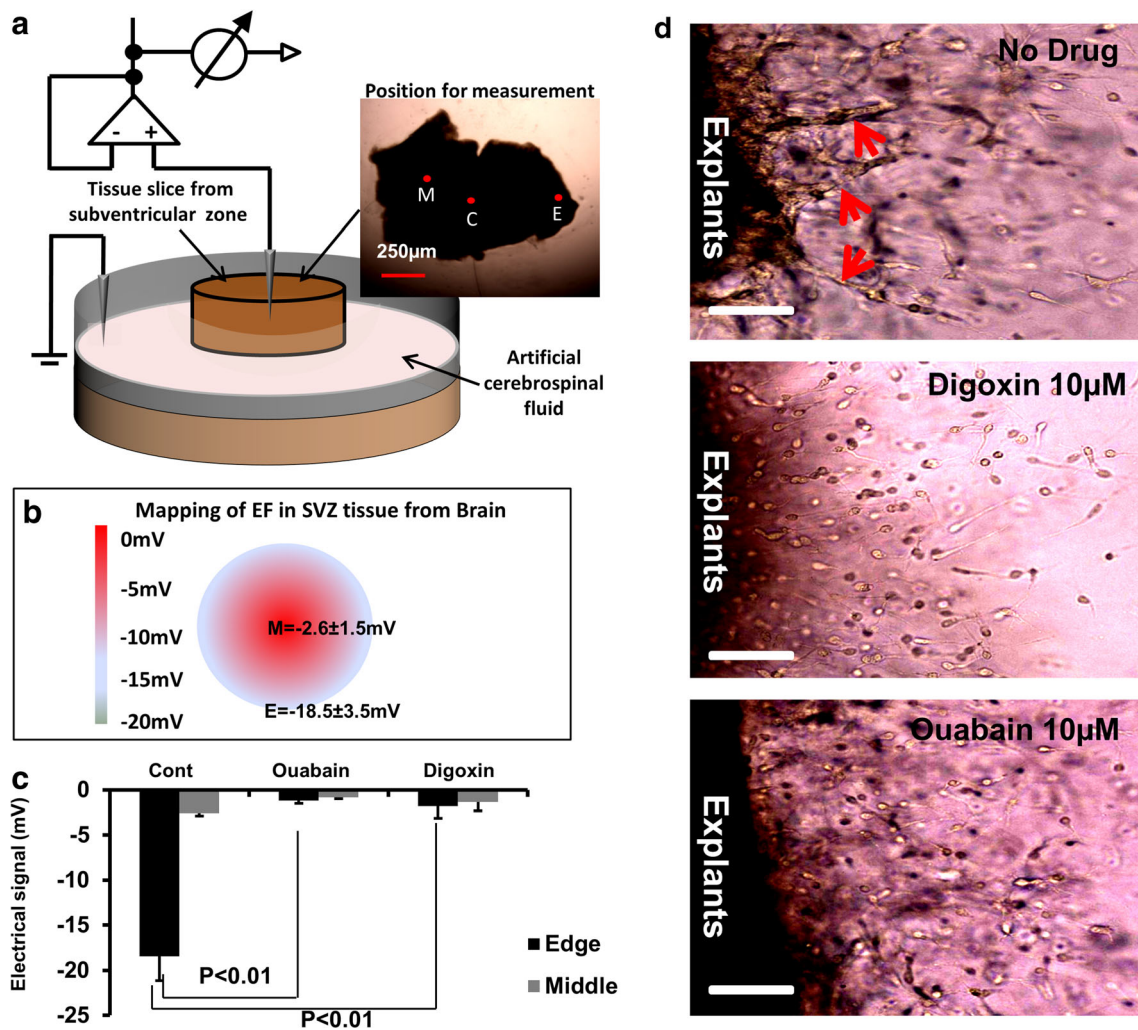


**Fig. 1** Inhibition of  $\text{Na}^+/\text{K}^+$ -ATPase effectively reduced both the endogenous voltage gradient and chain migration of neuroblast in SVZ explants culture. **a** Schematic diagram of the method used to measure the EF in brain slices. **c** (centre), M (middle) and E (edge) represent the points at which the detecting microelectrode measured the extracellular voltage. Reference electrode was located in the medium and connected to earth. **b** Results showed that a voltage drop of  $-2.6 \pm 0.8$  and  $-18.5 \pm 3.5$  mV were measured at middle (M) and edge (E) of the SVZ slice respectively. The distance between middle point and edge point is 0.4 mm. The voltage gradient between middle and edge is therefore  $31.8 \pm 4.5$  mV/mm.  $N=5$  for each experiment. Triplicate was performed. **c** In explant slices treated

with Ouabain or Digoxin, the voltage drops between middle and edge of brain slices were inhibited significantly. The average voltage drop in the middle was reduced from  $-18.5$  mV to  $-1.2$  mV and  $-1.8$  mV by Ouabain and Digoxin respectively.  $p < 0.01$ .  $N=5$  in one experiment and triplicate was performed. **d** SVZ explants were prepared from p7 mice and cultured for 3 days. In no treatment control (upper row), chain migrations formed close to the edge of cultured explant of SVZ as indicated by the red arrows. When the endogenous extracellular EF was inhibited using Digoxin and Ouabain (middle and lower panel), cells migrating out from explants did so individually, rather than migrating by forming cellular chains, as was seen in untreated controls (top panel). Bar is 100 µm

### Mimicking the endogenous electrical cue induced chain migration in cultured mouse neuroblasts

Chain migration is dynamic; cells within a chain extend and retract filopodia making repeatedly sustained, broken and re-established cell contacts over short time frames [42, 43]. When neurospheres were cultured in a dish, migration of neuroblasts was evident. Without growth factors and with Matrigel coating, neurones migrated away from the spheres randomly and independently with multi-polar morphologies

over 5 h (Fig. 2a upper panel, Movie S1). By contrast, when exposed to an applied EF of physiological strength, migrating cells had a simple bipolar morphology and formed chains of cells extending from the spheres (10 mV/mm, Fig. 2a lower panel, Movie S2). The directedness of cell migration ( $\text{Cos } \theta$ ) increased significantly from  $0.08 \pm 0.1$  to  $0.64 \pm 0.03$  ( $N=50$ ;  $p < 0.01$ ) in an applied EF of only 10 mV/mm, indicating strong cathodally-directed migration. In addition, the migration speed at 10 mV/mm showed no significant difference between EF and no EF control (Fig S1A). In short, the applied

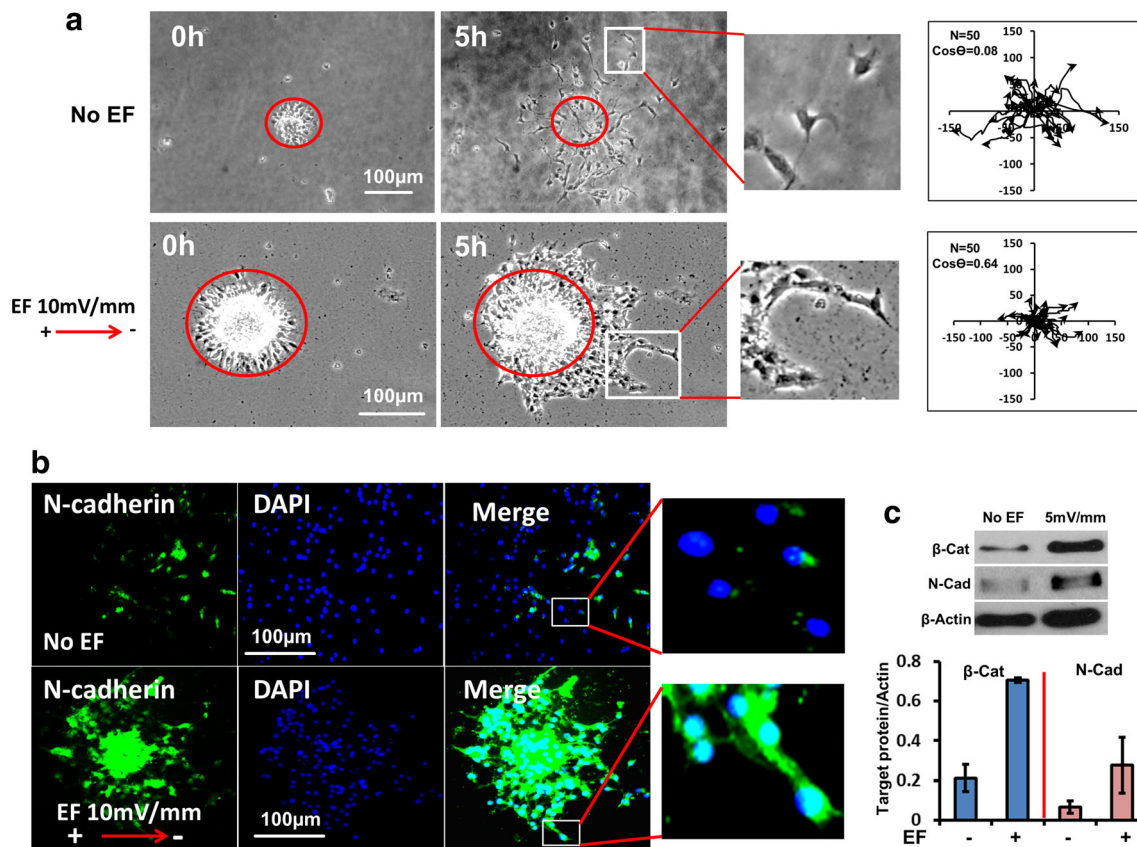


**Fig. 2** An applied physiological EF induced chain migration in neurospheres. **a** Neurospheres from mouse SVZ were cultured in electrotaxis chambers and an EF of physiological strength (10 mV/mm) was applied for 5 h. In upper row - no EF control, neuroblasts migrated in random directions and did so largely separated and scattered independently from each other (see enlarged image). Lower row - EF applied with cathode to the right. EF-stimulated neurospheres remained closely adherent to each other and migrated together in chains (see enlarged image at right). Tracks of neuroblast migration are shown in the plots at right. The migration of individual cells is plotted starting at the centre and lines radiate out to show the path and the end point of migration at 5 h. Axes are in  $\mu\text{m}$ . N is cell number and  $\text{Cos } \theta$  represents the directedness of cell migration. If  $\text{Cos } \theta = 1$ , it means all cells have migrated directly to the

cathode. Control plots (no EF - upper right) show that migration occurs in all directions, randomly. EF-exposed plots (lower right): by contrast migration was directed cathodally (*to the right*). **b** Neurospheres were seeded in electrotaxis chambers with/without an applied EF for 5 h and then the cells were fixed and stained immunofluorescently with an N-cadherin antibody. Cultures exposed to a very low physiological EF of 10 mV/mm (*lower row*) show strikingly enhanced N-cadherin staining compared to no EF controls (*upper row*). **c** A very low physiological EF (5 mV/mm) increased the expression of N-cadherin and  $\beta$ -catenin as determined by Western blotting (3 h exposure to EF). Actin is a loading control. The ratio of protein expression/actin is shown below the corresponding western blots

physiological EF clearly induced chains of cells to form and directed migration to the cathodal side in mouse neurospheres.

Next, we detected two molecules known as markers of typical chain migration in neuroblasts, N-cadherin [5] and  $\beta$ -catenin. Up-regulation of N-cadherin and  $\beta$ -catenin was seen only within the migrating chains exposed to an EF (Fig. 2b). In contrast, there was significantly lower expression of N-cadherin and  $\beta$ -catenin in no EF treated control cells (Fig. 2b). Protein analysis with Western blotting confirmed this (Fig. 2c), indicating that an applied physiological EF induced the formation of chain migration in cultured mouse neuroblasts by increasing cell-cell interaction. This was achieved by an EF-induced increased expression of N-cadherin and  $\beta$ -catenin which promoted and maintained cell-cell contacts and the extension of processes over the other cells in the migrating chains.

A physiological EF increased cell-cell contacts and directed migration in SH-SY5Y cells

SH-SY5Y is a human-derived cell line from neuroblastoma and resembles immature sympathetic neuroblasts in culture [44]. Here, we used this cell line to confirm and augment the data from mouse neurospheres. Firstly, we checked cell migration and found that an EF of 50 mV/mm induced significant cell cluster formation and directed migration to the cathode in SH-SY5Y cells (Fig. 3a to c, Movie S3 and S4). We further analysed quantitatively cell cluster formation in SH-SY5Y cells induced by a physiological EF by counting the proportion of single cells or of cell groups with less than 3 cells connected in a real-time recording stack. A reduction of single cells or groups with less than 3 cells connected would demonstrate an increase

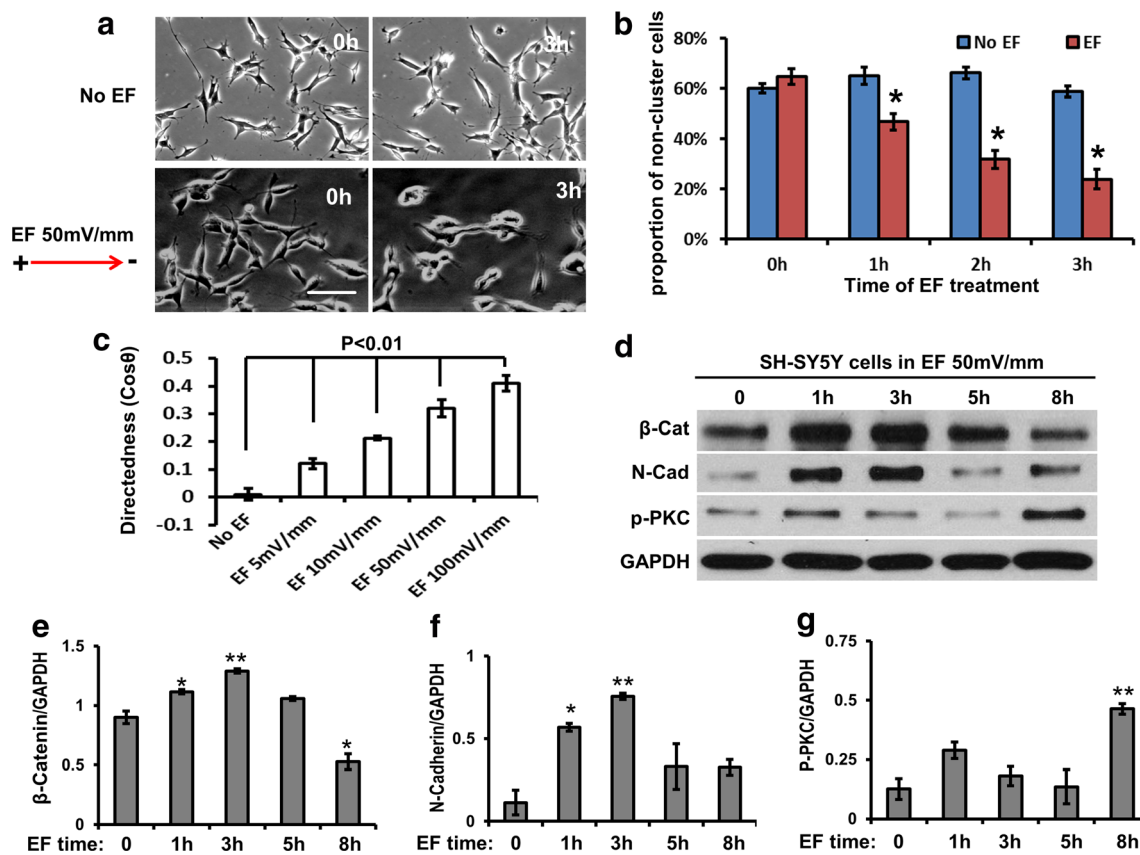


**Fig. 3** An applied physiological EF induced cell clustering and chain migration in SH-SY5Y. **a** An applied EF of 50 mV/mm (lower panels) significantly induced cells to cluster together and to migrate to the cathode. Upper panel – control (no EF); lower panel EF cathode at right. Bars: 20  $\mu$ m. **b** Cluster formation of SH-SY5Y cells was quantified by counting the percentage of single cell, or groups with less than 3 cells connected together. The reduction of these groups over 3 h in the EF indicates the continuing onset of cell cluster formation. The EF therefore significantly reduced the proportion of single cells due to more cell

clusters having formed (>3 cells connection). **c** The directedness (Cos  $\theta$ ) of SH-SY5Y cell migration was field strength dependent, showing significant increases from 5 mV/mm to 100 mV/mm. **d** Western blotting showed that the applied EF effectively increased the expression of N-cadherin and  $\beta$ -catenin at 1 h of EF exposure. The concentration of p-PKC was increased significantly after 8 h treatment by an applied EF. GAPDH is a loading control. (E, F and G) The ratio of protein expression/GAPDH is shown below the western blots for  $\beta$ -Catenin (E), N-cadherin (F) and p-PKC (G)

in cell-cell contacts and collective migration (chain migration). The results showed that an EF of 50 mV/mm significantly reduced single cell numbers and encouraged cell clustering and that these effects increased with longer exposure to the EF (Fig. 3b). In addition, the directedness (Cos  $\theta$ ) of collective cell migration was increased significantly and was dependent on both EF strength (from 5 to 100 mV/mm) and the duration of EF treatment (Fig. 3c).  $\theta$  is the angle between a line connecting the beginning and end points of cell migration and the X axis. The average directedness of random migration would be 0. The average directedness value would tend to 1 in fully directed migration [25]. Furthermore, our data showed that an applied EF significantly promoted the expression of  $\beta$ -catenin and N-cadherin within one hour and lasting for up to 5 h in SH-SY5Y cells (Fig. 3c, e and f). Since we had shown that the cell-cell adhesion molecules  $\beta$ -catenin and N-cadherin are up-regulated by an applied EF in cultured mouse neurospheres (Fig. 2c), these results are consistent. In this experiment, the applied EF effectively increased cell-cell connections and the cathode

directedness of SH-SY5Y cell migration at a physiological EF strength. This indicates that an EF induced chain migration in SH-SY5Y cells. Interestingly, at 8 h in an applied EF the expression of  $\beta$ -catenin and N-cadherin reduced significantly (Fig. 3d, e and f). This indicates that the EF-induced increase in the expression of  $\beta$ -catenin and N-cadherin is a short time function which enhances the maintenance of chain migration in vitro. For long term directed migration in EF (>5 h), other mechanisms, e.g. activation of PKC (Fig. 3d and g), may play a functional role.

#### P2Y1 Mediated the Chain Migration Induced by a Physiological EF

We have reported that an applied EF increases cathodally directed migration in mouse neuroblasts and that this is mediated by P2Y1 receptors [24]. Atypical protein kinase C (PKC) is required to establish and control cell polarity [45, 46]. In addition, we have reported that PKC played a key role

in cell polarity and directed cell migration induced by an applied EF [25, 47]. Inhibition of PKC in RMS neuroblasts disrupts their ability to reorient the centrosome and stabilize processes, and so leads to failure of directed neuronal

migration [48]. Here, we found that an applied EF increased the expression of P2Y1 receptors significantly and in a time dependent manner using both western blotting in SH-SY5Y cells and immunofluorescent staining in mouse neuroblasts

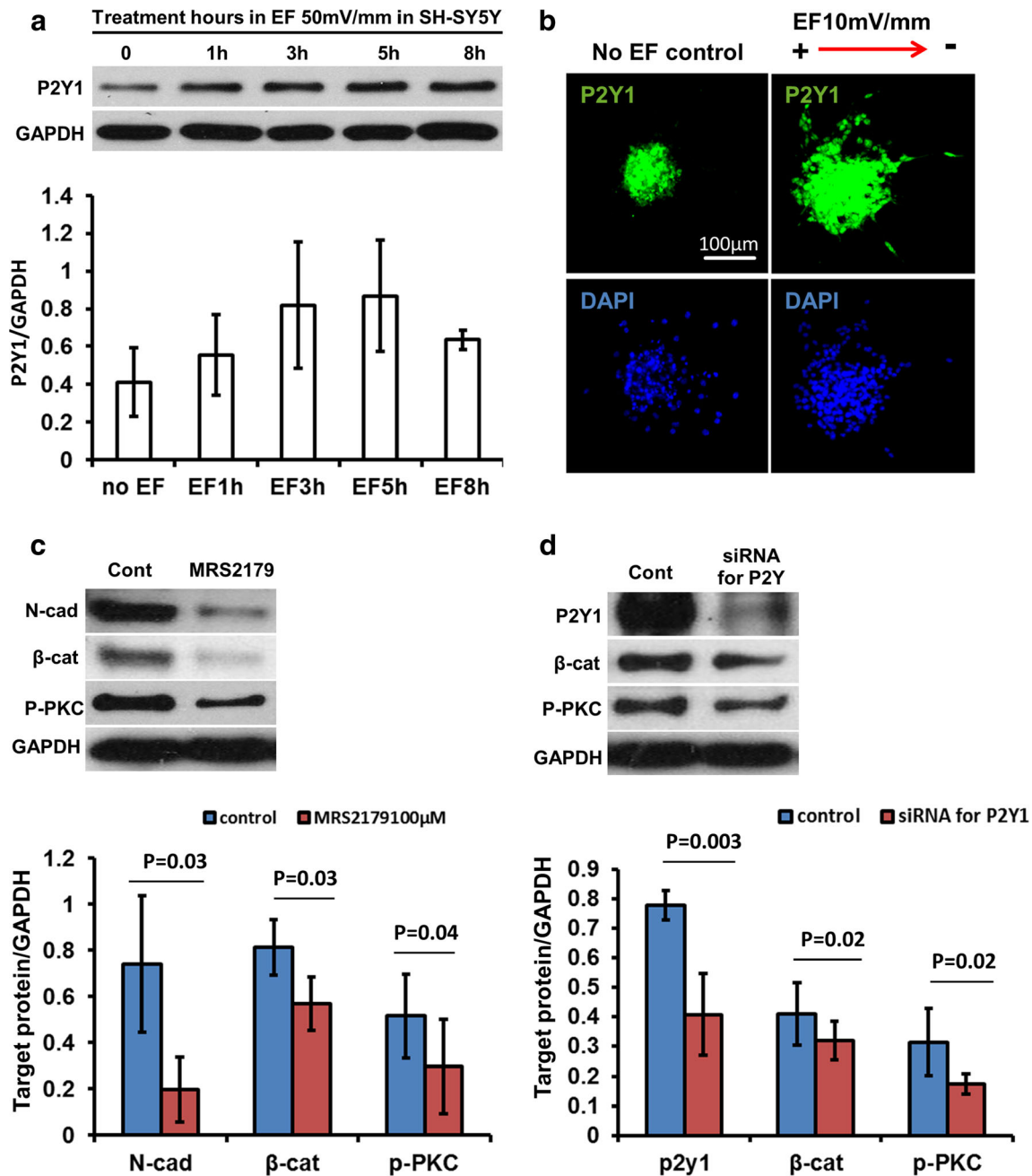


**Fig. 4** P2Y1 mediated neuronal chain migration induced by a physiological EF. **a** Western blotting showed the P2Y1 band at 45KD to be up-regulated in a time dependent manner by a physiological EF, with an increase evident within 1 h. **b** Neurospheres from mouse SVZ were seeded in electrotaxis chambers with/without an applied EF for 5 h and then cells were fixed and stained immunofluorescently with P2Y1 receptor antibody. The applied EF significantly increased the expression of P2Y1 in the cells which migrated out from the cultured mouse

neurosphere. **c** Inhibition of P2Y1 receptors with a specific inhibitor (100 μM MRS2179) significantly reduced the expression of N-cadherin and β-catenin and blocked the activation of PKC using western blotting and mouse neurospheres. **d** Inhibition of P2Y1 receptors with siRNA also effectively inhibited the expression of N-cadherin and activation of PKC. Graphs below C and D demonstrate corresponding quantification. All experiments were triplicate

(Fig. 4a and b). Furthermore, inhibition of P2Y1 receptors with MRS2179 and siRNA had similar effects in inhibiting the expression of N-cadherin,  $\beta$ -catenin and activation of PKC (Fig. 4c and d). This indicates that the chain migration induced by an applied EF in neuroblasts may be mediated by the P2Y1 receptor.

#### Extracellular ATP Increased EF-Directed Neuronal Migration

P2Y1 is a receptor for extracellular ATP which acts as a neurotransmitter and neuromodulator in the CNS. For example, ATP induces increases in calcium and neuronal excitation in various brain regions [49–52]. To confirm a functional role of the P2Y1 receptor in EF-induced chain migration of

neuroblasts, we next observed the migration of mouse neurospheres when P2Y1 was either activated or inhibited using extracellular ATP, or the specific inhibitor MRS2179 in SHSY5Y cells. We found that extracellular ATP (100  $\mu$ M) markedly increased both the directedness (from  $0.11 \pm 0.01$  to  $0.35 \pm 0.03$ ;  $p < 0.01$ ) and the migration speed (Tt/T) of SHSY5Y cells (from  $17.6 \pm 1.2$   $\mu$ m/h to  $29.7 \pm 2.1$   $\mu$ m/h;  $p < 0.01$ ) in a physiological EF of 100 mV/mm (Fig. 5a to c). Furthermore, when P2Y1 receptors were inhibited with siRNA in mouse neuroblasts (neurospheres), the directed migration induced by an EF was inhibited profoundly (directedness from 0.56 to 0.12; Fig. 5d – f). This suggests that EF regulated chain migration of neuroblasts may be mediated by the P2Y1 extracellular ATP receptor.

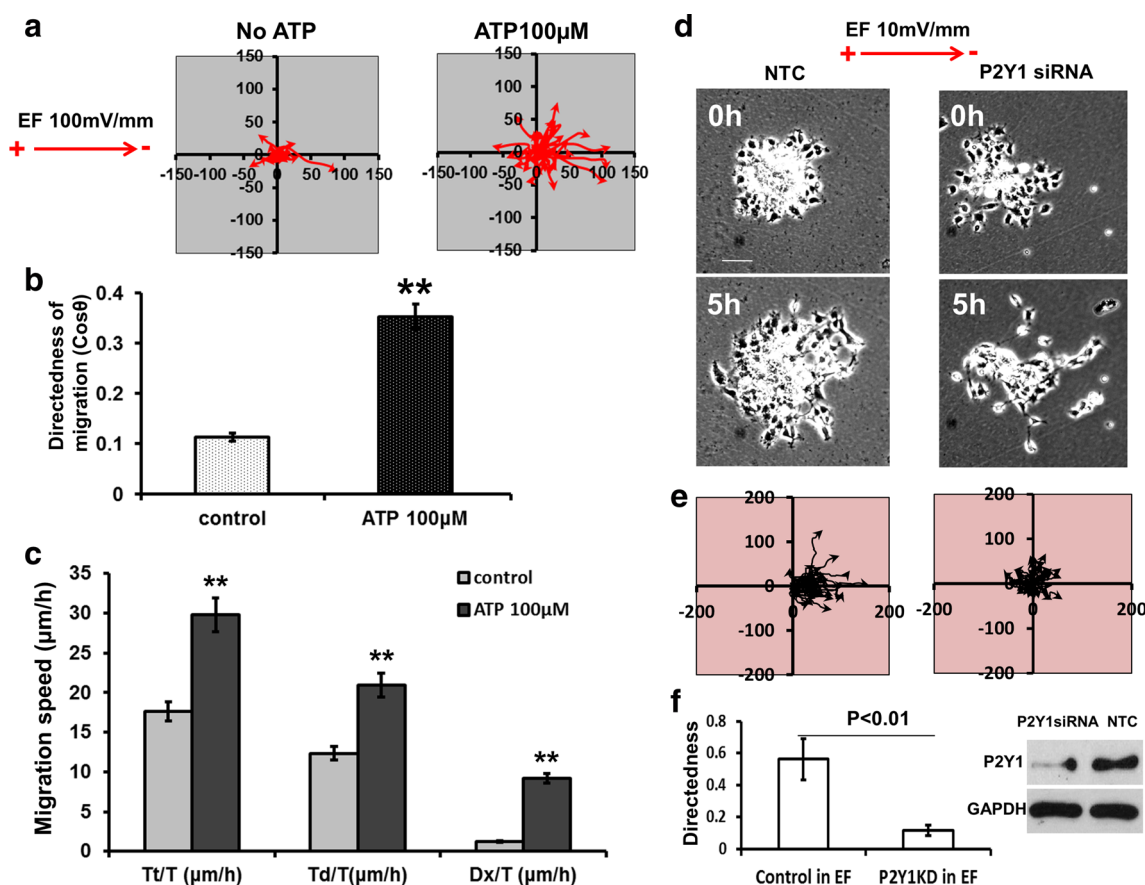


**Fig. 5** Extracellular ATP increased the directed migration of SH-SY5Y cells and knock down of P2Y1 receptors inhibited directed migration in mouse neurospheres. **a** to **c** In SHSY5Y cells (human), 100  $\mu$ M ATP significantly increased the directedness (Cos  $\theta$ ) of cells migration induced by an applied EF from 0.11 to 0.35 (EF=100 mV/mm,  $n=200$ ). The migration speed including Trajectory rate (Tt/T), Displacement rate (Td/T) and Displacement speed along the x-axis (Dx/T) also increased significantly: Tt/T from  $17.6 \pm 1.2$  to  $29.7 \pm 2.1$   $\mu$ m/h, Td/T from  $12.3 \pm 0.9$  to  $20.9 \pm 1.5$   $\mu$ m/h, Dx/T from  $1.2 \pm 0.09$  to  $9.2 \pm 0.6$   $\mu$ m/h. If cells migrated preferentially towards the right, an average directedness would be larger than 0 and approaching 1. Trajectory rate (Tt/T) is the total length of the migration trajectory of a cell (Tt) divided by the given period of time (T). Displacement rate (Td/T) is the straight-line distance between the start

and end positions of a cell (Td) divided by the time (T). Displacement speed along the x-axis (Dx/T) is a cell's displacement distance along the x-axis (Dx) divided by the time (T). **\*\*** $p < 0.01$ . **d** to **f** In cultured mouse neurospheres, knock down of P2Y1 receptor with siRNA (right column in D) significantly inhibited the directedness of cell migration compared with no siRNA control (left column in D). In E, the diagram of line plots showed cathodally directed cell migration to be reduced by inhibition of P2Y1 receptors with siRNA. Directedness (Cos  $\theta$ ) dropped from 0.56 to 0.12 ( $n=30\sim 35$ ,  $p < 0.01$ ).  $n$  is cell number. No EF control is shown in Fig. 2a. The western blot (right in F) shows down-regulation of P2Y1 receptor expression by siRNAP2Y1. NTC is no transfection control. GAPDH is loading control. All experiments were triplicate



## Discussion

In adult brain, neuroblasts are generated and complete their initial differentiation in the SVZ. They then migrate directionally as neuronal chains, sliding along each other in the RMS from SVZ to OB [53–55]. Upon arriving at the OB, the new neurons differentiate into olfactory interneurons, and integrate into the olfactory processing system. Chain migration is regulated by multiple cellular and molecular cues, the coordination of which is still unclear [4, 10, 56]. We report a novel mechanism in which extracellular electrical signals contribute to directed chain migration of neuroblasts through P2Y1 receptor signalling.

Early recordings showed that the cortical surface was 0.5 to 5.5 mV positive to the ventricle [57]. In addition, synchronous neuronal discharges within highly laminar structures such as the hippocampus generate substantial extracellular field potentials [41]. Turner et al. found extracellular EFs ranging from 6 to 31 mV/mm in adult rat hippocampus, whilst EFs ranged from 13 to 43 mV/mm in adult turtle cerebellum [58]. In the developing embryonic neural tube also, extracellular EFs of 10–100 mV mm<sup>-1</sup> have been recorded [13, 15, 16, 59]. Here, we detected an extracellular EF of 31.8±4.5 mV/mm in neonatal mouse SVZ slices (Fig. 1). Previously, we have measured directly an electric gradient of 5.7±1.2 mV/mm in the extracellular spaces along the rostral migratory stream [24]. Clearly extracellular electrical gradients are widespread in different developing, neonatal and adult brain locations although their physiological roles remain little recognised and poorly understood.

EFs are widespread also in other developing and regenerating tissues where they regulate cell division and directed cell migration [11, 12, 25, 38]. Intriguingly, most cell migrations in developing and damaged brain occur through tissues in which steady electrical signals exist [11]. For example, epileptic seizure, stroke, ischaemia, migraine and acute damage to the hippocampus all induce extracellular electrical signals in brain that persist for hours [19–23]. Thus, the endogenous EFs represent a novel and powerful signalling mechanism with the potential to guide cell migration. In addition, EF-induced directional re-orientation of the leading edge cells of large epithelial sheets is E-cadherin dependent [60]. To migrate at high speed over long distance within neuronal chains, the collective of neuroblasts needs to slide along each other efficiently [61] and for this, a consistent direction and maintained cell-cell contacts are essential. Here, we found that a physiological EF induced cathodal-directed migration and increased the expression of N-cadherin and  $\beta$ -catenin to promote and maintain the cell-cell connections between neuroblasts. Consistent with this, inhibition of the extracellular electrical signal in SVZ slices effectively disrupted the formation and directed migration of neuroblast chains. This is the first evidence that the natural extracellular

electrical gradients of the brain contribute to the formation, maintenance and directed migration of chains of neuroblasts.

Several proteins that regulate chain formation in RMS have been identified. For example, mice lacking the cell-surface receptors ErbB4 and ApoER2 lost chain migration in the RMS and new neurons arriving in the OB were reduced [62, 63]. Extracellular matrix-related molecules such as  $\alpha$ 6 $\beta$ 1-integrin and ADAM2 protease also are involved [64–66], indicating that both cellular receptor and extracellular matrix elements regulate neuroblast chain formation in brain. Additionally, extracellular signals such as ATP dynamically reorganize the cytoskeleton of each migrating neuroblast and regulate chemotaxis of microglia via Gi/o-coupled P2Y receptors [67, 68]. Early studies showed that electrical stimulation of axons liberated ATP [69, 70] and that extracellular ATP induces excitation and increases in calcium in neurons [49, 50, 71, 72], Erk activation [73], and calcium wave propagation [74]. This calcium signalling is essential for directed cell migration induced by an applied EF [75]. Furthermore, an applied EF transiently elevated extracellular ATP and caused Akt phosphorylation that was additive to insulin and inhibited by suramin (inhibitor of P2Y receptors) [76]. Tran et al. demonstrated a role for extracellular ATP, purinergic receptors and protein kinase signalling in enhancing N-cadherin expression indicating a role in cell-cell interactions [77]. We found that an applied electrical signal which mimicked that found in brain up-regulated the expression of P2Y1 receptors to increase expression of N-cadherin and  $\beta$ -catenin. Therefore, the mechanism of EF-induced chain migration of neuroblasts most likely involves activation of the ATP/P2Y1 signalling pathway through up-regulation of P2Y1 expression and increased release of ATP.

Increased neurogenesis and migration of progenitor cells have been observed in animal models of epilepsy, stroke, trauma, Alzheimer's disease, Parkinson's disease and Huntington's disease [78]. In addition, high expression of P2Y1 is required for neuroblast migration in brain [68]. We found that the exogenous EF promoted chain migration of neuroblasts through increasing the expression of P2Y1. This indicates that it may be possible to deliver neuroblasts to sites of brain injury and disease by directing their migration using an applied DC electric field. EFs have been used clinically in the treatment of human spinal cord lesions [79] and extending their use to brain lesions therefore is feasible.

## Conclusions

We showed previously that there is an extracellular EF between SVZ and the OB which contributes to guidance of neuroblast migration along the RMS [24]. Here, we show further that this endogenous EF regulates chain migration of neuroblasts by promoting and maintaining cell-cell

connections by up-regulating the expression of N-cadherin and  $\beta$ -catenin. In addition, we found that up-regulation of the P2Y1 receptor contributes to EF-induced chain migration. Our data indicate that this naturally occurring electrical gradient within the extracellular spaces of the RMS acts as a guidance cue directing chain migration of neuroblasts between the SVZ and the OB. These findings present a highly novel perspective of one of the mechanisms controlling and guiding neuroblast migration in a specific part of the mammalian brain.

**Acknowledgments** This work was supported by a grant from NHS Grampian.

**Conflict of Interest** The authors declare that they have no conflicts of interest.

**Open Access** This article is distributed under the terms of the Creative Commons Attribution License which permits any use, distribution, and reproduction in any medium, provided the original author(s) and the source are credited.

## References

- Alvarez-Buylla, A., & Garcia-Verdugo, J. M. (2002). Neurogenesis in adult subventricular zone. *The Journal of Neuroscience: the Official Journal of the Society for Neuroscience*, 22, 629–634.
- Lois, C., Garcia-Verdugo, J. M., & Alvarez-Buylla, A. (1996). Chain migration of neuronal precursors. *Science*, 271, 978–981.
- O'Rourke, N. A., Chenn, A., & McConnell, S. K. (1997). Postmitotic neurons migrate tangentially in the cortical ventricular zone. *Development*, 124, 997–1005.
- Wynn, M. L., Kulesa, P. M., & Schnell, S. (2012). Computational modelling of cell chain migration reveals mechanisms that sustain follow-the-leader behaviour. *Journal of the Royal Society Interface/the Royal Society*, 9, 1576–1588.
- Yagita, Y., Sakurai, T., Tanaka, H., Kitagawa, K., Colman, D. R., & Shan, W. (2009). N-cadherin mediates interaction between precursor cells in the subventricular zone and regulates further differentiation. *Journal of Neuroscience Research*, 87, 3331–3342.
- Tomasiewicz, H., Ono, K., Yee, D., Thompson, C., Goridis, C., Rutishauser, U., et al. (1993). Genetic deletion of a neural cell adhesion molecule variant (N-CAM-180) produces distinct defects in the central nervous system. *Neuron*, 11, 1163–1174.
- Bonfanti, L., & Theodosis, D. T. (1994). Expression of polysialylated neural cell adhesion molecule by proliferating cells in the subependymal layer of the adult rat, in its rostral extension and in the olfactory bulb. *Neuroscience*, 62, 291–305.
- Wang, Y., Kaneko, N., Asai, N., Enomoto, A., Isotani-Sakakibara, M., Kato, T., et al. (2011). Girdin is an intrinsic regulator of neuroblast chain migration in the rostral migratory stream of the postnatal brain. *The Journal of Neuroscience: the Official Journal of the Society for Neuroscience*, 31, 8109–8122.
- Delaloy, C., Liu, L., Lee, J. A., Su, H., Shen, F., Yang, G. Y., et al. (2010). MicroRNA-9 coordinates proliferation and migration of human embryonic stem cell-derived neural progenitors. *Cell Stem Cell*, 6, 323–335.
- Jacques, T. S., Relvas, J. B., Nishimura, S., Pytela, R., Edwards, G. M., Streuli, C. H., et al. (1998). Neural precursor cell chain migration and division are regulated through different beta1 integrins. *Development*, 125, 3167–3177.
- McCaig, C. D., Song, B., & Rajnicek, A. M. (2009). Electrical dimensions in cell science. *Journal of Cell Science*, 122, 4267–4276.
- McCaig, C. D., Rajnicek, A. M., Song, B., & Zhao, M. (2002). Has electrical growth cone guidance found its potential? *Trends in Neurosciences*, 25, 354–359.
- Hotary, K. B., & Robinson, K. R. (1991). The neural tube of the *Xenopus* embryo maintains a potential difference across itself. *Brain Research. Developmental Brain Research*, 59, 65–73.
- Shi, R., & Borgens, R. B. (1994). Embryonic neuroepithelial sodium transport, the resulting physiological potential, and cranial development. *Developmental Biology*, 165, 105–116.
- Hotary, K. B., & Robinson, K. R. (1990). Endogenous electrical currents and the resultant voltage gradients in the chick embryo. *Developmental Biology*, 140, 149–160.
- Shi, R., & Borgens, R. B. (1995). Three-dimensional gradients of voltage during development of the nervous system as invisible coordinates for the establishment of embryonic pattern. *Developmental Dynamics*, 202, 101–114.
- Borgens, R. B., Jaffe, L. F., & Cohen, M. J. (1980). Large and persistent electrical currents enter the transected lamprey spinal cord. *Proceedings of the National Academy of Sciences of the United States of America*, 77, 1209–1213.
- Jaffe, L. F., & Nuccitelli, R. (1974). An ultrasensitive vibrating probe for measuring steady extracellular currents. *The Journal of Cell Biology*, 63, 614–628.
- Marshall, W. H. (1959). Spreading cortical depression of Leao. *Physiological Reviews*, 39, 239–279.
- Jefferys, J. G. (1981). Influence of electric fields on the excitability of granule cells in guinea-pig hippocampal slices. *The Journal of Physiology*, 319, 143–152.
- Hadjikhani, N., Sanchez Del Rio, M., Wu, O., Schwartz, D., Bakker, D., Fischl, B., et al. (2001). Mechanisms of migraine aura revealed by functional MRI in human visual cortex. *Proceedings of the National Academy of Sciences of the United States of America*, 98, 4687–4692.
- Strong, A. J., Fabricius, M., Boutelle, M. G., Hibbins, S. J., Hopwood, S. E., Jones, R., et al. (2002). Spreading and synchronous depressions of cortical activity in acutely injured human brain. *Stroke; A Journal of Cerebral Circulation*, 33, 2738–2743.
- Reid, B., Nuccitelli, R., & Zhao, M. (2007). Non-invasive measurement of bioelectric currents with a vibrating probe. *Nature Protocols*, 2, 661–669.
- Cao, L., Wei, D., Reid, B., Zhao, S., Pu, J., Pan, T., et al. (2013). Endogenous electric currents might guide rostral migration of neuroblasts. *EMBO Reports*, 14, 184–190.
- Zhao, M., Song, B., Pu, J., Wada, T., Reid, B., Tai, G., et al. (2006). Electrical signals control wound healing through phosphatidylinositol-3-OH kinase-gamma and PTEN. *Nature*, 442, 457–460.
- Zhao, M. (2009). Electrical fields in wound healing—an overriding signal that directs cell migration. *Seminars in Cell & Developmental Biology*, 20, 674–682.
- Nishimura, K. Y., Isseroff, R. R., & Nuccitelli, R. (1996). Human keratinocytes migrate to the negative pole in direct current electric fields comparable to those measured in mammalian wounds. *Journal of Cell Science*, 109(Pt 1), 199–207.
- Fang, K. S., Ionides, E., Oster, G., Nuccitelli, R., & Isseroff, R. R. (1999). Epidermal growth factor receptor relocalization and kinase activity are necessary for directional migration of keratinocytes in DC electric fields. *Journal of Cell Science*, 112(Pt 12), 1967–1978.
- Rorth, P. (2009). Collective cell migration. *Annual Review of Cell and Developmental Biology*, 25, 407–429.
- Arvidsson, A., Collin, T., Kirik, D., Kokaia, Z., & Lindvall, O. (2002). Neuronal replacement from endogenous precursors in the adult brain after stroke. *Nature Medicine*, 8, 963–970.

31. Kokaia, Z., & Lindvall, O. (2003). Neurogenesis after ischaemic brain insults. *Current Opinion in Neurobiology*, *13*, 127–132.
32. Singec, I., Knoth, R., Meyer, R. P., Maciaczyk, J., Volk, B., Nikkhah, G., et al. (2006). Defining the actual sensitivity and specificity of the neurosphere assay in stem cell biology. *Nature Methods*, *3*, 801–806.
33. Brewer, G. J., & Torricelli, J. R. (2007). Isolation and culture of adult neurons and neurospheres. *Nature Protocols*, *2*, 1490–1498.
34. Song, B., Gu, Y., Pu, J., Reid, B., Zhao, Z., & Zhao, M. (2007). Application of direct current electric fields to cells and tissues in vitro and modulation of wound electric field in vivo. *Nature Protocols*, *2*, 1479–1489.
35. Chen, Y., Balasubramanian, V., Peng, J., Hurlock, E. C., Tallquist, M., Li, J., et al. (2007). Isolation and culture of rat and mouse oligodendrocyte precursor cells. *Nature Protocols*, *2*, 1044–1051.
36. Wei, D., Levic, S., Nie, L., Gao, W. Q., Petit, C., Jones, E. G., et al. (2008). Cells of adult brain germinal zone have properties akin to hair cells and can be used to replace inner ear sensory cells after damage. *Proceedings of the National Academy of Sciences of the United States of America*, *105*, 21000–21005.
37. Zhao, M., Agius-Fernandez, A., Forrester, J. V., & McCaig, C. D. (1996). Orientation and directed migration of cultured corneal epithelial cells in small electric fields are serum dependent. *Journal of Cell Science*, *109*(Pt 6), 1405–1414.
38. Pu, J., & Zhao, M. (2005). Golgi polarization in a strong electric field. *Journal of Cell Science*, *118*, 1117–1128.
39. Shinohara, R., Thumkeo, D., Kamijo, H., Kaneko, N., Sawamoto, K., Watanabe, K., et al. (2012). A role for mDia, a Rho-regulated actin nucleator, in tangential migration of interneuron precursors. *Nature Neuroscience*, *15*(373–380), S371–S372.
40. Wichterle, H., Garcia-Verdugo, J. M., & Alvarez-Buylla, A. (1997). Direct evidence for homotypic, glia-independent neuronal migration. *Neuron*, *18*, 779–791.
41. Turner, R. W., & Richardson, T. L. (1991). Apical dendritic depolarizations and field interactions evoked by stimulation of afferent inputs to rat hippocampal CA1 pyramidal cells. *Neuroscience*, *42*, 125–135.
42. Kasemeier-Kulesa, J. C., Kulesa, P. M., & Lefcort, F. (2005). Imaging neural crest cell dynamics during formation of dorsal root ganglia and sympathetic ganglia. *Development*, *132*, 235–245.
43. Kulesa, P. M., & Fraser, S. E. (1998). Neural crest cell dynamics revealed by time-lapse video microscopy of whole embryo chick explant cultures. *Developmental Biology*, *204*, 327–344.
44. Biedler, J. L., Roffler-Tarlov, S., Schachner, M., & Freedman, L. S. (1978). Multiple neurotransmitter synthesis by human neuroblastoma cell lines and clones. *Cancer Research*, *38*, 3751–3757.
45. Etienne-Manneville, S., & Hall, A. (2003). Cdc42 regulates GSK-3beta and adenomatous polyposis coli to control cell polarity. *Nature*, *421*, 753–756.
46. Yoshimura, T., Kawano, Y., Arimura, N., Kawabata, S., Kikuchi, A., & Kaibuchi, K. (2005). GSK-3beta regulates phosphorylation of CRMP-2 and neuronal polarity. *Cell*, *120*, 137–149.
47. Cao, L., Pu, J., & Zhao, M. (2011). GSK-3beta is essential for physiological electric field-directed Golgi polarization and optimal electrotaxis. *Cellular and Molecular Life Sciences: CMLS*, *68*, 3081–3093.
48. Higginbotham, H., Tanaka, T., Brinkman, B. C., & Gleason, J. G. (2006). GSK3beta and PKCzeta function in centrosome localization and process stabilization during Slit-mediated neuronal repolarization. *Molecular and Cellular Neurosciences*, *32*, 118–132.
49. Edwards, F. A., Gibb, A. J., & Colquhoun, D. (1992). ATP receptor-mediated synaptic currents in the central nervous system. *Nature*, *359*, 144–147.
50. Chen, Z. P., Levy, A., & Lightman, S. L. (1994). Activation of specific ATP receptors induces a rapid increase in intracellular calcium ions in rat hypothalamic neurons. *Brain Research*, *641*, 249–256.
51. Inoue, K., Koizumi, S., & Nakazawa, K. (1995). Glutamate-evoked release of adenosine 5'-triphosphate causing an increase in intracellular calcium in hippocampal neurons. *Neuroreport*, *6*, 437–440.
52. Nabekura, J., Ueno, S., Ogawa, T., & Akaike, N. (1995). Colocalization of ATP and nicotinic ACh receptors in the identified vagal preganglionic neurone of rat. *The Journal of Physiology*, *489*(Pt 2), 519–527.
53. Carter, S. B. (1967). Haptotaxis and the mechanism of cell motility. *Nature*, *213*, 256–260.
54. Theveneau, E., & Mayor, R. (2011). Collective cell migration of the cephalic neural crest: the art of integrating information. *Genesis*, *49*, 164–176.
55. Lois, C., & Alvarez-Buylla, A. (1994). Long-distance neuronal migration in the adult mammalian brain. *Science*, *264*, 1145–1148.
56. Thomas, L. B., Gates, M. A., & Steindler, D. A. (1996). Young neurons from the adult subependymal zone proliferate and migrate along an astrocyte, extracellular matrix-rich pathway. *Glia*, *17*, 1–14.
57. Goldring, S., & O'Leary, J. L. (1951). Experimentally derived correlates between ECG and steady cortical potential. *Journal of Neurophysiology*, *14*, 275–288.
58. Chan, C. Y., & Nicholson, C. (1986). Modulation by applied electric fields of Purkinje and stellate cell activity in the isolated turtle cerebellum. *The Journal of Physiology*, *371*, 89–114.
59. Hotary, K. B., & Robinson, K. R. (1994). Endogenous electrical currents and voltage gradients in *Xenopus* embryos and the consequences of their disruption. *Developmental Biology*, *166*, 789–800.
60. Li, L., Hartley, R., Reiss, B., Sun, Y., Pu, J., Wu, D., et al. (2012). E-cadherin plays an essential role in collective directional migration of large epithelial sheets. *Cellular and Molecular Life Sciences: CMLS*, *69*, 2779–2789.
61. Sawada, M., & Sawamoto, K. (2013). Mechanisms of neurogenesis in the normal and injured adult brain. *The Keio Journal of Medicine*, *62*, 13–28.
62. Andrade, N., Komnenovic, V., Blake, S. M., Jossin, Y., Howell, B., Goffinet, A., et al. (2007). ApoER2/VLDL receptor and Dab1 in the rostral migratory stream function in postnatal neuronal migration independently of Reelin. *Proceedings of the National Academy of Sciences of the United States of America*, *104*, 8508–8513.
63. Anton, E. S., Ghashghaei, H. T., Weber, J. L., McCann, C., Fischer, T. M., Cheung, I. D., et al. (2004). Receptor tyrosine kinase ErbB4 modulates neuroblast migration and placement in the adult forebrain. *Nature Neuroscience*, *7*, 1319–1328.
64. Belvindrah, R., Hankel, S., Walker, J., Patton, B. L., & Muller, U. (2007). Beta1 integrins control the formation of cell chains in the adult rostral migratory stream. *The Journal of Neuroscience: the Official Journal of the Society for Neuroscience*, *27*, 2704–2717.
65. Emsley, J. G., & Hagg, T. (2003). alpha6beta1 integrin directs migration of neuronal precursors in adult mouse forebrain. *Experimental Neurology*, *183*, 273–285.
66. Murase, S., Cho, C., White, J. M., & Horwitz, A. F. (2008). ADAM2 promotes migration of neuroblasts in the rostral migratory stream to the olfactory bulb. *The European Journal of Neuroscience*, *27*, 1585–1595.
67. Honda, S., Sasaki, Y., Ohsawa, K., Imai, Y., Nakamura, Y., Inoue, K., et al. (2001). Extracellular ATP or ADP induce chemotaxis of cultured microglia through Gi/o-coupled P2Y receptors. *The Journal of Neuroscience: the Official Journal of the Society for Neuroscience*, *21*, 1975–1982.
68. Liu, X., Hashimoto-Torii, K., Torii, M., Haydar, T. F., & Rakic, P. (2008). The role of ATP signaling in the migration of intermediate neuronal progenitors to the neocortical subventricular zone. *Proceedings of the National Academy of Sciences of the United States of America*, *105*, 11802–11807.

69. Holton, F. A., & Holton, P. (1953). The possibility that ATP is a transmitter at sensory nerve endings. *The Journal of Physiology*, *119*, 50P–51P.
70. Holton, P. (1959). The liberation of adenosine triphosphate on antidromic stimulation of sensory nerves. *The Journal of Physiology*, *145*, 494–504.
71. Shen, K. Z., & North, R. A. (1993). Excitation of rat locus coeruleus neurons by adenosine 5'-triphosphate: ionic mechanism and receptor characterization. *The Journal of Neuroscience: the Official Journal of the Society for Neuroscience*, *13*, 894–899.
72. Dubyak, G. R., & el-Moatassim, C. (1993). Signal transduction via P2-purinergic receptors for extracellular ATP and other nucleotides. *The American Journal of Physiology*, *265*, C577–C606.
73. Neary, J. T., Kang, Y., Bu, Y., Yu, E., Akong, K., & Peters, C. M. (1999). Mitogenic signaling by ATP/P2Y purinergic receptors in astrocytes: involvement of a calcium-independent protein kinase C, extracellular signal-regulated protein kinase pathway distinct from the phosphatidylinositol-specific phospholipase C/calcium pathway. *The Journal of Neuroscience: the Official Journal of the Society for Neuroscience*, *19*, 4211–4220.
74. Scemes, E., Suadicani, S. O., & Spray, D. C. (2000). Intercellular communication in spinal cord astrocytes: fine tuning between gap junctions and P2 nucleotide receptors in calcium wave propagation. *The Journal of Neuroscience: the Official Journal of the Society for Neuroscience*, *20*, 1435–1445.
75. Sauer, H., Stanelle, R., Hescheler, J., & Wartenberg, M. (2002). The DC electrical-field-induced Ca(2+) response and growth stimulation of multicellular tumor spheroids are mediated by ATP release and purinergic receptor stimulation. *Journal of Cell Science*, *115*, 3265–3273.
76. Osorio-Fuentealba, C., Contreras-Ferrat, A. E., Altamirano, F., Espinosa, A., Li, Q., Niu, W., et al. (2013). Electrical stimuli release ATP to increase GLUT4 translocation and glucose uptake via PI3Kgamma-Akt-AS160 in skeletal muscle cells. *Diabetes*, *62*, 1519–1526.
77. Tran, M. D., Wanner, I. B., & Neary, J. T. (2008). Purinergic receptor signaling regulates N-cadherin expression in primary astrocyte cultures. *Journal of Neurochemistry*, *105*, 272–286.
78. Parent, J. M. (2003). Injury-induced neurogenesis in the adult mammalian brain. *The Neuroscientist*, *9*, 261–272.
79. Shapiro, S., Borgens, R., Pascuzzi, R., Roos, K., Groff, M., Purvines, S., et al. (2005). Oscillating field stimulation for complete spinal cord injury in humans: a phase 1 trial. *Journal of Neurosurgery: Spine*, *2*, 3–10.

1 **Glioblastoma Cell Migration is Directed by Electrical Signals**

2 Hannah Clancy<sup>a</sup>, Michal Pruski<sup>a,b</sup>, Bing Lang<sup>a</sup>, Jared Ching<sup>a,c\*</sup>, Colin D. McCaig<sup>a\*</sup>

3 <sup>a</sup>*Institute of Medical Sciences, University of Aberdeen, Aberdeen*

4 <sup>b</sup>*School of Medicine, Tongji University, Shanghai*

5 <sup>c</sup>*John Van Geest Centre for Brain Repair, University of Cambridge, Cambridge*

6

7

8 *\*Joint corresponding authors:*

9 Jared Ching

10 [jared.ching@nhs.net](mailto:jared.ching@nhs.net)

11

12 Colin D. McCaig

13 [c.mccaig@abdn.ac.uk](mailto:c.mccaig@abdn.ac.uk)

14

15 *Preprint*

16 A preprint of this article has been deposited on a preprint server for science, bioRxiv. DOI:

17 <https://doi.org/10.1101/2020.09.09.290254>.(1) This pre-print has been made available under a CC-BY-

18 NC-ND 4.0 International License to bioRxiv.

19

20 *ORCID IDs*

21 HC: <https://orcid.org/0000-0001-9883-1395>

22

23 MP: <https://orcid.org/0000-0001-7582-1418>

24

25 BL: <https://orcid.org/0000-0002-0076-2094>

26 JC: <https://orcid.org/0000-0002-3562-8055>

27

28 CDM: <https://orcid.org/0000-0001-5151-8254>

29

30

31

32 **Abstract**

33 Electric field (EF) directed cell migration (electrotaxis) is known to occur in glioblastoma multiforme  
34 (GBM) and neural stem cells, with key signalling pathways frequently dysregulated in GBM. One such  
35 pathway is EGFR/PI3K/Akt, which is down-regulated by peroxisome proliferator activated receptor  
36 gamma (PPAR $\gamma$ ) agonists. We investigated the effect of electric fields on primary differentiated and  
37 glioma stem cell (GSCs) migration, finding opposing preferences for anodal and cathodal migration,  
38 respectively. We next sought to determine whether chemically disrupting Akt through PTEN  
39 upregulation with the PPAR $\gamma$  agonist, pioglitazone, would modulate electrotaxis of these cells. We  
40 found that directed cell migration was significantly inhibited with the addition of pioglitazone in both  
41 differentiated GBM and GSCs subtypes. Western blot analysis did not demonstrate any change in  
42 PPAR $\gamma$  expression with and without exposure to EF. In summary we demonstrate opposing EF  
43 responses in primary GBM differentiated cells and GSCs can be inhibited chemically by pioglitazone,  
44 implicating GBM EF modulation as a potential target in preventing tumour recurrence.

45

46 *Keywords: Glioblastoma, Glioma Stem Cells, Electric fields, Galvanotaxis*

47

48

49

50

51

52

53

54

55

56

57

58

59

60 **Introduction**

61 Glioblastoma multiforme (GBM) is the most frequent and aggressive primary brain tumour and is  
62 classified by the World Health Organisation as a Grade IV astrocytoma (2, 3). GBM occurs at all ages,  
63 however the majority of patients are diagnosed in later life, at a median age of 64 years (3). Without  
64 treatment, the expected survival of those diagnosed with GBM averages 3 months (4), and is extended  
65 to 10-15 months with combined surgical resection, chemo- and radiotherapy (5). Despite these  
66 therapeutic advancements and the significant progress in treating systemic cancers, disease recurrence  
67 renders GBM incurable. Recurrence is largely attributed to the highly infiltrative nature of GBM,  
68 leading to residual cells being inevitably spared by surgical resection (6).

69

70 Many of the malignant characteristics of GBM are thought to be attributed to glioma stem cells (GSCs),  
71 first isolated in 2002 (7-10). This subpopulation of GBM cells is considered highly tumourigenic due  
72 to stem-like properties of self-renewal, multilineage differentiation, dysregulated proliferation and  
73 increased resistance to apoptosis (11). The presence of GSCs in GBM has been shown to negatively  
74 impact survival (12, 13), and is implicated in the invasive behaviour of GBM (6). Therefore,  
75 understanding GSC migration and consequent invasion provides opportunities for targeted therapeutic  
76 strategies.

77

78 GBM cell migration occurs primarily along white matter tracts and perivascular regions within the  
79 brain, through a process whereby the cell becomes morphologically polarised due to underlying  
80 cytoskeletal changes (14-16). Interestingly, neural stem cell (NSC) migration has been shown to be  
81 directed by electrical fields (EFs), with cells migrating towards the cathode (17-23). EFs occur  
82 physiologically as a product of ionic, and consequent voltage, gradients established through spatial  
83 variations in ion channels, pumps and leaks (24). These have been demonstrated in the mammalian  
84 brain *ex vivo*, for example along the rostral migratory stream (RMS) (19). Furthermore, EF guided cell  
85 migration (electrotaxis) has been demonstrated in several types of cancer at endogenous voltages,  
86 including prostate, breast and more recently brain cancers (25-28). Limited research has been carried  
87 out on the electrotaxis of GBM. Li and colleagues reported cathodal migration in several immortalised

88 glioma cell lines (25), whilst Huang and colleagues demonstrated anodal GSC migration and cathodal  
89 migration of differentiated cells (28).

90

91 The PI3K/Akt signalling pathway is heavily implicated in electrotaxis (18, 21, 22, 25, 27, 29). One such  
92 mechanism involves a cathodal redistribution of epidermal growth factor receptors (EGFR), resulting  
93 in polarised activation of the PI3K/Akt pathway and subsequent polarised actin remodelling (21, 30).

94 This produces asymmetrical membrane protrusions and consequently migration in the direction of the  
95 cathode. This pathway is frequently dysregulated in GBM through EGFR overexpression and  
96 downregulation of the Akt inhibitor PTEN (31). We therefore sought to investigate the effect of an  
97 applied EF on the migration of primary GBM cell lines, both differentiated: HROG02-Diff, HROG05-  
98 Diff and HROG24-Diff; and de-differentiated, GSC-like: HROG02-GSC, HROG05-GSC; with the aim  
99 of providing a greater understanding of the infiltrative behaviour of GBM. This is the first time EF  
100 migration has been investigated in both differentiated and de-differentiated phenotypes of the same cell  
101 lines.

102

103 PPAR $\gamma$  activation has been shown to upregulate PTEN, causing downstream inhibition of Akt (32, 33).

104 PPAR $\gamma$  activation also has been shown to have anti-neoplastic activity on GBM cells (34, 35) and anti-  
105 proliferative effects on patient derived GSC lines, albeit heterogeneously (36). The potential role of Akt  
106 in GBM electrotaxis in conjunction with the high frequency of Akt activating mutations led us to  
107 investigate the effect of the PPAR $\gamma$  agonist pioglitazone in both differentiated (HROG02-Diff and  
108 HROG05-Diff) and GSC (HROG02-GSC and HROG05-GSC) primary GBM cell lines.

109

## 110 **Materials and Methods**

### 111 *Reagents*

112 Dulbecco's Modified Eagle's Medium, F12 nutrient, penicillin/streptomycin, 0.25% Trypsin-EDTA,  
113 Neurobasal-A medium, glutamine, B27, N2 and CO<sub>2</sub> independent medium were obtained from  
114 Invitrogen (Camarillo, CA, USA) and foetal calf serum, EGF,  $\beta$ FGF, heparin, donkey serum, Matrigel  
115 and agar were obtained from Sigma Aldrich (St. Louis, MO, USA). Silicone adhesive (3140 RTV



116 coating) and DC4 high vacuum grease were purchased from Dow Corning (Midland, MI, USA).  
117 Steinberg solution was prepared using NaCl and Tris Base sourced from Fisher Bioreagents (USA),  
118 KCl, Ca(NO<sub>3</sub>)<sub>2</sub>, and MgSO<sub>4</sub> obtained from Sigma Aldrich (St. Louis, MO, USA). Primary antibodies  
119 for sox-2 (MAB4423) and nestin (ABD69) were purchased from Millipore (USA), whilst primary  
120 antibodies for GFAP (G3893) were obtained from Sigma Aldrich (St. Louis, MO, USA), CD133 from  
121 Miltenyi Biotec (Germany). Alexa Fluor 594 donkey anti-mouse (R37115), Alexa Fluor 594 donkey  
122 anti-rabbit (R37119), Alexa Fluor 488 donkey anti-goat (A-11055) and Alexa Fluor 488 donkey anti-  
123 mouse (A-21202) were purchased from Molecular Probes (USA). Pioglitazone hydrochloride (E6910),  
124 GW9662 (M6493) and phenazine methosulfate was purchased from Sigma Aldrich (St. Louis, MO,  
125 USA) and XTT cell viability assay from Invitrogen (USA). Stock solutions of 10mM  
126 pioglitazone:DMSO and 10mM GW9662:DMSO were prepared. Lysis buffer solution was prepared  
127 using cell lytic lysis buffer obtained from Sigma Aldrich (St. Louis, MO, USA) and complete EDTA  
128 free and phosphostop protease inhibitors from Roche, (Switzerland). Western blotting was completed  
129 using 4-12% Bis-Tris pre-cast gels and MOPS running buffer purchased from Invitrogen (USA),  
130 Nitrocellulose membrane obtained from GE Healthcare (Amersham, United Kingdom), Anti-PPAR $\gamma$   
131 (E-8) (sc-7273) purchased from Santa Cruz, (USA), Anti- $\beta$ -Actin from Sigma Aldrich (A2228) (St.  
132 Louis, MO, USA) and 680 Alexa Fluor donkey anti-mouse IgG (A-10038) secondary antibodies  
133 purchased from Molecular Probes (USA).

134

### 135 *Cell Culture*

136 Primary GBM Cell lines, HROG02, HROG05 and HROG24, were kindly provided by Professor  
137 Linnebacher of the University of Rostock. HROG02 is characterised by methylated MGMT, TP53  
138 mutation and IDH wildtype, whilst HROG05 features methylated MGMT and both TP53 and IDH  
139 wildtype. These characteristics have been demonstrated to persist post cryo-preservation (37). Genetic  
140 data for HROG24 was not available. To produce the differentiated phenotype, cells were maintained in  
141 DMEM:F12 supplemented with 5% foetal calf serum and 1% penicillin/streptomycin at 37°C, 5%  
142 carbon dioxide. This produced three differentiated cell lines: HROG02-Diff, HROG05-Diff and  
143 HROG24-Diff. To achieve the de-differentiated, GSC phenotype, cells were cultured in Neurobasal-A

144 medium supplemented with 2mM glutamine, 1% penicillin/streptomycin, epidermal growth factor  
145 (20ng/mL), basic fibroblast growth factor (20ng/mL), heparin (2µg/mL), 2% B27 and 1% N2 at 37°C,  
146 5% carbon dioxide (38-40). De-differentiated cells formed neurospheres when seeded in ultra-low  
147 adhesion 6 well plates and were termed HROG02-GSC and HROG05-GSC. The above method is an  
148 established technique in producing the GSC-like phenotype demonstrated to produce tumours when  
149 implanted in vivo (38).

150

### 151 *Electrotaxis Assay*

152 Assays to assess cell electrotaxis were adapted from a previously described protocol (41). Electrotactic  
153 chambers were constructed by gluing No. 1 thickness cover glass slides to the base of a 10cm petri-dish  
154 using silicone adhesive; the resulting electrotactic region measured 10 x 40mm. Cells were seeded on  
155 top of a layer of 1% Matrigel within the electrotactic region and incubated at 37°C, 5% carbon dioxide  
156 overnight. High vacuum grease was used to apply a No. 1 thickness glass slide roof over the electrotactic  
157 region shortly before experimentation, and 5ml CO<sub>2</sub> independent medium added (CO<sub>2</sub> independent  
158 media replaced DMEM:F12 and Neurobasal-A medium in differentiated and GSC cultures,  
159 respectively). EFs were delivered via silver/silver chloride electrodes in reservoirs of Steinberg's  
160 solution, passing current through 2% Agar bridges into the insulated pools of CO<sub>2</sub> independent medium  
161 on the left (cathode) and the right (anode) side of the electrotactic chamber. Cells were exposed to either  
162 0 (control), 50, 100 or 200mV/mm for 3 hours, with images taken every 10 minutes using a Leica DM  
163 IRB inverted microscope, digital camera and Velocity software (Improvision, UK).

164

### 165 *Quantification of Electrotaxis*

166 Image J software (National Institution of Health, USA), was used to track cells manually, and  
167 Microsoft Excel used to calculate velocity (total distance/time) and directedness. Directedness was  
168 calculated by  $\text{Cosine}(\theta)$  where  $\theta$  is the angle formed between the cell trajectory and EF vector. This  
169 gives a value between +1 (perfect anodal migration) and -1 (perfect cathodal migration), with migration  
170 perpendicular to the EF vector producing a value of 0. Experiments were repeated three times, with 100  
171 cells tracked per experiment, n=300 for all velocity and directedness data. The Chemotaxis plugin (Ibidi

172 GmbH, Germany) for Image J was used to produce migration diagrams, animations and data for xFMI  
173 (proportion of cell migration in the x-axis) change over time. The number of cells migrating to either  
174 the anode or cathode was obtained from migration diagrams, resulting in three counts of migration for  
175 both directions, displayed as percentage (n=3 for cell count data). Some cells did not migrate and were  
176 included in this % analysis. This makes it more difficult for the data to reach statistical significance  
177 compared to the directedness values, since cells not migrating are included. However, their inclusion in  
178 the directedness measure with values of 0 would have little effect on values of anodal versus cathodal  
179 directedness.

180

### 181 *Immunocytochemistry*

182 Immunocytochemistry was completed concurrently on differentiated and corresponding de-  
183 differentiated primary GBM cell lines. Cells were seeded onto 1% Matrigel coated circular borosilicate  
184 cover slips and incubated at 37°C, 5% carbon dioxide overnight. Slides were fixed with 4%  
185 paraformaldehyde and permeabilised with 0.3% Triton-X-100. Cells were stained with primary  
186 antibodies for sox-2 (1:200), CD133 (1:50), nestin (1:500) and GFAP (1:400) overnight at 4°C. Slides  
187 were probed with Alexa Fluor fluorescent secondary antibodies and counterstained with Hoechst  
188 (1:2000). For fluorescent microscopy, a Zeiss imager M2 upright microscope with DAPI (Zeiss set 49),  
189 DsRed (Zeiss set 43) and FITC (Zeiss set 10) filters was used, with images captured using a high  
190 resolution microscope camera and Axiovision software (for all images except for HROG05-Diff and  
191 HROG05-GSC stained for Hoechst, GFAP and nestin). These later images were captured using a high  
192 resolution camera linked to a Zeiss Axio Observer Z1 inverted microscope using DAPI (Zeiss set 49),  
193 Texas Red (Semrock) and FITC (Zeiss set 10) filters, with axiovision software (Germany).

194 CD133, nestin and sox-2 positive cells are associated with the GSC phenotype, whilst GFAP staining  
195 is astrocyte specific and therefore indicates a differentiated phenotype (39, 42).

196

### 197 *Drug Treatments*

198 XTT viability assays were performed in triplicate, testing different concentrations of the PPAR $\gamma$  agonist  
199 pioglitazone and PPAR $\gamma$  antagonist GW9662. Cells were exposed to treatments for 24 hours at 37°C,

200 5% carbon dioxide, after which XTT/PMS solution was added and the absorbance of the individual  
201 wells read at 450nm. Online resource 1 represents data from the XTT assay that was used to guide  
202 subsequent the drug treatment concentrations that did not reduce GBM cell viability. Experimental  
203 conditions of 15 $\mu$ M pioglitazone + 5 $\mu$ M DMSO (pioglitazone treatment), 15 $\mu$ M pioglitazone + 5 $\mu$ M  
204 GW9662 (pioglitazone/GW9662 treatment) and 20 $\mu$ M DMSO control, exposed for 12 to 24 hours.  
205 Electrotaxis assays were completed as previously described. The cells were seeded into the electrotaxis  
206 chambers in media containing drug treatments, with the time of application noted. Upon  
207 experimentation, CO<sub>2</sub> independent media containing drug treatments were added and an EF of  
208 200mV/mm was applied for 3 hours. Total time of treatment exposure was recorded; there were no  
209 significant differences in total exposure times.

210

#### 211 *Western Blotting*

212 Collection of protein samples was achieved using the method described for the electrotaxis assay,  
213 however using a larger 40 x 60mm electrotactic region. This larger region resulted in increased voltage  
214 instability and temperature gain over a 3 hours period. Preliminary data concerning xFMI change with  
215 time showed that xFMI generally peaked after one hour of exposure to 200mV/mm EF, therefore this  
216 time period and field strength was applied to samples. This was repeated three times for EF completed  
217 simultaneously with a paired control condition, following an identical procedure but with no EF applied.  
218 Adherent cells were lysed using lysis buffer solution and separated by electrophoresis on 4-12% Bis-  
219 Tris pre-cast gels using MOPS running buffer and transferred onto nitrocellulose membrane.  
220 Membranes were cut and incubated with appropriate primary antibodies: anti-PPAR $\gamma$  (1:100) or  $\beta$ -actin  
221 (1:50000); and subsequently with 680 donkey anti-mouse secondary antibody. Membranes were  
222 visualised by infrared scanning (Li-Cor Odyssey, USA) and quantified using Odyssey 2.1 software  
223 (USA) to produce an Integrated Intensity value (II). PPAR $\gamma$  II was normalised to  $\beta$ -actin control.

224

#### 225 *Statistics*

226 All graphs and statistical analysis was performed using GraphPad Prism 5.04, (USA). All migration  
227 data was analysed by One-Way ANOVA and Tukey's multiple comparison post-hoc tests, with  $p < 0.05$

228 considered significant. Western blot data was tested using Unpaired T-tests, deemed significant at  
229  $p < 0.5$ . All data presented as mean  $\pm$  SEM. Results from Tukey's post-hoc test were given as follows: Ns  
230 = non-significant, \* = significant ( $0.01 < p < 0.05$ ), \*\* = very significant ( $0.001 < p < 0.01$ ), \*\*\* = extremely  
231 significant ( $p < 0.001$ ).

232

## 233 **Results**

### 234 *HROG02-GSC and HROG05-GSC express glioma stem cell markers*

235 In order to generate GSCs from differentiated GBM cells, we utilised established cell culture methods  
236 to recapitulate a stem-like cancer cell state as previously described (38), to produce neurospheres.  
237 Immunocytochemistry was undertaken to screen for several markers associated with GSCs (online  
238 resource 2). HROG02-Diff stained negatively for sox-2, CD133, weakly for nestin and positively for  
239 GFAP. In contrast, HROG02-GSC stained strongly for the GSC markers sox-2, CD133 and nestin,  
240 whilst demonstrating variable GFAP expression. This staining pattern is in keeping with the  
241 differentiated and GSC phenotypes. HROG05-Diff stained negatively for sox-2, CD133 and GFAP, but  
242 positively for nestin. HROG05-GSC in comparison stained positively for sox-2, CD133, nestin and  
243 GFAP, however again GFAP showed variable expression across repeated imaging. Since it is widely  
244 accepted that GBM cells exist as a continuum between highly stem like and differentiated, as opposed  
245 to a binary stem/non-stem state, our staining confirms our cultures as GSCs.

246

### 247 *Primary differentiated cell lines HROG02-Diff, HROG05-diff and HROG24-diff migrate anodally in a* 248 *voltage dependent manner*

249 To characterise the electrotaxis of differentiated GBM cells, we applied a direct current EF of 50-200  
250 mV/mm to the differentiated GBM cells. Figures 1a and 1b demonstrate a higher proportion of  
251 HROG02-Diff and HROG05-Diff cells migrated towards the anode when exposed to a greater EF.  
252 Figures 1d and 1e f show that with no EF cells did not migrate preferentially to either pole. However,  
253 application of EF induced predominantly anodal migration of cells in a voltage dependent manner, with  
254  $84.3 \pm 4.1\%$  (HROG02-Diff) and  $71.0 \pm 7.0\%$  (HROG05-Diff) of cells migrating towards the anode at  
255 200mV/mm. Figures 1c and 1e demonstrate a stepwise increase in directedness of cell migration

256 towards the anode in both differentiated cell lines, with statistically significant changes in the presence  
257 of an EF as low as 50mV/mm in HROG02-Diff and 100mV/mm in HROG05-Diff. Increasing EF was  
258 also associated with statistically significant increases in velocity at voltages as low as 50mV/mm, as  
259 shown in online resource 3. Online resource 3 also illustrates the change in xFMI over the duration of  
260 the experiment, with both cell lines showing a plateau in the proportion of migration towards the anode  
261 by approximately 60 minutes. Greater EF applied also produced increasingly anodal cell migration in  
262 the additional cell line HROG24-Diff (online resource 4). Here there was a statistically significant  
263 increase in directedness of migration towards the anode at field strengths as low as 50mV/mm with  
264  $89.7\pm0.9\%$  of cells migrating towards the anode at 200mV/mm. HROG24-Diff cells also demonstrated  
265 statistically significant increases in velocity associated with increased EF applied. Animations  
266 illustrating the migration of HROG02-Diff, HROG05-Diff and HROG24 with increasing EF applied  
267 can be found in online resource 5, 6 and 7 respectively. Overall, we show that differentiated primary  
268 GBM cells preferentially migrate to the anode when an EF is applied.

269

#### 270 *EF induces cathodal migration in GSC cell lines HROG02-GSC and HROG05-GSC*

271 To characterise the electrotaxis of GSCs, a direct current EF of 50-200 mV/mm was applied to GSCs.  
272 Application of greater EF resulted in a greater proportion of GSC line cells migrating towards the  
273 cathode (Fig. 2a and 2b). Increasing the EF applied caused a corresponding increase in the percentage  
274 of cells migrating towards the cathode, increasing from  $49.3\pm2.9\%$  of cells with no EF, to  $70.3\pm2.7\%$   
275 cells with an EF of 200mV/mm in HROG02-GSC, and from  $44.7\pm5.2\%$  cells with no EF present, to  
276  $68.3\pm3.7\%$  cells at 200mV/mm in HROG05-GSC (Fig. 2d and 2f). This was further reflected in  
277 directedness, which increased towards the cathode in the presence of an EF (Fig. 2c and 2e). Application  
278 of 50mV/mm to HROG02-GSC produced a statistically significant increase in directedness towards the  
279 cathode compared to control from  $0.15\pm0.04$  to  $-0.12\pm0.04$ , remaining at similar directedness when  
280 exposed to 100mV/mm ( $-0.11\pm0.04$ ), before significantly increasing to  $-0.28\pm0.04$  at 200mV/mm (Fig.  
281 2c). Application of an EF as low as 100mV/mm induced a significant increase in directedness of  
282 HROG05-GSC cell migration towards the cathode ( $-0.25\pm0.03$ ) when compared to no EF applied  
283 ( $0.17\pm0.04$ ) (Fig. 2e). Increasing the applied EF to 200mV/mm did not significantly increase

284 directedness compared to 100mV/mm. HROG02-GSC showed increased velocity of cell migration with  
285 increased field strength (online resource 8); mean cell velocity when exposed to 200mV/mm was  
286 approximately 60% higher than when no EF was applied. With increasing EF applied to HROG05-GSC  
287 cells, velocity initially decreased compared to control in an EF of 50mV/mm. However, subsequent  
288 increases in EF strength were correlated with greater migration velocities. Online resource 8 illustrates  
289 the change in xFMI over time in HROG02-GSC and HROG05-GSC respectively, demonstrating a  
290 plateau in xFMI reached by 60 minutes. Upon exposure to an EF of 100 and 200mV/mm, HROG05-  
291 GSCs initially appear to migrate towards the anode, a positive xFMI, in a similar manner to the control  
292 group, however by 30 minutes began to steadily migrate more cathodally. Animations illustrating the  
293 migration of HROG02-GSC and HROG05-GSC with increasing EF applied can be found in online  
294 resource 9 and 10 respectively. Interestingly, we confirmed that GSCs derived from the same  
295 differentiated cells respond in the opposite direction to an applied EF.

296

297 *Pioglitazone significantly alters EF guided migration of HROG05-Diff and HROG02-Diff primary*  
298 *GBM cell lines*

299 As it has been previously shown that the PI3K/Akt pathway is important in modulating electrotaxis, we  
300 sought to determine whether the PPAR $\gamma$  agonist pioglitazone, known to inhibit Akt signalling through  
301 PTEN, had an effect on GBM cell responses to EF. Application of differing pharmacological treatments  
302 induced a statistically significant change in the directedness of cell migration of HROG02-Diff and  
303 HROG05-Diff,  $p=0.0280$  and  $p<0.0001$  calculated respectively by One-Way ANOVA (Fig. 3c and 3e).  
304 Treatment of HROG02-Diff cells with pioglitazone was associated with a significant decrease in  
305 directedness of migration towards the anode when compared with pioglitazone/GW9662 treatment  
306 ( $p=0.048$ ). The percentage of HROG02-Diff cells migrating towards the anode decreased with  
307 pioglitazone treatment ( $67.0\pm 1.5\%$ ) compared to DMSO ( $76.7\pm 4.7\%$ ) and pioglitazone/GW9662  
308 ( $78.7\pm 4.2\%$ ) (Fig.3d). There was no significant change in HROG02-Diff cell migration velocity  
309 between treatment conditions ( $p=0.3592$ ) (online resource 11). HROG05-Diff cells showed a  
310 statistically significant decrease in anodal migration when treated with pioglitazone compared to both  
311 DMSO and pioglitazone/GW9662 treatments. This was represented as both a significant decrease in

312 both the directedness of anodal migration (Fig.3e) and the number of cells migrating towards the anode  
313 (Fig. 3f). Directedness with pioglitazone treatment was  $0.10\pm 0.04$ , whilst  $0.36\pm 0.04$  with DMSO and  
314  $0.39\pm 0.04$  with pioglitazone/GW9662; a statistically significant decrease (Fig.3e). Pioglitazone  
315 treatment also induced a significant decrease in HROG05-Diff cell velocity (online resource 11). Online  
316 resource 11 shows a similar pattern of xFMI change over time of HROG02-Diff between the three  
317 treatment conditions, however, after approximately 60 minutes, the xFMI of cells treated with  
318 pioglitazone slowly decreased. HROG05-Diff cells treated with pioglitazone showed minimal change  
319 in xFMI, reaching a peak of 0.05, compared to peaks of 0.34 and 0.35 with DMSO and  
320 pioglitazone/GW9662 treatments respectively. Animations illustrating the effect of PPAR $\gamma$  stimulation  
321 on migration of HROG02-Diff and HROG05-Diff cells in the presence of a 200mV/mm EF are provided  
322 in online resources 12 and 13 respectively.

323

324 *Pioglitazone significantly decreases directedness of cell migration in HROG02-GSC and HROG05-*  
325 *GSC cell lines*

326 The role of pioglitazone was then examined in the electroaxis of GSCs. Figure 4c shows treatment of  
327 HROG02-GSC cells with pioglitazone significantly decreased directedness of cell migration towards  
328 the cathode compared to both DMSO and pioglitazone/GW9662 treatments. Although fewer HROG02-  
329 GSC cells migrated towards the cathode when treated with pioglitazone, this did not reach statistical  
330 significance (Figures 4a and 4d; also see Methods). Velocity of cell migration was unaffected by  
331 different drug conditions ( $p=0.4484$ ; see online resource 14). Pioglitazone treatment alone diminished  
332 cathodal migration of HROG05-GSC cells demonstrated by a reversal in directional preference (Fig.  
333 4b and 4f), and in directedness of cell migration (Fig. 4e). Figure 4e shows both DMSO ( $-0.23\pm 0.04$ )  
334 and pioglitazone/GW9662 ( $-0.38\pm 0.04$ ) treatments produced cathodal migration, however pioglitazone  
335 was associated with minimal anodal migration ( $0.03\pm 0.04$ ); a statistically significant finding. Velocity  
336 of HROG05-GSC cell migration was significantly reduced when treated with pioglitazone compared to  
337 pioglitazone/GW9662 however there was no significant decrease in comparison to DMSO treatment,  
338 shown in online resource 14. Animations illustrating the effect of PPAR $\gamma$  stimulation on migration of



339 HROG02-GSC and HROG05-GSC cells in the presence of a 200mV/mm EF are provided in online  
340 resources 15 and 16 respectively.

341

342 *EF does not alter PPAR $\gamma$  expression in HROG02 or HROG05*

343 To determine whether the application of EF alters PPAR $\gamma$  expression in the differentiated GBM cells  
344 and GSCs, PPAR $\gamma$  expression was quantified with Western Blotting. Online resource 17 and 18 show  
345 infrared scans of western blots stained for PPAR $\gamma$  and  $\beta$ -actin expression in HROG02-Diff, HROG05-  
346 Diff, HROG02-GSC and HROG05-GSC cells respectively with and without EF application.  
347 Quantification of these reveal no statistically significant change in the normalised Integrated Intensity  
348 of PPAR $\gamma$  in any cell lines tested upon application of an EF ( $p \Rightarrow 0.5$ ) (Online resource 17 and 18)

349

## 350 **Discussion**

351 Herein we demonstrate for the first time that the application of an EF produces contrasting migratory  
352 responses in the differentiated and GSC-like states of primary GBM cell lines. Specifically, HROG02  
353 and HROG05 cells migrated anodally in the differentiated state but reversed to cathodal migration in  
354 the de-differentiated, GSC-like state. Crucially, electrotaxis occurred at a predefined physiological  
355 voltage gradient (50mV/mm)(21, 22). Our findings compliment recent evidence by Huang and  
356 colleagues (2016), who also demonstrate cathodal migration of 5 different patient derived brain tumour  
357 initiating cell lines in a 2-dimensional (2D) culture over poly-L-ornithine/laminin and in a 3D  
358 microfluidic device. However, Huang and colleagues were unable to recapitulate an opposing  
359 electrotactic response in the immortalised differentiated U87 GBM cell line, where no migratory  
360 response was elicited at 1V/cm, despite Li and colleagues reporting that U87MG cells migrate  
361 cathodally when exposed to 2V/cm (28, 43). Our observations indicate that GBM cells will migrate in  
362 opposite directions depending on their transition state (differentiated or stem-like) when exposed to an  
363 EF.

364

365 Similar contrasting electrotactic responses have been reported in other cancer types and are often related  
366 to metastatic potential. Prostate cancer cells, for example, with high and low metastatic potential

367 migrate cathodally and anodally, respectively (44). Further, a positive correlation between the  
368 metastatic potential and anodal migration has been reported in breast cancer cells (27). This migratory  
369 phenomenon may therefore represent a malignant feature of cancer; opposing responses of  
370 subpopulations of cancer cells induces selective migration away from the tumour bulk and less  
371 predictable infiltration. This may explain the diffuse infiltration typically seen in GBM. In theory, if an  
372 electrical gradient existed between the tumour and the surrounding brain parenchyma, a subpopulation  
373 of either differentiated or GSC GBM cells would migrate away from the tumour depending on the  
374 electrical gradient polarity. Therefore, if diffuse GBM cell migration is time dependent, preventing or  
375 reversing this process may be more feasible earlier in the disease course, however this concept has yet  
376 to be fully investigated and may not be clinically feasible based on the requirements for medical  
377 screening tests (45). Studying the electrical gradient polarity between brain and tumour in animal  
378 models would help elucidate this, where a recently discovered wild-type murine GBM model has been  
379 discovered and would be more representative than xenograft models (46).

380

381 However, the Food and Drug Administration approved in 2005 Novocure's Tumour Treatment Fields  
382 (renamed recently to Optune), which utilises alternating current across the cranium in recurrent post-  
383 surgical GBM in combination with chemotherapy (47). Optune utilises externally placed transducer  
384 arrays on a patient's scalp to induce apoptosis of tumour cells undergoing mitosis. Our results  
385 demonstrate pioglitazone can significantly reduce the directed cell migration of GSCs but not migration  
386 velocity. A possible therapeutic strategy to prevent the unregulated spread of GSCs would be to  
387 chemically disrupt directed cell migration, where migration velocity would play a less important role  
388 to achieve this goal. We estimate that the pioglitazone concentrations used in vitro in the present study  
389 are equivalent to subtherapeutic licensed dosages, however this would require in vivo studies to confirm  
390 whether directed cell migration is affected. As such, the use of a direct current EF or chemical disruption  
391 of electroaxis to manipulate GBM cell migration has yet to be optimised for clinical use.

392

393 Neural stem cells are known to be prone to transformation into GSCs (48) and have been demonstrated  
394 to reliably migrate in a cathodal direction in response to EFs in vitro and in vivo. (28, 49, 50). In contrast,

395 we and others find that GSCs migrate anodally, suggesting a pathological mechanism underlying this  
396 change in response (28). Previous evidence implicates PI3K in electrotaxis, where cytoskeletal  
397 rearrangements ultimately lead to directed migration via Src/PI3K/Akt and MAPK signalling pathways  
398 (21, 27, 29, 51). Huang and colleagues demonstrate that chemical inhibition of PI3K with LY294002  
399 decrease brain tumour initiating cells directed migration, where inhibition of Erk and each of its  
400 activating growth factors had no effect on electrotaxis (28). Recently, Lyon and colleagues identified  
401 putative electrotactic signalling pathways with transcriptomic analyses in differentiated U87MG  
402 spheroid aggregates, and subsequently found that PI3K, Akt, mTOR, ErbB2, ErbB3 and Src/Abl, but  
403 not MEK, HGF/VEGF and ROCK1/2, inhibition attenuates cathodal migration (52). However, PI3K  
404 inhibition with LY294002 did not affect cathodal migration, although BEZ235 abolished directed  
405 migration, which may be non-specifically accrued to its dual activity on PI3K/mTOR and more efficient  
406 downregulation of Akt (52, 53). Taken together, PI3K does not appear to be an efficient target to prevent  
407 directed cell migration in differentiated GBM cells with in vitro efficacy proven in GSCs but not  
408 differentiated GBM cells.

409

410 Based on findings that PPAR $\gamma$  agonists suppress Akt in both differentiated and GSC cells through  
411 PPAR $\gamma$  activation (32, 54), we utilised pioglitazone to determine whether EF migration is affected by  
412 Akt downregulation by PPAR $\gamma$ . We found that pioglitazone treatment significantly decreased the  
413 directedness of electrotaxis of primary GBM cell lines in both differentiated and de-differentiated states.  
414 This inhibitory effect was diminished by the PPAR $\gamma$  antagonist GW9662, directly implicating PPAR $\gamma$   
415 activation in suppression of EF guided migration of primary GBM cell lines. PPAR $\gamma$  activation inhibited  
416 electrotaxis in both differentiated and de-differentiated phenotypes, implying a common migratory  
417 pathway downstream of PPAR $\gamma$ , such as the PI3K/Akt pathway. This provides early evidence that  
418 inhibition of GBM directed cell migration reliant on electrotaxis may be targeted with drug therapies.  
419 Further investigation, including transcriptomics, selective chemical inhibition and in vivo experiments  
420 would be necessary to validate this. We present promising findings that a single drug can simultaneously  
421 inhibit differentiated and stem cell populations of the same primary GBM cells. As such PPAR $\gamma$   
422 agonists may have a further clinical role in preventing GBM recurrence in addition to anti-proliferative,

423 pro-differentiation of GSC and pro-apoptotic effects reported previously (55). Such findings need to be  
424 recapitulated in animal models of GBM to determine whether tumour infiltration can be reversed. Such  
425 a strategy holds clinical importance as patients with GBM present late in the disease, making cancer  
426 cell migration reversal using electric fields a more realistic approach as opposed to a containment  
427 strategy such as chondroitin sulfate proteoglycans modulation, which would not be able to target  
428 satellite GBM cells (56).

429

430 Physiological EFs have been demonstrated in the mammalian brain (19) and such EF's have been shown  
431 to occur in many other cancer types including ovarian, leukaemic, breast, cervical and prostate cancer  
432 cells. In these instances, depolarisation is positively correlated with the rate of proliferation (57).  
433 Recently, Jun-Feng and colleagues demonstrate that human neural stem cells implanted in the rat brain  
434 can be electrically guided along the rostral migratory stream (50). Not only does this have implications  
435 for neural regeneration but also for GBM treatment, where EF therapy may be useful as a treatment  
436 adjunct to prevent tumour recurrence. Interestingly, voltage-gated Na<sup>+</sup> channels have been implicated  
437 in tumour-parenchyma EF generation (57) and GBMs demonstrate an association between metastatic  
438 potential and Na<sup>+</sup> influx (58). Furthermore, epileptiform hyperexcitability has been demonstrated at the  
439 interface between GBM and normal brain tissue, peri-tumour, that is mediated by glutamate excess  
440 (59) . While tumour epilepsy does not occur universally in patients with GBM, EF generation at the  
441 peri-tumour caused by increased extracellular glutamate may contribute to driving cell migration away  
442 from the tumour (60).

443

444 The generation of a pathological EF between GBM and surrounding brain parenchyma may be  
445 dependent on high rates of cellular proliferation and deregulated sodium transport. This would produce  
446 a relatively depolarised tumour bulk which would act as an anode whilst the surrounding brain tissue  
447 acts as a cathode. The cathodal migration of GSC-like primary GBM cell lines that we report here  
448 demonstrates a pro-migratory mechanism of highly tumourigenic GBM cells that may be directed away  
449 from the tumour bulk *in vivo*. It is unknown how the presence of raised extracellular glutamate may

450 affect this electrochemical gradient and requires further investigation to clarify the underlying  
451 mechanisms.

452

453 In our study, we did not investigate physiological levels of EF of 3-5mV/mm as found previously in the  
454 RMS in *ex vivo* mouse brains (19). Instead, we focused on higher levels of EF from 50-200mV/mm that  
455 have been reported when culturing neural stem cells *in vitro*. Cao et al. reported that neuroblasts respond  
456 to EFs of 50mV/mm *in vitro* (19), Huang et al. demonstrated that GSC respond to EFs as low as  
457 50mV/mm (61) and Li et al. demonstrated that immortalised GBM cells respond to 200mV/mm (43).  
458 Using these EF strengths allowed us to determine whether they have therapeutic potential. Furthermore,  
459 we chose to utilise an EF of 200mV/mm in drug treatment experiments to screen for whether EF-  
460 mediated migration could be chemically targeted, where a lower EF may not provide the resolution to  
461 detect a difference. Understanding the tumour to brain voltage differentials will be critical in the future,  
462 where reports of a novel wild type GBM model may provide the ideal platform to measure this (46).

463

464 Surgically implanted neuro-stimulatory devices, including deep brain stimulation and vagal nerve  
465 stimulation, have been established in the fields of Parkinson's disease, epilepsy and depression.  
466 Applying direct current to a GBM tumor or resection cavity would require careful voltage tapering in  
467 animal models in the first instance before considering human use. The effect of a resection cavity must  
468 also be fully investigated, which can act as a cathode in theory, permitting GSC migration towards the  
469 cavity but promoting undesirable differentiated GBM cell outward migration. Concomitant  
470 glucocorticoid treatment with novel drug therapies should be considered carefully as dexamethasone is  
471 commonly prescribed in the early stages of GBM diagnosis, where this would be particularly relevant  
472 for PPAR $\gamma$  agonists. Further investigation including *in vivo* models and clinical trials will be required  
473 to prove whether electrotaxis of GBM and GSCs can be targeted chemically and/or surgically to add to  
474 the current armamentarium in brain tumour treatment.

475

476

477 **Conclusions**

478 We demonstrate for the first time that differentiated and stem cell state primary GBMs derived from  
479 the same cell populations migrate in opposing directions in an applied EF. The directedness of  
480 electrotaxis behaviours, irrespective of polarity, in both cell states was reduced markedly by the PPAR $\gamma$   
481 agonist pioglitazone. Regardless of the direction of EF present, cancer cells appear to migrate away  
482 from the tumour bulk. Further research into the generation and characteristics of tumour-brain EFs  
483 would provide invaluable insights into the pathology. Pathological EF disruption may represent a novel  
484 target to prevent tumour infiltration. Chemical or surgical interventions may be developed to take  
485 advantage of this potential susceptibility in the future.

486

## 487 **References**

- 488 1. Clancy H, Pruski M, Lang BVOP, Ching J, McCaig C. Glioblastoma Cell Migration is  
489 Directed by Electrical Signals. bioRxiv; 2020.
- 490 2. Louis DN, Perry A, Reifenberger G, von Deimling A, Figarella-Branger D, Cavenee WK, et  
491 al. The 2016 World Health Organization Classification of Tumors. *Acta Neuropathologica*.  
492 2016;131:803-20.
- 493 3. Ostrom Qt, Gittleman H, Liao P, Rouse C, Chen Y, Dowling J, et al. CBTRUS Statistical  
494 Report: Primary Brain and Central Nervous System Tumors Diagnosed in the United States in 2007–  
495 2011. *Neuro-oncology*. 2014;16:Suppl: iv1-iv63.
- 496 4. Thakkar JP, Dolecek TA, Horbinski C, Ostrom QT, Lightner DD, Bamholtz-Sloan JS, et al.  
497 Epidemiologic and Molecular Prognostic Review of Glioblastoma. *Cancer Epidemiology, Biomarkers  
498 & Prevention*. 2014;23(10):1985-96.
- 499 5. Stupp R, Hegi ME, Mason WP, van den Bent MJ, Taphoorn MJB, Janzer RC, et al. Eff ects of  
500 radiotherapy with concomitant and adjuvant temozolomide versus radiotherapy alone on survival in  
501 glioblastoma in a randomised phase III study: 5-year analysis of the EORTC-NCIC trial. *Lancet  
502 Oncology*. 2009;10:459-66.
- 503 6. Xie Q, Mittal S, Berens ME. Targeting adaptive glioblastoma: an overview of proliferation and  
504 invasion. *Neuro-Oncology*. 2014;16(12):1575-84.
- 505 7. Ignatova TN, Kukekov VG, Leywell ED, Suslov ON, Vrionis FD, Steindler DA. Human  
506 Cortical Glial Tumors Contain Neural Stem-Like Cells Expressing Astroglial and Neuronal Markers In  
507 Vitro. *GLIA*. 2002;39:193-206.
- 508 8. Singh SK, Clarke ID, Terasaki M, Bon VE, Hawkins C, Squire J, et al. Identification of a  
509 Cancer Stem Cell in Human Brain Tumors. *Cancer Research*. 2003;63:5821-8.

- 510 9. Hemmati HD, Nakano I, Lazareff JA, Masterman-Smith M, Geschwind DH, Bronner-Fraser  
511 M, et al. Cancerous stem cells can arise from pediatric brain tumors. *PNAS*. 2003;100(25):15178-83.
- 512 10. Galli R, Binda E, Orfanelli U, Cipelletti B, Gritti A, De Vitis S, et al. Isolation and  
513 Characterization of Tumorigenic, Stem-like Neural Precursors from Human Glioblastoma. *Cancer*  
514 *Research*. 2004;64:7011-21.
- 515 11. Lathia JD, Mack SC, Mulkearns-Hubert EE, Valentim CLL, Rich JN. Cancer stem cells in  
516 glioblastoma. *Genes and Development*. 2015;29:1203-17.
- 517 12. Shin JH, Lee YS, Hong Y, Kang CS. Correlation between the prognostic value and the  
518 expression of the stem cell marker CD133 and isocitrate dehydrogenase1 in glioblastomas. *Journal of*  
519 *Neurooncology*. 2013;115:333-41.
- 520 13. Pallini R, Ricci-Vitiani L, Banna GL, Signore M, Lombardi D, Todaro M, et al. Cancer Stem  
521 Cell Analysis and Clinical Outcome in Patients with GlioblastomaMultiforme. *Clinical Cancer*  
522 *Research*. 2008;14(24):8205-12.
- 523 14. Demuth T, Berens ME. Molecular Mechanisms of Glioma Cell Migration and Invasion. *Journal*  
524 *of Neuro-Oncology*. 2004;70.
- 525 15. Lefranc F, Brotschi J, Kiss R. Possible Future Issues in the Treatment of Glioblastomas: Special  
526 Emphasis on Cell Migration and the Resistance of Migrating Glioblastoma Cells to Apoptosis. *Journal*  
527 *of Clinical Oncology*. 2005;23:2411-22.
- 528 16. Paw I, Carpenter RC, Watabe K, Debinski W, Lo H. Mechanisms regulating glioma invasion.  
529 *Cancer Letters*. 2015;362:1-7.
- 530 17. Ariza CA, Fleury AT, Tormos CJ, Petruk V, Chawla S, Oh J, et al. The Influence of Electric  
531 Fields on Hippocampal Neural Progenitor Cells. *Stem Cell Reviews and Reports*. 2010;6:585-600.
- 532 18. Arocena M, Zhao M, Collinson JM, Song B. A Time-Lapse and Quantitative Modelling  
533 Analysis of Neural Stem Cell Motion in the Absence of Directional Cues and in Electric Fields. *Journal*  
534 *of Neuroscience Research*. 2010;88:3267-74.
- 535 19. Cao L, Wei D, Reid B, Zhao S, Pu J, Pan T, et al. Endogenous Electric Currents Might Guide  
536 Rostral Migration of Neuroblasts. *EMBO Reports*. 2013;14:184-90.
- 537 20. Li L, El-Hayek YH, Liu B, Chen Y, Gomez E, Wu X, et al. Direct-Current Electrical Field  
538 Guides Neuronal Stem/Progenitor Cell Migration. *Stem Cells*. 2008;26:2193-200.
- 539 21. Meng X, Arocena M, Penninger J, Gage FH, Zhao M, Song B. PI3K mediated electrotaxis of  
540 embryonic and adult neural progenitor cells in the presence of growth factors. *Experimental Neurology*.  
541 2011;227:210-7.
- 542 22. Yao L, Shanley L, McCaig C, Zhao M. Small Applied Electric Fields Guide Migration of  
543 Hippocampal Neurons. *Journal of Cellular Physiology* 2008;216:527-35.
- 544 23. Zhao H, Steiger A, Nohner M, Ye H. Specific Intensity Direct Current (DC) Electric Field  
545 Improves Neural Stem Cell Migration and Enhances Differentiation towards  $\beta$ III-Tubulin+ Neurons.  
546 *PLOS ONE*. 2015;10(6):1-21.

- 547 24. McCaig CD, Song B, Rajniecek AM. Electrical Dimensions in Cell Science. *Journal of Cell*  
548 *Science*. 2009;122:4267-76.
- 549 25. Li F, Chen T, Hu S, Lin J, Hu R, Feng H. Superoxide Mediates Direct Current Electric Field-  
550 Induced Directional Migration of Glioma Cells through the Activation of AKT and ERK. *PLOS ONE*.  
551 2013;8(4):1-11.
- 552 26. Mycielska ME, Djamgoz MBA. Cellular Mechanisms of Direct-Current Electric Field Effects:  
553 Galvanotaxis and Metastatic Disease. *Journal of Cell Science*. 2004;117.
- 554 27. Pu J, McCaig CD, Cao L, Zhao Z, Segall JE, Zhao M. EGF receptor signalling is essential for  
555 electric-field directed migration of breast cancer cells. *Journal of Cell Science*. 2007;120:3395-403.
- 556 28. Huang Y, Hoffmann G, Wheeler B, Schiapparelli P, Quinones-Hinojosa A, Searson P. Cellular  
557 microenvironment modulates the galvanotaxis of brain tumor initiating cells. *Scientific Reports*.  
558 2016;6(21583).
- 559 29. Zhao M, Song B, Pu J, Wada T, Reid B, Tai G, et al. Electrical signals control wound healing  
560 through phosphatidylinositol-3-OH kinase- $\gamma$  and PTEN. *Nature*. 2006;442:457-60.
- 561 30. Zhao M, Pu J, Forrester JV, McCaig CD. Zhao, M., Pu, Membrane lipids, EGF receptors and  
562 intracellular signals co-localize and are polarized in epithelial cells moving directionally in a  
563 physiological electric field. *Federation of American Societies for Experimental Biology*.  
564 2002;16(8):857-9.
- 565 31. Mezey G, Treszl A, Schally AV, Block NL, Vízkeleti L, Juhász A, et al. Prognosis in human  
566 glioblastoma based on expression of ligand growth hormone-releasing hormone, pituitary-type growth  
567 hormone-releasing hormone receptor, its splicing variant receptors, EGF receptor and PTEN genes.  
568 *Journal of Cancer Research and Clinical Oncology*. 2014;140:1641-9.
- 569 32. Ching J, Amiridis S, Stylli SS, Bjorksten AR, Kountouri N, Zheng T, et al. The peroxisome  
570 proliferator activated receptor gamma agonist pioglitazone increases functional expression of the  
571 glutamate transporter excitatory amino acid transporter 2 (EAAT2) in human glioblastoma cells.  
572 *Oncotarget*. 2015:1-14.
- 573 33. Patel L, Pass I, Coxen P, Downes CP, Smith SA, Macphee CH. Tumor suppressor and anti-  
574 inflammatory actions of PPAR $\gamma$  agonists are mediated via upregulation of PTEN. *Current Biology*.  
575 2001;11(10):765-8.
- 576 34. Cimini A, Cristiano L, Colafarina S, Benedetti E, Di Loreto S, Festucciar C, et al. PPARc-  
577 dependent effects of conjugated linoleic acid on the human glioblastoma cell line (ADF). *International*  
578 *Journal of Cancer*. 2005;117:923-33.
- 579 35. Zang C, Wachter M, Liu H, Posch MG, Fenner MH, Stadelmann C, et al. Ligands for PPAR $\gamma$   
580 and RAR cause induction of growth inhibition and apoptosis in human glioblastomas. *Journal of Neuro-*  
581 *Oncology*. 2003;65:107-18.
- 582 36. Cilibrasi C, Butta V, Riva G, Bentivegna A. Pioglitazone Effect on Glioma Stem Cell Lines:  
583 Really a Promising Drug Therapy for Glioblastoma? *PPAR Research*. 2016;2016(7175067):1-8.



- 584 37. Mullins CS, Schneider B, Stockhammer F, Krohn M, Classen CF, Linnebacher M.  
585 Establishment and characterization of primary glioblastoma cell lines from fresh and frozen material: a  
586 detailed comparison. *PLoS One*. 2013;8(8):e71070.
- 587 38. Fael Al-Mayhany TM, Ball SLR, Zhao J, Fawcett J, Ichmura K, Collins PV, et al. An efficient  
588 method for derivation and propagation of glioblastoma cell lines that conserves the molecular profile of  
589 their original tumours. *Journal of Neuroscience Methods*. 2009:192-9.
- 590 39. Pollard SM, Yoshikawa K, Clarke ID, Danovi D, Stricker S, Russell R, et al. Glioma Stem Cell  
591 Lines Expanded in Adherent Culture Have Tumor-Specific Phenotypes and Are Suitable for Chemical  
592 and Genetic Screens. *Cell*. 2009:568-80.
- 593 40. Chearwae W, Bright JJ. PPAR $\gamma$  agonists inhibit growth and expansion of CD133+ brain  
594 tumour stem cells. *British Journal of Cancer* 2008;99:2044-53.
- 595 41. Song B, Gu Y, Pu J, Reid B, Zhao Z, Zhao M. Application of direct current electric fields to  
596 cells and tissues in vitro and modulation of wound electric field in vivo. *Nature Protocols*.  
597 2007;2(6):1479-89.
- 598 42. Vik-Mo EO, Sandberg C, Olstom H, Varghese M, Brandal P, Ramm-Petersen J, et al. Brain  
599 tumor stem cells maintain overall phenotype and tumorigenicity after in vitro culturing in serum-free  
600 conditions. *Neuro-Oncology*. 2010;12(12):1220-30.
- 601 43. Li F, Chen T, Hu S, Lin J, Hu R, Feng H. Superoxide Mediates Direct Current Electric Field-  
602 Induced Directional Migration of Glioma Cells through the Activation of AKT and ERK *PLoS ONE*;  
603 2013. p. e61195.
- 604 44. Djamgoz M, Mycielska M, Madeja Z, Fraser SP, Korohoda W. Directional movement of rat  
605 prostate cancer cells in direct-current electric field: involvement of voltage-gated Na<sup>+</sup> channel activity. .  
606 *Journal of Cell Science*. 2001;114(14):2697-705.
- 607 45. Pinsky PF. Principles of Cancer Screening. *Surg Clin North Am*. 2015;95(5):953-66.
- 608 46. Hatcher A, Yu K, Meyer J, Aiba I, Deneen B, Noebels JL. Pathogenesis of peritumoral  
609 hyperexcitability in an immunocompetent CRISPR-based glioblastoma model. *J Clin Invest*.  
610 2020;130(5):2286-300.
- 611 47. Fabian D, Guillermo Prieto Eibl MDP, Alnahhas I, Sebastian N, Giglio P, Puduvalli V, et al.  
612 Treatment of Glioblastoma (GBM) with the Addition of Tumor-Treating Fields (TTF): A Review.  
613 *Cancers (Basel)*. 2019;11(2).
- 614 48. Vescovi AL, Galli R, Reynolds BA. Brain tumour stem cells. *Nat Rev Cancer*. 2006;6(6):425-  
615 36.
- 616 49. Feng JF, Liu J, Zhang XZ, Zhang L, Jiang JY, Nolte J, et al. Guided migration of neural stem  
617 cells derived from human embryonic stem cells by an electric field. *Stem Cells*. 2012;30(2):349-55.
- 618 50. Feng JF, Liu J, Zhang L, Jiang JY, Russell M, Lyeth BG, et al. Electrical Guidance of Human  
619 Stem Cells in the Rat Brain. *Stem Cell Reports*. 2017;9(1):177-89.

- 620 51. Sun Y, Do H, Gao J, Zhao R, Zhao M, Mogilner A. Keratocyte fragments and cells utilize  
621 competing pathways to move in opposite directions in an electric field. *Curr Biol.* 2013;23(7):569-74.
- 622 52. Lyon JG, Carroll SL, Mokarram N, Bellamkonda RV. Electrotaxis of Glioblastoma and  
623 Medulloblastoma Spheroidal Aggregates. *Sci Rep.* 2019;9(1):5309.
- 624 53. Maira SM, Stauffer F, Brueggen J, Furet P, Schnell C, Fritsch C, et al. Identification and  
625 characterization of NVP-BEZ235, a new orally available dual phosphatidylinositol 3-  
626 kinase/mammalian target of rapamycin inhibitor with potent in vivo antitumor activity. *Mol Cancer*  
627 *Ther.* 2008;7(7):1851-63.
- 628 54. Im CN. Combination Treatment with PPAR. *Biomed Res Int.* 2017;2017:5832824.
- 629 55. Ellis HP, Kurian KM. Biological Rationale for the Use of PPAR $\gamma$  Agonists in Glioblastoma.  
630 *Front Oncol.* 2014;4:52.
- 631 56. Silver DJ, Siebzehnruhl FA, Schildts MJ, Yachnis AT, Smith GM, Smith AA, et al. Chondroitin  
632 sulfate proteoglycans potently inhibit invasion and serve as a central organizer of the brain tumor  
633 microenvironment. *J Neurosci.* 2013;33(39):15603-17.
- 634 57. Yang M, Brackenbury J. Membrane Potential and Cancer Progression. *Frontiers in Physiology.*  
635 2013;4:1-10.
- 636 58. Berdiev BK, Xia J, McLean LA, Markert JM, Gillespie GY, Mapstone TB, et al. Acid-sensing  
637 Ion Channels in Malignant Gliomas. *The Journal of Biological Chemistry.* 2003;278(17):15023-34.
- 638 59. Buckingham SC, Campbell SL, Haas BR, Montana V, Robel S, Ogunrinu T, et al. Glutamate  
639 release by primary brain tumors induces epileptic activity. *Nat Med.* 2011;17(10):1269-74.
- 640 60. Yuen TI, Morokoff AP, Bjorksten A, D'Abaco G, Paradiso L, Finch S, et al. Glutamate is  
641 associated with a higher risk of seizures in patients with gliomas. *Neurology.* 2012;79(9):883-9.
- 642 61. Huang YJ, Hoffmann G, Wheeler B, Schiapparelli P, Quinones-Hinojosa A, Searson P. Cellular  
643 microenvironment modulates the galvanotaxis of brain tumor initiating cells. *Sci Rep.* 2016;6:21583.

644

645

646

647

648

649

650

651

652

653 *Acknowledgements*

654 We thank Dr Filipa Cunha, Dr Lin Cao and Dr Jin Pu for technical support in performing electroxis  
655 experiments. We thank Professor Michael Linnebacher for gifting primary brain tumour cell lines.

656

657 *Authors' contributions*

658 Conceptualisation, J.C., C.D.M.; Methodology, J.C., C.D.M.; Validation J.C. H.C., M.P.; Formal  
659 Analysis, H.C., M.P.; Investigation, J.C., H.C., M.P.; Data Curation, H.C., M.P., J.C.; Manuscript draft,  
660 H.C., M.P., J.C.; Manuscript final review, All; Supervision, C.D.M, J.C., B.L.; Funding, J.C., C.D.M.

661

662 *Ethics approval and consent to participate*

663 Ethical approvals were obtained from the National Research Ethics Service – North of Scotland, REC  
664 reference: 14/NS/0015, Protocol No.: 3/076/13, IRAS project ID: 138989.

665

666 *Consent for publication*

667 Not applicable.

668

669 *Data availability*

670 All data generated or analysed during this study are included in this published article and its  
671 supplementary information files.

672

673 *Conflict of interest*

674 The authors declare no conflict of interest.

675

676 *Funding*

677 Funding was provided by NHS Grampian Endowment Grants, Project Number: 14/17.

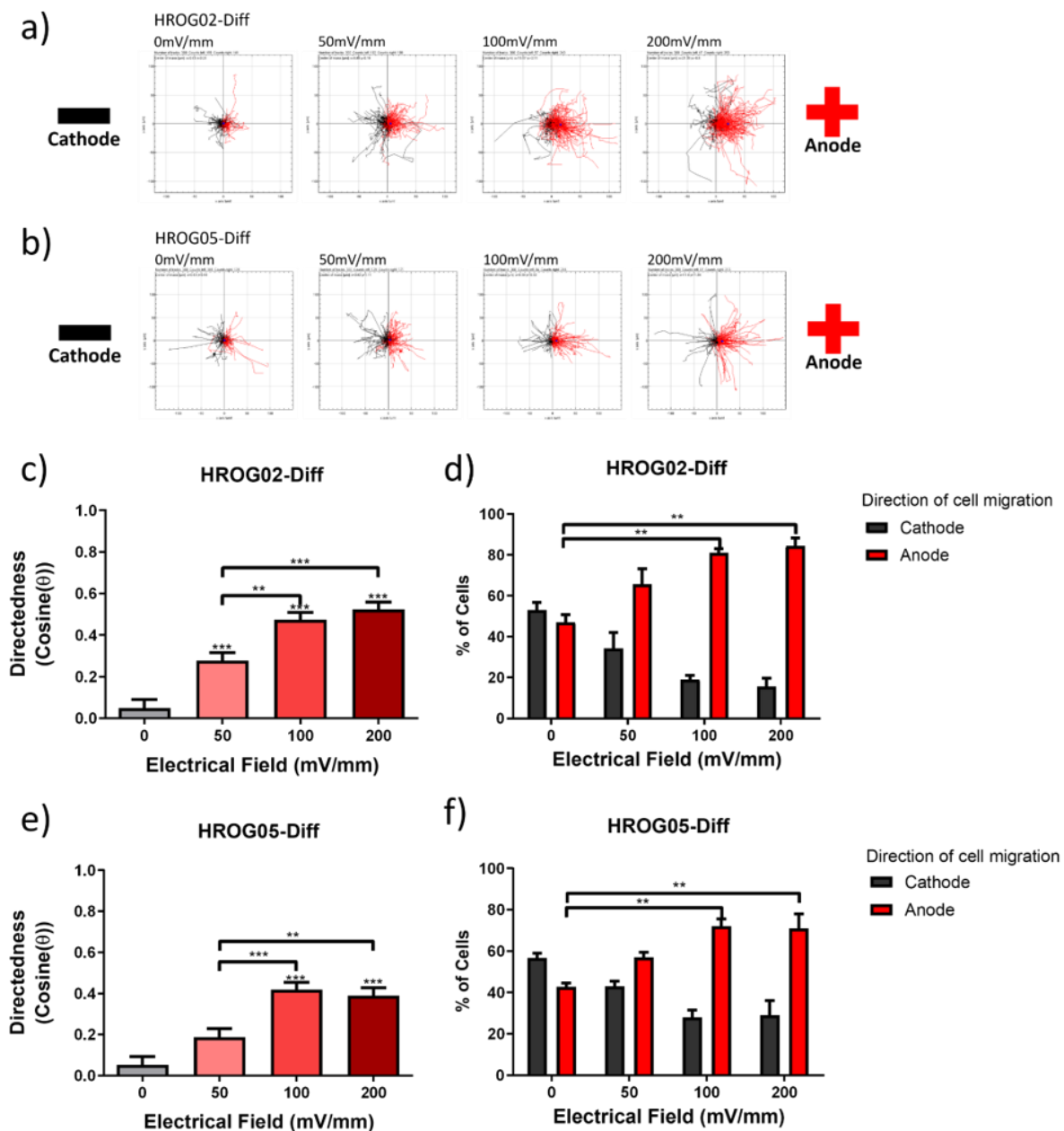
678

679

680

681

682 **Figures and Legends (NB: All images would require colour printing)**



683

684 **Figure 1**

685 HROG02-Diff and HROG05-Diff cell migration in electric fields. Panel (a) and (b) visualises the  
686 cellular movement that occurred under different field strengths for HROG02-Diff and HROG05-Diff,  
687 respectively. (c) and (e) show the effects of field strength on the directedness of migration for HROG02-  
688 Diff and HROG05-Diff, respectively. (d) and (f) show the percentage of cells that migrated towards  
689 each electrode for HROG02-Diff and HROG05-Diff, respectively. HROG02-Diff cells show an anodal

690 migration pattern (a;  $p=0.0022$  in d), with a statistically significant effect of the electric field on  
691 directedness (c,  $p<0.0001$ ); one-way ANOVA. HROG05-Diff cells show an anodal migration pattern  
692 (b;  $p=0.0035$  in f) with a statistically significant effect of the electric field on directedness (e,  $p<0.0001$ );  
693 one-way ANOVA. \*, \*\* and \*\*\* above bars represent Tukey's post-test comparisons with control (0  
694 mV/mm), while horizontal bars represent Tukey's results of comparisons between groups that have  
695 shown statistical significance.

696

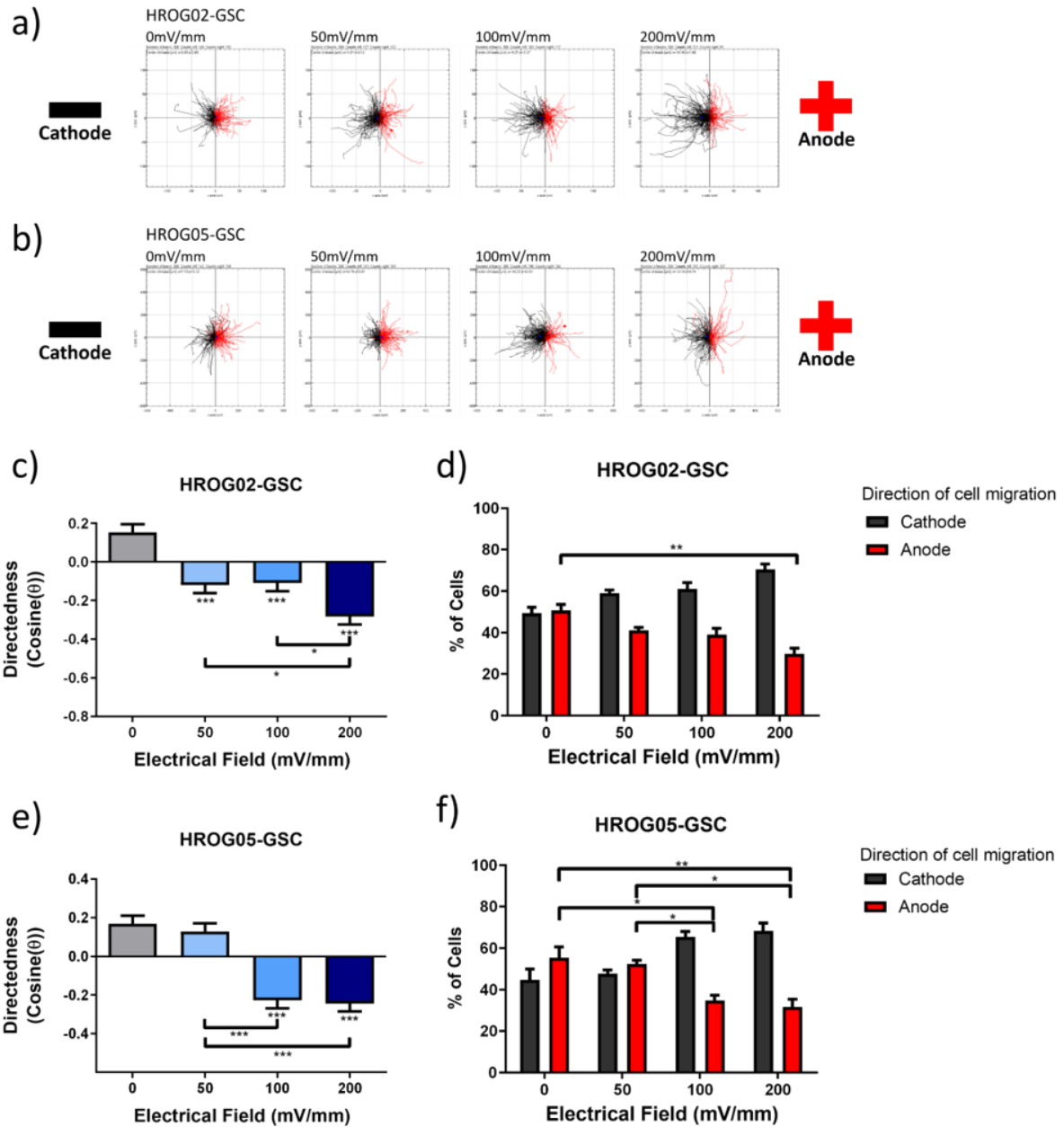
697

698

699

700

701



702

703 **Figure 2**

704 HROG02-GSC and HROG05-GSC cell migration in electric fields. Panel (a) and (b) visualises the

705 cellular movement that occurred under different field strengths of HROG02-GSC and HROG05-GSC,

706 respectively. (c) and (e) show the effects of field strength on the directedness of migration, and the

707 percentage of cells that migrated towards each electrode of HROG02-GSC and HROG05-GSC,

708 respectively. HROG02-GSC cells show a cathodal migration pattern (a;  $p=0.0034$  in d) with a

709 statistically significant effect of the electric field on directedness (c,  $p<0.0001$ ); one-way ANOVA.

710 HROG05-GSC cells show a cathodal migration pattern (b;  $p=0.0030$  in f) with a statistically significant

711 effect of the electric field on directedness (e,  $p < 0.0001$ ); one-way ANOVA \*, \*\* and \*\*\* above bars  
712 represent Tukey's post-test comparisons with control (0 mV/mm), while horizontal bars represent  
713 Tukey's results of comparisons between groups that have shown statistical significance.

714

715

716

717

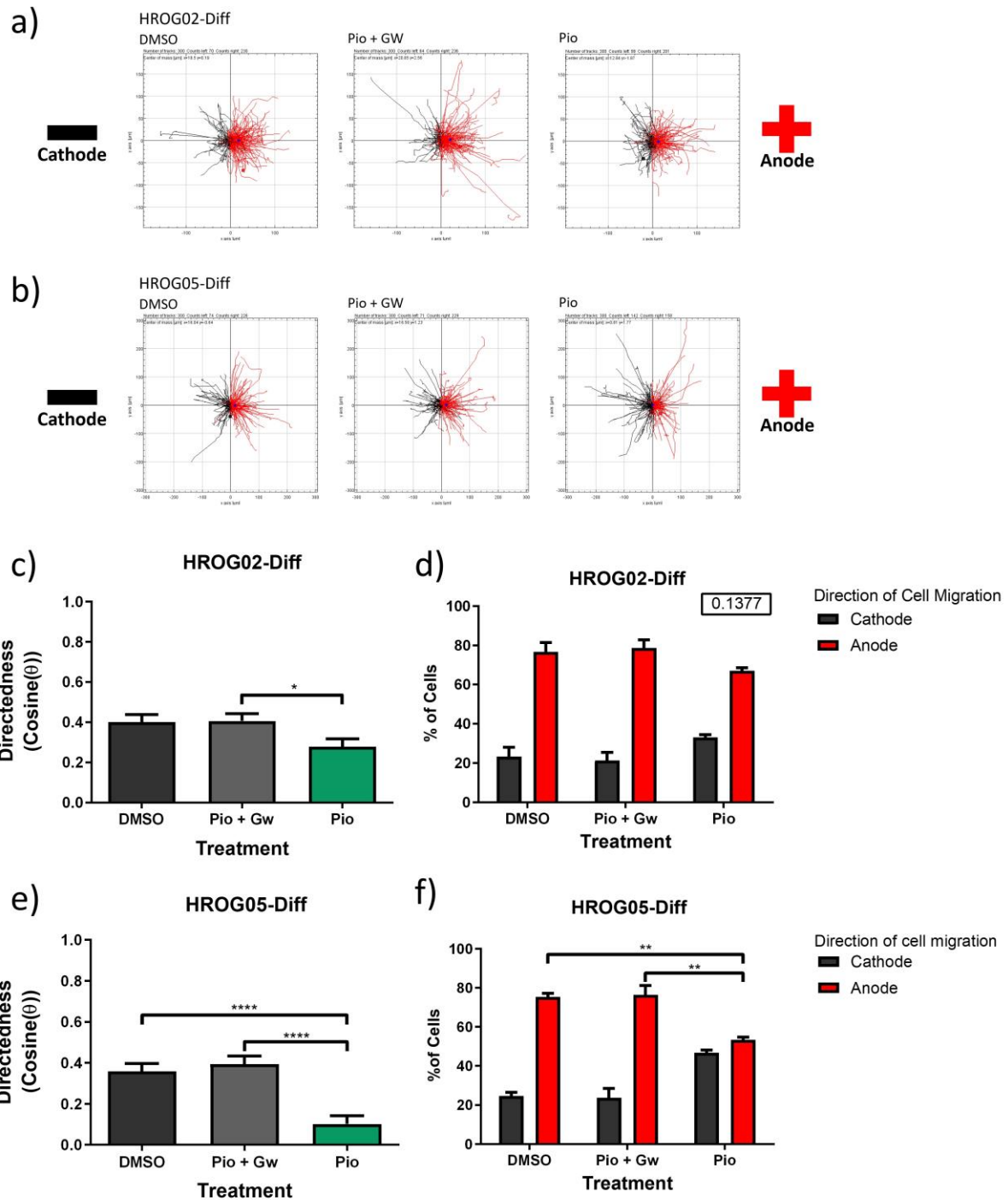
718

719

720

721

722



723

724 **Figure 3**

725 Effect of PPAR $\gamma$  stimulation on HROG02-Diff and HROG05-Diff cell migration in a 200mV/mm  
 726 electrical field. Panel (a) and (b) illustrates changes caused by the different treatments of DMSO (drug  
 727 vehicle) and PPAR $\gamma$  agonists (pioglitazone, “pio”) and antagonist (GW9662, “GW”). (c) and (e) show,  
 728 respectively, the effects PPAR $\gamma$  stimulation on directedness of HROG02-Diff and HROG05-Diff cell  
 729 migration. Treatment had a significant effect on the HROG02-Diff cells’ directedness (c,  $p=0.048$



730 between piogltazone and pioglitazone/GW9662 treatments. Treatment had a significant effect on the  
731 direction of HROG05-Diff cell migration (b; P=0.0034 in f), as well as on directedness (e, p<0.0001,)   
732 one-way ANOVA. \*, \*\* and \*\*\* above horizontal bars represent Tukey's results of comparisons  
733 between groups that have shown statistical significance. n= 300 for all analysis excluding (d) where  
734 n=3. Number in box in top right hand corner represents p value for one-way ANOVA (d).

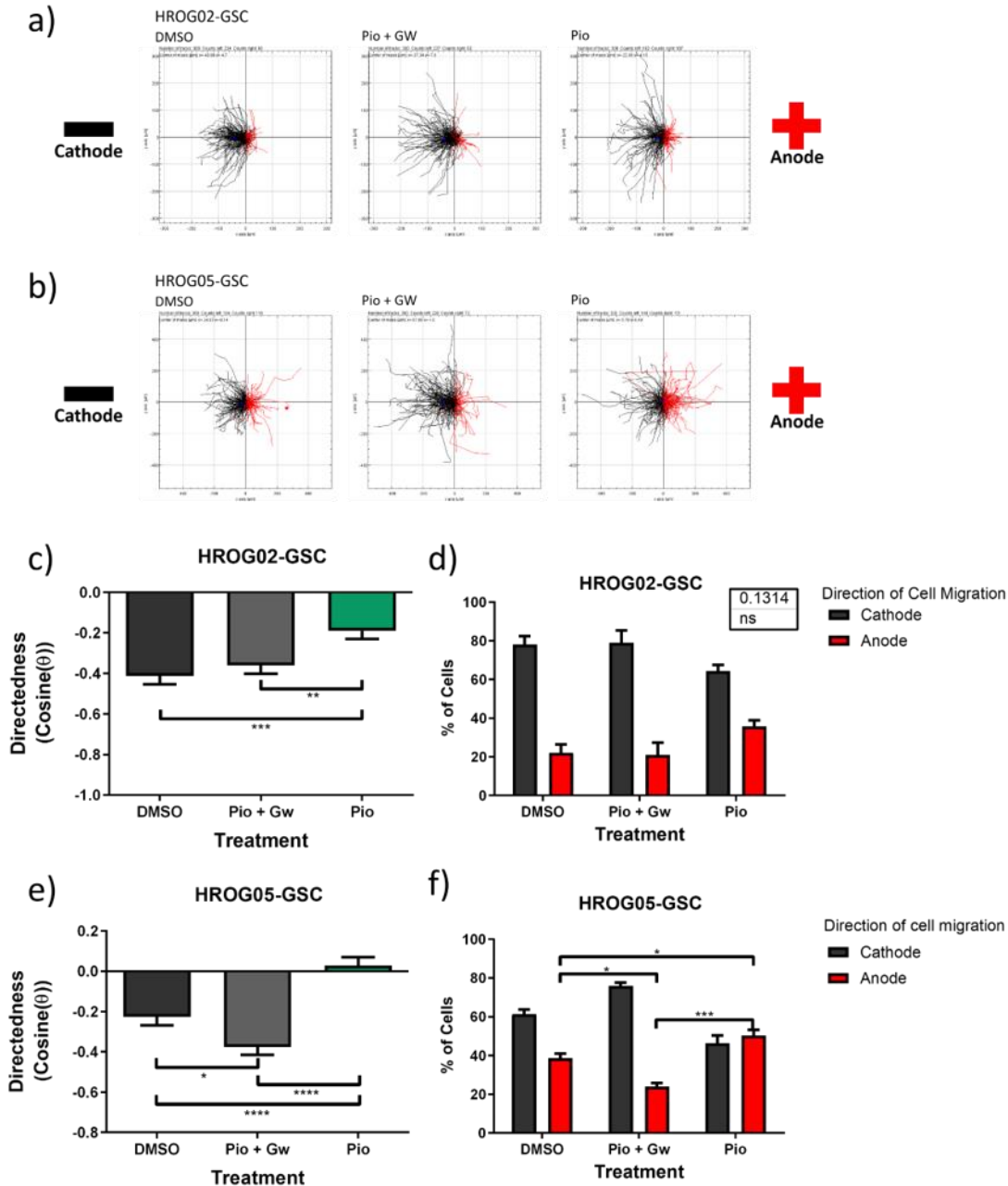
735

736

737

738

739



740

741 **Figure 4**

742 Effect of PPAR $\gamma$  stimulation on HROG02-GSC and HROG05-GSC cell migration in a 200mV/mm  
 743 electrical field. Panel (a) and (b) illustrates changes caused by the different treatments of DMSO (drug  
 744 vehicle) and PPAR $\gamma$  agonists (pioglitazone, “pio”) and antagonist (GW9662, “GW”). (c) and (e) show,  
 745 respectively, the effects of PPAR $\gamma$  stimulation on directedness of HROG02-GSC and HROG05-GSC  
 746 cell migration. Treatment significantly reduced the directedness of HROG02-GSC cell migration  
 747 towards the cathode. Treatment had a significant effect on direction of migration HROG05-GSC cells  
 748 (b; P=0.0008 in f; one-way ANOVA) as well as directedness (e, p<0.0001, one-way ANOVA). \*, \*\*

749 and \*\*\* above horizontal bars represent Tukey's results of comparisons between groups that have  
750 shown statistical significance. n= 300 for all analysis excluding (d) and (f) where n=3. Number in box  
751 in top righthand corner represents p value for one-way ANOVA (d).

752

753

754

755

756

757

758

759

760

761

762

763

764

765

766

767

768

769

770

771

772

773

774

775

776

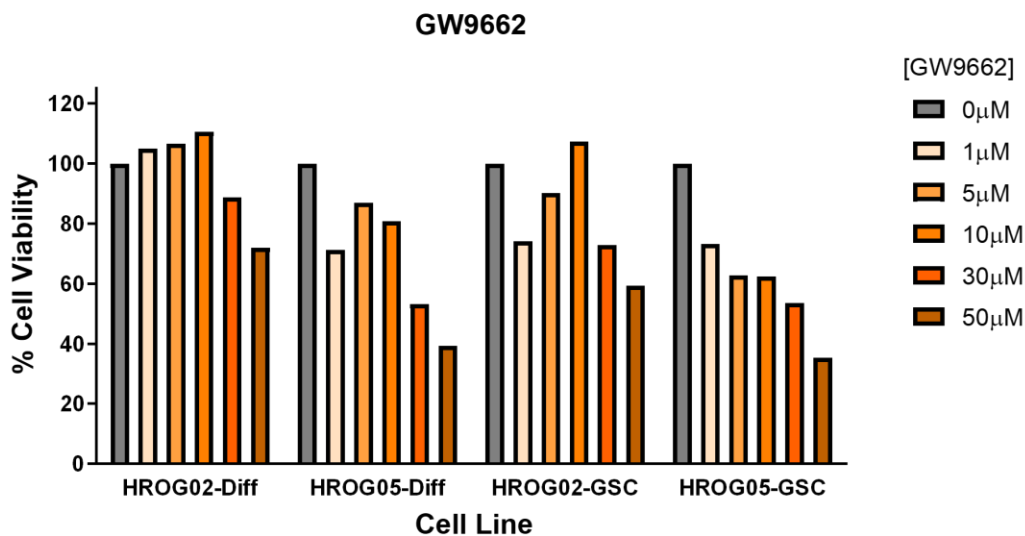
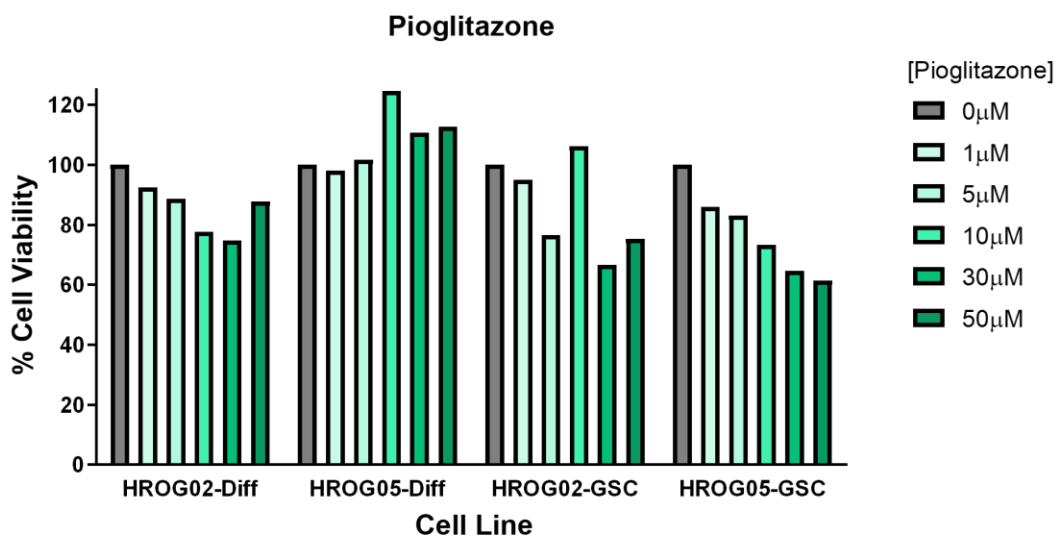
777 **Online Resource 1**

778 Effect of pioglitazone and GW9662 on cell viability of HROG02-Diff, HROG05-Diff,  
779 HROG02-GSC and HROG05-GSC cell lines using an XTT assay.

**Glioblastoma Cell Migration is Directed by Electrical Signals.** H. Clancy<sup>1</sup>, M. Pruski<sup>1,2</sup>, B. Lang<sup>1</sup>, J. Ching<sup>1,3\*</sup>, C. D. McCaig<sup>1\*</sup>

<sup>1</sup>Institute of Medical Sciences, University of Aberdeen, Aberdeen, <sup>2</sup>School of Medicine, Tongji University, Shanghai, <sup>3</sup>John Van Geest Centre for Brain Repair, University of Cambridge, Cambridge

\*Joint corresponding authors: Jared Ching, [jared.ching@nhs.net](mailto:jared.ching@nhs.net) and Colin D. McCaig, [c.mccaig@abdn.ac.uk](mailto:c.mccaig@abdn.ac.uk)



780

781

782 **Online Resource 2**

783 Immunocytochemistry staining of HROG02-Diff (a), HROG02-GSC (b), HROG05-Diff  
784 (c), and HROG05-GSC (d). Nuclei are visualised in blue (Hoechst staining), green

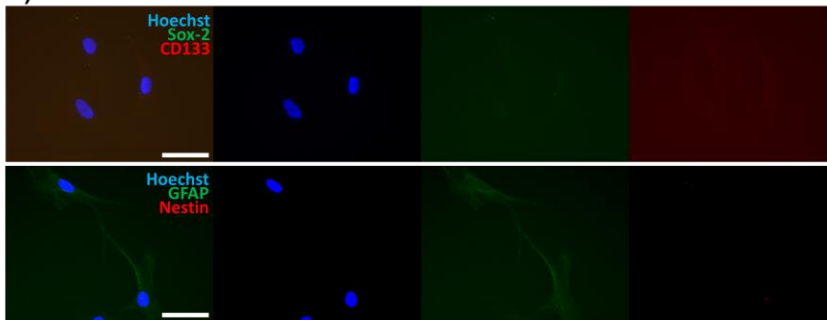
785 visualised either ant-Sox-2 or anti-GFAP, red visualises either anti-CD133 or anti-  
 786 Nestin. Scale bar represents 100  $\mu$ m. HROG02-Diff and HROG05-Diff showed  
 787 negative staining for sox-2 and CD133. HROG02-GSC and HROG05-GSC stained  
 788 positively for sox-2, CD133 and nestin. GFAP showed the most variability in staining

**Glioblastoma Cell Migration is Directed by Electrical Signals.** H. Clancy<sup>1</sup>, M. Pruski<sup>1,2</sup>, B. Lang<sup>1</sup>, J. Ching<sup>1,3\*</sup>, C. D. McCaig<sup>1\*</sup>

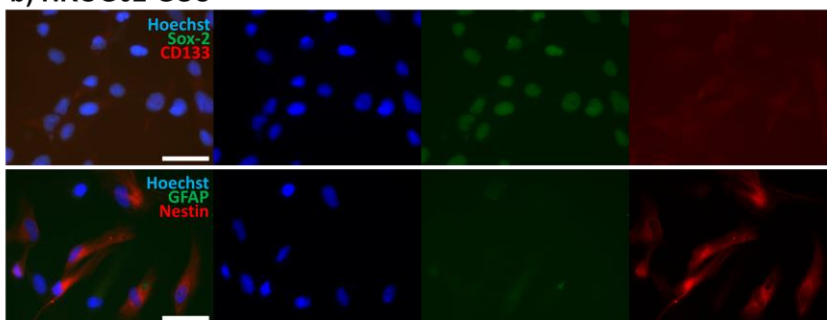
<sup>1</sup>Institute of Medical Sciences, University of Aberdeen, Aberdeen, <sup>2</sup>School of Medicine, Tongji University, Shanghai, <sup>3</sup>John Van Geest Centre for Brain Repair, University of Cambridge, Cambridge

\*Joint corresponding authors: Jared Ching, [jared.ching@nhs.net](mailto:jared.ching@nhs.net) and Colin D. McCaig, [c.mccaig@abdn.ac.uk](mailto:c.mccaig@abdn.ac.uk)

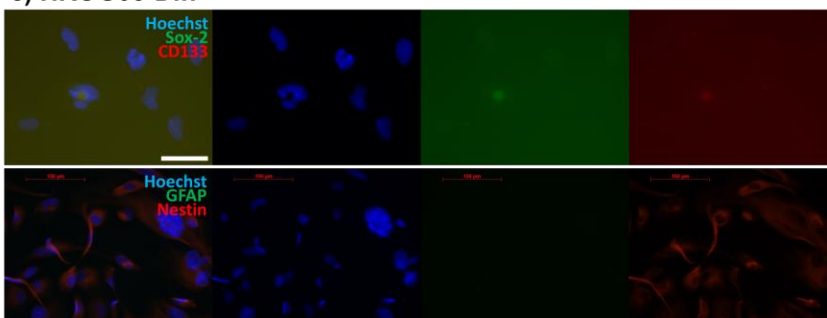
**a) HROG02-Diff**



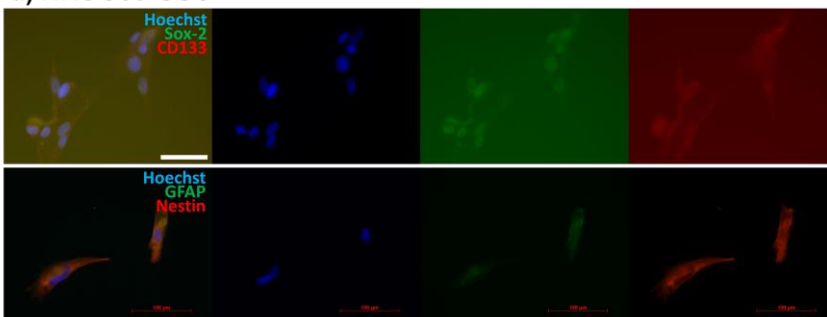
**b) HROG02-GSC**



**c) HROG05-Diff**



**d) HROG05-GSC**



789

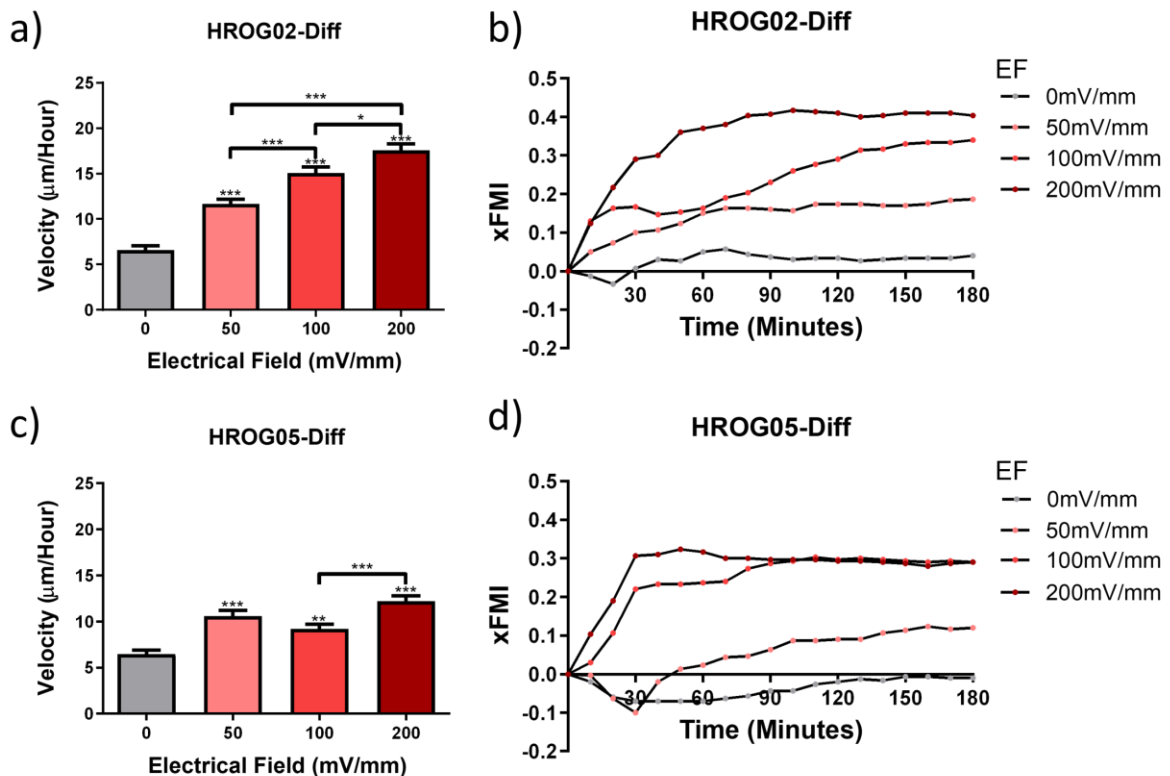
790 **Online Resource 3**

791 Additional results from HROG02-Diff and HROG05-Diff electrotactic experiments.  
 792 Panels (a) and (c) show, respectively, HROG02-Diff and HROG05-Diff cell velocity in  
 793 increasing field strengths. Panels (b) and (d) illustrates the effect of increasing field  
 794 strengths on x-Forward Migratory Index (x-FMI). \*, \*\* and \*\*\* above bars represent  
 795 Tukey's post-test comparisons with control (0 mV/mm), while horizontal bars represent  
 796 Tukey's results of comparisons between groups that have shown statistical  
 797 significance. n= 300 for (a) and (c)

**Glioblastoma Cell Migration is Directed by Electrical Signals.** H. Clancy<sup>1</sup>, M. Pruski<sup>1,2</sup>, B. Lang<sup>1</sup>, J. Ching<sup>1,3\*</sup>, C. D. McCaig<sup>1\*</sup>

<sup>1</sup>Institute of Medical Sciences, University of Aberdeen, Aberdeen, <sup>2</sup>School of Medicine, Tongji University, Shanghai, <sup>3</sup>John Van Geest Centre for Brain Repair, University of Cambridge, Cambridge

\*Joint corresponding authors: Jared Ching, [jared.ching@nhs.net](mailto:jared.ching@nhs.net) and Colin D. McCaig, [c.mccaig@abdn.ac.uk](mailto:c.mccaig@abdn.ac.uk)



798

799

800

801 **Online Resource 4**

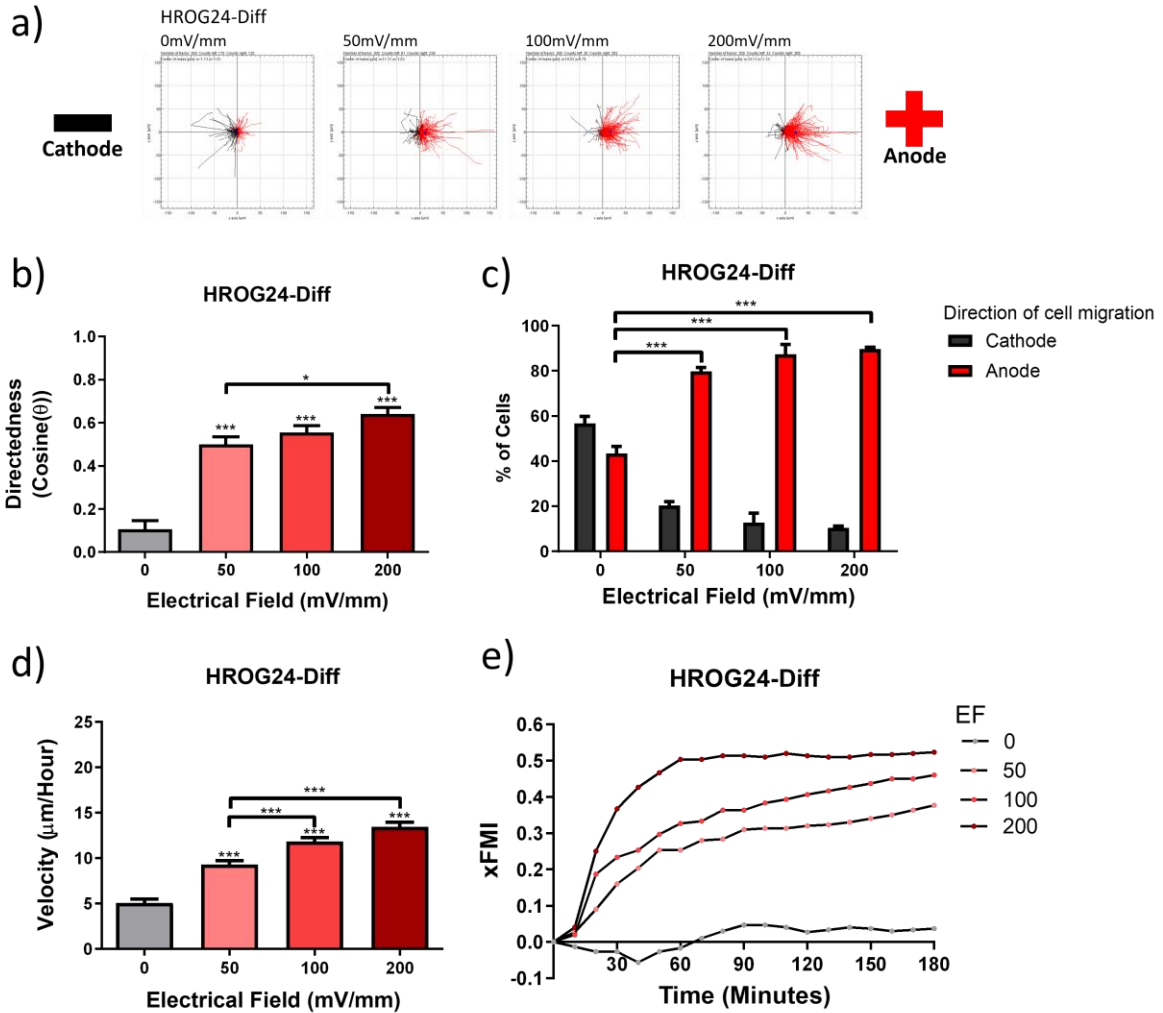
802 HROG24-Diff cell migration in electric fields. Panel (a) visualises the cellular  
803 movement that occurred under different field strengths. (b-e) show, respectively, the  
804 effects of field strength on the directedness of migration, the percentage of cells that  
805 migrated towards each electrode, cell velocity, and effect of field strength over time on  
806 the x-Forward Migration Index. Cells show an anodal migration pattern (a;  $p < 0.0001$   
807 in c) with a statistically significant effect of the electric field on directedness (b,  
808  $p < 0.0001$ ) and velocity (d,  $p < 0.0001$ ); one-way ANOVA. \*, \*\* and \*\*\* above bars  
809 represent Tukey's post-test comparisons with control (0 mV/mm), while horizontal bars  
810 represent Tukey's results of comparisons between groups that have shown statistical  
811 significance.  $n = 300$  for all analysis excluding (d) where  $n = 3$

## Glioblastoma Cell Migration is Directed by Electrical Signals.

H. Clancy<sup>1</sup>, M. Pruski<sup>1,2</sup>, B. Lang<sup>1</sup>, J. Ching<sup>1,3\*</sup>, C. D. McCaig<sup>1\*</sup>

<sup>1</sup>Institute of Medical Sciences, University of Aberdeen, Aberdeen, <sup>2</sup>School of Medicine, Tongji University, Shanghai, <sup>3</sup>John Van Geest Centre for Brain Repair, University of Cambridge, Cambridge

\*Joint corresponding authors: Jared Ching, jared.ching@nhs.net and Colin D. McCaig, c.mccaig@abdn.ac.uk



812

813

814

815

816

817

818

819



820 **Online Resource 5**

821 Video containing four animations illustrating migration of HROG02-Diff cells in  
822 response to increasing EF applied (0mV/mm, 50mV/mm, 100mV/mm and  
823 200mV/mm). Each animation contains 300 individual cell migratory pathways with the  
824 cathode (black coloured pathways) on the left, and anode (red coloured pathways) on  
825 the right

826



827

828

829

830

831

832

833

834

835

836 **Online Resource 6**

837 Video containing four animations illustrating migration of HROG05-Diff cells in  
838 response to increasing EF applied (0mV/mm, 50mV/mm, 100mV/mm and  
839 200mV/mm). Each animation contains 300 individual cell migratory pathways with the  
840 cathode (black coloured pathways) on the left, and anode (red coloured pathways) on  
841 the right

842



843

844

845

846

847

848

849

850

851

852 **Online Resource 7**

853 Video containing four animations illustrating migration of HROG24-Diff cells in  
854 response to increasing EF applied (0mV/mm, 50mV/mm, 100mV/mm and  
855 200mV/mm). Each animation contains 300 individual cell migratory pathways with the  
856 cathode (black coloured pathways) on the left, and anode (red coloured pathways) on  
857 the right

858



859

860

861

862

863

864

865

866

867

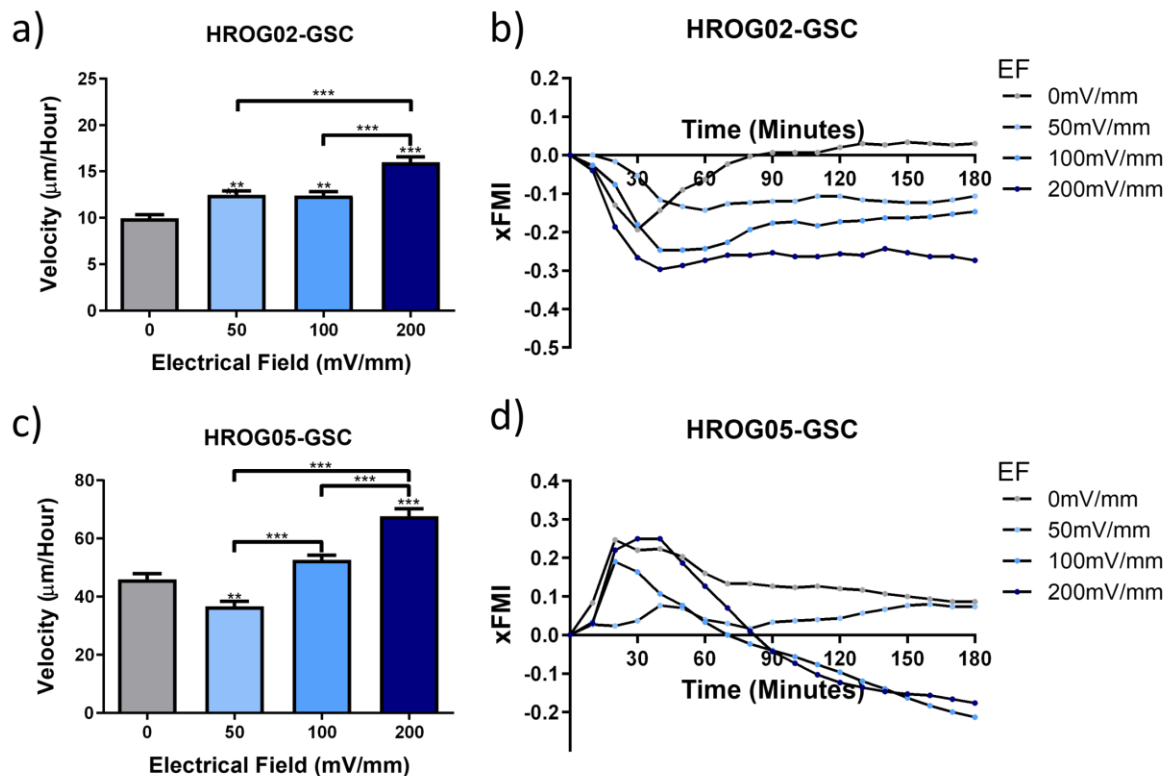
868 **Online Resource 8**

869 Additional results from HROG02-GSC and HROG05-GSC electrotactic experiments.  
870 Panels (a) and (c) show, respectively, HROG02-GSC and HROG05-GSC cell velocity  
871 in increasing field strengths. Panels (b) and (d) illustrates the effect of increasing field  
872 strengths on x-Forward Migratory Index (x-FMI). \*, \*\* and \*\*\* above bars represent  
873 Tukey's post-test comparisons with control (0 mV/mm), while horizontal bars represent  
874 Tukey's results of comparisons between groups that have shown statistical  
875 significance. n= 300 for (a) and (c)

**Glioblastoma Cell Migration is Directed by Electrical Signals.** H. Clancy<sup>1</sup>, M. Pruski<sup>1,2</sup>, B. Lang<sup>1</sup>, J. Ching<sup>1,3\*</sup>, C. D. McCaig<sup>1\*</sup>

<sup>1</sup>Institute of Medical Sciences, University of Aberdeen, Aberdeen, <sup>2</sup>School of Medicine, Tongji University, Shanghai, <sup>3</sup>John Van Geest Centre for Brain Repair, University of Cambridge, Cambridge

\*Joint corresponding authors: Jared Ching, [jared.ching@nhs.net](mailto:jared.ching@nhs.net) and Colin D. McCaig, [c.mccaig@abdn.ac.uk](mailto:c.mccaig@abdn.ac.uk)



876

877

878

879 **Online Resource 9**

880 Video containing four animations illustrating migration of HROG02-GSC cells in  
881 response to increasing EF applied (0mV/mm, 50mV/mm, 100mV/mm and  
882 200mV/mm). Each animation contains 300 individual cell migratory pathways with the  
883 cathode (black coloured pathways) on the left, and anode (red coloured pathways) on  
884 the right

885



886

887

888

889

890

891

892

893

894

895 **Online Resource 10**

896 Video containing four animations illustrating migration of HROG05-GSC cells in  
897 response to increasing EF applied (0mV/mm, 50mV/mm, 100mV/mm and  
898 200mV/mm). Each animation contains 300 individual cell migratory pathways with the  
899 cathode (black coloured pathways) on the left, and anode (red coloured pathways) on  
900 the right

901

Sample textGlioblastoma Cell Migration is Directed by Electrical Signals

H. Clancy<sup>1</sup>, M. Pruski<sup>1,2</sup>, B. Lang<sup>1</sup>, J. Ching<sup>1,3\*</sup>, C. D. McCaig<sup>1\*</sup>

<sup>1</sup>Institute of Medical Sciences, University of Aberdeen, Aberdeen,

<sup>2</sup>School of Medicine, Tongji University, Shanghai,

<sup>3</sup>John Van Geest Centre for Brain Repair, University of Cambridge, Cambridge

\*Joint corresponding authors:

Jared Ching, [jared.ching@nhs.net](mailto:jared.ching@nhs.net)

Colin D. McCaig, [c.mccaig@abdn.ac.uk](mailto:c.mccaig@abdn.ac.uk)

902

903

904

905

906

907

908

909

910

911 **Online Resource 11**

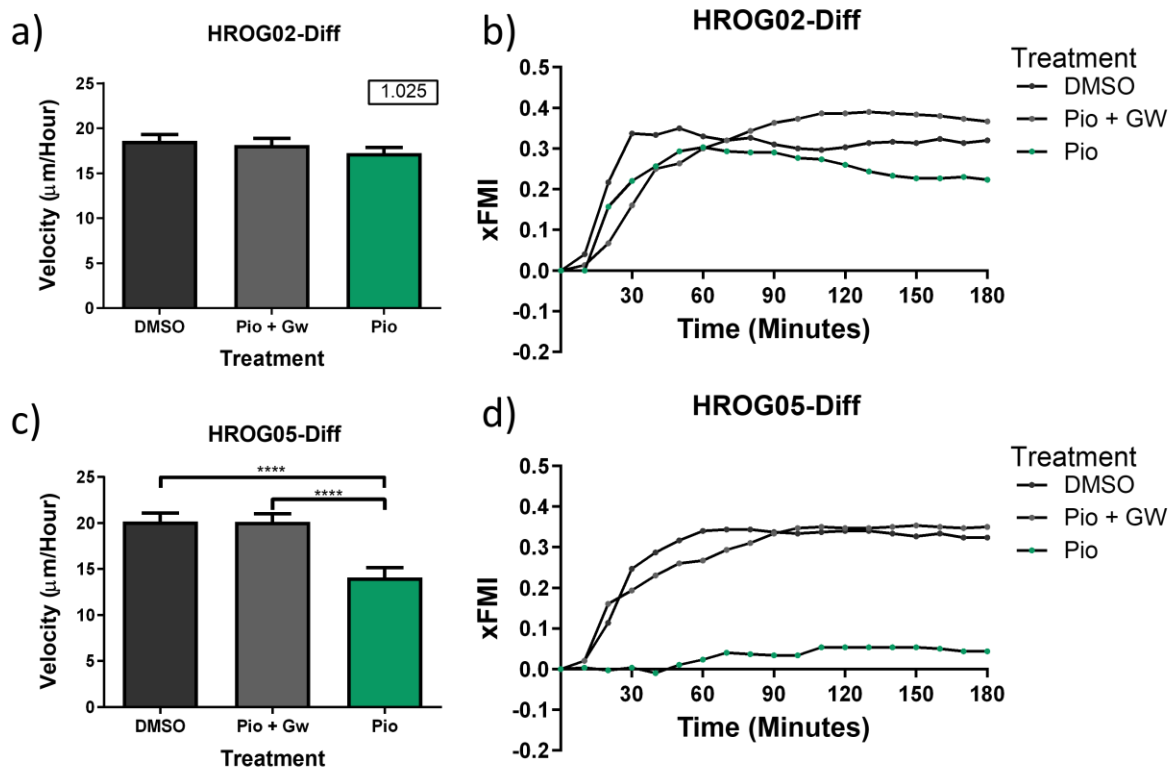
912 Additional results showing the effect of PPAR $\gamma$  stimulation on HROG02-Diff and  
913 HROG05-Diff cell migration in a 200mV/mm electric field. Panels (a) and (c) show,  
914 respectively, HROG02-Diff and HROG05-Diff cell velocity upon exposure to DMSO  
915 (drug vehicle) and PPAR $\gamma$  agonists (pioglitazone, “pio”) and antagonist (GW9662,  
916 “GW”). Panels (b) and (d) illustrates the effect of treatment over time on the x-Forward  
917 Migration Index. \*, \*\* and \*\*\* above bars represent Tukey’s post-test comparisons with  
918 control (0 mV/mm), while horizontal bars represent Tukey’s results of comparisons  
919 between groups that have shown statistical significance. n= 300 for (a) and (c)

**Glioblastoma Cell Migration is Directed by Electrical Signals.**

H. Clancy<sup>1</sup>, M. Pruski<sup>1,2</sup>, B. Lang<sup>1</sup>, J. Ching<sup>1,3\*</sup>, C. D. McCaig<sup>1\*</sup>

<sup>1</sup>Institute of Medical Sciences, University of Aberdeen, Aberdeen, <sup>2</sup>School of Medicine, Tongji University, Shanghai, <sup>3</sup>John Van Geest Centre for Brain Repair, University of Cambridge, Cambridge

\*Joint corresponding authors: Jared Ching, jared.ching@nhs.net and Colin D. McCaig, c.mccaig@abdn.ac.uk



920

921

922 **Online Resource 12**

923 Video containing three animations illustrating the effect of PPAR $\gamma$  stimulation on  
924 HROG02-Diff cell migration in a 200mV/mm electric field. Each animation contains  
925 300 individual cell migratory pathways with the cathode (black coloured pathways) on  
926 the left, and anode (red coloured pathways) on the right. "Pio" refers to pioglitazone,  
927 and "GW" GW9662  
928



929

930

931

932

933

934

935

936

937



938 **Online Resource 13**

939 Video containing three animations illustrating the effect of PPAR $\gamma$  stimulation on  
940 HROG05-Diff cell migration in a 200mV/mm electric field. Each animation contains  
941 300 individual cell migratory pathways with the cathode (black coloured pathways) on  
942 the left, and anode (red coloured pathways) on the right. "Pio" refers to pioglitazone,  
943 and "GW" GW9662  
944



945  
946  
947  
948  
949  
950  
951  
952  
953

954 **Online Resource 14**

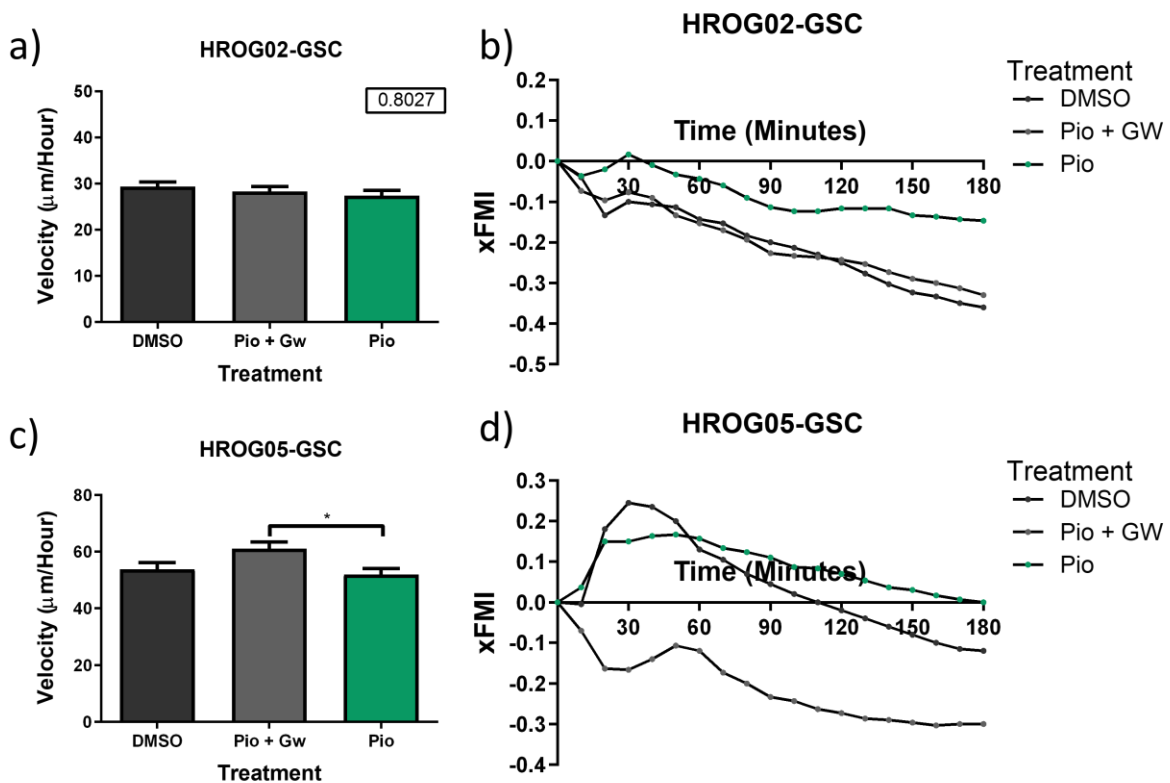
955 Additional results showing the effect of PPAR $\gamma$  stimulation on HROG02-GSC and  
956 HROG05-GSC cell migration in a 200mV/mm electric field. Panels (a) and (c) show,  
957 respectively, HROG02-GSC and HROG05-GSC cell velocity upon exposure to DMSO  
958 (drug vehicle) and PPAR $\gamma$  agonists (pioglitazone, “pio”) and antagonist (GW9662,  
959 “GW”). Panels (b) and (d) illustrates the effect of treatment over time on the x-Forward  
960 Migration Index. \*, \*\* and \*\*\* above bars represent Tukey’s post-test comparisons with  
961 control (0 mV/mm), while horizontal bars represent Tukey’s results of comparisons  
962 between groups that have shown statistical significance. n= 300 for (a) and (c)

**Glioblastoma Cell Migration is Directed by Electrical Signals.**

H. Clancy<sup>1</sup>, M. Pruski<sup>1,2</sup>, B. Lang<sup>1</sup>, J. Ching<sup>1,3\*</sup>, C. D. McCaig<sup>1\*</sup>

<sup>1</sup>Institute of Medical Sciences, University of Aberdeen, Aberdeen, <sup>2</sup>School of Medicine, Tongji University, Shanghai, <sup>3</sup>John Van Geest Centre for Brain Repair, University of Cambridge, Cambridge

\*Joint corresponding authors: Jared Ching, jared.ching@nhs.net and Colin D. McCaig, c.mccaig@abdn.ac.uk



963

964

965 **Online Resource 15**

966 Video containing three animations illustrating the effect of PPAR $\gamma$  stimulation on  
967 HROG02-GSC cell migration in a 200mV/mm electric field. Each animation contains  
968 300 individual cell migratory pathways with the cathode (black coloured pathways) on  
969 the left, and anode (red coloured pathways) on the right. "Pio" refers to pioglitazone,  
970 and "GW" GW9662

971



972

973

974

975

976

977

978

979

980

981 **Online Resource 16**

982 Video containing three animations illustrating the effect of PPAR $\gamma$  stimulation on  
983 HROG05-GSC cell migration in a 200mV/mm electric field. Each animation contains  
984 300 individual cell migratory pathways with the cathode (black coloured pathways) on  
985 the left, and anode (red coloured pathways) on the right. “Pio” refers to pioglitazone,  
986 and “GW” GW9662

987



988

989

990

991

992

993

994

995

996

997 **Online Resource 17**

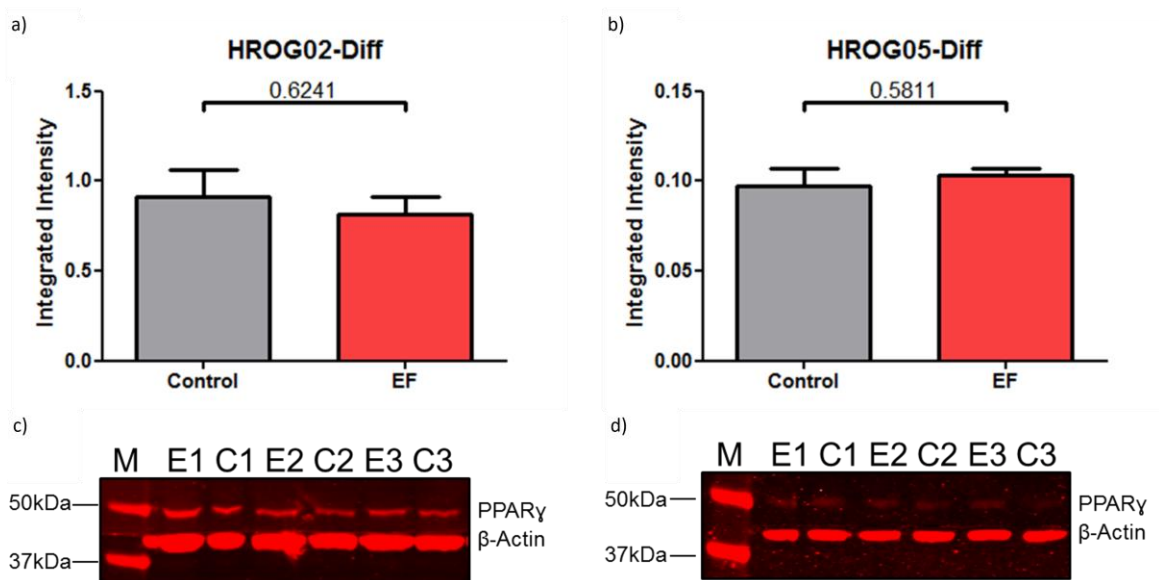
998 Effects of electric fields on PPAR $\gamma$  expression in HROG02-GSC and HROG05-GSC  
999 cells. (a) and (b) shows that a one hour application of a 200mV/mm field did not cause  
1000 a statistically significant change in PPAR $\gamma$  protein levels when compared to  $\beta$ -actin  
1001 expression of HROG02-GSC and HROG05-GSC respectively as demonstrated by  
1002 Integrated Intensity. (c) (d) shows the image used in the Western blot analysis of  
1003 HROG02-GSC and HROG05-GSC respectively; M indicates the protein ladder, E  
1004 indicates samples obtained from cells which were subjected to the electric field, C  
1005 indicates control samples (no EF applied). Number above horizontal bar indicates  
1006 unpaired T-Test analysis where n=3

**Glioblastoma Cell Migration is Directed by Electrical Signals.**

H. Clancy<sup>1</sup>, M. Pruski<sup>1,2</sup>, B. Lang<sup>1</sup>, J. Ching<sup>1,3\*</sup>, C. D. McCaig<sup>1\*</sup>

<sup>1</sup>Institute of Medical Sciences, University of Aberdeen, Aberdeen, <sup>2</sup>School of Medicine, Tongji University, Shanghai, <sup>3</sup>John Van Geest Centre for Brain Repair, University of Cambridge, Cambridge

\*Joint corresponding authors: Jared Ching, [jared.ching@nhs.net](mailto:jared.ching@nhs.net) and Colin D. McCaig, [c.mccaig@abdn.ac.uk](mailto:c.mccaig@abdn.ac.uk)



1007  
1008  
1009  
1010

1011 **Online Resource 18**

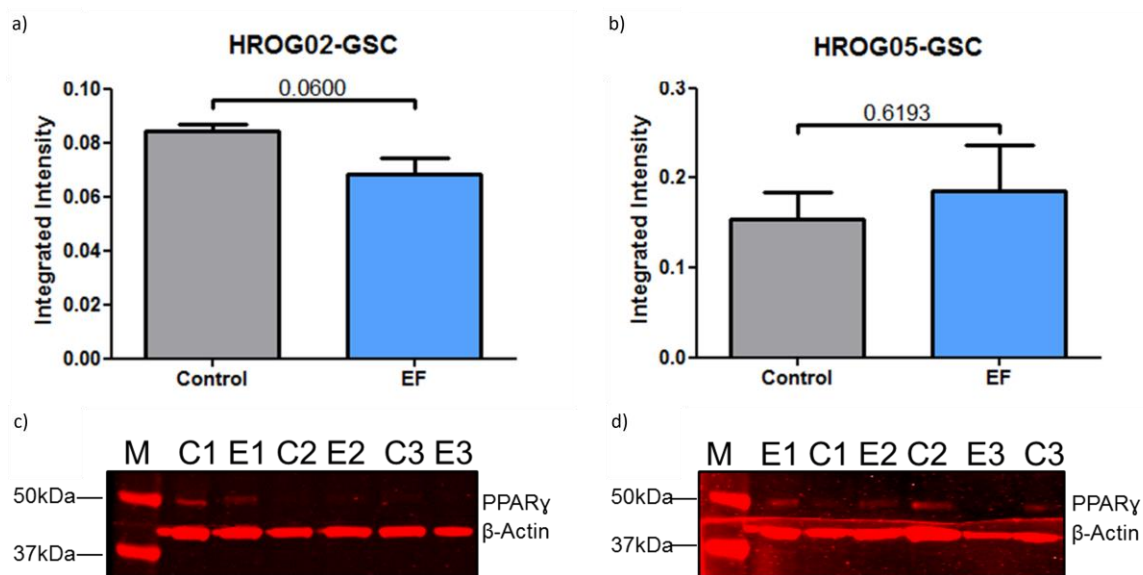
1012 Effects of electric fields on PPAR $\gamma$  expression in HROG02-GSC and HROG05-GSC  
1013 cells. (a) and (b) shows that a one hour application of a 200mV/mm field did not cause  
1014 a statistically significant change in PPAR $\gamma$  protein levels when compared to  $\beta$ -actin  
1015 expression of HROG02-GSC and HROG05-GSC respectively as demonstrated by  
1016 Integrated Intensity. (c) (d) shows the image used in the Western blot analysis of  
1017 HROG02-GSC and HROG05-GSC respectively; M indicates the protein ladder, E  
1018 indicates samples obtained from cells which were subjected to the electric field, C  
1019 indicates control samples (no EF applied). Number above horizontal bar indicates  
1020 unpaired T-Test analysis where n=3

**Glioblastoma Cell Migration is Directed by Electrical Signals.**

H. Clancy<sup>1</sup>, M. Pruski<sup>1,2</sup>, B. Lang<sup>1</sup>, J. Ching<sup>1,3\*</sup>, C. D. McCaig<sup>1\*</sup>

<sup>1</sup>Institute of Medical Sciences, University of Aberdeen, Aberdeen, <sup>2</sup>School of Medicine, Tongji University, Shanghai, <sup>3</sup>John Van Geest Centre for Brain Repair, University of Cambridge, Cambridge

\*Joint corresponding authors: Jared Ching, [jared.ching@nhs.net](mailto:jared.ching@nhs.net) and Colin D. McCaig, [c.mccaig@abdn.ac.uk](mailto:c.mccaig@abdn.ac.uk)



1021



[Click here to access/download](#)

**Supplementary material for online publication only**  
**Online Resource 7.mp4**





[Click here to access/download](#)

**Supplementary material for online publication only**  
**Online Resource 9.mp4**







[Click here to access/download](#)

**Supplementary material for online publication only**  
**Online Resource 10.mp4**





[Click here to access/download](#)

**Supplementary material for online publication only**  
Online Resource 12.mp4





[Click here to access/download](#)

**Supplementary material for online publication only**  
Online Resource 13.mp4





[Click here to access/download](#)

**Supplementary material for online publication only**  
**Online Resource 15.mp4**





[Click here to access/download](#)

**Supplementary material for online publication only**  
**Online Resource 16.mp4**





[Click here to access/download](#)

**Supplementary material for online publication only**  
**Online Resource 5.mp4**





[Click here to access/download](#)

**Supplementary material for online publication only**  
**Online Resource 6.mp4**



**Declaration of interests**

The authors declare that they have no known competing financial interests or personal relationships that could have appeared to influence the work reported in this paper.

The authors declare the following financial interests/personal relationships which may be considered as potential competing interests:



## **Glioblastoma Cell Migration is Directed by Electrical Signals**

### **CRedit author statement**

Conceptualization, J.C., C.D.M.; Methodology, J.C., C.D.M.; Validation J.C. H.C., M.P.;  
Formal Analysis, H.C., M.P.; Investigation, J.C., H.C., M.P.; Data Curation, H.C., M.P.,  
J.C.; Writing – original draft, H.C., M.P., J.C.; Writing – Review & Editing, All;  
Supervision, C.D.M, J.C., B.L.; Funding acquisition, J.C., C.D.M.